26 June 2009 | $10

Science

Stem Cells

AAAS

cell sciences

signal transduction

Research products for the study of the important signal transduction pathways…

www.cellsciences.com

Abl SH3 domain, inactive
ABL1
ACV-R1
ADRBK1
ADRBK2
Akt1
Akt1, inactive
Akt2
Akt3
ALK/P80
AMPK-alpha1
ARK5
ASK1
ATF-2
Aurora A
Aurora B
Aurora C
AXL
BLK
BMX
BRAF
BRK
BRSK1
BTK
C-JUN
C-Src
CAMK1 delta
CAMK1 gamma
CAMK2 beta
CAMK2 delta
CAMK4
CDC42BPA/MRCKA
CDC42BPB/MRCKB
CDK1/CycB
CDK1/CycE
CDK2
CDK2/CycA
CDK2/CycE
CDK3/CycE
CDK4
CDK4/CycD1
CDK4/CycD3
CDK5
CDK5/p25NCK
CDK5/p35NCK
CDK6/CycD1
CDK7/CycH/MAT1
CDK8, inactive
CDK9/CycT
CHK2
CK1 alpha 1
CK1 delta
CK1 gamma 1
CK1 gamma 2
CK1 gamma 3
CK2 alpha 1
CK2 alpha 2
CK2 beta
CK2 holoenzyme
CKBB
CKMB
CKMBI type 1
CKMBI type 2
CKMM
CKMM Type 1
CKMM Type 3
CLK1
CREB-1
CSK
DAPK1
DAPK2
DAPK3
DCAMKL2
DDR2
DEK
DMPK
EGFR
eIF2 alpha
ELK-1
EphA1
EphA2
EphA3
EphA4
EphA5
EphA7
EphA8
EphB1
EphB2
EphB3
EphB4
ERBB2
ERBB4
Erk1
Erk2
FAK
FER
FGF-R1
FGF-R2
FGF-R3
FGF-R4
FGR
Flt-1
Flt3 Kinase
FRK
GCK
GRK5
GRK6
GSK3
GSK3 beta
Hck SH3 domain, inactive
Hck
HGK
HIPK1
HIPK3
I kappa B alpha
IGF1-R
IKK-beta
IKK-epsilon
INS-R
IRAK1
IRAK4
ITK
JAK2 JH1 JH2
JAK2
JAK3
JNK1
JNK2 alpha 1
JNK2 alpha 2
KDR/VEGFR2
KHS1/MAP4K5
KIT
LCK SH3 domain, inactive
LCK
LTK
LYN B
MAPK9
MAPK11/p38 beta
MAPK12/p38 gamma
MAPK14
MAPK14/p38
MAPKAPK2
MAPKAPK3
MAPKAPK5
MARK1
MARK2
MARK3
MARK4
MATK
MEK1
MEK2
MEK3
MET
MERTK
MINK1
MLK1
MLK2
MLK3
MST2
MST4
MUSK
MYLK
MYLK2
NCK2
NCOR2/SMRT
NEK2
NEK3
NEK6
NEK7
NEK11
NFAT
NLK
p110 alpha/p85 alpha
p38 alpha
p38 beta
p38 delta
p38 gamma
p70S6K
PAK1
PAK2
PAK4
PAK6
PAK7
PBK
PDGFR-alpha
PDGFR-beta
PDK1
PHKG1
PHKG2
PI3K p110d/p85a
PI3K p110g
PI3K beta p110ß/p85a
PI3K p110a/p85a
PI3K p110g
PIM1
PIM2
PKA holoenzyme type Ia
PKA holoenzyme type IIa
PKA regulatory subunit Ia
PKA regulatory subunit IIa
PKAc alpha
PKAc beta
PKAc gamma
PKAR-I alpha
PKC alpha
PKC beta 1
PKC beta II
PKC delta
PKC epsilon
PKC eta
PKC gamma
PKC iota/lambda
PKC mu
PKC nu
PKC theta
PKC zeta
PKD2
PKG1 beta
PLK1
PLK2
PLK3
PP2C alpha
PRK1
PTK2B
PYK2
Raf1
RET
RIPK2
ROCK1
ROCK2
RPS6KB1/p70S6K
RPS6KB2/p70S6Kbeta
RSK1
RSK2
RSK3
RSK4
S6K
SAK
SGK1
SGK2
SGK3
SNARK
SNK
Sphingosine Kinase 1
Sphingosine Kinase 2
Src
SRPK1
SRPK2
STAT1
STAT3
STK3
STK16/TSF1
STK17A (DRAK1)
STK22B/TSSK2
STK23/MSSK1
STK24/MST3
STK33
SYK
TBK1
TGFB-R1
Tie2
TRKA
TSF1
TSSK1
TSSK2
TTK
TYRO3
VEGF-R1
VEGF-R2/KDR
VEGF-R3
VRK1
WEE1
WNK2
WNK3
YES
ZAP70

CELL SCIENCES INC • 480 NEPONSET STREET, BUILDING 12A, CANTON, MA 02021 • INFO@CELLSCIENCES.COM

TOLL FREE: (888) 769-1246 • TEL: (781) 828-0610 • FAX: (781) 828-0542 • WEB WWW.CELLSCIENCES.COM

Stemgent® Small Molecules. Essential Tools for Research in Differentiation, Self-Renewal, and Pluripotency.

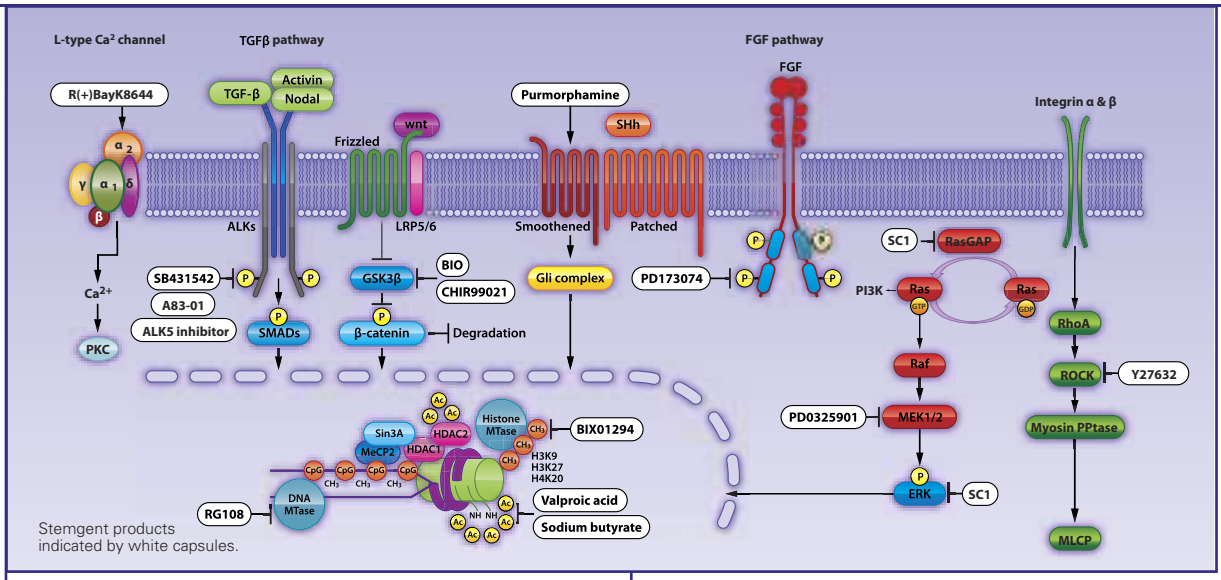

Stemgent products indicated by white capsules.

Precision Information About Where Your Stem Cells Are Headed.

Small molecules have proven to be invaluable as effectors of stem cells. To promote self-renewal and achieve precise control of stem cell differentiation, access to a vast library of small molecule modulators is an important research tool. Here are just a few reasons why.

- ❑ **Easy cell penetration.**
- ❑ **Very low antigenicity.**
- ❑ **Work across multiple cell signalling pathways.**
- ❑ **Easily effect epigenetic modifications.**

MORE www.stemgent.com/sml2

Stemolecules™. Reliability, Quality and Formulae Only Available Here.

Naturally you can count on the purity of all of the small molecule products in the Stemolecule line. You can also expect a growing number of small molecule products with special relevance to almost all stem cell researchers.

- ❑ **CHIR99021–GSK3β inhibitor used in maintaining pluripotency**
- ❑ **PD0325901–Mek inhibitor used in maintaining pluripotency**
- ❑ **Y27632–Rock I/II Inhibitor that increases stem cell survival after stress conditions**

MORE www.stemgent.com/sml4

We Are Your Partner In Small Molecule Research.

Whether your work involves differentiation of stem cells into different tissues, or you need to maintain pluripotency or more likely, both, Stemgent® is your trusted source for small molecules. Our inventory is substantial and we look forward to working with you directly to provide small molecules precisely prepared for your experimental needs.

- ❑ **Talk directly with a scientist in our small molecules group.**
- ❑ **Get the small molecules you need for your specific work.**
- ❑ **Our world-renowned Scientific Advisory Board keeps us on the cutting edge.**

MORE www.stemgent.com/sml6

Our purpose is to move stem cell science forward. The best way to do that is to make the research of world-class scientists available to you in ways that are reliable and useful. In that way, your work benefits from their work. And the future of stem cell research is accelerated. Come to www.stemgent.com/sci8 for more information. Or call 877-228-9783 (toll-free) or +1-617-245-0098 (international).

STEMGENT™

REPROGRAMMING THE REAGENT™

BOSTON | www.stemgent.com/sci8 | SAN DIEGO

ISSCR: BOOTH 38

MORE www.stemgent.com/xxx **About Stemgent Information Links**. Get to the precise information you need faster. When you see one of these link bars, go to Stemgent.com and add the /xxxx extension. It's a direct link to the info you need.

WHAT'S Next™

Biacore systems

from inspiration ...to publication

Highest quality, information-rich interaction data from Biacore™ systems deepen your understanding of molecular mechanisms and interaction pathways and enable you to add function to structure.

Select the perfect solution for your application and draw conclusions with confidence – from the company that continues to set the standard for label-free protein interaction analysis.

For further information or register to have one of our scientific experts contact you, please visit **www.gelifesciences.com/biacore-science**

Biacore T100
unmatched performance

Biacore X100
ready to run research system

Biacore Flexchip
array-based comparative profiling

imagination at work

SPECIAL SECTION

Stem Cells

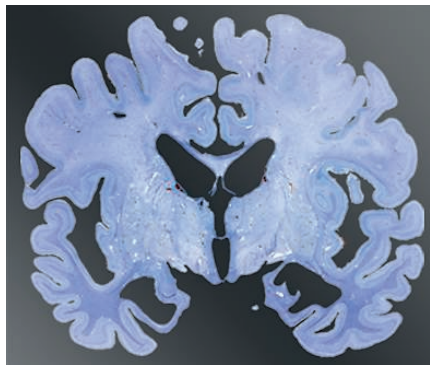

page 1634

INTRODUCTION

PERSPECTIVES

REVIEWS

EDITORIAL

NEWS OF THE WEEK

NEWS FOCUS

LETTERS

BOOKS *ET AL.*

POLICY FORUM

EDUCATION FORUM

PERSPECTIVES

CONTENTS continued >>

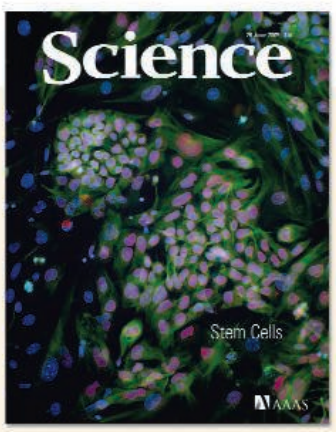

COVER

Colonies of human embryonic stem cells with differentiating cells at their edges, growing on mouse feeder cells. Cell nuclei are stained in blue, nuclear lamina in red, and cytoplasm in green (overlapping blue and red areas appear purple). The self-renewal capacity and pluripotency of human stem cells make them valuable for modeling human disease. These cells also display potential for transplantation medicine. See the special section beginning on page 1661.

Image: Oded Kopper and Nissim Benvenisty, The Hebrew University of Jerusalem

DEPARTMENTS

Published by AAAS

Rotor-Gene Q — pure detection

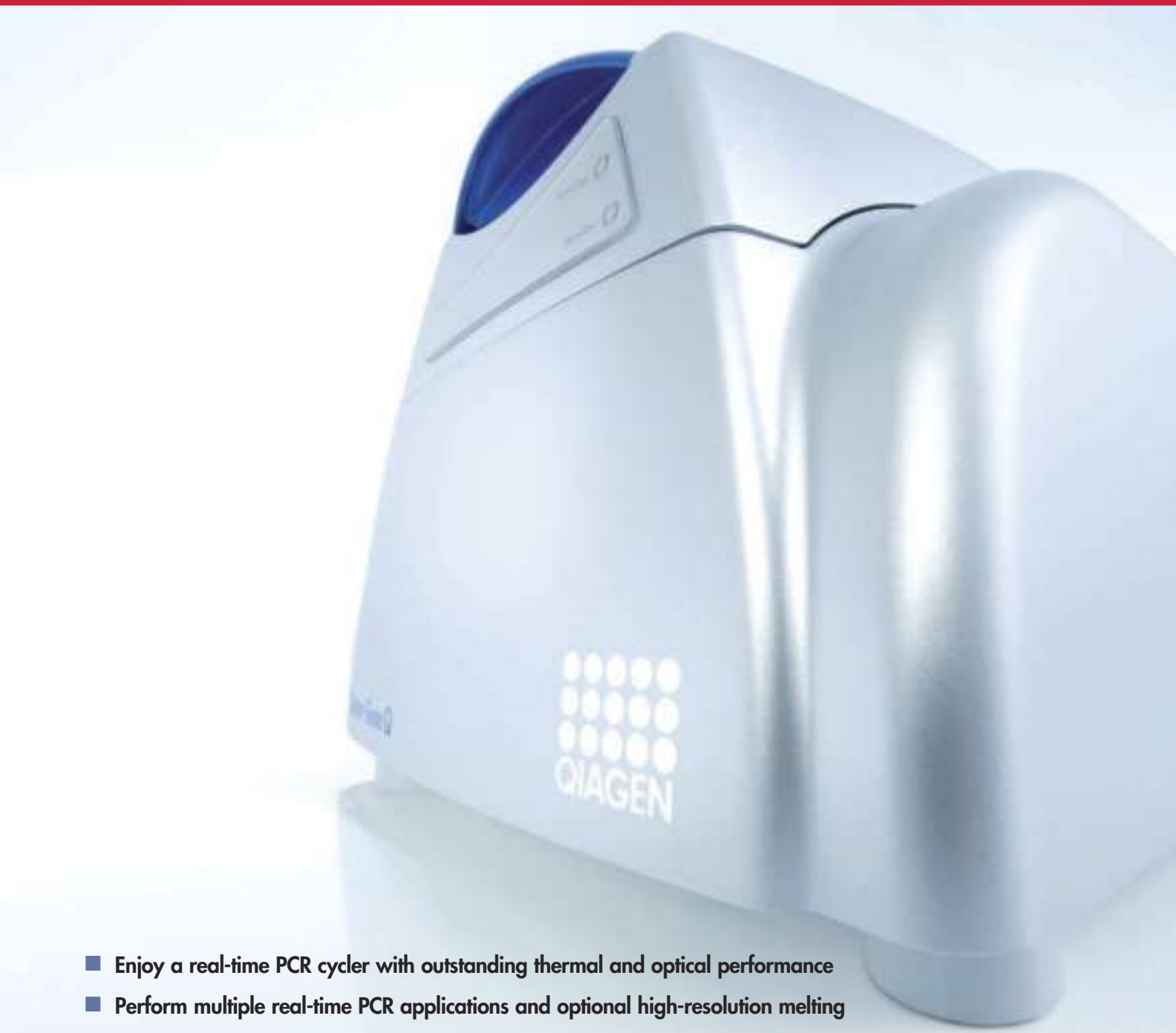

- Enjoy a real-time PCR cycler with outstanding thermal and optical performance
- Perform multiple real-time PCR applications and optional high-resolution melting
- Benefit from a variety of state-of-the-art analyses
- Experience unrivaled robustness and minimal maintenance
- Count on reliable results from QIAGEN kits and assays

Discover more at www.qiagen.com/goto/PureDetection.

QIAGEN®

Sample & Assay Technologies

AUTORotorgeneQ0109S1WW

REVIEW

BREVIA

RESEARCH ARTICLE

REPORTS

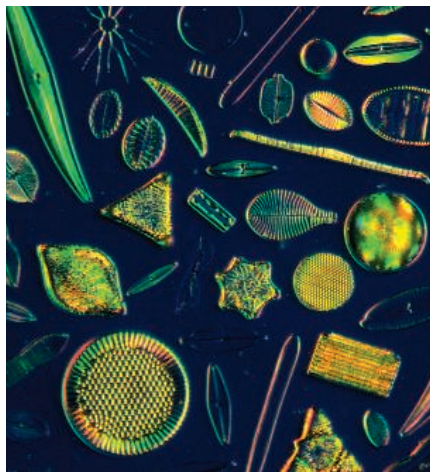

pages 1651 & 1724

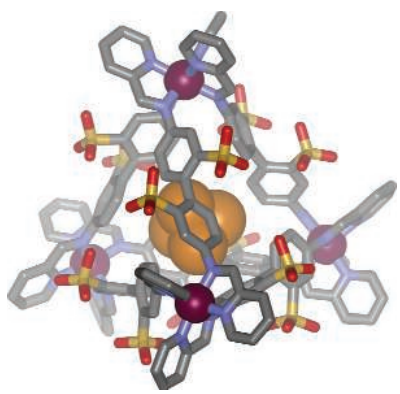

page 1697

CONTENTS continued >>

Published by AAAS

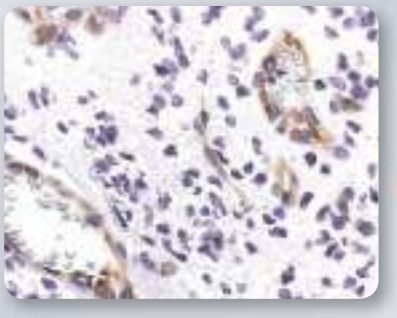

Immunohistochemical analysis of paraffin-embedded human astrocytoma using **VEGF Receptor 2 (55B11) Rabbit mAb #2479**.

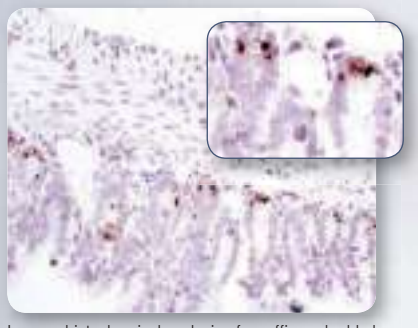

Immunohistochemical analysis of paraffin-embedded mouse small intestine using **MMP7 (D4H5) Rabbit mAb #3801**.

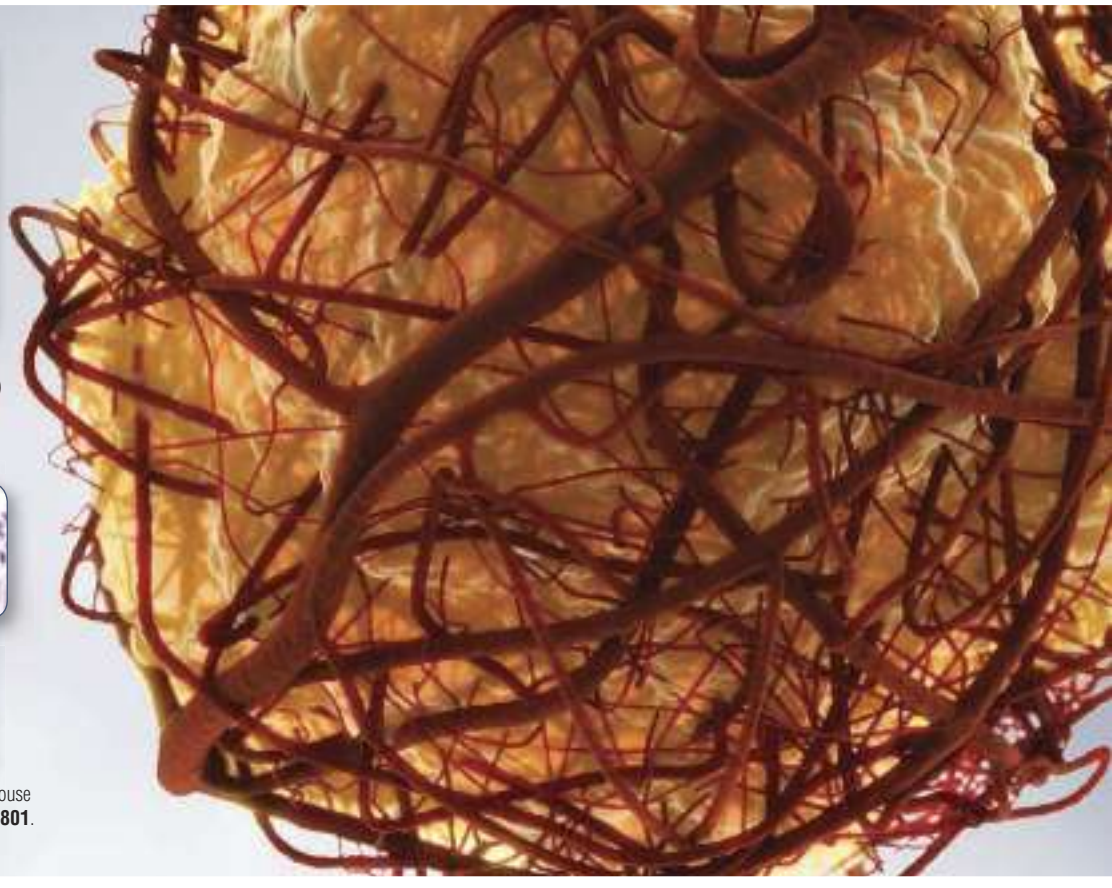

The Highest Quality Antibodies for the Study of

Angiogenesis

...from Cell Signaling Technology®

Unparalleled product quality, validation and technical support.

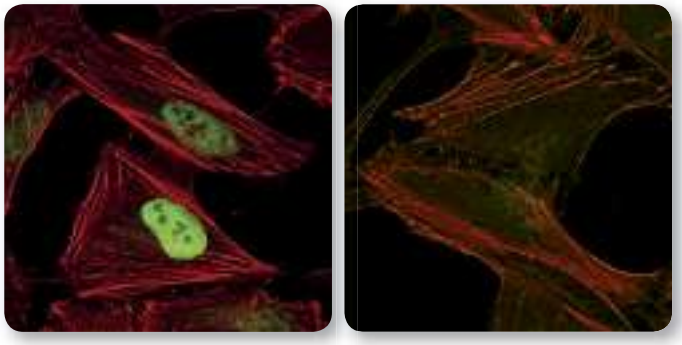

Confocal immunofluorescent analysis of HeLa cells, treated with either 10 µM MG132 (left) or 10 µM MG132 and 1 mM DMOG (right), using **Hydroxy-HIF-1α (Pro564) (D43B5) Rabbit mAb #3434** (green). Actin filaments have been labeled using DY-554 phalloidin (red).

- Cell Signaling Technology's innovative products offer unsurpassed sensitivity, specificity and performance.
- Extensive in-house validation means that optimization is not left up to you, the user.
- Technical support provided by the same scientists who produce and validate the products translates into a thorough, fast and accurate response.

for quality products you can trust...

www.cellsignal.com

Cell Signaling TECHNOLOGY®

SCIENCEONLINE

SCIENCEXPRESS
www.sciencexpress.org

String Theory, Quantum Phase Transitions, and the Emergent Fermi Liquid
M.Čubrović et al.

Mathematical methods developed in string theory to describe gravity are applied to complex condensed matter systems.
10.1126/science.1174962

Measuring the Cosmic Ray Acceleration Efficiency of a Supernova Remnant
E. A. Helder et al.

The pressure induced by cosmic rays produced by the explosion of a star exceeds the thermal pressure behind the shock wave.
10.1126/science.1173383

A Gene Network Regulating Lysosomal Biogenesis and Function
M. Sardiello et al.

Coordination of the genes that regulate lysosomal biogenesis occurs via a shared sequence motif and one transcription factor.
10.1126/science.1174447

An ER-Mitochondria Tethering Complex Revealed by a Synthetic Biology Screen
B. Kornmann et al.

A protein complex zippers mitochondria to endoplasmic reticulum for phospholipid transfer.
10.1126/science.1175088

DICER1 Mutations in Familial Pleuropulmonary Blastoma
D. A. Hill et al.

A rare form of lung cancer in children is associated with mutational disruption of an enzyme that generates small noncoding RNAs.
10.1126/science.1174334

SCIENCENOW
www.sciencenow.org
Highlights From Our Daily News Coverage

Atoms Speeding From the Moon
Scientists probing the outer reaches of our solar system have hit upon an unusual phenomenon much closer to home.

Tracking Killers of the Sea
Researchers borrow forensic geographic profiling methods to study how sharks hunt.

Fish Throws Away Its Genes as It Grows
Lamprey sheds one-fifth of its genome, but no one's sure why.

SCIENCESIGNALING
www.sciencesignaling.org
The Signal Transduction Knowledge Environment

RESEARCH ARTICLE: The Kinesin Protein Kif7 Is a Critical Regulator of Gli Transcription Factors in Mammalian Hedgehog Signaling
H. O.-L. Cheung et al.

Kif7 may be the functional equivalent of the *Drosophila* kinesin-like protein Costal2.

RESEARCH ARTICLE: PKC-θ Modulates the Strength of T Cell Responses by Targeting Cbl-b for Ubiquitination and Degradation
T. Gruber et al.

PERSPECTIVE: Activation of T Cells: Releasing the Brakes by Proteolytic Elimination of Cbl-b
M. L. Schmitz

Degradation of the ubiquitin E3 ligase Cbl-b in response to T cell costimulation depends on PKC-θ.

PODCAST
A. Levchenko and A. M. VanHook

A microfluidic device enables high-throughput analysis of signaling in individual cells.

SCIENCECAREERS
www.sciencecareers.org/career_magazine
Free Career Resources for Scientists

Career Renewal for Established Scientists
E. Pain

Staying engaged, motivated, and productive after tenure can be challenging.

Rejuvenation Tips for Tenured Faculty
E. Pain

Here are ways to rekindle a passion for science and inject new life into your research.

Revising Best-Laid Plans
S. Carpenter

Tenured scientists tell stories about how they managed to restart their research careers.

SCIENCEPODCAST
www.sciencemag.org/multimedia/podcast
Free Weekly Show

Download the 26 June *Science* Podcast to hear about new draft NIH guidelines for human stem cell research, investigating the neural basis of memory, your letters to *Science,* and more.

ORIGINSBLOG
blogs.sciencemag.org/origins
A History of Beginnings

SCIENCEINSIDER
blogs.sciencemag.org/scienceinsider
Science Policy News and Analysis

SCIENCESIGNALING
Extra digits without Kif7.

SCIENCECAREERS
Renewing your career after tenure.

SCIENCE (ISSN 0036-8075) is published weekly on Friday, except the last week in December, by the American Association for the Advancement of Science, 1200 New York Avenue, NW, Washington, DC 20005. Periodicals Mail postage (publication No. 484460) paid at Washington, DC, and additional mailing offices. The title SCIENCE is a registered trademark of the AAAS. Domestic individual membership and subscription (51 issues): $146 ($74 allocated to subscription). Domestic institutional subscription (51 issues): $835; Foreign postage extra: Mexico, Caribbean (surface mail) $55; other countries (air assist delivery) $85. First class, airmail, student, and emeritus rates on request. Canadian rates with GST available upon request, GST #1254 88122. Publications Mail Agreement Number 1069624. **Printed in the U.S.A.**

Change of address: Allow 4 weeks, giving old and new addresses and 8-digit account number. **Postmaster:** Send change of address to AAAS, P.O. Box 96178, Washington, DC 20090–6178. **Single-copy sales:** $10.00 current issue, $15.00 back issue prepaid includes surface postage; bulk rates on request. The identification code for *Science* is 0036-8075. *Science* is indexed in the *Reader's Guide to Periodical Literature* and in several specialized indexes.

AAAS
ADVANCING SCIENCE, SERVING SOCIETY

CREDITS: (*SCIENCE SIGNALING*) RONG MO/THE HOSPITAL FOR SICK CHILDREN; (*SCIENCE CAREERS*) AGRICULTURAL RESEARCH SERVICE/USDA

Welcome to Abcam

The largest catalog of the best antibodies in the world

Abcam provides more than 52,000 cutting edge antibodies with the most comprehensive and up-to-date datasheets including customer reviews and enquiries, fast delivery, customer service and scientific support. Check out all we have to offer:

- **Primary antibodies**
- **Secondary antibodies**
- **Kits**
- **Lysates**
- **Proteins/Peptides**
- **Slides**

www.abcam.com

Abpromise℠

Buy from Abcam for the reassurance of our expert scientific support and replacement or refund if the product does not perform as we say it should.

www.abcam.com/abpromise

Downloadable Pathways and Posters

We work hard to gather new pathways that complement our large range of antibodies. Check them out today.

- **Cancer**
- **Nuclear Signaling**
- **Cardiovascular**
- **Stem Cells**
- **Immunology**
- **Neuroscience**
- **Microbiology**
- **Chromatin**

www.abcam.com/poster

Abcam offers next day delivery

Order by 8pm EST Monday - Thursday and receive your product next day.

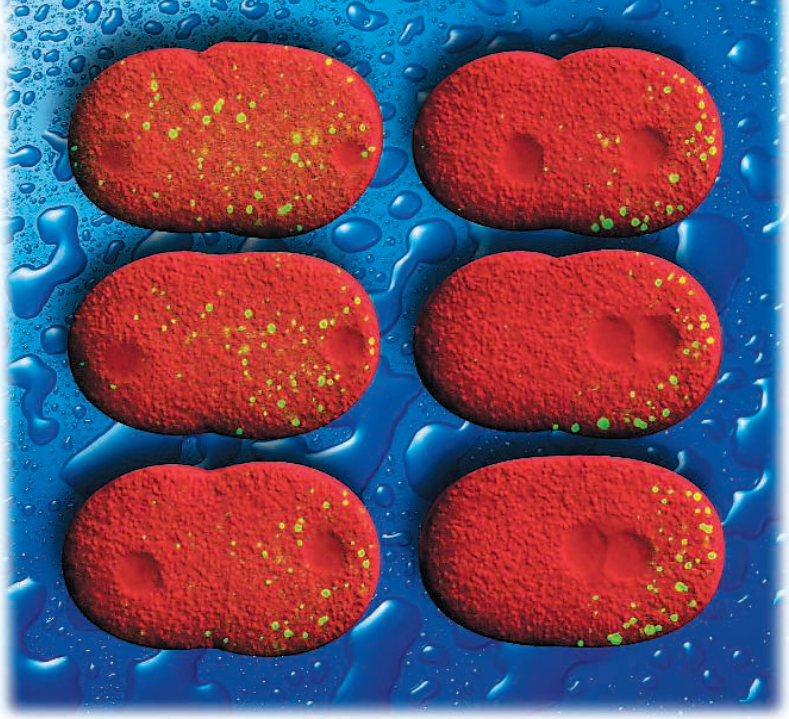

CREDITS (TOP TO BOTTOM): CLIFFORD BRANGWYNNE AND ISTOCKPHOTO.COM/SEBASTIAN VERA; MONICA ALANDETE-SAEZ/UNIVERSITY OF CALIFORNIA–DAVIS

<< P Granule Conundrum

In many organisms, the presumptive germ cells can be distinguished from somatic cells by the presence of distinctive cytoplasmic granules. In *Caenorhabditis elegans*, these P granules are more or less uniformly distributed in the oocyte and one-cell stage of the fertilized egg. By the end of the first cleavage, however, the anterior cell is essentially free of P granules, whereas the posterior cell still displays a prominent population of granules. Exactly how this process occurs and whether it involves directed migration of the granules is unclear. Now **Brangwynne *et al.*** (p. 1729, published online 21 May; see the Perspective by **Le Goff and Lecuit**) provide evidence that localization occurs by a quite different mechanism, controlled dissolution and condensation of granule components. This type of cytoplasmic remodeling by physicochemical mechanisms can now be looked for in other cellular and developmental systems.

Winner Takes All?

Competition between individual cells plays a role in normal animal development and cell homeostasis. **Johnston** (p. 1679) reviews two situations of cell competition in *Drosophila*, one involving epithelial cells in the wing and another involving germline or somatic stem cells. "Loss" in cell competition is evidenced by the "weaker" cell's death or displacement. On the other hand, winners may engulf the loser or display enhanced proliferation. Competitive interactions allow cells to sense and eliminate poor-quality cells during development.

Molecular Fire Quencher

Cage-shaped molecular assemblies can regulate the reactivity of smaller molecules trapped within them. **Mal *et al.*** (p. 1697) extend this approach to enable the protection of elemental white phosphorus (P_4), a substance that rapidly ignites on contact with oxygen. The tetrahedral cages self-assemble in aqueous solution through coordination of six ligands to four iron ions, and efficiently capture phosphorus from a suspension. The water-soluble host-guest constructs were stable in air for at least 4 months, but released intact P_4 rapidly on displacement by added benzene.

CO on a Chip

Microfluidics technology has facilitated remarkable miniaturization of chemical synthesis platforms; through electrically gated solution flow and mixing, molecular reactions can be carried out on chips several centimeters across. When it comes to more fundamental dynamics studies, though, which involve probing gas-phase molecules in specific quantum mechanical states, the experiments still tend to require much larger interaction areas. **Meek *et al.*** (p. 1699) take a step toward miniaturization in this latter regime by demonstrating the isolation of a cold gas-phase beam of CO molecules just above a microelectrode-decorated chip. The technique relies on rapidly modulated electric fields that trap and then slow down the incoming molecules through dipole interactions. Once brought to a stop, the molecules can be held on the chip for a discrete period and then released to a detector.

Flower Functionalization

The development of the specialized cells that make up the female reproductive unit in flowering plants, the gametophyte, requires the hormone auxin. However, auxin's function and movement to and within these cells are unclear. **Pagnussat *et al.*** (p. 1684, published online 4 June; see the Perspective **Friedman**) provide evidence that auxin is synthesized at specific positions within the female gametophyte and exerts a positional effect and that a gradient of auxin controls patterning of these specialized cells.

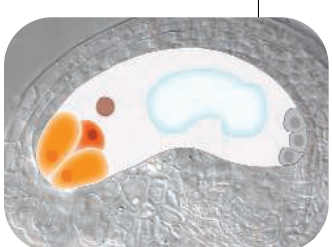

Going Faster

The concentrations of most tropospheric pollutants and trace gases are kept in check by their reactions with hydroxyl radicals (OH). OH is a short-lived, highly reactive species that is produced in the atmosphere by photochemical processes, and regenerated in the chain of chemical reactions that follows the oxidative destruction of those molecules. These regeneration mechanisms were thought to be fairly well understood, but now **Hofzumahaus *et al.*** (p. 1702, published online 4 June) present evidence of a pathway not previously recognized. In a study of atmospheric composition in the Pearl River Delta, a highly polluted region of China, greatly elevated OH concentrations were observed without the correspondingly high levels of ozone expected from current models. Thus, OH concentrations may be augmented by a process that speeds the regeneration of OH without producing ozone.

Two's a Crowd

The process by which males and females compete to maximize their individual fitness also affects the fitness of their offspring. Sexual selection largely results from polyandry (multiple mating by females), and several competing hypotheses attempt to explain the evolution of polyandry. **Bilde *et al.*** (p. 1705) staged double mating experiments in seed beetles to distinguish between the theories underlying cryptic female choice and sexual antagonism. Contrary to expectation, males of high genetic quality, as measured on the basis of the number of offspring sired when singly mated to a female, consistently produced fewer offspring when females were doubly mated to males of

Continued on page 1615

Published by AAAS

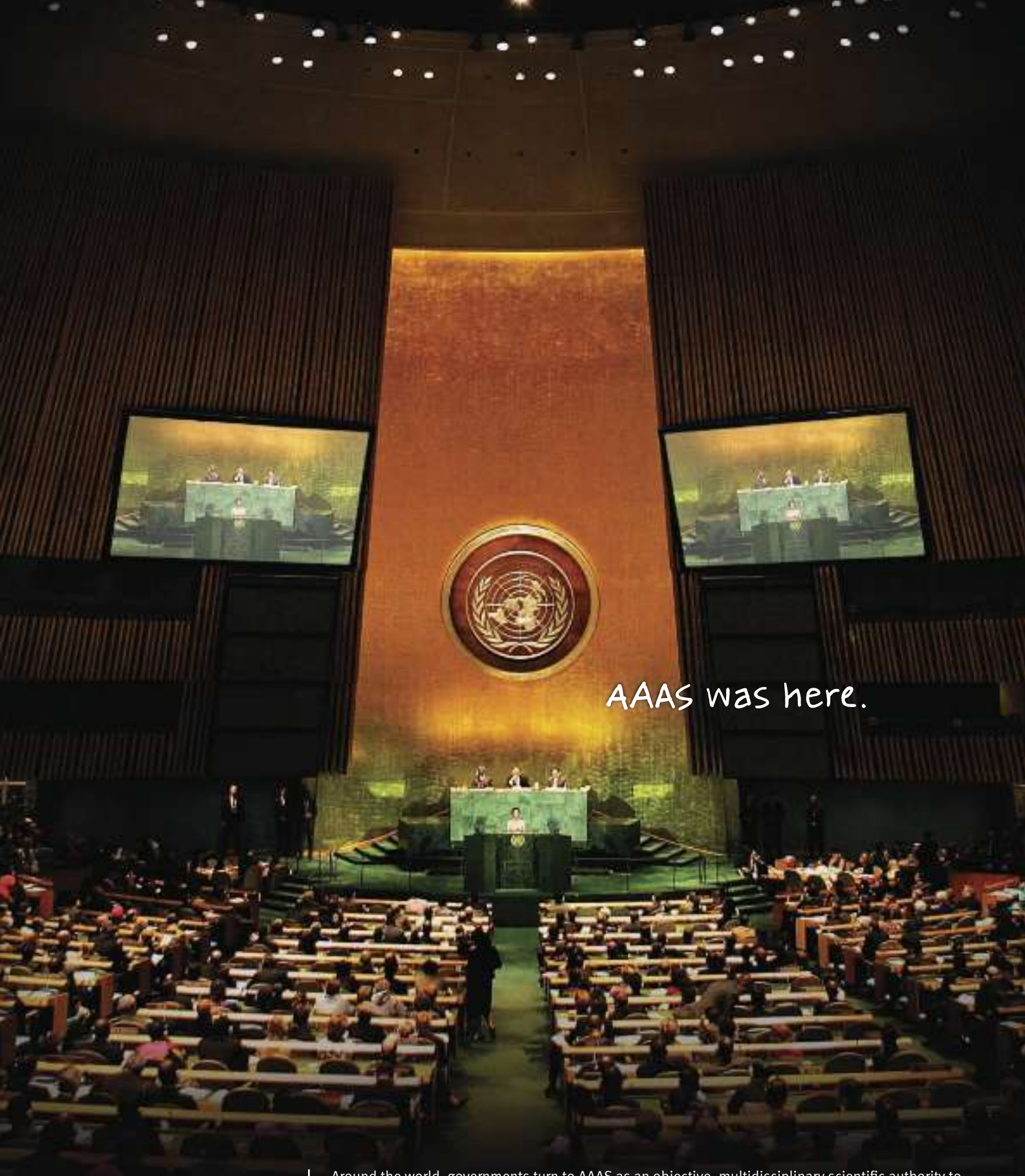

Science funding
Climate regulation
Human rights

Around the world, governments turn to AAAS as an objective, multidisciplinary scientific authority to educate public officials and judicial figures on today's most pressing issues. Our goal is to promote informed policy decisions that benefit society. And this is just one of the ways that AAAS is committed to advancing science to support a healthy and prosperous world.
Join us. Together we can make a difference. **aaas.org/plusyou**

AAAS + U = Δ

Continued from page 1613

both high and low genetic quality. Thus, postmating sexual selection can favor male genotypes with low fitness, and females risk genetic costs when mating with multiple males.

Of Life, Limb, and a Small RNA

Gene expression in mammals is controlled not only by proteins but by small noncoding RNAs called microRNAs. The involvement of these RNAs provides powerful clues about the molecular origins of human diseases and how they might be treated. Ischemic diseases arise from an inadequate blood supply. **Bonauer *et al.*** (p. 1710, published online 21 May) find that a specific microRNA that is expressed in the cells lining blood vessels (called miR-92a) functions to repress the growth of new blood vessels. MiR-92a probably acts through effects on expression of integrins, proteins involved in cell adhesion and migration. In mouse models in which an inadequate blood supply had caused damage either to heart or limb muscle, therapeutic inhibition of miR-92a led to an increase in blood vessel density in the damaged tissues and enhanced functional recovery.

Ras, STAT3, and Transformation

The STAT (signal transducer and activator of transcription) proteins are activated in response to receptor stimulation and act in the nucleus to regulate gene expression. **Gough *et al.*** (p. 1713) found that STAT3 functioned in transformation of cells by the oncogene Ras. However, this activity was maintained in mutants of STAT that fail to activate transcription. Instead, the active STAT3 appeared to be associated with mitochondria. Furthermore, modified STAT3 targeted to the mitochondria promoted transformation by Ras, and mitochondrial function was disrupted in Ras-transformed cells lacking STAT3. Such transformation-specific effects of STAT3 could be a useful target in developing anticancer therapies.

Cuprate Analysis

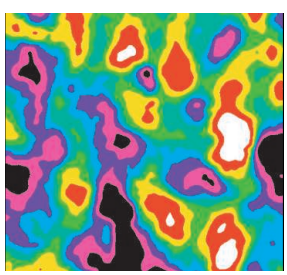

Despite more than 20 years of intensive effort, the mechanism providing superconductivity in the cuprates remains elusive and contentious, partly because the cuprates are inhomogeneous. Scanning tunneling spectroscopy (STS) and high-resolution, angle-resolved photoemission spectroscopy provide energy and momentum information about the excitations in the high-temperature cuprate superconductors. **Pushp *et al.*** (p. 1689, published online 4 June) provide a STS study of the cuprate $Bi_2Sr_2CaCu_2O_{8+\delta}$ over a range of doping levels and temperatures. This methodology for analyzing the spectra takes into account the inhomogeneity and may provide insight into how a superconducting pairing mechanism evolves from the parent insulating state.

CREDIT: PUSHP *ET AL.*

Green for Diatoms

Diatoms account for 20% of global carbon fixation and, together with other chromalveolates (e.g., dinoflagellates and coccolithophorids), represent many thousands of eukaryote taxa in the world's oceans and on the tree of life. **Moustafa *et al.*** (p. 1724; see the Perspective by **Dagan and Martin**) have discovered that the genomes of diatoms are highly chimeric, with about 10% of their nuclear genes being of foreign algal origin. Of this set of 1272 algal genes, 253 were, as expected, from a distant red algal secondary endosymbiont, but more than 1000 of the genes were derived from green algae and predated the red algal relationship. These protist taxa are important not only for genetic and genomic investigations but also for their potential in biofuel and nanotechnology applications and in global primary productivity in relation to climate change.

BDNF and Drug Dependence

Brain-derived neurotrophic factor (BDNF) is a growth factor involved in neuronal plasticity that is expressed after chronic administration of drugs of abuse and may play a crucial role in chronic opiate effects. **Vargas-Perez *et al.*** (p. 1732, published online 28 May) found that BDNF was directly involved in the switching mechanism in the ventral tegmental area, from an opiate-naïve, dopamine-independent drug reward substrate to an opiate-dependent, dopamine-dependent motivational substrate. In the ventral tegmental area, BDNF changed the action of GABA-A receptors from inhibitory to excitatory. This change led to behavioral changes that defined a neurobiological boundary between the acute phase of drug-taking and addiction.

Published by AAAS

Need to assess the novelty of substances?
SciFinder is the answer.

It includes CAS REGISTRY,SM the most comprehensive substance information available, integrated with relevant journal articles and patents.

Give your research team the highest quality and most timely scientific information resource.

Make SciFinder an essential part of your research process.

For more information about SciFinder, visit www.cas.org or e-mail help@cas.org.

SciFinder®—an essential Part of the process.™

CAS | SciFinder®

www.cas.org

CAS is a division of the American Chemical Society

Roger Pedersen is professor of Regenerative Medicine and director of the Anne McLaren Laboratory for Regenerative Medicine at the University of Cambridge, UK. E-mail: director@stemcells.cam.ac.uk.

Out With the Old, In With the New?

PRESIDENT OBAMA'S RECENT ANNOUNCEMENT OF A NEW POLICY FOR FEDERAL FUNDING OF STEM cell research changes the landscape for this important area of biomedicine in the United States. His Executive Order and the subsequent draft guidelines of the National Institutes of Health (NIH) remove a major existing limitation on federal support for research using pluripotent human embryonic stem cells (hESCs). These stem cells can specialize into all body cell types. Thus, in principle they can be used to produce a wide range of tissues for therapeutic use. In addition, their study will very likely generate new insights into human early developmental mechanisms. The new Obama policy promises to speed research by making many new hESC lines eligible for federally funded studies. But the draft NIH guidelines accompanying the new policy need revision, because their donor consent rules for embryos used to generate hESCs would make some—and perhaps even all—of the previously approved hESCs ineligible for further federal funding. This would needlessly hinder progress in the stem cell field, and reasonable exceptions should be made to correct this unintended outcome.

President Bush's stem cell funding policy, in place since 2001, made a total of 21 hESC lines eligible for federal research funding. Because all of those lines had been exposed to animal cells and serum during their derivation and growth, they have limited value for clinical applications. More recently, hESC lines have been generated without being exposed to animal products, and these are more likely to be compatible with therapeutic use. In addition, they provide greater genetic diversity, making them more representative of patient populations. The federal funding to be made available for hESC research under the new guidelines places U.S. stem cell researchers on an equal footing with researchers in the UK and elsewhere, who have enjoyed access to such new and improved hESC lines for the past 8 years. New collaborations now become possible that will speed the research in this field. These include basic research by multiple researchers using clinically compatible hESC lines, which can culminate in their therapeutic use. Thus, the new U.S. policy will be important both for stem cell research and for the patients who are its future beneficiaries.

The new policy and guidelines also attempt to correct shortcomings in donor consent for federally eligible hESC lines. Doubts about the ethical status of the previously eligible hESC lines were raised by Streiffer,* who obtained anonymized patient consents for all 21 eligible lines through the U.S. Freedom of Information Act. U.S. standards for donor consent in the derivation of hESCs from human embryos were established by the National Academy of Sciences (NAS) in 2005. None of the 21 lines meets all these standards, and some lines fall far short. But the previously eligible hESC lines have now been used in hundreds of studies, providing benchmarks for the pluripotent stem cell field. The NIH draft guidelines reaffirm most of the NAS consent requirements, seemingly making the previously eligible lines ineligible under the new policy. Revisions in the draft NIH guidelines are thus necessary to retain eligibility for federal funding for the less ethically problematic of the widely used hESC lines.

Many researchers have recently been redirecting their attention to pluripotent stem cells that are induced from specialized cells. First described in 2006 by Japanese researchers, induced pluripotent stem cells are appealing both for their unlimited genetic diversity and for their reduced ethical complexity. However, it is still unclear whether human induced pluripotent stem cells have the necessary properties to qualify them for future therapeutic uses. Therefore, caution is needed in drafting new U.S. stem cell funding policies to avoid the unintended consequence of reducing, rather than expanding, the options available for research on hESCs that could lead to treatment of diseases. **– Roger Pedersen**

*R. Streiffer, *Hastings Center Rep.* **38**, 40 (2008).

10.1126/science.1177267

MILLIPORE™

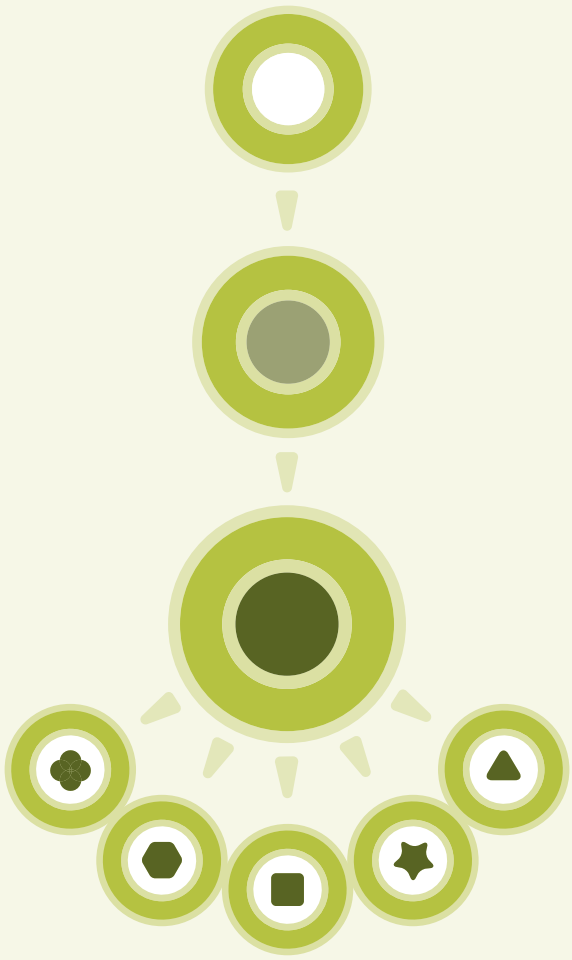

CELL BIOLOGY
CELL SIGNALING
DRUG DISCOVERY
IMMUNODETECTION
LAB WATER
PROTEIN BIOMARKERS
STEM CELL RESEARCH

NEXT GENERATION?

Give rise to controlled differentiation.

We stand with you in our investment in and commitment to stem cell research. By combining Upstate® and Chemicon® products and services with our years of experience supporting Life Science research, we successfully partner with the world's leading scientists to develop proven solutions for human and murine, adult and embryonic stem cell research.

ADVANCING LIFE SCIENCE TOGETHER™

Visit www.millipore.com/stem_cells for more information on this and other ways Millipore supports Life Science research.

THE EXPERTISE OF
CHEMICON® & UPSTATE®
IS NOW A PART OF MILLIPORE

PHOTO CREDIT (TOP): HUMBERTO OLARTE CUPAS/ALAMY

EVOLUTION

Going Farther with Sex

Plant mating systems are under pressure to produce the most and the best offspring (seeds) and to offer them the greatest opportunity to thrive in the absence of competition by dispersal. Self-pollination is one means by which plants can maximize their reproductive potential, but how it relates to dispersal is unclear. Plants that cannot self-fertilize have been linked to lower dispersal rates because it has been thought that if they were to disperse widely, the lack of a nearby pollen source would result in reproductive failure. Despite this theory, it has been noted that invasive species, those with fleshy fruits, and island colonizers—all of which typify plants with good dispersal systems—tend to have mating systems that separate the sexes or select against self-pollination.

Cheptou and Massol construct a metapopulation model that captures the evolution of dispersal and self-fertilization in environments defined by stochastic pollen limitation. Their calculations show that self-fertilization associates with no dispersal and that outcrossing goes with dispersal, contrary to some previous postulates. Based on these results, they explain the overrepresentation of dioecious plants (those with only male or female individuals) in flora, such as papaya, that have colonized islands. — LMZ

Am. Nat. **174**, 46 (2009).

PHYSIOLOGY

Growing Fat with Mom's Help

A mutation in the α subunit of the guanine nucleotide–binding protein G_s, which transduces signals from various hormone receptors, causes obesity and insulin resistance in the human disorder Albright hereditary osteodystrophy. These disease manifestations occur in individuals with mutations in the maternal allele of the gene encoding $G\alpha_s$, *GNAS*, because genomic imprinting causes expression primarily from the maternal allele of *GNAS* in some tissues. Chen *et al.* provide evidence that the differential expression of *GNAS* in the brain (the paraventricular nucleus of the hypothalamus) accounts for the metabolic effects of the disease. They observed that mice with a disrupted maternal $G\alpha_s$ allele became obese as a result of reduced energy expenditure. These animals also became insulin-resistant and diabetic even before they became obese. Loss of $G\alpha_s$ function mimicked some of the effects seen with loss of the MC4R melanocortin receptor; melanocortins function through $G\alpha_s$-coupled receptors to control energy expenditure and food intake. Specifically, effects of melanocortin on food intake operated independently of $G\alpha_s$. On the other hand, the stimulation of energy expenditure by melanocortin was diminished in animals carrying the mutant maternal allele. — LBR

Cell Metab. **9**, 548 (2009).

PLANT SCIENCE

Abstaining from Sex

When a desirable plant appears, featuring an unusual flower color or a valuable nutritional trait, it would be handy to be able to propagate identical versions of that individual, but apomixis (asexual reproduction through seeds) is uncommon in crop plants. d'Erfurth *et al.* have identified a gene in the sexual plant *Arabidopsis* that causes an omission of the second meiotic division (*OSD1*) during gametogenesis. Developing gametes that carry mutations in *OSD1* generate two diploid rather than four haploid cells. These gametes are functional and give rise after fertilization to plants with increased ploidy. Although aspects of recombination during the first meiotic division generated progeny not identical to the parent, by combining the *OSD1* mutation with two other mutations that alter the first meiotic division, the authors obtained gametes that carried the same genetic program as the parental plant, a promising start to engineering apomixis. — PJH

PLoS Biol. **7**, e1000124 (2009).

CHEMISTRY

Nuclear Glow

Traditional methods of detecting radioactivity rely on sampling the stream of photons and particles that are actually being radiated. The decay of unstable atomic nuclei sends forth a burst of fast-moving charges—at times accompanied by high-energy, very-short-wavelength gamma rays—and multiple sensing technologies are available to capture them. At the same time, the underlying nuclear transformation also leaves behind a slow heavy co-product, and it is this latter decay signature which Berezin *et al.* target for sensing. They present an indole-based dye that fluoresces in the near-infrared (760 nm peak emission wavelength) with an efficiency that varies depending on the identity of a coordinated metal ion. Copper (Cu) quenches the fluorescence, whereas zinc enhances it; nickel has little impact. Thus, decay of the unstable ^{64}Cu isotope to a mixture of nickel and zinc can give rise to a significant shift in the fluorescence intensity of the chelating dye. The

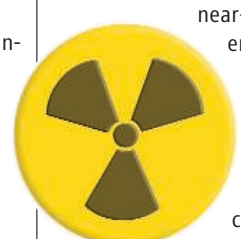

Continued on page 1621

No doctor alone can stop SIDS, childhood epilepsy or brain tumors. That's why we brought his team to Seattle.

Cure.

Dr. Nino Ramirez, Director of the Center for Integrative Brain Research at Seattle Children's Research Institute, is dedicated to finding cures for some of the most serious childhood diseases. A world-renowned researcher and Professor of Neurological Surgery at the University of Washington, Dr. Ramirez leads a team of top brain researchers at Seattle Children's.

At Seattle Children's, finding cures for tomorrow is as important as treating children today. With a focus on translational research, our teams collaborate daily, both within their own groups and with other leading researchers—in state-of-the-art laboratories with the most advanced technology available. To learn more, visit seattlechildrens.org/research.

Seattle Children's
HOSPITAL • RESEARCH • FOUNDATION

Continued from page 1619

approximately 12-hour half-life of this nucleus facilitated experimentation; the nuclear decay process does not disrupt coordination of the product ions, nor does it appear to damage the dye scaffold, which retains its primary absorption features throughout. Energy and charge transfer are put forward as the most likely mechanisms for the Cu-induced fluorescence quenching. The authors envision multiple molecular imaging applications. — JSY

J. Am. Chem. Soc. **131**, 10.1021/ja903685b (2009).

CANCER

Fat Feeds Tumors

Weight-loss campaigns emphasize the impact of obesity on the risk of heart disease and diabetes, but in reality the situation may be even grimmer. Emerging evidence suggests that obesity also increases the risk of developing common cancers such as breast and colorectal cancer and may be associated with a poorer prognosis if cancer occurs. The biological mechanisms by which obesity affects tumorigenesis are unclear, although research has centered on the concept that adipose tissue (fat) serves as a source of hormones, growth factors, and cytokines that promote tumor cell growth or invasiveness.

Zhang *et al*. provide evidence for an intriguing alternative in which adipose-derived cells rather than signaling molecules play a key role. Using mouse tumor models, they show that

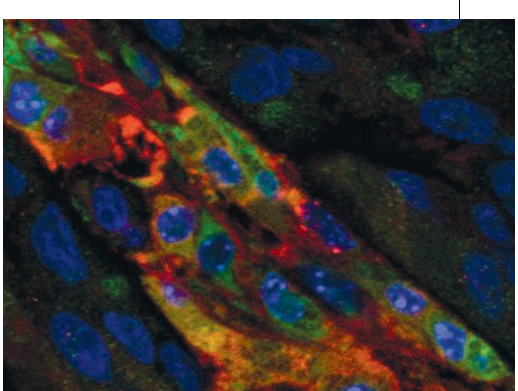

CREDIT: ZHANG *ET AL.*, *CANCER RES.* **69**, 5259 (2009)

stromal and endothelial cells derived from white adipose tissue (WAT) are recruited by tumors to help build the blood vessels required for tumor expansion. Mobilization of these cells (green) into the circulation and their engraftment into the tumor stroma and vasculature (red) were associated with an increase in tumor growth and progression in the mice. Whether WAT-derived cells function similarly in human tumors remains to be explored. — PAK

Cancer Res. **69**, 5259 (2009).

CHEMISTRY

Concentrating on Etching

The etching of nanometer-scale features on substrates is usually achieved with polymeric masks patterned by ultraviolet lithography, with resolution tied to the irradiation wavelength. Liu *et al.* report an alternative approach, whereby carbon nanotubes can act as catalysts for etching trenches in silicon dioxide 4 to 6 nm deep and about 60 nm in width. They first grew carbon nanotubes on silicon via chemical vapor deposition, with diameters of 1 to 4 nm. Immersion in basic solution led to etching rates that were about three times faster in the vicinity of the carbon nanotubes than elsewhere on the substrate, an effect which the authors attribute to the greater concentration of hydroxide groups that adsorb on the hydrophobic surface of the nanotubes in the electrical double layer. Atomic force microscopy revealed that most of the carbon nanotubes on the surface were released into solution after etching. — PDS

J. Am. Chem. Soc. **131**, 10.1021/ja903333s (2009).

CANCER

Partners in Repression

Chromosomal translocations are structural abnormalities caused by the breaking and aberrant joining of regions from two or more chromosomes. If portions of two genes become fused, the fusion gene may encode a protein that combines two functions and produces a deleterious outcome. In some diseases, a single gene can be linked to one of several partners: Whereas the common gene dictates a basic similarity in disease etiology, the partner's identity may define a distinctive mechanism of causation.

In patients with acute promyelocytic leukemia (APL), the retinoic acid receptor alpha (RARA) is expressed as a fusion protein with one of five different partners, such as PML or PLZF. Although most APL patients express RARA-PML and can be treated with all-trans retinoic acid, those carrying RARA-PLZF are resistant. Boukarabila *et al.* show that both fusion proteins inappropriately recruit the same Polycomb-repressive complex (PRC2) to mediate the silencing of retinoic acid–responsive genes. For RARA-PML, repression is reversed on treatment with retinoic acid; in contrast, RARA-PLZF also recruits PRC1, which contributes to tumorigenesis but is resistant to retinoic acid. Understanding the precise mechanisms of action of fusion proteins is important for the development of effective therapies. — HP

Genes Dev. **23**, 1195 (2009).

Published by AAAS

www.sciencemag.org

Science

1200 New York Avenue, NW
Washington, DC 20005
Editorial: 202-326-6550, FAX 202-289-7562
News: 202-326-6581, FAX 202-371-9227
Bateman House, 82-88 Hills Road
Cambridge, UK CB2 1LQ
+44 (0) 1223 326500, FAX +44 (0) 1223 326501

Subscription Services For change of address, missing issues, new orders and renewals, and payment questions: 866-434-AAAS (2227) or 202-326-6417, FAX 202-842-1065. Mailing addresses: AAAS, P.O. Box 96178, Washington, DC 20090-6178 or AAAS Member Services, 1200 New York Avenue, NW, Washington, DC 20005

Institutional Site Licenses please call 202-326-6755 for any questions or information

Reprints: Author Inquiries 800-635-7181
Commercial Inquiries 803-359-4578

Permissions 202-326-7074, FAX 202-682-0816

Member Benefits AAAS/Barnes&Noble.com bookstore www.aaas.org/bn; AAAS Online Store www.apisource.com/aaas/ code MKB6; AAAS Travels: Betchart Expeditions 800-252-4910; Apple Store www.apple/eppstore/aaas; Bank of America MasterCard 1-800-833-6262 priority code FAA3YU; Cold Spring Harbor Laboratory Press Publications www.cshlpress.com/affiliates/aaas.htm; GEICO Auto Insurance www.geico.com/landingpage/go51.htm?logo=17624; Hertz 800-654-2200 CDP#343457; Office Depot https://bsd.officedepot.com/portalLogin.do; Seabury & Smith Life Insurance 800-424-9883; Subaru VIP Program 202-326-6417; VIP Moving Services www.vipmayflower.com/domestic/index.html; Other Benefits: AAAS Member Services 202-326-6417 or www.aaasmember.org.

science_editors@aaas.org	(for general editorial queries)
science_letters@aaas.org	(for queries about letters)
science_reviews@aaas.org	(for returning manuscript reviews)
science_bookrevs@aaas.org	(for book review queries)

Published by the American Association for the Advancement of Science (AAAS), *Science* serves its readers as a forum for the presentation and discussion of important issues related to the advancement of science, including the presentation of minority or conflicting points of view, rather than by publishing only material on which a consensus has been reached. Accordingly, all articles published in *Science*—including editorials, news and comment, and book reviews—are signed and reflect the individual views of the authors and not official points of view adopted by AAAS or the institutions with which the authors are affiliated.

AAAS was founded in 1848 and incorporated in 1874. Its mission is to advance science, engineering, and innovation throughout the world for the benefit of all people. The goals of the association are to: enhance communication among scientists, engineers, and the public; promote and defend the integrity of science and its use; strengthen support for the science and technology enterprise; provide a voice for science on societal issues; promote the responsible use of science in public policy; strengthen and diversify the science and technology workforce; foster education in science and technology for everyone; increase public engagement with science and technology; and advance international cooperation in science.

Information for Authors
See pages 807 and 808 of the 6 February 2009 issue or access www.sciencemag.org/about/authors

Trusted!

SIGMA® Life Science

Insist on Sigma's FLAG® System…
Original and Proven Performance

FLAG is the established system for recombinant protein expression, purification, and detection. Don't settle for inferior systems.

- **Proven**: Cited in more than 2,000 publications
- **Ultrasensitive**: Antibodies detect as little as 100 femtomoles of protein
- **Comprehensive**: Complete systems in multiple formats

View the full range of FLAG products at ***sigma.com/flagtag***

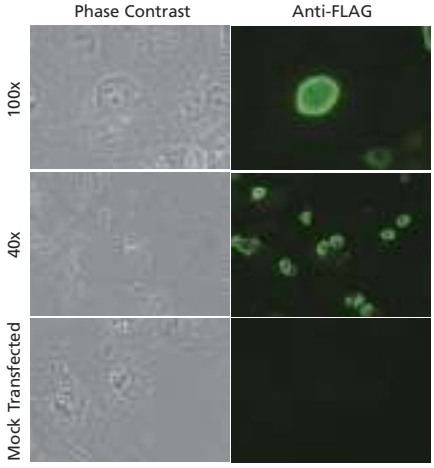

FLAG-p53 and mock transfected COS-7 cells were permeabilized, fixed, blocked, and incubated with anti-FLAG M2 antibody

Our Innovation, Your Research — Shaping the Future of Life Science

EDITED BY KELLI WHITLOCK BURTON

It's the Thought That Counts

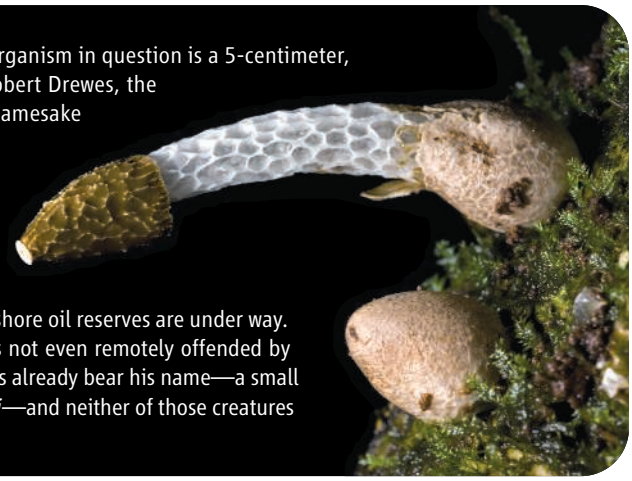

Ordinarily, having a species named after you is a great honor. But what if the organism in question is a 5-centimeter, phallus-shaped fungus that smells of rotting flesh? Still a great honor, says Robert Drewes, the curator of herpetology at the California Academy of Sciences and the proud namesake of *Phallus drewesii*, described in the July/August issue of *Mycologia*.

The name was chosen by mycologist Dennis Desjardin of San Francisco State University and his postdoc Brian Perry to acknowledge Drewes's role in inspiring researchers to survey biodiversity on São Tomé and Príncipe, the equatorial island nation off the west coast of Africa where the fungus was found. The islands have incredible biodiversity that scientists have scarcely begun to catalog, Drewes says. Time may be running out, as plans to tap vast offshore oil reserves are under way.

Drewes describes Desjardin as a "dear friend and colleague" and insists he's not even remotely offended by sharing his name with a diminutive phallic fungus. He notes that two other species already bear his name—a small moss frog, *Arthroleptella drewesii*, and a blind worm snake, *Leptotyphlops drewesi*—and neither of those creatures is particularly virile either.

Second Sight

Last December, when an angry Iraqi journalist hurled his shoes at then–U.S. President George W. Bush and Iraqi Prime Minister Nouri al-Maliki, some viewers cringed; others chuckled. Neuroscientists at Washington University in St. Louis, Missouri, wrote a paper that explains how the president reacted so quickly.

When you observe your surroundings, your focus moves like a spotlight, settling on what's most interesting and ignoring the rest. Scientists have believed that moving that spotlight requires conscious awareness. But dodging threats (such as airborne shoes) leaves no time for cogitation. This suggests that there are two independent pathways in the visual system—one for perception and the other for action—says Jeffrey Lin, lead author of the study, published in the 11 June issue of *Current Biology*. The action system allows you to focus your attention on threats before you consciously perceive them.

"If you look at the shoe-throwing video, you will see that the prime minister doesn't flinch at all," Lin says. "His brain has already categorized the shoe as nonthreatening." Bush's brain, in contrast, detected danger and ordered evasive maneuvers. If the men had consciously focused on the shoe, both might have dodged.

Lin and colleagues tested the hypothesis with a computer program that lobbed simulated baseballs toward viewers' heads. "When we throw two balls at you with very similar trajectories, they may look the same to your perceptual system," Lin says. "But your brain can automatically calculate which one is more threatening and trigger a dodging motion before you've even realized what has happened."

CREDITS (TOP TO BOTTOM): BRIAN PERRY; AP; PHOTOS.COM

They Take the Prize

The advent of summer saw a bumper crop of awards for achievements in science and technology.

This year's Kyoto Prize in Advanced Technology went to semiconductor scientist Isamu Akasaki, 80, for research that led to the development of the blue light-emitting diode. Akasaki holds professorships at both Nagoya University and Meijo University in Japan.

Peter and Rosemary Grant, both 72, became the first husband-and-wife team to receive the Kyoto Prize for Basic Sciences. The pair were recognized for their studies of rapid evolution caused by natural selection in response to environmental changes. The Grants are professors emeriti at Princeton University.

This year's Blue Planet Prize went to Hirofumi Uzawa, a professor emeritus at the University of Tokyo in Japan, and Nicholas Stern, a professor at the London School of Economics. Both were recognized for applying economic theories to environmental issues such as global warming.

Five researchers won Shaw Prizes. For astronomy: Frank H. Shu, an astrophysicist at the University of California, San Diego, for work that established a standard model of star formation. For life science and medicine: Douglas L. Coleman of the Jackson Laboratory in Bar Harbor, Maine, for research on obesity in mice, and Jeffrey M. Friedman of Rockefeller University in New York City, who identified the fat-regulation hormone leptin. And for mathematics: Simon K. Donaldson of Imperial College London and Clifford H. Taubes of Harvard University for advances in theoretical physics.

Recipients of the Kyoto and Blue Planet prizes each receive about $500,000; Shaw Prize recipients, $1 million.

NAMING RIGHTS

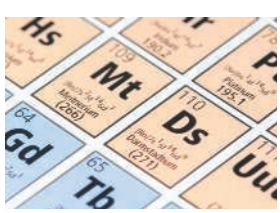

Get out your baby name books. Element 112 has been officially recognized by the International Union of Pure and Applied Chemistry, the official keepers of the periodic table of elements.

A team of 21 scientists led by researchers at the GSI Helmholtz Centre for Heavy Ion Research in Darmstadt, Germany, first produced element 112 in 1996 by firing a beam of zinc ions down a 120-meter-long particle accelerator into a lead target. Zinc and lead nuclei fused to produce a single atom of 112. Although scarce (only a handful of atoms of it have been detected), 112 is a stout beast, 227 times heavier than hydrogen and the heaviest element in the periodic table. It's also the sixth element created by the Darmstadt crew, which produced elements 107 to 111.

New elements are named by their discoverers. So far, the German scientists have named element 107 "bohrium," 108 "hassium," 109 "meitnerium," 110 "darmstadtium," and 111 "roentgenium." Perhaps it's time for something a little simpler. How about "Bob"?

Published by AAAS

Internet addiction: a suitable case for treatment?
1630

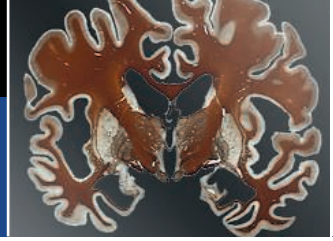

Digitizing a famous brain
1634

BIOSECURITY

Discovery of Untracked Pathogen Vials at Army Lab Sparks Concerns

Like forgotten ice cream in the back of a freezer, more than 9200 unlisted vials of dangerous pathogens and toxins have turned up in an inventory of biological materials at the U.S. Army Medical Research Institute of Infectious Diseases (USAMRIID) in Fort Detrick, Maryland. USAMRIID officials say most of the samples—representing about 13% of 70,000 vials housed in the institute—were left behind by researchers who worked at the institute before 2005. Officials say although they cannot be "100%" certain that no unlisted samples were lost or stolen, security measures at the institute make it unlikely.

The finding, announced by USAMRIID deputy commander Mark Kortepeter last week, has surprised some researchers and security experts, who say the institute may have violated federal rules by not conducting such an exhaustive inventory right after the enactment of the 2002 Bioterrorism Act. It has also left some wondering whether other biodefense labs might have incomplete databases of select agents.

"I am greatly shocked," says Janet Shoemaker, director of public affairs at the American Society for Microbiology in Washington, D.C., who helped draft the bioterrorism legislation after the 2001 anthrax letter attacks. However, "the fact that USAMRIID is releasing this information shows a new level of transparency, and that's refreshing," says Paul Keim, a microbiologist at Northern Arizona University (NAU) in Flagstaff.

The institute has been under intense public scrutiny since last summer, when the Federal Bureau of Investigation implicated former USAMRIID researcher Bruce Ivins in the 2001 anthrax attacks. On 4 February, institute commander John Skvorak ordered a full inventory of the materials after a spot inspection uncovered four vials of Venezuelan equine encephalitis that had never been entered into the institute's electronic database, created in 2005 (*Science*, 13 February, p. 861). Over the next 4 months, research at the institute stood still as scientists counted every vial in its 330-odd freezers and refrigerators. "The vast majority" of the unlisted samples were "working stocks that had accumulated over several decades," says Kortepeter.

The initial inventory for the electronic database 4 years ago had focused on vials that were in active use, Kortepeter says. The process failed to capture materials that had been pushed to the back of the freezers after the researchers working with them had left the institute. "It would have been better to do a complete inventory," concedes Sam Edwin, USAMRIID's inventory control officer.

Jam-packed. USAMRIID officials say documenting vials from every box in every freezer was a monumental task.

Shoemaker points out that one of the rules that went into effect after the 2002 Bioterrorism Act was passed, CFR 73.17, requires that labs permitted by the government to possess select agents maintain an "accurate, current inventory" for each agent, including the quantity and where it is stored. USAMRIID's failure to do so may have violated that rule, she says.

In addition, in late 2002, the Centers for Disease Control and Prevention (CDC) and the Department of Health and Human Services notified all labs across the country that they must dispose of any select agents in their possession or register under the select-agent program. The notification prompted some labs to autoclave their select agents or ship them to other facilities. Shoemaker finds it surprising that managers at USAMRIID "did not go into the institute's freezers" back then "to determine what they had in there."

Keim, whose lab at NAU handles anthrax and other pathogens, is surprised, too. After the notification, "we scrambled like crazy and had to divert people from other projects to do a 100% inventory," he says. "I remember spending hundreds of hours in the biocontainment suite over a 6-month period, putting bar codes on every vial."

The reason that was never done at USAMRIID was sheer volume, says Kortepeter, who insists that the institute broke no rules. "There may be some latitude in how the regulations regarding inventory are interpreted," he explains, adding that the rules don't specify accounting down to the vial level. And documenting every vial is tough, he says. "You open these small drawers, the vials are caked up in frost, it's dark," he says. "You can't hold the door open very long" because an increase in temperature could destroy samples.

Army spokesperson Michael Brady says the Army may decide to investigate whether any unlisted vials could have gone missing. He says all of the Army's other biodefense labs, which are much smaller than USAMRIID, have completed 100% inventories in recent months. From now on, says Brady, all Army labs, including USAMRIID, will have to do a complete inventory every year, and the Army will conduct random inspections every quarter.

Shoemaker says USAMRIID's case raises questions about lab inspections conducted by federal agencies to ensure compliance with select-agent rules. At least in USAMRIID's case, a CDC inspection in September 2008 failed to identify the problem of unlisted samples, say USAMRIID officials.

–YUDHIJIT BHATTACHARJEE

CREDIT: KATHLEEN CASHMAN/USAMRIID

Published by AAAS

Antibiotics' natural role
1637

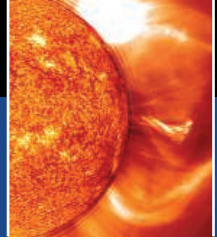

Predicting solar storms
1640

FUSION RESEARCH

ITER Gets the Nod for Slower, Step-by-Step Approach

The managers of the ITER fusion project are still scrambling to draw up a final design, schedule, and cost estimate for the massive reactor. But the international partners behind the effort agreed last week to build the project in stages so engineers can make corrections if something goes awry early on.

First, a simple stripped-down reactor will start producing a superhot hydrogen plasma in 2018; then components will gradually be added to prepare it for a power-producing plasma of deuterium and tritium by the end of 2026, some 18 months to 2 years later than previously planned. Member countries agreed to the new plan, known as scenario 1, at the half-yearly meeting of the ITER council in Mito, Japan, contingent on their accepting the full revised design, costing, and schedule, known as the baseline, at their next meeting in November. "We're learning as we go," says David Campbell, deputy head of ITER's fusion science and technology department. "There is some delay, but it's the first time we've done this."

ITER, originally called the International Thermonuclear Experimental Reactor, aims to prove that nuclear fusion, the process that powers the sun and other stars, could provide Earth-bound energy. Researchers spent about 15 years drawing up a design for ITER, and the ground is now prepared at Cadarache in southern France to begin construction this year. But when the ITER organization was officially created in October 2007, staff were working from a baseline drawn up in 2001. Researchers spent the next year working on a redesign incorporating the latest results from plasma physics.

But the physicists' wish list inevitably pushed up the price tag. The governments of the seven members—China, the European Union, India, Japan, South Korea, Russia, and the United States—were alarmed by early cost estimates, which insiders say ranged as high as twice the original €5 billion construction estimate (*Science*, 27 June 2008, p. 1707). "There's no question that costs have gone up," says Steven Cowley, director of the Culham Science Centre near Oxford, the U.K.'s fusion research lab, adding: "I'm pretty optimistic that we'll see a number of measures to bring down those costs."

Ready, set, ... The ground is prepared at Cadarache in southern France. Construction of ITER will begin this year.

CREDIT: © AGENCE ITER FRANCE

ITER managers proposed scenario 1 mainly to reduce technical risk, says Campbell. "We'll be able to shake down the core system, demonstrate first plasma, then integrate other systems," he says. "If something goes wrong, it's easier to get at it and fix it." Earlier fusion reactors, including JET at Culham, currently the world's largest, adopted a similar staged approach. The machine that researchers will fire up in 2018 will pretty much just comprise the vacuum vessel, superconducting magnets to hold the plasma in place, and a cryogenic system to cool the magnet coils. Researchers will first run the reactor with normal hydrogen inside to learn how to control the plasma, and there won't be any fusion reactions.

In following years, engineers will install diagnostic instruments, microwave and particle beam heating systems to raise the plasma's temperature, a metal blanket on the inside wall of the vessel to absorb neutrons from the fusion reactions, and a diverter to extract spent fuel. Only when all of those components are working properly will researchers fire up a plasma of deuterium and tritium and attempt to generate energy. Once they start, the vessel will be radioactive and harder to modify. Campbell says scenario 1 will delay the start of deuterium-tritium operation from early 2025 to late 2026. "Scenario 1 has a lot of attractions for a machine builder," says Cowley. "It's a better idea than the original idea."

Estimating ITER's cost remains a thorny issue and may be impossible to do accurately, project scientists say. In the 2001 baseline, researchers had calculated a value for ITER's various components so that they could be parceled out fairly to the partners to build and deliver to the site. Each partner decides for itself how much to spend on their components, depending on local market conditions and commodity prices. The ITER organization in Cadarache is in charge of only about 10% of spending. "We're trying to make the best estimate of the costs we're responsible for," says Campbell.

As part of that effort, after ITER staff presented the first results of the redesign at a council meeting in June 2008, the council ordered JET's former operations director, Frank Briscoe, to carry out an independent review of costs. As of last week's meeting, that review was still going on, and the council requested that a final revised baseline be presented at its next meeting in November.

Cowley thinks the council would not even consider scaling down the reactor to cut costs. "You would never get to fusion with anything less," he says. "ITER [as it stands] is the minimum possible." In the end, Cowley believes, the members are less concerned about the overall cost than about keeping annual expenditure steady. The phased construction plan has the added benefit that it avoids a huge peak in construction activity and spending during about 2015–16. **–DANIEL CLERY**

Published by AAAS

DEPRESSION GENE

Back to the Drawing Board for Psychiatric Genetics

Geneticists have long been immersed in an arduous and largely fruitless search to identify genes involved in psychiatric disorders. In 2003, a team led by Avshalom Caspi, now at Duke University in Durham, North Carolina, finally landed a huge catch: a gene variant that seemed to play a major role in whether people get depressed in response to life's stresses or sail through. The find, a polymorphism related to the neurotransmitter serotonin, was heralded as a prime example of "gene-environment interaction": whereby an environmental trigger influences the activity of a gene in a way that confers susceptibility.

"Everybody was excited about this," recalls Kathleen Merikangas, a genetic epidemiologist at the National Institute of Mental Health (NIMH) in Bethesda, Maryland. "It was very widely embraced." Because of the well-established link between serotonin and depression, the study offered a plausible biological explanation for why some people are so much more resilient than others in response to life stresses.

But an exhaustive new analysis published last week in *The Journal of the American Medical Association* suggests that the big fish may be a minnow at best.

In a meta-analysis, a multidisciplinary team headed by Merikangas and geneticist Neil Risch of the University of California, San Francisco, reanalyzed data from 14 studies, including Caspi's original, and found that the cumulative data fail to support a connection between the gene, life stress, and depression. It's "disappointing—of all the [candidates for behavior genes,] this seemed the most promising," says behavioral geneticist Matthew McGue of the University of Minnesota, Twin Cities.

The Caspi paper concluded from a longitudinal study of 847 New Zealanders that people who have a particular variant of the serotonin transporter gene are more likely to be depressed by stresses, such as divorce and job loss (*Science*, 18 July 2003, pp. 291, 386). The gene differences had no effect on depression in the absence of adversity. But those with a "short" version of the gene—specifically, an allele of the promoter region of the gene—were more likely to be laid low by unhappy experiences than were those with two copies of the "long" version, presumably because they were getting less serotonin in their brain cells.

Subsequent research on the gene has produced mixed results. To try to settle the issue, Merikangas says, "we really went through the wringer on this paper." The group started with 26 studies but eliminated 12 for various reasons, such as the use of noncomparable methods for measuring depression. In the end, they reanalyzed and combined data from 14 studies, including unpublished data on individual subjects for 10 of them.

When life gets you down … Serotonin-linked variant may not have a hand in it after all.

Of the 14 studies covering some 12,500 individuals, only three of the smaller ones replicated the Caspi findings. A clear relationship emerged between stressful happenings and depression in all the studies. But no matter which way they sliced the accumulated data, the Risch team found no evidence that the people who got depressed from adverse events were more likely to have the suspect allele than were those who didn't.

Caspi and co-author Terrie Moffitt, also now at Duke, defend their work, saying that the new study "ignores the complete body of scientific evidence." For example, they say the meta-analysis omitted laboratory studies showing that humans with the short allele have exaggerated biological stress responses and are more vulnerable to depression-related disorders such as anxiety and post-traumatic stress disorder. Risch concedes that his team had to omit several supportive studies. That's because, he says, they wanted to focus as much as possible on attempts to replicate the original research, with comparable measures of depression and stress.

Many researchers find the meta-analysis persuasive. "I am not surprised by their conclusions," says psychiatric geneticist Kenneth Kendler of Virginia Commonwealth University in Richmond, an author of one of the supportive studies that was excluded. "Gene discovery in psychiatric illness has been very hard, the hardest kind of science," he says, because scientists are looking for multiple genes with very small effects.

Dorrett Boomsma, a behavior geneticist at Amsterdam's Free University, points out that many people have questioned the Caspi finding. Although the gene was reported to have an effect on depression only in the presence of life stress, she thinks it is "extremely unlikely that it would not have an independent effect" as well. Yet recent whole-genome association studies for depression, for which scientists scan the genomes of thousands of subjects for tens of thousands of markers, she adds, "do not say anything about [the gene]."

Some researchers nonetheless believe it's too soon to close the book on the serotonin transporter. Psychiatric geneticist Joel Gelernter of Yale University agrees with Caspi that the rigorous demands of a meta-analysis may have forced the Risch team to carve away too much relevant material. And NIMH psychiatrist Daniel Weinberger says he's not ready to discount brain-imaging studies showing that the variant in question affects emotion-related brain activity.

Merikangas believes the meta-analysis reveals the weakness of the "candidate gene" approach: genotyping a group of subjects for a particular gene variant and calculating the effect of the variant on a particular condition, as was done in the Caspi study. "There are probably 30 to 40 genes that have to do with the amount of serotonin in the brain," she says. So "if we just pull out genes of interest, … we're prone to false positives." Instead, she says, most geneticists recognize that whole-genome scans are the way to go. McGue agrees that behavioral gene hunters have had to rethink their strategies. Just in the past couple of years, he says, it's become clear that the individual genes affecting behavior are likely to have "much, much smaller effects" than had been thought.

–CONSTANCE HOLDEN

INTERNATIONAL COLLABORATION

Bioscientists Slowly Bridge The Taiwan Strait

TAIPEI—At a recent conference here on bioscience, the presentation by Chen Pei-Jer, a molecular virologist at the National Taiwan University (NTU) College of Medicine in Taipei, attracted attention not just because of his solid work on hepatitis B but more importantly because it was one of very few reports resulting from a collaboration between scientists in Taiwan and the Chinese mainland. "It is quite natural to have those on both sides [of the Taiwan Strait] work together. Both not only share a common cultural heritage but also a very similar history of human disease loads," Chen says. Unfortunately, despite being natural, "there still is little cooperation."

The dearth of joint work among life scientists is puzzling because cross-strait ties in other fields are flourishing. The bottom line, researchers say, is that for various reasons, life scientists in Taiwan and the mainland just haven't had the chance to get to know each other yet, which was one of the objectives of the conference. "It's part of the mission of the Society of Chinese Bioscientists in America to foster scientific collaborations," says SCBA treasurer Dihua Yu, a molecular biologist at the University of Texas (UT) M. D. Anderson Cancer Center in Houston.

It took a while for Cold War tensions between Taiwan and the mainland to thaw. But economic and scientific links started growing in the 1990s, despite thickets of regulations (*Science*, 16 May 2003, p. 1074). Scientific cooperation has now become routine in many fields. The Academia Sinica Institute of Astronomy & Astrophysics in Taipei is working with astronomers at the Chinese Academy of Sciences (CAS) Purple Mountain Observatory in Nanjing to develop instruments for radio telescopes. Particle physicists on both sides of the strait are also working on each other's neutrino experiments.

In a recent advance, just after the May 2008 Wenchuan Earthquake devastated Sichuan Province, CAS president Lu Yongxiang wrote to his counterpart at Academia Sinica, Wong Chi-Huey, suggesting that Taiwanese experts share knowledge gained from the September 1999 earthquake that struck central Taiwan. It was the first ever official contact between the presidents of the two institutions, which both trace their roots to an organization founded on the mainland in 1928. Liu Chao-Han, Academia Sinica vice president for international affairs, led an 11-member team of engineers, geologists, psychologists, and lawyers that met with mainland counterparts last summer. That workshop led to "regular exchanges and joint studies related to earthquake engineering and reconstruction," says Liu. They are now discussing joint studies of typhoons and other topics.

"I realized the impact of our research would be bigger if it extended to the mainland."

—CHEN PEI-JER, NATIONAL TAIWAN UNIVERSITY

Meanwhile, the logistics of cross-strait cooperation have gotten easier. Since July 2008, there have been direct flights between the mainland and Taiwan, eliminating the need to change planes in Hong Kong. And although there are still some bureaucratic hurdles, researchers say such things as visa approvals are going through more smoothly.

Amid this progress, why is cooperation among life scientists lagging? One reason is that unlike physicists and astronomers, life scientists are less dependent on shared facilities and often work in small groups. And if they think of collaborations, many turn to U.S. contacts, in part because the infrastructure in Asia "is not even close to what is in the U.S.," says Wang Xiaodong, a biochemist at UT Southwestern Medical Center in Dallas who is also co-director of the National Institute of Biological Sciences in Beijing.

What promises to bring the two sides together is biomedicine. Given the genetics involved, "to answer questions about disease patterns in East Asia, we have to collaborate within the region," says Yang Pan-Chyr, dean of the NTU College of Medicine in Taipei. UT Southwestern's Wang notes that for clinical studies in general, "China offers so many patients."

Chen, for example, went to China to expand his studies of liver diseases, particularly cancer and viral hepatitis B. "I realized the impact of our research would be bigger if it extended to the mainland," Chen says. The point has been driven home by demand for a hepatitis B mouse model he developed in 2006: 80% of requests for the mice came from China, with the rest split between the United States and Europe.

Chen formed close ties with Xiamen University, on the mainland coast directly across from Taiwan, and is now codrafting an agreement for visits of graduate students and joint work on diagnostic kits and therapeutics. There are still hurdles. Chen wants to sequence the genome of a Taiwanese—hence ethnic Chinese—liver cancer victim. But the approvals needed to send samples directly to China look daunting, so he is considering working with U.S. colleagues.

Chen points to other examples: The lead investigator for an Asia-wide clinical trial of a liver cancer drug is his NTU colleague Cheng Ann-Lii, though many of the clinical sites are on the mainland. And Yang, dean of the NTU medical school, says NTU is also working with Guangzhou Institute of Respiratory Diseases on lung cancer studies.

Just when such collaborations will extend to more basic life science research remains a question, although researchers who gathered here for the conference professed to be interested in making them happen.

—DENNIS NORMILE

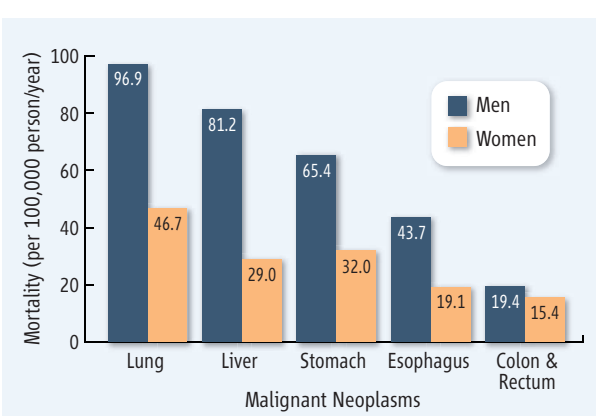

Deadly difference. According to a 2005 study, liver cancer is a more prominent cause of cancer deaths in China than in the West.

CREDITS (TOP TO BOTTOM): CHEN PEI-JER; ADAPTED FROM JIANG HE *ET AL.*, *NEW ENGLAND JOURNAL OF MEDICINE* **353**, 11

*The 12th Society of Chinese Bioscientists in America International Symposium: 14–18 June 2009.

Published by AAAS

SCIENCE IN SOCIETY

China Reins in Wilder Impulses in Treatment of 'Internet Addiction'

BEIJING—World of Warcraft was Sun Jiuqing's undoing. It began to take over his life last autumn, after the 18-year-old had transferred to a new high school with higher academic standards than his previous one. He struggled from the start. "I couldn't catch up to the other students," he says. Sun chose instead to escape. Before long, he was spending 10 hours a day playing World of Warcraft, an online game. Sun spurned pleas to stop. Finally, in late March, his father drove the young man a few hours from their home in Tianjin to a People's Liberation Army barracks in south Beijing and admitted him to the General Hospital of Beijing Military Region's Addiction Medicine Center (AMC).

Boot camp. For youth diagnosed with "Internet addiction disorder" at the Addiction Medicine Center, psychiatrist Tao Ran (*inset*) prescribes everything from drugs to military-style discipline.

No one doubts that logging long hours on the Internet can erode quality of life and on occasion can lead to ruinous consequences. "It's a global phenomenon," says AMC director Tao Ran, a psychiatrist and senior colonel. In China alone, Tao estimates, 5 million of the country's 300 million Internet users are "Internet addicts." Adolescents are especially vulnerable. "Youth who compulsively seek social contact on the Internet at the expense of offline activities may be finding it difficult to establish sufficiently gratifying social ties in their regular lives," says sociologist Zeynep Tufekci of the University of Maryland, Baltimore County.

But there is no meeting of the minds on whether Internet addiction (IA) is a genuine disorder. "Labeling these behaviors as deviant is being done by older generations who have very different experiences with technology," argues Shelia Cotten, a sociologist at the University of Alabama, Birmingham. Overlooking or ignoring social factors can result in unnecessary medical interventions for behaviors that "do not fit into the structure of our society as it happens to be now," adds Tufekci.

An American Psychiatric Association panel is now weighing whether to include IA in the fifth edition of the field's practices bible, the *Diagnostic and Statistical Manual of Mental Disorders* (*DSM-V*), planned for release in 2012. In an editorial in the March 2008 issue of *The American Journal of Psychiatry*, Jerald Block, a psychiatrist in Portland, Oregon, argued that IA "appears to be a common disorder that merits inclusion." But Cotten, for one, disagrees. She thinks it is premature to include IA in *DSM-V* given the lack of consensus about what constitutes IA or "whether Internet addiction disorder even exists."

In China, the official view appears to be that Internet addiction is a genuine disorder, but attitudes are shifting about how aggressively it should be treated. Last year, CCTV-12, a central government channel, ran a series of glowing reports on a clinic in Shandong Province in eastern China that has used electric shocks on unanesthetized IA patients as part of what the clinic's director, Yang Yongxin, has called a "holy crusade" to cure IA. Earlier this month, the state-owned newspaper *China Daily* ran an article raising questions about Yang's methods, indicating an official about-face on the use of electric shocks as a valid IA treatment.

Sizing up the beast

Several years ago, when parents started showing up at AMC claiming that their adolescent children were Internet junkies, "at first I was skeptical we were seeing a true disorder," says center psychologist Huang Xiuqin. But as cases accumulated, she and Tao, her boss, became convinced that IA is an authentic disorder. Of the more than 3000 cases they have chronicled, patients were spending on average 9 hours a day on the Net.

Tao has been trying to put diagnosis and treatment of IA on a more solid footing. Last November, his group released the first diagnostic criteria for IA; a paper outlining the guidelines is under review at the journal *Addiction*. The group classifies sufferers in three categories: simple IA (about 40% of cases), IA with accompanying symptoms such as anxiety or depression (30%), and IA with a second disorder, such as attention deficit hyperactivity disorder (30%). About 80% of patients are teenage boys.

Tao's group has defined seven IA symptoms, including preoccupation with the Internet, disregard of harmful consequences of spending too much time online, and loss of interest in other activities. "Only being on the Internet makes them happy," says Tao. To qual-

CREDITS: R. STONE/*SCIENCE*

ify for diagnosis as an Internet addict, they have proposed that a person must spend at least 6 hours a day on the Internet (for reasons other than business or academic work) for at least 3 months after showing symptoms.

In the vast majority of cases, Tao says, the culprit is online games, although female patients also often get hooked on online chat rooms. After arriving at AMC, "almost all" patients suffer withdrawal symptoms, Tao says, including anger, irritation, and restlessness, that fade after a few weeks. (Those reactions may not be too surprising: Adolescents are usually taken against their will to AMC, whose dormitory's entrance has steel bars—a state requirement of psychiatric wards.)

AMC's treatments include behavioral training, drug therapy for patients with mental symptoms, dancing and sports, reading, karaoke, and elements of the "12 step" program of Alcoholics Anonymous. A "very important" part of the regimen is family therapy, says Tao. "Internet addiction occurs because the parents are doing something wrong," he asserts. Patients tend to have parents who are strict authoritarians or demand perfection, or come from single-parent households or homes in which the parents are frequently fighting, Tao says. In the beginning, parents tend to blame their children, he says, but after treatment they recognize their failings.

Beyond the pale. As documented in a CCTV-12 program last year, Yang Yongxin administered electric shocks to "H" (*top*) with an electroconvulsive therapy machine (*bottom*).

In the absence of guidance from China's health ministry, which is considering but has not yet adopted the military hospital's IA definition, dubious clinics have sprouted up throughout the country. Some force IA patients to go on kilometers-long hikes day after day as therapy. "That's unscientific. It doesn't treat the nature of the disorder," says Tao.

The most infamous, perhaps, is the Yang Yongxin Center for IA Treatment at public hospital number four in Linyi, Shandong. Last year, a CCTV-12 segment recounted how the parents of a young man, "H," drugged him with a dozen sleeping pills and brought him to Yang's clinic. After "H" had woken up, he protested to Yang that he was over 18 years old and therefore they could not force him to stay without his consent. Yang bundled "H" into a room, and other patients restrained him on a bed, after which Yang administered shocks—for more than 1 hour, the narrator claimed—with a DX-IIA electroconvulsive therapy (ECT) machine, clearly shown in the program. In an 8 May article in *China Youth Daily*, Yang explained that he uses a weaker current than standard ECT and that the shocks, although "very painful," are "harmless."

After months of appeals from Tao and colleagues, last month three government entities—the central government's information ministry, Shandong Province government, and the Communist Youth League—launched an investigation of Yang's clinic. A Linyi hospital spokesperson declined to comment. She stated that as *Science* went to press, Yang was occupied with a CCTV interview and would not be available to speak with *Science*.

Cracking down on extreme treatments is unlikely to alter views in China that IA is a disorder. At the barracks in Beijing's Daxing district, Sun has taken a break from drills in AMC's courtyard. It was difficult, he says, adapting to waking at sunrise, lights out at 9 p.m., and other elements of the center's strict regimen. But after nearly 3 months, he says, "I feel normal now," and adds that he and his father, who has stayed in Beijing the whole time, are communicating much better with each other.

In a few days, Sun will return to the real world. Tao's statistics show that there is a 40% chance the teenager will relapse. But for now, Sun is eager to get back to school—and face down the temptation of losing himself, once again, to the Internet.

–RICHARD STONE

CREDIT (RIGHT): PHOTO COURTESY OF JERAMIAH SMITH

ScienceNOW.org

From *Science*'s Online Daily News Site

Serial Killers of the Sea
A criminal investigation tool used to place a suspect at the scene of a crime is now being applied to track vicious killers in the ocean—great white sharks. Typically used in serial crime cases, geographic profiling evaluates crime-scene locations to determine the most likely area of the perpetrator's residence. Now, for the first time, a research team has used the tool to study sharks hunting Cape fur seals off the coast of South Africa. http://tinyurl.com/kosakk

Atoms Speeding From the Moon
Scientists probing the outer reaches of our solar system have hit upon an unusual phenomenon much closer to home. Instruments aboard a NASA spacecraft have detected fast-moving hydrogen atoms emanating from the moon. The atoms, which originated as protons from the sun, may help scientists study the lunar surface and other solar system objects in greater detail than believed possible. When the solar wind hits the moon, most particles stick to the surface, but as many as 10% of solar protons are bouncing back as hydrogen atoms. http://tinyurl.com/nsrond

Fish Throws Away Its Genes as It Grows
Whether it's its extraterrestrial looks or status as a "living fossil," there's always been something fishy about the sea lamprey. Now scientists have added another oddity to the creature's repertoire: The lamprey jettisons 20% of its genome during development. http://tinyurl.com/n9dlow

A Yawn From the Napping Sun
Maybe old Sol didn't hear the alarm clock. After a mysterious 2-year delay, the next 11-year solar cycle seems ready to begin, scientists say. That means the reemergence of sunspots and with them periodic electromagnetic assaults on global navigation, communications, and power supplies—as well as brilliant auroras in the polar regions. http://tinyurl.com/nqpox8

Read the full postings, comments, and more on **sciencenow.sciencemag.org**.

Published by AAAS

BIODIVERSITY

Biodiversity Databases Spread, Prompting Unification Call

LONDON—"For millennia, researchers have hoarded data, because essentially data [are] power," says Norman MacLeod, keeper of paleontology at London's Natural History Museum. That attitude has faded in recent years, as scientists increasingly recognize the value of collaborative, open-access data sharing for understanding the world. But there's still a wide gap between wanting to share and figuring out how to do it right, discovered those who attended an international meeting on biodiversity here this month.

MacLeod was one of the organizers of e-Biosphere 09*, a meeting for creators and users of the Encyclopedia of Life (EOL), the Consortium for the Barcode of Life (CBOL), the Catalogue of Life (CoL), and other major efforts to build and manage open-access biodiversity databases. CoL now lists more than 1.1 million species, for example, and EOL has compiled more than 150,000 vetted species pages and 1.4 million short articles, called "stubs," that will be expanded as information on each species is gathered. "At e-Biosphere, many groups demonstrated they are now providing actual services, around the clock, with interfaces that large numbers of people can use," says Jesse Ausubel, program director of the Alfred P. Sloan Foundation in New York City. The goal of the conference was to figure out how to combine data from at least 100 systems into one gigantic, online, open-access database that will eventually cover all life on Earth, with lots of information, including primary research.

But whether these researchers are ready to create one-stop shopping for biodiversity remains to be seen. They are behind in gathering data, some may soon be strapped for cash, and not everyone is eager to share information. "None of the groups has a permanent, sustainable business model," says Rainer Froese, coordinator of FishBase, a comprehensive database on fish.

Many of the individual projects have run short of funding or underestimated how long it would take to meet their targets. Begun in 2007 with $12.5 million, EOL hoped to profile 700,000 to 1 million species by 2011 (*Science*, 11 May 2007, p. 818). But 2 years into the project, it has just 150,000 on its computers and will be happy to hit between 500,000 and 700,000 by that point. CoL, essentially a species list that provides a "taxonomic backbone" for many of the other databases, including EOL, has pushed back by 3 years its 2011 goal of covering all 1.75 million known species. It won't say how much it's spent so far but now needs new money to complete the job.

Funding has also been an issue for the International Barcode of Life (iBOL) project, a yet-to-launch international project based at the University of Guelph in Canada that is building a database of DNA bar codes—short sequences of DNA that can be used to "tag" species (*Science*, 18 February 2005, p. 1037). iBOL needs $60.7 million for the next 6 years. It has promises of $24 million from various Canadian agencies but this year got only $1.7 million of $21.7 million expected from the government's Genome Canada. Paul Hebert of iBOL is confident the other $20 million will be awarded by next February, but that still leaves the project searching for another $15 million or so. iBOL's barcoding centers around the world will have to come up with their own funding as well.

Pick a species. Like baseball cards, species pages from the Encyclopedia of Life give the vital statistics on an organism.

Tagged. The bar codes for the Great Horned Owl (*above, left*) and the Barn Owl show great variation in the mitochondrial gene sequenced from these two birds. A global bird bar-code database is under construction.

Scientists have also discovered that making the databases comprehensive is a tough process. The Global Biodiversity Information Facility (GBIF) Web site, for example, allows users to generate biodiversity maps. "If you look at [maps on] the GBIF Web site, you'll see a lot of blank spots," says CBOL's executive secretary, David Schindel. "Those are either countries that don't have a lot of digital records or for some reason have decided not to share their data."

Converting scientists from data hoarders to data sharers can still be a problem, says MacLeod. Yet combining data across disciplines can be quite useful. One, for example, can link a species' global-positioning data with its biological makeup, and then with climate-modeling data, to get a clearer picture of threats to its existence.

Because funding is often an issue, projects

CREDITS (BOTTOM): SUZ BATESON/BIODIVERSITY INSTITUTE OF ONTARIO

Published by AAAS

that have something to offer government agencies may have an easier time keeping afloat. The Fish Barcode of Life Initiative is developing bar codes for commercial fish for the Regulatory Fish Encyclopedia at the U.S. Food and Drug Administration and also for the National Oceanic and Atmospheric Administration. "In general, we are seeing more interest from government agencies [in bar coding]," says Schindel, who hopes these agencies will eventually provide funding for these efforts.

But even if the projects can meet their targets, how will they then ensure that they have sustainable funding to maintain the databases and continue to add new species and primary research data? At the London meeting, the participants agreed that some of their efforts may be short-lived. "A lot of competition is going on, and [some] people are creating similar sorts of tools," says Schindel.

For projects that do survive, funding will remain a key concern. Dave Roberts of the European Distributed Institute of Taxonomy says that it's "unrealistic to give guarantees" for funding of many projects in the current economic climate—a sentiment echoed by many of the project leaders in attendance. However, many hope they can make a good case for sustained funding, citing the 27-year history of GenBank, a public archive of DNA sequence data. "We know GenBank will still be there 10 years from now," says CoL's Frank Bisby. "I believe this will also be true of the CoL and several other key components of the biodiversity informatics community."

For some of the projects, public involvement and interest outside of the scientific community will be crucial to their sustainability. For EOL, allowing access to update pages and add pictures will help keep the project relevant to the wider world, says EOL's species page group director, Cynthia Sims Parr. But access will be controlled to some extent to avoid "the Wikipedia problem," which is caused when users introduce errors into articles unchecked. EOL is now recruiting site curators for various groups of species; they will monitor and verify if information added is correct.

But as researchers try to fix problems facing individual projects, they need to also figure out how to integrate these initiatives. Bisby notes, for example, that GBIF failed to include species added this year because it was still using last year's version of CoL's species checklist. In general, scientists must now navigate each database site separately to pull together information needed on a species. But aligning software from all the databases to enable interoperability will be a huge challenge, involving reformatting large amounts of data into a standardized form.

After the conference ended, a smaller working group from the major initiatives discussed a "digital road map" of how to connect the databases on the Web. The first steps they agreed upon included completing a list of global species names, on which many other databases can be built, and reaching out to potential collaborators in the computer science community to help construct the road map. Initial progress will be presented either at October's GBIF GB16 meeting in Copenhagen or the Taxonomic Database Working Group's November 2009 meeting in Montpellier, France. The e-Biosphere working group doesn't have any milestones set yet but hopes to present incremental progress and outline new action items toward creating the road map. Ballpark estimates are that the "virtual laboratory" envisioned will take 10 years to construct. But EOL Executive Director James Edwards says that the "guts" of the system, an integrated database incorporating the largest projects such as EOL, GBIF, and CoL, should be available within 2 years. **–CLAIRE THOMAS**

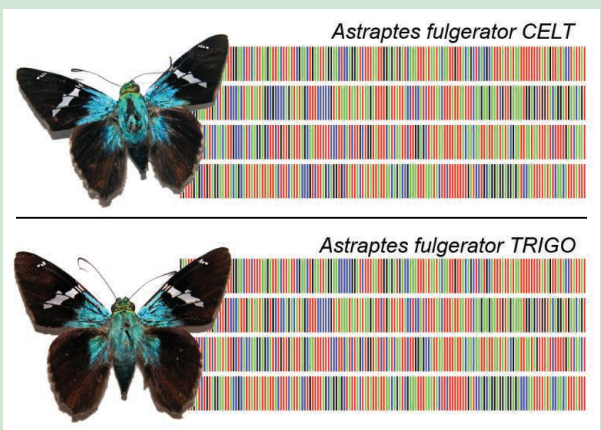

Two in one. They look alike, but these two butterflies are two species—so says their different bar codes—an observation confirmed by watching what their caterpillars eat.

CREDITS: DAN JANZEN/BIODIVERSITY INSTITUTE OF ONTARIO

*The e-Biosphere 09 International Conference on Biodiversity Informatics, London, 3–5 June, www.e-Biosphere09.org.

ScienceInsider

From the *Science* Policy Blog

*Science*Insider this week reported on a U.S. government official's prediction that **H1N1 flu will continue unabated** during the summer and into the fall, a decision by the **G8 nations to skip science** at their summit meeting in Italy this month, and an **interruption of clinical trials** caused by procedural errors at two U.S. cancer centers.

*Science*Insider also highlighted a warning that the continuity of **U.S. weather data is "at extreme risk"** because a program to develop new Earth-observing equipment is poorly managed. The effort to replace older satellites is well under way, but the National Polar-orbiting Operational Environmental Satellite System, as it is called, has doubled in cost to $14 billion.

Two large companies have offered to provide **free vaccine against the H1N1 flu** to people in developing countries who can't afford to pay. An offer of 100 million free doses came from Sanofi-Aventis shortly after a similar pledge was announced by GlaxoSmithKline.

A widely debated **plan to change the way the U.K. government doles out research funds** to universities has been shot down. The proposal to switch from live peer review to evaluation based on citation analysis and other bibliometric data—both complex and controversial—has been sidelined indefinitely.

The U.S. Congress is fighting over changes to a $2 billion research program to **tap the creativity of small businesses**, with the goal of reaching agreement before the program expires next month. Also this week, four legislators asked the U.S. National Academies to tell them what the government needs to do **to keep U.S. academic research strong**. A similar 2005 letter spawned the influential *Rising Above the Gathering Storm* report.

Keep up with the latest science policy news at **blogs.sciencemag.org/scienceinsider**.

Published by AAAS

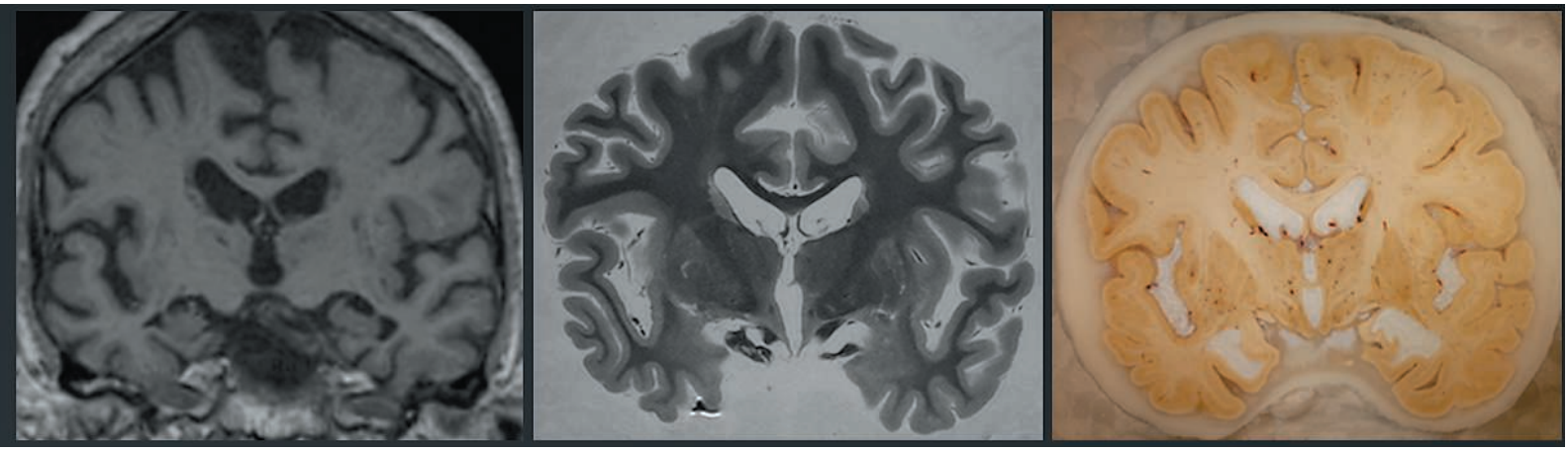

The Brain Collector

Jacopo Annese plans to create an open-access digital brain library—starting with the most famous amnesic patient of all time

The refrigerators against the back wall of Jacopo Annese's lab are filled with human brains. Some float in tubs of formaldehyde; others have been sliced into ultrathin sections to be treated with stains that will reveal various anatomical features. One of the tubs is labeled HM, after Henry Molaison, the most studied human being in the history of psychology. In 1953, an experimental brain surgery intended to correct a devastating seizure disorder left Molaison unable to form new memories. At age 27, he became frozen in time. He could remember facts he'd learned and names of people he'd encountered before the surgery but virtually nothing after it. For half a century, until his death last December, Molaison gamely cooperated with psychologists and neuroscientists, and his case reshaped scientific thinking on the neural basis of memory.

Annese, 42, is a neuroanatomist at the University of California, San Diego (UCSD), and he has been charged with preserving Molaison's brain for perpetuity. He takes this responsibility seriously. Among other precautions, the fridge containing Molaison's brain has an alarm system that calls Annese's office, home, and cell phones if the temperature deviates too far from the set point. He has also taken certain security measures he's loath to discuss on the record. "It probably sounds a bit paranoid," he says, "but we've tried to think of anything that could go wrong and eliminate the risk."

With funding from the Dana Foundation, a New York City nonprofit that supports research in neuroscience, and the National Science Foundation, Annese plans to create a digital, zoomable atlas of Molaison's brain and make it freely available online, the first entry in what he hopes will become an open-access brain library to be used by scientists, students, or anyone with an Internet connection and an interest in neuroanatomy. Ultimately, the library will include donated brains from people with Alzheimer's disease and other neurological disorders, Annese says, as well as a collection of healthy brains of different ages. But for now, Molaison's brain is the star attraction.

"More was learned about memory by research with just that one patient than was learned in the previous 100 years of research on memory," says Vilayanur Ramachandran, a behavioral neurologist at UCSD who is not directly involved with Annese's project. Postmortem anatomical studies could reveal new clues about the cause of Molaison's amnesia by revealing more precisely the extent of his surgical lesions, as well as subsequent degeneration, Ramachandran says. Preserving the donated brains of such unique patients has both historical and scientific value, he says.

Online
sciencemag.org
Podcast interview with author Greg Miller.

A long history

Molaison's story begins decades before Annese got involved. Henry Gustav Molaison was born in 1926 and grew up in and around Hartford, Connecticut. His seizures began at age 10. The cause is uncertain, but his father's family had a history of epilepsy, and a collision with a passing bicycle rider had once knocked Henry unconscious for several minutes. The seizures worsened through his teens and 20s until frequent blackouts and increasingly severe convulsions left him unable to continue his work repairing electric motors, despite high doses of anticonvulsant drugs. He ended up in the care of William Beecher Scoville, a neurosurgeon at Hartford Hospital.

Because of the incapacitating nature of Molaison's seizures, Scoville decided to try what he later described as a "frankly experimental operation." He removed, via suction, a finger-sized piece of the temporal lobes on both sides of the brain, including most of the hippocampus, amygdala, and nearby parahippocampal gyrus. Scoville had previously performed such bilateral medial temporal lobotomies on dozens of psychiatric patients, hoping to calm their psychosis without the personality changes associated with the more drastic frontal lobotomies that were beginning to fall out of favor at the time. By coincidence, two of Scoville's previous patients had been prone to seizures, and those diminished postsurgery, says Suzanne Corkin, a neuroscientist at the Massachusetts Institute of Technology in Cambridge who worked with Molaison for 46 years and is writing his biography. As a last resort, Scoville thought the surgery was worth a try with Molaison.

In a landmark 1957 paper, Scoville and Canadian psychologist Brenda Milner reported that although Molaison's seizures had diminished greatly, he now exhibited profound amnesia. He easily recalled events prior to his operation but had virtually no lasting memories of anything that had happened since. A half-hour after hav-

CREDIT: (BANNER) JACOPO ANNESE, PETER J. CHON, AND ALEX GHATAN

Published by AAAS

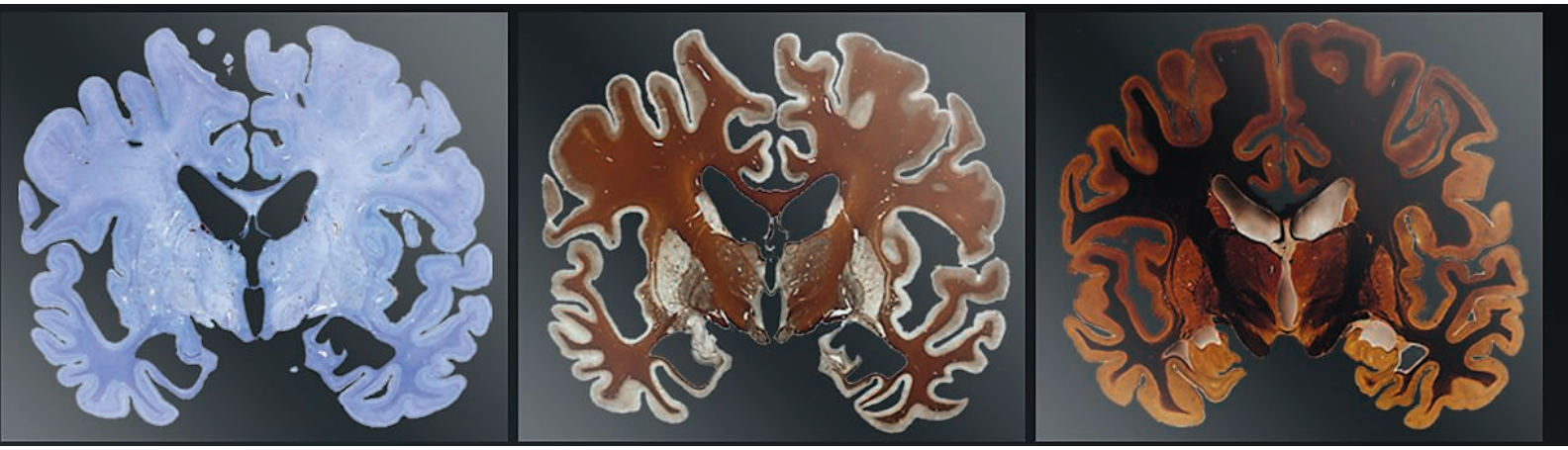

Multimodal. A new brain library will archive multiple views of individual human brains, including MRI scans, photographs, and thin slices dyed to reveal detailed anatomy.

ing lunch with Milner in the hospital cafeteria, for example, he couldn't name a single thing he had eaten and did not even remember eating. The paper also described moderate to severe memory deficits in seven other patients with similar surgeries, mainly for schizophrenia. In the coming years, Scoville urged other surgeons not to perform this surgery on both sides of the brain.

Memory lessons

Molaison's case startled memory researchers. Conventional wisdom at the time held that memory could not be pinned to any specific location in the brain. This view sprang largely from the work of Karl Lashley, an American physiologist who in the 1930s and '40s had searched in vain for the "engram," or neural trace of memory, by removing different regions of the cerebral cortex of rats to see whether this would destroy a previously learned memory, such as the location of food in a maze. Because removing even large swaths of cortex did not render the rodents amnesic, Lashley concluded that memory traces must be widely distributed.

Molaison's case suggested otherwise. His ability to learn and retain new facts, what researchers now call declarative memory, had been devastated by removing a relatively small part of his brain. (Lashley, certain he would find the engram in the cerebral cortex, never tried removing the hippocampus.)

Further studies provided additional clues about the biology of memory. Although Molaison was unable to create long-lasting new memories, his recollection of distant events—World War II, for example—demonstrated that older memories must reside outside the medial temporal lobes. At the same time, he also retained a fleeting short-term memory: He could remember a string of numbers or words for 30 seconds, about the same as someone with an intact brain. And in another widely cited study, Milner reported in 1962 that Molaison could learn and remember a new skill. She asked him to trace a double star design while watching his hand in a mirror.

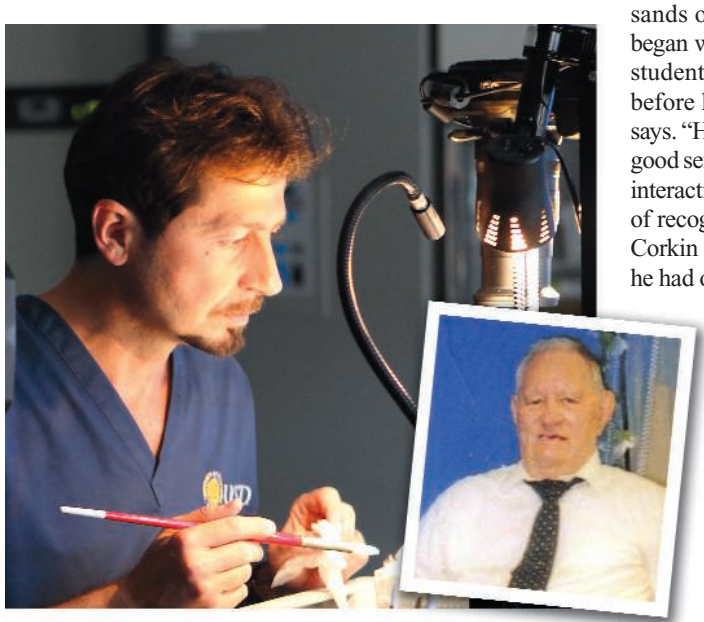

Painstaking work. Jacopo Annese aims to digitally reconstruct the brain of amnesic patient Henry Molaison (*inset*).

Over several days, his drawings improved substantially, demonstrating a memory of previous practice sessions. Yet he always insisted that he'd never done this task before and seemed surprised that it turned out to be easier than he'd thought.

Molaison's case helped establish several modern tenets of memory research, including the notion that there are different types of memory that depend on different brain regions, and the concept of memory consolidation, which holds that new memories formed by the hippocampus are later archived in the cerebral cortex for long-term storage.

Molaison was interviewed by at least 100 researchers and has been mentioned in thousands of journal articles, says Corkin, who began working with him as Milner's graduate student in 1962 and continued until shortly before his death. "Everyone liked him," she says. "He was soft-spoken, polite, and he had a good sense of humor." Yet despite thousands of interactions, Molaison displayed only a flicker of recognition, sometimes saying he'd known Corkin in high school. "Whatever knowledge he had of me was very sketchy," she says. "He never really knew who I was."

In 2002, Corkin set up a committee, which included Annese, to plan for Molaison's eventual death. Molaison, who had no immediate living family, and a distant relative who acted as his conservator signed paperwork agreeing to donate his brain. Corkin delivered Cryopaks to his nursing home in Windsor Locks, Connecticut. "They kept them in the freezer so that the moment he died they could wrap his head to preserve the brain," she says. When Molaison died of respiratory failure at 5:05 p.m. on 8 December 2008, the plan sprang into action. A hearse took his body to Massachusetts General Hospital (MGH) in Charlestown, where researchers began collecting anatomical magnetic resonance imaging (MRI) scans of his brain at about 9 p.m.—and continued until 6 a.m. the next day, when Annese arrived on a red-eye flight from San Diego.

Annese assisted MGH neuropathologist Matthew Frosch in removing the brain. "I

CREDITS: JACOPO ANNESE, PETER J. CHON, AND ALEX GHATAN; (INSET) COURTESY OF SUZANNE CORKIN

was sweating bullets," Annese says. But the delicate procedure went smoothly, and for the next 2 months, the brain remained at MGH. A fresh brain is the consistency of Jell-O that has barely begun to set. Only when fixed in formaldehyde would it be firm enough to transport safely.

Artistic anatomy

Annese grew up in Florence, Italy, and the Renaissance city's cultural sensibilities seem to have rubbed off on him. His office décor includes old anatomical prints and antique microscopes. Issues of an artsy cooking magazine and the Italian-language version of *The New York Review of Books* fill a magazine rack in the common area of the lab, and an espresso machine stands ready to jolt sleepy anatomists back into action.

On a large touch-screen monitor, a student scrolls through the MRI scans of Molaison's head taken the night he died. A green outline shows the software's best guess at the contours of the brain, and he uses a stylus to make adjustments here and there where the computer got it wrong. Once corrected, these MRI data will yield a three-dimensional image Annese likens to the globe that appears on the opening screen of Google Earth—a starting point for navigation. Digital photographs and histological images will provide more detailed neuroanatomical maps, down to the level of individual cells.

In February, Annese flew back to Boston to collect Molaison's brain. In these security-conscious days, it took some advance planning to arrange to bring the brain—in an ice-packed cooler—as carry-on luggage. An official from the Transportation Security Administration escorted Annese through the security checkpoint. Jet Blue reserved the front row for him. He flew back to San Diego with Molaison's brain sitting beside him in the window seat.

The brain now soaks in a mixture of formaldehyde and sucrose, which will help prevent ice crystals from forming and poking holes in the tissue when Annese freezes it for slicing. Using a microtome, he will slice the brain into very thin sections. "Like prosciutto," he says, but less than 1/20 the thickness and a lot more fragile. Annese aims to slice the brain whole instead of first cutting it into smaller chunks as is more routinely done. Small chunks are much easier to work with, but the resulting slices are hard to keep in register with one another. Whole-brain slices will keep more of the tissue intact and result in a more faithful reconstruction of the brain, he says.

Annese estimates he will end up with about 2600 slices of Molaison's brain. He and his colleagues will mount some of these, perhaps every 12th one to start, on extra-large glass slides—13 by 18 centimeters—and treat them with a stain that colors cell bodies purple. A camera attached to a microscope will photograph each slice at 20× magnification, sufficient to distinguish different cell types. At that magnification, photographing a single slice will require a mosaic of about 40,000 individual images. An automated system Annese designed will carry out the tedious job of moving the slice for each photo, focusing, triggering the shutter, and sending the shot to the San Diego Supercomputer Center, which will store the data and stitch the images together into a composite for each slice.

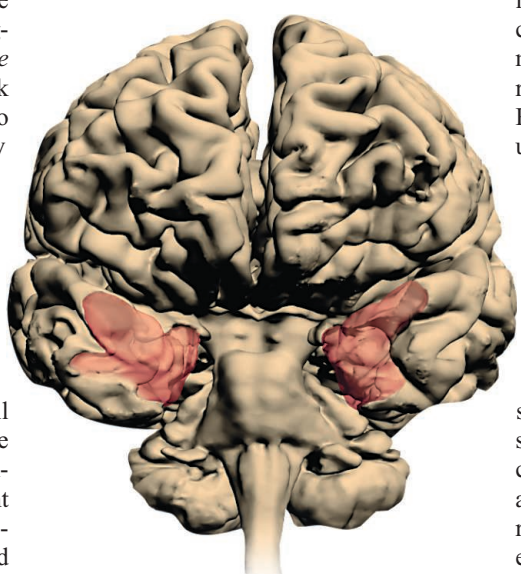

A memorable brain. A preliminary reconstruction of Molaison's surgical lesion (red), based on MRI scans.

Other memory researchers are eager for a better look at Molaison's brain. "The main thing we will all look to is exactly where the boundaries of the surgical lesion were," says Larry Squire, a neuroscientist and veteran memory researcher at UCSD. Knowing the precise location of the lesion "will sharpen the brain-behavior correlation," says Corkin, and may shed light on some lingering puzzles. Despite his well-documented declarative memory deficits, for example, Molaison every once in a while surprised researchers with a newly learned fact. "He knew that Archie Bunker's son-in-law was called Meathead" in the 1970s sitcom *All in the Family*, Corkin says. "When he came up with stuff like that, everyone's jaw just dropped to the ground." MRI scans lack the resolution to determine with certainty which bits of tissue survived Scoville's surgery and may have provided such residual memory function, Corkin says. Annese's work will provide a much clearer view.

Comparing Molaison's brain with those of other amnesic patients may yield additional insights, Squire says. He has entrusted Annese with the donated brains of three amnesic patients his group has studied. One, known as E.P., died in early 2008. Viral encephalitis had ravaged his medial temporal lobes in 1992 and left him with memory deficits strikingly similar to Molaison's. Subtle differences in the two cases, paired with anatomical comparisons, might help clarify the function of different regions within the temporal lobes. UCSD's Ramachandran, who works on a variety of unusual neurological conditions, says several of his patients have agreed to donate their brains, which he will send to Annese.

Annese hopes others will follow suit. But he sees the project as a two-way street, an experiment in open-access science. "The lab is not going to be a fortress," he says. "Everything is going to be up online and discussed with colleagues." His Web site (thebrainobservatory.ucsd.edu) will soon include a blog where other scientists can offer advice on methodological issues, ask him to photograph a particular brain region with higher magnification, suggest experiments, or request tissue samples. Nonscientists will be welcome, too. Just as amateur archaeologists have found undiscovered sites by combing Google Earth, Annese says, amateur neuroscientists might make discoveries that have eluded experts.

Even the slicing will be viewable online in real time, Annese says. His head technician, Natalie Schenker, finds this a bit daunting. "How about a 5-second delay?" she suggests. Annese laughs and says he'll consider it. He plans to slice the brain himself in a marathon 30-hour session, probably sometime in July. If it goes well, all but the most die-hard viewers will be bored silly as he cuts slice after slice and transfers each one from the blade of the microtome to a fluid-filled well in a plastic tray. But a lot could go wrong. The MRI scans reveal deterioration of the white matter, Annese says, which might make the slices especially delicate and prone to tearing. An even more nightmarish scenario is a cracked brain, he says. Sometimes, a brain will freeze unevenly and break apart—destroying it before it can be sliced. Annese is taking every precaution, but he's not taking anything for granted. "Cutting will make or break the project," he says. "But if the brain cracks, I go back to Italy."

–GREG MILLER

CREDIT: JACOPO ANNESE, PETER J. CHON, AND ALEX GHATAN

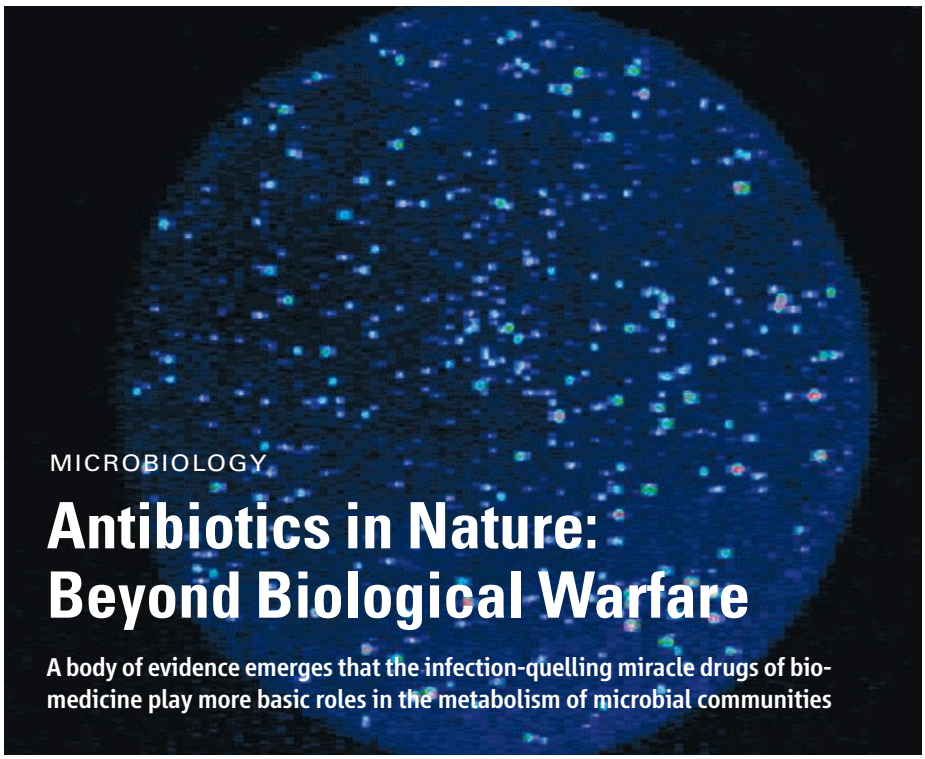

MICROBIOLOGY

Antibiotics in Nature: Beyond Biological Warfare

A body of evidence emerges that the infection-quelling miracle drugs of biomedicine play more basic roles in the metabolism of microbial communities

Signal lights. Engineered *Salmonella* cells light up in response to low levels of compounds produced during the crosstalk of the microbial community in a sediment sample. Some of the detected compounds may lead to new antibiotics.

At the beginning of World War II, Hollywood released the movie *Dr. Ehrlich's Magic Bullet*, depicting the life of turn-of-the-20th-century German microbiologist Paul Ehrlich and his quest to develop an antibiotic drug to treat syphilis. It was Ehrlich who originated the idea of medical "magische Kugeln," launching the warfare metaphor that has clung to such drugs ever since. Even their generic name—antibiotics—has a weaponlike ring to it. The compounds are widely regarded simply as microbe-killers, both in medicine and in nature, where they are produced by soil-dwelling fungi and bacteria. "You still read all the time [about] biological warfare in the soil," says microbiologist Roberto Kolter of Harvard Medical School in Boston.

But there's scant evidence that bacteria or fungi deploy antibiotics to kill or ward off other microbes. What researchers know about antibiotic-producing microbes comes mainly from studying them in high numbers as pure cultures in the lab—artificial conditions compared with the numbers and diversity found in soil. And in the past 15 years, Kolter and other researchers, with Julian Davies of the University of British Columbia at the forefront, have become convinced that natural antibiotics are doing other things in the complex world of microbial communities. These molecules, they assert, may be less weapons for competition or combat than tools of communication, or even essential cogs in their producers' own metabolism.

Kolter's team, for example, recently reported a possible "peaceful" role for the commonly prescribed drug nystatin, a molecule with potent antifungal properties isolated in the 1940s from a soil bacterium. When certain bacteria are exposed to nystatin, the microbes form slimelike communities known as biofilms. Kolter, who has also teased out the novel mechanism by which nystatin triggers this transformation, believes this may be just one of the molecule's natural roles.

Microbiologists' shift away from the biomedical view of antibiotics is no less than "a Copernican turn-about for the role of antibiotics in nature," José Martínez of the Campus Universidad Autónoma de Madrid and his co-workers have written. Beyond reworking the tenets of microbial ecology, understanding the true roles "antibiotics" play has practical potential, researchers say: It could provide a way to manage the increasing problem of resistance to these once-miraculous drugs and lead to discovery of new pathogen-fighters.

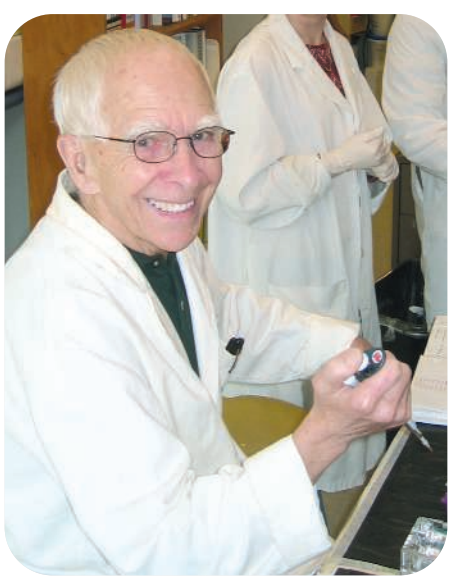

Antimicrobial hunter. Julian Davies is looking for new antibiotics by screening for microbial signals.

Fossil molecules repurposed

The term "antibiotic" was coined by Selman Waksman, who shared the 1952 Nobel Prize in physiology or medicine for discovering streptomycin, the first effective treatment for tuberculosis. And it was streptomycin, one of thousands of antibiotics produced by soil bacteria known as actinomycetes, that caught the attention of the Welsh-born Davies, who was trained in organic chemistry but had always been interested in biologically produced natural compounds. (In grammar school, he memorized the structure of penicillin.) While at Harvard Medical School in the early 1960s, Davies figured out that streptomycin inhibits the growth of bacteria such as *Mycobacterium tuberculosis* by latching onto a part of the ribosome, so the cell can no longer make protein.

Davies spent the next decades studying antibiotics and antibiotic resistance. By the 1980s, after investigating a class of antimicrobial peptides composed of unusual amino acids that have also been detected on meteorites, he started wondering what antibiotics did in soils and other microbial communities. In 1990, Davies wrote a provocative though little-noticed review proposing that the compounds are evolutionarily old—"fossil molecules" that predate proteins—and could have originated in the primordial soup as "effectors" that interacted with early nucleic acids in a variety of reactions. He theorized that as the protein-making RNA-based machinery of early cells was honed and evolved into the ribosome, these effector molecules were kept around because their bioactivity proved useful in the microbial communities taking shape.

In the past decade, as researchers started sequencing actinomycete genomes, Davies found more evidence that antibiotics play peaceful roles in nature: An individual actinomycete genome can code for many more apparent antibiotic compounds than scien-

CREDITS: (TOP) JULIAN DAVIES; (BOTTOM) VIVIAN MIAO

Published by AAAS

tists had realized, sometimes upward of 25. It didn't make evolutionary sense to Davies that an organism would maintain such an arsenal. It made even less sense when he looked beyond the actinomycetes to the vast genetic diversity of the microbial world. "There are millions and millions of small molecules out there [made by microbes]," says Davies. "I couldn't believe they were all weapons." (Antibiotics are considered "small" molecules because of their size relative to enzymes and many other cellular proteins.) Davies also noted that the microbes producing these molecules live mainly in the soil, whereas most of the pathogens the antibiotics can inhibit thrive on animals. "They would never see each other" in nature, says Davies.

There are exceptions, of course. One place where microbes do clearly produce antibiotics that ward off threats from other microbes is the rhizosphere, the nutrient-rich area around plant roots. Linda Thomashow leads a group in the U.S. Department of Agriculture's Agricultural Research Service lab at Washington State University, Pullman, that has demonstrated that wheat plants provide a nurturing habitat on their roots for *Pseudomonas* bacteria, which in turn produce antibiotics that suppress fungi harmful to the plants. In a similar three-way interaction, Cameron Currie's group at the University of Wisconsin, Madison, has shown that bacterial symbionts living in insects produce antibiotics that suppress fungi that would otherwise harm the insects (*Science*, 3 October 2008, p. 63).

But most attempts to detect microbes in their natural environments making antibiotics at the relatively high concentrations needed to inhibit or kill other microbial cells have come up short. So Davies took a cue from a phenomenon known as hormesis (*Science*, 17 October 2003, p. 376). Many agents, from sunlight to caffeine, can have stimulating effects on cells at low concentrations and lethal effects at high ones. Davies wondered if the same held true for antibiotics in nature.

In a seminal 2002 study, Davies's group collaborated with Michael Surette at the University of Calgary in Canada to examine what low concentrations of microbially produced antibiotics such as erythromycin and rifampicin did to other microbes. They used a large library of *Salmonella typhimurium* colonies, each one engineered so that it would bioluminesce the way fireflies do if a specific *Salmonella* gene promoter was activated.

The antibiotics put on an unexpected light show, indicating they can repress or activate scores of promoters and thereby influence the activity of many microbial genes, the researchers discovered. "Any given antibiotic will affect as many as 200 promoters," says Davies, "and different compounds affect different promoters." The affected genes are involved in a variety of cellular activities, from transport of molecules to DNA repair, Davies and his colleagues have found.

To Davies, those findings suggested that there is a whole lot of chemical communication going on in the soil, with microbes secreting many compounds at low concentrations that turn on or off the genes of other microbes and orchestrate the growth of the community. "I thought that was exactly right on," says Melvin Simon, a microbiologist at the University of California, San Diego, who cites the 2002 study as an example of "a really good idea … where you say 'Of course.' "

"These compounds are signals," Simon adds, "and a sort of language that microorganisms have that allows them to interact with each other."

The complex molecular interchanges might explain why so few microbes—less than 1% of the known diversity—can be grown in pure cultures in a laboratory. The microbes likely depend on compounds produced by other members of the community, whether for nutrition, signaling with other cells, or other activities.

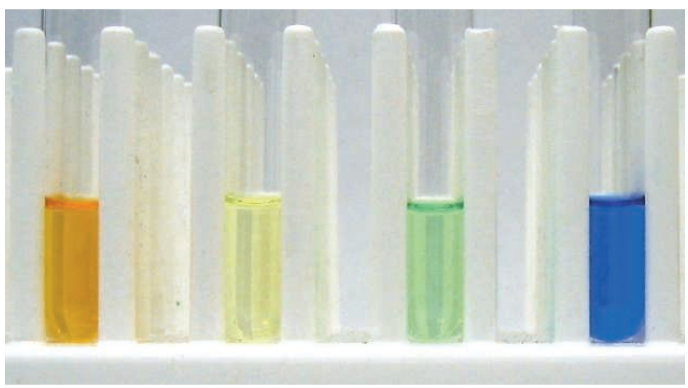

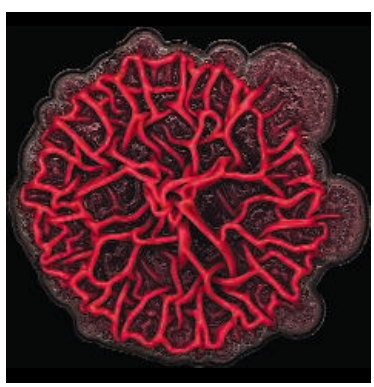

Color-coordinated. *Pseudomonas* bacteria make an array of colorful phenazines (*above*) that are toxic to other cells but play key roles in their producers' metabolism, including handling electrons when oxygen becomes unavailable. With a mutation that disrupts their ability to make phenazines, *Pseudomonas* cells that normally grow into a smooth dome form a wrinkled colony (*right*), an arrangement that seems to allow the cells better access to oxygen.

An antibiotic's true colors

Davies wasn't the only one at the time finding unexpected roles for antibiotics. Dianne Newman was a new professor in geosciences at the California Institute of Technology in Pasadena whose research into how microbes shape the planet's geochemistry had, almost by accident, turned to include antibiotics.

Newman started her career with an interest in how bacteria use minerals in their metabolism. Instead of consuming oxygen in respiration as plants and animals do, some bacteria turn to iron or other mineral compounds to handle the electrons that get moved about in the course of burning fuel, a process known as reduction-oxidation, or redox. Newman's group figured out how *Shewanella* bacteria use quinone compounds in soil humus as a shuttle to ferry electrons out of the cellular interior and ultimately to iron in the soil. The researchers noticed something striking: The structure of the quinone-containing shuttle looked a lot like those of phenazines, antibiotics naturally made by *Pseudomonas* bacteria. These antibiotics also have the thermodynamic capacity to handle electrons in redox reactions, and in doing so they change colors as they accept or release electrons.

The structural similarity of the quinone redox shuttle and the phenazines was "a light-bulb moment," recalls Newman, who is now at the Massachusetts Institute of Technology in Cambridge. Suspecting that the antibiotics could function as electron shuttles, not just as weapons, Newman and her co-workers turned their full attention to the phenazines and the *Pseudomonas* bacteria.

The well-studied *P. aeruginosa* can cause infections in people, particularly those with cystic fibrosis, whose lungs are filled with mucus that allows the bacterium to thrive. Infected patients often have blue sputum, an indicator of one particular phenazine that can be toxic to other bacteria as well as to lung cells.

Researchers in the 1930s had suggested

CREDITS (TOP TO BOTTOM): ALEXA PRICE-WHELAN; LARS DIETRICH

that the pigments play a role in bacterial metabolism, but that idea faded once their toxicity was discovered. Newman's group has revived this interpretation, and in a series of papers, including one last year in *Science* (29 August 2008, p. 1203), they describe the complex ways *P. aeruginosa* uses phenazine. The microbe begins to produce phenazine at a late stage of growth, which is typical for all antibiotic-producing microbes and the reason such molecules have been labeled "secondary metabolites." At this point, cells have piled up to form a biofilm, resulting in pockets of more or less oxygen. With oxygen running out, phenazine can step in to handle the electrons, changing color in the process.

Using *P. aeruginosa* mutants unable to make phenazine, the researchers connected this metabolic turning point to a change in the appearance of the biofilm's cell colonies, which typically remain smooth even as they reach their maximum size. But when the bacteria can't produce phenazine, the colonies become wrinkly and spread out to cover a larger area, allowing all cells to access oxygen. "It's like living in Los Angeles or New York," says Newman. "If you're crowded for breathing room, you either move out to the suburbs or build skyscrapers."

Newman's studies indicate that phenazine is a key architect in determining how *P. aeruginosa* communities get built. "Clearly, [phenazine plays] a role that's different from weaponry here," says biochemist Bruce Demple of the Harvard School of Public Health in Boston. Understanding that role, he adds, offers the potential for disrupting biofilm formation in *Pseudomonas* infections.

Newman's group has found that phenazines can increase or decrease the activity of a number of *Pseudomonas* genes, including signaling genes that appear to lead to the cells' excreting biofilm-related polymers. Phenazines can even improve a microbe's ability to access iron by transferring electrons to the metal. "Phenazines are functioning at many levels," says Newman. Rather than being "secondary," she says, these antibiotics are central to the metabolism of their producers.

In addition to community building with its own phenazines, *P. aeruginosa* can also "listen" to antibiotics produced by other microbes. In 2005, Samuel Miller of the University of Washington, Seattle, and his co-workers reported that aminoglycosides, a class of antibiotics including streptomycin that are often used to treat *P. aeruginosa* infections, can at lower concentration actually induce the microbe to form biofilms, another apparent example of hormesis. And Martínez and his co-workers reported in 2006 that low concentrations of other antibiotics such as tetracycline also turn on *P. aeruginosa* genes involved in biofilm formation.

Kolter's nystatin story, reported in the 6 January issue of the *Proceedings of the National Academy of Sciences*, is one of the latest connections between antibiotics and biofilms, but with an unexpected twist. Named after New York state—where in the 1940s public health department microbiologists Rachel Brown and Elizabeth Hazen isolated it from a culture of soil bacteria—nystatin is one of the oldest drugs available for fungal infections. Yet Kolter's team surprisingly found that nystatin has an effect on bacteria in addition to fungi.

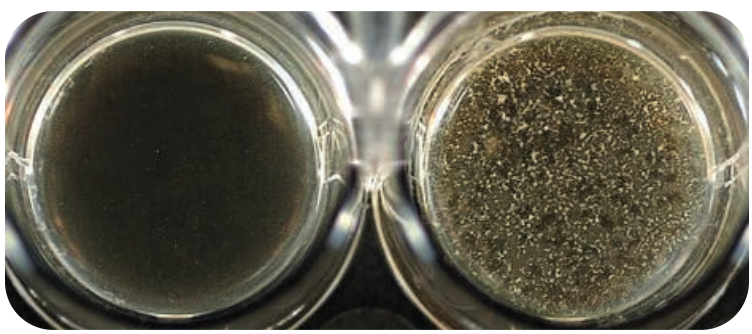

Triggers of mass construction. *Bacillus subtilis* growing in broth (*left*) clump together when the antibiotic nystatin is added (*right*).

CREDIT: COURTESY OF ROBERTO KOLTER

Nystatin jolts *Bacillus subtilis*, another soil dweller, into synthesizing the sugar and protein mix that allows the cells to stick together as a biofilm. The researchers further discovered that nystatin does this by creating pores in the bacterial cell that allow potassium ions to flow out. The rapid departure of the potassium ions turns on a key enzyme, which leads to creation of the extracellular material for the biofilm.

"It's almost like neurons," says Kolter, referring to how the flow of charged ions in and out of nerve cells allows them to signal each other. Kolter suspects that this antibiotic-induced potassium leakage will turn out to be a common mechanism for translating signals from other cells, so his team is looking for it in other microorganisms. "It makes sense," says Miller, and uncovering this novel mechanism "is an important contribution."

Volume control

If serving as signals is more commonly the natural role of antibiotics rather than killing or inhibiting growth, then the medical problem of antibiotic resistance may really be an issue of volume control. Although genes that confer resistance to antibiotics, including ones that encode molecular pumps or enzymes that dismantle the drugs, are most often found in microbes in hospitals or other clinical settings, they're also counterintuitively present in soil microbes that live in pristine environments little exposed to pharmaceuticals. In a commentary last year, Martínez suggested that such "resistance determinants," rather than serving as a defensive countermeasure, fine-tune the communication role of antibiotics in a natural community (*Science*, 18 July 2008, p. 365).

Davies shares this perspective, adding that these genes "might be one way of modulating the signal another organisms is producing, one way to mute the response of another." Given that premise, Davies advocates turning to soil to address the antibiotic-resistance problem. He believes that soil contains an abundance of yet-to-be-discovered signaling molecules made by microbes and that screening for ones with bioactivity at lower concentrations—drug companies looking for antibiotics typically screen for activity that depends on high concentrations of compounds—will yield leads that ultimately turn into new infection-fighting drugs. Kolter agrees: "Scan widely for signaling and you might find other antibiotics."

Davies's group is currently doing just that, using its library of bioluminescent bacteria to screen soil itself. They are finding that various colonies do react—lighting up, says Davies, "like stars against the sky"—indicating that compounds or organisms in the soil are activating a range of specific gene promoters in *S. typhimurium*.

Thanks to the work of Davies and others, no one now suggests that antibiotics made by microbes perform a single function in nature. It's increasingly clear that the molecules are more often a part of microbial crosstalk rather than crossfire. It's just a lucky, lifesaving accident for us that the right dose of a microbial signal can make it a poison, too.

–CHRISTINE MLOT

Christine Mlot is a science writer based in Madison, Wisconsin.

SPACE WEATHER FORECASTING

Are We Ready for the Next Solar Maximum? No Way, Say Scientists

Forecasters testing their skills against the sun's mounting ferocity find themselves still in the early days of space weather prediction

The Big One for space physicists struck on 28 August 1859. The sun had blasted a billion-ton magnetic bubble of protons and the like right at Earth. On smashing into the planet's own magnetic cocoon at several million kilometers per hour, the bubble dumped its energy, pushing the solar-driven aurora from its customary arctic latitudes to overhead of Cuba. This once-in-500-years "solar superstorm" crippled telegraph systems for a day or two across the United States and Europe but otherwise was mainly remembered for its dramatic light show.

Now that our world has evolved into a so-called cyberelectrosphere of modern electronics, we can hardly hope to fare as well. Today, the charged-particle radiation and electromagnetic fury of a geomagnetic superstorm would fry satellites, degrade GPS navigation, disrupt radio communications, and trigger continent-wide blackouts lasting weeks or longer. Even a storm of the century would wreak havoc. That's why space physicists are so anxious to forecast space weather storms accurately. If predicting a hurricane a few days ahead can help people prepare for a terrestrial storm's onslaught, they reason, predicting solar storms should help operators of susceptible systems prepare for an electromagnetic storm.

And space weather forecasters' next challenge is coming up soon. The next peak in the 11-year sunspot cycle of solar activity looms in 2012 or 2013. A space weather symposium* last month asked, "Are we ready for Solar Max?" The unanimous answer from participants was "No." "I think we are better off" than a decade ago, says space physicist Daniel Baker of the University of Colorado, Boulder. Back then, researchers were about to launch their first concerted effort to predict space weather the way meteorologists predict terrestrial weather, using computer models. "But we probably aren't as ready as we ought to be," Baker adds.

In fact, space forecasters are about where their meteorological colleagues were in the 1960s: making useful but unimpressive forecasts in the short term and lacking computer models able to improve on longer-term predictions by human forecasters. And even the short-term forecasts could go by the boards if the sole but aging early-warning satellite fails before a replacement—as yet unfunded and unplanned—arrives in orbit.

High-tech target

While researchers have been working to improve their forecasting skills, the world has, if anything, become more susceptible to space weather. "The general trend would be increasing vulnerability to the effects of space storms," says Baker, who chaired a December 2008 workshop report on the subject by the Space Studies Board of the U.S. National Academies. "In general, the systems are becoming softer." The power grid operates more efficiently, he says, but that gives it less margin for error and less capacity to buffer a storm's disruptions. The surging power-line currents induced by a severe solar storm could push the grid into uncharted territory. GPS technology, especially the highest-precision variety, has become commonplace since the last solar maximum—for navigating planes more autonomously, for example—but it comes with new codes and new signals untested by the ionospheric disturbances of a major solar storm. Now-ubiquitous cell phones are no less vulnerable.

The academies' report put a huge price tag on a repeat of the 1859 superstorm. Judging by the costs of smaller incidents in recent decades, the panel estimated the economic cost in just the first year after such an extreme storm at $1 trillion to $2 trillion. Full recovery would take 4 to 10 years. Disturbances in the high-altitude ionosphere would disrupt radio communications and GPS for days; surges induced in the power grid could destroy expensive and hard-to-replace trans-

*The 2009 Space Weather Enterprise Forum, 19–20 May, Washington, D.C.

CREDITS: SOHO (ESA & NASA)

Published by AAAS

Solar assailant. The sun violently ejects magnetically confined bubbles of charged particles (*left*) that collide with Earth's magnetic field (*right*), triggering geomagnetic storms.

formers. Satellites that survived could cost $100 million apiece to put back into operation. Even a recurrence of the lesser superstorm of May 1921 could lead to blackouts affecting 130 million Americans and half of North America, the panel reported.

Status quo

If you pity the poor weatherman, then your sympathies for the space weather forecaster should be unbounded. In May 1996, Ernest Hildner—then director of the National Oceanic and Atmospheric Administration's Space Environment Center in Boulder, Colorado—told an audience that when it comes to predicting space weather, "we don't do very well. We're several decades behind weather forecasters."

A big part of the problem, Hildner said, was a dearth of observations. Space weather forecasters used ground-based telescopes to observe sunspots, solar flares, and other signs that the sun was primed to launch solar-storm-inducing disturbances toward Earth. But forecasters had no spacecraft between the sun and Earth to record the passage of threatening solar disturbances, much less whether they were actually going to hit Earth. It was "like predicting Washington, D.C., weather with one weather station in San Francisco," Hildner said.

Enter ACE. In 1997, the Advanced Composition Explorer arrived at its station, L1 or Lagrangian point 1, about 1.5 million kilometers sunward of Earth. There it could monitor the high-speed bubbles of protons and other charged particles—called coronal mass ejections (CMEs)—that would slam into the bulbous end of Earth's teardrop-shaped magnetosphere 30 to 60 minutes after passing ACE. The speed and density of a CME reflects its total energy. But ACE also reports the orientation of the magnetic field embedded in a CME, which must be opposite that of Earth's magnetic field if the CME's power is to gain entry to the magnetosphere and drive a storm.

ACE made the first short-term storm warnings possible in 1999. Issued only 20 to 60 minutes ahead of a storm's arrival by the Space Weather Prediction Center (SWPC, the former Space Environment Center), the warnings have fallen far short of perfection. One-third of major storms arrive unheralded and almost one-quarter of the warnings turn out to be false alarms, according to SWPC's own analysis. More severe storms are so rare that it's hard to say how much skill forecasters have in predicting them, says Christopher Balch, acting head of SWPC's forecast office.

ACE can offer no help with forecasting storms a day ahead. Next-day SWPC forecasts of geomagnetic activity based on observations of the sun have performed better than simply assuming that the current day's conditions would persist into the next day. But next-day forecasts performed no better than if forecasters assumed the next day would be like the average of the previous 30 days. Accurate forecasting 8 hours to 1 day ahead, Baker concludes, "is just not in the cards right now."

Playing catch-up

To push useful space weather forecasting beyond a few minutes ahead, geophysicists are emulating terrestrial weather forecasters. From the 1950s onward, meteorologists built and refined computer models that ingested a torrent of observations and produced a picture of current weather around the globe. The models could then calculate how the weather would evolve. Over several decades, the models surpassed human forecasters at short-range prediction and pushed useful forecasts out beyond 7 days.

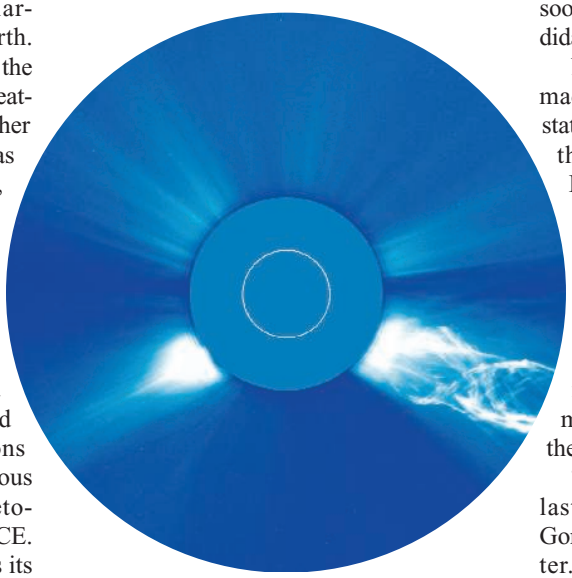

Coming out blazing. The sun (masked here to reveal faint features) will be blasting more coronal mass ejections (*lower right*) Earth's way as the sun enters its next cycle of rising activity.

Space weather forecasters face extra hurdles. There's still a severe dearth of observations to feed into the models. And rather than evolving within one relatively uniform atmosphere, space weather progresses from the near-vacuum of a million-degree solar corona—where magnetic fields rule—to Earth's relatively dense, cold upper atmosphere and eventually the ground: "sun to mud," as they say. That forces researchers to develop a dozen submodels to make a chain linking the sun to Earth. Space scientists hoping to transfer their research models to the forecasting arena should "expect to have your egos hurt," magnetospheric physicist W. Jeffrey Hughes of Boston University (BU) said at the May meeting of the American Geophysical Union. "It's a painful process."

To ease the pain of moving from research modeling to day-to-day forecasting, the American space weather community has developed a loose structure for creating and testing forecast models. Two 8-year-old centers—one at the University of Michigan (UM), Ann Arbor, and the other an 11-institution consortium headed by BU—vie in friendly competition to develop physics-based, sun-to-Earth models. A 10-year-old interagency modeling center at NASA's Goddard Space Flight Center (GSFC) in Greenbelt, Maryland, is evaluating 30 contributed submodels. Finally, a test bed will soon be created at SWPC for debugging candidate submodels before they go operational.

No model—not even a submodel—has made it through this system to operational status. A submodel called ENLIL is leading the pack, says SWPC Director Thomas Bogdan. ENLIL forecasts how newly formed CMEs will propagate from the sun to ACE. But it won't become operational for 2 to 3 years, around the time of solar max, when it will be run on the same supercomputer National Weather Service forecasters use. Models carrying the disturbance into and through the magnetosphere and the atmosphere and to the ground all trail ENLIL.

"We've made very good progress in the last decade," says space physicist Tamas Gombosi, director of the UM modeling center. "But can we forecast? No. We have a long way to go. My hope is that not this solar max but the next, physics-based forecasting" will be a reality.

In the meantime, scientists are keeping their fingers crossed for ACE. At 12 years old, it has entered satellite old age. It and the 14-year-old SOHO satellite that images CMEs near the sun "can fail any time, no one knows," notes Michael Hesse, director of the modeling center at GSFC. Although enough time remains to build and launch a backup for ACE's monitoring system, none has been proposed, much less funded.

–RICHARD A. KERR

CREDIT: SOHO (ESA & NASA)

Published by AAAS

From cooperative childcare
1646

Regulating stem cell research
1648

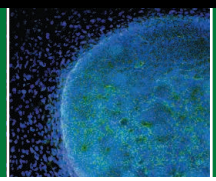

LETTERS

edited by Jennifer Sills

The Global Alliance for Chronic Diseases

APPROXIMATELY 35 MILLION PEOPLE WILL DIE THIS YEAR FROM CHRONIC, NONCOMMUNICABLE diseases (CNCDs) worldwide (*1*, *2*). CNCDs include cardiovascular disease and stroke, cancer, diabetes, and chronic respiratory diseases. CNCDs account for 60% of all deaths worldwide, of which 80% occur in low- and middle-income countries (LMICs) (*3*). Yet, until now there has been no coordinated effort by major global health research councils to address these specific needs.

To this end, we announce a new global health initiative, the Global Alliance for Chronic Diseases (GACD). The first alliance of its kind among government health research councils, the GACD was launched on 15 June 2009 in Seattle, Washington, coincident with the meeting of Heads of International Biomedical Research Organizations. The GACD has a global reach, bringing together an initial formative group of six major national health research councils. These agencies together represent about 80% of all public research funding in the world. Member agencies are Australia's National Health and Medical Research Council; the Canadian Institutes of Health Research; the Chinese Academy of Medical Sciences; the U.K. Medical Research Council; and the U.S. National Institutes of Health, specifically its National Heart, Lung, and Blood Institute and Fogarty International Center. In addition, the Indian Council of Medical Research has been invited to be a Member agency of the Alliance.

Allies. Global Alliance for Chronic Diseases signatories make the Alliance official [back row, left to right: Depei Liu (China), Warwick Anderson (Australia), Abdallah Daar (University of Toronto), Stig Pramming (Oxford Health Alliance), and Leszek Borysiewicz (United Kingdom); front row, left to right: Elizabeth Nabel (United States) and Alain Beaudet (Canada)].

The GACD intends to coordinate research activities that address the prevention and treatment of chronic diseases on a global scale (*2*). It will collectively seek to identify common approaches to develop the evidence base needed to guide policy, develop and share best practices for fighting chronic diseases, and foster a sustainable and significant reduction of illness, disability, and death around the world. A significant focus is on the CNCDs in LMICs and among low-income and indigenous populations of the more developed countries to support collaborative, coordinated research on low-cost interventions and to build capacity in research, training, and healthcare delivery.

This initial group will expand to involve other research funders, including philanthropic foundations, from around the world with an interest in the Alliance's agenda. Industry has an important role in solving some of these problems, ensuring the public-private aspect of this venture. The World Health Organization (WHO) has joined in an Observer status and, in addition to the Grand Challenges priorities (*2*), GACD will consider the WHO 2008–2013 Action Plan for the Prevention and Control of Noncommunicable Diseases in setting priorities (*4*).

The following priorities have been proposed by some GACD founding members, but exact research priorities await further discussion and will develop as the Alliance evolves: prevention of cardiovascular diseases; public health measures for the control of diabetes and obesity; characterization, quantification of risk factors (tobacco and environmental pollution), and development of control measures for chronic obstructive airways disease, cancer, cardiovascular disease and other disorders; and implementation research of interventions to address these and other priorities. A future Alliance research priority is likely to be in the area of mental health.

The creation of the GACD brings to fruition a global commitment to urgently increase the resources and attention to CNCDs. With concerted action, many millions of premature deaths can be averted in the decades ahead.

ABDALLAH S. DAAR,[1,2]* ELIZABETH G. NABEL,[1,3] STIG K. PRAMMING,[1] WARWICK ANDERSON,[4] ALAIN BEAUDET,[5] DEPEI LIU,[6] V. M. KATOCH,[7] LESZEK K. BORYSIEWICZ,[8] ROGER I. GLASS,[9] JOHN BELL[1]

[1]Preparatory Committee, Oxford Health Alliance, London, UK. [2]McLaughlin-Rotman Centre for Global Health, UHN/University of Toronto, Toronto, ON, Canada. [3]National Heart, Lung, and Blood Institute, Bethesda, MD, USA. [4]National Health and Medical Research Council, Canberra, ACT, Australia. [5]Canadian Institutes of Health Research, Ottawa, ON, Canada. [6]Chinese Academy of Medical Sciences, Beijing, China. [7]Indian Council of Medical Research, New Delhi, India. [8]Medical Research Council, London, UK. [9]Fogarty International Center, Bethesda, MD, USA.

*To whom correspondence should be addressed. E-mail: a.daar@utoronto.ca

References

1. "The maladies of affluence," *The Economist* (11 August 2007).
2. A. S. Daar *et al.*, *Nature* **450**, 494 (2007).
3. A. D. Lopez *et al. Global Burden of Disease and Risk Factors* (Oxford Univ. Press and World Bank, Washington, DC, 2006).
4. World Health Organization, 2008–2013 Action Plan for the Global Strategy for the Prevention and Control of Noncommunicable Diseases (www.who.int/nmh/Actionplan-PC-NCD-2008.pdf).

CREDIT: KEVIN P. CASEY FOR THE GLOBAL ALLIANCE FOR CHRONIC DISEASES

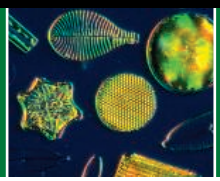

Diatom evolution
1651

Auxin in evolution
1652

Current Brazilian Law on Animal Experimentation

LAST YEAR, *SCIENCE* PUBLISHED A STORY ON THE Brazilian scientific community's battle against a series of local attempts to ban laboratory animal experimentation and the hope for a federal law addressing laboratory animal research that would put a stop to such local bans (*1*). The Brazilian Federal Law on Animal Experimentation (Law 11794) was enacted on 8 October 2008.

Law 11794 establishes procedures for the scientific use of animals and abrogates the previous Law 6638/1979, which was ineffective because it was not regulated by the Brazilian Executive Power. Without regulation, many issues remained ill-defined, including operational procedures and responsibilities such as licensing, accreditation, and institutional compliance inspection. The new law states that scientific research activities include basic and applied science, technological development, production and quality control of drugs and medications, food, immunobiological agents, and instruments tested on animals. The law does not extend to the procedures applied to animal experimentation in the course of veterinary, agricultural, or laboratory animal husbandry practices and procedures for the identification of animals for scientific purposes, should they cause no lasting harm.

Only universities and biomedical technical schools are entitled to use laboratory animals in teaching. The term "biomedical" is not defined within the text of the Law, which may generate difficulties given that it does not have a specific meaning in the context of education. Law 11794 does not indicate whether animal experimentation is allowed by students under 18 years old, unlike Law 6638/1979.

Law 11794 establishes The National Animal Experimentation Control Board (CONCEA), under the presidency of the Ministry of Science and Technology (MCT). Law 11794 does not clearly specify in which ministry CONCEA, as a public administrative unit, belongs. That is, there is no legal disposition tying CONCEA to the MCT. This means that CONCEA will have difficulties implementing its norms, procedures, and resolutions due to lack of ministerial power.

Only institutions accredited by CONCEA can breed or use laboratory animals for teaching and research. CONCEA is primarily an advisory body, and its powers are limited. CONCEA accreditation requires the previous establishment of an ethics committee on the use of animals (CEUA) by the license-seeking institution. CEUA is the body formally responsible for the care and use of research and teaching animals within the institution. All proposals involving laboratory animals have to be submitted and reviewed by CEUA, which has the authority to halt any teaching or research practice that

Published by AAAS

does not comply with the legislation. CEUA must ensure that the facility standards and the care of animals are in accordance with CONCEA resolutions. The Committee is composed of veterinarians and biologists, professors and researchers of a specific area, and one representative of a legally established Animal Protection Society within the country. The number of members is left open with exception of the mandatory Animal Protection Society member. Considering the heterogeneous geographical distributions of researchers within the Brazilian Territory, a large variability in the number and profile of CEUA members among institutions is expected, which is problematic.

It is CEUA's duty to keep an institutional database of researchers and procedures that use laboratory animals in research and teaching and to report the data to CONCEA. Law 11794 does not mention whether the information retrieved by CONCEA will be made available to the public. The value of public access to information has been stressed by the Federal Constitution (Article 5, XXXIII). Accountability and transparency in animal experimentation are practices yet to be learned by Brazilian research institutions and governmental bodies. The changing process will demand from CONCEA and CEUA communication skills far above those previously required.

Law 11794 places less emphasis on alternatives to animal experimentation than was previously treated legislatively and is expected by the Animal Protection Societies. A requirement that animal experimentation projects must demonstrate the relevance of their results for the progress of science and show that alternative, equally effective methods do not exist was also deleted from one of the substitutive bills proposed.

For Brazilian scientists, Law 11794 undoubtedly represents improvement. It can also support the democratic process of closing the gap between science and society. Nevertheless, its limits and potentialities will depend on the regulatory process in progress. The challenging issues that were left open by Law 11794 may lead to subjective interpretation of its content. In addition, the adoption of research practices that take into account animal welfare will depend on a government long-term action plan regarding the many and complex aspects related to human resources, training and education on animal care, management and housing, animal research facilities, replacement techniques on animal experimentation, and communication and information systems.

CARLOS JOSÉ SALDANHA MACHADO, ANA TEREZA PINTO FILIPECKI,* MÁRCIA TEIXEIRA

Fundação Oswaldo Cruz, Rio de Janeiro, Rio de Janeiro 21040-361, Brazil.

*To whom correspondence should be addressed. E-mail: afilipecki@fiocruz.br

Reference

1. M. Enserink, *Science* **319**, 1319 (2008).

Letters to the Editor

Letters (~300 words) discuss material published in *Science* in the previous 3 months or issues of general interest. They can be submitted through the Web (www.submit2science.org) or by regular mail (1200 New York Ave., NW, Washington, DC 20005, USA). Letters are not acknowledged upon receipt, nor are authors generally consulted before publication. Whether published in full or in part, letters are subject to editing for clarity and space.

Creationist Beliefs in Europe

A RECENT NEWS OF THE WEEK STORY ("CREationist beliefs persist in Europe," A. Curry, 27 February, p. 1159) referred to a lack of regionwide studies on creationist beliefs in Europe, while ignoring most of the European research project BIOHEAD-Citizen (Biology, Health, and Environmental Education for Better Citizenship CIT2-CT-2004-506015, 2004–2008). This project involved data collection from 7050 teachers in 19 countries, 13 of which were in Europe (*1*).

In each country, the sample was a balanced set of primary and secondary school teachers who taught biology or the national language. This study differentiated between anti-evolutionist creationist teachers, teachers who are creationist and evolutionist, and teachers who are evolutionists. There was a large contrast across countries: from 2% anti-evolutionist creationists in Estonia or France to more than 80% in Morocco or Algeria. In Europe, results revealed 47% anti-evolutionist creationists in Romania, 30% in Poland, and more than 25% in Cyprus and Malta. Creationist beliefs were more likely in those with greater belief in God or greater religious observance, regardless of religion. Biology teachers were more evolutionist than their colleagues in only half of the countries surveyed. The longer a teacher trained at a university, the greater the acceptance of evolutionist ideas.

PIERRE CLÉMENT[1]* AND MARIE-PIERRE QUESSADA[2]

[1]LEPS-LIRDHIST, Université Lyon 1, Villeurbanne 69622, France. [2]LIRDEF, IUFM Nîmes, Université Montpellier 2, Nîmes 30000, France.

*To whom correspondence should be addressed. E-mail: Pierre.Clement@univ-lyon1.fr

Reference

1. P. Clément, M. P. Quessada, *Nat. Sci. Soc.* **16**, 154 (2008).

Sex in *Leishmania*

IN THEIR REPORT "DEMONSTRATION OF GENETIC exchange during cyclical development of *Leishmania* in the sand fly vector" (10 April, p. 265), N. S. Akopyants *et al*. provided evidence for sexual recombination. The next priority should be to apply high-resolution imaging with molecular markers to determine when, where (i.e., in which part of sand fly gut), and how the "mating" events occur.

Genetic exchange is crucial for adaptation to stressful environments. However, in *Leishmania*, exposure to specific stressful conditions in the sand fly gut is likely to induce genetic exchange. Access to the sand fly genome is now urgently required to facilitate the search for factors that stimulate *Leishmania* sex.

The epidemiological consequences of genetic exchange in *Leishmania* are potentially alarming. Akopyants *et al.* demonstrate two distinct virulence traits among hybrid *Leishmania* clones but do not document the effect of genetic exchange on development of *Leishmania* in the vector. There is, however, proof that sex enhances *Leishmania* fitness and transmission in the sand fly. *Leishmania infantum* and *L. major* are divergent species, transmitted by different vectors to different mammalian reservoirs. Nevertheless, *L. infantum*/*L. major* hybrids (*1*) complete the life cycle in *Phlebotomus papatasi*, the specific vector of *L. major* that does not support *L. infantum*. Hybrids thrive in the aggressive, widespread human-biting *P. papatasi*, as well as in a principal vector of *L. infantum*, *Lutzomyia longipalpis* (*2*). Other naturally occurring interspecific *Leishmania* hybrids may spread to new vectors, with geographical expansion and carriage of traits such as visceralization and metastasis in humans.

PETR VOLF* AND JOVANA SADLOVA

Department of Parasitology, Charles University in Prague, Prague 128 44, Czech Republic.

*To whom correspondence should be addressed. E-mail: volf@cesnet.cz

References

1. C. Ravel *et al.*, *Int. J. Parasitol.* **36**, 1383 (2006).
2. P. Volf *et al.*, *Int. J. Parasitol.* **37**, 589 (2007).

HUMAN EVOLUTION

Caring Cooperators

Gillian R. Brown

Early hominin families are traditionally portrayed as a mother sitting by a campfire, tending to her offspring, while the father is away hunting for meat (*1*). This version of human evolutionary history has dominated anthropology and shaped our views of human sex roles for the past century. In *Mothers and Others*, Sarah Hrdy challenges a key assumption of this model—that childcare was centered wholly on the mother—and, in doing so, provides us with a strikingly different perspective on human evolution. Using evidence from diverse research fields (including ethnography, archaeology, developmental psychology, primatology, endocrinology, and genetics), Hrdy (an anthropologist at the University of California, Davis) builds an engaging and compelling argument for an evolutionary history of cooperative offspring care that requires us to rethink entrenched views about how we came to be human.

Mothers and Others
The Evolutionary Origins of Mutual Understanding
by Sarah Blaffer Hrdy
Harvard University Press, Cambridge, MA, 2009. 430 pp. $29.95, £19.95, €21. ISBN 9780674032996.

Perhaps the most convincing line of evidence that human beings have evolved as a cooperatively breeding species (that is, a species in which individuals other than the mother assist in the care and provisioning of young) comes from comparing the reproductive lives of women with those of other extant primates. In hunter-gatherer populations, Hrdy reports, women have an interval of three to four years between births, which is much shorter than the interbirth interval of six to eight years in other great apes. Hrdy argues that, in human beings, "[s]uch hyperfertility would have been feasible only if mothers in ancestral populations had been able to count on alloparental assistance." In great apes, mothers are extremely unwilling to allow conspecifics to carry, or even touch, their infants during their first few months. In contrast, human mothers are very tolerant and trusting in allowing other individuals, alloparents, to have access to their offspring. For example, in the Hadza of Tanzania, Hrdy notes, children during their first four years spend around 33% of their contact hours with individuals other than their mothers. Ethnographic data indicate that helpers have positive effects on offspring survival in many parts of the world (*2*). Although in some human populations, such as the Aka of the Central African Republic, fathers play a very important role in childcare, Hrdy argues that paternal investment could not be relied on by mothers. She stresses that "[f]lexibility was, and continues to be, the hallmark of the human family."

The consequences of viewing humans as having an evolutionary history of cooperative breeding are potentially profound. For instance, Hrdy argues that if early hominin mothers relied on the assistance of alloparents, infants that were better at gauging the intentions of others, and engaging with them, would also be better at eliciting care and more likely to survive. She goes on to claim that these selection pressures acting on infants led humans to become so adept at theorizing about the mental states and intentions of others. She suggests that infants' interest in human faces, their ability to follow eye gaze, and their attractive features are all traits that have been advantageous in an environment of shared care. Hrdy contrasts her version of the evolution of shared intentionality and prosociality with other theories that emphasize conflict and competition both within and between groups. Her ideas will certainly provoke strong debate among researchers interested in the evolution of theory of mind and altruism in human beings, by challenging them to rethink the selective environments in which such traits might have evolved.

Hrdy convincingly argues that during hominin evolution, cooperative breeding predated the expansion of the brain. Indeed, the extended period of dependency that accompanies cooperative breeding in other animals could have lessened selection pressures acting against brain expansion in the human ancestral line. While discussing the implications of a history of cooperative breeding for our understanding of brain evolution, Hrdy inquires "whether there is some interaction between a deep history of cooperative breeding and offspring that grow up to be especially good at learning from others." Although Hrdy doesn't expand on the idea that a history of cooperative breeding allowed for selection of key human traits such as social learning, teaching, and language, other researchers have begun to pursue these ideas (*3*, *4*). Many questions still surround the relationship between cooperative breeding and the evolution of the human brain, including the issue of whether cooperative care enhanced cultural learning processes; these questions will occupy researchers for some time to come. Hrdy's careful use of archaeological evidence and broad comparative perspective provides an outstanding example of how to go about producing testable evolutionary hypotheses without recourse to an unspecified environment of evolutionary adaptedness. As Hrdy argues, pinpointing the sequence of evolutionary events in our hominin ancestry will be crucial to understanding the co-evolution of human traits.

Social care. Hadza women and children around a cooking fire, Tanzania.

CREDIT: BETH WALD/AURORA/GETTY IMAGES

The reviewer is at the School of Psychology, University of St. Andrews, South Street, St. Andrews, Fife KY16 9JP, UK. E-mail: grb4@st-andrews.ac.uk

Published by AAAS

Mothers and Others provides a fascinating, readable account of how our hominin ancestors might have negotiated the obstacles to raising offspring. Hrdy presents a well-argued case for human evolutionary history being characterized by cooperative offspring care, which opens fresh avenues of research into the history of our species. In addition, she prompts readers to consider far-reaching questions, such as whether the nuclear family is the "best" unit in which to raise children and how learned parenting practices might determine the future of human evolution. Her thought-provoking book will interest students, specialists, and general readers alike and should focus attention on the neglected roles of mothers and others within human evolutionary theory.

References

1. C. O. Lovejoy, *Science* **211**, 341 (1981).
2. R. Sear, R. Mace, *Evol. Hum. Behav.* **29**, 1 (2008).
3. W. J. E. Hoppitt *et al.*, *Trends Ecol. Evol.* **23**, 486 (2008).
4. W. T. Fitch, in *Emergence of Communication and Language*, C. Lyon, C. L. Nehaniv, A. Cangelosi, Eds. (Springer, London, 2007), pp. 29–51.

10.1126/science.1175159

SOCIOLOGY

Buying So Children Belong

Sandra L. Hofferth

I just returned from a Mother's Day visit to my parents' home in Lancaster, Pennsylvania. On the outskirts of town, we passed a succession of black horse-drawn buggies belonging to Amish families returning from religious gatherings on a beautiful spring afternoon. Boys in pastel shirts and black pants and their sisters in brightly colored dresses peered out of the open rear window of one buggy. As I pondered the tremendous gap between this close-knit community with its 19th-century ways and 21st-century society, I could not help but think about the questions raised by Allison Pugh's modest but thoughtful tome, *Longing and Belonging*. Why does buying for children invite so much anxiety and concern? And, knowing what they do, why do parents capitulate?

Pugh (a sociologist at the University of Virginia) conducted in-depth interviews with 54 families in three schools in a large urban school district in northern California: a public school in a low-income area, a public school in a high-income area, and a private school. The book reviews children's conversations about consumer goods and parental responses to children's requests in low- and middle-income families.

Longing and Belonging
Parents, Children, and Consumer Culture

by Allison J. Pugh

University of California Press, Berkeley, 2009. 319 pp. $55, £37.95. ISBN 9780520258433. Paper, $21.95, £14.95. ISBN 9780520258440.

In the not-so-distant past, having common experiences such as growing up on a farm, entering the military, or attending church formed the foundation for a common culture or set of meanings. Today, the argument goes, consumption goods build culture. The desire to belong to a group is so strong (the "longing" of the title) that children continually attempt to show their worthiness through conversations and status displays. In the economy in which children participate, one must have something others want or envy and be able to share it. Pugh argues that consumer goods form the scrip children use to feel more similar to other children, which allows them to participate more equally with their peers in everyday child culture, to belong. Not having those goods creates outsider status. This she calls "the economy of dignity."

The author describes parents who know that children are consuming too many of the family's scarce resources but don't know what to do. Upper-middle-class families respond by greatly restricting their children's consumption in various ways—"symbolic deprivation," consisting of providing an allowance or otherwise limiting children's spending while being sensitive to when an item is too important to ignore. Low-income families, in contrast, struggle to provide minimal consumption items so that their child can achieve some degree of dignity in the school setting.

So how are the Amish able to do without the accoutrements of modern popular culture? The Amish have a strong community wrapped around their shared religious beliefs (*1*). Consumer goods are not important indicators of status. In a fine historical treatment of childhood (*2*), Steven Mintz argued that children have been increasingly segregated in a peer culture, becoming less involved in overall family and community life. Parents' lives no longer require children's participation. Through the media, the children's separate world has become integrated in consumer culture.

Immigrant families offer a contrast to this separation of childhood. Among immigrants, children are often integrated through chores or involvement in family businesses. Pugh describes an immigrant family who simply refused to go along with the consumption pressures. Their goal of buying a home took precedence over individual wants and needs. All children participated in the family economy, shopping together, for example. This family preserved its values and the goals to the detriment of the individual child. To them, the culture of dignity was not something to be left to children but one to be defined by adults. Any failure to participate was borne by the child, not the adult.

From my own research and personal experience, families who have successfully reared and launched children have done so in a strong community with strong beliefs and values. They participated as a family, whether the activity involved playing music, hiking and camping, or team sports. In this context, children learn about adult roles, about ethics and values, and contribute to the family economy (*3*).

The author sees an inherent contradiction between individual development and a longing to belong. Consumption provides belongingness. However, Pugh does not spend much time examining "pathway consumption," a common parental focus on developing skills that allow young people to both be independent and belong to a group, to a larger society. If children are involved in extracurricular, family, or community-oriented activities, they will not need to consume to belong. Parents find it much harder to share time as a family than to buy things and activities for their children. I speculate that they feel guilty for giving their children less time than they believe they should. Thus spending money, rather then time, has become an indicator of caring.

Pugh is correct about the problem, but the solution is not merely cutting back consumption. Rather, parents must establish shared family goals and involve children in family activities and decision-making. Families who have found a balance between children's needs and family needs are generally successful. We could learn from examining contemporary groups such as the Amish that manage to maintain low-consumption life-styles amid the plenty that characterizes America.

References

1. J. A. Hostetler, *Amish Society* (Johns Hopkins Univ. Press, Baltimore, ed. 4, 1993).
2. S. Mintz, *Huck's Raft: A Story of American Childhood* (Harvard Univ. Press, Cambridge, MA, 2004).
3. S. L. Hofferth, D. A. Kinney, J. S. Dunn, *The Hurried Child: Myths vs. Reality* (Iota, Bethesda, MD, 2009).

10.1126/science.1173386

The reviewer is at the Department of Family Science, University of Maryland, College Park, MD 20742, USA. E-mail: hofferth@umd.edu

RESEARCH ETHICS

The NIH Draft Guidelines on Human Stem Cell Research

New guidelines have positive aspects, but challenges remain in relation to previously approved stem cell lines, informed consent, oversight, and research embryos.

Mary A. Majumder and Cynthia B. Cohen[2]

With new draft guidelines to govern federal funding of human stem cell research, including human embryonic stem cell (hESC) research, the National Institutes of Health (NIH) have again taken on one of the most contentious endeavors of the day (*1*). There are positive aspects of the guidelines (*2*), but concern is growing that prior approvals of many widely used cell lines may not be in accord with specific wording requirements in the draft guidelines; such cell lines would need to be "grandfathered in" if research is to continue unimpeded (*3*). There are also several surprising omissions, surprising because they come in areas that are thoroughly addressed in the guidelines of the U.S. National Academies of Sciences (NAS) (*4*–*6*), which have become the gold standard for the conduct of stem cell research in the United States. Further, there has been little comment on the kind of initiative that would support future policy development.

Grandfathering Previously Approved Lines

As standards related to informed consent and hESC research evolve, many stem cell lines derived according to earlier requirements may not conform to new ones and may therefore be disqualified for use in federally funded research. The final NIH guidelines will need to address this problem, as the NAS guidelines do. They categorically "grandfather in" or permit continuation of research on cell lines previously approved by NIH; they also allow the use of other previously derived cell lines if investigators provide a local Embryonic Stem Cell Research Oversight (ESCRO) committee with documentation that establishes use of an informed consent process that this oversight body considers acceptable (*5*, *6*). Sugarman and Siegel (*7*, *8*) have outlined a systematic approach to determining the acceptability of nonconforming hESC lines, and Taylor has recently endorsed this general framework (*9*).

Informed Consent

The NIH draft guidelines, despite devoting attention to informed consent (see table, right), do not require consent from gamete donors, but only from the individual(s) who sought reproductive services [i.e., in vitro fertilization (IVF) treatment]. Here, they are at odds with the NAS guidelines and the current consensus in the field (*7*). We recommend that the final NIH guidelines emulate those in other jurisdictions by expressly requiring evidence of gamete donor consent to research use. However, gamete donors should not be given full control over subsequent use of embryos to which they contribute.

The informed consent provisions of the NIH draft guidelines also fail to say enough about potential research uses of hESCs derived from donated embryos. In contrast, the 2000 NIH guidelines (*10*) required a statement informing potential embryo donors that research uses might include human transplantation research. Moreover, the NAS guidelines call for explicit

Comparison of U.S. National Stem Cell Research Guidelines

	NIH 2009 (*1*)	NAS 2008 (*7*)	NIH 2000 (*10*)
Grandfathering Nonconforming hESC lines			
Criteria for use of preexisting hESC lines		●	
Criteria for use of non-U.S. hESC lines		●	
Informed Consent: Process/Statements			
All options for spare embryo disposition explained to donors	●	●	
No inducements offered	●	●	●
Attending physician and researcher not the same person	●*	●*	●
Limited to frozen embryos			●
Approach about consent to research use only at time of disposition			●
Consent obtained at time of donation	●	●	●
Consent to research use given by any donors of gametes		●	
Statements to embryo donors:			
Alternative options understood	●†		
Right to withdraw until actual use	●	●	
Quality of care unaffected	●	●	
No restriction of direction regarding beneficiaries	●†	●‡	●
No intent to provide direct medical benefit to donors	●†	●‡	●
Commercial potential but no related benefit to donors	●†	●	●
Description of outcome for donated embryos	●†	●	●
Description of possible research uses		●	●
Cell lines may be maintained for many years	●†	●	●
Commitment to adhere to best practices		●	
Whether identifiying information will be retained	●†	●	●
Risk to donors		●	
Required Oversight			
IRB		●§	●‖
ESCRO		●	
National body		●¶	●
Ineligible or Prohibited Research			
Derivation of hESCs	●		●
Using hESCs derived from research embryos	●#		●
Introducing human pluripotent stem cells into nonhuman embryos	●**	●**	●
Breeding animals with possible germline contribution	●	●	

*Qualified by "whenever it was/is practicable." †Statement must be in written consent form. ‡Except in case of autologous donation. §For procurement of gametes, somatic cells, or blastocysts. ‖For derivation of hESCs. ¶Charged with reviewing policies and guidelines rather than specific research protocols or proposals. #Includes somatic cell nuclear transfer, parthenogenesis, and/or IVF embryos created for research purposes. **Limited to human-nonhuman primate blastocysts.

PHOTO CREDIT: ALAN TROUNSON

[1]Center for Medical Ethics and Health Policy, Baylor College of Medicine, Houston, TX 77030, USA. [2]Kennedy Institute of Ethics, Georgetown University, Washington, DC 20057, USA.
*Author for correspondence. E-mail: majumder@bcm.edu

Published by AAAS

reference to possible research uses involving genetic manipulation and human-nonhuman chimeras, as well as exploration of donor objections to "any specific forms of research" [(*6*) App. A, p. 29]. In these and other ways, the earlier guidelines link transparency to the fundamental ethical principle of respect for persons. States that have devoted substantial resources to addressing informed consent in regulations governing publicly funded hESC research, such as California (*11*), offer useful models for national standards. The final NIH guidelines should urge a similar transparency regarding potential research uses in light of evidence of the information that embryo donors want about research aims and types (*12*–*14*).

The NIH guidelines go beyond prior efforts in specifying that certain statements be included in written consent forms. Such forms help to create a floor for disclosure of significant information, serve as a platform for discussion, and ultimately provide documentation of the informed consent process. However, it is important not to lose sight of informed consent as an "ongoing, interactive dialogue" [(*15*), p. 120] and to avoid overcrowding forms with legalese driven by the needs of institutions rather than (potential) human subjects.

Oversight

In authorizing the expansion of federal funding for hESC research, President Obama made an explicit commitment to strict oversight (*16*). Yet, in the draft NIH guidelines, it is difficult to find a trace of the strong local and national oversight provisions developed by the NAS (see table). This is perplexing, as support of local and national oversight was also clear in the 2000 NIH guidelines and the 1999 report on stem cell research issued by the National Bioethics Advisory Commission (NBAC) (*17*).

For local oversight, the 2000 NIH guidelines relied on existing Institutional Review Boards (IRBs). This was a natural, but problematic, choice. Considerable evidence has emerged that IRBs are overburdened and face difficulties in discharging their core duties under the federal regulations governing human subjects research (*15*). Further, IRB members do not necessarily have specialized expertise in the field of hESC research. The NAS guidelines incorporate the idea of local oversight of hESC research, but introduce a new body, the ESCRO committee, with members who have the specialized expertise to fill in gaps of oversight by IRBs and other institutional committees. The NAS guidelines retain a role for IRBs in reviewing new procurements of gametes, blastocysts, or somatic cells. ESCRO committees are charged with providing oversight of issues related to derivation and use of hESCs, passing on the scientific merit of research protocols, addressing compliance with applicable regulations and the NAS guidelines, maintaining registries of research and cell lines, and facilitating investigator education. ESCRO committees already have experience in resolving the problem of grandfathering in previously approved cell lines.

Since many institutions now have or have access to an ESCRO committee (*18*), an NIH endorsement of this system would not force a radical change from current practice. However, instead of adopting this approach, the NIH draft guidelines do not require any local oversight of hESC research (apart from stating that an institutional official must provide assurances of compliance with the guidelines and maintenance of documentation).

Further, the NIH draft guidelines do not provide any form of oversight of hESC research at the national level. Perhaps there is a case to be made for moving away from stem cell research exceptionalism in this regard. However, the NIH has not offered one, and there are good ethical and pragmatic reasons for favoring a coordinated, two-tiered local and national approach to oversight of research in this area, reasons that have proved persuasive to NBAC, the NIH task force responsible for the 2000 guidelines, the NAS, and most countries with well-developed stem cell research programs. Further, the standardization of criteria for hESC use that a national oversight body provides can facilitate collaborative research among stem cell investigators at different institutions. We therefore recommend that the NIH take advantage of this opportunity to establish a national stem cell research panel to help guide federal efforts to foster progress in this dynamic field. This panel would not engage in routine protocol review but would focus on larger topics, such as special ethical and policy issues, development and dissemination of best practices, and establishing a statistical coordinating center.

Further Considerations

Many of those who understand the difference between cloning for reproduction and for research believe there is a morally significant difference between using spare embryos for research and specifically creating embryos for research. Given this context, it is not surprising that the NIH has fallen back on Clinton-era policy in this regard (see table) and has simply avoided the issue. The absence of discussion, however, is regrettable.

We echo the International Society for Stem Cell Research in urging the NIH to "open discussions on funding research carried out with human pluripotent stem cell lines derived from sources other than excess reproductive IVF embryos" (*19*). The NIH has been authorized by President Obama to make decisions about federal funding of hESC research within the constraints of current law. Depending on its interpretation, the Dickey amendment (*20*) either prohibits the creation and destruction of human embryos in federally funded research or prohibits both, as well as the use of hESCs in federally funded research. In 1999, the NIH adopted the first interpretation; this interpretation was also implicitly accepted by the Bush administration when it authorized the use of certain already derived stem cell lines in federally funded research. We agree that under the first interpretation, the NIH could not fund the creation and subsequent destruction of research embryos. However, under the same interpretive logic that allows the NIH to fund research on stem cell lines previously derived from spare embryos using nonfederal funds, the NIH could fund research on stem cell lines previously derived from research embryos using nonfederal funds. Those at NIH responsible for developing the final guidelines and setting the future course now have an extraordinary opportunity to lay out the relevant ethical and policy considerations.

References and Notes

1. NIH, Draft NIH guidelines for human stem cell research. *Fed. Regist.* **74**, 18578 (2009); http://stemcells.nih.gov/policy/2009draft.
2. C. Holden, *Science* **323**, 1412 (2009).
3. R. Stein, *Washington Post*, 25 May 2009, p. A9.
4. National Research Council (NRC), *Guidelines for Human Embryonic Stem Cell Research* (National Academies Press, Washington, DC, 2005).
5. NRC, *2007 Amendments to the National Academies' Guidelines for Human Embryonic Stem Cell Research* (National Academies Press, Washington, DC, 2007).
6. NRC, *2008 Amendments to the National Academies' Guidelines for Human Embryonic Stem Cell Research* (National Academies Press, Washington, DC, 2008).
7. J. Sugarman, A. W. Siegel, *Science* **322**, 379 (2008).
8. J. Sugarman, A. W. Siegel, *Cell Stem Cell* **3**, 238 (2008).
9. P. L. Taylor, *Cell Stem Cell* **4**, 479 (2009).
10. NIH Guidelines for research using human pluripotent stem cells. *Fed. Regist.* **65**, 51976 (2000); http://stemcells.nih.gov/news/newsArchives/stemcellguidelines.asp.
11. 17 Cal. Code of Regs. § 100100 (2009).
12. A. D. Lyerly, R. R. Faden, *Science* **317**, 46 (2007).
13. K. Hug, *Fertil. Steril.* **89**, 263 (2008).
14. C. B. Cohen, *Stem Cell Rev.*, **5**, 116 (2009).
15. Institute of Medicine, *Responsible Research: A Systems Approach to Protecting Research Participants* (National Academies Press, Washington, DC, 2002).
16. B. H. Obama, remarks for delivery of stem cell executive order, 9 March 2009; www.whitehouse.gov/the_press_office/.
17. NBAC, *Ethical Issues in Human Stem Cell Research* (NBAC, Washington, DC, 1999).
18. R. O. Hynes, *Nat. Rev. Mol. Cell Biol.* **9**, 993 (2008).
19. International Society for Stem Cell Research, ISCCR comments on NIH draft guidelines for embryonic stem cell funding, 22 May 2009; www.isscr.org/press_releases/nihcomments.html.
20. Omnibus Appropriations Act, H.R. 1105, Division F, Title V, § 509 (Public Law 111-8).

10.1126/science.1176253

INFORMATION TECHNOLOGY

Innovating Education in Croatia

Reforms that are raising the quality of IT in Croatian science and education aim to create a knowledge-based society.

Dragan Primorac

To make Croatian science and education the most competitive in Eastern Europe by 2010, the Croatian Ministry of Science, Education, and Sports (the Ministry) has undertaken major reforms in the past 4 years (*1*) to develop information technology (IT) as the essential infrastructure for a knowledge-based society (*2*). Since 1993, IT projects have improved the quality of learning and teaching (*2*–*4*) and have created equal learning opportunities for all students (*3*). As a result, primary and secondary school students can access educational content from their homes or dormitories. The infrastructure for implementing new technologies in the education system has been developed and maintained by the Croatian Academic and Research Network—CARNet (www.carnet.hr). CARNet connects all universities and research institutions in Croatia with access speed ranging from 2 Mbp/s to 10 Gbp/s. It also connects to academic institutions in Bosnia and Herzegovina through cooperation with BIHARNET, the Academic and Research Network of Bosnia and Herzegovina, and throughout Europe via GÉANT, the pan-European data communication network (*4*). CARNet is free for all authorized users and provides each with a unique, electronic identifier.

CARNet equipped all scientific and academic libraries, 650 school libraries, 700 branch elementary schools (of 1367 in total), all secondary school staff rooms (391 in total), and all high school dormitories (54 in total) in Croatia with computer equipment and Internet access (*5*). This includes a room-based videoconference system, with 34 teleconferencing classrooms in 15 cities. Since the 2006–07 school year, 280 of 391 secondary schools have been equipped with SmartBoards, touch-sensitive whiteboards, on which a computer's video output can be displayed. Efforts are focused on using Web-based IT to connect remote parts of Croatia, such as its archipelago of 1000 islands. Croatia's "e-islands" project connects 21 island schools via a videoconference system (see figure).

To promote computer literacy, users have access to electronic content via the "Nikola Tesla" National Portal for Distance Learning (lms.carnet.hr), which includes the European Computer Driving License (ECDL). Courses on information-communication technologies are available, as well as interactive education content for high schools in mathematics, physics, biology, and chemistry. In a step toward computerization of educational resources and records, undergraduates use the Information System of Higher Education Institutions (ISVU) IT system (www.srce.hr/english/isvu.html) to sign up for exams via the Internet, check teaching and exam schedules, access records, and receive other related services. ISVU has been introduced in 82 public institutions in Croatia, and currently contains data on ~80% (around 135,000) of all undergraduates.

Video-conferencing for education.

The e-Matica system, implemented in 2008, is a database of primary and secondary educational institutions, their employees, students, programs, and activities. It contains around 30,000,000 records. E-Matica serves as the base for the Education Management Information System (*6*), a database of standardized data from pedagogical documentation and education statistics. E-Matica is also used in implementation of free textbook distribution through schools.

Starting in 2010, criteria for general secondary school students and 4-year vocational students to attend higher education institutions will include the State Matura Exam (SME). Currently under development is the National Information System for Application at Higher Education Institutions, in which data from e-Matica, ISVU, SME results, and elsewhere will be used to create student ranking lists.

Benefits and Challenges

Investment in development of IT in education and research totaled €133,300,000 (~$184,400,000) over the last 5 years. This amounted to ~2% of the Ministry's budget per year. Although the largest investments were in hardware, the fastest growing investments have been in software and education.

The Croatian government believes that providing access to information via the Internet leads to higher-quality education (*7*), especially in geographically isolated or economically underdeveloped areas. Remote learning should be embraced with traditional education as of equal importance. However, a serious obstacle is the lack of adequately trained staff. To overcome this, in the last 4 years, 20,000 employees in the education sector have completed ECDL training. Future efforts must address fear of new technologies and lack of motivation.

Other small countries that have made heavy investments in science and education (such as Israel, Ireland, and Finland) have shown how a small country can find an efficient strategy to become globally competitive. As Danish Crown Prince Christian VIII said in 1813 [(*8*), p. 242)], when the budget for education was increased despite Denmark's having declared bankruptcy following war with England, "If we now become foolish, we may say goodbye to the idea of surviving as a state."

Ministry of Science, Education, and Sports of the Republic of Croatia, 10000 Zagreb, Croatia. E-mail: dragan.primorac@st.t-com.hr

References and Notes

1. Ministry of Science, Education, and Sports (MSES), *Science and Technology Policy 2006–2010* (MSES, Zagreb, Croatia, 2006).
2. D. Primorac, *Public Service Rev. Eur. Union* **14**, 153 (2007).
3. E. Marshall, "Croatia: Aiming high"; http://blogs.sciencemag.org/newsblog/2008/07/croatia-aiming.html.
4. M. Petrovečki, V. Paar, D. Primorac, *Croat. Med. J.* **47**, 809 (2006).
5. D. Primorac, *EMBO Rep.* **9**, 596 (2008).
6. MSES, *Education Sector Development Plan 2005–2010* (MSES, Zagreb, Croatia, 2005).
7. National scores for 2007–08 were analyzed in schools that had had computers for student use for 1 to 4 years. A significant correlation was obtained between the number of years computers were available in schools and the national exam scores in chemistry, informatics, and physics. However, a more systematic investigation of these relations is necessary.
8. Croatian Heritage Foundation, *Hrvatski iseljenički zbornik 2007* (Croatian emigrant almanac 2007), (Croatian Heritage Foundation, Zagreb, Croatia, 2007), 368 pp.
9. I thank Z. Stanić, D. Schwarz, Z. Paldi, V. Mornar, A. Marušić, A. Mišak, I. Bošnjak, and. D. Bonacci.

10.1126/science.1167183

MICROBIOLOGY

Seeing Green and Red in Diatom Genomes

Diatom genomes contain remnants of both green and red algal genomes, hinting at a complex evolutionary past.

Tal Dagan and William Martin

The genomes of eukaryotes, particularly algae, are providing more and more evidence for the workings of endosymbiosis, an evolutionary source of complex cell organization where one cell (the symbiont) comes to live within another (the host). Some of that evidence is expected, but other evolutionary findings emerging from genomes are unanticipated. On page 1724 of this issue, Moustafa *et al*. (*1*) uncover such an evolutionary surprise from diatom genomes. The results are likely to be controversial.

Endosymbiotic theory predicts that a substantial fraction of the plant genome was likely acquired from the endosymbiont that made plants what they are—photosynthetic. Early in eukaryote evolution, one lineage aquired a cyanobacterial endosymbiont that became stably integrated into its host cell and eventually turned into a plastid (the photosynthetic compartment of plant cells that transforms solar energy, carbon dioxide, and water into sugar). Plastids still have their own DNA as testimony to their endosymbiotic origin, but that DNA contains only ~1 to 3% as many genes as found in cyanobacteria; yet plastids typically contain about as many proteins as their cyanobacterial cousins. This observation led to the expectation that the plant genome should contain many genes of cyanobacterial origin that were transferred during the course of evolution from the endosymbiont genome to the host genome through a type of lateral gene transfer (the spread of genetic information across species boundaries) called endosymbiotic gene transfer (the transfer of genes from endosymbiont to host).

Moustafa *et al*. (*1*) set out to look for evidence for gene transfer from organelles to the nucleus in the evolutionary history of diatom genomes. To do so they compared the thousands of genes in two completely sequenced diatom genomes to all genes from hundreds of other sequenced genomes (the search set), and created individual phylogenetic trees for all these genes. They then determined, for each diatom gene, which gene among the search set appears as the sister to the diatom gene in the phylogenetic tree, and hence is most likely to be the progenitor of the diatom nuclear gene.

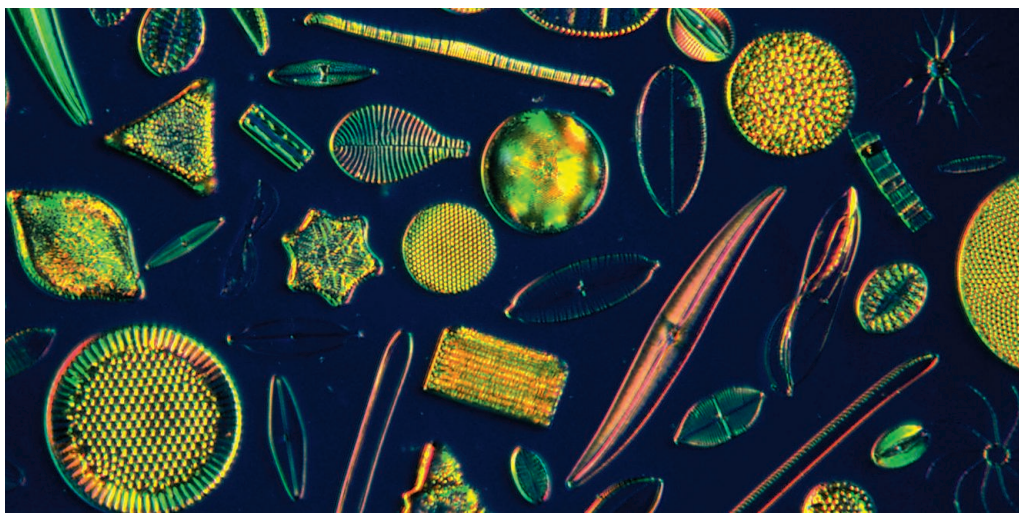

CREDIT: PHOTOTAKE INC./ALAMY

Diatom diversity. Based on a comparative study of diatom genomes, Moustafa *et al*. provide evidence for a previously unknown endosymbiotic event early in the evolution of diatoms.

Given that diatoms are known to have acquired their plastids from red algae via a process known as secondary endosymbiosis (*2*–*4*), one would have expected their search to uncover many nuclear genes with a red algal origin. Yet, the authors find that most symbiont-derived genes in the diatom genome have a green algal origin; only a small minority derive from red algae. To account for this unexpected find, the authors consider several possibilites. They favor the following scenario: The diatom lineage once possessed a green algal endosymbiont that donated green genes to the nucleus. This green plastid was later replaced by an endosymbiotic event that gave rise to the contemporary red plastid. The molecular evidence for this green plastid disappearing act lies in the genes that it left behind in the nucleus.

The outright replacement of well-established plastids by fresh ones of different origin through endosymbiosis might sound unlikely to some readers, but such things do happen during algal evolution, for example, among the dinoflagellates (*2*–*4*). Like lateral gene transfer among prokaryotes, endosymbiosis among algae is a normal and widespread mechanism of natural variation, but one that does not strictly adhere to Darwin's metaphor of a universal "tree of life" (*5*). Algal genomes are chimaeras whose constituent parts have different origins, and approaches to unraveling their genome evolution must take that into account. The approach of looking at all gene histories individually does just that.

The report raises many questions. First and foremost, did the authors make some serious error in their analysis? If they did, then everyone else is making the same error. If we read the fine print of both diatom genome sequence papers (*6*, *7*), both teams evidently saw that there was something suspiciously green about the diatom genome data, which on all counts was supposed to be purely red. Even the genome of the oomycete *Phytophthora infestans*—supposed to be descended from the same red algal symbiosis as the diatoms—contains genes of inexplicably green origin (*8*). Moustafa *et al*.'s suggestion of a lost green endosymbiont would account for these green evolutionary traces, but at the same time would date the shared green endosymbiotic event back to their common ancestor.

Another question is whether the small size of the red algal genome used for comparison, that of *Cyanidioschyzon merolae* (*9*), might bias the results. With 5300 protein coding genes, it harbors only about one-fifth as many genes as most genomes from the green lineage do. Hence, one possibility is that this is biasing our view of things. Moustafa *et al*. (*1*)

Institut für Botanik III, Heinrich-Heine Universitaet Duesseldorf, Universitaetsstrasse 1, 40225 Duesseldorf, Germany. E-mail: w.martin@uni-duesseldorf.de

Published by AAAS

looked into that by checking the cases where genes from both the green and red lineages were present in the same tree and found that even there, the green signal came through; thus, it cannot readily be explained away by the tininess of the red algal genome. More data from red algae would soothe all concerns; if anyone is searching for a reason to sequence larger red algal genomes, there it is.

Another question is whether the green signal is spurious. When we are dealing with thousands of trees, as in the present study, some trees will give erroneous results purely by chance, because that is the nature of phylogenetic inference (*10*). So, might the green signal just be phylogenetic noise?

The ciliate genome highlights the problem of distinguishing signal from noise in gene evolution studies. Ciliates are a group of eukaryotes that lack plastids but, like the oomycetes, are relatives of the diatoms (*2*–*4*). The ciliates may have had plastids in the past, the same plastids as diatoms, but later lost them. If so, then ciliate genomes should harbor genes reflecting that photosynthetic past. In the first ciliate genome sequences, Eisen *et al*. (*11*) uncovered a few dozen genes among 27,000 (~0.1% of the genome) harboring potential evidence for a photosynthetic past. According to Eisen *et al*., that signal does not rise above background noise, but Moustafa *et al*. found a few dozen of their green diatom genes in the ciliate genome.

Are a few dozen positive results among tens of thousands of cases more than one would expect by chance? That issue is not fully resolved to everyone's satisfaction so far. Thus, what constitutes "evidence" in the analysis of thousands of gene trees remains subjective. Moreover, trees are made from alignments, and alignments themselves can be a burgeoning source of phylogenetic error. Tools to help separate phylogenetic signal from noise at the level of alignments (*12*) are only slowly coming into use.

On the reassuring side, Moustafa *et al*. (*1*) are not talking about a dozen genes: They are talking about ~1000 green genes, or ~16% of the diatom genome. A phylogenetic signal of that magnitude surely tells us something important about algal evolution. Like much other recent data from genomes (*13*, *14*), the present findings do not fit comfortably into current theories for algal evolution (*2*–*4*). Recent advances in eukaryote phylogeny (*15*) are bringing order to chaos among the protists that lack plastids, where the evolutionary process is mostly tree-like in nature. But among algae, the lines of descent are becoming more tangled all the time.

References

1. A. Moustafa, *et al*., *Science* **324**, 1724 (2009).
2. S. B. Gould, R. F. Waller, G. I. McFadden, *Annu. Rev. Plant Biol.* **59**, 491 (2008).
3. T. Kleine, U.-G. Maier, D. Leister, *Annu. Rev. Plant Biol.* **60**, 115 (2009).
4. J. M. Archibald, *Curr. Biol.* **19**, R81 (2009).
5. W. F. Doolittle, E. Bapteste, *Proc. Natl. Acad. Sci. U.S.A.* **104**, 2043 (2007).
6. E. V. Armbrust, *et al*., *Science* **306**, 79 (2004).
7. C. Bowler, *et al*., *Nature* **456**, 239 (2008).
8. B. M. Tyler, *et al*., *Science* **313**, 1261 (2006).
9. M. Matsuzaki, *et al*., *Nature* **428**, 653 (2004).
10. O. Deusch, *et al*., *Mol. Biol. Evol.* **25**, 748 (2008).
11. J. A. Eisen, *et al*., *PLoS Biol.* **4**, e286 (2006).
12. G. Landan, D. Graur, *Mol. Biol. Evol.* **24**, 1380 (2007).
13. M. V. Sanchez-Puerta, C. F. Delwiche, *J. Phycol.* **44**, 1097 (2008).
14. I. B. Rogozin, M. K. Basu, M. Csürös, E. V. Koonin, *Genome Biol. Evol*. doi:10.1093/gbe/evp011 (2009).
15. A. J. Roger, A. G. B. Simpson, *Curr. Biol.* **19**, R167 (2008).

10.1126/science.1175765

EVOLUTION

Auxin at the Evo-Devo Intersection

William E. Friedman

The female gametophyte of flowering plants may have evolved through iteration of a modular structure and a gradient of the hormone auxin.

"Alles ist Blatt." With this simple but profound assertion ("All is leaf"), Johann Wolfgang von Goethe launched the modern age of comparative biology (*1*–*3*). By articulating the concept that plants can be broken down into modular and iterative variants of an archetypal structure (the leaf, in the form of bud scales, spines, petals, stamens and so forth), Goethe propelled the analysis of plant and animal structure (*4*) for the next two centuries and beyond. The idea that variant forms of a basic organ "type" are homologous (morphologically equivalent) within an organism and between organisms has emerged as a central conceptual (and testable) framework in the burgeoning field of comparative molecular analyses of development. On page 1684 of this issue, a study by Pagnussat *et al*. (*5*) brings together a remarkable set of experiments that bear on the developmental biology and modular construction of the microscopic egg-producing structure (female gametophyte or embryo sac) buried deep within a flowering plant's reproductive tissues. The findings have great importance for understanding and further examining the evolutionary developmental history of flowering plants.

Pagnussat *et al*. demonstrate in the flowering plant *Arabidopsis thaliana* that the phytohormone auxin is a key determinant of cell fates within the angiosperm female gametophyte. The embryo sac contains seven cells and eight nuclei: an egg cell, two synergids (one of which will receive the pollen tube bearing two sperm cells), a binucleate central cell, and three sterile antipodal cells at the opposite pole from the egg (see the figure). The egg cell and central cell serve as female gametes and, upon receipt of the two sperm from a pollen tube during the process of double fertilization, will yield a diploid zygote and a triploid endosperm, the embryo-nourishing tissue within the seed. Pagnussat *et al*. show that the distribution of auxin within the developing embryo sac is polarized, and they propose that gradient-based variation in the concentration of auxin determines the identity that cells will assume during the transition from a single-celled syncytium to a seven-celled, eight-nucleate mature structure. This finding is seminal, as auxin's centrality to patterning and differentiation in the angiosperm female gametophyte—or, for that matter, any land plant gametophyte—had not been anticipated.

Following the recent discovery that the earliest flowering plants likely produced a female gametophyte with only four cells and four nuclei, it was proposed that the angiosperm female gametophyte is a modular and iterative structure involving quartets of nuclei (*6*–*9*) (see the figure). Development of a basic angiosperm female gametophyte module was hypothesized to involve three ontogenetic stages: positioning of a single nucleus within a developmentally autonomous cytoplasmic domain of the female gametophyte; two nuclear division events to yield four nuclei within that domain; and par-

Department of Ecology and Evolutionary Biology, University of Colorado, Boulder, CO 80309, USA. E-mail: ned@colorado.edu

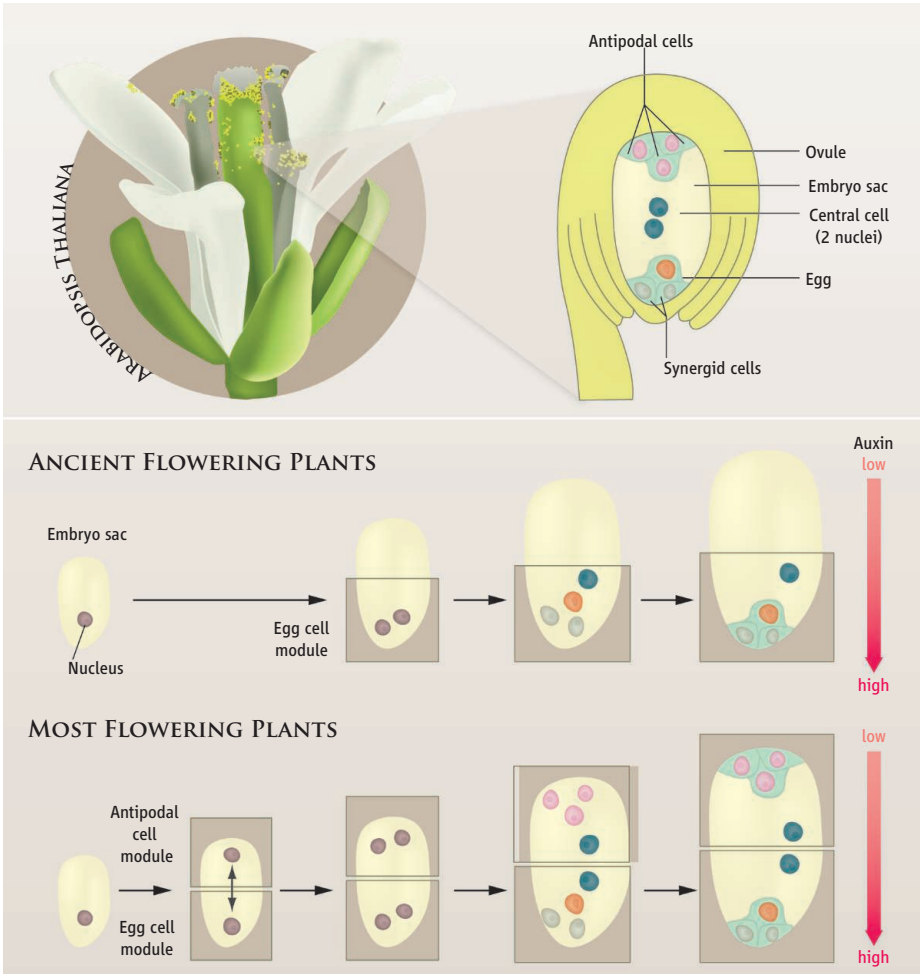

Module model. The female gametophyte of most angiosperms, including *Arabidopsis*, contains seven cells and eight nuclei. **(Top)** The ancestral angiosperm female gametophyte is hypothesized to form a quartet of nuclei and a single egg cell module within a gradient of auxin. (**Bottom**) Insertion of a nuclear migration event at the two-nucleate stage of development, in the presence of a gradient of auxin, is predicted to have led to the creation of two autonomous cytoplasmic domains that formed a two-module, seven-celled, eight-nucleate female gametophyte. This would have transformed the fertile egg apparatus into a set of three sterile antipodal cells. The second polar nucleus would behave as the original polar nucleus because both come into direct contact and share the same proximate cytoplasmic environment. In this scenario, an egg cell module and antipodal cell module develop and the evolution of triploid endosperm is the key functional outcome of this transition.

CREDIT: N. KEVITIYAGALA/*SCIENCE*

titioning of three uninucleate cells such that the fourth nucleus is confined to the central cell of the female gametophyte. Specifically, it was postulated that the first flowering plant female gametophytes (as well as those of some of the most ancient extant angiosperm clades) were constructed of a single fertile module (the egg cell module) and that duplication of this basic module gave rise to the seven-celled, eight-nucleate female gametophyte of most extant angiosperm species (*9*). This modular duplication event thus would have led to the creation of the antipodal cell module in the common ancestor of monocots, magnoliids, and eudicots (these three clades constitute more than 99% of extant angiosperms) about 115 million years ago.

As with all serial homologs, homeosis—the transformation of one form of organ type (e.g., petal leaf) into another form (sepal leaf or stamen leaf)—remains a key test of morphological equivalence. The observation of Pagnussat *et al*. that the identities of cells of the antipodal cell module can be transformed into cell identities characteristic of the egg cell module when proximate auxin concentrations are raised can be argued to constitute evidence of homeosis and hence modularity (serial homology). Moreover, the findings of Pagnussat *et al*. generate a clear set of testable predictions. If the first angiosperms produced a female gametophyte with a single egg cell module, and an auxin gradient was present, creation of an additional module at the opposite (low concentration of auxin) pole of the female gametophyte might well have led immediately to the formation of a sterile egg apparatus (egg plus two synergids) that we now recognize as the antipodal cells (*5*). Contribution of the fourth nucleus of this new ectopically expressed module to the central cell would have placed this nucleus in the same cytoplasmic environment as the original single polar nucleus and hence would have resulted in its participation in the second fertilization event to create triploid endosperm. As such, the origin of triploid endosperms in flowering plants from ancestral diploid endosperms may have a mechanistic explanation in which auxin plays a central role.

What is needed next are comparative studies of auxin concentrations and gradients in the female gametophytes of diverse eudicots and monocots as well as the most ancient lineages of flowering plants that bear four-celled, four-nucleate, single-module female gametophytes (Austrobaileyales and Nymphaeales). For now, we can begin to envision a working model of one of the key evolutionary transitions in flowering plant history: the shift from single-module female gametophytes that produce diploid endosperms to two-module female gametophytes that yield triploid endosperms.

All too often, organismic biology (specifically morphology and embryology) is thought to be a descriptive science. In fact, morphology, as Goethe showed, is a predictive science that generates testable hypotheses. The work by Pagnussat *et al*. confirms the view that morphological concepts can be supported or undercut by molecular data. The study reminds us of the truly co-dependent (in the best sense) relationship between organismic and molecular biology that remains, although often unacknowledged, at the heart of the field of evolutionary developmental biology.

References

1. J. W. Goethe, *Versuch die Metamorphose der Pflanzen zu erklären* (Ettinger, Gotha, Germany, 1790).
2. D. R. Kaplan, *Am. J. Bot.* **88**, 1711 (2001).
3. M. C. Dornelas, O. Dornelas, Braz. *J. Plant Physiol.* **17**, 335 (2005).
4. E. Coen, *C. R. Acad. Sci. Paris* **324**, 523 (2001).
5. G. C. Pagnussat, M. Alandete-Saez, J. L. Bowman, V. Sundaresan, *Science* **324**, 1684 (2009); published online 4 June 2009 (10.1126/science.1167324).
6. J. H. Williams, W. E. Friedman, *Nature* **415**, 522 (2002).
7. W. E. Friedman, J. H. Williams, *Evolution* **57**, 216 (2003).
8. W. E. Friedman, E. N. Madrid, J. H. Williams, *Int. J. Plant Sci.* **169**, 79 (2008).
9. W. E. Friedman, K. C. Ryerson, *Am. J. Bot.* **96**, 129 (2009).

10.1126/science.1176526

DEVELOPMENTAL BIOLOGY

Phase Transition in a Cell

The polarized distribution of P granules in a worm embryo is achieved, not by movement of the granules, but by a condensation process.

Loïc Le Goff and Thomas Lecuit

Most eukaryotic cells divide into equal halves, but cell division can be asymmetric when the two daughter cells acquire different cell fate determinants by unequal segregation of RNAs, proteins, and/or organelles. Asymmetric division controls cell diversification required for embryonic development (*1*) or the homeostasis of adult tissues (*2*), and in some animals, such as the nematode *Caenorhabditis elegans*, it can occur as early as the one-cell stage fertilized egg (zygote). On page 1729 in this issue, Brangwynne *et al*. (*3*) report an unusual strategy for polarizing the cytoplasm in the one-cell stage *C. elegans* embryo.

In the *C. elegans* zygote, sperm entry is thought to weaken a contractile cytoskeletal cortex, triggering a cortical flow of PAR polarity proteins and the asymmetric segregation of PAR-1 and PAR-3 (*4*) (see the figure). This break in cortical symmetry is then propagated to the cytoplasm, leading, for example to the posterior shift of the mitotic spindle, a major cytoskeletal (microtubule) structure. In most cases of cellular polarization, asymmetric segregation of RNAs, proteins, and organelles requires microtubules. A vivid example of this is the net redistribution of lipid droplets in the early fruit fly (*Drosophila melanogaster*) embryo by regulated changes in directed transport along microtubules (*5*, *6*). Such is also the case during asymmetric cell division. However, Brangwynne *et al*. report a different mechanism.

Brangwynne *et al*. studied the mechanism underlying localization of P granules—ribonucleoprotein organelles that specify germ cells–to the posterior side of the early *C. elegans* embryo. To address how symmetry breaking of the PAR-1–PAR-3 complex is transmitted into segregation of P granules, the authors labeled P-granule components with green fluorescent protein and tracked their movement by imaging the particles. Although individual trajectories of the P granules closely matched cytoplasmic flows, they could not account for their posterior accumulation overall, because as many granules moved toward the anterior as moved toward the posterior. Thus, no appreciable net transport to the posterior side is achieved.

The authors also observed that granules have an intrinsic dynamic: They either shrink (dissolution) or grow (condensation), or even do both sequentially. Furthermore, these dynamics are spatially biased: Granules in the anterior part of the embryo shrink, whereas granules in the posterior tend to grow. Brangwynne *et al*. propose that this polarized dynamic is the basis for the steady-state posterior accumulation of P granules. Indeed, they find that the spatial pattern in condensation dynamics is concurrent with symmetry breaking by PAR proteins, whether in wild-type situations or in conditions where the asymmetric segregation of PAR proteins is delayed.

What is it about symmetry breaking at the cortex that affects P-granule condensation and localization? By characterizing the spatial distribution of known regulators of P granules, Brangwynne *et al*. observed that MEX-5, a protein implicated in P-granule stability, forms a gradient with its lowest concentration at the posterior end of the embryo, where P granules condense. In embryos depleted of MEX-5 (by RNA interference), P-granule dissolution was reduced and became uniform along the anterior-posterior embryo body axis. Conversely, in embryos depleted of PAR-1, in which MEX-5 cytoplasmic accumulation is high and uniform, P granules do not condense. Thus, one model of P-granule distribution involves asymmetric PAR-1 localization, which induces a MEX-5 countergradient in the cytoplasm, and results in biased P-granule dissolution in the anterior and condensation in the posterior (see the figure).

The findings raise an interesting analogy between P-granule dynamics and liquid-gas phase transition. When the concentration of a gas increases above a certain threshold (the saturation concentration), liquid droplets nucleate in the gas and grow by exchange of molecules between the two phases. Similarly, the growth dynamics of P granules suggest that P-granule components exchange between a dense phase—the P granules themselves—and a dilute phase distributed throughout the cytoplasm. Brangwynne *et al*. propose that removal of MEX-5 from the posterior embryo lowers the saturation concentration there, inducing P-granule condensation. Lowering the saturation concentration is likely to occur through a change of affinities among RNAs and proteins comprising P granules. In response to shear stress, P granules behaved as viscous fluids, and their surface tension—the energetic cost of

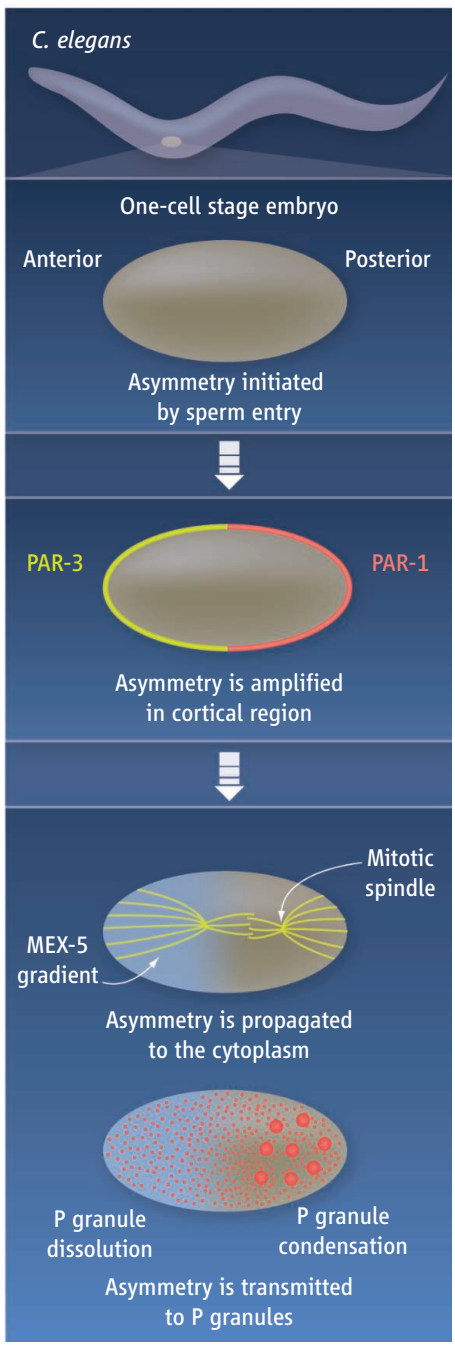

Propagating polarization. In the one-cell-stage *C. elegans* embryo, symmetry breaking is initiated by sperm entry, leading to the segregation of PAR-1 and PAR-3 proteins. This asymmetry is then transmitted to other cellular components, yielding posterior movement of the mitotic spindle, MEX-5 gradient formation, and posterior accumulation of P granules. P granule posterior accumulation in the embryo occurs through biased condensation of P-granule constituents.

CREDIT: N. KEVITIYAGALA/*SCIENCE*

IBDML, UMR6216 CNRS–Université de la Méditerranée. Campus de Luminy case 907, 13288 Marseille Cedex 09, France. E-mail: lecuit@ibdml.univ-mrs.fr

Published by AAAS

creating a new liquid-gas interface—was very small, indicating that the granules are highly deformable structures and are easy to nucleate.

The demixing transition described by Brangwynne *et al*. occurs only at the scale of the ribonucleic complexes that constitute P granules and not at the scale of the solvent (water and salts). Such mesoscopic phase transition can often be seen in soft-matter physics, where systems are driven by weak affinities (*7*). In a cell, a number of forces can affect molecular affinities, such as electrostatics or hydrogen bonds (*8*). Fine tuning these interactions could induce a similar demixing phase transition for other complexes.

The study of Brangwynne *et al*. may influence how we think about transport in the cytoplasm. Proteins might be thought of as exchanging between solid, liquid, and gas phases characterized by high-, low-, and zero-affinity interactions, respectively. Although proteins are usually considered to be freely diffusing in the cytoplasm, potentially in search of high-affinity partners, Brangwynne *et al*. remind us that they inhabit a more complex environment, and physics should have a say in describing this organization and how it affects the functional compartmentalization of protein activity.

References and Notes

1. P. Gönczy, *Nat. Rev. Mol. Cell Biol.* **9**, 355 (2008).
2. J. A. Knoblich, *Cell* **132**, 583 (2008).
3. C. P. Brangwynne *et al. Science* **324**, 1729 (2009); published online 21 May 2009 (10.1126/science.1172046).
4. E. Munro, J. Nance, J. R. Priess, *Dev. Cell* **7**, 413 (2004).
5. M. A. Welte, S. P. Gross, M. Postner, S. M. Block, E. F. Wieschaus, *Cell* **92**, 547 (1998).
6. G. T. Shubeita *et al.*, Cell **135**, 1098 (2008).
7. D. G. Aarts *et al.*, *Science* **304**, 847 (2004).
8. J. Israelachvili, *Intermolecular and Surface Forces* (Academic Press, London, 1992).

9. The authors' research was supported by the CNRS, the Agence National de la Recherche, Association pour la recherche contre le cancer, Fondation recherche médicale, and Human Frontier Science Program.

10.1126/science.1176523

CHEMISTRY

Rate Control and Reaction Engineering

A concept for evaluating the relative importance of steps in complex reactions may guide the development of better catalysts.

J. K. Nørskov, T. Bligaard, J. Kleis

A simple explanation for the acceleration of reactions by catalysts is that they speed up the rate-determining step. However, many reactions of practical importance are complex, multistep processes, and assessing the role that each step may play in controlling the overall rate of the reaction is not trivial. In a recent paper, Stegelmann *et al*. (*1*) have introduced a useful concept for characterizing such reactions: the general degree of rate control. Identifying the elementary steps that exert the greatest control on the overall rate of a chemical reaction offers the possibility of finding an appropriate catalyst or improving existing ones.

To illustrate the approach of Stegelmann *et al*., consider a catalyzed chemical reaction that takes place in several steps (see the figure). The overall rate of the reaction, r, depends on all maxima and minima in free energy, G_n. The minima define the stability of the reactants, intermediates, and products in the reaction, and the maxima define transition states that must be traversed for the reaction to proceed. In transition-state theory, the rates of each of these elementary reaction steps is determined from the activation free energies—that is, the free-energy differences between the transition states (TSs) and the immediately preceding minima.

Stegelmann *et al*. now define the generalized degree of rate control, X_{RC}, as the relative change of the net rate r when the stability of any free-energy extremum is varied while keeping all other extremum free energies, G_n, fixed:

$$X_{RC,}(i) = 1/r\,[\partial r/\partial\,(-G_i/k_BT)]_{G_{n\neq i}}$$

where k_B is Boltzmann's constant and T is temperature. Although there are other measures of the sensitivity of a rate on rate constants for elementary reactions (*2*, *3*), the one defined by Stegelmann *et al*. relates directly to the free energy of the intermediates and the transition states. It thus makes it easier to compare experimental results to theoretical calculations, which can determine free energies anywhere along the reaction coordinate.

The concept of the degree of rate control is useful in several ways. First, it quantifies concepts like the rate-determining step. In cases where one well-defined reaction step is the most difficult, the X_{RC} value of that transition state energy is 1, and all other values are 0. However, the example shown in the figure—the steam-reforming of methane, $CH_4 + H_2O \rightarrow CO + 3H_2$—is more complex. The activation of the first C–H bond in CH_4 is almost but not completely rate-determining. For the conditions shown in the figure, the degree of rate control of this step, $X_{RC}(CH_4\text{-TS})$, is 0.8, and the overall rate will decrease if the transition-state energy of this step is increased. Other values of X_{RC} in this reaction are nonzero. For example, the rate control value for the stability of adsorbed carbon atoms, $X_{RC}(C)$, is −0.26. The rate increases when adsorbed carbon is

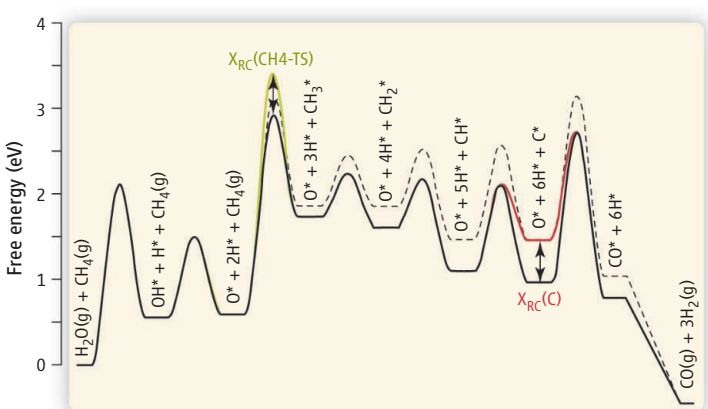

Sensitive reaction steps. The concept of degree of rate control is illustrated for the steam-reforming reaction ($CH_4 + H_2O \rightarrow CO + 3H_2$) over a stepped ruthenium surface. The changes in free energy are plotted for the progression of elementary steps, and the effect of changing the free energy of adsorbed C and the transition state for CH_4 dissociation is shown. The dashed line shows the free-energy diagram when the C adsorption energy is changed and we include the correlations that are found between the C adsorption energy and the other energies of relevance. The plot has been constructed from density functional theory calculations of enthalpies, as well as normal-mode analysis for determining entropies. The pressure-corrected free energies were then calculated for a reaction temperature of 1123 K (*10*).

Center for Atomic-Scale Materials Design, Department of Physics, Technical University of Denmark, Lyngby, DK-2800 Denmark. E-mail: norskov@fysik.dtu.dk; bligaard@fysik.dtu.dk; kleis@fysik.dtu.dk

destabilized, because the barrier for the formation of CO decreases.

The concept of the degree of rate control can be used to examine ways to improve a catalyst. For the steam-reforming reaction shown in the figure, a catalyst that lowers the activation free energy for CH_4 dissociation should be useful. This free energy has the largest value of X_{RC}, and if this barrier is decreased without affecting the other extrema, the maximum effect will be obtained. One of the challenges in changing the stability of individual extrema is that there are many correlations between them. For example, it may not be possible to change the stability of the CH_4 transition state without affecting the strength of the surface-C bond. Because $X_{RC}(CH_4\text{-TS})$ and $X_{RC}(C)$ have opposite signs, further analysis would be necessary to predict the net effect.

There are different ways of changing the stability of a transition state. For reactions catalyzed by transition-metal surfaces, changing the surface structure through particle size or shape changes can influence stability. The electronic structure can also be modified by adding another metal (alkali metals and other promoters often increase reaction rates) or by changing or alloying the transition metal. In the latter case, transition-state energies for surface reactions tend to scale with overall reaction energies (*1*, *4*–*7*).

Furthermore, the adsorption energy of different intermediates scale with each other (*8*). The interrelations between different G_n values often mean that there may be far fewer independent free energies than extrema. If the relations between different extrema are known, the kinetics can be expressed in terms of a reduced set of underlying independent descriptors, G_j. A possible extension of the generalized degree of rate control concept would then be to define a degree of catalyst control, X_{CC}, in terms of these mutually independent underlying descriptors (*9*).

For the steam-reforming reaction, there are approximate scaling relations between most intermediates and transition states for different transition-metal catalysts, including alloys, allowing the C and O adsorption energies to be used as the only independent variables (*10*). As indicated by the dashed line in the figure, a change in the C adsorption energy by choosing a new metal surface as catalyst will change a number of energy barriers. When all the correlations between the C adsorption energy and the energy of various intermediates and transition states are included, a value of $X_{CC}(C) = 0.11$ results. The dependence of the total rate on the C adsorption energy is relatively weak because two opposite effects compete: Weaker C binding increases the barrier for CH_4 dissociation, but also lowers the barrier for CO formation. The effect is weak because ruthenium is close to being the optimum catalyst for this process, and the rate is relatively insensitive to effects that change the free energy of the catalyst. The degree of catalyst control limits the problem to those degrees of freedom that can be modified, and finding the material for which all $X_{CC}(i)$ are zero corresponds to finding the optimal catalyst.

Developing better catalysts is a daunting task, but is critical for many problems in drug discovery, material synthesis, and energy technology (*11*). The beauty of simple reaction descriptors such as Stegelmann *et al.*'s degree of rate control, X_{RC}, is that they allow us to quantify which reaction steps we need to control and provide guidance for the design of new catalysts.

References and Notes

1. C. Stegelmann, A. Andreasen, C. T. Campbell, *J. Am. Chem. Soc.* **131**, 8077 (2009).
2. J. A. Dumesic, G. W. Huber, M. Boudart, in *Handbook of Heterogeneous Catalysis*, G. Ertl, H. Knozinger, F. Schuth, J. Weitkamp, Eds. (Wiley-VCH, Weinheim, Germany, ed. 2, 2008), p. 1445.
3. H. Meskine, *et al.*, *Surf. Sci.* **603**, 1724 (2009).
4. V. Pallassana, M. Neurock, *J. Catal.* **191**, 301 (2000).
5. J. K. Nørskov, *et al.*, *J. Catal.* **209**, 275 (2002).
6. Z.-P. Liu, P. Hu, *J. Am. Chem. Soc.* **125**, 1958 (2003).
7. R. Alcalá, M. Mavrikakis, J. A. Dumesic, *J. Catal.* **218**, 178 (2003).
8. F. Abild-Pedersen, *et al.*, *Phys. Rev. Lett.* **99**, 016105 (2007).
9. We define $X_{CC}(i) = 1/r[dr/d(-G_i/k_BT)] = 1/r \sum_n [\partial r/\partial(-G_n/k_BT)](dG_n/dG_j)$, where the relations between the G_n and the specific G_j in question are included explicitly in the differentiation.
10. G. Jones *et al.*, *J. Catal.* **259**, 147 (2008).
11. J. K. Nørskov, T. Bligaard, J. Rossmeisl, C. H. Christensen, *Nat. Chem.* **1**, 27 (2009).

10.1126/science.1174885

COMPUTER SCIENCE

Building an Open Cloud

Michael R. Nelson

As the Internet is increasingly used not only for communication but also for computing, issues of protocol, security, and openness need to be addressed.

The Internet is entering an exciting, third phase, as important as its second phase, the World Wide Web. Thanks to paradigms for distributed computing such as Web 2.0, Web Services, and Software as a Service, the Internet is becoming a platform for computing as well as communications. This new platform, the Cloud (*1*), is a many-to-many medium that can link millions of users to thousands of computers simultaneously (see the figure). It represents a fundamental shift in how computing is done. To quote Eric Schmidt, the CEO of Google, "We're moving into the era of 'cloud' computing, with information and applications hosted in the diffuse atmosphere of cyberspace rather than on specific processors and silicon racks. The network will truly be the computer" (*2*).

In Cloud computing, users rely on data and software that both reside on the Internet. Typical applications include Google Apps for word processing, virtual worlds such as Second Life that enable users to build three-dimensional environments, and grid computing. Cloud computing has the potential to be widely adopted because it can reduce the cost and the power required to do routine computing tasks and computationally intensive research problems (*3*), foster collaboration, and dramatically reduce the cost and complexity of developing new applications. Without the economies of scale enabled by Cloud computing, it will be increasingly difficult to deal with growing data and traffic volumes: A factor of >30 increase in the total amount of traffic on the Internet by 2015 is anticipated (*4*), and the total amount of research data available online will grow even more (*5*).

It is feasible that within the next 5 years, more than 80% of the world's computing and data storage could occur "in the Cloud." But many things will affect how, and how quickly, the Cloud will develop. We are at a critical point in the development of the Internet (*6*). The standards and policy framework for the Cloud will be defined in the next 2 or 3 years. If this is not done properly, in a way that enables innovation and competition, the full potential of Cloud computing may never be realized. A number of challenges must be addressed, including open standards, collaboration between cloud service providers, security and privacy, online copyright, liability, user resistance, organizational inertia, and law enforcement and national security concerns. Cloud computing has reached a point in its evolution similar to where the World Wide Web was in 1993: The key standards are in place, the first exciting commercial applications are taking off, there are concerns about security, and, most important, it is not clear how and where

Communication, Culture and Technology Program, Georgetown University, Washington, DC 20057, USA. E-mail: mnelson@pobox.com

this new, disruptive technology will be applied. But it is clear that decisions taken now by businesses and governments could limit the options and opportunities.

The research and library communities have a key role to play in shaping the development of the Cloud, just as they did with the Web in the mid-1990s (*7*). They were early adopters of the technology, helping to find solutions to concerns about Web security and privacy. They pushed for an interoperable Web that was based on open standards and open-source software. Users rejected efforts to create proprietary browser standards that would have segmented the World Wide Web by requiring the use of a particular Web browser to reach certain Web sites viewable only with that browser (*8*). These communities need to play a similar role today.

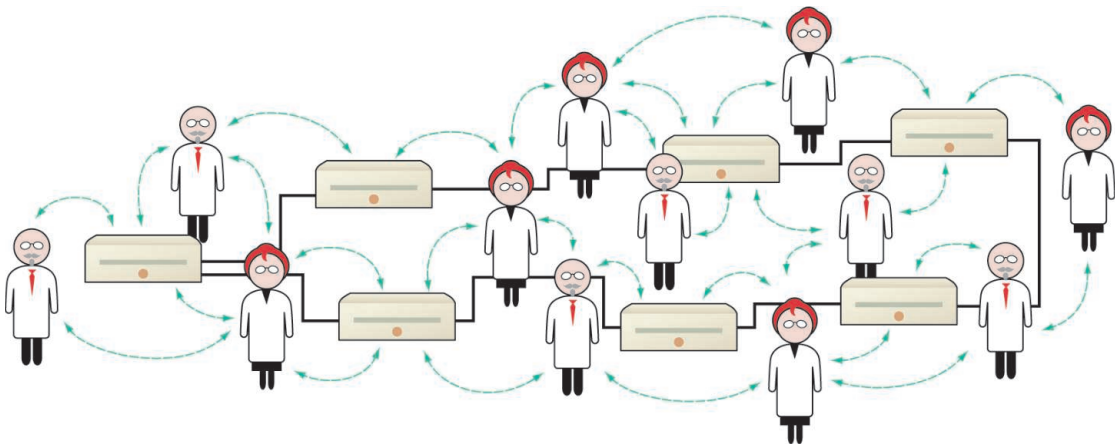

I see three possible scenarios for the Cloud. The first, the "Many Clouds" scenario, will result if a handful of companies are able to take advantage of economies of scale, proprietary standards, and government policies to control the market. They are likely to create separate, unconnected cloud platforms based on proprietary technologies. This scenario would provide some efficiencies, but it would be very difficult for data and software on one company's cloud to be combined with that from another cloud. The potential for new applications and closer collaboration would thus be lost.

The second scenario, "Hazy Skies," would still be dominated by large cloud service providers using proprietary systems. Data, but not software, could move between the different clouds. Common middleware, such as single sign-on authentication, would be absent, making it difficult for users to combine data and services operating in different clouds.

The third scenario, the "Open Cloud" (or "Blue Skies"), would use open standards, open interfaces, and open-source software to enable thousands of different organizations to link their infrastructure into a single, global Cloud. The Cloud would be like the Internet, a "network of networks" made up of more than 100,000 different subsystems run by different companies and organizations. This scenario would maximize collaboration, enabling users to assemble software and data into services that meet their particular needs. New authentication, security, and privacy-enhancing technologies could then be deployed throughout the cloud (*9*). In order to understand how the cloud is developing, we need accurate data on how Cloud computing is being used, as well as economic and social science research on innovation sparked by the Cloud. In addition, policy makers need advice on how existing telecommunication and information policy should be adapted so as not to slow its adoption.

In the 1980s, the Internet user community, and academic researchers in particular, worked to ensure that the Internet became a truly interoperable "network of networks" (*10*). Users embraced the Internet Protocol, which was based on open standards and could be implemented in open-source software. By adopting Cloud services built using similar open standards, users can provide a counterforce to the tendency of companies to differentiate their service by using proprietary technologies and to lock in customers.

Numerous organizations and companies have embraced the Open Cloud, including the Open Grid Forum (*11*), the Open Science Grid (*12*), an academic consortium (*13*) led by Google and IBM, and almost 200 companies and organizations that have endorsed the Open Cloud Manifesto (*14*). However, a number of forces are arrayed against the development of an Open Cloud. Governments wishing to censor the information that their citizens can view online and the services that they can use may try to limit access to and development of the Open Cloud. Poorly designed efforts to increase Internet security could limit the flexibility needed for the Cloud to grow and evolve (*15*). Proposals to impose filtering requirements on Internet service providers in order to detect the transmission of copyrighted material could eliminate many of the potential benefits of the Cloud.

Government procurements could either foster open Cloud standards or, by favoring one or two vendors, increase the likelihood of the Many Clouds or Hazy Skies scenarios. The academic and research communities can use their role as "early adopters," the results of their economics and policy research, and their access to the media to highlight the need for policies and practices that favor the development of an Open Cloud, interoperability, and competition.

CREDIT: ADAPTED FROM MICHAEL R. NELSON

References

1. "Let It Rise," ***The Economist***, 23 October 2008 (www.economist.com/specialreports/displaystory.cfm?story_id=12411882).
2. E. Schmidt, "Don't Bet Against the Internet," ***The Economist***, 16 November 2006 (www.economist.com/theworldin/business/displayStory.cfm?story_id=8133511&d=2007).
3. M. Armbrust ***et al., Above the Clouds: A Berkeley View of Cloud Computing***, University of California at Berkeley, Technical Report UBS/EECS-2009-28, 10 February 2009 (www.eecs.berkeley.edu/Pubds/TechRpts/2009/EECS-2009-28.html).
4. B. Swanson, G. Gilder, "Estimating the Exaflood: The Impact of Video and Rich Media on the Internet—a 'zettabyte' by 2015?", Discovery Institute, 29 January 2008 (www.discovery.org/a/4428).
5. G. Bell, T. Hey, A. Szalay, *Science* **323**, 1297 (2009).
6. D. E. Atkins *et al., Revolutionizing Science and Engineering Through Cyberinfrastructure: Report of the National Science Foundation Blue-Ribbon Advisory Panel on Cyberinfrastructure*, January 2003 (www.nsf.gov/od/oci/reports/atkins.pdf).
7. C. L. Borgman, *Scholarship in the Digital Age: Information, Infrastructure, and the Internet* (MIT Press, Cambridge, MA, 2007), p. 3.
8. See http://en.wikipedia.org/wiki/Browser_wars (as viewed on 11 June 2009).
9. M. R. Nelson, M. Schunter, M. R. McCullough, J. S. Bliss, "Trust and On Demand: Enabling Privacy, Security, Transparency, and Accountability in Distributed Systems," Telecommunications Policy Research Conference, 2005 (http://intel.si.umich.edu/tprc/archive-search-abstract.cfm?PaperID=460).
10. J. D. Rogers, *Inf. Soc.* **14**, 213 (1998).
11. Open Grid Forum (www.ogf.org/About/abt_overview.php).
12. Open Science Grid (www.opensciencegrid.org).
13. National Science Foundation Press Release 09-082, 23 April 2009 (www.nsf.gov/news/news_summ.jsp?cntn_id=114686&org=NSF&from=news).
14. Open Cloud Manifesto (www.opencloudmanifesto.org/supporters.htm).
15. J. Zittrain, *The Future of the Internet—And How to Stop It* (Yale Univ. Press, New Haven, CT, 2009).

10.1126/science.1174225

SCIENCE AND HEALTH

Personalized Medicine: Successes Tempered by Significant Challenges

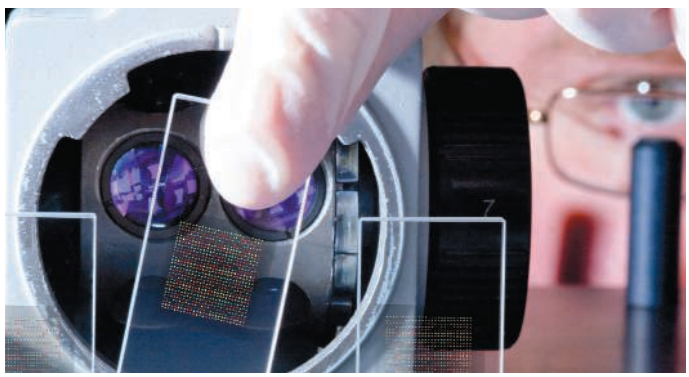

Future diagnosis. Rapid screening of the genome has helped researchers identify clinically important biomarkers for a range of medical conditions.

Since the decoding of the human genome in 2000, researchers and clinicians have sought to translate the new wealth of genetic information into custom-tailored treatments for patients. But the practice of personalized medicine still faces significant scientific and policy challenges, experts said at a recent colloquium co-organized by the Food and Drug Law Institute and AAAS.

Even the most successful forays into individualized diagnoses have had mixed results, the speakers agreed. And issues of regulation, physician training, and insurance have clouded at least the immediate future of the field.

While promising molecular discoveries and new diagnostic tests proliferate, said Dietrich Stephan, president of the Ignite Institute for Individualized Health, there has been "very little oversight on what's real and what's not real" in the realm of personalized medicine.

Speakers paid particular attention to the quest for biomarkers—molecular signposts for disease or a patient's response to a drug that are gleaned from roughly 20,000 to 25,000 human genes. The approach offers a way to circumvent some of the false starts and lengthy searches common with the trial-and-error method of drug discovery.

The challenge, said Rick Hockett, chief medical officer for the biotechnology company Affymetrix, is to sift through "this vast ocean of stuff"—millions of small segments of DNA and huge numbers of proteins—for biomarkers connected to an actual medical condition.

It's a task, agreed Klaus Lindpaintner of Roche Molecular Medicine Laboratories, "about as difficult, or perhaps even more difficult, than finding a new drug."

There have been some promising early developments. A woman with breast cancer can now discover whether her tumor is overproducing a gene product called HER-2. If she tests positive for the biomarker, she is a good candidate for a drug called Herceptin that targets the excess HER-2 and cuts the risk of disease recurrence nearly in half.

Another biomarker test can tell whether a patient has a particular genetic combination of liver enzymes, known as cytochrome P450, that help metabolize more than half of all drugs. The test can be used to fine-tune drug dosage based on a person's metabolism rather than on cruder factors such as body weight.

Even when good diagnostic tests are available, many health care professionals can have difficulty interpreting the tests and explaining genetic risks to patients, said Joseph McInerney, executive director of the National Coalition for Health Professional Education in Genetics. He cited a 2007 U.S. and Canadian study which found that three-quarters of the 112 medical schools responding taught medical genetics in the first year of course work, usually with an emphasis on general concepts rather than practical clinical applications.

The regulatory picture for these tests is also complicated. Tests distributed by commercial manufacturers must be reviewed by the U.S. Food and Drug Administration before marketing, said Courtney C. Harper, head of the FDA's Office of In Vitro Diagnostic Device Evaluation and Safety. But tests developed for use in a single lab—even those intended for personalized medicine—do not need to undergo FDA premarket review.

As personalized medicine enters the mainstream, insurers will face decisions on whether to cover novel tests and procedures. Pamela Sankar, a medical ethicist at the University of Pennsylvania, noted that CIGNA decided late last year not to cover the cytochrome P450 test because the insurer considered it to be "experimental, investigational, or unproven."

Louis B. Jacques, director of the division of items and devices at the U.S. Centers for Medicare & Medicaid Services, said that the agency will be looking for clear evidence of clinical benefit as it decides on Medicare coverage for genetic tests. And if a test "is not ordered by a physician," he said, "we won't pay for it."

Despite these obstacles, many consumers have an interest in participating in personalized medicine, the experts agreed, and some are turning to commercial gene-testing companies to learn more about their propensity for particular diseases. States such as California have acted to halt unlicensed Internet sales of genetic tests to their residents.

Sankar cautioned against overly optimistic projections for personalized medicine. Some of the resources now devoted to personalized medicine research, she suggested, might be better spent on pressing national health issues such as infant mortality, AIDS, and obesity.

The colloquium "brought together diverse views on an important topic that merges science, ethics, and policy," said Mark S. Frankel, director of AAAS's Scientific Freedom, Responsibility and Law Program. "We wanted to provide the public with a balanced assessment of an emerging issue that will affect their lives."

—Earl Lane and Becky Ham

COMMUNICATION

Screeners Needed for Journalism Awards

Volunteer scientists are needed to review entries in the prestigious AAAS Kavli Science Journalism Awards program. Scientists residing in the Washington, D.C., area, or who will be in the area in mid-August to mid-September, are invited to help screen print, online, radio, and television reports for scientific accuracy. If interested, please contact Molly McElroy (202-326-6434; mmcelroy@aaas.org) in the AAAS Office of Public Programs.

Winners of the awards, which are sponsored by The Kavli Foundation, will be honored at a ceremony in February 2010 at the AAAS Annual Meeting in San Diego. Members of the screening committees will be recognized in the awards booklet distributed during the ceremony.

Published by AAAS

INTERNATIONAL

Mapping the Frontiers of Science and Diplomacy

LONDON—With a growing corps of nations embracing science and technology as essential to future prosperity, influential research and policy leaders from around the world met here to explore the promise and potential obstacles of science diplomacy as a means for addressing challenges and easing tensions on a global scale.

A question of capacity. Mohamed Hassan urged more opportunities for researchers from developed and developing nations to work together.

Hosted by the Royal Society and co-sponsored by AAAS, the 2-day meeting offered S&T leaders a chance to explore the facets of science and diplomacy—ranging from science education and national security to research in the Islamic world and the environmental future of the Arctic. Speakers suggested that the meetings would help create a foundation for future efforts in science diplomacy and research collaboration.

Even during the Napoleonic Wars of the 19th century, French and British scientists maintained working contacts, said Lorna Casselton, foreign secretary of the Royal Society. Today, she said, science remains a means of "rising above political and diplomatic affairs."

"The discussions in London made clear that science diplomacy is a tremendously timely concept," added Alan I. Leshner, chief executive officer of AAAS and executive publisher of *Science*. "So many of our great challenges have science and technology at their cores, and they cannot be solved by any one country working alone. And scientific collaboration allows nongovernmental organizations to help build constructive relationships among peoples of the world, even when governmental ties are strained."

The London meeting, held 1 to 2 June, was evidence of a growing interest in employing science diplomacy more systematically. The meeting attracted nearly 200 speakers and participants from two dozen countries in Asia, the Middle East, Africa, South and North America, and Europe. Among the speakers were prominent researchers, NGO leaders, and top government science advisers.

The emerging sense of possibility for science diplomacy was underscored when U.S. President Barack Obama used his 4 June address in Cairo to announce science research and education initiatives with the Muslim world that will focus on health, technology, job creation, and additional scientific collaboration. Others say that science diplomacy could be critical in the run-up to the December climate change conference in Copenhagen.

Journalists are interested, too: While in London, Leshner and Ehsan Masood, who has written extensively on science and Islam, were interviewed at length on BBC Radio 3's "Night Waves" program. Leshner also took part in a news briefing on the prospects for science diplomacy in the Arctic.

To be sure, many academic institutions, NGOs, and governmental bodies are already engaged in ongoing joint international projects. But speakers described the efforts as "fragmented" and "patchwork." And, some said, the needs are so great in fields such as climate, food production, infectious disease, and science education that efforts must be undertaken now to build S&T relationships that link the developed world and the developing world.

Mohamed Hassan, executive director of the Academy of Sciences for the Developing World, said that north-south partnerships shaped at centers of excellence such as Nairobi-based ICIPE—the International Center of Insect Physiology and Ecology—could produce both excellent research and increased research capacity in the developing world.

During the conference, several speakers expressed concern that the term "science diplomacy" could provide cover for manipulative political activity that undermines the integrity of research efforts. John Beddington, chief scientific adviser to the U.K. government, and Nina Fedoroff, science and technology adviser to U.S. Secretary of State Hillary Clinton, both warned against efforts to use science as a political tool in foreign relations.

But they and other speakers suggested that protocols and safeguards built into the scientific enterprise could help manage such risks.

Norman P. Neureiter, senior adviser to the AAAS Center for Science Diplomacy, acknowledged the need for semantic nuance. "Diplomacy" can imply government use of science for political purposes, he said. "Soft power" suggests that science could be used as a competitive tool, and science "engagement," to some, connotes military action.

Neureiter's solution: "For now, I'm going to stick with 'science diplomacy': the employment of science for building better relationships throughout the world."

AAAS

New Dues Rates Approved for 2010

The AAAS Board of Directors has approved a dues increase for 2010. The Board authorizes increases to cover two kinds of expenses: unavoidable costs associated with running AAAS and publishing ***Science,*** and new expenses that add value to membership. Postage and paper increases and improving online resources are examples of the kinds of expenses the Board anticipated in setting the 2010 rates.

The new rates are effective for membership terms beginning after 31 December 2009. As listed below, they do not include postage or taxes for international members, which are additional.

Regular professional members	$146
Postdocs and K–12 teachers	$99
Emeritus members who receive print ***Science***	$115
Students	$75
Patrons	$310
Institutional rate for print for high schools and public libraries	$360
All other institutions receiving print	$910

For further information, including subscription rates for ***Science*** Online, librarians should contact AAAS or their subscription agents, or go to the ***Science*** Online Web site.

All members will be advised of the new dues rates on their renewal notices for 2010. Member dues and voluntary contributions form the critical financial base for a wide range of AAAS activities. For more information, contact the AAAS Membership Office at 202-326-6417, or www.aaas.org/membership/.

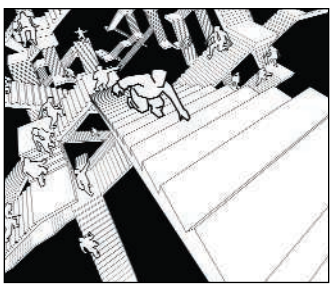

INTRODUCTION

Steps to the Clinic

"RESEARCHERS ANNOUNCE MAJOR STEP IN STEM CELL RESEARCH!" THIS NOW familiar claim extols the virtues of fresh research propelling us yet another step toward the clinic. We greet the news with excitement and then follow with "So how much farther?" Well, it's hard to say. The stairwell leading to the clinic seems to display twists, turns, and bifurcations and often lacks handrails. In addition, many of the building materials (progenitor cells or differentiated cell types), technologies (such as delivery method), and destinations (optimal regenerative tissues) are undefined as yet. To make the climb even more challenging, not all steps are created equal, with some treads and landings missing structural elements, leading to the occasional stumble.

But basic researchers serve as able guides for the climb. Their research on model organisms provides a firm grounding in stem cell biology. Such research is exemplified in a Review by Stappenbeck and Miyoshi (p. 1666), which describes stromal stem cells as they function in wound repair, and in a Review by Johnston (p. 1679), which tells of cell competition in somatic and germline cells of *Drosophila*. In addition, collaborative interdisciplinary efforts enable us to reach greater heights at an expedited pace. As Discher *et al.* (p. 1673) outline, new technologies can be used to parse complicated in vivo mechanisms to elucidate biophysical properties of stem cells and their microenvironment.

Cellular events occasionally go awry, as in cancer. There is much current interest in the biological properties of cancer cells with relevance to stem cell biology. Rosen and Jordan (p. 1670) tell how research on cancer stem cells, despite being an area of considerable controversy, is revealing potential targets for cancer therapy.

Safeguards for stem cell research are supported by regulatory bodies such as the U.S. Food and Drug Administration (FDA). In a Perspective, Fink (p. 1662) explains the role of the FDA in evaluating the safety of stem cell–based products intended for clinical application. Additional guidelines are even now being established by the National Institutes of Health [see the related Editorial by Pedersen (p. 1617) and Policy Forum by Majumder and Cohen (p. 1648)]. Guidelines and regulations are critically necessary, but, all too frequently, patients and their families feel that not enough progress is being made. The associated heartfelt urgency may lead to poor medical decisions taken by those who want to scale flights quickly when there is limited time. In a Perspective, Lindvall and Hyun (p. 1664) distinguish between responsibly extending the stairway into uncharted territory—the course of medical innovation—and taking leaps into the unknown that are driven more by hope than thought.

Although the steps to the clinic are still under construction, we are seeing exciting progress. The ascent is made easier through interdisciplinary research and improved communication among researchers, clinicians, and bioengineers. All the while, consultation with policy-makers and ethicists is crucial. Now we press onward, taking care to test our steps and build as we go.

– BEVERLY A. PURNELL AND PAMELA J. HINES

Stem Cells

CONTENTS

Perspectives

Reviews

See also related Editorial on p. 1617, Policy Forum on p. 1648, Review on p. 1679, and Report on p. 1707; Science *Podcast.*

Published by AAAS

PERSPECTIVE

FDA Regulation of Stem Cell–Based Products

Donald W. Fink Jr.

Cell self-renewal and the capacity to differentiate into multiple cell types (pluripotency) are biological attributes casting stem cells as attractive candidates for development of therapies targeting indications that involve functional restoration of damaged tissues. In the United States, clinical trials designed to demonstrate the safety and effectiveness of stem cell–based products are regulated by the U.S. Food and Drug Administration (FDA). To ensure that subjects enrolled in a clinical study involving stem cell–based products are not exposed to significant and unreasonable risk, the FDA reviews medical and scientific information that encompasses delineation of product-specific characteristics and preclinical testing to determine whether there is sufficient safety assurance to permit initiation of human clinical studies.

Evaluating the safety profile of an investigational stem cell–based product intended for clinical study within the United States is the responsibility of the U.S. Food and Drug Administration (FDA) (*1*). FDA has more than two decades of experience regulating cellular therapies, including stem cell–based products, gained through evaluation of proposals to perform clinical trials, conducting of intramural research, participation in scientific workshops and symposiums, and convening of advisory committee meetings on the topic of stem cells. To determine whether it is reasonable to grant permission for a clinical trial to proceed, FDA evaluates potential risk based on results derived from analytical assessment of product characteristics as well as preclinical proof-of-concept and safety testing, which, collectively, are considered within the context of a proposed clinical study (*2*). From a regulatory perspective, FDA considers stem cell–based products to be somatic cellular therapies that do not warrant a distinct regulatory approach. In contrast to therapies composed of differentiated, lineage-restricted somatic cells, some stem cell–based products are capable of cell self-renewal and differentiation into multiple types of specialized cells. Due to the extent of their proliferative and differentiation potential, there is a spectrum of safety concerns that relate to a specific stem cell–based product.

Clinical studies involving investigational stem cell–based products, which may include one or more of a variety of stem cell types derived from various physiologic sources, have been submitted to FDA for review. Embryonic stem (ES) cells with their potential for limitless self-renewal and the capacity to give rise to all differentiated cell types within the body raise a specific set of questions related to the safety of stem cell–based products. Pluripotency of undifferentiated ES cells demonstrated by spontaneous formation of teratoma-like masses composed of differentiated cells from the three somatic germ layers after injection in adult, immunodeficient mice (*3*, *4*) requires the attention of preclinical testing. FDA review experience involving stem cell–based products that includes strategies to enrich the target cell population indicates it is likely that some small but detectable proportion of undifferentiated ES cells with the potential to form a teratoma will remain in cellular products that result from differentiation of ES cells. Although these are classified histologically as benign, it is important to evaluate the teratoma-forming potential of differentiated cellular products derived from ES cells, because the appearance of a teratoma in an anatomically sensitive location such as the central nervous system, joint capsule, or myocardium could pose a considerable safety concern.

Other safety issues germane to stem cell–based products include the potential for spontaneous malignant transformation due to protracted, ex vivo culture expansion (*5*), a propensity for cells to migrate from the original site of administration, development of immunogenicity resulting from eventual expression of the cell/tissue donor human leukocyte antigen molecules (*6*), and the biologic impact of nontarget cellular impurities within the differentiated cell product.

The advent of induced pluripotent stem (iPS) cells generated by reprogramming of nonpluripotent, differentiated, adult somatic cells (*7*–*9*) has kindled interest in the possible use of such cells to generate autologous cellular products. The specific cellular reprogramming process selected for generating an iPS cell line may present novel risks for use of cellular products derived from that cell line requiring evaluation that involves both detailed product characterization and preclinical testing to support a proposed clinical use. At this time, reports describing new reprogramming methodologies are appearing in the scientific literature at a rapid pace; thus, additional safety issues that may need to be addressed remain to be fully delineated.

Safety assurance is achieved, in part, through comprehensive characterization of stem cell–based products. Because of the biological complexity exemplified by cellular composition heterogeneity, FDA suggests a multiparametric testing approach for characterization of stem cell–based products. This involves development of quantitative analytical techniques for conducting a panel of tests such as morphologic evaluation, detection of phenotype-specific cell surface antigens, assessment of unique biochemical markers, and genomic/proteomic analysis. In addition to relying on tests that target cell types within a stem cell–based product possessing desirable attributes, it is of equal importance to establish a panel of analytical tests that permits assessment of the cellular impurities profile. For example, analytical tests with sufficient sensitivity to detect discrete populations of cells with unwanted features are important when performing an impurities profile analysis of a cellular product derived from human embryonic stem cells. Testing could include detection of biomarkers for undifferentiated stem cells that have been linked with tumorigenesis. With respect to spontaneous transformation resulting from extended ex vivo cell culture, karyotypic analysis, routine evaluation of in vitro cell growth kinetics, and assessment of differentiation potential represent examples of tests that may be useful for detection of accumulating anomalies within a cell culture and may allow for establishment of parametric constraints on the cell expansion process. Undoubtedly, continued research efforts in cellular, molecular, and developmental biology will identify additional markers of value as well as improve on the specificity and sensitivity of tests used to characterize stem cell–based products. Given the potential for heterogeneity that results from multiple states of differentiation and/or cell lineages present within a single stem cell–based product, developing test methods that identify unique characteristics capable of anticipating clinical effectiveness poses further challenges.

Additional safety information pertaining to a stem cell–based product may be provided by execution of rigorous, well-designed studies conducted in appropriately sensitive preclinical experimental systems. Because cellular therapies are not readily retrievable once administered, the principles of conventional pharmacokinetics, namely, absorption, distribution metabolism, and excretion, are not applicable.

There are a number of important elements to consider when designing preclinical animal studies. They include (i) selection of relevant disease/injury models, (ii) testing of the product intended for clinical administration, (iii) using a route and method of delivery comparable to what is planned clinically, (iv) optimal timing of product adminis-

Cell Therapy Branch, Division of Cellular and Gene Therapies, Office of Cellular, Tissue, and Gene Therapies, Center for Biologics Evaluation and Research, U.S. Food and Drug Administration, 1401 Rockville Pike, Suite 200N, Mail Code HFM-720, Rockville, MD 20852–1448, USA. E-mail: donald.fink@fda.hhs.gov

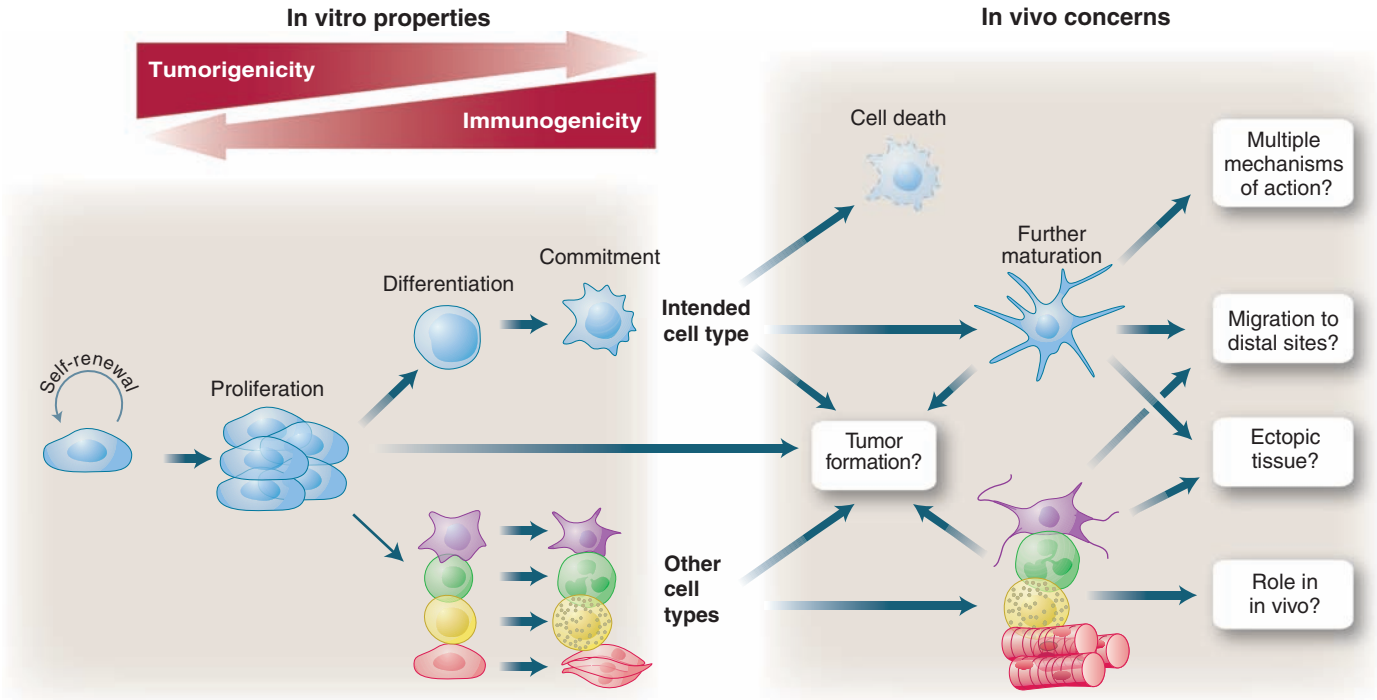

Fig. 1. Risk assessment of stem cell–based products. The potential for tumor formation (tumorigenicity) represents a concern correlated with the self-renewal of undifferentiated cells, whereas cells at other levels of maturation may also pose risk. Many stem cell–based therapies will not consist of a pure, homogeneous target cell population, which raises additional questions about risks that nontarget cells may present, as well as their physiologic role after administration. Ectopic tissue formation and migration from the site of transplantation are also concerns, particularly when stem cell–based products are introduced to anatomically sensitive sites. Additionally, differentiation of stem cell–based products that are allogeneic with respect to the recipient results in increased immunologic incompatibility due to expression of foreign nonself antigens. Death of large proportions of the transplanted cell population, not unique to stem cells, may constitute further risk.

tration with respect to disease/injury onset, and (v) an appropriate study duration that permits simultaneous assessment of potential adverse safety events and provides evidence of durable biological activity. Observable changes in animal behavior, physiologic function, and tissue morphology serve as indicators of cell survival and engraftment after administration, further in vivo cellular differentiation, physiologic integration, unchecked proliferation, migration to nontarget sites, ectopic tissue formation due to cell type impurities, and tumorigenesis (Fig. 1).

When extrapolating preclinical testing results to the intended clinical setting, it is important to recognize and appreciate both the relevant attributes and the limitations of a selected animal model of disease/injury. In those circumstances when well-developed animal models of injury/disease are available, evidence for robust proof-of-concept preclinical test results is valuable and informative, particularly in situations when the targeted clinical indication calls for administration of the stem cell–based product into a highly vulnerable anatomic site such as the central nervous system, a joint capsule, or the myocardium.

Additional challenges posed by immunological discordance encountered when testing human stem cell–based products in preclinical animal models of disease are an important consideration. Obtaining meaningful information pertaining to safety and biological activity derived from preclinical testing of human stem cell–based products necessitates immunocompetence modification of the animal disease model. Moreover, if use of an immunosuppressive regimen during execution of the clinical study is contemplated to support engraftment of the investigational stem cell–based product, this fact is to be taken into account during the preclinical testing stage of the product's development.

Efforts are under way at FDA to promote communication and exchange of scientific information between the agency and its stakeholders, with the goal of facilitating development of safe and effective stem cell–based products. To achieve this objective, several mechanisms are under consideration, including FDA-led translational science workshops and establishment of collaborative partnerships with the stem cell research community. The acquisition of additional analytical tools to enable elucidation of product characteristics, creation of new animal-based or in vitro preclinical models that recapitulate human disease conditions with greater fidelity, and development of noninvasive imaging methodologies with sufficient sensitivity to monitor migration and ectopic tissue formation after administration (*10*) will require cooperative interdisciplinary efforts that involve the broader research community and serve to ensure further patient safety.

References and Notes

1. D. W. Fink, S. R. Bauer, in *The Essentials of Stem Cell Biology*, R. Lanza, J. Gearhart, B. Hogan, D. Melton, R. Pedersen, J. Thomson, E. Thomas, M. West, Eds. (Elsevier, Burlington, MA, 2005), pp. 503–511.
2. M. Moos, *Trends Pharmacol. Sci.* **29**, 591 (2008).
3. J. A. Thomson *et al.*, *Science* **282**, 1145 (1998).
4. A. H. Brivanlou *et al.*, *Science* **300**, 913 (2003).
5. J. Garcia-Castro *et al.*, *Cancer Res.* **65**, 3035 (2005).
6. O. Preynat-Seauve *et al.*, *J. Cell. Mol. Med.*; published online 13 March 2009 (10.1111/j.1582-4934.2009.00746.x).
7. J. Yu *et al.*, *Science* **318**, 1917 (2007).
8. W. E. Lowry *et al.*, *Proc. Natl. Acad. Sci. U.S.A.* **105**, 2883 (2008).
9. J. Yu *et al.*, *Science* **324**, 797 (2009).
10. C. M. Long, J. W. Bulte, *Expert Opin. Biol. Ther.* **9**, 293 (2009).
11. The author acknowledges the important contributions of colleagues in the Office of Cellular, Tissue, and Gene Therapies, in particular S. Bauer, K. Benton, T. Chen, T. Finn, B. McCright, and M. Serabian.

29 April 2009; accepted 1 June 2009
10.1126/science.1173712

PERSPECTIVE

Medical Innovation Versus Stem Cell Tourism

Olle Lindvall[1]* and Insoo Hyun[2]*

Stem cell tourism is criticized on grounds of consumer fraud, blatant lack of scientific justification, and patient safety. However, the issues are complex because they invoke questions concerning the limits of acceptable medical innovation and medical travel. Here we discuss these issues and articulate conditions under which "unproven" therapies may be offered to patients outside of regular clinical trials.

Stem cell tourism is a worrying new form of medical travel driven by hope and pretense. Clinics around the world are offering unproven stem cell–based therapies to desperate patients for an array of intractable medical conditions. Such stem cell clinics have come under attack by scientists, clinicians, and bioethicists on grounds that they exploit seriously ill patients and threaten legitimate progress in the stem cell field (*1*). These concerns have found support in two recent publications. An analysis by Lau *et al*. (*2*) of online advertisements for stem cell therapies reveals that many clinics worldwide overpromise the benefits of their purported treatments and grossly downplay or ignore their attendant risks. And none backs up their claims with credible preclinical studies or other published scientific evidence. This is not simply another case of buyer beware; at stake is the potential for serious harm to vulnerable patients, many of whom may be too young to opt out of the proffered treatment. As a case in point, Amariglio *et al*. (*3*) report of a child who developed tumors in his brain and spinal cord after being treated with a series of poorly defined fetal stem cell transplants administered at a stem cell clinic. One might conclude from these examples that stem cell tourism—as the travel metaphor suggests—is teeming with medical tourist traps selling inauthentic representations of real medical treatment to unsuspecting consumers. The solution, many would argue, is for scientists to work with regulatory bodies to tighten regulations in offending locales and better educate patients.

These are sensible responses, but we must proceed carefully. The difficulty lies in being able to distinguish clearly between objectionable stem cell tourism and legitimate attempts at medically innovative stem cell–based interventions. This is crucial for two reasons: First, failure to draw such a distinction makes it difficult to sanction against objectionable stem cell tourism and may hinder the development of ethically and scientifically responsible avenues for innovative stem cell–based care for patients with few or no acceptable alternatives. We must discourage objectionable stem cell tourism without eliminating the possibility of responsible medical innovation.

Second, the general issue of medical travel is complex, and demonizing all stem cell tourism runs the risk of giving short shrift to patients' legitimate ethical motivations for such travel. Patients are not to blame, since medical travel may represent for them their last grasp at hope. Indeed, medical travel occurs in other areas of medicine, often involving highly innovative interventions at great cost to seriously ill patients, as happens today in cardiac centers of excellence all over the United States. Likewise, medical travel now and in the future may include "proven stem cell therapies," i.e., stem cell–based treatments that have been established in the clinic and accepted by the scientific and clinical community. Such treatments, e.g., hematopoietic stem cell transplantation for leukemia, may not be available to patients in their own country. In due course, other proven treatments may be banned for political or religious reasons because of their use of human embryonic stem cells. Patients should remain free to travel to clinics offering established stem cell–based therapies. Thus, we must be able to distinguish between acceptable medical travel for innovative or proven therapies and problematic stem cell tourism.

The key question, therefore, is what are the hallmarks of an innovative stem cell–based medical intervention? To answer this question, we have to clarify the central difference between research, as carried out in a clinical trial process, and medical innovation. As explained in the seminal U.S. research ethics document, the Belmont Report, research aims at scientifically generalizable results (not patient care), whereas the goal of medical innovation is the benefit of the individual patient (*4*–*6*). Because of these disparate aims, the regulatory requirements for clinical research do not serve as a proper surrogate for the ethical standards appropriate for attempts at medically innovative therapies (*7*). In short, the ethics of medical innovation is the ethics of patient care, not research. The research ethics paradigm views innovative treatment as a departure from standard treatment and overlooks clinical situations in which the currently accepted treatments are ineffective or burdensome (*7*).

From many patients' point of view, consenting to medically innovative care may be preferable to enrolling in a clinical trial, especially where patient care is decidedly not the purpose of the trial—expanding knowledge is. Patients with precious little time might not care much about expanding knowledge; what they care about is getting better and surviving. Demonizing stem cell tourism will never squelch this vital instinct. Acceptable channels must be made available to seriously ill patients.

There are additional reasons why we must reserve space for stem cell–based medical innovations. One may not be able to rely solely on the clinical trials process—moving from Phase I, through Phase II, to Phase III trials to demonstrate safety, efficacy, and possible advantages compared to available treatments—to advance the field. We believe medically innovative care could be a powerful route, in combination with the clinical trials process, for developing proven therapies if conducted with rigorous oversight and scientific integrity. There exists an enormous array of possible stem cell–based interventions, depending, e.g., on cell type, homologous or nonhomologous use, site of delivery, autologous or allogeneic transplantation, and disease indication. The result of this plurality is that some stem cell–based interventions may be more akin to a drug intervention amenable to a multistage clinical trials approach, whereas others may align more along a surgical or transplantation paradigm, for which a clinical trials approach may be practically quite difficult to use, at least initially. In the last 40 years, only 10 to 20% of all surgical techniques were developed through a clinical trials process. Some specialties, such as cardiac transplant and laparoscopic surgery, developed entirely without clinical trials (*8*). Responsible medical innovation could be an important avenue for the development of stem cell–based therapies that follow a surgical paradigm or otherwise do not fit neatly into the square peg of the clinical trials process. Other approaches may evolve through the "off-label" use of approved stem cell–based interventions outside of a clinical trial, as has happened with many medical innovations in the past. In either of these cases, tough standards must be set forth to protect patients.

Developing a stem cell–based therapy via medical innovation alone is, however, not optimal. The clinical trials process enables one to compare the results of a procedure with the long-term outcome of alternative interventions, which is particularly relevant for stem cell–based therapies. These are in

[1]Laboratory of Neurogenesis and Cell Therapy, Wallenberg Neuroscience Center, and Lund Stem Cell Center, University Hospital, SE-221 84 Lund, Sweden. [2]Department of Bioethics, Case Western Reserve University School of Medicine, Cleveland, OH 44106–4976, USA.

*E-mail: olle.lindvall@med.lu.se; insoo.hyun@case.edu

most cases meant to be replacement or regenerative therapies, for which long-term survival, lasting efficacy, and lack of serious side-effects are essential. The stem cell–based therapies must also be clinically competitive. Compared to available treatments, stem cell–based therapies have to offer more pronounced clinical improvement, fewer side effects, and/or lower costs.

Given the importance of both clinical trials and medical innovation, how should we proceed? The *Guidelines for the Clinical Translation of Stem Cells* (*9*), drafted by the International Society for Stem Cell Research (ISSCR), emphasize the clinical trials process in the absolute majority of translational stem cell studies (Fig. 1, left track). The principles include consistent starting materials, tests in animal models, review of protocols, and informed consent from patients.

Similarly, the ISSCR Guidelines offer standards for stem cell–based medical innovation. Currently, almost all stem cell–based approaches—aside from hematopoietic stem cell transplantation for blood disorders—are "unproven." But there are important differences. The "magic cure by stem cells" approach (Fig. 1, right track), for which there is no scientific rationale or preclinical evidence of efficacy and safety, must be condemned in all circumstances. If there are no chances of improvement, the "therapy" is both unethical and scientifically and clinically unacceptable. Stem cell–based medical innovation (Fig. 1, middle track) encompasses approaches where there is a scientific rationale and for which efficacy without serious side effects has been demonstrated in animal models but the approach has not yet been established clinically. This may be due to poor availability of cells, limiting the number of patients who can be transplanted, or to rapid scientific development with a need of further optimization before formal clinical trials should be started. This category should be acceptable outside formal clinical trials in few seriously ill patients who lack good therapeutic options. Although this proposal may seem radical to some, this is not a unique approach to medical advancement. As others have argued, efforts must often be made to advance a procedure to the point at which a formal research protocol can be developed (*7*, *10*). These initial efforts may include clarifying the types of patients who might benefit from the proposed intervention and standardizing the procedures (*7*).

We emphasize, however, that stem cell–based medical innovations should be subject to a combined scientific and ethical review and proper patient protections (*9*). Again, this is not a new concept. In surgery, where medical innovation is both widespread and necessary for improving patient care, medical professional societies have previously wrestled with similar questions. As a result of this vital dialogue, The Society of University Surgeons recently issued ethical guidelines for surgical innovation (*10*). According to these guidelines, surgical innovators ought to submit a proposal to a local surgical innovations committee, which, like an ethical research board, would provide appropriate oversight, but within the context of patient care (*10*, *11*). An analogous process for stem cell–based innovations has to be sensitive to the complexities of stem cell science. There should be a written plan that includes a scientific rationale, available evidence of efficacy and safety from preclinical studies in animal models as well as from applications of this intervention for other indications in humans, full characteristics of the cells to be delivered, and description of mode of cell delivery and of clinical follow-up. This plan should be approved through a review process performed by experts, and there should then be a rigorous voluntary informed consent. Transparency of this review process and institutional accountability are also desirable and crucial for continued public support of the stem cell field. Following the experience with the medically innovative procedure, the physician-scientists should, whenever possible, initiate a clinical trials process. Due to the complexity of stem cell–based approaches and their strong foundation on basic research, medical innovations should only be applied by clinicians who are experts in the field and with close links to stem cell laboratories. Our recommendation here echoes the concept of "field strength" advanced by some writing in the liver transplantation field—namely, that the team performing the innovative procedure should have proven successes in relevantly similar procedures (*12*).

Given the current state of our knowledge about stem cells and their actions, patients should continue to be counseled against medical travel for unproven stem cell–based therapies at this time. In the near future, however, there will be a need to articulate further the acceptable conditions under which "unproven" stem cell therapies for specific diseases may be attempted, as medical innovation, in patients outside of clinical trials. In a world already flattened by the Internet and easy travel, this task will become increasingly difficult, especially as authoritative preclinical stem cell studies and legitimate clinical trials begin to offer promising results to the public. Thus, the public's interest in stem cell tourism is likely to increase as stem cell science advances toward the clinic. There is much work ahead for the international community of researchers, clinicians, patient advocates, and regulators.

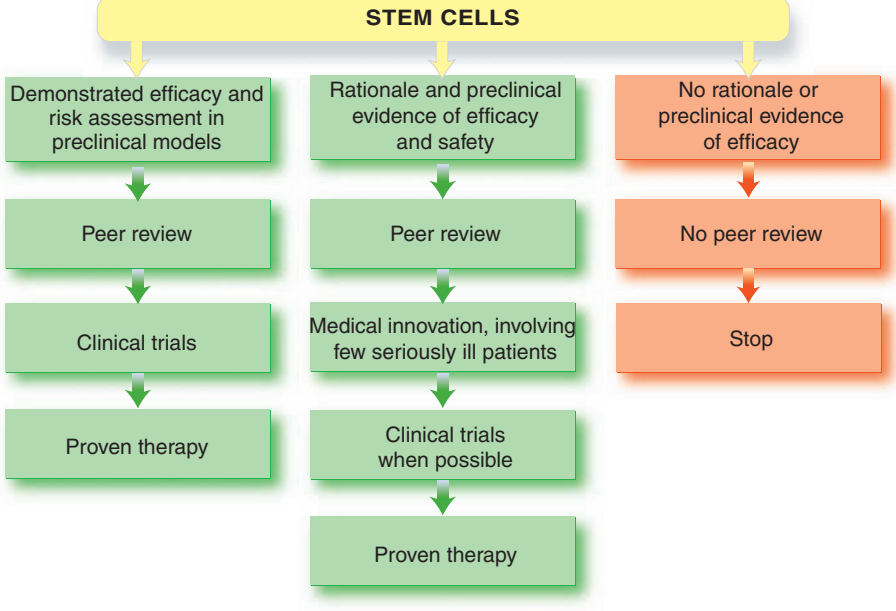

Fig. 1. Different steps in alternative processes for developing new stem cell–based therapies.

References and Notes

1. I. Hyun *et al.*, *Cell Stem Cell* **3**, 607 (2008).
2. D. Lau *et al.*, *Cell Stem Cell* **3**, 591 (2008).
3. N. Amariglio *et al.*, *PLoS Med.* **6**, e1000029 (2009).
4. The Belmont Report; available at http://ohsr.od.nih.gov/guidelines/belmont.html.
5. C. E. Margo, *J. Med. Ethics* **27**, 40 (2001).
6. H. Morreim, *Am. J. Bioeth.* **5**, 42 (2005).
7. G. J. Agich, *J. Med. Ethics* **27**, 295 (2001).
8. D. M. Cosgrove, *Cleve. Clin. J. Med.* **75** , S6 (2008).
9. International Society for Stem Cell Research (ISSCR), *Guidelines for the Clinical Translation of Stem Cells*; available at www.isscr.org.
10. W. L. Biffl *et al.*, *J. Am. Coll. Surg.* **206**, 1204 (2008).
11. A. M. Reitsma, J. D. Moreno, Eds., *Ethical Guidelines for Innovative Surgery* (University Publishing Group, Hagerstown, MD, 2006).
12. D. C. Cronin, J. M. Millis, M. Siegler, *N. Engl. J. Med.* **344**, 1633 (2001).

13. We are grateful to E. Borgelt for research assistance on this paper.

10.1126/science.1171749

REVIEW

The Role of Stromal Stem Cells in Tissue Regeneration and Wound Repair

Thaddeus S. Stappenbeck* and Hiroyuki Miyoshi

The process of wound repair in epithelium-lined organs of mammals is complex and is influenced by numerous secreted factors including cytokines, growth factors, and chemokines. However, the cellular organizers of this process are still not understood. Recent studies of tissue regeneration in organisms with simpler development have uncovered details about the activity of stem cells in the mesenchyme (the blastema) during this process. These blastemal cells are well positioned to interpret cues from the environment and to execute decisions about the direction of wound repair. In mammalian wounds, stromal stem cells appear to be positioned to perform functions similar to those of blastemal cells, including communication with both the overlying epithelium and the inflammatory cells in the mesenchyme.

Nearly two millennia ago, Aulus Cornelius Celsus (*1*) was apparently the first to characterize how human tissue responds to injury, using the terms tumor, rubor, calor, and dolor (swelling, redness, heat, and pain). Since that time, our understanding of the process of the acute response to wounding has become increasingly more sophisticated, and our current level of understanding has been detailed in many excellent textbooks on pathology [e.g., (*2*)]. Briefly, in this acute phase, soluble mediators are released in the wound and act on (i) the local vascular system to increase permeability and vasodilation; (ii) leukocytes (in particular, neutrophils) to stimulate their chemotaxis into the wound bed; (iii) platelets to aggregate during clotting; and (iv) microbes in order to tag them for removal by macrophages through a process called opsonization. This initial phase is critical to stabilize the wound and allow for a second phase of regenerative activity to occur.

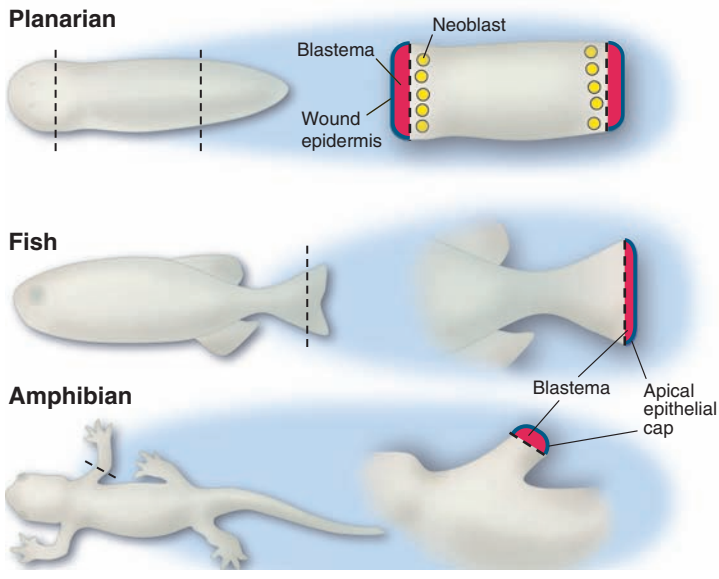

Fig. 1. Regeneration after transection in various model organisms requires specific stem cells in the mesenchyme. Planarians (head or tail), fish (fin), and amphibians (limbs) show regeneration after transection of specific sites. In all cases, a blastema (red) forms at the site of injury. In planarians, the blastema consists of neoblasts; in fish and amphibians, it consists of cells that have undergone dedifferentiation.

The regenerative phase of wound repair is characterized by the presence of fibroblasts, new blood vessels (created through a process of angiogenesis), and chronic inflammatory cells (consisting predominantly of macrophages) in the wound bed. Understanding the precise role of each cell type in this process is currently an intense area of investigation (*3*–*5*). One goal of this research is to promote the ideal outcome of wound repair, whereby damaged or lost specialized cells are replaced by cells with functional characteristics and organization similar to those represented before injury. In cases when a chronic damaging stimulus or infection is present, less than satisfactory outcomes of wound repair occur, including altered tissue organization, fibrosis or scarring, and metaplasia (replacement of cellular elements with inappropriate alternative cellular elements), all of which can affect normal function. One method to make wound repair more efficient and minimize undesirable outcomes would be to manipulate the cell type(s) that control this overall process. Stromal stem cells in the wound bed may fulfill this requirement if they can both mediate regeneration and coordinate their actions with the immune system to promote efficient wound repair while preventing infection of the wound bed.

The interplay of stromal stem cells and the immune system is most obvious in epithelium-lined organs that expose the host vascular and immune cells to the environment during injury. The skin and the cornea have emerged as useful systems for study because they are easily accessible and their healing can be observed in a longitudinal manner. Removal or damage of focal areas of skin is typically performed using a punch or incisional biopsy (*5*); the cornea can be focally damaged by both chemical and physical means (*6*, *7*). Other epithelium-lined organs that are amenable to damage and study of wound repair include mucosa-lined structures such as the lung and gut, which offer unique challenges and perspectives concerning this process. Because the key function of both the lung and gut is the physiologic exchange of either gas or nutrients with the environment, only a single layer of epithelial cells is present to act as a barrier to a numerous and diverse group of microbes [e.g., (*8*) for the intestine]. This epithelium can be damaged experimentally by well-defined chemical or physical means (*9*–*11*). A variety of studies have detailed the secreted factors that influence wound healing, identifying well-known families of growth factors such as epidermal growth factor (EGF), fibroblast growth factor (FGF), platelet-derived growth factor (PDGF), transforming growth factor–β (TGF-β), and vascular endothelial growth factor (VEGF). Various other hormones, growth factors, cytokines, and chemokines also influence wound repair (*12*).

Our knowledge of how this myriad of secreted factors is coordinated at the cellular level during injury repair remains incomplete. Much attention has been placed on the definition and behavior of epithelial stem cells that are responsible for the maintenance of this part of the barrier. However, it is not completely clear how mesenchymal elements are organized and regenerated in wound repair and to what extent they play a role in the proper regeneration of the epithelium. One reason why this has been difficult to discern is that injury sites in mice and humans typically contain a

Departments of Pathology and Immunology, Washington University School of Medicine, St. Louis, MO 63110, USA.

*To whom correspondence should be addressed. E-mail: stappenb@pathology.wustl.edu

robust inflammatory infiltrate that is intermingled with these mesenchymal cells. The thesis of this review is that lessons from the study of tissue regeneration in simpler developmental systems that point to undifferentiated mesenchymal elements as the key to this process will be instructive for investigators studying mammalian repair. These undifferentiated mesenchymal cells in simpler organisms are similar to mammalian mesenchymal stem cells (MSCs) (*13*) that are currently being studied in experimental models of injury and are being used to treat a growing number of chronic diseases in which wound repair is deficient (*14*). The more primitive mesenchymal cells may also be in a position in the wound bed to communicate with the immune system to ensure an appropriate level of inflammation.

Lessons from Regeneration in Model Organisms

In its simplest form, regeneration can be performed by resident, totipotent stem cells that normally maintain homeostasis by replenishing cells lost to turnover. Many simple organisms such as planarians, hydra, and starfish use this strategy for large-scale regeneration of substantial portions of their body plan after resection (*15*) (Fig. 1). The planarian *Schmidtea mediterranea* offers experimental advantages because its genome has been sequenced and RNA interference can be used to study gene functions (*16*, *17*). The planarian stem cell, the neoblast, is radiation-sensitive and is solely responsible for regeneration after resection (*18*, *19*). After resection of either the head or the tail of the planarian, neoblasts respond by proliferation and migration to the site of the injury, where in aggregate they form a blastema (a structure composed of undifferentiated cells). The blastema is the nidus for the formation of all the excised structures in a given region of the planarian, including the ectoderm, rudimentary gut, and reproductive system.

Analysis of mRNA microarray profiles of planarian neoblasts showed that >75% of their enriched mRNAs (with known mammalian homologs) could be classified into categories of protein biosynthesis, RNA binding, transcription, and DNA binding (*20*). All four of these categories represent intracellular processes that have been shown to be enriched in a variety of stem cells isolated from both mouse and human organs and embryos (*21*).

Even in this simplest case, neoblasts in transected planarians require instructive cues so that regeneration proceeds correctly. During regeneration, loss of Wnt signaling affects the anteroposterior axis recognition: Treatment of planarians with small interfering RNAs that abrogate Wnt signaling after tail resection results in a spectacular phenotype of a second "head" that is regenerated in place of the tail (*22*–*24*). The specification of an anteroposterior axis during regeneration also appears to require Wnt signaling in another model system, the hydra (*25*). Loss of bone morphogenetic protein (BMP) signaling affects proper mediolateral regeneration that is manifested by a lack of regeneration in this area of the planarian (*26*, *27*). An important emerging lesson from this recent work is that cell position and spatial orientation are critical to shape the activity of stem cells so that their actions are properly coordinated with the needs of the organism. Additional studies in this experimental system that determine the source of Wnt and BMP signals, as well as the cells that respond to them, will likely provide new ideas about how stem cells can shape regeneration.

Regeneration of higher-order organisms requires the coordinated action of multiple stem cell types. Fish and urodele amphibians (salamanders and newts) have the well-recognized ability to regenerate epithelium-covered appendages that have been amputated (Fig. 1; fins in fish and limbs in amphibians). Both systems are characterized by a phase of cellular dedifferentiation at the wound site, involving both mesenchymal and epithelial elements, that occurs soon after amputation. Epidermal cells dedifferentiate and migrate to close off the wound site from the environment. When this apical epithelial cap forms, undifferentiated cells in the mesenchyme then proliferate to form a blastema, which, as a structure, is morphologically similar to the limb bud in early development (*28*). Blastemal cells most likely are derived from local, mature dermal cells that dedifferentiate, although there appears to be a contribution of

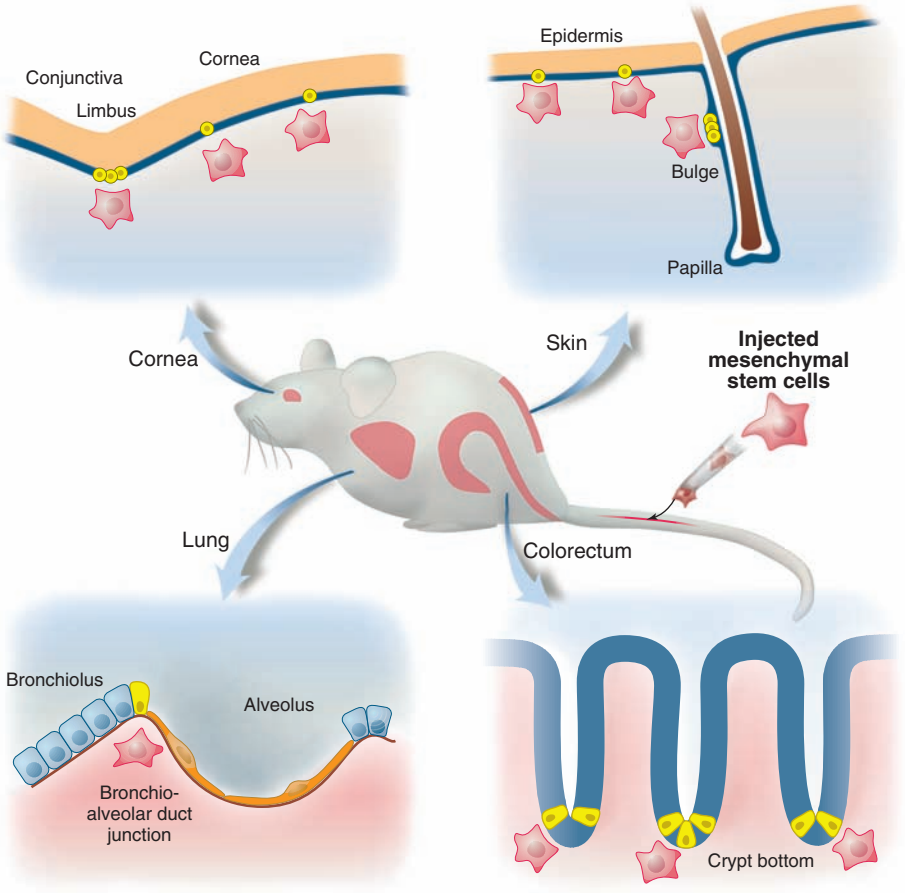

Fig. 2. Injected mesenchymal stem cells (MSCs) home to various sites of injury in mice. MSCs injected into the vascular system can home to various epithelium-lined organs including lung, gut, skin, and cornea (red). Corneal and skin epithelium contain multiple layers (orange, superficial; blue, basal layer). Stem cells are yellow and are present in the limbus of the cornea and hair follicle bulge of skin, although these cells also appear to be located in the cornea away from the limbus and in the interfollicular areas of skin as well in the basal layer. The lung and gut epithelium are single cell layers. The lung epithelium transitions from cuboidal-shaped cells to flat cells (blue and orange, respectively). The stem cell (yellow) may be located at the junction of these cell types. The colonic epithelium contains a layer of tall columnar-shaped cells (blue). The colonic stem cells (yellow) are located at the base of invaginations of this epithelium called crypts of Lieberkühn. In all cases, MSCs migrate to the mesenchyme of injured organs. Their as yet unproven interaction with stem cells in each organ is depicted.

dedifferentiated cells from muscle and bone as well (*28*).

The amphibian limb blastema is exquisitely organized. Transplantation studies during amphibian limb regeneration have shown that the proximal blastema gives rise to the proximal portion of the limb, and the distal blastema likewise gives rise to the distal limb (*29*). Blastemal cells, although morphologically indistinct, seem to be functionally distinct, programmed to know where they are placed in an organism or wound. Blastemal cells are "proximalized" by retinoic acid, which induces the expression of Meis homeobox domain proteins (*30*). This concept appears to have application in adult mammalian organs as well. A similarly seemingly indistinct cell type, the stromal fibroblast isolated from skin, is provided the equivalent of a "hometown address" simply on the basis of its location in the body. This idea was generated by an array analysis of mRNAs from human mesenchymal fibroblasts isolated from different areas of the body that showed differential expression of specific genes, notably the Hox family (*31*). Furthermore, skin fibroblasts from a single location also contain geographic specificity. Superficial skin fibroblasts (with respect to the organ surface) have distinct properties of growth, collagen gel contraction, and growth factor production relative to skin fibroblasts isolated from deeper within the organ [reviewed in (*32*)].

In salamander limb regeneration, the blastema requires instructive cues from differentiated cells located nearby. For example, denervated limbs in this system do not regenerate (*33*), reflecting an interdependence between blastemal stem cells and nearby nerves that depends on a gradient of Prod1 present on the cell surface of blastemal cells and its ligand, AG, which is secreted by Schwann cells that make up the nerve sheath (*34*). Blastemal proliferation in the regenerating zebrafish fin is also regulated by a number of growth factors including FGFs. MicroRNA-133 levels (normally high in the uninjured fin) are quickly depleted by FGF signaling to promote appendage restoration through the expression of Mps1 kinase, which stimulates blastemal proliferation (*35*). MicroRNAs regulate mRNAs (in part by controlling stability) in the progeny of stem cells (*36*) during development and seemingly during wound repair as well.

Application to Mammalian Wound Repair

In mice and humans, the scope of tissue regeneration is much more limited. "Limb" regeneration is restricted to the distal tip of digits (*28*). In mice, this process requires the transcription factor Msx1 and BMP signaling (*37*). After injury, the epithelium overlying the lost digit tip induces mesenchymal expression of Msx1, which stimulates dedifferentiation of a variety of mesenchymal cell types (*38*). These dedifferentiated mesenchymal cells are an important source of the regeneration in this system. It remains unknown why limb regeneration exists in principle but is in actuality so limited in mice and humans.

In mammals, the concept of regeneration can be extended if one considers the restoration of morphologically distinct epithelial stem cell–containing substructures located within an organ. Examples of such "mini" organs include hair follicles in skin, crypts in the intestine, and the limbus in the cornea. Hair follicle regeneration in response to punch biopsy wounds in skin depends on Wnt signals (*39*). Like the planarian regeneration system, Wnt signaling is required for the patterning of this "mini" organ during its regeneration (analogous to regeneration of one end of the planarian). However, also like the planarian, the precise cellular source(s) and target(s) of the Wnt signals have not been completely defined. In particular, defining the role of Wnt signaling within the mesenchyme itself will be quite important. Crypts and glands that line the gut are thought to regenerate, in part through a process of crypt fission (*40*), although the molecular triggers of this process are not yet clear. In the cornea, loss of Notch function in the epithelium has profound consequences during corneal wound regeneration, such that the mesenchyme no longer transmits appropriate signals back to the epithelium, resulting in abnormal epithelial differentiation (*41*).

A key unanswered question in all of these mammalian organ systems is the cell type that communicates with the epithelium to modulate wound repair. No morphologic blastema has been recognized to form in mammalian wounds. However, injected MSCs may be able to coordinate wound repair. MSCs, initially isolated on the basis of their ability to quickly adhere to tissue culture plastic, can differentiate into multiple mesenchymal lineages depending on available growth factors (*14*). Many studies have used injection of these cells (derived mostly from bone marrow and fat) to show that they can migrate to a variety of wound sites including the skin, cornea, gut, and lung (*42*–*46*) (Fig. 2). The homing of MSCs to certain anatomic locations requires specific glycosylation states of CD44 on the MSCs (*47*).

Because of the crude method of isolating MSCs, there is substantial interest in determining the cell type or types that they represent. Recently, multiple investigators have proposed that fibroblasts isolated from a variety of tissues appear to have very similar properties to these MSCs, including the ability to differentiate into multiple mesenchymal lineages (*48*, *49*). Thus, MSCs when injected into the bloodstream of a human or mouse may represent a mobilized form of a tissue-

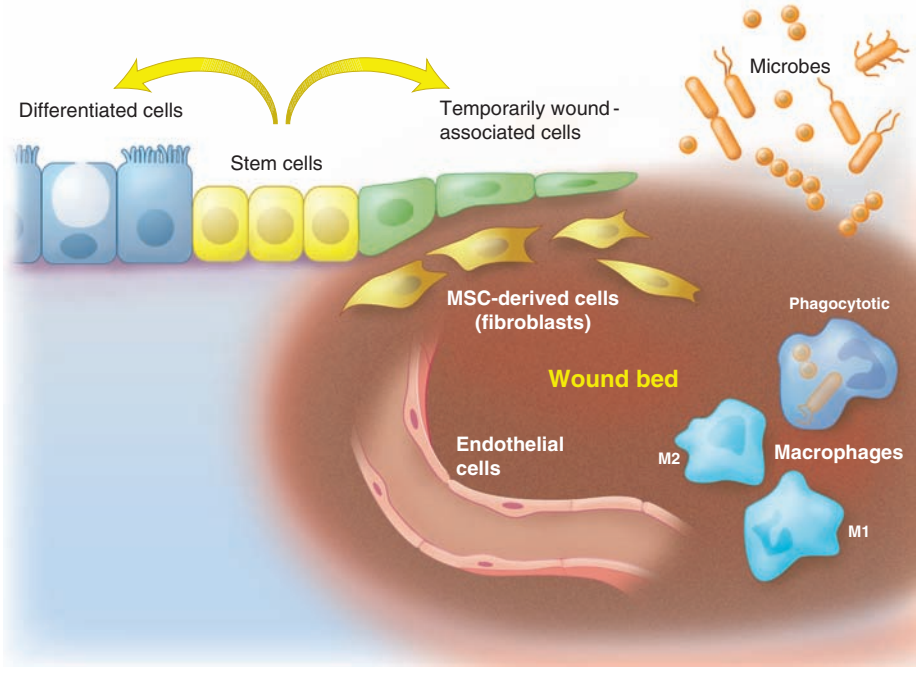

Fig. 3. Model of a potential role of tissue-resident fibroblasts in wound repair of epithelium-lined organs. The wound bed consists primarily of fibroblasts, new blood vessels, and macrophages, as labeled. The epithelium consists of stem cells that produce differentiated cells away from the wound bed and produce less differentiated cells that are associated with the wound bed. The timing and balance between wound repair and elimination of microbes in the wound bed must be properly orchestrated. The fibroblast may be in position to mediate this function by communication with overlying epithelial cells and macrophages within the wound bed.

resident fibroblast. Another intriguing proposal is that MSCs are pericytes (*50*), a supporting cell for blood vessels. This idea raises an intriguing connection between these cells and the microvasculature that undergoes such marked physiologic changes early in healing and must be remodeled in the late stage of healing. Finally, additional organ-resident, multipotent stromal stem cells with overlapping but distinct properties relative to MSCs have been isolated and characterized. An example is skin-derived precursors (SKPs) that are present in the adult and can differentiate not only into mesenchymal lineages but also neural lineages in vitro (*51*).

The primary function of MSCs in wound repair appears to depend on the site and type of injury. MSCs either can provide daughter cells that differentiate and then directly participate in the structural repair of a wound, or can supply secreted factors that support wound repair and modulate the immune system [e.g., (*46*, *52*, *53*)]. It is possible that MSCs, which can be isolated from virtually all tissue types, nonetheless may feature distinctive properties (including the ability to repair wounds) and markers when isolated from different tissues (*54*, *55*). This implies that MSCs may function within a tissue during injury repair, although they have not yet been observed to localize to a particular area of the wound. It is not known whether MSCs "dedifferentiate" during injury repair, or whether they simply divide and increase their representation in the wound bed. In any case, these cells may be strategically placed to communicate with overlying epithelial stem cells and the remainder of the wound-associated mesenchyme. To test this idea, it will be critical to develop novel tools to perform lineage-tracing studies of tissue-specific stromal cells as well as to knock out genes within them.

One cell type with which MSCs communicate under a variety of circumstances is macrophages (Fig. 3). Macrophages are often a dominant cell type in the mature wound bed and perform the critical function of killing and clearing any invading microbes. MSCs can secrete factors such as prostaglandin E2 (PGE_2) that down-modulate inflammatory cytokines that are produced by macrophages in response to encounters with microbes (*56*, *57*). Interestingly, PGE_2 can also potentiate Wnt signaling during repair in various organs (*58*), thus potentially linking immune and stem cell modulation. It is not clear whether the communication of MSCs (or any other cell type, for that matter) can program macrophages so that they aid in wound repair, as first suggested by Ross and colleagues in 1975 (*59*). This idea has led to the proposal that alternatively activated macrophages (through stimulation with interleukins IL-4 and IL-13) secrete factors that promote wound repair, whereas conventionally activated macrophages secrete a variety of pro-inflammatory cytokines that can inhibit wound repair (*60*). In support of this idea, Trem-2 knockout mice showed diminished expression of markers of alternatively activated macrophages in the wound bed of biopsy-injured mouse colons and showed diminished ability to heal wounds (*11*). However, the key test of this idea is to study mice that lack tissue-resident macrophages. In support of a positive role for macrophages in the response to tissue injury, colonic epithelial progenitors showed cell cycle arrest in $Csf1^{op/op}$ mice (which lack macrophages in many organs, including the gut) when injured with dextran sodium sulfate (*61*). Evidence that does not support a positive role of macrophages in injury repair comes from the study of skin injury using $PU.1^{-/-}$ mice [which also lack macrophages (*62*)]. Additional studies will obviously be required to further understand the role of macrophages and MSC-macrophage interactions in wound repair.

Understanding the mechanisms that underlie normal wound repair is of profound medical importance, because many disease states include elements of nonhealing or poorly healing lesions. Given the role of MSCs in wound repair of developmental systems and their emerging use as therapeutic agents, we propose that MSCs may be a critical, manipulable component of wound repair in humans. Understanding the role of MSCs within the tissue where a wound occurs will be quite valuable. What we lack are methods to specifically mark and trace the lineage of resident MSCs. Such methods, when developed, will help us to determine the extent to which MSCs act as stem cells or as sources of secreted factors, as well as to dissect this cell type into distinct and functional subpopulations.

References

1. A. C. Celsus, *On Medicine*, W. G. Spencer, Trans. (Harvard Univ. Press, Boston, 1935), Vol. 1, Books 1–4, pp. 219–351.
2. V. Kumar, N. Fausto, A. Abbas, Eds., *Robbins and Cotran Pathologic Basis of Disease* (Elsevier, Burlington, MA, ed. 7, 2008).
3. G. C. Gurtner, S. Werner, Y. Barrandon, M. T. Longaker, *Nature* **453**, 314 (2008).
4. M. Schäfer, S. Werner, *Annu. Rev. Cell Dev. Biol.* **23**, 69 (2007).
5. P. Martin, *Science* **276**, 75 (1997).
6. L. D. Ormerod, M. B. Abelson, K. R. Kenyon, *Invest. Ophthalmol. Vis. Sci.* **30**, 2148 (1989).
7. S. E. Wilson, R. R. Mohan, R. Ambrosio, R. R. Mohan, in *Wound Healing: Methods and Protocols*, L. A. DiPietro, L. A. Burns, Eds. (Humana, Totowa, NJ, 2003), pp. 67–82.
8. S. R. Gill *et al.*, *Science* **312**, 1355 (2006).
9. H. M. Wang, M. Bodenstein, K. Markstaller, *Eur. Surg. Res.* **40**, 305 (2008).
10. S. Wirtz, C. Neufert, B. Weigmann, M. F. Neurath, *Nat. Protocols* **2**, 541 (2007).
11. H. Seno *et al.*, *Proc. Natl. Acad. Sci. U.S.A.* **106**, 256 (2009).
12. S. Barrientos, O. Stojadinovic, M. S. Golinko, H. Brem, M. Tomic-Canic, *Wound Repair Regen.* **16**, 585 (2008).
13. M. F. Pittenger *et al.*, *Science* **284**, 143 (1999).
14. D. G. Phinney, D. J. Prockop, *Stem Cells* **25**, 2896 (2007).
15. K. D. Birnbaum, A. Sánchez Alvarado, *Cell* **132**, 697 (2008).
16. A. Sánchez Alvarado, P. A. Newmark, S. M. Robb, R. Juste, *Development* **129**, 5659 (2002).
17. A. Sánchez Alvarado, P. A. Newmark, *Proc. Natl. Acad. Sci. U.S.A.* **96**, 5049 (1999).
18. H. Randolph, *J. Morphol.* **7**, 317 (1892).
19. C. R. Bardeen, F. H. Baetjer, *J. Exp. Zool.* **1**, 191 (1904).
20. G. T. Eisenhoffer, H. Kang, A. Sánchez Alvarado, *Cell Stem Cell* **3**, 327 (2008).
21. J. M. Doherty, T. S. Stappenbeck, J. C. Mills, *Stem Cells* **26**, 2124 (2008).
22. K. A. Gurley, J. C. Rink, A. Sánchez Alvarado, *Science* **319**, 323 (2008); published online 4 December 2007 (10.1126/science.1150029).
23. C. P. Petersen, P. W. Reddien, *Science* **319**, 327 (2008); published online 6 December 2007 (10.1126/science.1149943).
24. T. Adell, E. Saló, M. Boutros, K. Bartscherer, *Development* **136**, 905 (2009).
25. M. Broun, L. Gee, B. Reinhardt, H. R. Bode, *Development* **132**, 2907 (2005).
26. P. W. Reddien, A. L. Bermange, A. M. Kicza, A. Sánchez Alvarado, *Development* **134**, 4043 (2007).
27. M. D. Molina, E. Saló, F. Cebrià, *Dev. Biol.* **311**, 79 (2007).
28. M. Han *et al.*, *Anat. Rec.* **287B**, 14 (2005).
29. K. Echeverri, E. M. Tanaka, *Dev. Biol.* **279**, 391 (2005).
30. N. Mercader, E. M. Tanaka, M. Torres, *Development* **132**, 4131 (2005).
31. J. L. Rinn, C. Bondre, H. B. Gladstone, P. O. Brown, H. Y. Chang, *PLoS Genet.* **2**, e119 (2006).
32. J. M. Sorrell, A. I. Caplan, *J. Cell Sci.* **117**, 667 (2004).
33. B. M. Carlson, *Principles of Regenerative Biology* (Elsevier, London, 2007).
34. A. Kumar, J. W. Godwin, P. B. Gates, A. A. Garza-Garcia, J. P. Brockes, *Science* **318**, 772 (2007).
35. V. P. Yin *et al.*, *Genes Dev.* **22**, 728 (2008).
36. A. J. Giraldez *et al.*, *Science* **312**, 75 (2006); published online 15 February 2006 (10.1126/science.1122689).
37. M. Han, X. Yang, J. E. Farrington, K. Muneoka, *Development* **130**, 5123 (2003).
38. G. Hu, H. Lee, S. M. Price, M. M. Shen, C. Abate-Shen, *Development* **128**, 2373 (2001).
39. M. Ito *et al.*, *Nature* **447**, 316 (2007).
40. H. S. Park, R. A. Goodlad, N. A. Wright, *Am J. Pathol.* **147**, 1416 (1995).
41. S. Vauclair *et al.*, *Dev. Cell* **13**, 242 (2007).
42. M. Sasaki *et al.*, *J. Immunol.* **180**, 2581 (2008).
43. J. Y. Oh *et al.*, *Stem Cells* **26**, 1047 (2008).
44. X. Fu, L. Fang, X. Li, B. Cheng, Z. Sheng, *Wound Repair Regen.* **14**, 325 (2006).
45. F. Tanaka *et al.*, *Life Sci.* **83**, 771 (2008).
46. M. A. González, E. Gonzalez-Rey, L. Rico, D. Büscher, M. Delgado, *Gastroenterology* **136**, 978 (2009).
47. R. Sackstein *et al.*, *Nat. Med.* **14**, 181 (2008).
48. M. A. Haniffa *et al.*, *J. Immunol.* **179**, 1595 (2007).
49. K. Sudo *et al.*, *Stem Cells* **25**, 1610 (2007).
50. M. Crisan *et al.*, *Cell Stem Cell* **3**, 301 (2008).
51. K. J. Fernandes *et al.*, *Nat. Cell Biol.* **6**, 1082 (2004).
52. Y. Wu, L. Chen, P. G. Scott, E. E. Tredget, *Stem Cells* **25**, 2648 (2007).
53. C. Toma *et al.*, *Circulation* **105**, 93 (2002).
54. L. da Silva Meirelles, P. C. Chagastelles, N. B. Nardi, *J. Cell Sci.* **119**, 2204 (2006).
55. S. Zhang *et al.*, *J. Cell. Biochem.* **99**, 1132 (2006).
56. K. Németh *et al.*, *Nat. Med.* **15**, 42 (2009).
57. S. Aggarwal, M. F. Pittenger, *Blood* **105**, 1815 (2005).
58. W. Goessling, T. E. North, S. Loewer, A. M. Lord, *Cell* **136**, 1136 (2009).
59. S. J. Leibovich, R. Ross, *Am. J. Pathol.* **78**, 71 (1975).
60. S. Gordon, *Nat. Rev. Immunol.* **3**, 23 (2003).
61. S. L. Pull, J. M. Doherty, J. C. Mills, J. I. Gordon, T. S. Stappenbeck, *Proc. Natl. Acad. Sci. U.S.A.* **102**, 99 (2005).
62. P. Martin *et al.*, *Curr. Biol.* **13**, 1122 (2003).

10.1126/science.1172687

REVIEW

The Increasing Complexity of the Cancer Stem Cell Paradigm

Jeffrey M. Rosen[1] and Craig T. Jordan[2]

The investigation and study of cancer stem cells (CSCs) have received enormous attention over the past 5 to 10 years but remain topics of considerable controversy. Opinions about the validity of the CSC hypothesis, the biological properties of CSCs, and the relevance of CSCs to cancer therapy differ widely. In the following commentary, we discuss the nature of the debate, the parameters by which CSCs can or cannot be defined, and the identification of new potential therapeutic targets elucidated by considering cancer as a problem in stem cell biology.

In 1994, John Dick and colleagues published their seminal paper that human acute myeloid leukemia is organized as a hierarchy that originates from a primitive hematopoietic cell, as shown in Fig. 1 (*1*, *2*). This report became the paradigm for later studies, which suggested that a similar model existed for solid tumors with cancer stem cells (CSCs) at the top of a hierarchical pyramid (*3*). These studies were based on a similar approach that uses fluorescence-activated cell sorting (FACS) of primary human cells with antibodies directed at defined cell-surface markers followed by limiting dilution transplantation, usually into an orthotopic site in immunocompromised mice (the xenograft model). Thus, the CSC paradigm refers to the ability of a subpopulation of cancer cells to initiate tumorigenesis by undergoing self-renewal and -differentiation, like normal stem cells, whereas the remaining majority of the cells are more "differentiated" and lack these properties.

Why Is There a Debate?

The concept that a specific subpopulation of tumor cells possesses distinct stem cell properties implies that CSCs arise as an intrinsic property of tumor biology and development (Fig. 2). However, the surrounding microenvironment (stromal fibroblasts, adipocytes, and endothelial cells, as well as the extracellular matrix) and the immune system are known to play important roles in cancer progression (*4*, *5*). Consequently, one caveat to the intrinsic model in the context of a xenograft is the lack of an appropriate microenvironment because of differences between the mouse and human and the lack of an intact immune system when evaluating the tumor-initiating capacity of these human cancer cells. Thus, it is possible that the subpopulation of cells that appeared nontumorigenic might actually be tumorigenic in the presence of the appropriate microenviroment. In other words, tumor cells might be functionally homogeneous, with heterogeneous potential arising as a consequence of extrinsic cues or the lack thereof (Fig. 2).

Strasser and colleagues attempted to test the original CSC hypothesis by using an alternative approach to the xenograft system. They used two transgenic mouse models in which the Eμ enhancer was used to express either the c-*myc* or N-*ras* oncogenes to induce B or T cell lymphomas, respectively (*6*). Upon the analysis of transplants, these authors concluded that "tumor growth need not be driven by rare cancer stem cells" based upon >10% of the transplanted cells, giving rise to tumors in syngeneic mice. Alternatively, recent studies by Guo *et al*. used a mouse model in which deletion of the *Pten* tumor suppressor gene in hematopoietic stem cells resulted in a myeloproliferative disorder followed by acute T-lymphoblastic leukemia (*7*). Using this model of a human leukemia, these investigators demonstrated by limiting dilution transplantation that a rare population of leukemia stem cells (LSCs) was responsible for leukemia development. Taken

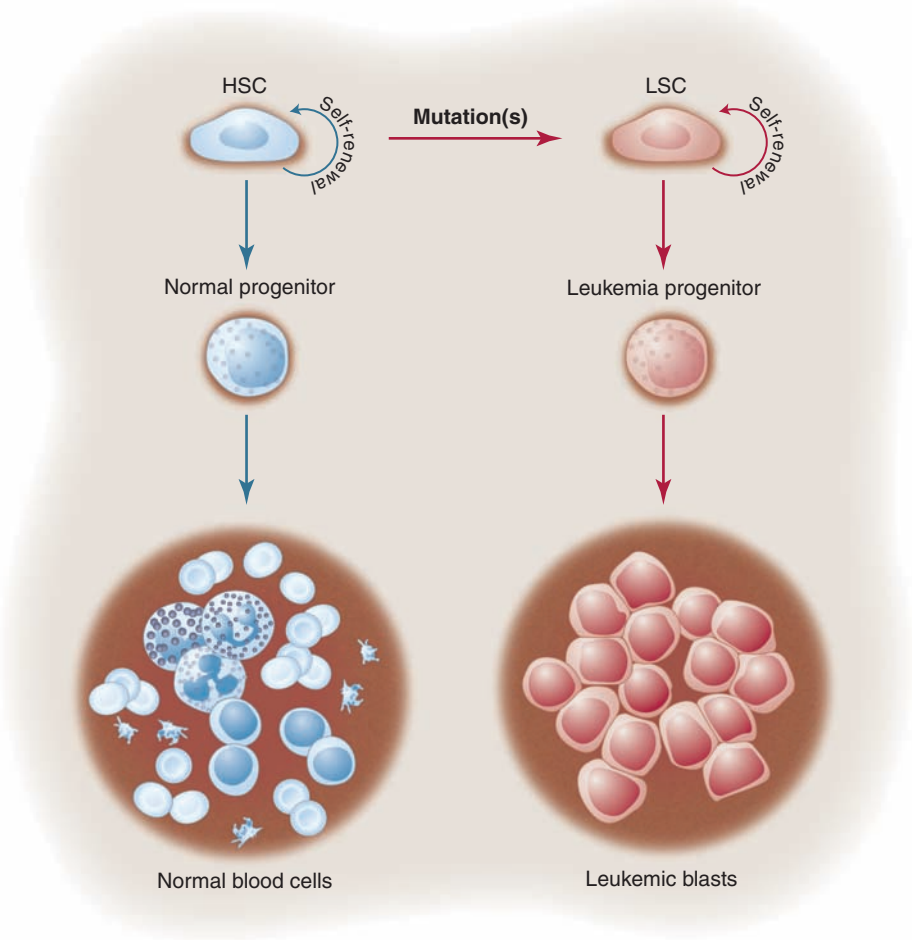

Fig. 1. Initial studies in leukemia provided the paradigm for the general CSC model. As shown on the left side of the figure, a hematopoietic stem cell (HSC) gives rise to normal progenitors and mature blood cells. The original model suggests that the HSC undergoes mutation(s) that give rise to its malignant counterpart, the leukemia stem cell (LSC). The LSC retains some degree of developmental potential, generating the leukemia progenitor and leukemic blast cells, which differ in their biological properties from the parent LSC. As in normal hematopoiesis, the stem cell maintains the ability to undergo self-renewal and thereby perpetuate the leukemia population.

[1]Department of Molecular and Cellular Biology, Baylor College of Medicine, Houston, TX 77030, USA. [2]James P. Wilmot Cancer Center, University of Rochester School of Medicine, Rochester, NY 14642, USA.

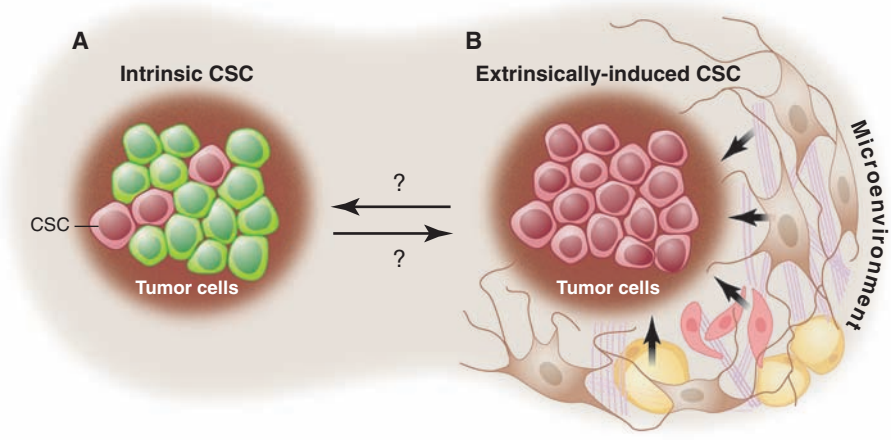

Fig. 2. CSC models. (**A**) The intrinsic model suggests that specific subpopulations within a tumor (pink cells) possess the functional properties of CSCs. (**B**) The extrinsic model proposes that all tumor cells are functionally equivalent and display heterogeneous behaviors as a function of extrinsic (microenvironmental) cues.

together, these findings indicate that the relative frequency and role of malignant stem cells can vary considerably as a function of the specific experimental system as well as perhaps the particular oncogenes or tumor suppressor genes used. However, for at least some forms of leukemia, stem cell properties reside within a relatively rare (<1%) subset of the tumor population, a finding that is consistent in both the xenograft and syngeneic models (*8*, *9*).

What Is the Situation in Solid Tumors?

In 2003, Michael Clarke and colleagues adapted to breast cancer the methods (*10*) used in leukemias and demonstrated the existence of a subpopulation of tumorigenic cells isolated primarily from breast cancer pleural effusions by limiting dilution transplantation of $CD44^{+}/CD24^{-/lo}/lineage^{-}$ cells into the mammary fat pad of immunocompromised nonobese diabetic–severe combined immunodeficiency (NOD-SCID) mice. A year later, Peter Dirks and colleagues reported the identification of human brain tumor–initiating cells again with FACS analysis but using a different cell surface marker CD133 (also called prominin1) and orthotopic intracranial transplantation into NOD-SCID mice (*11*). These reports led to a flurry of similar studies in other solid tumors [reviewed in (*3*)].

FACS and xenotransplantation of viable single cells from solid tumors require modifications of the approaches used for hematologic cancers because of the need to dissociate solid tissues into single cells, which are larger and more fragile than the hematopoietic cells usually isolated by these methods. Such procedures require several manipulations that may affect cell viability or behavior. Thus, the frequency of CSCs calculated in limiting dilution experiments can be markedly influenced by these parameters as well as the duration of the experiment performed to assess tumorigenicity. In addition, the nature of the immunocompromised host can also play a critical role in the efficiency of tumor formation. This is illustrated by the recent studies on human melanoma cells in which modified xenotransplantation conditions, including the use of more highly immunocompromised NOD/SCID interleukin-2 receptor γ chain null mice, increased the detection of tumorigenic melanoma cells by several orders of magnitude (*12*). Approximately one in four of the unselected melanoma cells formed tumors in these studies, which argues that the CSC population is not necessarily always rare and leads investigators to question, "Have we been studying these cells all along?" These studies highlight that the relative frequency of CSCs may vary as a function of both the tumor type and the specific experimental system used.

Once again, the use of syngeneic mouse models for analysis of CSCs has helped clarify the role of the microenvironment for solid tumors. As an example, two studies using mouse breast cancer models, the p53 null transplantation and the MMTV-Wnt1 models, have demonstrated by limiting dilution transplantation analysis that a small subpopulation of tumor cells are CSCs, whereas the bulk of the tumor cells are nontumorigenic (*13*, *14*). The secondary tumors that arise from isolated CSCs phenocopy the original tumors and give rise to the heterogeneous cell types observed in the primary tumors. This type of cell heterogeneity is not observed in all genetically engineered mouse models of breast cancer, so it is probable that in some models the frequency of CSCs may be quite high, similar to the observations made by Strasser and his colleagues using the Eμ lymphoma models. Studies using the same p53 null mouse breast cancer model and improved FACS protocols found tumors formed with a more than 10-fold higher frequency than previously reported (*14*), thus illustrating that the absolute CSC frequencies are highly dependent on the experimental conditions used. Although the calculated frequencies of CSCs may therefore vary depending on the methods used to isolate and transplant these cells, the fold enrichment observed between the CSCs and bulk tumor population was quite similar. Most importantly, >90% of the bulk tumor cells were nontumorigenic even after more than a year after transplantation. Thus, like the findings from hematologic cancers, the data from solid-tumor analyses demonstrate a high degree of variability depending on the specific experimental system. However, despite concerns noted for the use of xenografts, data from syngeneic models demonstrate the existence of subpopulations of cells in at least some solid tumors, satisfying the functional criteria of CSCs.

Why Is the CSC Paradigm Becoming More Complex?

Perhaps the most challenging issue facing the field is the fact that CSCs in primary tumors do not always display the properties classically used to define normal stem cells, cells with the ability to self-renew and -differentiate into multiple cell types. The cell-surface immunophenotype of primary tumors, as well as the frequency of functionally defined CSCs, can vary dramatically among different patients. In some cases, CSCs are relatively rare, whereas in others CSCs can constitute a substantial proportion of the tumor mass (*12*). So, why are tumor CSCs so variable? In normal steady-state systems, one can expect reasonably well-conserved development behavior, but upon any kind of substantial genetic or epigenetic perturbation, the rules that define cell and tissue behavior are not easily predicted and must be defined empirically. Thus, in the context of inherently unstable conditions such as cancer, the fact that CSCs display varying behaviors is no surprise. Moreover, the properties of CSCs appear to be influenced by both the specific genetic aberrancies in a given tumor as well as the stage of disease progression and the types of drugs used to challenge tumor growth (Fig. 3). Consequently, for any particular type of cancer the patient-to-patient variability of CSCs may be quite substantial. Taken together, these issues make any consistent definition of CSC properties difficult and suggest that being overly rigid in how CSCs are defined is not realistic. Furthermore, the variability in CSC properties introduces problems when developing new therapies.

A genetic program that might account in part for the diversity of abundance of CSCs in solid tumors is the ability of cells to undergo an epithelial-to-mesenchymal transition (EMT). Recent studies have suggested that induction of EMT in immortalized human mammary epithelia cells results in cells with stem-like properties, such as " an increased ability to form mammospheres, a property associated with mammary epithelial stem cells" (*15*). A number of studies

have suggested that cells at the leading invasive edge of solid cancers, such as colon, breast, and pancreatic tumors, exhibit more mesenchymal features and are characterized by the expression of CSC markers (*16*–*18*). Thus, there has been a convergence of the well-established concept that EMT is associated with tumor progression with the more recent hypothesis of migratory cancer stem cells (*19*, *20*). So how might this process be regulated in CSCs? Recent studies have implicated transcription factors, such as Zeb1 and -2 and Twist, which are known inducers of EMT (*21*), and a negative feedback pathway involving transforming growth factor–β (TGFβ) (*16*, *22*). So, changes in the surrounding microenvironment that influence expression of TGFβ family members as well as other cytokines expressed by mesenchymal stem cells or other cells in the microenvironment may influence both EMT and the reverse process of mesenchymal-to-epithelial transition, which is most likely critical for metastasis and colonization at distant sites (*23*). If true, then the CSC state may be transitory in certain circumstances, with tumor cells acquiring more of a stem-like phenotype upon stimulation with the appropriate environmental cues.

Studies of putative tumor stem cells have also served to highlight the potential clinical importance of the relationship between EMT and CSCs. For example, using the same subpopulation of tumorigenic breast cancer cells identified in (*10*), we reported the intrinsic resistance of these cells to chemotherapy studied in paired breast cancer biopsies (*24*). We also identified a TGFβ-like tumorigenic gene signature in a molecular subtype of human breast tumors characterized by expression of many mesenchymal-associated genes. Tumors resistant to conventional treatments were enriched for cells bearing this signature, and increased mesenchymal markers were observed in the posttreatment specimens. These data support a growing body of evidence for a mesenchymal-like phenotype in breast and possibly other solid tumors that may be responsible for invasion, metastases, and even treatment resistance.

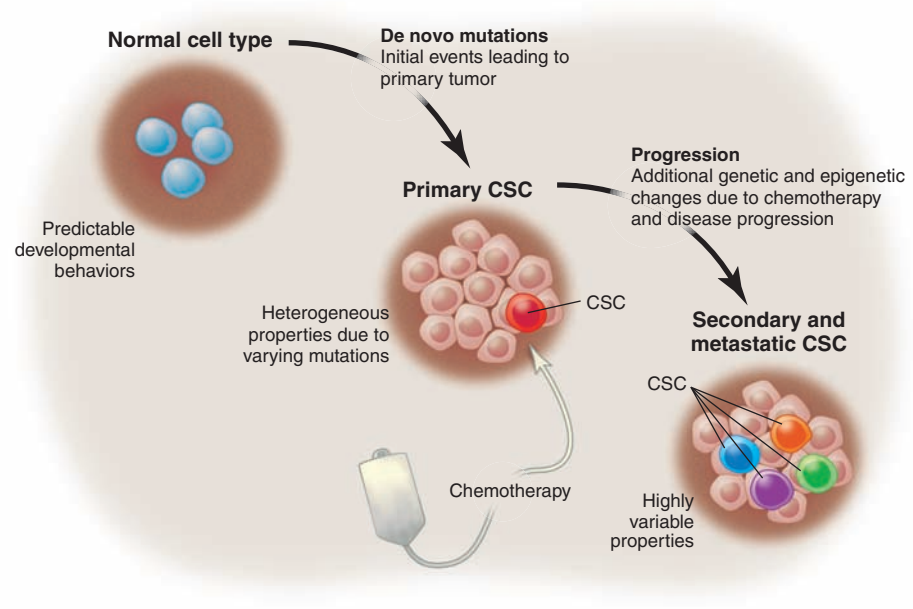

Fig. 3. Stages of CSC evolution. For many tumor types, the de novo mutations leading to primary CSC are varied. Thus, one would expect that the biology of primary CSCs may also be heterogeneous. Properties such as CSC frequency, cell-surface phenotype, and drug sensitivity may vary as a function of the specific mutations as well as the nature of the normal cell type in which the primary events occur. Next, neoplastic progression may occur either as a consequence of intrinsic tumor pathogenesis and/or challenge with chemotherapy. Selective pressures associated with neoplastic progression may lead to a higher frequency of functionally defined CSC in secondary or metastatic stages as well inter-patient and intra-patient variability of CSC properties.

To understand the relationship between CSCs and normal stem cells, bioinformatic studies compared the transcriptional programs in embryonic stem cells (ESCs) with adult tissue stem cells and human cancers (*21*). The ESC-like transcriptional program shown to be activated in diverse human epithelial cancers was a predictor of metastasis and death. The oncogene c-Myc, but not other oncogenes, appeared to be sufficient to activate this ESC-like program and could increase the fraction of CSCs. These authors concluded that "Activation of an ESC-like transcriptional program in differentiated adult cells may induce pathologic self-renewal characteristic of cancer stem cells." Further, Weinberg and colleagues have reported that a subset of ESC-associated transcriptional regulators are more frequently overexpressed in poorly differentiated tumors (*25*). These authors concluded "that these genes contribute to stem cell–like phenotypes shown by many tumors." Such data imply that some poor-prognosis tumors may possess higher frequencies of CSCs.

New Directions Resulting from the Study of CSCs

The controversy about CSCs has had the unexpected benefit of stimulating research in areas that previously were not the focus of cancer therapeutics. Pathways known to be important for stem-cell self-renewal, such as the Wnt, Notch, and Hedgehog (Hh) (which were previously identified as relevant to cancer as well as developmental biology), are now of increased interest because of their potential role in CSCs. For example, the first clinical trial using gamma-secretase inhibitors to block the Notch pathway in combination with chemotherapy in the neoadjuvant setting for breast cancer has recently been initiated. Another example is the recent report that Hh signaling is essential for maintenance of CSCs in myeloid leukemia (*26*).

The indication that there were distinctive subpopulations of cells within tumors with stem-like properties, which could be isolated using a variety of cell-surface markers, has led investigators to identify the specific signaling pathways in these cells as compared with the bulk tumor cells and their normal counterparts. Studies have suggested there might be selective effects of inhibiting the Pten/Akt and nuclear factor κB (NF-κB) pathways in LSCs as compared with normal hematopoietic stem cells (*27*–*29*). These studies have been extended to solid tumors with the observation that brain (and possibly breast) CSCs may be preferentially sensitive to Akt inhibitors (*30*). Studies of the mechanisms by which parthenolide, an NF-κB pathway inhibitor, might induce apoptosis in LSCs have suggested a role for increased reactive oxygen species (ROS) (*31*). In fact, recent studies have suggested an association of ROS levels and radioresistance in CSCs (*32*). Variability in the response of CSCs to conventional chemotherapy and radiation therapy have led to investigations of the differences in cell-cycle checkpoint and DNA-repair pathways in CSCs versus the bulk of tumor cells (*14*, *33*, *34*). An exciting new approach is the use of chemical genetic screens of drug libraries against CSCs with the possibility of discovering drugs to target CSCs that may already be approved for alternative clinical use (*35*). Another interesting approach will be to use synthetic lethal screens to search for new agents that may sensitize resistant tumor-cell subpopulations to conventional chemo- and radiation therapies (*36*). Finally, pharma and

biotech companies now have active programs to develop therapeutics so as to target many of these pathways.

Whether the CSC model is relevant to all cancers or not, it is clear that we need new approaches to target tumor cells that are resistant to current therapies and give rise to recurrence and treatment failure. Notwithstanding our ability to sequence the cancer genome(s) and to create personalized targeted therapies, it is apparent that combination therapies, which target the CSC subpopulation as well as the bulk of the tumor cells, will be required to effectively manage cancer treatment (*37*). One pressing need is the development of improved preclinical models to test these therapies because determining the appropriate doses and combinations as well as the order of addition of these agents will be critical for success in the clinic. The fact that these concepts are steadily making their way into the clinic is exciting and suggests that the recent interest in CSCs may yield beneficial outcomes in potentially unexpected ways.

References and Notes

1. T. Lapidot *et al.*, *Nature* **367**, 645 (1994).
2. J. E. Dick, *Blood* **112**, 4793 (2008).
3. J. E. Visvader, G. J. Lindeman, *Nat. Rev. Cancer* **8**, 755 (2008).
4. M. J. Bissell, M. A. Labarge, *Cancer Cell* **7**, 17 (2005).
5. A. Mantovani, *Nature* **457**, 36 (2009).
6. P. N. Kelly, A. Dakic, J. M. Adams, S. L. Nutt, A. Strasser, *Science* **317**, 337 (2007).
7. W. Guo *et al.*, *Nature* **453**, 529 (2008).
8. D. Bonnet, J. E. Dick, *Nat. Med.* **3**, 730 (1997).
9. S. J. Neering *et al.*, *Blood* **110**, 2578 (2007).
10. M. Al-Hajj, M. S. Wicha, A. Benito-Hernandez, S. J. Morrison, M. F. Clarke, *Proc. Natl. Acad. Sci. U.S.A.* **100**, 3983 (2003).
11. S. K. Singh *et al.*, *Nature* **432**, 396 (2004).
12. E. Quintana *et al.*, *Nature* **456**, 593 (2008).
13. R. W. Cho, M. F. Clarke, *Curr. Opin. Genet. Dev.* **18**, 48 (2008).
14. M. Zhang *et al.*, *Cancer Res.* **68**, 4674 (2008).
15. S. A. Mani *et al.*, *Cell* **133**, 704 (2008).
16. U. Burk *et al.*, *EMBO Rep.* **9**, 582 (2008).
17. C. Ginestier *et al.*, *Cell Stem Cell* **1**, 555 (2007).
18. P. C. Hermann *et al.*, *Cell Stem Cell* **1**, 313 (2007).
19. J. P. Thiery, *Nat. Rev. Cancer* **2**, 442 (2002).
20. T. Brabletz, A. Jung, S. Spaderna, F. Hlubek, T. Kirchner, *Nat. Rev. Cancer* **5**, 744 (2005).
21. D. J. Wong *et al.*, *Cell Stem Cell* **2**, 333 (2008).
22. P. A. Gregory, C. P. Bracken, A. G. Bert, G. J. Goodall, *Cell Cycle* **7**, 3112 (2008).
23. A. E. Karnoub *et al.*, *Nature* **449**, 557 (2007).
24. X. Li *et al.*, *J. Natl. Cancer Inst.* **100**, 672 (2008).
25. I. Ben-Porath *et al.*, *Nat. Genet.* **40**, 499 (2008).
26. C. Zhao *et al.*, *Nature* **458**, 776 (2009).
27. Q. Xu, S. E. Simpson, T. J. Scialla, A. Bagg, M. Carroll, *Blood* **102**, 972 (2003).
28. M. L. Guzman *et al.*, *Blood* **98**, 2301 (2001).
29. O. H. Yilmaz *et al.*, *Nature* **441**, 475 (2006).
30. C. E. Eyler *et al.*, *Stem Cells* **26**, 3027 (2008).
31. M. L. Guzman *et al.*, *Blood* **105**, 4163 (2005).
32. M. Diehn *et al.*, *Nature* **458**, 780 (2009).
33. S. Bao *et al.*, *Nature* **444**, 756 (2006).
34. W. A. Woodward *et al.*, *Proc. Natl. Acad. Sci. U.S.A.* **104**, 618 (2007).
35. P. Diamandis *et al.*, *Nat. Chem. Biol.* **3**, 268 (2007).
36. A. W. Whitehurst *et al.*, *Nature* **446**, 815 (2007).
37. W. A. Woodward, M. S. Chen, F. Behbod, J. M. Rosen, *J. Cell Sci.* **118**, 3585 (2005).

38. The authors thank W. Woodward, M. Zhang, Y. Li, M. Guzman, and J. Dick for their helpful comments and apologize to investigators for the failure to cite many other important contributions in this field because of space limitations. These studies were supported by NIH grants R37-CA16303 and R01-CA122206.

10.1126/science.1171837

REVIEW

Growth Factors, Matrices, and Forces Combine and Control Stem Cells

Dennis E. Discher,[1] David J. Mooney,[2] Peter W. Zandstra[3]

Stem cell fate is influenced by a number of factors and interactions that require robust control for safe and effective regeneration of functional tissue. Coordinated interactions with soluble factors, other cells, and extracellular matrices define a local biochemical and mechanical niche with complex and dynamic regulation that stem cells sense. Decellularized tissue matrices and synthetic polymer niches are being used in the clinic, and they are also beginning to clarify fundamental aspects of how stem cells contribute to homeostasis and repair, for example, at sites of fibrosis. Multifaceted technologies are increasingly required to produce and interrogate cells ex vivo, to build predictive models, and, ultimately, to enhance stem cell integration in vivo for therapeutic benefit.

Control over stem cell trafficking, survival, proliferation, and differentiation within a complex in vivo milieu is extremely challenging. In studies of animal models and humans where stem cell engraftment has been quantified after injection, only a few percent of cells remain after several days or weeks [e.g. (*1*)]. Many clinical trials are nonetheless under way, particularly with adult bone marrow–derived mesenchymal stem cells (MSCs), which are being investigated as treatments for diseases of nonhematopoietic tissues—primarily, myocardial infarction and peripheral ischemia (*2*). Although U.S. Food and Drug Administration approval for human testing of cells differentiated from embryonic stem cells (ESC) is a recent landmark for the field (*3*), two widely reported clinical cases highlight some of the technical opportunities and challenges with stem cells in soft tissue repair. One patient in Spain was successfully transplanted with a re-engineered trachea in 2008; donor trachea was first decellularized by using a detergent (without denaturing the collagenous matrix), and then, this scaffold was recellularized in a rotating bioreactor using MSC-derived cartilage-like cells (*4*). Long-term safety and efficacy will be important to monitor and understand. Indeed, in a second case, the cerebellum of a boy with ataxia telangiectasia (AT) was injected with human fetal neural stem cells (NSCs), and 4 years later, a glio-neuronal brain tumor of stem cell origin was found (*5*). Upon implantation, stem cells and their derived lineages encounter a multitude of cues that can influence cell fate. Efforts to parse the molecular mechanisms for translation from bench to clinic will increasingly benefit from a wide range of new and established technologies. Here we briefly review salient features of microenvironments, mechanics, and material systems that are being pursued to control stem cells for both basic insight and application.

Niche Interactions and in Vitro Designs

The niche is the in vivo microenvironment that regulates stem cell survival, self-renewal, and differentiation. Key niche components and interactions include growth factors, cell-cell contacts, and cell-matrix adhesions (Fig. 1A). The interplay of these niche factors is particularly important to comprehend if any desired stem cell response is to be made robust for therapy, i.e., resistant to the many types of perturbations encountered by cells delivered in vivo.

Growth factors added to culture or secreted by stem cells and nearby niche cells are often potent in their effects on cell fate, and so, in embryonic development, growth factors are tightly regulated in space and time (*6*). In culture, one means of controlling niche interactions in two dimensions is with micropatterns of extracellular matrix (ECM) islands, which limit diffusion of secreted growth factors within and between islands and also limit the modulating effects of matrix and cell contacts. With human ESCs (hESCs), for ex-

[1]Biophysical Engineering and Nanobiopolymers Laboratory, School of Engineering and Applied Science, University of Pennsylvania, Philadelphia, PA 19104, USA. E-mail: discher@seas.upenn.edu [2]Laboratory for Cell and Tissue Engineering, School of Engineering and Applied Sciences, Harvard University, Cambridge, MA 02138, USA. E-mail: mooneyd@seas.harvard.edu [3]Stem Cell Bioengineering Laboratory, Institute of Biomaterials and Biomedical Engineering, Centre for Biomedical and Biomolecular Research, University of Toronto, Toronto, ON M5S 3E1, Canada. E-mail: peter.zandstra@utoronto.ca

ample, islands of ECM made by microstamping onto a substrate (Fig. 1B) have demonstrated a minimal island size for maintenance and expansion of the pluripotent state; the mechanism is based in part on an antagonism between two different members of the transforming growth factor–β (TGFβ) superfamily (*7*). Such factors can affect the secreting cell (autocrine) or other cells (paracrine), and so, for spatiotemporal control of concentrations, microfluidic devices have been made that might need to come into contact before a given cell type will respond to locally secreted factors.

The ECM not only mediates cell attachment and presents key cues to cells (see below), but it often also binds growth factors and so limits their diffusion. This can be mimicked by synthetically tethering a growth factor to a substrate (*9*), which has been used to enhance survival of MSCs (*10*) and to regulate select transcriptional networks in mouse ESCs (mESCs) (*11*).

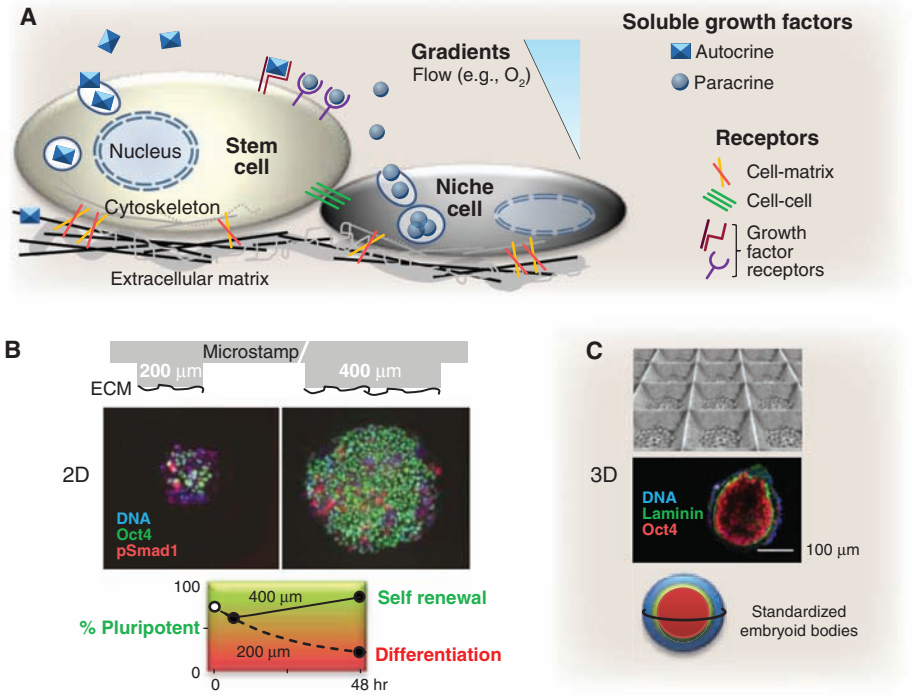

Fig. 1. Stem cell niche and designs. (**A**) Soluble and matrix-bound factors combine with cell-cell contact, cell-matrix adhesion, and gradients to direct cell fate. (**B**) Substrates with micropatterns of ECM control the size of ESC colonies and pluripotency based on immunofluorescence for the transcription factor Oct4 (in two dimensions, 2D) (*7*). (Plot) Large islands increase the pluripotent population; small islands inhibit with a time constant of 24 hours. (**C**) Substrates with microwells help to standardize the diameter of quasi-spherical embryoid bodies (*15*). Cells and ECM (laminin) exhibit a spherically symmetric pattern (in three dimensions, 3D), with pluripotent cells in the inside.

continuously wash away secreted factors while perfusing known concentrations of active factors. With human NSCs (hNSCs), for example, microfluidic control of growth factor within a single culture chamber showed very clearly that the amount of proliferation and the fraction of differentiated cells follow a strict inverse relation (*8*). Indeed, most terminally differentiated cells do not proliferate, whereas stem cells and progenitor cells do, but this distinction can be difficult to sort out in standard culture, where most cells crawl around semirandomly, dynamically changing both exposure to any gradients in growth factor and contact with other cells. In order to assess directly any modulating role of cell-cell contacts in soluble-factor signaling, micromechanical devices have been made to move cells reversibly into contact (*7*). The results suggest that different cell types

Adhesion of MSCs and ESCs to matrix or other cells is essential for viability—individual cells do not survive in suspension, but adhesive signals might be controlled just as well or better with synthetic mimics. Such materials could conceivably replace nonhuman niche cells or animal-derived matrix products (e.g., Matrigel) in common use with human stem cells. In an early combinatorial study with hESCs and muscle-derived stem cells, rigid spots of 576 different combinations of 25 different acrylate-based polymers were arrayed and found to combine with soluble factors in exerting wide-ranging effects on cell attachment, proliferation, and lineage induction (*12*). For three-dimensional cultures, cross-linked hyaluronic acid (HA) hydrogels proved unique in supporting hESC growth in undifferentiated masses (i.e., embryoid bodies), possibly because HA is a prominent ECM polymer in embryonic development (*13*). Embryoid bodies can also be sculpted to well-controlled diameters with polymer microwells and other methods (Fig. 1C) (*14*, *15*). Size control is important to minimize gradients in oxygen and other physical or chemical factors that regulate stem cell fate (*16*). Nonetheless, cell segregation and differentiation within embryoid bodies (and embryos, too) still need to be understood more deeply, with mechanisms likely rooted in the multiple pathways that a cell uses to sense its microenvironment (*17*).

Forces, Matrix Elasticity, and Fibrosis

Whether in vitro or in vivo, cells generate force and are often exposed to force—and both can influence stem cell fates. The very first stages of cell differentiation in embryogenesis are indeed blocked after knockout of ubiquitous force-generating myosins (*18*). Flowing fluids also generate forces on any object in the flow (you feel such forces when you hold your hand out of a car window), and fluid forces typical of blood flow have been found to initiate an endothelial program in isolated ESCs (*19*). Mechanical deformations or strains are also common in solid tissues (e.g., beating heart or dilating arteries), and imposing substrate strains of just 5% can induce MSC differentiation toward smooth muscle (*20*). Mechanistically, a force f will strain any physically linked protein and affect the kinetic rate k of a protein-protein interaction or of a conformation change (*21*), as

$$k \sim k_o \exp(f/f_o)$$

Stem cells may well have more than the typical ensemble of force-coupled signaling pathways as a means to sensitize themselves to microenvironments that range—physically—from flowing fluids and strained tissues to solid tissues of varied elasticity (Fig. 2A). Indeed, when MSCs are grown on firm gels that mimic the elasticity of muscle and that are coated with collagen I, myogenic markers are upregulated, whereas when MSCs are grown on rigid gels that mimic precalcified bone, the cells appear osteogenic (*21*). Added induction factors can either augment or oppose this programming of MSCs by matrix, whereas cell lines that are already committed to muscle or bone appear less responsive to the same cues. With NSCs, neuron differentiation is favored on soft matrices that mimic normal brain, whereas differentiation into glia is promoted on harder matrices that typify glial scars (*22*). These latter examples—and topographical patterns as well (*23*)—suggest not only physical contributions to differentiation but also that carefully made materials can help prime the expansion of specific progenitors.

In vivo, when stem cells egress from their niche into the circulation (*24*) or when stem cells are injected intravenously as part of a therapeutic regimen, fluid forces push and drag the cells (Fig. 2A); fluid forces oppose adhesion to the vessel wall, whereas tissue entry requires stem cell mo-

tility and might benefit from the high deformability of stem cell nuclei (*25*). The processes are similar to those widely studied with leukocytes and metastatic cancer cells [e.g., (*26*)]. The latter comparison is especially intriguing in that metastatic "capture" depends strongly on at least one matrix fibrosis factor (lysyl oxidase, which catalyzes cross-linking of collagen), and fibrotic scarring is a challenge common to many regenerative goals with stem cells.

Recent mechanical measurements of fibrotic scars that develop after an acute myocardial infarction (*27*) or with more chronic stimuli (*28*) show that the fibrotic tissue is locally rigidified by at least several-fold compared with normal tissue. Atomic force microscopy probing gives cell-scale elasticities of $E \approx 20$ to 60 kPa for fibrotic wounds (*27*, *29*), which exceeds E for soft tissues and overlaps with cartilage and precalcified bone (Fig. 2B).

Rigid fibrotic tissue can, in and of itself, contribute a homing signal. As seen from the use of various gel matrices with well-controlled elasticity and nonlimiting ligand density, most, if not all, cells are found to adhere, to spread, to assemble their cytoskeleton (Fig. 2C), and to anchor more strongly to stiff substrates compared with soft substrates (*30*). In a gradient of elasticity, cells therefore accumulate on stiffer substrates in a process called "durotaxis" (*31*), which might constitute a biophysical basis for why MSCs home to sites of injury and fibrosis (*1*). Matrix can also be a more potent differentiation cue for MSCs than standard induction cocktails (*32*, *33*). Whereas MSCs in an infarct scar in mice have been reported to generate bone in the heart (*34*), MSCs are also often found to attenuate scar formation (*1*, *27*). Recent models of a "scar in a dish" have shown that the well-studied differentiation of fibroblasts to myofibroblasts requires both a stiff matrix ($E >$ 20 kPa) and TGFβ, with growth factor release from the ECM dependent on cell contraction–driven unfolding of the ECM complex that sequesters the TGFβ (*29*). Although growth factor regulation by matrix and cell force has yet to be reported for stem cells, developmentally critical cell-cell interactions are hypothesized to mediate forced unfolding of another type of conserved membrane-based signaling system involving Notch. Force on this receptor exposes a cryptic site that is cleaved by protease to liberate a Notch fragment, and this fragment diffuses into the nucleus to ultimately affect transcription (*35*).

Materials pervade stem cell biology, often unintentionally. Isolation and growth of stem cells on rigid tissue culture plastic tend to promote spreading of cells rich in actin-myosin stress fibers. With similarly rigid surfaces, if the area of MSC contact is controlled with adhesive patterns (*36*), it is found that mixed induction cocktails that induce both fat and bone lead to adipogenesis on small islands (which minimize matrix contact) and osteogenesis on large islands (which maximize contractile anchorage). Mechanisms for sensing of matrix as well as for stem cell trafficking, continue to be clarified, but growth factor– and integrin-coupled roles for Rac and Rho in stem cell motility, contractility, and anchorage appear clear (Fig. 2C). In hematopoietic stem cells (HSCs), Rac isoforms are key regulators of engraftment and marrow retention, with Rac activation occurring via β_1-integrin adhesion to matrix coupled to stimulation by factors including stromal cell–derived factor (SDF-1), which binds ECM and a heterotrimeric guanine nucleotide–binding protein–coupled chemokine receptor (CXCR4) that is conserved in development (*37*). A similar, prototypical coupling of anchorage signaling pathways is also revealed in the phosphoproteome of MSCs induced by growth factors (*38*).

Consistent with the strict requirement for nonmuscle myosin in differentiation within embryos (*18*), pharmacological inhibition of myosin in MSCs blocks all lineages on both rigid and compliant substrates (*21*, *36*), with measurable effects on folding and assembly of the proteome (*39*). Inhibition of the Rho kinase effector, ROCK, resulting in deactivation of myosin, selectively blocks rigidity-directed osteogenesis (*21*, *36*), although not on compliant substrates (*21*). Inhibition of ROCK in dissociated hESCs (*40*) also dramatically enhances survival; no effects on ESC differentiation have been reported. Such

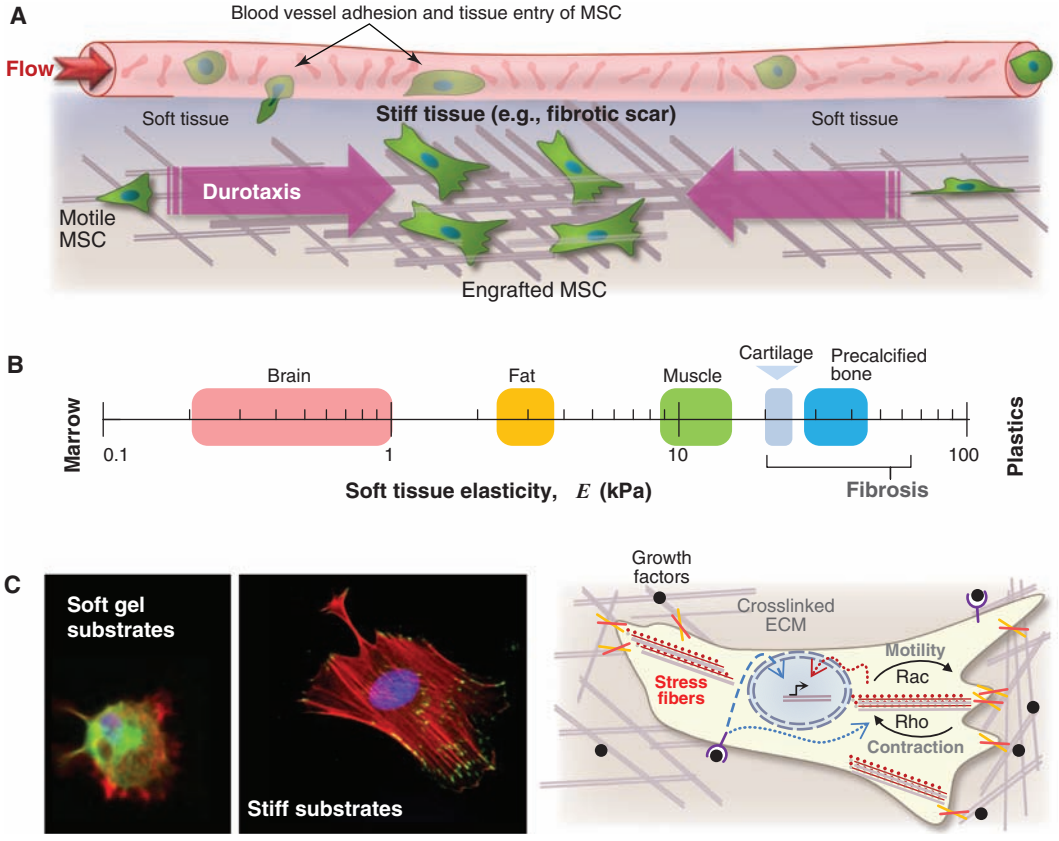

Fig. 2. Forces and ECM in stem cell trafficking. (**A**) To extravasate from the circulation and invade a tissue, stem cells must adhere strongly to the vessel wall and withstand high flow forces. Within a tissue, additional physical factors can direct motile cells, including durotaxis into stiff, fibrotic regions of tissue where cells engraft. (**B**) Soft tissue elasticity scale ranging from soft brain (*72*), fat (*73*), and striated muscle (*21*), to stiff cartilage [$E \approx 20$ to 30 kPa at the scale of adhesions (*74*, *75*)] and precalcified bone (*21*). (**C**) In vitro substrates that mimic soft and stiff tissue microenvironments (left) show that cells anchor more strongly to stiff substrates, building focal adhesions and actin-myosin stress fibers. (Right) Matrix adhesion and growth factors influence both cell physiology and lineage. Signals from growth factor receptors not only propagate into the nucleus (dashed blue arrow) and direct transcription (black arrow), but also affect Rho-GTPase (guanosine triphosphatase) activity (dotted blue arrow). Rac drives motility forward, and Rho regulates contraction of stress fibers (red), and both can also influence gene expression (dotted red arrow).

pharmacological perturbations of the cytoskeleton have been known for years to affect mesenchymal lineages such as chondrocytes (*41*), but effects can couple to matrix. The recent success in trachea reconstruction (*4*) likely benefited from suitable matrix signals for chondrogenesis in the detergent-decellularized donor trachea. Although detergents might preserve tissue mechanics, not all tissue regeneration can use such methods.

Physical perspectives on normal and diseased tissues help to generate new hypotheses. As a leading cause of death, heart disease is a principal target of stem cell therapies (*2*), but cardiogenesis involves a complex interplay of mechanochemical factors. Embryo-derived cardiomyocytes maintain their spontaneous beating on substrates with elasticity less than or equal to that of normal heart tissue, but the cells stop beating on rigid matrices that mechanically mimic a fibrotic scar (*42*). Studies of neonatal cardiomyocytes further show that ROCK inhibition selectively blocks cell dysfunction on rigid substrates (*43*). Therefore, future experiments with cardiomyocytes derived from ESCs or induced pluripotent stem cells require close attention to the matrix microenvironment.

Synthetic Niches in Vivo

An original assumption in the stem cell field was that transplanted cells would directly participate in the building of tissues; however, it is now clear that paracrine effects are also important (*44*). Advanced clinical applications of MSCs are seen with immune and/or inflammatory conditions including Crohn's disease of the bowel and graft versus host disease (GVHD), which can result from bone marrow transplants (*1*). The MSC treatments do not exploit tissue-building abilities but, instead, appear to exert immunomodulatory functions that extend to wound-healing and reduced scar formation. These applications serve to highlight again the importance of tight control over stem cell purity and differentiation, a need for strategies to enhance survival and engraftment of transplanted cells, and the possibility that distinct strategies may be useful for transplantation, depending on the specific functional outcome(s) sought.

An appealing approach to address some of the challenges involved in stem cell transplantation is the development and use of materials systems that create specialized niches for the cells. Limitations of conventional cell infusions or injections include poor delivery and retention of cells at the intended site or cell death due to loss of anchorage (anoikis). A variety of naturally derived materials and synthetic polymers are currently in development as vehicles for stem cell transplantation because of their ability to provide adhesion for interacting cells; control over the presentation of adhesion sites (e.g., density of peptides to bind integrins) by these materials improves transplanted cell survival and participation in tissue regeneration (*45*, *46*). Material architecture can be used to further pattern the structure of tissues (Fig. 3, A and B) formed from interacting stem cells (*47*), an approach that has been used to form tissue patches to enhance cardiac function in animal models (*48*) and to format a new mandible in a human patient (*49*). There has not yet been a demonstration that substrate mechanical properties regulate stem cell fate in vivo, although the demonstration that gel mechanical properties regulate capillary formation in vivo (*50*) supports this concept. One complication is that the mechanical properties and degradation rates of synthetic niches are typically coupled, and the degradation rate has been demonstrated to enhance bone regeneration by transplanted stem cells (*51*).

Growth factors or cytokines can be provided in a localized manner either with controlled release particle systems [e.g., (*52*)] or from the material scaffolds used as synthetic niches. Cardiomyocyte function has been dramatically

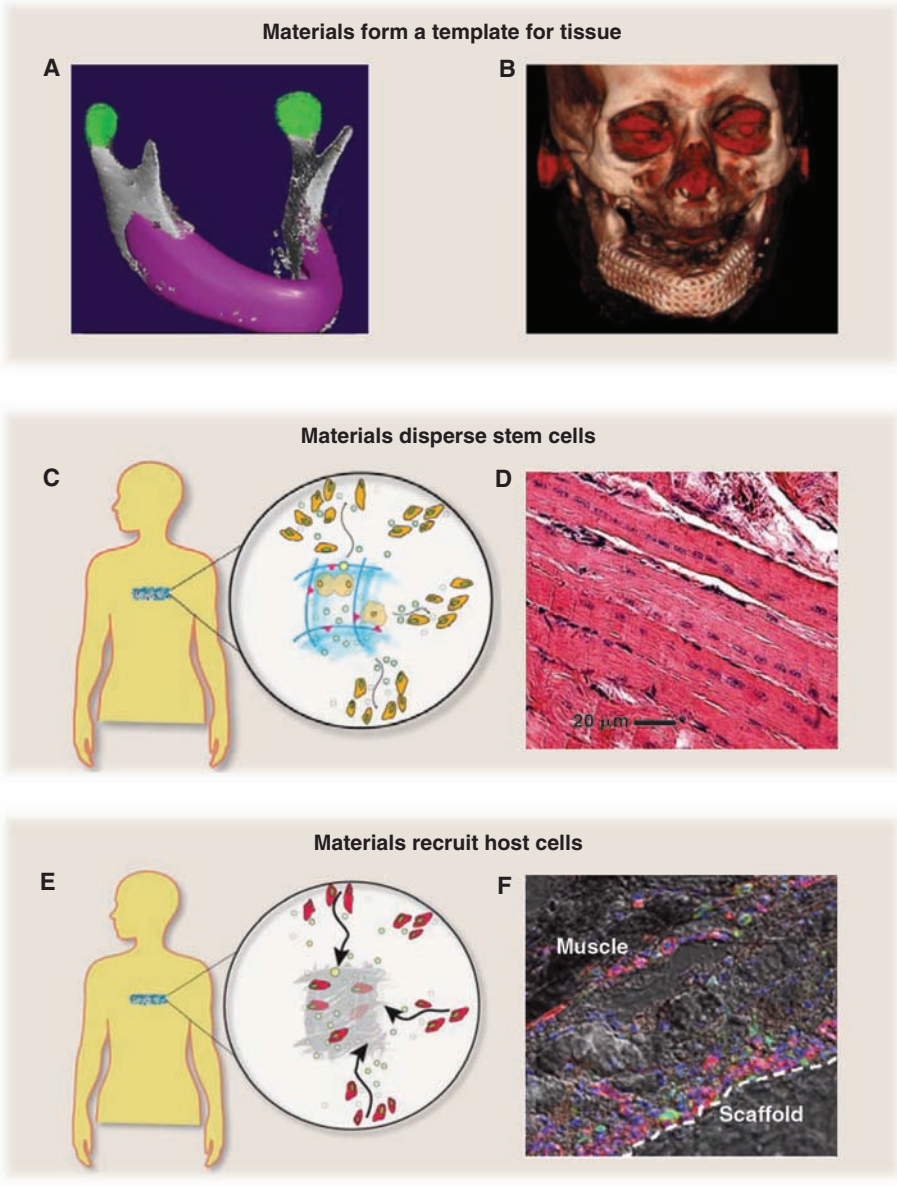

Fig. 3. Synthetic niches in vivo. (**A**) Materials can fill a specific anatomic defect (pink) to localize transplanted cells and serve as a scaffolding for formation of new tissue. (**B**) A mandible formed in a patient used a metal and polymer structure that was seeded with MSCs and cytokines (*49*). (**C**) A designed material niche maintains stem cell viability and proliferation, while promoting outward migration at an appropriate stage of differentiation. (**D**) Dispersion of stem cells from a niche into regenerating skeletal muscle (*61*). (**E**) Recruitment of host stem cells for subsequent homing to sites of tissue injury. (**F**) Mice with green fluorescent protein–labeled bone marrow-derived cells (green) show regenerating muscle infiltrated with cells that are dual-labeled for endothelial cell marker CD31 (red), which indicates neovascularization (*76*).

improved by coordinated release of insulin-like growth factor from the transplantation vehicle (*46*), as has bone formation by mesenchymal stems with release of TGFβ family proteins (*53*). However, full regeneration will only result from mechanical, vascular, and neural integration of the regenerating and surrounding tissues. Materials presenting angiogenic factors can enhance local vascularization (*54*) and can increase the survival of transplanted stem cells and subsequent regeneration (*55*). Materials may also be used as carriers of ESC-derived endothelial cell progenitors that form new vascular networks (*56*). Nervous system integration can also be enhanced by materials that provide gradients of neurotrophic factors (*57*) and by implantation adjacent to a transected nerve (*58*).

Instead of anchoring transplanted cells to a specific location with a material, stem cell niches might be mimicked to regulate the proliferation, differentiation, and dispersal of daughter cells into the surrounding tissue to participate in regeneration or to provide trophic factors over a large volume (Fig. 3, C and D). Because the stage of cell differentiation, exposure to morphogens and cytokines, and implant site conditions all regulate stem cell function after transplantation (*59*, *60*), this niche approach seems broadly useful. The ability of satellite cell–derived myoblasts to promote skeletal muscle regeneration after injury was recently enhanced with a material that activated resident cells but prevented terminal differentiation until the cells exited the material (*61*). This approach may be most useful in the wide dispersion of stem cell populations that secrete trophic factors that influence host cells. Material-directed endothelial progenitors will even orchestrate regional revascularization and salvage of necrotic limbs (*62*).

Potentially useful cell populations already exist in the body, and attracting these cells to a desired anatomic site (Fig. 3, E and F) has the potential to provide new therapeutic options. Cost and complexity should be reduced compared with approaches that use ex vivo bioreactors. With bone repair for example, implantation of simple biomaterials without growth factors has shown how potent the in vivo milieu can be in generating native-like bone (*63*), in spite of risks of implantation injury. Mobilization of endothelial progenitor cells from bone marrow with either granulocyte colony-stimulating factor or drugs such as statins is also being tested in ischemic conditions (*1*).

Systems Biology in Translation

Fate decisions in vivo with HSCs and MSCs appear tightly regulated by physiological demand. In addition to all of the extracellular cues highlighted earlier, stimulus-response can be complicated by tissue-specific patterns of ligand and receptor expression (*64*), as well as by sequential autocrine and paracrine inductive loops (*65*) that arise as cell populations develop and adapt (*66*). Genome-wide studies (*67*) and mathematical models (*68*) have begun to generate relevant network models, but only a few attempts have been made to unravel intercellular signaling (*69*, *70*). Cells (as opposed to proteins or genes) could be considered nodes in networks that are linked by cell contact, by shared matrix, and by secreted factors. Integrating immune cells, particularly natural killer cells and macrophages, into such networks will be important to understand how implanted cells either engraft and contribute to tissue or else are cleared (*71*).

Stem cell studies beyond those cited offer important perspectives on the opportunities and challenges that lie ahead. Soluble factor strategies combined with attention to cell adhesion and mechanics seem likely to synergize with both synthetic material niches and reengineered, tissue-derived matrices to play essential roles in making stem cell therapies safe, efficacious, and routine.

References and Notes

1. M. F. Pittenger, B. J. Martin, *Circ. Res.* **95**, 9 (2004).
2. NIH, http://clinicaltrials.gov (2009).
3. J. Alper, *Nat. Biotechnol.* **27**, 213 (2009).
4. P. Macchiarini *et al.*, *Lancet* **372**, 2023 (2008).
5. N. Amariglio *et al.*, *PLoS Med.* **6**, e1000029 (2009).
6. C. E. Murry, G. Keller, *Cell* **132**, 661 (2008).
7. R. Peerani *et al.*, *EMBO J.* **26**, 4744 (2007).
8. B. G. Chung *et al.*, *Lab Chip* **5**, 401 (2005).
9. E. E. Hui, S. N. Bhatia, *Proc. Natl. Acad. Sci. U.S.A.* **104**, 5722 (2007).
10. V. H. Fan *et al.*, *Stem Cells* **25**, 1241 (2007).
11. K. Alberti *et al.*, *Nat. Methods* **5**, 645 (2008).
12. D. G. Anderson, S. Levenberg, R. Langer, *Nat. Biotechnol.* **22**, 863 (2004).
13. S. Gerecht *et al.*, *Proc. Natl. Acad. Sci. U.S.A.* **104**, 11298 (2007).
14. T. C. McDevitt, S. P. Palecek, *Curr. Opin. Biotechnol.* **19**, 527 (2008).
15. M. D. Ungrin, C. Joshi, A. Nica, C. Bauwens, P. W. Zandstra, *PLoS One* **3**, e1565 (2008).
16. K. Parmar, P. Mauch, J. A. Vergilio, R. Sackstein, J. D. Down, *Proc. Natl. Acad. Sci. U.S.A.* **104**, 5431 (2007).
17. A. J. Engler, P. O. Humbert, B. Wehrle-Haller, V. M. Weaver, *Science* **324**, 208 (2009).
18. M. A. Conti, S. Even-Ram, C. Liu, K. M. Yamada, R. S. Adelstein, *J. Biol. Chem.* **279**, 41263 (2004).
19. K. Yamamoto *et al.*, *Am. J. Physiol. Heart Circ. Physiol.* **288**, H1915 (2005).
20. K. Kurpinski, J. Chu, C. Hashi, S. Li, *Proc. Natl. Acad. Sci. U.S.A.* **103**, 16095 (2006).
21. A. J. Engler, S. Sen, H. L. Sweeney, D. E. Discher, *Cell* **126**, 677 (2006).
22. K. Saha *et al.*, *Biophys. J.* **95**, 4426 (2008).
23. M. J. Dalby *et al.*, *Nat. Mater.* **6**, 997 (2007).
24. S. C. Pitchford, R. C. Furze, C. P. Jones, A. M. Wengner, S. M. Rankin, *Cell Stem Cell* **4**, 62 (2009).
25. J. D. Pajerowski, K. N. Dahl, F. L. Zhong, P. J. Sammak, D. E. Discher, *Proc. Natl. Acad. Sci. U.S.A.* **104**, 15619 (2007).
26. J. T. Erler *et al.*, *Nature* **440**, 1222 (2006).
27. M. F. Berry *et al.*, *Am. J. Physiol. Heart Circ. Physiol.* **290**, H2196 (2006).
28. P. C. Georges *et al.*, *Am. J. Physiol. Gastrointest. Liver Physiol.* **293**, G1147 (2007).
29. P. J. Wipff, D. B. Rifkin, J. J. Meister, B. Hinz, *J. Cell Biol.* **179**, 1311 (2007).
30. D. E. Discher, P. Janmey, Y. L. Wang, *Science* **310**, 1139 (2005).
31. C. M. Lo, H. B. Wang, M. Dembo, Y. L. Wang, *Biophys. J.* **79**, 144 (2000).
32. K. P. Bennett *et al.*, *BMC Genomics* **8**, 380 (2007).
33. D. S. W. Benoit, M. P. Schwartz, A. R. Durney, K. S. Anseth, *Nat. Mater.* **7**, 816 (2008).
34. M. Breitbach *et al.*, *Blood* **110**, 1362 (2007).
35. R. Kopan, M. X. G. Ilagan, *Cell* **137**, 216 (2009).
36. R. McBeath, D. M. Pirone, C. M. Nelson, K. Bhadriraju, C. S. Chen, *Dev. Cell* **6**, 483 (2004).
37. D. A. Williams, Y. Zheng, J. A. Cancelas, *Methods Enzymol.* **439**, 365 (2008).
38. I. Kratchmarova, B. Blagoev, M. Haack-Sorensen, M. Kassem, M. Mann, *Science* **308**, 1472 (2005).
39. C. P. Johnson, H. Y. Tang, C. Carag, D. W. Speicher, D. E. Discher, *Science* **317**, 663 (2007).
40. K. Watanabe *et al.*, *Nat. Biotechnol.* **25**, 681 (2007).
41. N. C. Zanetti, M. Solursh, *J. Cell Biol.* **99**, 115 (1984).
42. A. J. Engler *et al.*, *J. Cell Sci.* **121**, 3794 (2008).
43. J. G. Jacot, A. D. McCulloch, J. H. Omens, *Biophys. J.* **95**, 3479 (2008).
44. M. Gnecchi, Z. P. Zhang, A. G. Ni, V. J. Dzau, *Circ. Res.* **103**, 1204 (2008).
45. E. Alsberg *et al.*, *J. Dent. Res.* **82**, 903 (2003).
46. M. E. Davis *et al.*, *Circulation* **111**, 442 (2005).
47. R. Langer, J. P. Vacanti, *Science* **260**, 920 (1993).
48. W. H. Zimmermann *et al.*, *Nat. Med.* **12**, 452 (2006).
49. P. H. Warnke *et al.*, *Lancet* **364**, 766 (2004).
50. A. Mammoto *et al.*, *Nature* **457**, 1103 (2009).
51. C. A. Simmons, E. Alsberg, S. Hsiong, W. J. Kim, D. J. Mooney, *Bone* **35**, 562 (2004).
52. N. Takehara *et al.*, *J. Am. Coll. Cardiol.* **52**, 1858 (2008).
53. H. Park, J. S. Temenoff, Y. Tabata, A. I. Caplan, A. G. Mikos, *Biomaterials* **28**, 3217 (2007).
54. D. Trentin, H. Hall, S. Wechsler, J. A. Hubbell, *Proc. Natl. Acad. Sci. U.S.A.* **103**, 2506 (2006).
55. Y. C. Huang, D. Kaigler, K. G. Rice, P. H. Krebsbach, D. J. Mooney, *J. Bone Miner. Res.* **20**, 848 (2005).
56. S. Levenberg *et al.*, *Nat. Biotechnol.* **23**, 879 (2005).
57. T. A. Kapur, M. S. Shoichet, *J. Biomed. Mater. Res. A* **68**, 235 (2004).
58. V. Dhawan, I. F. Lytle, D. E. Dow, Y. C. Huang, D. L. Brown, *Tissue Eng.* **13**, 2813 (2007).
59. C. A. Collins *et al.*, *Cell* **122**, 289 (2005).
60. M. A. Laflamme *et al.*, *Nat. Biotechnol.* **25**, 1015 (2007).
61. E. Hill, T. Boontheekul, D. J. Mooney, *Proc. Natl. Acad. Sci. U.S.A.* **103**, 2494 (2006).
62. E. A. Silva, E. S. Kim, H. J. Kong, D. J. Mooney, *Proc. Natl. Acad. Sci. U.S.A.* **105**, 14347 (2008).
63. M. M. Stevens *et al.*, *Proc. Natl. Acad. Sci. U.S.A.* **102**, 11450 (2005).
64. Y. Kluger *et al.*, *Proc. Natl. Acad. Sci. U.S.A.* **101**, 6508 (2004).
65. K. A. Janes, D. A. Lauffenburger, *Curr. Opin. Chem. Biol.* **10**, 73 (2006).
66. D. C. Kirouac, P. W. Zandstra, *Curr. Opin. Biotechnol.* **17**, 538 (2006).
67. F. J. Muller *et al.*, *Nature* **455**, 401 (2008).
68. V. Chickarmane, T. Enver, C. Peterson, *PLoS Comp. Biol.* **5**, e1000268 (2009).
69. Z. Frankenstein, U. Alon, I. R. Cohen, *Biol. Direct* **1**, 32 (2006).
70. M. Rendl, L. Lewis, E. Fuchs, *PLoS Biol.* **3**, e331 (2005).
71. K. Takenaka *et al.*, *Nat. Immunol.* **8**, 1313 (2007).
72. L. A. Flanagan, Y. E. Ju, B. Marg, M. Osterfield, P. A. Janmey, *Neuroreport* **13**, 2411 (2002).
73. P. N. Patel, C. K. Smith, C. W. Patrick, *J. Biomed. Mater. Res. A* **73**, 313 (2005).
74. M. Stolz *et al.*, *Nat. Nanotechnol.* **4**, 186 (2009).
75. F. Guilak *et al.*, *Ann. Biomed. Eng.* **33**, 1312 (2005).
76. C. Fischbach *et al.*, *Proc. Natl. Acad. Sci. U.S.A.* **106**, 399 (2009).

77. Grants from the NIH and NSF are very gratefully acknowledged. Images of MSCs in Fig. 2C courtesy of A. Zajac (University of Pennsylvania). Assistance of E. Silva (Harvard) with Fig. 3 is acknowledged.

10.1126/science.1171643

The David Starr Jordan Prize
For Innovative Contributions to the Study of
Evolution, Ecology, Population and Organismal Biology

In 1986, Cornell, Indiana and Stanford Universities established a joint endowment to fund a prize in honor of David Starr Jordan, a scientist, educator and institution builder of enormous influence on higher education in the United States who had important ties to each of these universities. The prize is international in scope and presented approximately every three years to a young scientist (40 years of age or less) who is making novel innovative contributions in one or more areas of Jordan's interest: evolution, ecology, population and organismal biology.

The intent of this prize is to recognize young scientists who are making research contributions likely to redirect the principal foci of their fields. In addition to a cash award, the recipient will receive a commemorative medal, will attend an awards ceremony, visit each of the sponsoring institutions and give scholarly presentations of his/her work. The selection of the prize winner will be made by a committee composed of representatives from each of the three institutions.

The sixth David Starr Jordan Prize will carry a prize of $20,000.00 and will be announced in Fall of 2009. This year the award ceremony will be held at Cornell University.

Nomination forms are posted on the David Starr Jordan Prize Website (www.davidstarrjordan.org). Nomination forms with supporting materials should be submitted by email. Questions should be directed to:

Dr. William L. Crepet, Chair
Plant Biology Department
412 Mann Library Building
Cornell University
Ithaca, New York 14853
(607-255-2131 - FAX 607-255-5407) - email WLC1@cornell.edu

All nomination materials must be received prior to August 15, 2009.
For more information including a list of previous prize winners and their accomplishments, visit: **www.davidstarrjordan.org**.

Competitive Interactions Between Cells: Death, Growth, and Geography

Laura A. Johnston

Competitive interactions between cells are the basis of many homeostatic processes in biology. Some of the best-described cases of competition between cells occur in *Drosophila*: cell competition, whereby somatic cells within a growing epithelium compete with one another for contribution to the adult, and stem cell competition, in which germline or somatic stem cells vie for residency in the niche. Both types of competition are conserved physiological processes, with much to tell us about how cellular neighborhoods influence cell behavior, and have importance to stem cell biology, regeneration and transplantation, and cancer.

Competition is pervasive at every level of life—in ecology, economics, between countries and states, and in families—and helps to determine order, status, and survival. Competition also occurs at a cellular level, where it plays roles in tissue homeostasis, organ size control, and stem cell maintenance. In this Review, I focus on two examples of competition currently under intense study: cell competition, which occurs between somatic cells within a growing epithelium, and niche competition, between either germline or somatic stem cells. Although the ultimate fate of the "winners" and "losers" of each type of competition differs, both competitive processes are local and both can alter a cell's contribution to the adult. Competitive interactions provide a subtle yet powerful mechanism that senses and eliminates vulnerable, mispatterned, or potentially dangerous cells during normal tissue growth. Much of the work I discuss is carried out in *Drosophila* because of the genetic advantages this organism provides. However, both cell competition and niche competition appear to be ancient processes, occurring in diverse animals, and are relevant to regeneration and transplantation biology and to cancer.

Cell Competition: A Homeostatic Mechanism

Cell competition occurs when, within a growing tissue, two cell populations with different metabolic properties or growth rates confront each other, and results in growth of the stronger population at the expense of the weaker. It was discovered in the early 1970s when researchers used dominant, viable, slow-growing mutants, deficient in a ribosomal protein (Rp)–encoding gene [collectively known as *Minutes* (*1*)], to study cell lineages in *Drosophila*. Using mitotic recombination and genetic tricks to follow growth of marked cells, they generated mosaics where clones of wild-type (+/+) cells grew in a background of *Minute* (*M*/+) cells and unexpectedly found that the wild-type cells could overtake half (but never more than half) of the wing (*2*). Two aspects of this discovery were remarkable: First, the wild-type cells colonized areas of the wing that would have been filled by the *M*/+ cells, which suggests that the two cell populations—born from the same mother—competed for space in the wing; second, that expansion of the wild-type population was limited by an invisible but bona fide boundary dividing the wing into two "compartments" of cells with different developmental ancestry. Discovery of the boundary was of enormous importance for understanding development (*3*), but the realization that sibling cells compete for contribution to the adult had implications of great consequence to tissue growth. Cell competition was thus defined as a struggle between slow-growing *M*/+ cells (termed "losers") and faster-growing wild-type cells ("winners") for territory in the adult.

These experiments were possible because of the genetic tools in *Drosophila* and the simple architecture of the wing imaginal disc, the organ from which the wing develops. The wing disc is a proliferating epithelium that grows in the larva and differentiates adult wing structures during metamorphosis. Early in wing development, disc cells are multipotent, and cell division is stochastic and indeterminate. These properties provide a high degree of flexibility, so that cells lost through damage are rapidly replaced by proliferation of surviving cells. Early work from Morata and Simpson established key features of cell competition: It occurs locally, between clonal populations of wild-type and *M*/+ cells, and its severity is proximity-dependent (*4*, *5*). Elimination of the *M*/+ cells is accompanied by compensatory proliferation of wild-type cells, and a large clone of wild-type cells in a *M*/+ disc can fill an entire compartment. Remarkably, despite large territories of cells growing at different rates, the size and shape of the adult wing remains normal (*5*). These elegant genetic experiments established that a cell's potential for proliferation and survival—and ultimately its contribution to a fully developed tissue—is determined by its interactions with its neighbors. That cells sense and respond to each other's growth rate suggested that the sensing mechanism contributes to control of tissue and organ size (*6*), an idea that was recently confirmed (*7*).

Group dynamics yield winners and losers. Apoptosis is the principal cause of the growth disadvantage of loser cells: Loser cells die and are eliminated from the epithelium (Fig. 1) (*7*–*12*). Inactivation of many genes can lead to death and cell loss during development, often due to a cell-autonomous requirement for the gene for survival or a particular developmental process. However, cell competition is not an intrinsic property of cells: It relies completely on cell-cell interactions. It is these interactions that establish one cell as relatively weaker or stronger than another. Competition is

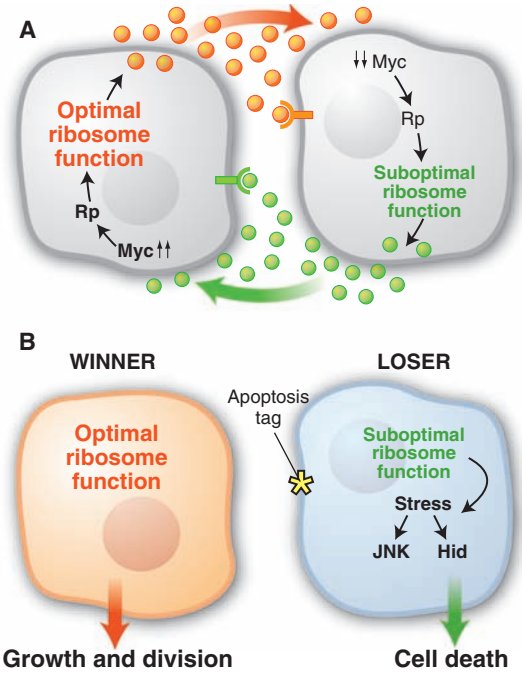

Fig. 1. A model of cell competition. (**A**) Neighboring epithelial cells recognize relative differences in ribosome function through a sensing mechanism that may involve the production of secreted factors by each cell (orange and green dots). (**B**) Once a difference is sensed, cells acquire "winner" or "loser" status, determined by their relative ribosome function. Loser cells sense stress and activate the JNK signaling pathway and expression of the proapoptotic factor, Hid. Hid induces apoptosis and leads to loser-cell death. Winner cells, with optimal ribosome function, are stimulated to proliferate faster. They also can activate genes required for cell engulfment, leading them to engulf dying loser cells (asterisk). Arrows depict genetic relationships rather than direct biochemical interactions.

CREDIT: KATHARINE SUTLIFF/*SCIENCE*

Department of Genetics and Development, College of Physicians and Surgeons, Columbia University, New York, NY 10032, USA. E-mail: lj180@columbia.edu

identified by strict experimental criteria, and thus far, only two genetic contexts are legitimately so defined: differences in Rp gene dosage, as in mosaics of *M*/+ flies and in chimeric *Belly spot and tail* (*Bst*) mice, a mouse "Minute" (*13*); or in Myc, the transcription factor and well-known oncogene (*7*, *9*). Several hallmarks distinguish cell competition from other processes that involve cell death and compensatory proliferation. First, competition is context-dependent—cells acquire "winner" or "loser" identity only when in confrontation; each is viable in a homotypic environment. Second, loser apoptosis is triggered by interactions with winner cells. This contrasts cell competition with compensatory proliferation occurring during regeneration, where cells are killed by physical damage or surgery. Finally, competition does not cross the boundaries of developmental compartments (Fig. 2). Rp- and Myc-induced competition share all of the traits that define cell competition, with minor variations. An interesting difference is that Myc-induced competition occurs over a greater distance—up to 10 cells—than *M*/+-induced competition, which occurs extremely locally (*7*, *12*).

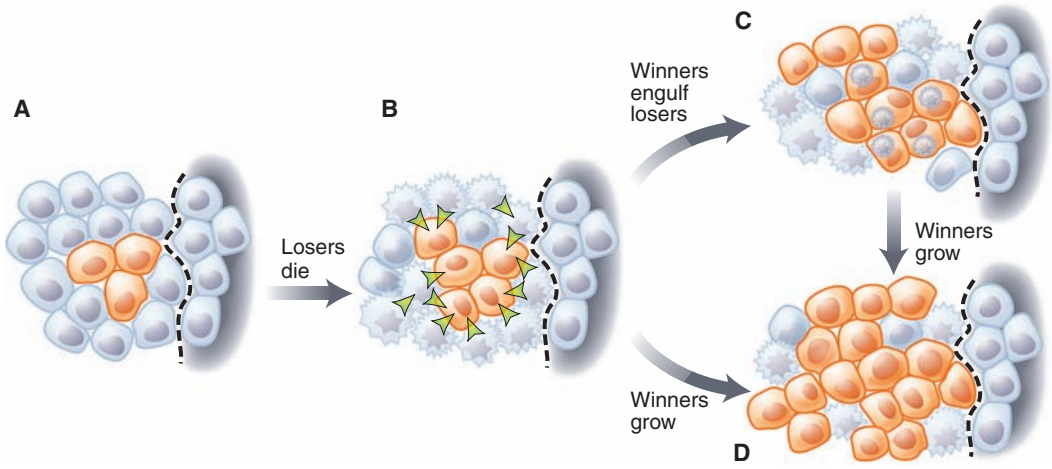

Fig. 2. Cells are insulated from competition by compartment boundaries. (**A**) Cell competition occurring on one side (left) of a compartment boundary (dotted line) does not affect cells on the other side (right). Gray cells, losers; orange cells, winners. (**B**) Local interactions between cells identify relative metabolic status, triggering apoptosis in losers. Signals from dying cells (arrowheads) may stimulate the growth of winner cells. Cells to the right of the compartment boundary are completely protected. (**C**) Loser cells can be engulfed by winner cells. This process promotes winner-cell proliferation. (**D**) Winner cells expand their territory at the expense of loser cells. However, this expansion is limited to one compartment, because cells in the opposite compartment (right of the dotted line) remain insulated. The geographic limits of competition help stabilize organ size.

The cell-intrinsic signaling pathways leading to apoptosis are highly conserved and use prodeath regulatory factors to overcome inhibition of caspases by IAP (inhibitor of apoptosis) proteins. Hid, a *Drosophila* prodeath protein, is a dose-dependent effector of loser-cell death during competition between cells that differ in Myc expression and is required for competition to occur (*7*, *10*). What signals Hid induction in loser cells is unknown but may be partially due to activation of the Jun N-terminal kinase (JNK) stress-response pathway (*7*–*9*). However, JNK's role is not entirely clear, because Hid expression and competition-induced apoptosis occur even in its absence (*7*, *11*). Although losers of cell competition die, winner cells survive and proliferate more, and these two processes are precisely balanced so that wing size is maintained. Expression of the caspase inhibitor, P35, in *M*/+ loser cells prevents their death and simultaneously reduces growth of wild-type winner cells (*12*), suggesting that the two processes are mechanistically tightly linked. Even without overt competition, preventing apoptosis—particularly that induced by Hid—alters wing growth and causes fluctuating asymmetry, an indicator of developmental instability (*7*, *14*, *15*). These are strong indicators that competition, with its growth and death outcomes, is an essential part of the homeostatic mechanism that stabilizes wing size.

Cell fitness surveillance. The basis of cell competition is that within a field of growing cells, the contribution of a cell and its progeny to a tissue is altered by neighboring cells that possess different growth or metabolic properties. However, such differences do not always lead to competition, indicating an intriguing level of discrimination (*7*). How do cells sense, compare, and relay their growth or metabolic status to their neighbors? This sensing requires that cells monitor their own metabolic state vis-à-vis their neighbors; thus, molecular sensors of cell competition presumably report cellular fitness. A common denominator in the two characterized examples of cell competition is a local difference in ribosome biogenesis or function. *Minute* mutations directly reduce Rp expression, impairing ribosome synthesis (*1*). Myc controls expression of numerous genes that contribute to ribosome synthesis, including Rps and rRNA (*16*, *17*). An inadequate supply of functional ribosomes is dangerous to cells by interfering with their ability to rapidly regulate translation in response to environmental changes. The nucleolus is a ribosome assembly factory but also contains cell cycle regulators, stress sensors (p53), tumor suppressors (Arf), stem cell factors (Nucleostemin), and transcription factors (Myc), many of which play roles in sensing cellular stress (*18*). Ribosome vigor may therefore be continually monitored and perhaps reported by a dedicated signaling pathway.

A paucity of ribosomes is potentially stressful, but not necessarily lethal. Both *M*/+ flies and *Bst*/+ mice grow slowly but develop into adults (*1*, *13*). However, confrontation between two populations that differ in ribosomal vigor could be perceived as stress. Our understanding of the requirements for sensors of competition is still limited, and no molecular sensors of cell competition have been unequivocally identified. However, several recent advances shed light on the process.

Ligand-capture–mediated cell competition. As a determinant of a cell's contribution to the adult, cell competition is closely tied to organ growth (*7*). Initially, it was suspected that cells in imaginal discs compete for growth or survival factors, as postulated for neurons (*19*). One such factor, the bone morphogenetic protein and transforming growth factor–β family member Dpp, is a secreted protein critical for pattern formation, cell survival, and growth of imaginal discs (*20*). High Dpp activity stimulates growth (*21*), whereas low levels activate JNK signaling and apoptosis (*22*); thus, if potential loser cells were ineffective at capturing Dpp, their survival and growth might be impaired. Some experiments supported this view (*8*, *9*), but the selectivity associated with competition argues against it (*7*). Furthermore, suppressors of *M*/+ and +/+ cell competition isolated in a genetic screen do not require Dpp activity to prevent it (*11*). Some of these suppressors augmented Dpp activity in loser cells and increased their proliferation, but death was not reduced, so Dpp-stimulated proliferation might just outpace their death (*11*). However, loser cells are protected from competition by overexpression of the endocytosis-promoting, small guanosine triphosphatase (GTPase) Rab 5 (*9*). Since numerous cell survival- and growth-promoting factors rely on receptor-mediated endocytosis, further investigation of this intriguing finding should be informative.

Mutual sensing mediated by soluble factors. Recent work suggests that cells recognize competitive status using a mutual sensing mechanism involving production of diffusible factors. In the wing disc, wild-type cells can sense Myc-expressing winner cells up to 10 cell diameters away, suggesting that signaling between the cells is short-range (*7*). In a cell culture model of competition with *Drosophila* S2 cells engineered to express different levels of Myc, cocultures induced

apoptosis specifically in cells with less Myc (*10*). This did not require cell-cell contact, which suggests mediation by soluble factors. Medium conditioned from competing cocultures was found to contain two activities: One caused Hid-dependent death of naïve, wild-type cells, turning them into "losers," whereas a second activity turned naïve Myc-expressing cells into "winners" that proliferated faster than normal. A cell's potential to be a winner or loser was determined by its ability to deregulate Myc expression (*10*), and production of both activities required reciprocal recognition by each cell type—potential winners and potential losers—suggesting that each activates a sensor that reports the other's metabolic status (Fig. 1).

Winners eat losers. Cell competition generates dead cells. In the fly, engulfment of dying or dead cells is typically carried out by hemocytes, migratory macrophage-like cells that are dedicated phagocytes. During competition, however, dying *M/+* loser cells are engulfed by nearby wild-type cells (Fig. 2C), possibly driving *M/+* cell death to completion (*12*). The death tendency of *M/+* cells is overcome if neighboring winner cells lack factors that regulate cell engulfment (including Draper, a *ced-1* homolog and scavenger receptor), WASp (Wiscott-Aldrich Syndrome protein), PSR (phosphatidylserine receptor), RAC (a small GTPase required for cytoskeletal rearrangements) and MBC (myoblast city, a SH3-domain–containing protein) (*12*). Perhaps the weak metabolic status of *M/+* cells triggers apoptosis, flagging them as "garbage." The sensing mechanism is unclear, though, because PSR, which recognizes PS exposure on the outer membrane of apoptotic cells, does not drive engulfment in *Drosophila* but inhibits apoptosis by suppressing Hid function and JNK signaling (*23*). Intriguingly, forced WASp activation stimulates engulfment without prior signaling from dying cells (*12*). Blocking loser engulfment by winner cells also prevented extra winner growth, adding to the evidence that loser death stimulates the growth of winner cells (Fig. 2) (*12*). Interestingly, loss of Croquemort, the *Drosophila* homolog of the CD36 macrophage receptor for dying cells, did not prevent engulfment nor prevent cell competition (*12*), suggesting that stimulation of competition-induced engulfment is qualitatively different from that induced in hemocytes. Still, *M/+* cells are not all engulfed by winners, as many delaminate from the epithelium for phagocytosis by hemocytes, and the importance of neighbor cell engulfment in Myc-induced competition is unclear (*7*, *8*, *12*). Nonetheless, loser cells are clearly perceived as dangerous to the tissue, and a local mechanism is deployed for their removal. The misregulation of wing size that can occur when loser cells cannot die (*7*) implies that engulfment is critical to the homeostatic function of cell competition.

"Danger Signals" and cell competition. Cell competition appears to proceed through a series of discrete steps: local sensing and recognition of cellular differences, production of diffusible factors, signaling that activates stress pathways and apoptotic suicide of loser cells, deployment of an engulfment program, and growth stimulation of winner cells (Fig. 2). This process is conceptually similar to the innate immune system's recognition of infectious pathogens, which activates a defensive cellular response that destroys invaders and restores homeostasis (*24*). Interestingly, the cohort of receptors and signaling modules of the innate immune system are also stimulated by endogenous "danger" signals, released upon tissue damage (*24*, *25*). Does cell competition contribute to an organism's ability to sense and respond to danger derived from itself? The answer to this question awaits further research.

Niche Occupancy: Competition Among Stem Cells

Competition of a different flavor occurs in the *Drosophila* gonad, where both somatic stem cells and germline stem cells (GSCs) vie for occupancy of their particular niche, or microenvironment (*26*, *27*). Like cell competition in somatic epithelia, stem cell competition pits cells against each other, but cells are displaced from the niche rather than killed. In the end, competing stem cells both contribute to formation of the ovary, although to different processes.

The GSC niche: *Adhesion-based residency.* In *Drosophila*, egg chambers arise within the germarium, a structure at the anterior end of the developing ovary. The germarium contains many different cell types in relatively close proximity, including stem cells and their accompanying support cells, the differentiating daughters of stem cells, follicle cells (FCs), and an egg chamber. The GSC niche, at the anterior-most end of the germarium, consists of three somatic cell types: cells in the terminal filament, escort cells, and cap cells (Fig. 3A). GSCs associate directly with cap cells via adherens junctions and are anchored firmly with E-cadherin–dependent interactions (*28*, *29*). This association is dependent upon E-cadherin, and loss of E-cadherin leads to a deficit of GSCs. The tight GSC–cap cell association ensures that the GSC receives proximity-dependent signals from the niche: For example, Dpp signal transduction is very high in the GSC but quite low even one cell diameter away (*30*, *31*). This high Dpp activity is required to repress expression of two differentiation-promoting genes, *bam* (*bag of marbles*) and *bgcn* (*benign gonial cell neoplasm*), in the GSC. GSCs divide asymmetrically, allowing one daughter to remain in the niche while the other moves away from the niche, derepresses *bam* expression, and differentiates into a cystoblast. Niche residency is imperative for a functional GSC and for continued production of new daughter cells (*32*).

GSCs lacking *bam* or *bgcn* cannot differentiate, and the germarium fills with extra GSCs. *bam* mutant GSCs out-compete wild-type GSCs for niche residency; possibly, loss of Bam increases E-cadherin expression, tightening the association between the mutant GSC and the cap cell. After GSC division, daughters are pushed from the niche (Fig. 3B); because *bam* mutant GSCs divide faster than wild-type GSCs, a larger pool of mutant daughters could increase the chance of their niche occupancy. Competition may also be enhanced because, unable to differentiate, mutant GSCs retain stem cell identity. *bam* mutant GSCs require neither Dpp or Myc to compete with wild-type GSCs, although too much Myc leads to GSC loss (*27*); however, Myc expression may facilitate competition between wild-type GSCs (*33*). GSCs appear to compete primarily based on their ability to adhere to cap cells, which, perhaps as a proxy for "fitness" and stem cell identity, ensures that they receive signals for their continual renewal (*27*).

FSC competition: Dynamic niches, migratory stem cells. Niche space for somatic follicle stem cells (FSCs), the progenitors of the follicular epithelium that surrounds the germline cysts, is also

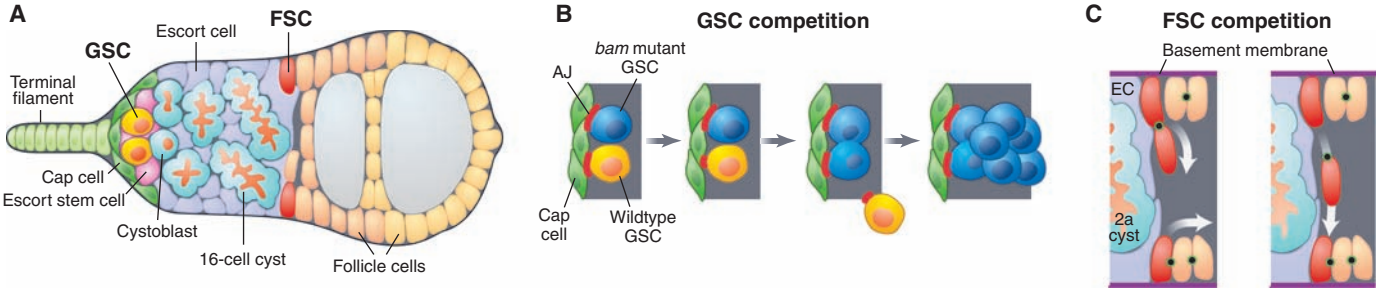

CREDIT: KATHARINE SUTLIFF/*SCIENCE*

Fig. 3. Stem cells compete for their niche. (**A**) Depiction of the germarium (adapted from *26*). (**B**) GSC competition. GSCs (blue and yellow) adhere to cap cells (green) in the niche via strong E-cadherin interactions. *bam*-mutant GSCs (blue) cannot differentiate, and they retain strong adherens junction (AJ) connections that can displace wild-type GSCs from the niche. (**C**) FSC competition. FSCs occupy a niche composed of the lateral edge of a 2a cyst encased in an escort cell (EC), the basement membrane (magenta line), and the FSC (red). Green circles are ring canal bridges. Arrows show direction of movement of the newly born FSC. The FSC can move posteriorly (bottom arrow) or toward the opposite niche (top arrows), where it can displace the resident FSC.

subject to competition. Each of two FSCs in the germarium resides in a small niche on opposite sides of the ovariole (Fig. 3, A and C). This niche is ill-defined, but quite different from the GSC niche because it lacks permanent, nondividing stromal cells that anchor the FSC in place. It appears to consist of an FSC, a 2a cyst, and an underlying basement membrane (Fig. 3C). After asymmetric division of the FSC, the daughter moves to the proximate posterior position or sometimes migrates laterally toward the opposite side of the ovariole. Although the niche is not a fixed entity, it is always established in the same general location, which apparently provides the necessary microenvironment to maintain stem cell identity and activity (*26*).

One component of the microenvironment might be signals that direct the cross-migration of FSC daughter cells. Laterally migrating FSC daughters move toward the opposite niche and can compete with the resident FSC (*26*). Displacement of a resident FSC by an incoming daughter is rare, however. Potential barriers to niche competition include E-cadherin- and Beta-catenin–mediated anchoring mechanisms between FSCs and differentiated FCs (*29*), ring canal bridges between FSCs and their daughters, and attachments with basement membrane (*26*). The fact that stem cell displacement and replacement is rare despite regular cross-migration of FSC daughters suggests that these mechanisms are quite robust, and occasional displacement by essentially equivalent FSCs may represent opportunistic, rather than competitive, behavior. However, the mechanisms that secure niche residency could encourage competition if one FSC acquired a mutation altering its anchoring ability or its ability to differentiate. In this case, FSC competition could lead to expansion of mutant FSCs and potentially to cancer (*26*).

Themes and Perspectives

The existence of cell competition tells us that decisions that cells make to grow, die, or differentiate are local and can be communal. Competition between stem cells and their daughters may ensure that functional stem cells reside in the niche (*26*, *32*), whereas competition between disc epithelial cells weeds out the relatively weak, including cells carrying a potentially harmful mutation. Whether destructive and leading to cell death, or instructive, determining order and status, both types of competition serve as subtle but important policing mechanisms that promote homeostasis.

Competition allows plasticity during growth, but this plasticity is not without limits. The stem cell niche strictly regulates stem cell numbers by restricting housing space, providing a geographic limitation that protects against deregulated stem cell proliferation. In epithelia such as the wing disc, mutual sensing of cellular status keeps both growth and death in check: In the absence of recognized differences, death is minimal and proliferation proceeds at the normal rate. Cell competition is also restrained in disc epithelia by specific insulating mechanisms. Cells in one developmental compartment are completely insulated from ongoing competition across its boundary (Fig. 2) (*4*, *7*), protecting each territory and the disc as a whole from unrestrained competition and unrestrained growth. Nutrient deprivation and cell cycle exit also protect against competition (*14*, *34*). How these protective mechanisms operate is unknown, but they limit competition geographically and stabilize organ size, preventing both detrimental overgrowth of winner cells and excessive loss of loser cells.

A fundamental difference distinguishes stem cell competition from cell competition. The goal in both types of competition is to acquire prime real estate, but competition for niche occupancy is adhesion-based, whereas competition between disc epithelial cells is established by a direct cell-cell comparison of metabolic status. In the latter, we still lack information about what molecules are measured, but the mechanism may well be conserved. Competitive-like interactions have been noted between transplanted wild-type cells and diseased host liver cells during liver regeneration in rats (*35*), highlighting its potential utility in therapeutic transplantations. In diverse animals, the expansion of one cell population at the expense of another is a common outcome in chimeras, and is also a hallmark of cancer (*36*–*38*). Indeed, both stem cell competition and cell competition are emerging models for tumorigenesis. A few rogue, mutant cells in a tissue or organ could enhance their own growth by killing off their neighbors (*39*–*41*). Likewise, mutations that increase adhesiveness or "stemness" of winner stem cells could out-compete wild-type stem cells and lead to tumors. Study of cell and stem cell competition offers a novel route to identify genes that report winner (precancerous) cells and loser (noncancerous) status in tissues harboring an incipient tumor. The continued use of *Drosophila* to discover such genes and the development of models of competition in vertebrate systems promise to reveal new and fascinating ways whereby cell fitness is sensed and communicated and homeostasis is maintained in local cellular communities.

References and Notes

1. A. Lambertsson, *Adv. Genet.* **38**, 69 (1998).
2. G. Morata, P. Ripoll, *Dev. Biol.* **42**, 211 (1975).
3. P. A. Lawrence, G. Struhl, *Cell* **85**, 951 (1996).
4. P. Simpson, *Dev. Biol.* **69**, 182 (1979).
5. P. Simpson, G. Morata, *Dev. Biol.* **85**, 299 (1981).
6. P. Bryant, P. Simpson, *Q. Rev. Biol.* **59**, 387 (1984).
7. C. de la Cova, M. Abril, P. Bellosta, P. Gallant, L. A. Johnston, *Cell* **117**, 107 (2004).
8. E. Moreno, K. Basler, G. Morata, *Nature* **416**, 755 (2002).
9. E. Moreno, K. Basler, *Cell* **117**, 117 (2004).
10. N. Senoo-Matsuda, L. A. Johnston, *Proc. Natl. Acad. Sci. U.S.A.* **104**, 18543 (2007).
11. D. M. Tyler, W. Li, N. Zhuo, B. Pellock, N. E. Baker, *Genetics* **175**, 643 (2007).
12. W. Li, N. E. Baker, *Cell* **129**, 1215 (2007).
13. E. R. Oliver, T. L. Saunders, S. A. Tarle, T. Glaser, *Development* **131**, 3907 (2004).
14. R. Neto-Silva, B. Wells, L. Johnston, *Annu. Rev. Cell Dev. Biol.* **25**, 1139 (2009).
15. P. A. Parsons, *Heredity* **68**, 361 (1992).
16. S. S. Grewal, L. Li, A. Orian, R. N. Eisenman, B. A. Edgar, *Nat. Cell Biol.* **7**, 295 (2005).
17. C. Grandori *et al.*, *Nat. Cell Biol.* **7**, 311 (2005).
18. C. Mayer, H. Bierhoff, I. Grummt, *Genes Dev.* **19**, 933 (2005).
19. M. C. Raff, *Nature* **356**, 397 (1992).
20. R. Burke, K. Basler, *Development* **122**, 2261 (1996).
21. C. Martin-Castellanos, B. A. Edgar, *Development* **129**, 1003 (2002).
22. T. Adachi-Yamada, M. B. O'Connor, *Dev. Biol.* **251**, 74 (2002).
23. R. J. Krieser *et al.*, *Development* **134**, 2407 (2007).
24. R. Medzhitov, *Nature* **454**, 428 (2008).
25. P. Matzinger, *Science* **296**, 301 (2002).
26. T. Nystul, A. Spradling, *Cell Stem Cell* **1**, 277 (2007).
27. Z. Jin *et al.*, *Cell Stem Cell* **2**, 39 (2008).
28. T. Xie, A. C. Spradling, *Science* **290**, 328 (2000).
29. X. Song, T. Xie, *Proc. Natl. Acad. Sci. U.S.A.* **99**, 14813 (2002).
30. T. Xie, A. C. Spradling, *Cell* **94**, 251 (1998).
31. E. Kawase, M. D. Wong, B. C. Ding, T. Xie, *Development* **131**, 1365 (2004).
32. A. C. Spradling *et al.*, *Cold Spring Harb. Symp. Quant. Biol.* **73**, 49 (2008).
33. C. Rhiner *et al.*, *Development* **136**, 995 (2009).
34. P. Simpson, *J. Embryol. Exp. Morphol.* **65**, 77 (1981).
35. M. Oertel, A. Menthena, M. D. Dabeva, D. A. Shafritz, *Gastroenterology* **130**, 507 (2006).
36. D. S. Stoner, B. Rinkevich, I. L. Weissman, *Proc. Natl. Acad. Sci. U.S.A.* **96**, 9148 (1999).
37. I. M. de Alboran *et al.*, *Immunity* **14**, 45 (2001).
38. B. E. Miller, F. R. Miller, D. Wilburn, G. H. Heppner, *Cancer Res.* **48**, 5747 (1988).
39. C. de la Cova, L. A. Johnston, *Semin. Cancer Biol.* **16**, 303 (2006).
40. E. Moreno, *Nat. Rev. Cancer* **8**, 141 (2008).
41. N. E. Baker, W. Li, *Cancer Res.* **68**, 5505 (2008).

42. Work on cell competition in our laboratory has been supported by NIH (grants HD42770 and GMO78464), the Rita Allen Foundation, and the Uehara Memorial Foundation.

10.1126/science.1163862

Elevated CO_2 Enhances Otolith Growth in Young Fish

David M. Checkley Jr.,* Andrew G. Dickson, Motomitsu Takahashi,† J. Adam Radich, Nadine Eisenkolb,‡ Rebecca Asch

A large fraction (0.3 to 0.5) of the carbon dioxide (CO_2) added to the atmosphere by human burning of fossil fuels enters the ocean (*1*). This causes ocean acidification by increasing the concentrations of oceanic CO_2, bicarbonate (HCO_3^-) and hydrogen (H^+) ions and decreasing the concentration of carbonate (CO_3^{2-}) ion and hence the saturation state of calcium carbonate (Ω) (*1*). Addition of CO_2 to the atmosphere and ocean may thus influence the rates of formation and dissolution of aragonite and calcite, biominerals that are critical to diverse marine taxa. Although some recent studies have shown that elevated CO_2 enhances structural calcification in coccolithophores and invertebrates, most studies have shown a slowing of structural calcification (*2*). Otoliths are bony structures used by fish to sense orientation and acceleration and consist of aragonite-protein bilayers, which document fish age and growth. We hypothesized that otoliths in eggs and larvae reared in seawater with elevated CO_2 would grow more slowly than they do in seawater with normal CO_2. To test our hypothesis, we grew eggs and prefeeding larvae of white sea bass (*Atractoscion nobilis*) under a range of CO_2 concentrations and measured the size of their sagittal otoliths by using a scanning electron microscope (Fig. 1, A to C) (*3*).

In each experiment, we incubated eggs and larvae in seawater under control (380 μatm of CO_2, 1 atm = 101.325 kPa) and treatment (993 or 2558 μatm of CO_2) atmospheres. Initial experiments 1 and 2 used 2558 μatm of CO_2 to test whether elevated CO_2, resulting in aragonite undersaturation in the seawater, affected otolith size. Experiments 3 and 4 used 993 μatm of CO_2, an atmospheric concentration ~2.5 times the present concentration that may occur by 2100 (*4*). Contrary to expectations, the otoliths of fish grown in seawater with high CO_2, and hence lower pH and $\Omega_{aragonite}$, were significantly larger than those of fish grown under simulations of present-day conditions (Fig. 1D and table S1). For 7- to 8-day-old fish grown under 993 and 2558 μatm of CO_2, the areas of the otoliths were 7 to 9% and 15 to 17% larger, respectively, than those of control fish grown under 380 μatm of CO_2. Assuming otolith density is constant and that volume is proportional to area$^{1.5}$ (*3*), we estimate otolith masses were 10 to 14% and 24 to 26% greater, respectively, for fish under 993 and 2558 μatm of CO_2. The dry mass of fish did not vary with CO_2 (*3*), and thus fish of the same size had larger otoliths when grown under elevated CO_2.

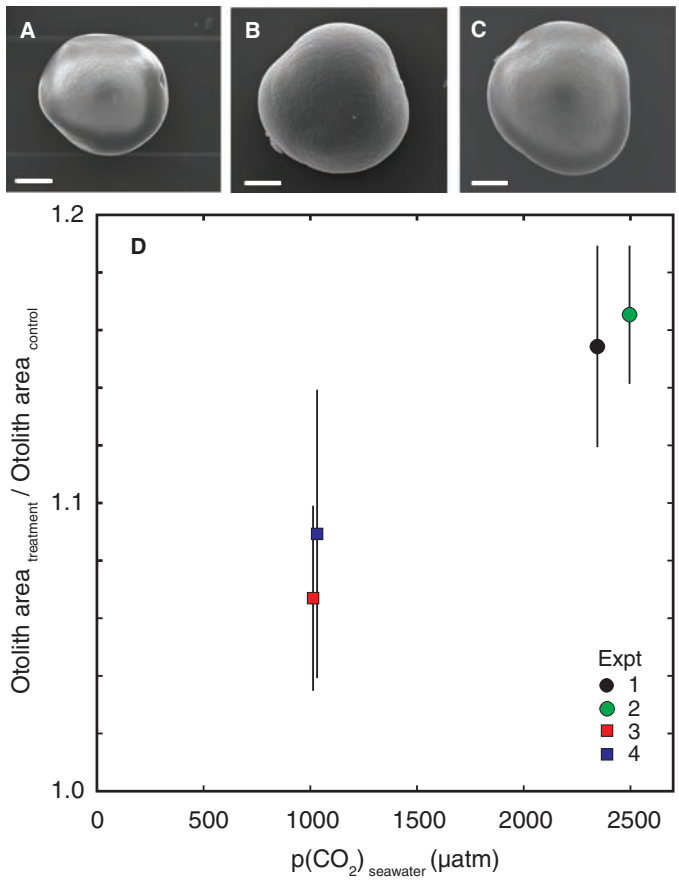

Fig. 1. Dorsal view of sagittal otoliths of 7-day-old white sea bass grown at (**A**) 430, (**B**) 1000, and (**C**) 2500 μatm $p(CO_2)_{seawater}$. Scale bars indicate 10 μm. (**D**) Ratio (treatment/control) of otolith area in relation to $p(CO_2)_{seawater}$. Mean ratios and their associated uncertainties (*3*) are plotted. The control level $p(CO_2)_{seawater}$ was ~430 μatm [$p(CO_2)_{atmosphere}$ ~ 380 μatm], for which otolith area ratio = 1.

Our results are consistent with young fish being able to control the concentration of ions (H^+ and Ca^{2+}), but not the neutral molecule CO_2, in the endolymph surrounding the otolith. Gases in tissues of fish eggs and larvae equilibrate rapidly with seawater by cutaneous exchange (*5*) but may also be affected by acid-base regulation (*6*). In the endolymph, with constant pH, elevated CO_2 increases CO_3^{2-} concentration and thus the $\Omega_{aragonite}$, accelerating formation of otolith aragonite. This is a fundamentally different effect of elevated CO_2 on marine biomineralization than those in previous reports on acidification (*1*, *2*).

We do not know whether our results apply to other taxa with aragonite sensory organs, such as squid and mysids (statoliths) or other fish species. Nor do we know whether larger otoliths have a deleterious effect, although we do know that asymmetry between otoliths can be harmful (*7*).

Our results indicate the need to understand the diverse effects of elevated CO_2 on biomineralization over taxa and developmental stages. The specific effects of elevated CO_2, not simply acidification, should be considered. Calcification and dissolution of calcium carbonate occur sequentially and often at different locations and under different conditions. Whatever the organism, to predict the effects of elevated CO_2, we need to know the mechanisms of production and dissolution and their relationships to changing seawater chemistry.

References and Notes

1. J. C. Orr *et al.*, *Nature* **437**, 681 (2005).
2. S. C. Doney *et al.*, *Annu. Rev. Mar. Sci.* **1**, 169 (2009).
3. Materials and methods are available as supporting material on *Science* Online.
4. Intergovernmental Panel on Climate Change (IPCC), *Climate Change 2007: Synthesis Report* (IPCC, Geneva, 2007).
5. B. Pelster, *Comp. Biochem. Physiol. A* **124**, 407 (1998).
6. H. O. Pörtner, A. P. Farrell, *Science* **322**, 690 (2008).
7. M. Gagliano *et al.*, *Proc. R. Soc. London Ser. B* **275**, 527 (2008).
8. We thank Hubbs-SeaWorld Research Institute for providing fertilized fish eggs. E. York assisted with electron microscopy. V. Fabry, G. Somero, V. Vaquier, and two anonymous reviewers improved the manuscript. Supported by the Academic Senate of the University of California, San Diego. Data available at http://repositories.cdlib.org/sio/techreport/97/.

Supporting Online Material

www.sciencemag.org/cgi/content/full/324/5935/1683/DC1
Materials and Methods
SOM Text
Table S1
References

15 December 2008; accepted 7 May 2009
10.1126/science.1169806

Scripps Institution of Oceanography, University of California, San Diego, CA 92093, USA.

*To whom correspondence should be addressed. E-mail: dcheckley@ucsd.edu
†Present address: Seikai National Fisheries Research Institute, Fisheries Research Agency, 1551-8, Taira-machi, Nagasaki-shi, Nagasaki 851-2213, Japan.
‡Present address: Department of Biological Sciences, University of Southern California, Los Angeles, CA 90089, USA.

Auxin-Dependent Patterning and Gamete Specification in the *Arabidopsis* Female Gametophyte

Gabriela C. Pagnussat,[1]* Monica Alandete-Saez,[1] John L. Bowman,[1,2] Venkatesan Sundaresan[1,3]†

The female reproductive unit of flowering plants, the haploid female gametophyte, is highly reduced relative to other land plants. We show that patterning of the *Arabidopsis* female gametophyte depends on an asymmetric distribution of the hormone auxin during its syncitial development. Furthermore, this auxin gradient is correlated with location-specific auxin biosynthesis, rather than auxin efflux that directs patterning in the diploid sporophytic tissues comprising the rest of the plant. Manipulation of auxin responses or synthesis induces switching of gametic and nongametic cell identities and specialized nonreproductive cells to exhibit attributes presumptively lost during angiosperm evolution. These findings may account for the unique egg cell specification characteristic of angiosperms and the formation of seeds with single diploid embryos while containing endosperm that can have variable numbers of parental haploid genomes.

The highly reduced female gametophyte of flowering plants (*1*, *2*), with specialized gametes to enable double fertilization, constitutes a microcosm of pattern formation and gamete specification for which the underlying mechanisms have remained elusive (*3*–*7*). In *Arabidopsis* and most other flowering plants, the female gametophyte, referred to as the embryo sac, first develops as a syncitium, a structure that contains eight nuclei, which are later partitioned into seven cells consisting of four cell types. These are the egg cell and central cell that form the gametes for double fertilization, two accessory synergid cells positioned next to the egg cell, and three antipodal cells. Manifestation of cell identity is concomitant with cellularization, suggesting that cell fates are programmed before this stage. Moreover, it has been shown that unusual positioning of the nuclei during embryo sac development, as observed in the *eostre* mutant, can lead to both morphological and functional defects, including the production of an extra functional egg cell in place of a synergid (*8*). These observations suggested that, in angiosperms, the determination of egg cell fate may depend on a location-specific mechanism within the syncitial female gametophyte. Additional support for this conjecture comes from observations of the maize *indeterminate gametophyte* mutant in which extra cells are generated that appear to assume specific cell fates correlated with their position (*9*). On the basis of these findings, we hypothesize that positional information within the syncitium might rely on the asymmetric distribution of a morphogenetic determinant as described in animals such as the development of the *Drosophila* embryo (*10*).

Auxin, auxin response, and cell specification. The phytohormone auxin regulates cell division, elongation, and differentiation in plants. Local accumulation of auxin provides positional signals for multiple developmental processes, such as establishment of the shoot and root meristems along the apical-basal axis, organogenesis, and vascular differentiation (*11*–*14*). In order to determine whether auxin acts as a positional determinant regulating cell specification during megagametogenesis in *Arabidopsis*, we followed the distribution of auxin by DR5-driven expression in the synthetic reporters *DR5::GFP* and *DR5::GUS* (GFP is green fluorescent protein, and GUS is β-glucuronidase) (*14*, *15*). Auxin signaling output was traced to megasporogenesis, the stage at which a signal was detectable at the distal tip of the nucellus (fig. S1A). At gametophyte developmental stage FG1, when a functional megaspore is visible, the signal is strong in the nucellus, outside the

[1]Department of Plant Biology, University of California, Davis, CA 95616, USA. [2]School of Biological Sciences, Monash University, Melbourne, Victoria 3800, Australia. [3]Department of Plant Sciences, University of California, Davis, CA 95616, USA.

*Present address: Instituto de Investigaciones Biológicas, Universidad Nacional de Mar del Plata, 7600 Mar del Plata, Argentina.

†To whom correspondence should be addressed. E-mail: sundar@ucdavis.edu

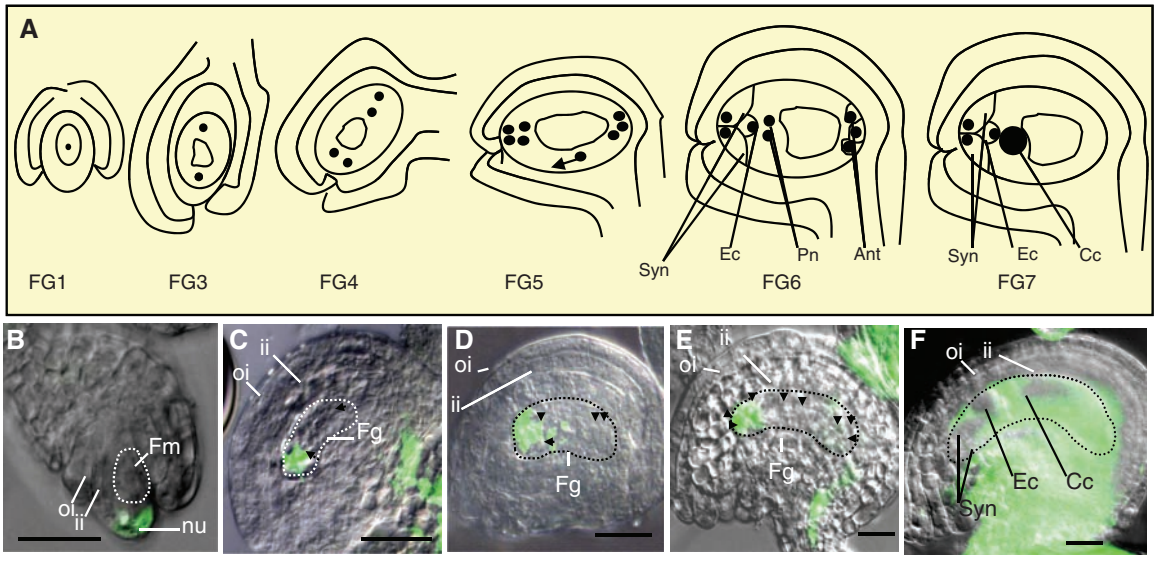

Fig. 1. Expression of the synthetic reporters *DR5::GFP* during female gametophyte development. (**A**) Scheme showing the developmental stages during wild-type female gametophyte development in *Arabidopsis*. Ant indicates antipodal cells; Cc, central cell; Ec, egg cell; Fg, female gametophyte; Fm, functional megaspore; ii, inner integument; nu, nucellus; oi, outer integument; Pn, polar nuclei; and Syn, synergid. (**B**), At FG1, the signal is strongly detected in the nucellus, outside the embryo sac. Scale bar indicates 25 μm, and the developing embryo sac is delimited by a dashed line. (**C**) At FG3 stage, the signal is detectable inside the embryo sac at the micropylar pole. (**D**) As the female gametophyte continues to develop, a strong *DR5::GFP* signal is localized to the micropylar end of the embryo sac by stage FG4. Small black arrowheads indicate nuclei inside the developing embryo sac. (**E**) A *DR5::GFP* activity maximum at the micropylar end of the embryo sac could be detected up to FG5 stage. (**F**) At FG6 stage the distribution of the *DR5::GFP* signal becomes less polarized. Signals outside the developing embryo sac in (C), (E), and (F) correspond to vascular tissues in the sporophytic ovule, particularly the funiculus.

developing embryo sac (Fig. 1, A and B, and fig. S1B). At the FG3 stage, after the first mitotic division and when the two resulting nuclei are separated by a small vacuole, the signal is detectable at the micropylar pole inside the embryo sac where one of the two nuclei is located (Fig. 1, A and C, and fig. S1C). As the female gametophyte developed, a strong signal was localized to the micropylar end of the developing embryo sac by stage FG4, after the second mitotic division, with one pair of nuclei located at the chalazal end of the gametophyte and the other pair at the micropylar end (Fig. 1, A and D). The *DR5::GFP* activity maximum at the micropylar end of the female gametophyte could be detected up to the FG5 stage, in which the third mitotic division was completed and eight nuclei were localized along the gametophyte (Fig. 1, A and E). These observations suggest that an auxin maximum is formed at the micropylar pole of the developing embryo sac. At late stages, that is, after cellularization, the distribution of the *DR5::GFP* signal appeared less polarized than in earlier stages and was detectable in all cells of the mature embryo sac (stage FG6, Fig. 1, A and F).

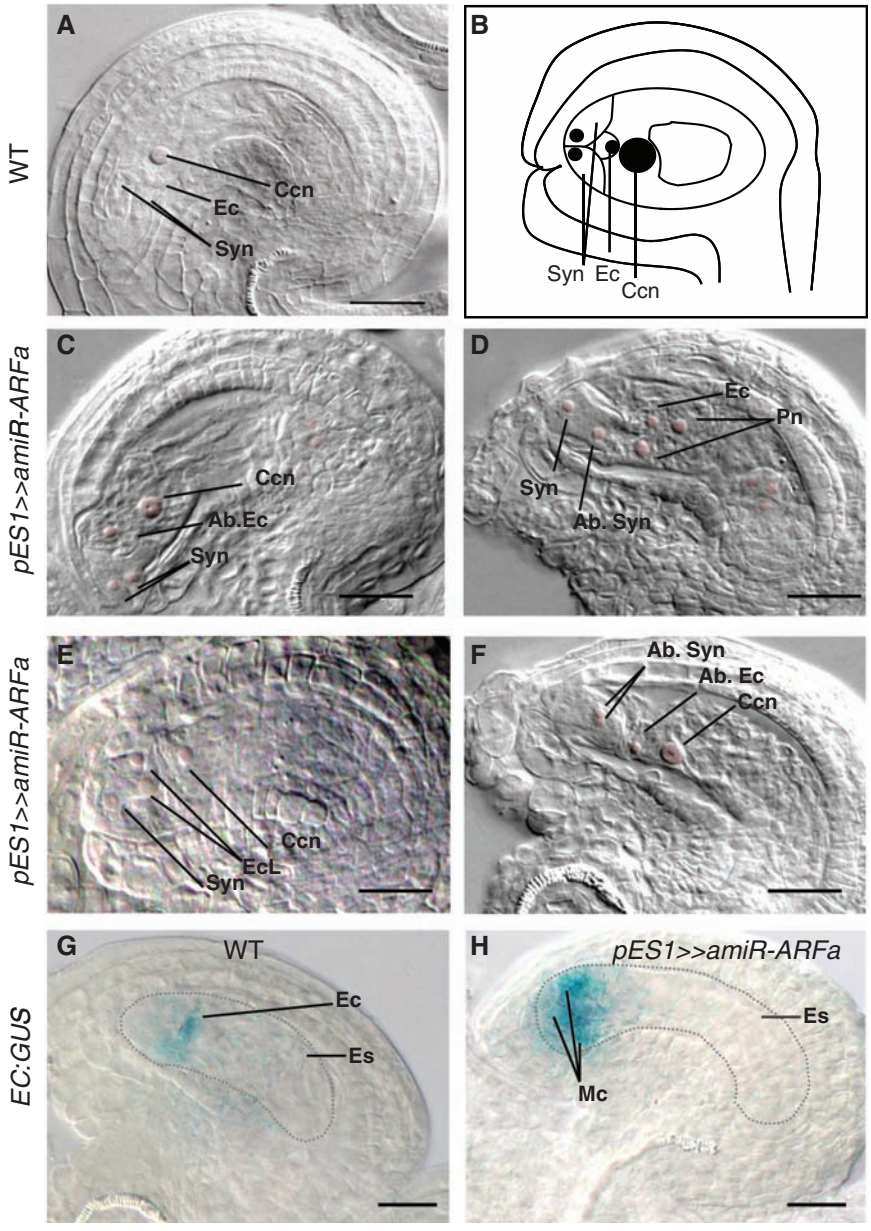

Fig. 2. When several ARF genes were down-regulated with an artificial miRNA expressed specifically in the embryo sac identity, defects in micropylar cells were observed. Scale bars, 25 μm. (**A**) DIC image of a wild-type (WT) embryo sac. Ccn, central cell nucleus; Ec, egg cell; and Syn, synergid. (**B**) Scheme of a WT female gametophyte. (**C**) Mature embryo sac showing an abnormal egg cell (Ab. Ec) with a centrally located nucleus. (**D**) Embryo sac showing unfused polar nuclei (Pn) and an abnormal synergid (Ab. Syn) cell, with a nucleus located toward the chalazal end of the embryo sac. (**E**) Embryo sac exhibiting two egglike cells. EcL, egg cell–like cell. (**F**) Embryo sac showing three cells morphologically similar to egg cells. (**G**) Expression of an egg cell–specific marker in a WT embryo sac. The developing embryo sac (Es) is delineated by a dashed line. (**H**) Expression of an egg cell–specific marker in all three micropylar cells of an ARF–down-regulated embryo sac. Mc, micropylar cell.

To determine whether the auxin maximum observed in the developing syncitial embryo sac conveys positional information for cell specification, we down-regulated genes involved in the auxin response with an artificial microRNA (miRNA) called *amiR-ARFa* targeting a subset of the auxin response factor genes (*ARFs*), a family of transcriptional regulator proteins that mediate responses to auxin by using a sequence highly conserved in ARFs from two major clades (fig. S5). Because many ARFs have essential functions in sporophyte development, we constructed transgenic plants carrying a pOp/LhG4 system to restrict the expression of *amiR-ARFa* to the embryo sac (*16*). This system was driven by the embryo sac promoter *pES1* (*8*), which is uniformly expressed during early female gametophyte development (stage FG1) to the mature embryo sac (stage FG7). To confirm that expression of *amiR-ARFa* by *pES1* results in down-regulation of the auxin response in the embryo sac, these transgenic plants were crossed to plants carrying the DR5::GFP auxin reporter. By scoring for DR5::GFP expression in the unfertilized pistils of the progeny, we showed that GFP-expressing embryo sacs were reduced by the predicted fraction, indicating down-regulation of the auxin response by *amiR-ARFa* (fig. S2 and table S1).

We observed that *ARF* down-regulation resulted in F1 plants with defective embryo sacs at ratios close to the expected 0.25 for co-inheritance of the driver and miRNA transgenes (table S2). Examination of the lines showing the greatest penetrance of the miRNA constructs revealed that defective embryo sacs developed to maturity but were unfertilized. Differential interference contrast (DIC) microscopy of mature defective embryo sacs revealed that the three cells at the micropylar end had identity defects (i.e., could not be recognized as egg cells or synergids) or had more than one cell exhibiting features characteristics of an egg cell (i.e., nucleus toward the chalazal end of the embryo sac and a large vacuole toward the micropylar end of the embryo sac) (Fig. 2, A to D).

We introduced cell-type specific GUS markers into the *pES* driven *amiR-ARFa* background to further examine cell identity. We observed that, although two micropylar cells were GUS positive for the expression of a synergid-specific marker [ET884 (*6*)] in wild-type embryo sacs, this marker was not detected in abnormal embryo sacs (fig. S2, A and B, and table S3). Concordantly, none of the mutant embryo sacs attracted pollen tubes, which is consistent with the loss of synergid cell identity (fig. S3E). For the egg cell–specific marker [ET119 (*6*)], we could detect expression of the marker in all three micropylar for 10 out of 489 embryo sacs examined (where 61 embryo sacs are expected to inherit all three transgenes; table S3), suggesting that synergid identity had been

replaced with egg cell identity (Fig. 2, E and F). Markers for the central cell [pMEA-GUS (*6*)] and the antipodal cells [*pAt1g36340-GUS* (*7*)] were also tested in transgenic embryo sacs; however, GUS-staining patterns for these markers were similar in both phenotypically wild-type and abnormal embryo sacs (fig. S2, C and D, and table S3). Importantly, we observed no abnormalities in nuclear positioning at earlier stages of embryo sac development, and the overall positioning of nuclei at maturity was similar to that of wild-type embryo sacs (Fig. 2 and fig. S3). Therefore, it appears that auxin may not regulate nuclear positioning during embryo sac development but instead regulates cell fate specification at cellularization.

Auxin efflux and biosynthesis in developing female gametophytes. In order to determine the origin of the discrete auxin maxima observed, the expression of different auxin efflux facilitators (PINs) was studied in the developing embryo sac. Plants carrying fusions of *PIN1*, *PIN2*, *PIN3*, *PIN4*, and *PIN7* to GFP were used to study *PIN* expression in wild-type female gametophytes. No *PIN* expression was observed in the female gametophyte, but *PIN1* was expressed in the nucellus until the FG1 stage (fig. S4, A to C). The pattern of localization of *PIN1* suggests that auxin flux may occur in the nucellus, establishing an auxin maximum at the distal tip during the earliest stages of embryo sac development (fig. S4D). Later in development, *PIN1* expression was not observed in the gametophyte or the immediately adjacent sporophytic ovule tissues (fig. S4E).

YUCCA (*YUC*) genes encode key enzymes in auxin biosynthesis (*17*–*19*), and transgenic plants carrying *YUC::GUS* constructs (*17*, *18*) showed that *YUC1* and *YUC2* expression overlapped with the auxin response signal in the ovules during megagametogenesis (Figs. 1 and 3). For both genes, *YUC* expression appears first at the micropylar region of the nucellus outside the embryo sac at FG1 and then localizes to the micropylar pole of the gametophyte from FG2 through the later stages, while being undetectable in the nucellus (Fig. 3). This suggests that auxin might be synthesized initially at the nucellus and subsequently at the micropylar pole of the embryo sac during early embryo sac development, by at least these *YUC* genes.

To distort the polarized distribution of auxin observed in the embryo sac toward higher auxin levels, we expressed *YUC1* in the whole megagametophyte with the *Op-LhG4* transactivation system (*16*). Because YUC1 expression was driven by *pES1* throughout developing embryo sacs from FG1 to FG7 (*20*), we predicted that auxin would be distributed throughout the developing embryo sac if YUC1 substrates were present in the embryo sac. As expected *YUC1*-overexpressed female gametophytes did not establish a discernible auxin gradient, and *DR5::GFP* activity was detected in the entire female gametophyte from stages FG1 to FG5 (Fig. 4A and fig. S5). F1 plants overexpressing *YUC1* in the embryo sacs had about 25% defective ovules as identified by embryo sacs with micropylar cells with abnormal polarities as well as unfused polar nuclei and collapsed embryo sacs (Fig. 4, B and C, and table S4). Furthermore, antipodal cells that did not degenerate were detected in 34 of out of 268 overexpressed-YUC ovules examined (Fig. 4J).

We examined expression of a synergid-specific marker [ET884 (*6*)] normally expressed in wild-type embryo sacs only in the synergid cells. In YUC-overexpressing embryo sacs, the synergid marker was expressed in multiple cells, including those normally specified as egg cell, central cell, and the antipodals at the chalazal pole of the embryo sac (Fig. 4, D to F, and table S5). Equally frequently, in the YUC-overexpressing embryo sacs, an egg cell–specific marker [ET119 (*6*)] was also detected in the antipodal cells (Fig. 4H and table S5). In some cases this marker was exclusively expressed at the chalazal pole of the embryo sac, where the antipodal cells are usually located (Fig. 4I). It may be that, in these *YUC1*-overexpressing embryo sacs, the cell at the position of the WT egg cell has assumed synergid attributes (Fig. 4, C and F).

Markers for the central cell and the antipodal cells in YUC-overexpressing embryo sacs showed similar GUS staining patterns in both wild-type and YUC-overexpressing embryo sacs with the pMEA-GUS central cell marker (*6*), indicating that overall central cell identity is maintained (table S5). Thus, the central cell seems to be less responsive to changes in local auxin concentrations than other female gametophytic cells, although, as noted, some central cells did express synergid markers. In addition, after fertilization we detected isolated embryo sacs that lacked endosperm development and had a morphological structure resembling a zygote at the position of the central cell, suggesting that the central cell might have switched to an egg cell fate (Fig. 4L). In contrast, the antipodal-specific marker *pAt1g36340-GUS* (*20*) showed expression only in a small fraction of the expected *YUC*-overexpressing embryo sacs carrying the GUS reporter (~10%, table S5). These observations were consistent with the reduction in the characteristic cell death after maturity that typifies antipodal cells.

We also ascertained whether the extra synergid-like cells observed in *YUC*-overexpressing embryo sacs interfered with normal pollen tube growth. When *YUC1*-overexpressing pistils were pollinated with wild-type pollen, two pollen tubes approaching and entering the female gametophyte were detected in 44 ovules out of 428 examined, of which 107 were predicted to contain embryo sacs carrying the two transgenes required to overexpress *YUC1*. By comparison, only 0.5% of wild-type ovules had more than one pollen tube enter the female gametophyte (*21*). These observations show that high auxin levels throughout the embryo sac alters cell identities, resulting in the conversion of chalazal cell identities to micropylar

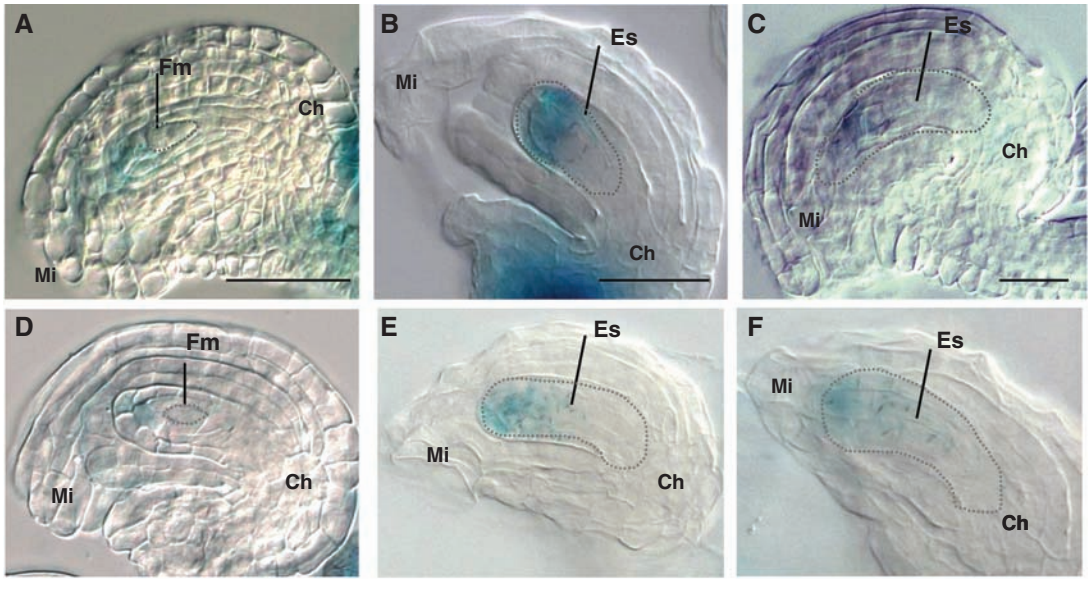

Fig. 3. Expression of *YUCCA* genes in transgenic plants carrying *YUC1::GUS and YUC2::GUS* constructs suggests a role for auxin biosynthesis in gametophyte development. (**A** to **F**) Expression of *YUC1* (A to C) and *YUC2* (D to F) in wild-type embryo sacs. Scale bars, 25 μm. (A) *YUC1* expression in the nucellus at FG1 stage. (B) *YUC1* expression at the micropylar end of the embryo sac at stage FG3. (C) *YUC1* expression at the micropylar end of the embryo sac at stage FG4. (D) *YUC2* expression in the nucellus at FG1 stage. (E) *YUC2* expression at the micropylar end of the embryo sac at stage FG3. (F) *YUC2* expression at the micropylar end of the embryo sac at stage FG4.

cell identities. As with the ARF–down-regulation experiments, we observed no abnormalities in nuclear positioning during embryo development arising from YUC1 overexpression (fig. S5), further confirming that nuclear positions within the syncitium are insensitive to auxin.

Auxin signaling and embryo sac development. We then examined mutants in auxin signaling for defects in cell specification. The *tir1 afb1 afb2 afb3* quadruple mutants have mutations in four genes of the *TIR* auxin receptor family and a significantly attenuated auxin response (*22*). From a total of 399 *tir1-1 afb1-1 afb2-1 afb3-1* embryo sacs examined, 82 showed defects in egg cell and synergid morphology, whereas 26 aborted at the 1 nuclear FG1 stage. The defective embryo sacs contained an additional egg cell–like cell replacing one of the two synergids, suggesting a switch of synergid to egg-cell fate (fig. S7A). We confirmed that at least some of these egg cell–like cells can function as gametic egg cells that form zygotelike structures after fertilization. By using embryonic markers introduced through the pollen, we demonstrated that the fertilized embryo sacs contain two embryos, together with an absence of fertilized endosperm, indicating that the two sperm cells have fertilized two egg cells (fig. S7, B and C).

Models for patterning of the female gametophyte in *Arabidopsis* by auxin. Thus, our results suggest that cell-type specification arises from the positional information conferred by the distance of the different nuclei from a micropylar auxin source in the syncitial embryo sac. The early auxin flux in the nucellus, as indicated by the location of PIN1 expression, might be involved in establishing an initial sporophtyic auxin source, which could then provide the trigger for events establishing gametophyte patterning. The trigger could be auxin itself or another patterning factor that is generated within the nucellus at that location. In either case, we can consider two alternative models for the subsequent events. In one model, the sporophytic signal leads to auxin sources specified within the gametophyte at the micropylar pole that result in a gradient of auxin along the micropylar-chalazal axis (Fig. 5, A to C). The outcome is the graded specification of different cell types, with the highest auxin concentrations specifying synergids, followed by egg cells, and the cells receiving the lowest amount of auxin developing into antipodal cells (Fig. 5D). In this model, all cells in the embryo sac might have the competence to differentiate into any of the different cell types composing the embryo sac, but the gradient of auxin directs the fate of each of the cells along the female gametophyte according to position. The positioning is determined by nuclear migration, which does not appear to be auxin-dependent, but may use other mechanisms (*8*). This proposed function of auxin in the embryo sac implies that it acts as a morphogen, that is, a source-derived gradient directing a concentration-dependent specification of different cell types, a concept for which support has been found in sporophytic root development (*23*, *24*). One difference is that the gametophytic auxin appears to be synthesized locally and in this respect resembles more closely the classical morphogen systems in animals.

Alternatively, gametophytic auxin might not be the primary instructive signal but might instead

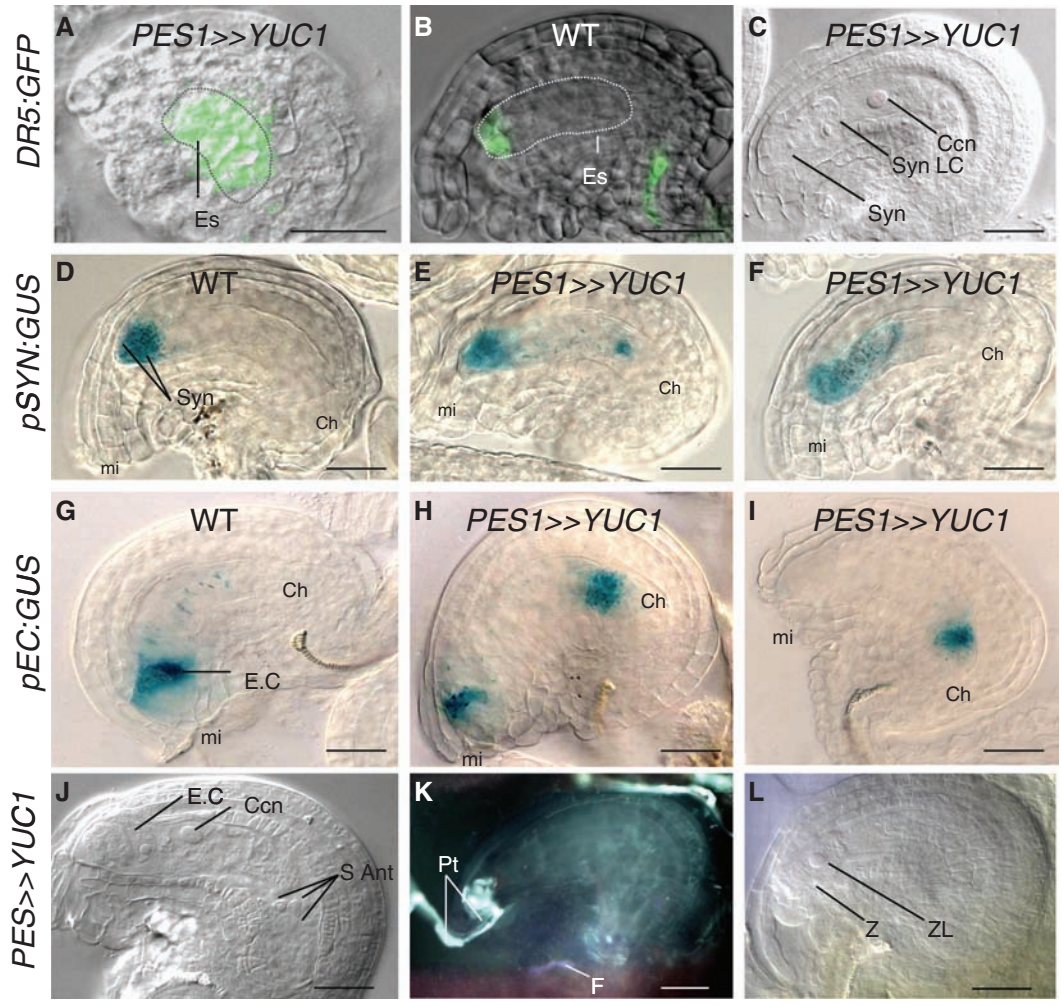

Fig. 4. Phenotype of *YUC1*-overexpressing embryo sacs and two alternative models for auxin-dependent cell specification in the female gametophyte. Scale bars, 25 μm. (**A**) DR5::GFP activity is localized in the whole embryo sac (Es) of *YUC1*-overexpressing embryo sacs at FG5. (**B**) Polarized DR5::GFP activity detected in a WT embryo sac at FG5. Ccn, central cell nucleus; Syn, synergid cells; and Syn LC, synergid-like cell. (**C**) A *YUC1*-overexpressing embryo sac with a synergid-like cell at a position in which the egg cell is usually located. (**D**) WT embryo sac showing the expression of a specific synergid marker. Ch, chalazal end of the embryo sac, and mi, micropylar end of the embryo sac. (**E**) Expression of the synergid marker in a *YUC1*-overexpressing embryo sac shows signal in the positions of both the synergid cells and the antipodal cells. (**F**) Expression of the synergid marker is detected in cells at the positions of synergids, egg cell, and central cell in a *YUC1*-overexpressing embryo sac. (**G**) Wild-type embryo sac showing the expression of an egg cell (E.C)–specific marker. (**H**) *YUC1*-overexpressing embryo sac exhibiting expression of the egg cell marker in a cell at the position of the egg cell and a cell at the antipodal position. (**I**) *YUC1*-overexpressing embryo sac showing expression of the egg cell marker only in a cell at the antipodal position. (**J**) Mature and unfertilized *YUC1*-overexpressing embryo sac from an emasculated flower showing surviving antipodal cells (S Ant) 2 days after emasculation. (**K**) Two pollen tubes (Pt) enter the micropyle of a *YUC1*-overexpressing embryo sac and continue to grow within the embryo sac. F, funiculus. (**L**) Fertilized *YUC1*-overexpressing embryo sac showing no endosperm development and a structure that morphologically resembles a zygote at the position of the central cell. EcL, egg cell–like cell; Z, zygote, and ZL, zygotelike cell.

act downstream of an undiscovered patterning factor "X" acting at the micropylar pole, which then induces *YUC* expression in the micropylar nuclei, resulting in the observed asymmetric auxin distribution (Fig. 5, E to H). In this model, high auxin might promote synergid cell fate, whereas egg-cell fate might be the consequence of lower levels of X that then result in lower auxin (Fig. 5H). The central cell and antipodals could then be specified by secondary auxin-independent mechanisms. The observation that central cell specification appears to be less susceptible to auxin levels than the other cells is consistent with the latter model. However, the relative stability of central cell fate to auxin perturbations can also be reconciled with the auxin as morphogen model. Because the central cell nucleus normally results from the fusion of two polar nuclei initially located at opposite sides of the female gametophyte, and these nuclei are hypothesized to be exposed to quite different auxin concentrations that are nonetheless intermediate between the egg apparatus and antipodals, specification of central cells might occur within a broader concentration range. Cells at this position are in fact capable of assuming synergid or egg cell attributes in high auxin (Fig. 4, F and L). Further studies will be needed to discriminate between these alternative models for patterning.

The maintenance of an auxin gradient within the syncitial embryo sac is unexpected. The localization of YUC gene expression, as well as the auxin GFP reporter, might be explained by the observation that the embryo sac syncitium is partitioned into cytoplasmic domains (*25*, *26*); such partitioning may restrict translation of messenger RNAs to the domain containing the nucleus where the transcript originated. However, auxin has a diffusion constant two orders of magnitude greater than GFP and is likely to diffuse rapidly even with cytoplasmic partitioning. Thus, it is probable that other mechanisms maintain a polarized auxin distribution, such as non-PIN auxin carriers or through the inactivation of auxin by conjugation or degradation at the chalazal pole.

Implications. This study provides support for the modular hypothesis of female gametophyte evolution (*1*, *2*, *27*). If the seven-cell/eight-nucleate *Polygonum*-type embryo sac that characterize the majority of the angiosperms is the result of a four-nuclei/cell module duplication, then cells in each of the modules might have conserved the capacity to differentiate into egg cells and synergids despite the loss of these functions at time of divergence of the basal angiosperm lineages >120 million years ago (*2*). Our observation that synergid and egg cell attributes can be generated at both poles of the embryo sac is consistent with this prediction. We hypothesize that, after the initial duplication, the potential egg apparatus located at the chalazal pole would be within a field of low auxin because of its distal position relative to the micropylar auxin source, leading to acquisition of a default cell fate as antipodal cells as a side effect (*2*). This study may also provide insights into the variation observed among angiosperm embryo sacs. Although the eight nuclear *Polygonum*-type embryo sac predominates, a wide variety of embryo sacs with 4 to 16 nuclei have been documented; yet in all such cases a unique egg cell develops and results in monozygotic seed when fertilized, although the number of haploid nuclei within the endosperm varies (*28*, *29*). This can be explained if the egg apparatus is always specified by its proximal location to the micropylar auxin source, which itself may be initially specified by the sporophyte. The formation of a single embryo in fertilized seeds, combined with variation in maternal genotype and ploidy of endosperm tissue, may determine fitness by affecting both the paternal genome dosage and the effects of imprinting that control seed size, as well as the relatedness between the endosperm and embryo (*29*).

Lastly, it is interesting to consider our results within the framework of the ancestral function of auxin in gametophyte patterning. Analyses of extant land plants and paleobotanical evidence indicate that the reduced female gametophyte of angiosperms is derived from an ancestral, complex, free-living gametophyte (*30*). Although little is known about the genetic basis of pattern formation of extant land plants with complex gametophytes, pharmacological experiments implicate that auxin is an important factor (*31*), despite evidence that polar auxin transport may be restricted to the sporophyte in several mosses studied (*31*, *32*). We hypothesize that localized auxin synthesis, along with the induction of sequential sources combined with auxin degradation/conjugation, rather than PIN-mediated transport might have been more important in establishing the patterning of lower plant gametophytes. Given their evolutionary history, it is likely that genetic programs patterning the female gametophytes of angiosperms were inherited from those patterning the complex three-dimensional tissues of ancestral gametophytes.

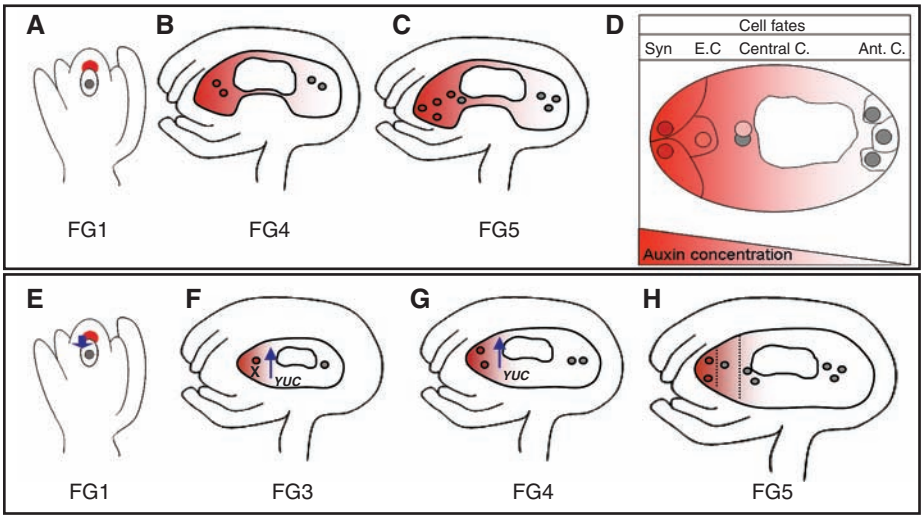

Fig. 5. Models for patterning of the female gametophyte. (**A** to **D**) Auxin gradient model for patterning. (A) At FG1 stage, the auxin source is sporophytic and is derived from the nucellus. (B) Subsequently, a secondary auxin source is specified locally within the gametophyte at the micropylar pole. (C) Auxin gradient with a maximum at the micropylar pole of the embryo sac. (D) Auxin concentration determines cell fates, with the highest auxin concentrations specifying synergids (Syn), followed by egg cells (E.C), and the lowest auxin resulting in antipodal (Ant.) cells. Central C., central cell. (**E** to **H**) Model for patterning by a nonauxin molecule acting through auxin. (E) Nucellus generates a signal (block arrow), which might originate from the auxin source. (F) This signal induces a factor X at the micropylar pole, which then induces auxin synthesis by activating *YUCCA* gene expression in the nucleus located at that pole. (G) Continued synthesis of auxin at micropylar pole. (H) Two of the micropylar nuclei are in the high auxin zone and differentiate into synergids, whereas the third micropylar nucleus in lower auxin differentiates into the egg cell. In this model, the central cell and antipodal cell fates could be specified by auxin-dependent or auxin-independent mechanisms.

References and Notes

1. M. W. Frohlich, M. W. Chase, *Nature* **450**, 1184 (2007).
2. J. H. Williams, W. E. Friedman, *Plant Cell* **16**, S119 (2004).
3. C. A. Christensen, E. J. King, J. R. Jordan, G. N. Drews, *Sex. Plant Reprod.* **10**, 49 (1997).
4. C. A. Christensen, S. Subramanian, G. N. Drews, *Dev. Biol.* **202**, 136 (1998).
5. J. M. Moore, J. P. V. Calzada, W. Gagliano, U. Grossniklaus, *Cold Spring Harbor Symp. Quant. Biol.* **62**, 35 (1997).
6. R. Gross-Hardt *et al.*, *PLoS Biol.* **5**, e47 (2007).
7. G. C. Pagnussat *et al.*, *Development* **132**, 603 (2005).
8. G. C. Pagnussat, H. J. Yu, V. Sundaresan, *Plant Cell* **19**, 3578 (2007).
9. M. M. S. Evans, *Plant Cell* **19**, 46 (2007).
10. D. Umulis, M. B. O'Connor, H. G. Othmer, *Curr. Top. Dev. Biol.* **81**, 65 (2008).
11. E. Benkova *et al.*, *Cell* **115**, 591 (2003).
12. J. Friml *et al.*, *Nature* **426**, 147 (2003).
13. J. Mattsson, W. Ckurshumova, T. Berleth, *Plant Physiol.* **131**, 1327 (2003).
14. S. Sabatini *et al.*, *Cell* **99**, 463 (1999).
15. T. Ulmasov, J. Murfett, G. Hagen, T. J. Guilfoyle, *Plant Cell* **9**, 1963 (1997).
16. Materials and methods are available as supporting material on *Science* Online.

17. Y. Cheng, X. H. Dai, Y. D. Zhao, *Genes Dev.* **20**, 1790 (2006).
18. Y. Cheng, X. H. Dai, Y. D. Zhao, *Plant Cell* **19**, 2430 (2007).
19. Y. Zhao *et al.*, *Science* **291**, 306 (2001).
20. H. J. Yu, P. Hogan, V. Sundaresan, *Plant Physiol.* **139**, 1853 (2005).
21. N. Huck, J. M. Moore, M. Federer, U. Grossniklaus, *Development* **130**, 2149 (2003).
22. N. Dharmasiri *et al.*, *Dev. Cell* **9**, 109 (2005).
23. O. Leyser, *Cell* **121**, 819 (2005).
24. C. Galinha *et al.*, *Nature* **449**, 1053 (2007).
25. R. C. Brown, B. C. Lemmon, *EMSA Bull* **22**, 48 (1992).
26. R. C. Brown, B. C. Lemmon, *Protoplasma* **165**, 155 (1991).
27. W. E. Friedman, J. H. Williams, *Evolution* **57**, 216 (2003).
28. V. Brukhin, M. D. Curtis, U. Grossniklaus, *Curr. Sci.* **89**, 1844 (2005).
29. W. E. Friedman, E. N. Madrid, J. H. Williams, *Int. J. Plant Sci.* **169**, 79 (2008).
30. P. Kenrick, P. R. Crane, *The Origin and Early Diversification of Land Plants: A Cladistic Study* (Smithsonian Series in Comparative Evolutionary Biology, Smithsonian Institution, Washington, DC, 1997).
31. T. J. Cooke, D. Poli, A. E. Sztein, J. D. Cohen, *Plant Mol. Biol.* **49**, 319 (2002).
32. T. Fujita *et al.*, *Evol. Dev.* **10**, 176 (2008).
33. We thank U. Grossniklaus for providing the cell-specific marker lines used in this study; B. Sheres, J. Friml, and M. Tasaka for providing plants carrying PIN::GFP fusions; Y. Zhao for providing YUC::GUS reporter lines and YUC1 cDNA; N. Dharmasiri for seeds of the *tir1afb* quadruple mutant; M. Yu and A. Krishnan for technical assistance; and G. Ruvkun, D. Hanahan, members of the Gasser, Bowman, and Sundaresan labs, and three anonymous reviewers for valuable suggestions. Funded by NSF grants IOS-0313501 (V.S.), IOS-0745167 (V.S.), and IOB-0515435 (J.L.B.).

Supporting Online Material

www.sciencemag.org/cgi/content/full/1167324/DC1
Materials and Methods
Figs S1 to S7
Tables S1 to S5
References

17 October 2008; accepted 28 April 2009
Published online 4 June 2009;
10.1126/science.1167324
Include this information when citing this paper.

Extending Universal Nodal Excitations Optimizes Superconductivity in $Bi_2Sr_2CaCu_2O_{8+\delta}$

Aakash Pushp,[1,2]* Colin V. Parker,[1]* Abhay N. Pasupathy,[1]† Kenjiro K. Gomes,[1]‡ Shimpei Ono,[3] Jinsheng Wen,[4] Zhijun Xu,[4] Genda Gu,[4] Ali Yazdani[1]§

Understanding the mechanism by which *d* wave superconductivity in the cuprates emerges and is optimized by doping the Mott insulator is one of the major outstanding problems in condensed-matter physics. Our high-resolution scanning tunneling microscopy measurements of the high–transition temperature (T_c) superconductor $Bi_2Sr_2CaCu_2O_{8+\delta}$ show that samples with different T_c values in the low doping regime follow a remarkably universal *d* wave low-energy excitation spectrum, indicating a doping-independent nodal gap. We demonstrate that T_c instead correlates with the fraction of the Fermi surface over which the samples exhibit the universal spectrum. Optimal T_c is achieved when all parts of the Fermi surface follow this universal behavior. Increasing the temperature above T_c turns the universal spectrum into an arc of gapless excitations, whereas overdoping breaks down the universal nodal behavior.

Central to the current debate on the mechanism underlying high-temperature superconductivity is the question of whether pairing strength in the cuprates is diminished as these systems approach the Mott insulator limit with reduced hole density. The panoply of physical phenomena in lightly doped cuprates near the Mott state uncovered over the last two decades—from observation of the pseudogap behavior (*1*, *2*) to fluctuating superconductivity (*3*) above the transition temperature (T_c) to the possibility of other competing orders (*4*–*6*)—have made addressing this question challenging. In a simple *d* wave superconductor, a single energy scale suffices to completely describe the excitation spectrum, the associated pairing energy gap (including its angular and temperature dependence), as well as the T_c of the sample. In the underdoped cuprates, however, there is increasing evidence (*7*–*12*) that a single energy scale is insufficient to describe the anisotropy of the energy gap because different behavior is seen near the node (45° to the Cu–O bond direction) and the anti-node (along the Cu–O bond direction). The temperature evolution of the spectroscopic measurements has also shown a dichotomy between nodal and anti-nodal gaps, showing different temperature dependence (*8*, *10*, *13*). Theoretical proposals for addressing these phenomena include those based on phase fluctuations of preformed pairs (*14*–*16*), incipient order (*5*), breakup of the Fermi surface due to umklapp scattering (*17*), and incoherence of anti-nodal quasi-particles (*18*). Although it is clear that the gap near the anti-node increases as one approaches the Mott insulator (*19*), the behavior of the gap near the node still remains debated, with different measurements showing both increasing (*19*–*21*) and decreasing (*7*, *8*, *22*) trends with underdoping. Whether pairing gaps associated with nodal excitations track the samples' T_c, as expected for simple *d* wave superconductors, is an unresolved question that deeply affects our understanding of superconductivity in the cuprates. The answer to this question can determine if the pairing is derived from the strong electronic correlations of the Mott state and can identify the mechanism by which *d* wave superconductivity is optimized in proximity to an insulating ground state.

To elucidate the nature of the nodal and anti-nodal gaps as a function of doping and temperature, we performed atomically resolved scanning tunneling microscopy (STM) measurements on $Bi_2Sr_2CaCu_2O_{8+\delta}$ (BSCCO) in the doping range of $0.07 < x < 0.24$ (where x is the nominal hole doping) and a temperature range from 5 to 120 K. Spectroscopic measurements in our home-built scanning tunneling microscope can be performed with sub–millielectron volt energy resolution on the same atomic location as a function of temperature (*9*, *23*). Although STM spectroscopy does not have intrinsic angular resolution, information about the nodal gap can be obtained from the spectrum near the Fermi energy, whereas the anti-nodal excitations occur at higher energy. We can use this information to extract the behavior of the nodal gap.

The complexity of the excitation spectrum in underdoped BSCCO samples (Fig. 1A) is seen in lattice-tracking spectroscopy (*9*, *23*) measurements, in which we track the temperature evolution of tunneling spectra at a given atomic location. This spectrum (typical for this sample) shows a higher energy gap, Δ_0, (black arrow in Fig. 1A), a smaller "kink" within the higher energy gap (red arrow in Fig. 1A), and an overall background, all of which are position dependent. Δ_0, determined by the maximum conductance on the positive side, shows strong spatial inhomogeneity (*24*, *25*) on the sample (Fig. 1C). The spatial average of the higher energy gap compares well with angle-resolved

[1]Joseph Henry Laboratories and Department of Physics, Princeton University, Princeton, NJ 08544, USA. [2]Department of Physics, University of Illinois at Urbana-Champaign, Urbana, IL 61801, USA. [3]Central Research Institute of Electric Power Industry, Komae, Tokyo 201-8511, Japan. [4]Condensed Matter Physics and Materials Science, Brookhaven National Laboratory (BNL), Upton, NY 11973, USA.

*These authors contributed equally to this work.
†Present address: Department of Physics, Columbia University, New York, NY 10027, USA.
‡Present address: Department of Physics, Stanford University, Stanford, CA 94305, USA.
§To whom correspondence should be addressed. E-mail: yazdani@princeton.edu

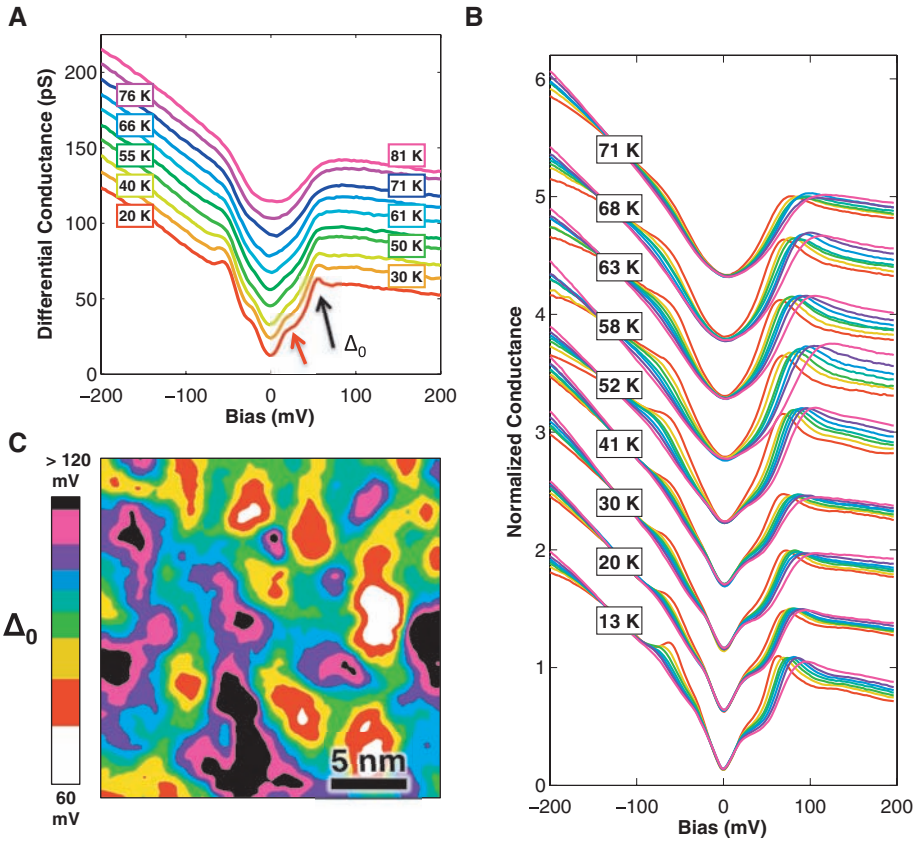

Fig. 1. (**A**) Spectra taken at one atomically resolved location on an underdoped $Bi_2Sr_2CaCu_2O_{8+\delta}$ sample (T_c = 61 K, UD61) at various temperatures. The spectra show two features at low temperature, the smaller of which (red arrow) disappears at higher temperatures. The higher-energy feature Δ_0 (black arrow) compares well with the anti-nodal gap measurements from ARPES. (**B**) Δ_0 sorted, averaged spectra at 13 K from 8192 spectral measurements on another underdoped $Bi_2Sr_2CaCu_2O_{8+\delta}$ sample (T_c = 58 K, UD58), for different temperatures and values of Δ_0. The spectra are normalized by the mean over the whole bias range shown (each offset by 0.5). (**C**) A spatial map at 13 K showing the variation of Δ_0. The colored regions represent areas where Δ_0 is nearest to the correspondingly colored spectrum in (B).

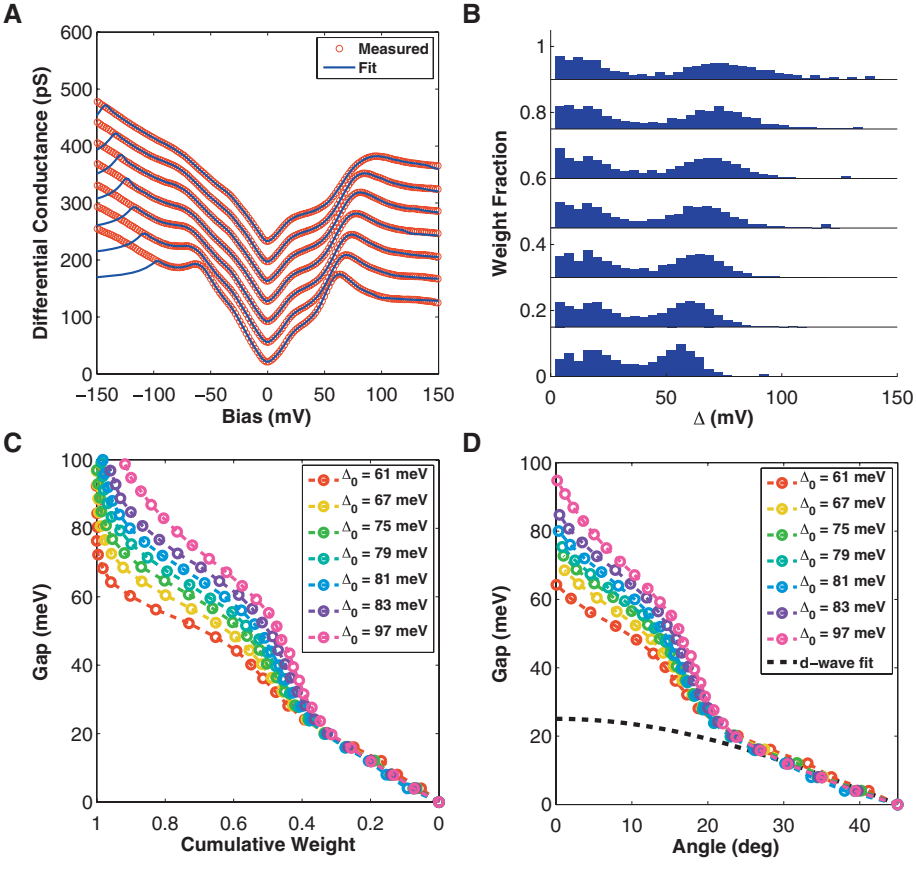

Fig. 2. (**A**) Average *dI/dV* spectra (orange circles) from Δ_0 sorted spectra on sample UD58 and the fit (solid blue line) as described in the text. The procedure is applied separately to the positive and negative sides. The curves are offset by 35 pS. (**B**) The weights of the corresponding positive side fits in (A), expressed as a fraction of the total weight for each gap size (each offset by 0.15). (**C**) Cumulative weights (*x* axis) obtained by summing the corresponding histogram for each gap size (*y* axis). The *x* axis would be proportional to the angle around the Fermi surface for a cylindrical band structure. (**D**) Gap as a function of angle as extracted from the fits, using the ARPES band structure (*27*).

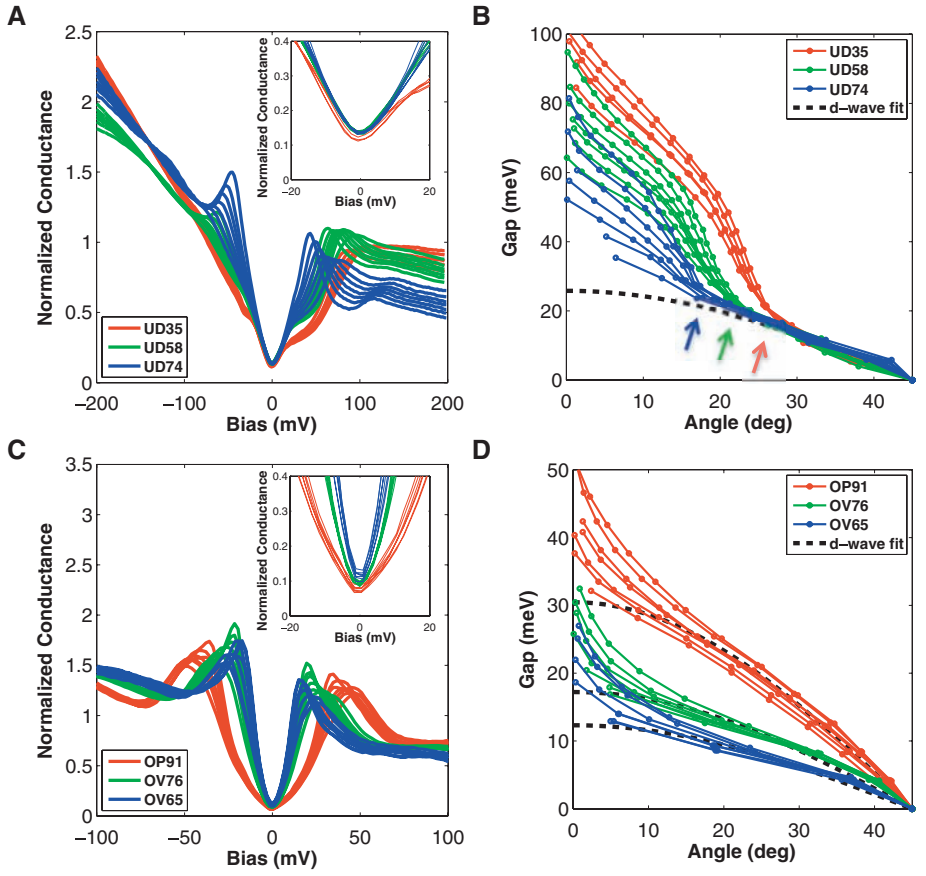

Fig. 3. (**A**) Average normalized *dI*/*dV* spectra for different Δ_0 values on three underdoped samples with T_c values of 35, 58, and 74 K taken at 8, 13, and 20 K, respectively. (Inset) Low-bias region, where the spectra follow a universal behavior. The normalization is done by averaging over the whole bias range. (**B**) Gap as a function of angle for the same samples as in (A). The low-bias universal behavior can be seen at angles near the nodes in all samples and agrees with a simple *d* wave form. At different points marked by colored arrows, the spectra deviate sharply from the universal behavior, leading to the kinks in the raw spectra. (**C**) Average normalized *dI*/*dV* spectra for different Δ_0 values on an optimally doped (OP91) and two overdoped samples with T_c values of 76 K (OV76) and 65 K (OV65), all taken at 8 K. (Inset) Low-bias region, where the universal behavior is lost. (**D**) Gap as a function of angle for the same samples as in (C). No universal behavior is seen at angles near the nodes.

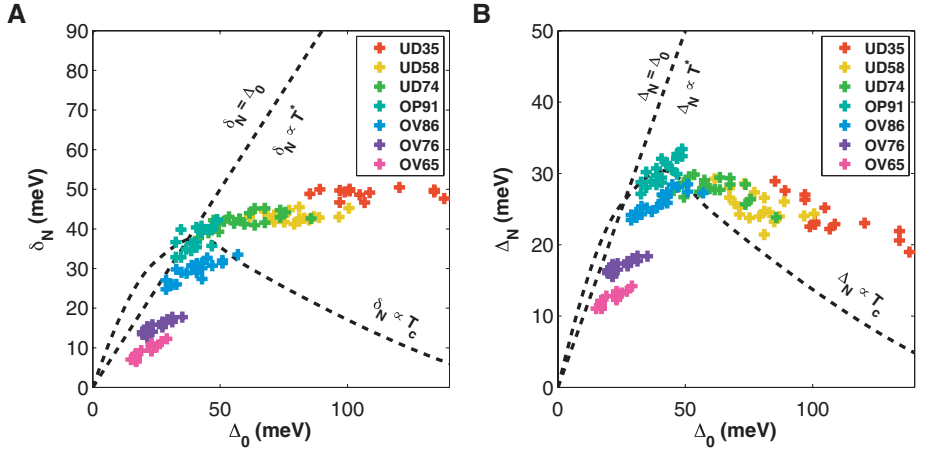

Fig. 4. (**A**) The inverse nodal slope (δ_N) extracted from a parabolic fit to the low bias region of the raw spectrum, plotted against the anti-nodal gap (Δ_0) extracted from the maximum in *dI*/*dV* on the positive side of the raw spectrum. For a *d* wave gap, the inverse nodal slope from a normalized *dI*/*dV* measurement is equal to the gap. (**B**) The nodal gap (Δ_N) extrapolated from the gap versus angle fits versus Δ_0. Dotted lines indicate the behavior expected for Δ_N tracking T_c or pseudogap temperature T^*. Note that both methods of determining the nodal behavior indicate a saturation at low doping, and neither quantity tracks T_c or T^*.

photoemission spectroscopy (ARPES) measurements of the anti-nodal gap (*19*, *20*), and, therefore, we identify it as such. Δ_0 shows relatively small temperature dependence and evolves smoothly through T_c into the anti-nodal pseudogap (*9*), whereas the kink shows strong temperature dependence (Fig. 1A). We show this contrast by averaging spectra from locations of the sample with the same Δ_0 and plotting the resultant spectra (Fig. 1B) as a function of temperature. At low temperatures, the low-energy spectra (below the kink) are substantially more homogeneous than the Δ_0 (*24*, *25*). However, the low-energy homogeneity is lost upon raising the temperature through T_c.

The shape of the tunneling spectra in underdoped samples (Fig. 1) cannot be fit to a simple *d* wave cos(2Θ) form (where Θ is the Fermi surface about (π, π) in momentum space), as it can be for overdoped samples (*23*). To quantitatively understand the shape of the energy gap in momentum space, we model the spectrum using an angle-dependent Bardeen-Cooper-Schrieffer (BCS)–like gap where we allow the gap function to deviate from the cos(2Θ) form while maintaining overall *d* wave symmetry. With evidence (*19*, *26*) from ARPES measurements showing that the spectral function is BCS-like at the node as well as at the anti-node, we model our spectra using a sum of BCS-like gaps. If we assume that the gap varies monotonically from the node to the anti-node and that the lifetime broadening is small at low temperatures, then we can fit the spectra uniquely with high accuracy (Fig. 2A). The fitting procedure described below allows us to extract the energy gap as a function of angle from the measured spectra in Fig. 2.

To fit the spectra shown in Fig. 2A, we assume that the differential conductance at a voltage bias V and temperature T is given by a sum of BCS gaps

$$\frac{dI}{dV}(V) = \int dE \frac{df(E+V,T)}{dE} \times \sum_{j=1}^{N} \mathrm{Re} \frac{(E - i\Gamma)}{\sqrt{(E - i\Gamma)^2 - \Delta_j^2}} \times W_j \quad (1)$$

Here, E is the energy, f is the Fermi function, N is the desired number of bins, i is the square root of –1, Δ_j are gaps each with a weight W_j, and Γ is the inverse of quasi-particle lifetime (a small nonzero value of Γ ~ 3 to 5 meV is required to match the experimentally observed conductance at the Fermi energy). Fitting the experimental spectrum then reduces to finding the weighting coefficients W_j, which can be done with the use of a simple least-squares fit. Figure 2B shows the weights obtained from these fits to the spectra shown in Fig. 2A.

The generalized approach in extracting the distribution of W_j from the spectra by using the model in Eq. 1 allows us to determine the angular dependence of Δ(Θ) from the STM spectra and, more precisely, to isolate the universal be-

havior of the low-energy excitation spectrum (*27*). The cumulative weight $C_j = \sum_{j'=1}^{j} W_{j'}$ is proportional to $\Theta(\Delta)$ in the case of a simple cylindrical Fermi surface. Figure 2C shows experimentally determined C_j for an underdoped sample with T_c = 58 K. With a more realistic model of the background density of states based on modeling of the ARPES data, information in Fig. 2C can be used to arrive at $\Delta(\Theta)$, as shown in Fig. 2D (*27*). Another way to view the results of the fitting procedure is that the functions $\Delta(\Theta)$ plotted in Fig. 2D provide the most accurate fit to the spectra shown in Fig. 2A and can capture all of the energy and spatial dependence of the data. Slightly different results are obtained from fits to the unoccupied (positive) and occupied (negative) side of the spectrum, but the trend is consistent between both (*27*). We will describe results from the unoccupied side.

The uniformity and shape of the spectra at low energy are the results of a position-independent $\cos(2\Theta)$ form of $\Delta(\Theta)$ near the node, whereas the kink in the spectra at higher energies signals the deviation of $\Delta(\Theta)$ from the $\cos(2\Theta)$ form at an angle away from the node. Previous attempts to extract gap versus angle with the use of quasiparticle interference (*28*) have not yielded results on the nature of nodal quasi-particles. The deviation of $\Delta(\Theta)$ for underdoped BSCCO reported here from STM measurements is very similar to recently reported ARPES measurements in other underdoped samples (*12*, *29*, *30*). However, systematic study of the $\Delta(\Theta)$ with doping and temperature uncovers its universal structure, its connection to samples' T_c values, and the Fermi arc behavior in underdoped samples.

To understand the behavior of the nodal gap with diminishing doping, we have measured STM spectra on a range of underdoped samples at $T << T_c$. Figure 3A shows spectra (spatially averaged by anti-nodal gap size) taken from three underdoped samples with T_c = 74, 58, and 35 K. We can clearly see that each sample displays a low-energy region, where the spectra are relatively homogeneous, and large inhomogeneity beyond the kink energy. We have normalized the tunneling conductance measured on different samples to their average value over the entire range shown, although the agreement of the low-bias region in the spectra is independent of the normalization (*27*). For a *d* wave superconductor, the slope of the spectrum near zero bias is inversely proportional to the value of the nodal gap. As the spectra shown in Fig. 3A line up, not only within a sample but across samples, we conclude that the nodal gap is uniform over the entire doping range shown in Fig. 3A (see inset for expanded view).

Based on the simple analysis of the shape of the spectra near zero bias, our conclusions regarding the nodal gap can be put on a firmer footing by using the extraction procedure to determine the gap versus angle for each spectrum. The results of this analysis (Fig. 3B) show that our simple expectation for the nodal gap is correct; all the spectra for these samples follow a universal curve near the node. We find that spectra for the different samples break away from this universal line in a doping dependent fashion (marked by the arrows in Fig. 3B): The sample with the lowest T_c breaks away at the smallest angle from the node, whereas the sample with the highest T_c continues along this line for the largest angle. The universality of the nodal spectrum and the doping-dependent breaking away from the universal *d* wave form constitute our principal results.

We contrast these results obtained for underdoped samples with the overdoped case. In the spectra obtained from an optimally doped sample (T_c = 91 K) and two overdoped samples with T_c values of 76 and 65 K (Fig. 3C), we can see that there is a variation in the near zero bias slope among spectra obtained on these samples (expanded view in the inset of Fig. 3C). The results of the $\Delta(\Theta)$ extraction procedure on these spectra (Fig. 3D) show that the universality of the nodal gap function is lost in these samples, as anticipated. Instead, there is substantial inhomogeneity in the nodal gaps, both within a sample as well as between dopings. The gap function in these samples is much closer to a $\cos(2\Theta)$ form as compared with that observed for the underdoped samples, although very close to the anti-nodal region, there is still some deviation from $\cos(2\Theta)$ dependence. This high-energy behavior is most likely associated with deviations from a pure *d* wave form caused by coupling to a bosonic mode (*20*, *23*). This coupling causes the conductance to increase above the *d* wave value at energies above the true anti-nodal gap, for which the fit compensates by adding a small weight for these oversized gaps.

To compare results for the nodal gap across the phase diagram, we define two measures of the nodal gap. The first measure is the inverse slope of the normalized *dI*/*dV* spectra near the Fermi energy δ_N (Fig. 4A) as a function of the maximum anti-nodal gap Δ_0 observed for each spectrum. Ideally, we would determine the slope as close to zero bias as possible, but to avoid broadening effects, we determine the slope at 10 mV bias from a parabolic fit. For anti-nodal gaps smaller than ~50 mV (optimal and overdoped samples), the nodal gap increases along with the anti-nodal gap. However, once the anti-nodal gap increases beyond 50 mV, the nodal gap is essentially saturated. A more quantitative estimate of the nodal gap is obtained from our $\Delta(\Theta)$ extraction procedure for each spectrum by extrapolating the shape of the near nodal gap following the universal *d* wave $\cos(2\Theta)$ curve to the anti-node. We refer to this as the universal nodal gap Δ_N, which characterizes the strength of pairing experienced by excitations near the node. We plot this quantity as a function of the anti-nodal gap (Fig. 4B) and once again see that, for optimal and overdoped samples, there is a strong correlation between Δ_N and Δ_0 (for a simple *d* wave, $\Delta_N = \Delta_0$). However, as Δ_0 increases into the underdoped regime, Δ_N saturates. Altogether, our results show that the evolution of the nodal gap with doping is very different from that of a simple BCS *d* wave supercon-

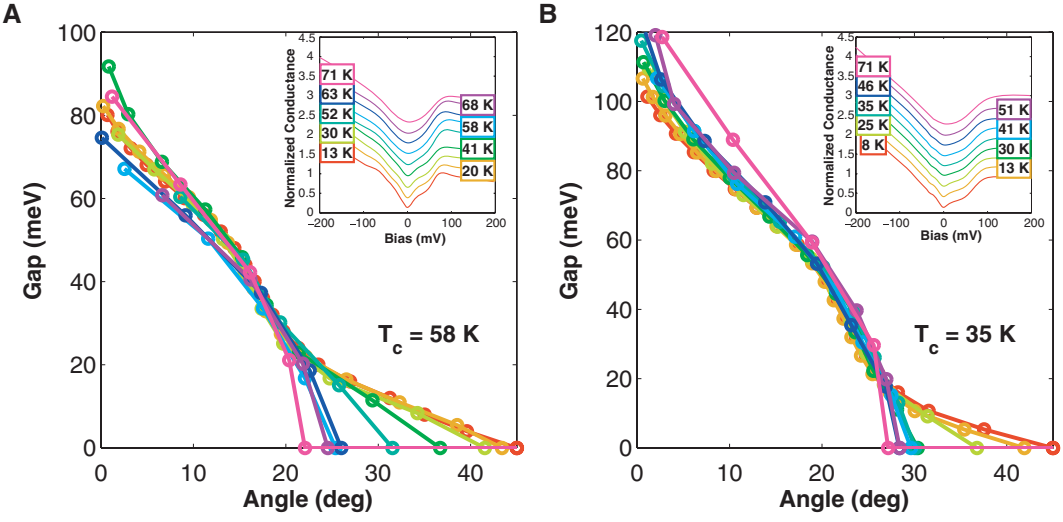

Fig. 5. Temperature evolution of the gap as a function of angle for the UD58 sample (**A**) and UD35 sample (**B**), obtained from the corresponding sample-averaged spectra (insets), showing the collapse of the nodal gaps near T_c. The gap strength at the point of deviation from *d* wave is not diminished with temperature.

ductor. On the overdoped side, the nodal gap, on average, tracks the T_c of the sample, although there is strong local inhomogeneity that gives rise to local patches of pairing, even above T_c (*9*, *23*). The data on the underdoped side show that pairing associated with nodal excitations does not increase in strength beyond its value at optimal doping and does not track T_c, yet the angular range of universal nodal *d* wave excitations is systematically suppressed as doping is reduced.

Examination of the temperature evolution of the tunneling spectra across T_c demonstrates an important connection between the universal *d* wave structure we find at low temperatures and the Fermi arc behavior that has long been the hallmark of underdoped cuprates (*13*). The angular extraction procedure for $\Delta(\Theta)$ previously used at low temperature can also be applied to determine the temperature dependence of $\Delta(\Theta)$. Figure 5, A and B, shows the temperature evolution of the extracted $\Delta(\Theta)$ for two underdoped samples (T_c = 58 and 35 K), whereas the insets show the corresponding sample-averaged spectra. As the temperature is raised above T_c, the gaps around the node vanish leading to an arc of gapless excitations, whereas the anti-node is relatively unchanged. The value of the lifetime broadening, Γ, for these fits is determined at the lowest temperature. The destruction of the gap can imply that either the amplitude of the gap is zero or the lifetime broadening exceeds the gap magnitude (*14*, *15*).

Although the nodal gaps disappear above T_c in underdoped samples, the temperature dependence of the gaps is very different from that of a conventional *d* wave BCS superconductor. As the temperature is raised, the nodal points do not reduce continuously as a function of temperature and disappear at T_c, but rather they develop into an arc whose length increases with increasing temperature. The observation of the Fermi arc above T_c is in accord with previous ARPES measurements that ubiquitously show this phenomenon in the underdoped cuprates (*13*, *19*); however, the $\Delta(\Theta)$ from STM measurements shown in Fig. 5 provides a new perspective on the relation between the arc and the *d* wave nodal gap. For both underdoped samples, the angular region over which the arc occurs immediately above T_c is the same as the universal *d* wave region we observed at temperatures well below T_c. As the doping is reduced (the two dopings shown in Fig. 5), both the arc regions as well as the universal *d* wave region decrease together.

Our measurements of the behavior of the nodal gaps with doping and temperature suggest a new picture of superconductivity in BSCCO. In overdoped samples, the nodal gaps, on average, increase with T_c, as one would expect for an inhomogeneous *d* wave superconductor, and collapse at a range of temperatures above T_c, correlating with the local variation of the pairing interaction (*9*, *23*). The anisotropic shape of the gap follows that of a simple *d* wave order parameter, and it is reasonable to assume that the entire Fermi surface contributes to bulk superconductivity. Below optimal doping, the anti-nodal gap continues to increase with decreasing hole doping, as has been measured in several previous experiments (*7*–*10*, *12*, *19*). However, our measurements demonstrate that the nodal gap does not change with reduced doping. The pairing strength does not get weaker or stronger as the Mott insulator is approached; rather, it saturates. There are strong deviations from the universal *d* wave excitation spectrum, which occur closer to the node with reduced doping. For each doping, the deviation point coincides with the Fermi arc observed above T_c. These observations are consistent with the hypothesis that only the areas of the Fermi surface that follow the universal *d* wave spectrum contribute to bulk superconductivity. Such a reduction in the *d* wave region also reduces the superfluid density, which, in turn, could make the systems susceptible to phase fluctuations (*31*), thereby reducing T_c. Although the origin of the anti-nodal gap remains unclear, optimal T_c is achieved when excitations follow the universal *d* wave characteristic along the entire Fermi surface.

References and Notes

1. T. Timusk, B. Statt, *Rep. Prog. Phys.* **62**, 61 (1999).
2. P. A. Lee, N. Nagaosa, X.-G. Wen, *Rev. Mod. Phys.* **78**, 17 (2006).
3. Y. Wang *et al.*, *Phys. Rev. Lett.* **95**, 247002 (2005).
4. V. J. Emery, S. A. Kivelson, J. M. Tranquada, *Proc. Natl. Acad. Sci. U.S.A.* **96**, 8814 (1999).
5. M. R. Norman, D. Pines, C. Kallin, *Adv. Phys.* **54**, 715 (2005).
6. D. LeBoeuf *et al.*, *Nature* **450**, 533 (2007).
7. M. Le Tacon *et al.*, *Nat. Phys.* **2**, 537 (2006).
8. K. Tanaka *et al.*, *Science* **314**, 1910 (2006); published online 15 November 2006 (10.1126/science.1133411).
9. K. K. Gomes *et al.*, *Nature* **447**, 569 (2007).
10. W. S. Lee *et al.*, *Nature* **450**, 81 (2007).
11. M. C. Boyer *et al.*, *Nat. Phys.* **3**, 802 (2007).
12. T. Kondo, R. Khasanov, T. Takeuchi, J. Schmalian, A. Kaminski, *Nature* **457**, 296 (2009).
13. A. Kanigel *et al.*, *Nat. Phys.* **2**, 447 (2006).
14. M. R. Norman, A. Kanigel, M. Randeria, U. Chatterjee, J. C. Campuzano, *Phys. Rev. B* **76**, 174501 (2007).
15. P. W. Anderson, preprint available at http://arxiv.org/abs/0807.0578v1.
16. C.-C. Chien, Y. He, Q. Chen, K. Levin, preprint available at http://arxiv.org/abs/0901.3151.
17. C. Honerkamp, M. Salmhofer, N. Furukawa, T. M. Rice, *Phys. Rev. B* **63**, 035109 (2001).
18. P. W. Anderson, P. A. Casey, preprint available at http://arxiv.org/abs/0902.1980v1.
19. J. C. Campuzano, M. R. Norman, M. Randeria, in *The Physics of Superconductors*, K. H. Bennemann, J. B. Ketterson, Eds. (Springer, Berlin, 2004), pp. 167–265.
20. A. Damascelli, Z. Hussain, Z.-X. Shen, *Rev. Mod. Phys.* **75**, 473 (2003).
21. M. Sutherland *et al.*, *Phys. Rev. B* **67**, 174520 (2003).
22. J. L. Tallon, J. W. Loram, *Physica C* **349**, 53 (2001).
23. A. N. Pasupathy *et al.*, *Science* **320**, 196 (2008).
24. C. Howald, P. Fournier, A. Kapitulnik, *Phys. Rev. B* **64**, 100504 (2001).
25. K. McElroy *et al.*, *Phys. Rev. Lett.* **94**, 197005 (2005).
26. A. Kanigel *et al.*, *Phys. Rev. Lett.* **99**, 157001 (2007).
27. See supporting data on *Science* Online.
28. Y. Kohsaka *et al.*, *Nature* **454**, 1072 (2008).
29. T. Yoshida *et al.*, preprint available at http://arxiv.org/abs/0812.0155v1.
30. R.-H. He *et al.*, *Nat. Phys.* **5**, 119 (2009).
31. V. J. Emery, S. A. Kivelson, *Nature* **374**, 434 (1995).

32. We gratefully acknowledge discussions with P. W. Anderson, N. P. Ong, M. R. Norman, and M. Randeria. The work at Princeton is supported by the U.S. Department of Energy (DOE) under contract DE-FG02-07ER46419 and NSF through the Princeton Center for Complex Materials and through an NSF-Instrumentation grant. The work in BNL is supported by DOE under contract DE-AC02-98CH10886.

Supporting Online Material

www.sciencemag.org/cgi/content/full/1174338/DC1
SOM Text
Figs. S1 to S4
References

31 March 2009; accepted 21 May 2009
Published online 4 June 2009;
10.1126/science.1174338
Include this information when citing this paper.

High-Resolution NMR in Magnetic Fields with Unknown Spatiotemporal Variations

Philippe Pelupessy,[1]* Enrico Rennella,[2] Geoffrey Bodenhausen[1,3]

Nuclear magnetic resonance (NMR) experiments are usually carried out in homogeneous magnetic fields. In many cases, however, high-resolution spectra are virtually impossible to obtain because of the inherent heterogeneity of the samples or living organisms under investigation, as well as the poor homogeneity of the magnets (particularly when bulky samples must be placed outside their bores). Unstable power supplies and vibrations arising from cooling can lead to field fluctuations in time as well as space. We show how high-resolution NMR spectra can be obtained in inhomogeneous fields with unknown spatiotemporal variations. Our method, based on coherence transfer between spins, can accommodate spatial inhomogeneities of at least 11 gauss per centimeter and temporal fluctuations slower than 2 hertz.

Nuclear magnetic resonance (NMR) is arguably one of the most versatile and ubiquitous forms of spectroscopy. Year after year, magnetic resonance imaging (MRI) reveals surprising insights into morphology, function, and metabolism. Most applications, regardless of whether they are concerned with inanimate solids or liquids or with living organisms, rely

on the use of very homogeneous magnetic fields B_0 with spatial variations below about 10^{-9}, so that subtle differences in the environment of various nuclei, leading to chemical shifts and couplings, can be made apparent. However, it is often not possible to work under ideal conditions. For example, sufficiently homogeneous fields are difficult to achieve in ex situ NMR, where the object under investigation is placed outside the magnet (*1*, *2*); in very high fields induced by resistive or hybrid magnets (*3*, *4*); and in samples (including animals and human beings) that are moving because of pulsating arteries or respiration, not to mention discontinuities of magnetic susceptibility due to voids and surgical implants (*5*, *6*).

Many techniques have been proposed to acquire high-resolution spectra under adverse conditions. Spin echoes (*7*, *8*) can refocus the effects of inhomogeneous B_0 fields and reveal couplings that lead to echo modulations (*9*–*11*). If the field's spatial distribution is known, the B_0 inhomogeneity may be compensated by using a radio-frequency (rf) field designed to have a similar, spatially correlated profile. Two such approaches have been described. In the first one, the rf-field $B_1(r)$ profile is designed to match the $B_0(r)$ profile (*12*–*14*). The dephasing caused by the rf field can then be refocused by rephasing in the main B_0 field. In the second approach, the inhomogeneities are compensated by manipulating the phases of the magnetization vectors associated with different voxels in the presence of a known gradient, in the manner of multidimensional single-scan experiments (*15*, *16*). In either case, the field $B_0(r)$ must be time-independent, and its spatial profile must be known, which constitutes a serious handicap.

We obtained high-resolution spectra in inhomogeneous fields by tracking the differences of the precession frequencies (*17*, *18*) of two spins in a single scan, in a way that is closely related to the ultrafast multidimensional experiments developed by Frydman and co-workers (*19*) and improved in our laboratory (*20*). The experiment functions regardless of the B_0 field profile. Spatial inhomogeneities of at least 11 G/cm can be accommodated. This corresponds to a frequency distribution of about 42 kHz (or 70 ppm for a 600-MHz resonance frequency) for a spherical sample 1 cm in diameter. Combining this technique with the *J*-modulated detection scheme of Giraudeau and Akoka (*21*) adds a second dimension that reveals multiplets due to scalar couplings.

As in the two-dimensional (2D) single-scan experiments, the evolution under the chemical shifts needs to be intertwined with gradient encoding (*22*). Let *S* and *I* constitute a homonuclear pair of spins. When a linearly swept adiabatic refocusing pulse is applied in the presence of a gradient to a coherence S_+ with coherence order $p = +1$ belonging to the manifold of *S*-spin transitions (Fig. 1A), the resulting phase at time t_1 is given by

$$\varphi_1 = \alpha\{\Omega_S + \delta\omega(r) + \Gamma_E(r)\}^2 \qquad (1)$$

(*20*), where Ω_S is the chemical shift of the *S* spin, $\delta\omega(r) = -\gamma_S B_0(r)$ is the (unknown) spatially dependent frequency induced by the inhomogeneous B_0 field, $\Gamma_E(r) = \gamma_S \mathbf{G}_E \cdot r$ is the (known) frequency induced by the encoding gradient $\mathbf{G}_E = \{G_{Ex}\mathbf{k}, G_{Ey}\mathbf{i}, G_{Ez}\mathbf{j}\}$, and $\alpha = \tau_{ad}/\Delta\omega_{ad}$ is the ratio of the duration τ_{ad} and sweep width $\Delta\omega_{ad}$ of the adiabatic inversion pulse. A second identical pulse combined with an opposite gradient then leads to a phase at time t_2:

$$\varphi_2 = 4\alpha\{\Omega_S + \delta\omega(r)\}\Gamma_E(r) \qquad (2)$$

The coherence can then be transferred (in the example of Fig. 1 by a simple $\pi/2$ pulse) from S_+ to I_- with coherence order $p = -1$ through any spin-spin coupling, exploiting (for example) a scalar interaction J_{IS}. If there are no scalar couplings, it might be possible to use demagnetizing fields, which can manifest themselves as intermolecular dipolar interactions (*23*, *24*). After an identical block comprising two more pulses and gradients, the total accumulated phase at time t_4 will be

$$\varphi_4 = 4\alpha\{\Omega_S + \delta\omega(r)\}\Gamma_E(r) - 4\alpha\{\Omega_I + \delta\omega(r)\}\Gamma_E(r) = 4\alpha\{\Omega_S - \Omega_I\}\Gamma_E(r) \qquad (3)$$

This phase does not depend on the spatial variation $\delta\omega(r)$ due to the inhomogeneous static field. The phase φ_4 can be refocused by a decoding gradient G_D. A gradient echo will be formed at an instant in time that will be delayed in proportion to the difference $\Omega_S - \Omega_I$

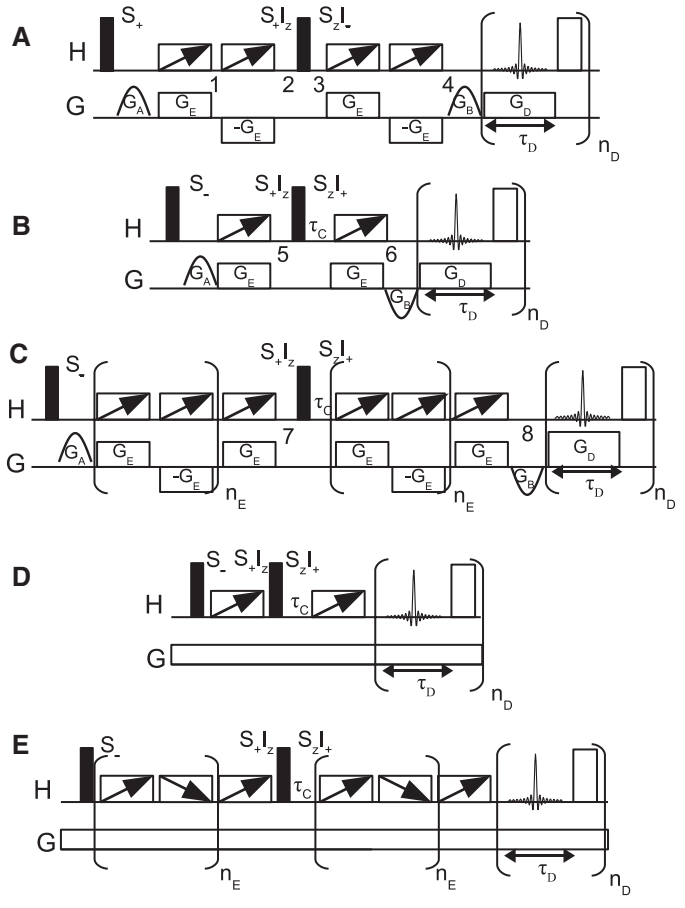

Fig. 1. Pulse sequences to obtain high-resolution spectra in a single scan in arbitrarily inhomogeneous, slowly fluctuating magnetic fields with unknown spatiotemporal distributions. Solid and open vertical rectangles represent $\pi/2$ and π pulses. The rectangles with sloping arrows indicate adiabatic frequency-swept refocusing pulses. G_E and G_D are encoding and decoding gradients. The gradients G_A and G_B of equal area serve to select the desired coherence pathways [they must be identical for (**A**) and opposite for (**B**) and (**C**)]. The delay τ_C serves to compensate for the evolution under the inhomogeneous B_0 field during G_A and G_B. Increasing G_B and prolonging τ_C by $\tau_D/2$ shifts the signals at zero frequency toward the center of the gradient G_D. Sequences (**D**) and (**E**) are adaptations of (B) and (C), respectively, for situations where a permanent gradient is dominant. Adiabatic pulses with down-pointing arrows have reversed sweep directions. The phases of the π pulses during decoding are alternated between x and $-x$ every two pulses (*21*). In these examples, $\pi/2$ pulses are used to achieve transfer of coherence, so that the spins need to be scalar-coupled. Other sequences can be used, such as total correlation spectroscopy (TOCSY). The signals during even (or odd) decoding gradients are arranged in sequential order to yield a 2D array. The gradient echoes that are formed during each decoding gradient appear in a temporal sequence that corresponds to the peaks in the spectrum. The scalar coupling pattern in the other dimension is obtained by performing a Fourier transformation as a function of the index of the decoding gradients.

[1]Département de Chimie Associé au CNRS, Ecole Normale Supérieure, 24 rue Lhomond, 75231 Paris Cedex 05, France. [2]Department of Biomedical Sciences and Technologies, Università degli Studi di Udine, I-33100 Udine, Italy. [3]Institut de Sciences et Ingénierie Chimiques, Ecole Polytechnique Fédérale de Lausanne, Batochime, 1015 Lausanne, Switzerland.

*To whom correspondence should be addressed. E-mail: philippe.pelupessy@ens.fr

between the frequencies of spins S and I. Although this feature is reminiscent of zero-quantum spectroscopy, it should be noted that the echoes arise simply from the differential evolution of two single-quantum coherences (*18*). During the decoding gradient G_D in the scheme of Fig. 1A, the coherences will continue to precess under the field inhomogeneities, thus preventing complete refocusing. An improved scheme is shown in Fig. 1B. Instead of applying two adiabatic pulses before and after coherence transfer, only one is applied, which leads to a phase:

$$\varphi_6 = \alpha\{\Omega_S + \delta\omega(r) + \Gamma_E(r)\}^2 - \alpha\{\Omega_I + \delta\omega(r) + \Gamma_E(r)\}^2 = \alpha\Omega_S^2 - \alpha\Omega_I^2 + 2\alpha(\Omega_S - \Omega_I)\{\Gamma_E(r) + \delta\omega(r)\} \quad (4)$$

The difference $\Omega_S - \Omega_I$ between the chemical shifts of spins I and S is now encoded not only by the gradient G_E but also by the B_0 inhomogeneity. During a decoding gradient G_D with the same amplitude as the encoding gradient G_E, the phase is then

$$\varphi_D(t_D) = \alpha\Omega_S^2 - \alpha\Omega_I^2 + 2\alpha(\Omega_S - \Omega_I)\{\Gamma_E(r) + \delta\omega(r)\} - t_D\{\Omega_I + \Gamma_E(r) + \delta\omega(r)\} \quad (5)$$

At $t_D = 2\alpha(\Omega_S - \Omega_I)$, an echo results because the phase is independent of $\delta\omega(r)$. Thus, a spectrum of frequency differences is obtained in the time domain in a single scan. The phase of this echo is

$$\varphi_D\{t_D = 2\alpha(\Omega_S - \Omega_I)\} = \alpha\Omega_S^2 + \alpha\Omega_I^2 - 2\alpha\Omega_I\Omega_S = \alpha(\Omega_S - \Omega_I)^2 \quad (6)$$

A hybrid scheme is shown in Fig. 1C. A bipolar gradient pair with adiabatic pulses that is repeated n_E times is inserted before each adiabatic pulse of Fig. 1B. The resulting phase at time t_7 is

$$\varphi_7 = 2n_E\alpha(\Omega_S - \Omega_I)\Gamma_E(r) + \alpha\Omega_S^2 - \alpha\Omega_I^2 + 2\alpha(\Omega_S - \Omega_I)\{\Gamma_E(r) + \delta\omega(r)\} = \alpha\Omega_S^2 - \alpha\Omega_I^2 + 2\alpha(\Omega_S - \Omega_I)\{(2n_E + 1)\Gamma_E(r) + \delta\omega(r)\} \quad (7)$$

The decoding gradient should have an amplitude that is $(2n_E + 1)$ times the encoding gradient—$G_D = (2n_E + 1)G_E$—in order to cancel the effects of the inhomogeneities $\delta\omega(r)$. The sequence of Fig. 1C is less sensitive to translational diffusion than the experiment of Fig. 1B (*25*).

As can be seen from Eq. 5, the scheme shown in Fig. 1B does not require any switched field gradients, provided the inhomogeneities are sufficiently large to cause sharp echoes. This

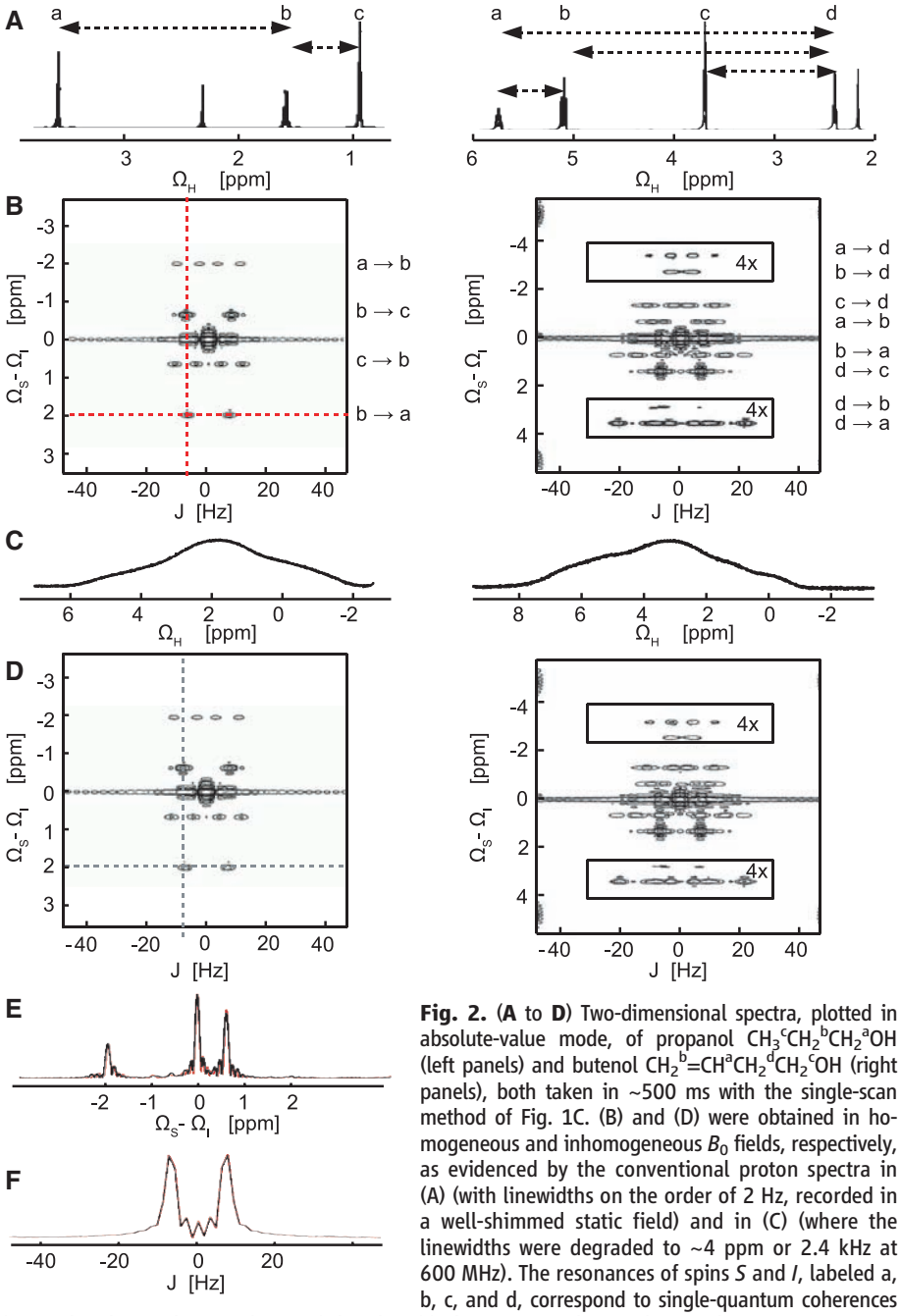

Fig. 2. (**A** to **D**) Two-dimensional spectra, plotted in absolute-value mode, of propanol $CH_3^cCH_2^bCH_2^aOH$ (left panels) and butenol $CH_2^b{=}CH^aCH_2^dCH_2^cOH$ (right panels), both taken in ~500 ms with the single-scan method of Fig. 1C. (B) and (D) were obtained in homogeneous and inhomogeneous B_0 fields, respectively, as evidenced by the conventional proton spectra in (A) (with linewidths on the order of 2 Hz, recorded in a well-shimmed static field) and in (C) (where the linewidths were degraded to ~4 ppm or 2.4 kHz at 600 MHz). The resonances of spins S and I, labeled a, b, c, and d, correspond to single-quantum coherences that evolve during the encoding and decoding blocks of Fig. 1; their scalar coupling patterns appear along the horizontal dimension and carry the same labels ($S \rightarrow I$). The arrows in (A) indicate all difference frequencies between scalar-coupled spins that can be observed; the top arrows correspond to the outer lines in the spectrum, the bottom arrows to the smallest frequency differences (inner lines). The line at zero frequency corresponds to coherences that are refocused but not transferred from one spin to another. Both spectra were recorded with $n_E = 1$, gradients applied simultaneously along directions z and y with strengths $G_E = 0.8$ G/cm and $G_D = 2.4$ G/cm. The adiabatic pulses of 6 ms had a wideband uniform rate and smooth truncation (WURST) profile (*28*) and sweep widths of 14 and 20 kHz for propanol and butenol, respectively. (**E**) Columns taken parallel to the vertical t_1 or ω_1 domain, taken along the dotted lines of the 2D spectra of propanol in homogeneous (red lines) and inhomogeneous fields (black lines), showing differences of chemical shifts in the spectrum of propanol. (**F**) Rows taken parallel to the horizontal ω_2 domain, showing a multiplet due to scalar couplings with a full width at half height of 3.5 Hz, for $n_D = 64$ ($t_2^{max} = 337$ ms).

could have implications for measurements in stray magnetic fields (*26*) or other permanent gradients. Shown in Fig. 1, D and E, are adaptations of Fig. 1, B and C, for situations with a permanent gradient. In Fig. 1E the sweep direction of the second adiabatic pulse in each repeated block is inverted. Both schemes lead to a phase φ_6 of Eq. 4, but the latter limits losses due to diffusion (*25*).

All schemes can be extended from one to two dimensions by appending n_D repetitions of a block comprising a decoding gradient followed by a π pulse in order to observe a train of spin echoes (*21*). A Fourier transformation of this echo train reveals (convoluted) multiplets due to scalar couplings in a second dimension. This option requires ~500 instead of ~50 ms for the basic 1D experiment. The simplest 1D spectrum corresponds to the signal acquired during the first decoding gradient.

Shapira *et al*. (*4*) proposed schemes for measurements in fluctuating resistive magnets. The resolution of correlation spectra can be improved, either by compensating for (known) inhomogeneities with tailored rf fields, or by exploiting echoes following coherence transfer from carbon-13 to proton nuclei. The latter scheme is related to our method, although in their case the effects of inhomogeneities are canceled only at one point in the acquisition period.

The experiments of Fig. 1C have been tested by applications to samples containing 5% 1-propanol ($CH_3CH_2CH_2OH$) and 5% 3-buten-1-ol (CH_2=$CHCH_2CH_2OH$, henceforth simply called butenol) in $CDCl_3$. The spectra in Fig. 2, A and B, have been obtained in a carefully shimmed homogeneous field. The resonances labeled a through d give rise to combination lines (differences in chemical shifts, i.e., four peaks in propanol and eight in butenol). In the vertical dimension, the spectra are symmetric with respect to $\omega_1 = 0$, because each transfer from spin *S* to *I* is accompanied by a transfer in the opposite direction. The central peak at $\omega_1 = 0$ arises from magnetization that is refocused but not transferred from one spin to another.

Shown in Fig. 2, C and D, are spectra obtained with the same method in an inhomogeneous field after deliberately missetting the shim currents. Yet the results of our single-scan experiments are virtually indistinguishable. The experiments have been repeated using several shim settings, invariably leading to similar spectra, as can be seen from the cross sections in Fig. 2, E and F. As with all 2D single-scan experiments, the signal-to-noise ratio decreases in proportion to the square root of the number of points observed in the indirect dimension, relative to a 1D spectrum taken under properly shimmed conditions. If the signal-to-noise ratio is poor, the experiments can be repeated for signal averaging, even if the B_0 inhomogeneities vary in time, provided the fluctuations are slow relative to the time it takes to acquire each scan. For a simple 1D spectrum, about 50 ms is sufficient. Thus, if we assume that the information must be acquired within 10% of the period of the fastest fluctuations, the spectrum of the stochastic variations must be limited to 2 Hz. This should be useful for NMR spectra obtained in resistive Bitter or hybrid magnets, which suffer from random fluctuations due to the power supply and to low-frequency vibrations associated with the circulation of cooling water.

The resolution, as measured by the full linewidth at half height in the vertical (chemical shift) dimension (t_1 or ω_1) of 1-propanol in Fig. 2E, is 60 μs, for a decoding gradient G_D of 4 ms. This corresponds to a resolution of 76 Hz (0.13 ppm) over a frequency range of ±2500 Hz (±4.2 ppm). The resolution of the spectra can be improved by increasing the amplitudes of both encoding and decoding gradients (provided the frequency sweep of the adiabatic pulses covers the frequency range induced by the encoding gradients) or, as shown in Fig. 3, by increasing n_E and the strength of the decoding gradients. The frequency range can be increased by extending the sweep width of the adiabatic pulses, albeit at the expense of the resolution, unless one also increases the strength of both encoding and decoding gradients (*27*). The resolution in the ω_2 dimension is determined by the number n_D of points acquired in the t_2 dimension, as in other forms of 2D spectroscopy.

To mimic a gradient that cannot be switched off, we have applied the scheme of Fig. 1D in the presence of a permanent gradient, or more accurately, a pulsed field gradient that was switched on before the experiment and stopped immediately after observing the signals. The echo corresponding to zero frequency appears at a delay τ_C after the start of signal acquisition. Only 1D spectra revealing combinations of chemical shifts in propanol were recorded (to avoid using prolonged strong gradients). The sample height was decreased to 18 mm, so that the line shape was further deteriorated by susceptibility effects at the edges. Figure 4A shows the resulting spectra in the presence of a gradient G_z = 2.75 G/cm (~35 ppm or 21 kHz across the sample). Signals arising from coherence transfer are indicated by arrows. The duration of the adiabatic pulses was 18 ms and their sweep width was 40 kHz. When the gradient strength was doubled to 5.5 G/cm (~70 ppm or ~42 kHz) together with a doubling of the adia-

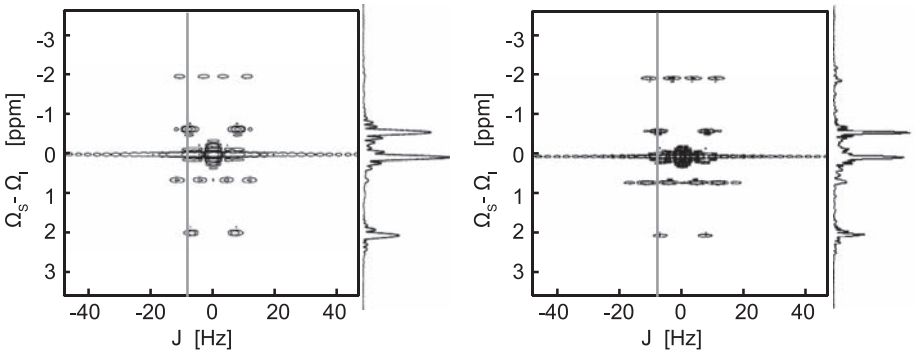

Fig. 3. Left panel: Same spectrum as in the left part of Fig. 2D, taken with n_E = 1 and G_D = 2.4 G/cm. Right panel: Spectrum taken under the same conditions, except that n_E = 2 and G_D = 4 G/cm. The columns shown on the right exemplify the gain in resolution that can be obtained by increasing the number of encoding gradients. The linewidth has improved from 76 Hz (0.13 ppm) on the left to 41 Hz (0.07 ppm) on the right.

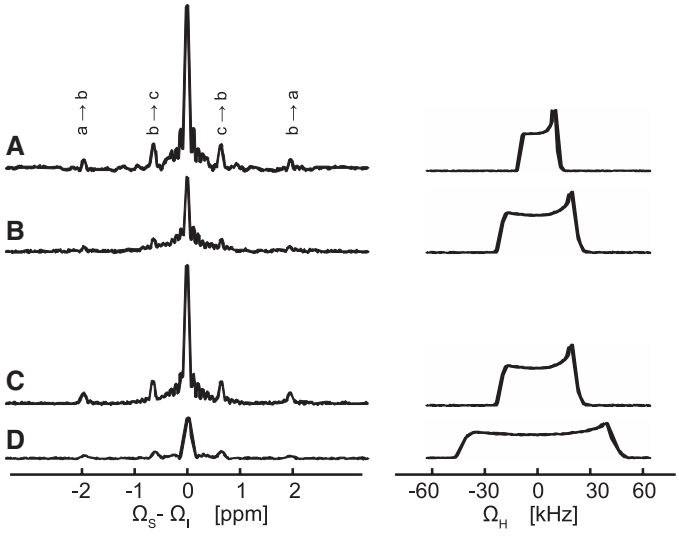

Fig. 4. (**A**) Spectrum of propanol recorded with the method shown in Fig. 1D, with a permanent gradient of 2.75 G/cm applied along the *z* axis throughout the entire sequence, without switching the decoding or encoding gradients. The adiabatic rf pulses had durations of 18 ms and sweep widths of 40 kHz. (**B**) Same as (A), but with twice the amplitude of the permanent gradient (5.5 G/cm) and twice the rf sweep width. (**C**) Same as (B), but each adiabatic pulse is replaced by three 6-ms adiabatic pulses as in Fig. 1E. (**D**) Same as (C), but with a permanent gradient of 11 G/cm and twice the sweep width of the adiabatic pulses. On the right are the corresponding single-quantum spectra.

batic sweep width, there was some loss of intensity due to diffusion (Fig. 4B). These losses could be reduced with the scheme of Fig. 1E, as shown in Fig. 4C for a total of six adiabatic pulses of 6-ms duration (instead of two otherwise identical pulses of 18 ms each, as in Fig. 4B). The linewidth in Fig. 4C is about 70 Hz. Increasing the gradient strength further to 11 G/cm (~140 ppm or ~84 kHz) led to the spectrum in Fig. 4D. In this case, the signal amplitude suffers not only from diffusion losses, but also from the limited rf amplitude (25 kHz) of the initial $\pi/2$ pulse. In stronger gradients, one should use a large number of short inversion pulses that cover a very broad bandwidth with the desired phase profile. In addition, the (possibly frequency-swept) $\pi/2$ pulses should excite the full bandwidth uniformly, bearing in mind that a linear dependence of the phase with respect to offset is allowed.

References and Notes

1. G. Eidmann, R. Savelsberg, P. Blumler, B. Blümich, *J. Magn. Reson. A* **122**, 104 (1996).
2. B. Blümich, J. Perlo, F. Casanova, *Prog. Nucl. Magn. Reson. Spectrosc.* **52**, 197 (2008).
3. Y.-Y. Lin *et al.*, *Phys. Rev. Lett.* **85**, 3732 (2000).
4. B. Shapira, K. Shetty, W. W. Brey, Z. Gan, L. Frydman, *Chem. Phys. Lett.* **442**, 478 (2007).
5. I. J. Cox *et al.*, *J. Magn. Reson.* **70**, 163 (1986).
6. C. E. Mountford, S. Doran, C. L. Lean, P. Russell, *Chem. Rev.* **104**, 3677 (2004).
7. E. L. Hahn, *Phys. Rev.* **80**, 580 (1950).
8. H. Y. Carr, E. M. Purcell, *Phys. Rev.* **94**, 630 (1954).
9. E. L. Hahn, D. E. Maxwell, *Phys. Rev.* **88**, 1070 (1952).
10. R. L. Vold, S. O. Chan, *J. Chem. Phys.* **53**, 449 (1970).
11. R. Freeman, H. D. W. Hill, *J. Chem. Phys.* **54**, 301 (1971).
12. C. A. Meriles, D. Sakellariou, H. Heise, A. J. Moulé, A. Pines, *Science* **293**, 82 (2001).
13. V. Demas *et al.*, *Concepts Magn. Reson. B* **29B**, 137 (2006).
14. J. Perlo *et al.*, *Science* **308**, 1279 (2005); published online 7 April 2005 (10.1126/science.1108944).
15. B. Shapira, L. Frydman, *J. Am. Chem. Soc.* **126**, 7184 (2004).
16. B. Shapira, L. Frydman, *J. Magn. Reson.* **182**, 12 (2006).
17. A. Wokaun, R. R. Ernst, *Chem. Phys. Lett.* **52**, 407 (1977).
18. K. Nagayama, K. Wüthrich, R. R. Ernst, *Biochem. Biophys. Res. Commun.* **90**, 305 (1979).
19. L. Frydman, T. Scherf, A. Lupulescu, *Proc. Natl. Acad. Sci. U.S.A.* **99**, 15858 (2002).
20. P. Pelupessy, *J. Am. Chem. Soc.* **125**, 12345 (2003).
21. P. Giraudeau, S. Akoka, *J. Magn. Reson.* **186**, 352 (2007).
22. L. Frydman, A. Lupulescu, T. Scherf, *J. Am. Chem. Soc.* **125**, 9204 (2003).
23. S. Vathyam, S. Lee, W. S. Warren, *Science* **272**, 92 (1996).
24. G. Galiana, R. T. Branca, W. S. Warren, *J. Am. Chem. Soc.* **127**, 17574 (2005).
25. P. Giraudeau, S. Akoka, *J. Magn. Reson.* **195**, 9 (2008).
26. P. J. McDonald, *Prog. Nucl. Magn. Reson. Spectrosc.* **30**, 69 (1997).
27. P. Pelupessy, L. Duma, G. Bodenhausen, *J. Magn. Reson.* **194**, 169 (2008).
28. E. Kupce, R. Freeman, *J. Magn. Reson. A* **115**, 273 (1995).

29. Supported by CNRS, the Agence Nationale pour la Recherche, the Integrated Infrastructure Initiative (I3) of the 6th Framework Program of the EC (contract RII3-026145, EU-NMR), the Fonds National de la Recherche Scientifique (Switzerland), and the Commission pour la Technologie et l'Innovation (Switzerland).

17 April 2009; accepted 14 May 2009
10.1126/science.1175102

White Phosphorus Is Air-Stable Within a Self-Assembled Tetrahedral Capsule

Prasenjit Mal,[1] Boris Breiner,[1] Kari Rissanen,[2] Jonathan R. Nitschke[1]*

The air-sensitive nature of white phosphorus underlies its destructive effect as a munition: Tetrahedral P_4 molecules readily react with atmospheric dioxygen, leading this form of the element to spontaneously combust upon exposure to air. Here, we show that hydrophobic P_4 molecules are rendered air-stable and water-soluble within the hydrophobic hollows of self-assembled tetrahedral container molecules, which form in water from simple organic subcomponents and iron(II) ions. This stabilization is not achieved through hermetic exclusion of O_2 but rather by constriction of individual P_4 molecules; the addition of oxygen atoms to P_4 would result in the formation of oxidized species too large for their containers. The phosphorus can be released in controlled fashion without disrupting the cage by adding the competing guest benzene.

Microenvironment alters behavior in chemical systems; encapsulation within the inner phase (*1*–*3*) of a molecular container can accelerate a reaction (*4*–*7*), change a reaction's course (*7*–*11*), perturb equilibria (*11*–*13*), or prevent the oligomerization of a reactive species such as a cyclotrisiloxane (*14*) or cyclobutadiene (*15*). The lifetimes of such fleeting molecules as hemiaminals (*16*), benzyne (*17*), and cycloheptatriene (*18*) may also be extended long enough to permit spectroscopic observation. Here, we show how encapsulation can render molecules of white phosphorus (P_4) air-stable through a constrictive mechanism.

The P-P bonds of tetrahedral P_4 (white phosphorus) are weak (200 kJ mol^{-1}) (*19*), leading to a low activation barrier to oxidation, and the P-O bonds of combustion products are strong (330 to 650 kJ mol^{-1}) (*19*), releasing substantial energy during their formation. P_4 is thus violently pyrophoric; its slow chemiluminescent combustion when O_2 is limited ["phosphorescence," the meaning of which has since changed (*20*)] defined the element's essence for the first chemists.

We have described the preparation of tetrahedral cage **1** in aqueous solution from the subcomponents shown in Fig. 1 (*21*). When an aqueous solution of **1** was left in contact with solid white phosphorus, uptake of P_4 converted **1** into the host-guest complex $P_4\subset$**1** (Fig. 1) (*22*). Vapor diffusion of acetone into an aqueous solution yielded crystalline $P_4\subset$**1** in 91% yield.

Incorporation of P_4 into **1** was marked by changes in the ^{1}H nuclear magnetic resonance (NMR) chemical shifts of **1** (fig. S1) and by the appearance of a single resonance in the ^{31}P NMR spectrum at –510 parts per million (ppm). Single crystals of sufficient quality for x-ray diffraction were grown by vapor diffusion of 1,4-dioxane into an aqueous solution of $P_4\subset$**1**. Its x-ray crystal structure is shown in Fig. 2.

The quality and resolution of the diffraction data, although limited, allow for unambiguous assignment of the cage's conformation and the placement of the guest within the cage, where it is disordered between two orientations (only one of

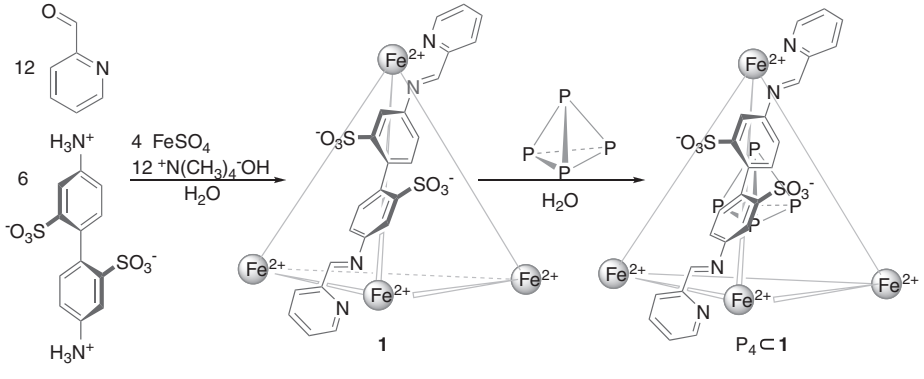

Fig. 1. Synthesis of tetrahedral cage **1** and subsequent incorporation of P_4.

[1]Department of Chemistry, University of Cambridge, Lensfield Road, Cambridge CB2 1EW, UK. [2]Department of Chemistry, Nanoscience Center, University of Jyväskylä, Post Office Box 35, 40014 JYU, Finland.

*To whom correspondence should be addressed. E-mail: jrn34@cam.ac.uk

which is shown in Fig. 2) (*22*) and stabilized through van der Waals interactions with the hydrophobic phenylene groups lining the cage's interior (*23*, *24*). Apart from crystalline white phosphorus (*25*), previous structures of intact P_4 tetrahedra have involved tight coordination to a transition-metal fragment (*26*–*28*).

Within **1**, P_4 became water-soluble and air-stable; ^{1}H NMR spectra of solid samples and aqueous solutions of P_4⊂**1** were unchanged after contact with the atmosphere over 4 months. This behavior contrasts markedly with that of naked P_4, infamous for its pyrophoric nature. Inspection of the crystal structure of P_4⊂**1** reveals a pore of 1.0 Å radius in each face of the tetrahedron; although this distance is smaller than the radial cross-section of O_2 (1.4 Å), thermal fluctuations in **1** would be expected to transiently open the cage sufficiently to let O_2 inside, analagously to what presumably occurs during P_4 uptake. We thus attribute encapsulated P_4's remarkable O_2 stability not to the cage's ability to exclude dioxygen but rather to the constriction applied by the confining capsule: The reaction of O_2 with P_4 would generate an intermediate product too large for the cavity of **1**. Modeling suggests that even the insertion of a single oxygen atom into a P-P bond of P_4, or the capping of one P atom of P_4 with an oxygen atom to create a P=O moiety, would require a transition state that could not fit within the hollow of **1** without deformation. This hypothesis is supported by the observation that P_4 within **1** did not react with the single–oxygen atom transfer reagents nitrous oxide or pyridine N-oxide after prolonged exposure (*22*). This constrictive stabilization of a reactive solid thus serves as a counterpoint and complement to the high effective gas pressures that may be observed within molecularly confined spaces (*29*).

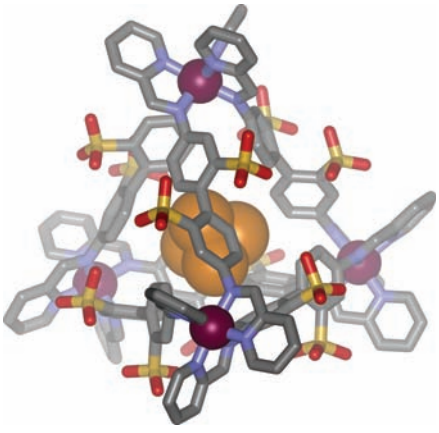

Fig. 2. Crystal structure of P_4⊂**1**. Solvent molecules, counterions, and hydrogen atoms are omitted for clarity. Fe, violet; N, blue; C, gray; O, red; S, yellow; P, orange.

Although P_4 appeared to be indefinitely stable within **1**, extracting guest from host through the addition of a competing guest proved to be straightforward. As illustrated in Fig. 3C, the addition of an equal volume of benzene to an aqueous solution of P_4⊂**1** resulted in the quantitative extraction of P_4 from **1** into the benzene layer, as evidenced by the appearance of a ^{31}P NMR peak at –520 ppm with concomitant formation of aqueous C_6H_6⊂**1**, as observed by ^{1}H NMR. (Cyclohexane was also demonstrated to work; see fig. S2.) The essential role played by benzene as a competing guest is highlighted by the outcome of an analogous experiment carried out with *n*-heptane (Fig. 3C), which resulted in no extraction of P_4 from **1**, despite the solubility of P_4 in this solvent. Heptane is a poor guest for **1**, whereas benzene is a good one: Extraction of P_4 thus requires not only the "pull" of a solvent that can extract P_4, but also the "push" of a competing guest that is capable of displacing it.

P_4, once extracted into benzene, regained its air-sensitivity. After exposure to the atmosphere for 24 hours at 323 K, no further evidence was observed by ^{31}P NMR for P_4 in the benzene layer. The aqueous layer, however, showed a new ^{31}P NMR resonance at 0 ppm, attributed to phosphoric acid. Benzene thus mediated the oxidation of P_4, although all phosphorus came from, and ended up in, the aqueous phase.

Only 3.5% phosphorus by mass is contained within P_4⊂**1**; however, our capsule is reusable, and the safety benefits of using **1** as a carrier are substantial: **1** could facilitate the handling and use of white phosphorus and could potentially be used directly as a means of cleaning up highly dangerous phosphorus spills. More generally, the method of constrictive encapsulation could find applications in the protection and controlled release of sensitive molecules or alternatively the protection of the environment through the sequestration of hazardous substances. Larger analogs of **1**, whose preparations are currently underway, may serve to stabilize and isolate larger and more complex guest species.

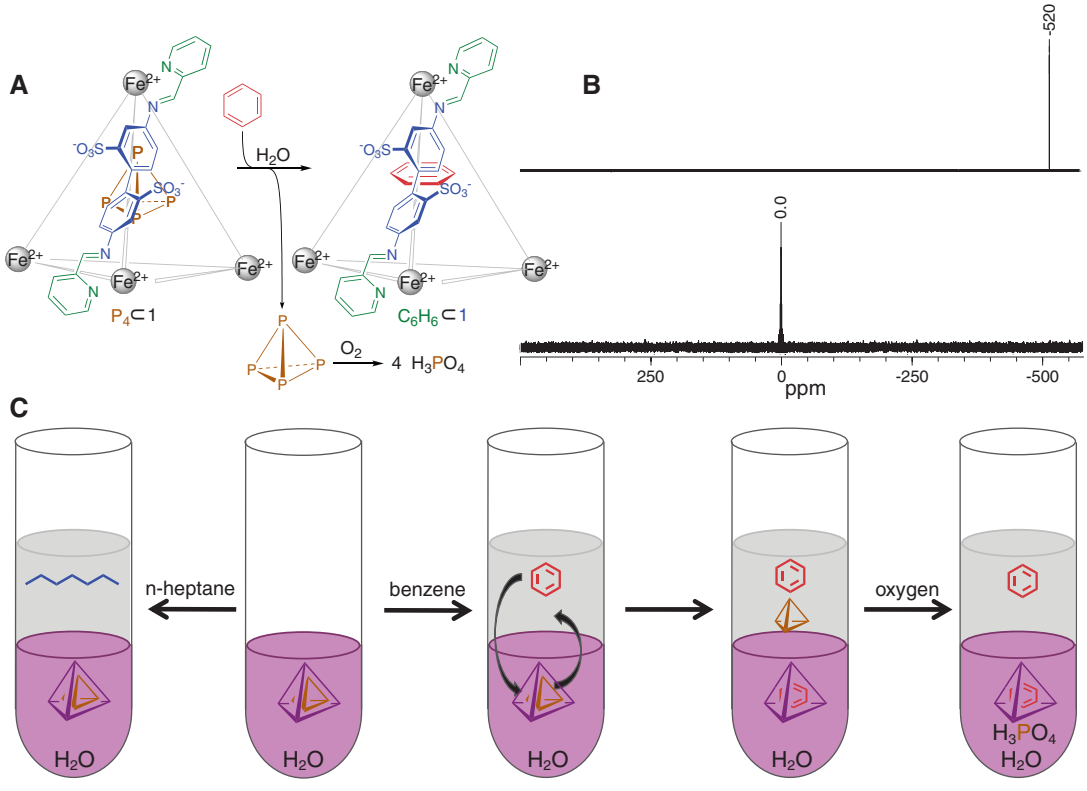

Fig. 3. Extraction of P_4 from **1** by *n*-heptane is not possible, whereas replacing P_4 with another suitable guest (benzene or cyclohexane) results in the facile removal of P_4 into the organic solvent. (**A**) Reaction scheme. (**B**) ^{31}P NMR spectra of P_4 extracted into the benzene layer (top) and phosphoric acid found in the aqueous layer after reaction of P_4 in benzene with oxygen (bottom). (**C**) Schematic representation of the extraction process.

References and Notes

1. D. J. Cram, *Nature* **356**, 29 (1992).
2. D. M. Vriezema *et al.*, *Chem. Rev.* **105**, 1445 (2005).
3. L. R. MacGillivray, J. L. Atwood, *Angew. Chem. Int. Ed.* **38**, 1018 (1999).
4. J. M. Kang, G. Hilmersson, J. Santamaria, J. Rebek, *J. Am. Chem. Soc.* **120**, 3650 (1998).
5. M. Marty, Z. Clyde-Watson, L. J. Twyman, M. Nakash, J. K. M. Sanders, *Chem. Commun. (Camb.)* 2265 (1998).
6. C. J. Hastings, D. Fiedler, R. G. Bergman, K. N. Raymond, *J. Am. Chem. Soc.* **130**, 10977 (2008).
7. M. Yoshizawa, M. Tamura, M. Fujita, *Science* **312**, 251 (2006).
8. M. Yoshizawa, Y. Takeyama, T. Okano, M. Fujita, *J. Am. Chem. Soc.* **125**, 3243 (2003).
9. D. R. Benson, R. Valentekovich, F. Diederich, *Angew. Chem. Int. Ed. Engl.* **29**, 191 (1990).
10. M. Kuil, T. Soltner, P. van Leeuwen, J. N. H. Reek, *J. Am. Chem. Soc.* **128**, 11344 (2006).
11. M. D. Pluth, R. G. Bergman, K. N. Raymond, *Science* **316**, 85 (2007).
12. V. M. Dong, D. Fiedler, B. Carl, R. G. Bergman, K. N. Raymond, *J. Am. Chem. Soc.* **128**, 14464 (2006).
13. L. Trembleau, J. Rebek, *Science* **301**, 1219 (2003).
14. M. Yoshizawa, T. Kusukawa, M. Fujita, K. Yamaguchi, *J. Am. Chem. Soc.* **122**, 6311 (2000).
15. D. J. Cram, M. E. Tanner, R. Thomas, *Angew. Chem. Int. Ed. Engl.* **30**, 1024 (1991).
16. T. Iwasawa, R. J. Hooley, J. Rebek Jr., *Science* **317**, 493 (2007).
17. R. Warmuth, *Angew. Chem. Int. Ed. Engl.* **36**, 1347 (1997).
18. R. Warmuth, M. A. Marvel, *Angew. Chem. Int. Ed.* **39**, 1117 (2000).
19. F. S. Dainton, *Trans. Faraday Soc.* **43**, 244 (1947).
20. P. R. Lewis, C. Price, *Polymer (Guildf.)* **12**, 258 (1971).
21. P. Mal, D. Schultz, K. Beyeh, K. Rissanen, J. R. Nitschke, *Angew. Chem. Int. Ed.* **47**, 8297 (2008).
22. Materials and methods are available as supporting material on *Science* Online.
23. C. L. D. Gibb, B. C. Gibb, *J. Am. Chem. Soc.* **126**, 11408 (2004).
24. E. Botana, E. Da Silva, J. Benet-Buchholz, P. Ballester, J. de Mendoza, *Angew. Chem. Int. Ed.* **46**, 198 (2007).
25. D. E. C. Corbridge, E. J. Lowe, *Nature* **170**, 629 (1952).
26. A. P. Ginsberg, W. E. Lindsell, K. J. McCullough, C. R. Sprinkle, A. J. Welch, *J. Am. Chem. Soc.* **108**, 403 (1986).
27. M. Peruzzini *et al.*, *Eur. J. Inorg. Chem.* 931 (1999).
28. I. Krossing, L. Van Wullen, *Chem. Eur. J.* **8**, 700 (2002).
29. D. Ajami, J. Julius Rebek, *Angew. Chem. Int. Ed.* **47**, 6059 (2008).

30. This work was supported by the Walters-Kundert Charitable Trust, the Royal Society, the Marie Curie IIF scheme of the 7th European Union Framework Program (to P.M.), and the Academy of Finland (project 212588, to K.R.). The authors also thank D. S. Wright for helpful discussions and a gift of white phosphorus and J. K. M. Sanders for useful comments on the manuscript. Mass spectra were provided by the Engineering and Physical Sciences Research Council National Mass Spectrometry facility at Swansea. CCDC-727817 contains the supplementary crystallographic data for this paper. These data can be obtained free of charge from the Cambridge Crystallographic Data Centre via www.ccdc.cam.ac.uk/data_request/cif.

Supporting Online Material

www.sciencemag.org/cgi/content/full/324/5935/1697/DC1
Materials and Methods
Figs. S1 to S3
References

22 April 2009; accepted 1 June 2009
10.1126/science.1175313

Trapping Molecules on a Chip

Samuel A. Meek, Horst Conrad, Gerard Meijer*

Magnetic trapping of atoms on chips has recently become straightforward, but analogous trapping of molecules has proved to be challenging. We demonstrated trapping of carbon monoxide molecules above a chip using direct loading from a supersonic beam. Upon arrival above the chip, the molecules are confined in tubular electric field traps ~20 micrometers in diameter, centered 25 micrometers above the chip, that move with the molecular beam at a velocity of several hundred meters per second. An array of these miniaturized moving traps is brought to a standstill over a distance of only a few centimeters. After a certain holding time, the molecules are accelerated off the chip again for detection. This loading and detection methodology is applicable to a wide variety of polar molecules, enabling the creation of a gas-phase molecular laboratory on a chip.

The manipulation of atoms above a chip using magnetic fields produced by current-carrying wires is a mature field of research (*1*). This field was inspired by the notion that miniaturization of magnetic field structures enables the creation of large field gradients, i.e., large forces and steep potential wells for atoms. Modern microelectronics technology makes it possible to integrate the multiple tools underlying these experiments onto a compact surface area. Such atom chips have been used to demonstrate rapid Bose-Einstein condensation (*2*) and have found applications in matter-wave interferometry and in inertial and gravitational field sensing (*3*). Likewise, the engineering of miniaturized electric field structures holds great promise for the manipulation of polar molecules above a chip (*4*). The latter might enable, for instance, the implementation of proposed schemes of quantum computation that use polar molecules as qubits (*5*, *6*). Here, we experimentally demonstrate a method for loading and detecting molecules on a chip, adding to the recent advances in the taming of molecular beams (*7*).

A schematic of the experimental setup with an expanded view of the chip with the array of microelectrodes, all contained in a compact high-vacuum machine, is shown in Fig. 1. The chip consists of a total of 1254 equidistant 10-μm-wide gold electrodes with a 40-μm center-to-center distance deposited onto a glass substrate, forming a structure that is 5 cm long (micro resist technology GmbH). All electrodes extend over a central 4-mm region, whereas outside this region the electrodes extend alternately to the left or right and terminate at three different lengths. Via the square pads and the nickel wires that are connected to every third electrode on either side of the array, six different potentials are applied to the electrodes. These potentials are described by $\pm V_0[1 + \cos(2\pi\nu t + \phi_n)]$, with exclusively positive (or negative) potentials applied to a given side of the array. Within each polarity set, three different phases ϕ_n with a mutual phase difference of $\pm 2\pi/3$ are used. In this way, tubular minima of electric field strength are generated every 120 μm, and these minima move over the chip with a speed given by 120 μm × ν (in MHz) at a constant height of about 25 μm. The diameter of the tubular electric field minima is about 20 μm, and with V_0 = 80 V, their depth is about 4 kV/cm. The two ends of the 4-mm-long tubular minima are closed in the present design by the fringe fields near the ends of the electrodes. A detailed description of the generation of the moving tubular electric field traps above this particular chip is given elsewhere (*4*, *8*); a pictorial representation of the tubular traps above the chip, indicated in blue, is shown in the lower panel of Fig. 1.

The experiments here were performed with CO molecules in the low-field–seeking levels of the metastable $a^3\Pi_1$ ($v' = 0, J' = 1$) state. For these molecules, the electric field minima correspond to traps with a depth of about 50 mK when a constant frequency ν is applied. When the frequency ν is changed linearly in time, i.e., when a constant acceleration is applied, the diameter and depth of the traps decrease but three-dimensional confinement is maintained up to an acceleration of about 1.5×10^6 m/s^2. In the low–electric field region around the long axis of the trap, molecules can be lost due to nonadiabatic transitions to nontrappable degenerate states (*9*). In magnetic traps for atoms on a chip, this hole at the center of the trap is commonly plugged by adding a homogeneous magnetic field. An offset magnetic field could also be added in the present setup. For molecules in electric traps, however, there often exists the unique alternative solution to simply select an isotopologue with a favorable hyperfine level structure such that there is no degeneracy between trappable and nontrappable states in zero electric field (*10*). The most abundant carbon monoxide isotopologue, $^{12}C^{16}O$, has no hyperfine structure, and the low-field–seeking $M\Omega = -1$ level of the $a^3\Pi_1$ ($v' = 0, J' = 1$) state is degenerate with the $M = 0$ level in zero electric field, making this species susceptible to nonadiabatic transitions. In $^{13}C^{16}O$, however, the coupling of the nuclear spin of the ^{13}C nucleus with the orbital angular momentum results in a lifting of this degeneracy. As shown in the inset of Fig. 2, the low-field–seeking

Fritz-Haber-Institut der Max-Planck-Gesellschaft, Faradayweg 4-6, D-14195 Berlin, Germany.

*To whom correspondence should be addressed. E-mail: meijer@fhi-berlin.mpg.de

levels never come closer to the nontrappable level than 53 MHz in any electric field for ^{13}CO (*11*), effectively preventing nonadiabatic transitions from occurring.

In Fig. 2, the measured arrival-time distributions of metastable ^{13}CO molecules are shown for four different sets of wave forms of the potentials applied to the chip. When the molecules with an initial velocity of 312 m/s have just arrived above the chip, the external potentials are switched on. When wave forms with a constant frequency of ν = 2.6 MHz are used, the traps move at a constant velocity of 312 m/s while transporting the molecules to the other end of the chip. The total time that it takes the molecules to travel the complete 30-cm distance from the excitation point to the detector is about 0.96 ms in that case. With increasing accelerations, the molecules are slowed down from their initial velocity of 312 m/s to the indicated final velocities of 240, 168, or 96 m/s and arrive ever later on the detector. The broad background that is observed at early times results from metastable CO molecules in the $M = 0$ level that are hardly influenced by the electric fields. For comparison, the results for the guiding at 312 m/s and for the gentle deceleration of ^{12}CO molecules to 240 m/s are shown on the same scale as well (in gray). The dramatic loss in signal when going from ^{13}CO to ^{12}CO indicates the importance of nonadiabatic transitions even during the less than 200-μs residence time of the molecules in the electric field traps. All other experiments have therefore been performed with ^{13}CO.

In Fig. 3, measurements are shown to demonstrate how the longitudinal phase-space distribution of the ^{13}CO molecules can be manipulated in a three-step process to achieve both the maximum number of trapped molecules on the chip and the optimum detection sensitivity. In the inset, the corresponding longitudinal phase-space distributions are given at eight different times (A to H). Distribution (A) depicts the initial 1-mm-long distribution directly after laser excitation, just before the skimmer, whereas (B) is the same distribution after 0.6 ms of free flight. First, for optimum loading on the chip, a velocity-focusing deceleration is applied to sweep the velocities of all molecules of the incoming beam together (B to D). An array of about 250 electric field traps is loaded on the chip, one after the other, in this way. Second, a rapid deceleration is applied to bring all these traps to the desired final velocity on the chip (D to E). The chosen final velocity is 180 m/s in this particular measurement, but could be tuned to any velocity, including standstill. Third, for optimum detection of the molecules, a space-focusing acceleration is applied (E to G) to eject the molecules off the chip with velocities such that they all arrive at the same time on the detector (H), irrespective of their original position on the chip. The required values for the velocity-focusing deceleration and the space-focusing acceleration are determined by the geometry of the experimental setup. The gray curve in Fig. 3 is the measurement when the time sequence (A to E) is as described here, but when no acceleration is applied to eject the molecules off the chip. Despite the narrow velocity distribution achieved for the trapped molecules, the range of distances from the detector they exhibit leads to a broad distribution of arrival times (H′). The black curve is obtained when the optimum loading and detection strategy (A to H) is used.

The observed integrated signal intensity of the measurements shown in Fig. 3 is about 25 counts per pulse. As it is estimated that about one count is obtained for every hundred metastable CO molecules that hit the detector, this integrated value implies that there are ~10 CO molecules per electric field trap on the chip. The density in the traps is thus on the order of 10^7 molecules/cm^3, similar to the densities that have been obtained in macroscopic traps after beam deceleration (*7*). This density is given by the original density in the molecular beam at the entrance of the chip and can be several orders of magnitude higher when more intense pulsed sources are used or when the chip is brought closer to the beam source; the latter can readily be done with the chip but is less straightforward for larger-scale decelerators. The total volume of the simultaneously loaded tubular traps on the chip is ~0.25 mm^3, which is only between one and two orders of magnitude less than the volume of the typical macroscopic electrostatic traps that have been used thus far (*7*). The ejection of the molecules off the chip and their spatial focusing further downstream is ideal for any laser-based

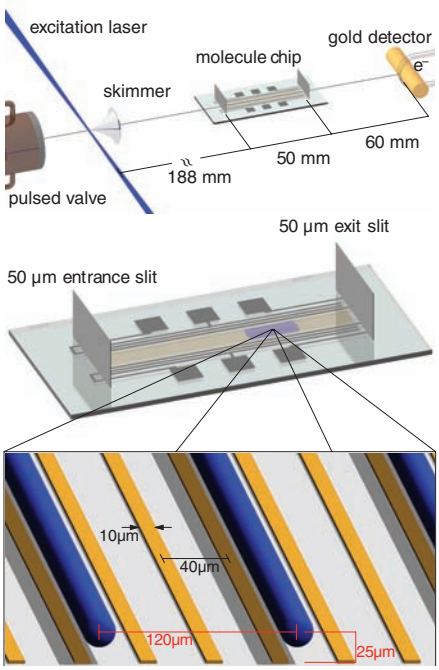

Fig. 1. Schematic of the experimental setup with an enlarged view of the chip. A pulsed beam (10 Hz) of ground-state CO molecules with a mean velocity of about 310 m/s is produced by expanding a mixture of 20% CO in krypton through a cooled valve in vacuum. Just before passing through the skimmer, CO molecules are prepared in the upper Λ-doublet level of the $a^3\Pi_1$ ($v' = 0$, $J' = 1$) state by direct laser excitation from the electronic ground state. The pulsed laser (5-ns pulse) is weakly focused (1-mm diameter) onto the molecular beam, creating a well-defined packet of metastable CO molecules. About 19 cm downstream from the laser excitation point, the molecules pass through a 50-μm-high entrance slit and then travel closely above the chip over its full 5-cm length. At the end of the chip, the molecules have to pass through another 50-μm-high exit slit to then fly freely to a gold surface that is positioned 6 cm further downstream. The arrival-time distribution of the molecules on the gold surface is measured via recording of the Auger electrons that are emitted when the metastable CO molecules impact there.

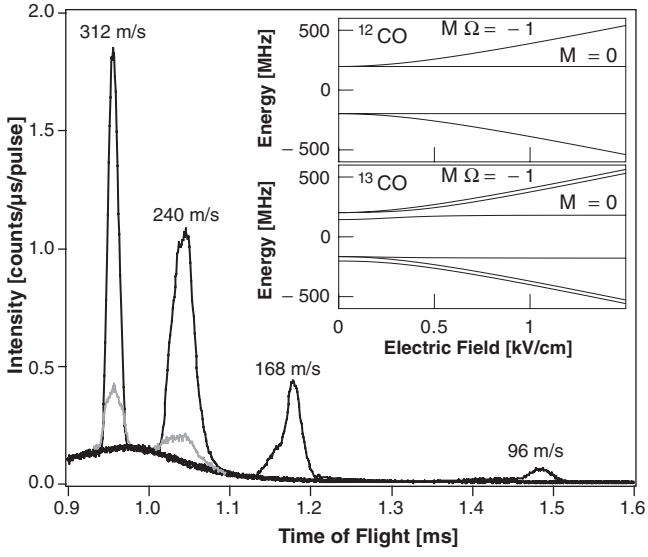

Fig. 2. Arrival-time distributions of ^{13}CO (black curves) and ^{12}CO (gray curves) molecules on the detector. The time scale is relative to the time of laser excitation, and the vertical scale is in counts per microsecond and per pulse. The initial frequency of the wave forms is 2.6 MHz in all cases, and this frequency is either kept constant or ramped down linearly in time while the molecules are above the chip. Ramping down to a final frequency of 2.0, 1.4, and 0.8 MHz results in final velocities of 240, 168, and 96 m/s and corresponds to accelerations of 0.40×10^6, 0.70×10^6, and 0.89×10^6 m/s^2, respectively. Each measured trace is averaged over 2 hours (at 10 Hz). (**Inset**) The levels of the $a^3\Pi_1$ ($v' = 0$, $J' = 1$) state of ^{12}CO and ^{13}CO, calculated from spectroscopic data (*11*), are shown in low electric fields.

detection scheme. When resonant laser ionization in combination with mass-selective ion detection is being used, the overall detection efficiency can approach unity. This makes the method outlined here applicable to a wide variety of molecules like (various isotopologues of) the hydroxyl radical, ammonia, water, and formaldehyde. All these molecules can be decelerated and trapped in their electronic ground state, in ro-vibrational levels that are well populated in a molecular beam, and for which sensitive laser-based detection schemes are available (*12*). To more generally prevent losses due to nonadiabatic transitions in these molecules, an offset magnetic field, directed parallel to the long axis of the trap and thereby always perpendicular to the electric fields above the chip, might be required.

In Fig. 4, a series of arrival-time measurements is shown that has been recorded after the ^{13}CO molecules have been held for certain times in stationary electrostatic traps on the chip. An important advantage of the present scheme is that the loading of stationary traps on the chip involves simply bringing already existing, fast-moving traps to a standstill. This is fundamentally different from trap-loading schemes using conventional Stark decelerators (*7*) because the effective traps that are present in those decelerators disappear at low velocities. In the measurements shown in Fig. 4, an array of about 60 electric field traps has been loaded and brought to a stop. After a variable holding time in the 0- to 2.5-ms range, these traps have been accelerated again and the molecules have been space-focused on the detector. In the inset, the integrated signal intensity is shown as a function of the holding time. The observed decrease of the signal as a function of time is consistent with the expected decay based on the known 2.6-ms lifetime of the $a^3\Pi_1$ ($v' = 0, J' = 1$) state of CO (*13*). Clearly, measurements like the one shown in Fig. 4 can be used to determine lifetimes of molecules in long-lived electronically or vibrationally excited states, something that is notoriously difficult to do without trapping and for which thus far large experimental machines had to be constructed (*13*–*15*). The presently achieved densities of the molecules on the chip are in principle already sufficient for this (one actually does not want the densities to be too high, to prevent collisions between the trapped molecules), but for accurate measurements the statistics still need to be improved to some degree, either by increasing the density or implementing more sensitive ionization detection schemes.

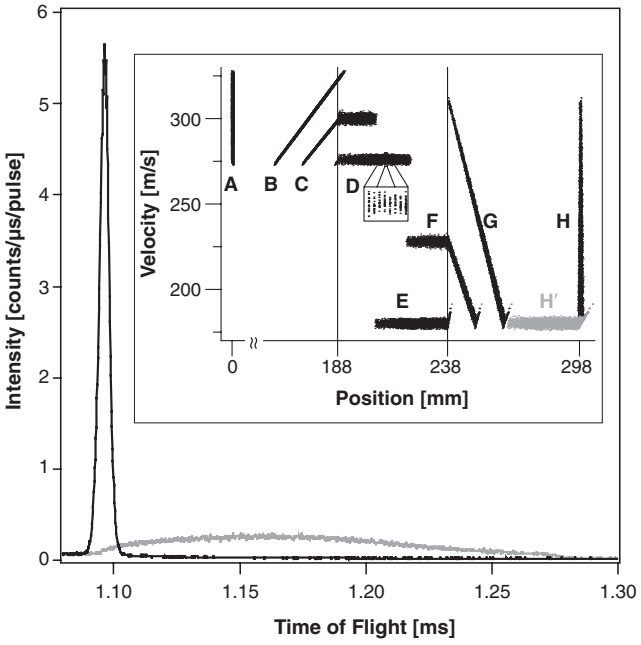

Fig. 3. Arrival-time distribution of ^{13}CO molecules ejected from about 250 simultaneously loaded electric field traps on the chip, both with (black curve) and without (gray curve) space focusing them on the detector. The time scale is relative to the time of laser excitation, and the vertical scale is in counts per microsecond and per pulse. Each measured trace is averaged over 2 hours (at 10 Hz). (**Inset**) The corresponding longitudinal phase-space distributions are shown at eight different times in the loading and detection cycle (A to H). By using a velocity-focusing deceleration of about 0.5×10^6 m/s^2 (B to D) followed by a rapid further deceleration of 1.20×10^6 m/s^2 (D and E), the molecules are brought to a velocity of 180 m/s on the chip. The edges of the chip are 188 and 238 mm away from the excitation point, indicated by vertical lines. An expanded view of the phase-space distribution at time (D), in which the individual electric field traps can be recognized, is shown as well.

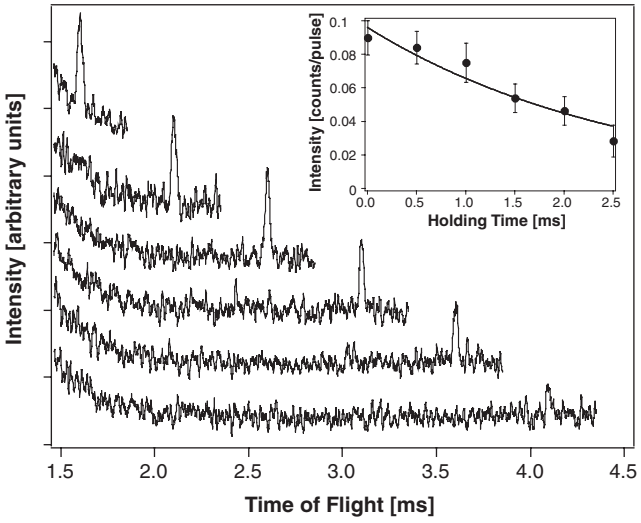

Fig. 4. Arrival-time distribution of ^{13}CO molecules ejected from about 60 simultaneously loaded stationary electric field traps on the chip after holding times ranging from 0 to 2.5 ms, in steps of 0.5 ms (from top to bottom). In these measurements, space focusing on the detector is used. The horizontal scale is relative to the time of laser excitation, and the curves have been given a vertical offset for clarity. Each measured trace is averaged over 4 hours (at 10 Hz). (**Inset**) The integrated intensity of the signal in counts per pulse is shown as a function of holding time, together with the expected dependence when only the phosphorescent decay of the metastable molecules is taken into account (*13*). The indicated error bars are determined from the 2σ noise on the baseline of the individual traces.

Many of the advances that were foreseen for microscopic magnetic traps for neutral atoms (*16*) and integrated atom optics on a chip (*17*) about a decade ago have now become a reality. The decisive advantage of the versatility of the lithographic wire structures can also be exploited for molecules. The ability of a molecule to rotate and vibrate allows for coupling to photons over an enormous range of frequencies. Coupling at microwave frequencies, in particular, provides a convenient interface between quantum optic and solid-state technologies (*6*). The use of miniaturized traps with inherent high trapping frequencies brings quantum degeneracy for samples of polar molecules considerably closer. A tight trap permits fast adiabatic changes of the confining potential, and via compression of a cloud of trapped molecules, increased thermalization rates and shortened times for forced evaporative cooling can be achieved. Here, we have experimentally demonstrated an integrated experimental approach to confine molecules in miniaturized traps on a chip and subsequently detect them, thereby opening up these fascinating research possibilities.

References and Notes

1. J. Fortágh, C. Zimmermann, *Rev. Mod. Phys.* **79**, 235 (2007).
2. W. Hänsel, P. Hommelhoff, T. W. Hänsch, J. Reichel, *Nature* **413**, 498 (2001).
3. T. Schumm *et al.*, *Nat. Physics* **1**, 57 (2005).
4. S. A. Meek, H. L. Bethlem, H. Conrad, G. Meijer, *Phys. Rev. Lett.* **100**, 153003 (2008).
5. D. DeMille, *Phys. Rev. Lett.* **88**, 067901 (2002).
6. A. André *et al.*, *Nat. Physics* **2**, 636 (2006).
7. S. Y. T. van de Meerakker, H. L. Bethlem, G. Meijer, *Nat. Physics* **4**, 595 (2008).
8. S. A. Meek, H. Conrad, G. Meijer, *N. J. Phys.* **11**, 055024 (2009).
9. M. Lara, B. L. Lev, J. L. Bohn, *Phys. Rev. A* **78**, 033433 (2008).
10. M. Kirste, B. G. Sartakov, M. Schnell, G. Meijer, *Phys. Rev. A* **79**, 051401(R) (2009).

11. R. H. Gammon, R. C. Stern, M. E. Lesk, B. G. Wicke, W. Klemperer, *J. Chem. Phys.* **54**, 2136 (1971).
12. The advantage of using metastable CO in the present experiments is that these molecules are prepared with a pulsed laser at a well-defined time and at a well-defined position in a single quantum state with the appropriate Stark shift. By detecting the Auger electrons when the metastable CO molecules impact on the Au surface, the full arrival-time distribution of the molecules can be recorded in a single pulse, and the schemes to manipulate the longitudinal phase-space distribution demonstrated in Fig. 3, for instance, can be rapidly tested and optimized. Even though the detection efficiency for metastable CO is not as good now as it can be for ionization detection, the multiplex nature of the trap-loading and detection scheme already enables us to detect down to one metastable CO molecule per hundred traps on the chip.
13. J. J. Gilijamse *et al.*, *J. Chem. Phys.* **127**, 221102 (2007).
14. S. Y. T. van de Meerakker, N. Vanhaecke, M. P. J. van der Loo, G. C. Groenenboom, G. Meijer, *Phys. Rev. Lett.* **95**, 013003 (2005).
15. W. C. Campbell, G. C. Groenenboom, H.-I. Lu, E. Tsikata, J. M. Doyle, *Phys. Rev. Lett.* **100**, 083003 (2008).
16. J. D. Weinstein, K. G. Libbrecht, *Phys. Rev. A* **52**, 4004 (1995).
17. E. A. Hinds, I. G. Hughes, *J. Phys. D Appl. Phys.* **32**, R119 (1999).
18. We acknowledge the help of B. G. Sartakov in the calculation of the hyperfine structure of ^{13}CO and the design of the electronics by G. Heyne, V. Platschkowski, and T. Vetter. This work has been funded by the European Community's Seventh Framework Program FP7/2007-2013 under grant agreement 216 774.

27 March 2009; accepted 26 May 2009
10.1126/science.1175975

Amplified Trace Gas Removal in the Troposphere

Andreas Hofzumahaus,[1] Franz Rohrer,[1]* Keding Lu,[1,2] Birger Bohn,[1] Theo Brauers,[1] Chih-Chung Chang,[3] Hendrik Fuchs,[1] Frank Holland,[1] Kazuyuki Kita,[4] Yutaka Kondo,[5] Xin Li,[1,2] Shengrong Lou,[1,6] Min Shao,[2] Limin Zeng,[2] Andreas Wahner,[1] Yuanhang Zhang[2]*

The degradation of trace gases and pollutants in the troposphere is dominated by their reaction with hydroxyl radicals (OH). The importance of OH rests on its high reactivity, its ubiquitous photochemical production in the sunlit atmosphere, and most importantly on its regeneration in the oxidation chain of the trace gases. In the current understanding, the recycling of OH proceeds through HO_2 reacting with NO, thereby forming ozone. A recent field campaign in the Pearl River Delta, China, quantified tropospheric OH and HO_2 concentrations and turnover rates by direct measurements. We report that concentrations of OH were three to five times greater than expected, and we propose the existence of a pathway for the regeneration of OH independent of NO, which amplifies the degradation of pollutants without producing ozone.

The central role of hydroxyl radicals (OH) in atmospheric chemistry was recognized by Levy in the early 1970s (*1*). Since then it has become more and more evident how OH radicals govern the degradation processes of air pollutants. OH radicals are short-lived (<1 s), and their formation and loss must be essentially balanced. OH is primarily formed through the photolysis of ozone, nitrous acid, and hydrogen peroxide and is consumed by a multitude of reactions with trace gases that can be oxidized. In this way, OH controls the removal of most atmospheric pollutants such as carbon monoxide (CO) and volatile organic compounds (VOCs). The OH reactions with CO and VOCs produce hydroperoxy (HO_2) and organic peroxy (RO_2) radicals, respectively. In continental air, with nitrogen oxides (NO_x) present, RO_2 is converted to HO_2 through reaction with NO. HO_2 further reacts with NO, thereby recycling OH. The ultimate loss of OH is the reaction with NO_2, forming nitric acid. These are the key processes that are believed to determine the self-cleaning ability of the troposphere (*2*, *3*). OH recycling enhances the efficiency of atmospheric oxidation, even at moderate NO concentrations. As a side effect, reactions of HO_2 or RO_2 with NO form NO_2, which produces ozone upon photolysis. This is the generally accepted, exclusive mechanism for the photochemical formation of ozone in the troposphere (*4*). OH formation through photolysis, HO_2 to OH recycling with NO, and OH loss with NO_2 have been established through a small number of well-understood reactions. In contrast, OH reactions with VOCs and the subsequent organic radical reactions are diverse and introduce enormous complexity into tropospheric chemistry, which is far from being fully explored (*5*, *6*).

The current understanding of tropospheric OH chemistry has been tested in a number of field campaigns, where the concentrations of OH and trace gases and meteorological parameters were observed simultaneously (*7*). However, OH observations are still too sparse, owing to the difficulty of measuring its extremely small and highly variable concentration, to provide a conclusive picture of the photochemistry in the entire troposphere (*8*–*10*). More experimental studies in different chemical environments are necessary to explore the various factors influencing the self-cleaning capability of the atmosphere. In this paper, we present concentration measurements of OH and HO_2 radicals in China (*11*), together with simultaneously measured mixing ratios of atmospheric trace gases and photolysis frequencies (*12*) (fig. S1). Complementary to direct measurements of VOCs, we also measured the total OH reactivity, k'_{OH}, corresponding to the inverse chemical lifetime of OH (*13*, *14*). Our measurements were part of an intense field campaign in a rural area, about 60 km NW of Guangzhou City, in the heavily populated Pearl River Delta (PRD) (*12*).

The diurnal dependences of the measured OH and HO_2 concentrations and k'_{OH} are shown

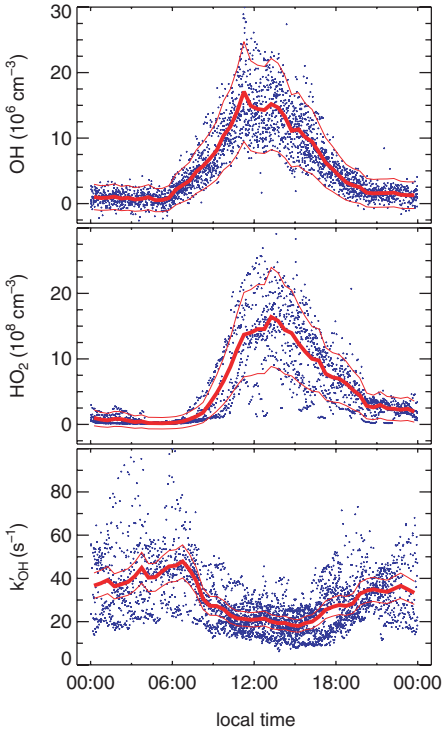

Fig. 1. Diurnal variation of OH, HO_2, and k'_{OH} near Guangzhou in the PRD, China, between 5 and 25 July 2006. Blue symbols denote individual data, and the thick red line the half-hourly mean diurnal profile. The enclosing thin red lines represent the maximum data variability caused by the measurement instrument (about 46% at noon), calculated as the sum of the 2σ measurement precision and the 2σ variability of its calibration. Campaign average calibration factors were used to convert measured OH and HO_2 signals into ambient concentrations.

[1]Forschungszentrum Jülich, Institut für Chemie und Dynamik der Geosphäre–2: Troposphäre, 52425 Jülich, Germany. [2]College of Environmental Sciences and Engineering, Peking University, Beijing 100871, China. [3]Research Center for Environmental Changes, Academic Sinica, Taipei, China. [4]Faculty of Science, Ibaraki University, Ibaraki 310-8512, Japan. [5]Research Center for Advanced Science and Technology, University of Tokyo, Tokyo 153-8904, Japan. [6]School of Environmental Science and Technology, Shanghai Jiaotong University, Shanghai 200240, China.

*To whom correspondence should be addressed. E-mail: f.rohrer@fz-juelich.de (F.R.); yhzhang@pku.edu.cn (Y.Z.)

in Fig. 1. The scatter of individual data points at a given time of day is caused by instrumental error (envelope lines in Fig. 1) and the variability of atmospheric conditions. In the following, we refer to the mean diurnal profiles, which have an improved measurement precision for OH and HO_2 of about 5%. The most striking feature is the high average OH concentration of 15×10^6 cm^{-3} around noon, which is maintained despite a large OH reactivity of about 20 s^{-1}. Most of that OH reactivity can be attributed to the heavy load of VOCs, with a substantial amount of isoprene, whereas only about 20% is explained by measured CO and NO_x [supporting online material (SOM) text]. Another remarkable feature is the very high noontime HO_2 concentration, yielding an HO_2/OH ratio of about 100, which is normally found only in clean air at low concentrations of NO_x (*15*). Although the air at the PRD was rich in VOCs, the level of NO at noon was surprisingly low, with an average of about 200 parts per trillion (ppt).

Figure 2A presents the total OH loss rate, calculated as the product of the OH concentration, [OH], and k'_{OH}. The high [OH] coinciding with a large OH reactivity at noontime causes a loss rate of approximately 40 parts per billion (ppb)/hour, which corresponds to an equivalent turnover in CO and VOCs. These values exceed recent observations in Mexico City (*16*) by a factor of 1.7. To maintain a steady state in [OH] requires an equally large OH production rate. We find that at the PRD, the OH production from all known sources cannot balance the large consumption rate of OH when NO drops to low values in the late morning (Fig. 2B). For instance, at noontime the OH recycling rate through the NO + HO_2 reaction is about 8 ppb/hour (Fig. 2A) and the primary OH production is 4 ppb/hour only (Fig. 2C). Apparently, the photochemical mix at the PRD maintains a hitherto unknown source of OH of about 28 ppb/hour, which is about two times larger than that of the known OH production processes displayed in Fig. 2 and sustains a highly efficient removal of trace gases by OH. This conclusion is based entirely on measurements and does not depend on modeled parameters.

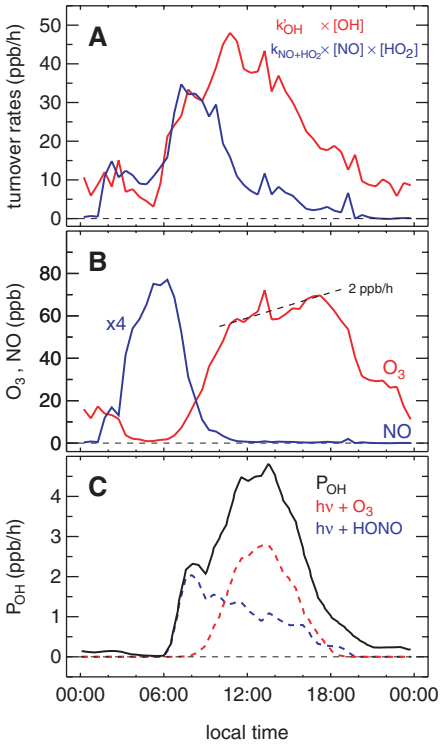

Fig. 2. Analysis of mean diurnal OH production and loss rates derived from measurements at the PRD in July 2006. (**A**) The red line denotes the total OH loss rate, the blue line the OH recycling rate from the reaction of HO_2 with NO, and (**C**) the black line the total primary OH production rate (P_{OH}) from photolysis and ozonolysis processes. The major contributions from the photolysis of ozone and HONO are shown by the red and blue dashed lines, respectively. (**B**) Mean diurnal profiles of ozone and NO.

Additionally, we performed chemical box-model calculations (*12*) for OH and HO_2, which are displayed in Fig. 3 as mean diurnal profiles, together with the experimental data. The model yields an excellent description of the measured HO_2 for the entire day, indicating that the ratio of the production to destruction rates of HO_2 is simulated correctly. Concentrations of OH, however, match only in the early morning to about 10:00; that is, as long as NO remains above 1 ppb. Thereafter, the measured [OH] is significantly larger than predicted by the model by a factor of 3 to 5 at low NO levels (<1 ppb). The discrepancy cannot be explained by the systematic experimental and modeling errors of 20 and 40%, respectively (fig. S6), and an experimental OH interference of the necessary magnitude is highly unlikely (SOM text). The measured OH reactivities are well described by the model during daytime (fig. S4). This and the failure of the model to reproduce the observed [OH] correctly is synonymous with our conclusion from Fig. 2, that the known OH sources are not enough to sustain the observed reaction rate of OH with pollutants.

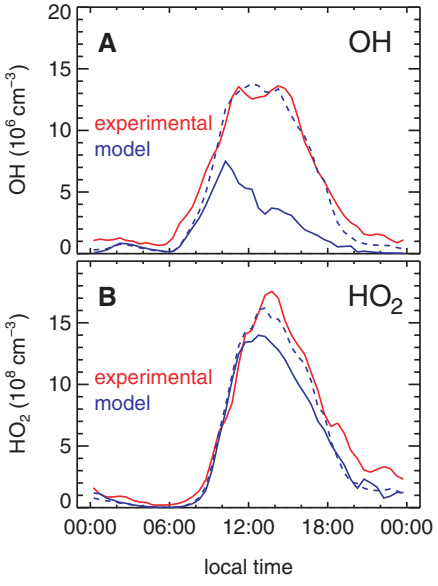

Fig. 3. Comparison of measured and modeled mean diurnal profiles of (**A**) OH and (**B**) HO_2. Red lines represent experimental data, blue solid lines the Regional Atmospheric Chemistry Mechanism (RACM) results (base case), and blue dashed lines the results from the extended RACM model with enhanced HO_2 and RO_2 recycling. The figure uses a subset of field campaign data, in which all required measurements are simultaneously available over full diurnal cycles.

In further simulations, we extended the model by various generic radical-production processes that might explain the measured diurnal variations of both OH and HO_2. Based on these model runs, we can exclude additional primary sources of OH or HO_2 to explain the observations. They would increase both species by a similar factor, because the partitioning of OH and HO_2 is largely maintained. An additional source in the model to match the measured OH would result in a significant overprediction of HO_2. Incidentally, the reaction of excited NO_2 with H_2O, a recently recognized new OH source (*17*), is too small to make a difference in our model results.

Additional recycling of peroxy radicals to OH is another way to increase the modeled [OH]. Peroxy reactions such as $RO_2 + HO_2 \rightarrow \alpha \times OH$ have been proposed to be a potentially significant source of atmospheric OH at low NO conditions (*10*, *18*). Laboratory studies provided α values up to 0.6 for specific RO_2 (*19*–*21*). Even at α = 1 for all RO_2 species, this process can explain only 15 to 30% of the additionally required OH, because most RO_2 (70 to 80%) reacts with NO (100 to 200 ppt) rather than with HO_2 (up to 60 ppt; SOM text). Lelieveld *et al.* (*10*) explained unexpectedly high [OH] in an isoprene-rich, low-NO (~20 ppt) environment, assuming α = 2 to 4 for the reaction of isoprene peroxy radicals. In contrast to the laboratory work, this requires additional photolysis of reaction products. Again, this hypothesis cannot explain our observations at the PRD, given the significantly larger rate of the competing RO_2 + NO reaction. Another possible path of HO_2 to OH by reaction with halogen oxides (BrO and IO) was observed in marine air at Cape Verde (*22*). This route can be discarded here as highly unlikely, because the required halogen oxide concentrations exceed all tropospheric observations, and no halogen sources were noted at the PRD (SOM text).

In order to reach the measured [OH] but maintain the level of observed HO_2, the mechanism needs to include reactions that as a net effect convert RO_2 to HO_2 and HO_2 to OH. The actual chemical mechanism of the proposed OH

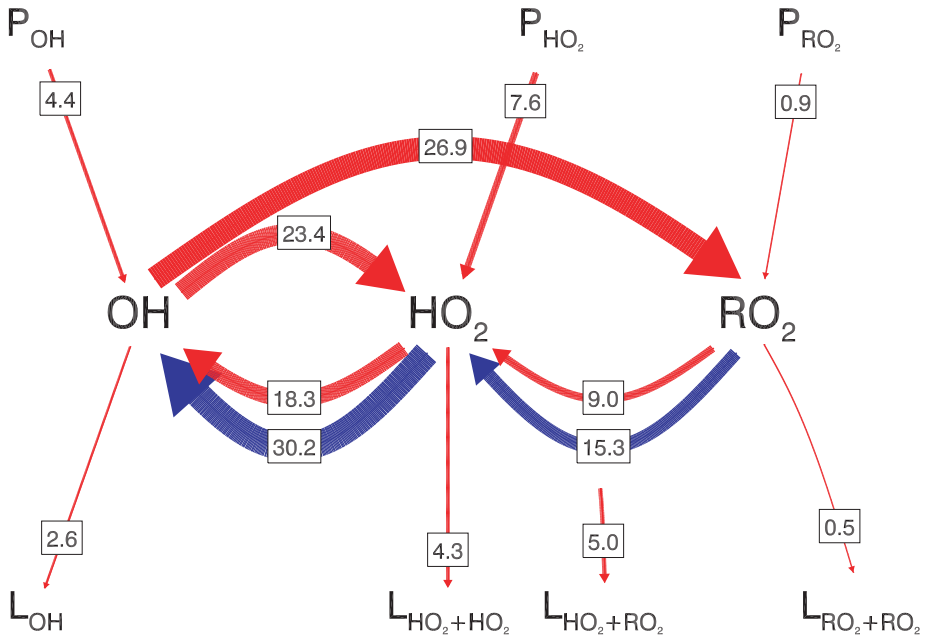

Fig. 4. Generic chart of the chemistry of tropospheric OH radicals. The arrows represent chemical processes which generate (P→), remove (→L), or interconvert (A→B) radicals. The width of the arrows scales with the reaction rates (in parts per billion per hour), given by the numbers in boxes, at 12:00 local time at Guangzhou in July 2006. Red arrows represent known reaction pathways of the RACM model and blue arrows the additional recycling processes needed to maintain the observed high [OH]. The total OH loss rate, $k'_{OH} \times [OH]$, corresponds to the sum of arrows OH → HO_2, OH → RO_2, and OH → LOH. The OH recycling by NO, $k_{HO_2 + NO} \times [NO] \times [HO_2]$, is represented by the red arrow HO_2 → OH.

recycling is not clear. In the most simple case, there could be two reactions, $RO_2 + X \rightarrow HO_2$ and $HO_2 + X \rightarrow OH$, both of similar rate, as in the case of the corresponding NO reactions. Another possibility would be reactions with several reactants, each of which makes a small contribution, summing up to a large OH source. Including the two reactions with a single reactant X as formulated above and assuming for X a reactive equivalent of 0.85 ppb of NO [obtained from an optimization (*12*)], the model is able to reproduce the mean diurnal cycles of both OH and HO_2 at high- and low-NO_x conditions during daytime surprisingly well (Fig. 3). The corresponding radical conversion rates at noon and in the afternoon are illustrated in Fig. 4 and fig. S7, respectively, quantifying the important role of the assumed recycling process for maintaining a high [OH].

In case of OH recycling with a single species X, a strong source of X would be required during the noon and afternoon hours. It could be direct emission, conversion from a large reservoir, or a recycling process of X. Steps toward the identification of the unknown OH recycling mechanism require further field and laboratory experiments to identify the reactions and chemical species involved, which are missing from current tropospheric chemistry models.

The existence of an additional radical-recycling mechanism has a potentially important implication for our ability to predict the photochemical formation of tropospheric ozone (*18*). In the current understanding, in which OH is recycled only by NO reactions, the oxidation of a CO or VOC molecule with OH can produce one or up to three ozone molecules, respectively (*23*). For a high turnover rate of 40 ppb/hour of OH as observed at the PRD at noontime (Fig. 2A), the classical mechanism would yield, with sufficient NO, a net production of ozone of about 60 ppb/hour. The observed trend of the mean diurnal ozone profile, however, is only 2 ppb/hour at noon and shortly thereafter (Fig. 2B). This suggests that the unknown radical-recycling process is not likely to produce much ozone, because the estimated loss by transport (<2 ppb/hour) cannot dissipate a potential net production of 60 ppb/hour (SOM text). If we run the extended model (Fig. 3) and assume that the proposed recycling mechanism does not form ozone, we calculate a chemical ozone increase of 7 ppb/hour, which is roughly in line with the observed ozone trend.

Unexplained high [OH] was observed previously in the presence of high VOC mixing ratios and at low to moderate NO_x levels in rural forested North America (*9*, *24*) and above the tropical rainforest in Surinam (*10*). In these regions, biogenic VOCs, mostly isoprene, are abundant and contribute significantly to the atmospheric OH reactivity, as in our observations at the PRD field site. Measured [OH] under clean air conditions (*25*) (low NO_x and low VOCs) and in highly polluted areas (*16*) (high NO_x and high VOCs), however, can be explained reasonably well by current models. Thus, the shortcoming of photochemistry models by underestimating tropospheric [OH], seems to apply only to low-NO_x and high-VOC regions, as encountered in the northern part of the PRD, and thus probably to large areas where a major portion of natural VOCs is emitted globally.

Current atmospheric chemistry models predict large formation of secondary pollutants such as ozone in strong correlation to trace gas degradation. Our observations suggest that the proposed recycling mechanism does not produce ozone but increases the stability of the [OH] and amplifies the oxidation capacity in the troposphere.

References and Notes

1. H. Levy II, *Science* **173**, 141 (1971).
2. D. H. Ehhalt, *Phys. Chem. Chem. Phys.* **1**, 5401 (1999).
3. G. P. Brasseur, R. G. Prinn, A. P. Pszenny, Eds., *Atmospheric Chemistry in a Changing World, Global Change—The IGAC Series* (Springer Verlag, Berlin, 2003).
4. S. C. Liu *et al.*, *J. Geophys. Res.* **92**, 4191 (1987).
5. B. Aumont, S. Szopa, S. Madronich, *Atmos. Chem. Phys.* **5**, 2497 (2005).
6. A. H. Goldstein, I. E. Galbally, *Environ. Sci. Technol.* **41**, 1514 (2007).
7. D. E. Heard, M. J. Pilling, *Chem. Rev.* **103**, 5163 (2003).
8. F. Rohrer, H. Berresheim, *Nature* **442**, 184 (2006).
9. X. R. Ren *et al.*, *J. Geophys. Res.* **113**, D05310 (2008).
10. J. Lelieveld *et al.*, *Nature* **452**, 737 (2008).
11. F. Holland, A. Hofzumahaus, R. Schäfer, A. Kraus, H. W. Pätz, *J. Geophys. Res.* **108**, 8246 (2003).
12. Information on measurement methods, modeling, and chemical conditions is available as supporting material on *Science* Online.
13. P. Di Carlo *et al.*, *Science* **304**, 722 (2004).
14. Y. Sadanaga, A. Yoshino, S. Kato, Y. Kajii, *Environ. Sci. Technol.* **39**, 8847 (2005).
15. D. J. Creasey, G. E. Evans, D. E. Heard, J. D. Lee, *J. Geophys. Res.* **108**, 4475 (2003).
16. T. R. Shirley *et al.*, *Atmos. Chem. Phys.* **6**, 2753 (2006).
17. S. Li, J. Matthews, A. Sinha, *Science* **319**, 1657 (2008).
18. J. A. Thornton *et al.*, *J. Geophys. Res.* **107**, 10.1029/2001JD000932 (2002).
19. A. S. Hasson, G. S. Tyndall, J. J. Orlando, *J. Phys. Chem. A* **108**, 5979 (2004).
20. M. E. Jenkin, M. D. Hurley, T. J. Wallington, *Phys. Chem. Chem. Phys.* **9**, 3149 (2007).
21. T. J. Dillon, J. N. Crowley, *Atmos. Chem. Phys.* **8**, 4877 (2008).
22. K. A. Read *et al.*, *Nature* **453**, 1232 (2008).
23. L. I. Kleinman *et al.*, *J. Geophys. Res.* **107**, 4733 (2002).
24. D. Tan *et al.*, *J. Geophys. Res.* **106**, 24407 (2001).
25. T. Brauers, M. Hausmann, A. Bister, A. Kraus, H.-P. Dorn, *J. Geophys. Res.* **106**, 7399 (2001).

26. We thank the PRiDe PRD 2006 campaign team (2002CB410801), especially L. J. Zhong, M. Hu, N. Takegawa, Y. Miyazaki, M. Koike, R. Häseler, and A. Oebel, for technical help and support at the field site, and J. L. Wang for help in the in situ measurement of VOCs. C.C. thanks Academic Sinica, Taiwan, for financial support of this work. Discussions with S. C. Liu and D. H. Ehhalt are gratefully acknowledged.

Supporting Online Material

www.sciencemag.org/cgi/content/full/1164566/DC1
Methods
SOM Text
Figs. S1 to S9
References

12 August 2008; accepted 21 May 2009
Published online 4 June 2009;
10.1126/science.1164566
Include this information when citing this paper.

Postmating Sexual Selection Favors Males That Sire Offspring with Low Fitness

Trine Bilde,[1,2]* Anne Foged,[2] Nadia Schilling,[2] Göran Arnqvist[1]

Despite the costs of mating, females of most taxa mate with multiple males. Polyandrous females are hypothesized to gain genetic benefits for their offspring, but this assumes paternity bias favoring male genotypes that enhance offspring viability. We determined net male genetic effects on female and offspring fitness in a seed beetle and then tested whether fertilization success was biased in favor of high-quality male genotypes in double mating experiments. Contrary to expectations, high-quality male genotypes consistently had a lower postmating fertilization success in two independent assays. Our results imply that sexually antagonistic adaptations have a major and unappreciated influence on male postmating fertilization success. Such genetic variation renders indirect genetic benefits an unlikely driver of the evolution of polyandry.

Our understanding of the evolution of multiple mating by females (i.e., polyandry) in the face of the costs of mating is limited (*1*, *2*), despite a massive empirical effort (*3*, *4*). Polyandry is adaptive in cases where females receive material benefits from males (*3*), but in many cases such direct benefits are lacking. Thus, it is commonly believed that females gain genetic (or indirect) benefits for their offspring by mating with multiple males (*4*). Theory suggests that genetic benefits in the form of genetic diversification or genetic bet-hedging (i.e., various forms of genetic risk-spreading) are unlikely to contribute to the evolution of polyandry (*5*). Instead, the genetic benefits of polyandry rely on a positive relationship between male postmating fertilization success and the viability of offspring carrying his genes (*5*, *6*). Cryptic female choice, which occurs through the success of certain males over others by female traits that bias postmating fertilization (*7*), would promote this relationship if it favors males carrying alleles with high fitness or alleles that are more compatible with the female genotype because of epistatic interactions (*1*, *6*, *8*). Females can maximize offspring fitness by choosing both types of genetic variation in fitness simultaneously (*8*). We thus define male genetic quality as the net viability effects of his genes in the offspring of a given female genotype. Under this wide definition, male genetic quality may vary across female genotypes and will be the sum of additive (i.e., good genes) and nonadditive (i.e., compatibility) genetic quality (*8*).

The relationship between male genetic quality and fertilization success plays a key role for the evolution of polyandry (*9*–*12*). Polyandrous females can reduce the cost of inbreeding by cryptic female choice for genetically compatible males (*12*–*14*). However, except for documented cases of inbreeding avoidance, very limited evidence supports the assumption that fertilization is generally biased toward males with a genotype that enhances offspring viability (*1*, *11*, *15*).

[1]Department of Ecology and Evolution, Evolutionary Biology Centre, University of Uppsala, Norbyvägen 18d, SE - 752 36 Uppsala, Sweden. [2]Department of Biological Sciences, University of Aarhus, Ny Munkegade 1540, 8000 Aarhus C, Denmark.

*To whom correspondence should be addressed. E-mail: trine.bilde@biology.au.dk

We tested whether males of high genetic quality are also favored in postmating sexual selection in the seed beetle *Callosobruchus maculatus*. This species is polyandrous and shows both differential sperm competition success across male genotypes and cryptic female choice, as evidenced by the fact that sperm competition success of specific male genotypes varies across female genotypes (*16*, *17*). Reciprocal crosses between a large number of discrete isogenic genotypes were used to establish both female fitness and female offspring fitness (lifetime reproductive success) in crosses between genotypes (*18*). For each female genotype, we ranked males according to their net genetic quality, that is, the net additive and nonadditive effect of a male genotype on fitness (*18*). Focal females were then mated with two males, each representing a high- and a low-quality male, in two independent assays of postmating fertilization success (*19*). In the first assay, male quality rank was assessed from paternal effects on the lifetime number of adult offspring produced by a given female genotype (Fig. 1). In the second, male quality rank examined paternal effects on the lifetime number of adult offspring produced by the daughters of a specific cross (*18*). Paternal genetic effects on the fitness of their mates and parental genetic effects on the fitness of their daughters are sizeable and significant in this species (*18*).

The first assay showed that males that conferred a relatively low fitness on their mates had a significantly higher rate of fertilization success [generalized linear mixed models (GLMM), $F_{1,266.4} = 15.44$, $P < 0.001$] (Fig. 2). Studies of the genetic architecture of fitness among these genotypes (*18*) showed that variance in the effects of male genotype on female fitness (i.e., female lifetime offspring production) is due both to direct effects, such as variance in ejaculate composition (*20*) or costs of mating (*21*, *22*), and to indirect genetic effects affecting juvenile survival (*18*). On

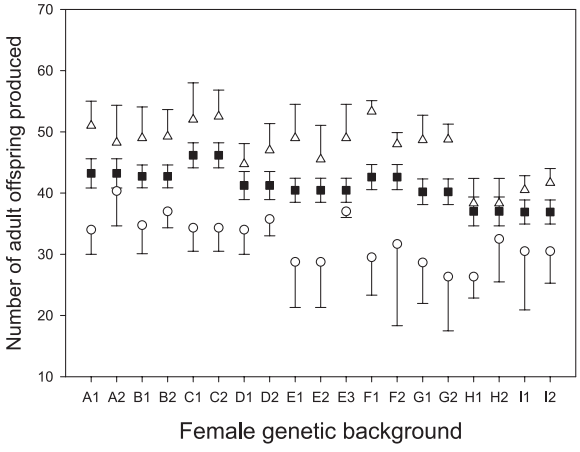

Fig. 1. The average number of adult offspring produced (■ ±SE) (lifetime reproductive success, LRS) by isogenic females across all isogenic males. Male genotypes that conferred a high lifetime offspring production (Δ +SE) were considered high-quality males, and those that conferred a low lifetime offspring production (○ −SE) were designated low-quality males. Females enjoyed higher fitness when reproducing with high- compared with low-quality males (mixed model analysis of variance, effect of male quality: $F_{1,108} = 68.13$, $P < 0.001$).

Fig. 2. Estimates of the average (with 95% confidence intervals) proportion of eggs fertilized by a second male mated with a female. Males were categorized as high or low quality on the basis of either their net effect on female lifetime offspring production (●) or their paternal net genetic contribution to offspring fitness (○). In both assays, low-quality males sired a higher proportion of offspring.

average, females were 18% more fit (95% confidence interval = 13 to 28%) when reproducing with high-quality males relative to low-quality males. We expect then that females would benefit if they biased paternity toward high-quality males. This is supported by the fact that cryptic female choice for specific male genotypes has been demonstrated in this species (*17*, *23*). Yet, the pattern of paternity bias that we observed was the opposite of what is expected to benefit females. In fact, our data show that males that confer a low fitness on their mates gain the highest share of paternity. This observation is consistent with the fact that male traits that increase success in sperm competition may, as a direct negative pleiotropic side effect, depress the fitness of their mates. Such sexually antagonistic male sperm competition adaptations are known from many different taxa (*24*), including seed beetles (*21*). Both male effects on female lifetime offspring production (*18*) and male postmating fertilization success (*17*, *23*) are partly determined by male genotype–by–female genotype interactions in seed beetles. Our data suggest that these two types of interactions may be related, given the causal link between the paternal effects affecting a particular female genotype, and thus female fitness, and sperm competition success in that female genotype. We note that we expect to observe similar results whenever the efficacy of a sexually antagonistic male sperm competition adaptation (e.g., an accessory gland protein in the male seminal fluid) depends on the female traits with which it interacts (e.g., female receptors) (*24*).

In the second assay, males that fathered offspring with relatively low fitness sired a significantly higher proportion of eggs than did males of high quality. This was true whether females that did not produce any offspring of the second male to which they were mated were excluded (GLMM, $F_{1,58.9} = 8.9$, $P = 0.004$) or included (GLMM, $F_{1,162.3} = 15.9$, $P < 0.001$) (Fig. 2) in the analyses. On average, females produced daughters with 17% (95% confidence interval = 13 to 23%) higher lifetime reproductive success when reproducing with high-quality compared with low-quality males (*18*). A quantitative genetic study of the genetic architecture of fitness with these genotypes show that the fitness of daughters is dominated by both additive and nonadditive (dominance/epistatic) genetic variance (*18*). Females can gain indirect genetic benefits when their daughters have elevated reproductive success, and they can influence this by favoring genetically compatible males and/or males with a higher breeding value for offspring fitness (*8*). Thus, our results are again opposite to that expected under cryptic female choice for males carrying good or compatible genes for general viability (*1*). The apparent lack of precopulatory female mate choice in this species (*25*) strongly suggests that females are unable to negate this detrimental effect by exercising control before mating.

The observed negative relationship between male postmating fertilization success and the fitness effects of his genes in female offspring could be due to genes with either additive or nonadditive effects (*18*). If additive effects dominate, our results support that some degree of intralocus sexual conflict is occurring: the presence of sexually antagonistic genes with opposite effects on fitness when expressed in the two sexes (*26*). Intralocus sexual antagonism has been documented in other insects (*27*, *28*). If common, such genes will result in successful males siring unsuccessful daughters (*29*). This predicts that the relationship between male quality and offspring fitness would be negative in daughters but positive in sons. However, the quantification of sex-specific genetic effects was not the aim of this study: Our primary goal was to determine the scope for nonrandom fertilization success among males to build genetic associations (i.e., linkage disequilibrium) between alleles coding for polyandry and those encoding high viability, thus generating indirect selection on female mating rate by a "good genes" process (*5*, *15*, *18*). Although intralocus sexual conflict can nullify indirect genetic benefits in one sex (*28*, *29*), it is highly unlikely that sex-specific indirect effects would alter our main result. Because indirect selection is generally weak relative to direct selection (*18*, *30*) and because males successful in sperm competition fathered offspring with low juvenile survival in both sexes and with low fitness in daughters (*18*), sex-specific benefits to sons would need to be very large indeed to result in appreciable net indirect selection for polyandry (*15*, *30*). This possibility lacks empirical support (*31*). If nonadditive genetic effects dominate the fitness effects seen, they involve interactions between maternal and paternal genotypes affecting fertilization success in the parental generation and offspring fitness in the next generation. This could occur if, for example, particular combinations of sex-specific traits associated with high male paternity within a female reproductive tract are also associated with low fitness in daughters at other developmental stages.

Classic cryptic female choice (*1*, *7*) and theory based on sexual antagonism (*24*, *26*) make contrasting predictions with regards to the relationship between male genetic quality and paternity bias. If sexually antagonistic adaptations and/or sexually antagonistic alleles (i.e., where the direction of selection on a given allele expressed in both sexes depends on the sex in which it resides) are common and polymorphic, as is apparently the case in seed beetles, postmating sexual selection will not reward polyandrous females with the genetic benefits required to outweigh the costs of mating. Females may even suffer genetic costs from mating with multiple males in such situations, and any female benefits of polyandry must come from elements other than the paternal genetic contribution to offspring.

References and Notes

1. L. W. Simmons, *Annu. Rev. Ecol. Evol. Syst.* **36**, 125 (2005).
2. T. R. Birkhead, A. P. Møller, *Sperm Competition and Sexual Selection* (Academic Press, London, 1998).
3. G. Arnqvist, T. Nilsson, *Anim. Behav.* **60**, 145 (2000).
4. M. D. Jennions, M. Petrie, *Biol. Rev. Camb. Philos. Soc.* **75**, 21 (2000).
5. Y. Yasui, *Trends Ecol. Evol.* **13**, 246 (1998).
6. T. Tregenza, N. Wedell, *Mol. Ecol.* **9**, 1013 (2000).
7. W. G. Eberhard, *Female Control: Sexual Selection by Cryptic Female Choice* (Monographs in Behavior and Ecology, Princeton Univ. Press, Princeton, NJ, 1996).
8. M. Puurtinen, T. Ketola, J. S. Kotiaho, *Trends Ecol. Evol.* **20**, 157 (2005).
9. M. A. Dziminski, J. D. Roberts, L. W. Simmons, *Evolution* **62**, 879 (2008).
10. J. P. Evans, F. Garcia-Gonzalez, D. J. Marshall, *Evolution* **61**, 2832 (2007).
11. D. O. Fisher, M. C. Double, S. P. Blomberg, M. D. Jennions, A. Cockburn, *Nature* **444**, 89 (2006).
12. T. Tregenza, N. Wedell, *Nature* **415**, 71 (2002).
13. J. A. Zeh, D. W. Zeh, *Nature* **439**, 201 (2006).
14. T. Bilde, A. A. Maklakov, N. Schilling, *J. Evol. Biol.* **20**, 1237 (2007).
15. G. Arnqvist, M. Kirkpatrick, *Am. Nat.* **165**, S26 (2005).
16. G. Arnqvist, T. Nilsson, M. Katvala, *Behav. Ecol.* **16**, 123 (2005).
17. N. Wilson, S. C. Tubman, P. E. Eady, G. W. Robertson, *Proc. R. Soc. London Ser. B* **264**, 1491 (1997).
18. T. Bilde, U. Friberg, A. A. Maklakov, J. D. Fry, G. Arnqvist, *BMC Evol. Biol.* **8**, 10.1186/1471-2148-8-295 (2008).
19. Materials and methods are available as supporting material on *Science* Online.
20. J. L. Ronn, M. Katvala, G. Arnqvist, *J. Evol. Biol.* **21**, 461 (2008).
21. C. Hotzy, G. Arnqvist, *Curr. Biol.* **19**, 404 (2009).
22. J. Ronn, M. Katvala, G. Arnqvist, *Proc. Natl. Acad. Sci. U.S.A.* **104**, 10921 (2007).
23. D. K. Dowling, U. Friberg, G. Arnqvist, *J. Evol. Biol.* **20**, 2113 (2007).
24. G. Arnqvist, L. Rowe, *Sexual Conflict* (Monographs in Behavior and Ecology, Princeton Univ. Press, Princeton, NJ, 2005), p. 330.
25. U. M. Savalli, C. V. Fox, *Ethol. Ecol. Evol.* **11**, 49 (1999).
26. A. K. Chippindale, J. R. Gibson, W. R. Rice, *Proc. Natl. Acad. Sci. U.S.A.* **98**, 1671 (2001).
27. K. M. Fedorka, T. A. Mousseau, *Nature* **429**, 65 (2004).
28. A. Pischedda, A. K. Chippindale, *PLoS Biol.* **4**, 2099 (2006).
29. K. Foerster *et al.*, *Nature* **447**, 1107 (2007).
30. M. J. Wade, S. M. Shuster, J. P. Demuth, *Am. Nat.* **162**, 403 (2003).
31. C. W. Fox, R. C. Stillwell, J. Moya-Larano, in *Sex, Size, and Gender Roles*, D. J. Fairbairn, W. U. Blanckenhorn, T. Szekely, Eds. (Oxford Univ. Press, Oxford, 2007), pp. 88–96.

32. We thank E. B. Rasmussen for assistance; C. W. Fox for providing the beetle population used; and I. M. Horsman, D. Grand, and P. Schjerbeck at Aarhus University Hospital for their extensive help and flexibility with irradiating males. U. Friberg, T. Tregenza, M. Olsson, and J. Schneider provided valuable comments. Funded by a Marie Curie fellowship (MC MEIF-CT-2006-023645) (T.B.), the Carlsberg Foundation (T.B.), and the Swedish Research Council (G.A.).

Supporting Online Material

www.sciencemag.org/cgi/content/full/324/5935/1705/DC1
Materials and Methods
References

30 January 2009; accepted 12 May 2009
10.1126/science.1171675

Dynamic Signaling Network for the Specification of Embryonic Pancreas and Liver Progenitors

Ewa Wandzioch and Kenneth S. Zaret*†

Studies of the formation of pancreas and liver progenitors have focused on individual inductive signals and cellular responses. Here, we investigated how bone morphogenetic protein, transforming growth factor–β (TGFβ), and fibroblast growth factor signaling pathways converge on the earliest genes that elicit pancreas and liver induction in mouse embryos. The inductive network was found to be dynamic; it changed within hours. Different signals functioned in parallel to induce different early genes, and two permutations of signals induced liver progenitor domains, which revealed flexibility in cell programming. Also, the specification of pancreas and liver progenitors was restricted by the TGFβ pathway. These findings may enhance progenitor cell specification from stem cells for biomedical purposes and can help explain incomplete programming in stem cell differentiation protocols.

Although stem cells are defined by their ability to self-renew and to differentiate down specific cell lineages, there are limitations in the capability of stem cells to be programmed in vitro. Cells differentiated in culture often lack the full spectrum of properties normally exhibited by their in vivo counterparts (*1*, *2*). One reason for the limitation could be a lack of understanding of how inductive signals interrelate to properly program, for example, pancreas and liver progenitors (*1*–*3*).

In the mouse embryo, progenitors to the pancreatic beta cell and hepatocyte lineages arise from neighboring domains of ventral foregut endoderm. *Pdx1* (*Ipf1*) and *alb1* (*Alb*) are activated at the seventh and eighth somite pair (7-8S) stage in nascent pancreas and hepatocyte progenitors, respectively, in mouse development (*4*–*7*). At the same stage and spanning both the pancreatic (*Pdx1*+) and hepatic (*alb1*+) domains, the regulatory genes *Hnf1b* (*Tcf2*), *Hnf6* (*Onecut1*), and *Prox1* are induced; each is required for the subsequent development of both the liver and pancreatic buds (*8*–*12*). We focused on the signaling network that induces all five of these earliest genes specific to the pancreatic and hepatic lineages.

Embryonic tissue explant studies have established that the different progenitor cell domains are induced by signals emitted from overlying mesoderm cells (*6*, *13*–*16*). In mouse and zebrafish embryos, redundant fibroblast growth factors (FGFs) and bone morphogenetic proteins (BMPs) secreted from the cardiac mesoderm and septum transversum mesenchyme, respectively, induce *alb1* in the ventral endoderm and suppress *Pdx1* (*5*, *17*–*21*). How these signals coordinately feed into the induction of *Hnf1b*, *Hnf6*, and *Prox1* is not known, nor is their relationship to TGFβ signaling, which is also present in the foregut (*22*).

Establishing a foregut endoderm fate map (*23*) is crucial for monitoring endoderm signaling events before cell type specification. Paired lateral domains of endoderm cells move ventrally at the anterior intestinal portal, helping to close off the developing foregut and contribute to the liver bud (Fig. 1, A and B). The liver bud is also constituted from a distinct population of medial endoderm cells (Fig. 1, A and B); the prospective lateral and medial hepatic domains fuse near the heart at the 7-9S stage (Fig. 1C) (*23*). Ventral pancreatic progenitors reside in the caudal-most domain of lateral liver progenitors; they migrate toward the midline during gut closure and reside caudal to the liver and heart domains at 7-8S (*23*). To examine BMP, TGFβ, and FGF signaling within ventral endoderm before pancreatic and liver specification, we stained embryos at different stages (*24*) with antibodies specific to the phosphorylated pathway intermediates SMAD1,5,8 (for the BMP pathway), Smad2 (for the TGFβ pathway), and extracellular signal–regulated kinases ERK1 and 2 [for the mitogen-activated protein kinase (MAPK) pathway, downstream of FGF (*17*)]. The staining patterns were blocked by pathway inhibitors to ensure specificity of the antibodies (fig. S1).

Whole-mount immunofluorescence of 3-4S embryos revealed that the prospective lateral hepatic progenitors contained activated FGF-MAPK signaling (Fig. 1D), as reported previously (*17*). The ventral-medial endoderm, also containing prospective hepatic progenitors, was negative for phosphorylated ERK (pERK) at 3-4S (Fig. 1D). Activated BMP signaling exhibited the opposite pattern: pSMAD1,5,8 was evident in ventral-medial endoderm at 3-4S and not in the ventral-lateral endoderm (Fig. 1G). Thus, the prospective ventral-medial hepatic progenitors have activated BMP signaling (as evidenced by SMAD1,5,8) at the 3-4S stage, but these progenitors do not yet have an active FGF-MAPK pathway, whereas prospective ventral-lateral hepatic progenitors have activated FGF-MAPK at the 3-4S stage, but no active BMP signaling.

A few hours later in development (5-6S), activated MAPK signaling tracked with the prospective lateral hepatic progenitors as they moved ventral-medially (Fig. 1E). During this period, *Bmp4* and *Bmp2* were expressed in septum transversum mesenchyme across the ventral-medial region (*20*, *25*) (fig. S2, A and B), and

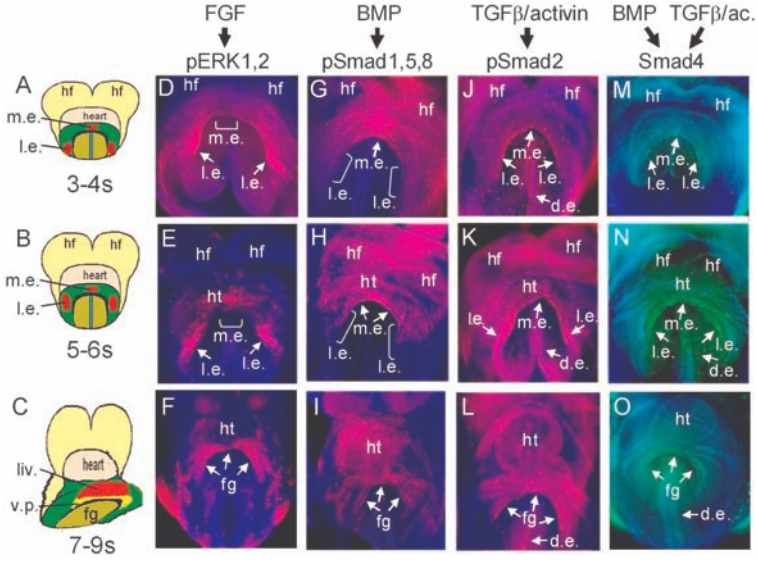

Fig. 1. Dynamic signal transduction molecule activation in the foregut endoderm revealed by whole-mount immunofluorescence (IF). (**A** to **C**) Fate map of foregut endoderm at different stages (*23*). (**D** to **O**) Images with the foregut facing the viewer. Arrows indicate regions with positive signal; brackets indicate regions lacking signal. m.e., medial endoderm; l.e., lateral endoderm; d.e., dorsal endoderm; hf, head fold; ht, heart; fg, foregut; liv., liver; v.p., ventral pancreas.

Cell and Developmental Biology Program, Fox Chase Cancer Center, 333 Cottman Avenue, Philadelphia, PA 19111, USA.

*Present address: Department of Cell and Developmental Biology, University of Pennsylvania, 421 Curie Boulevard, Philadelphia, PA 19104, USA.

†To whom correspondence should be addressed. E-mail: zaret@upenn.edu

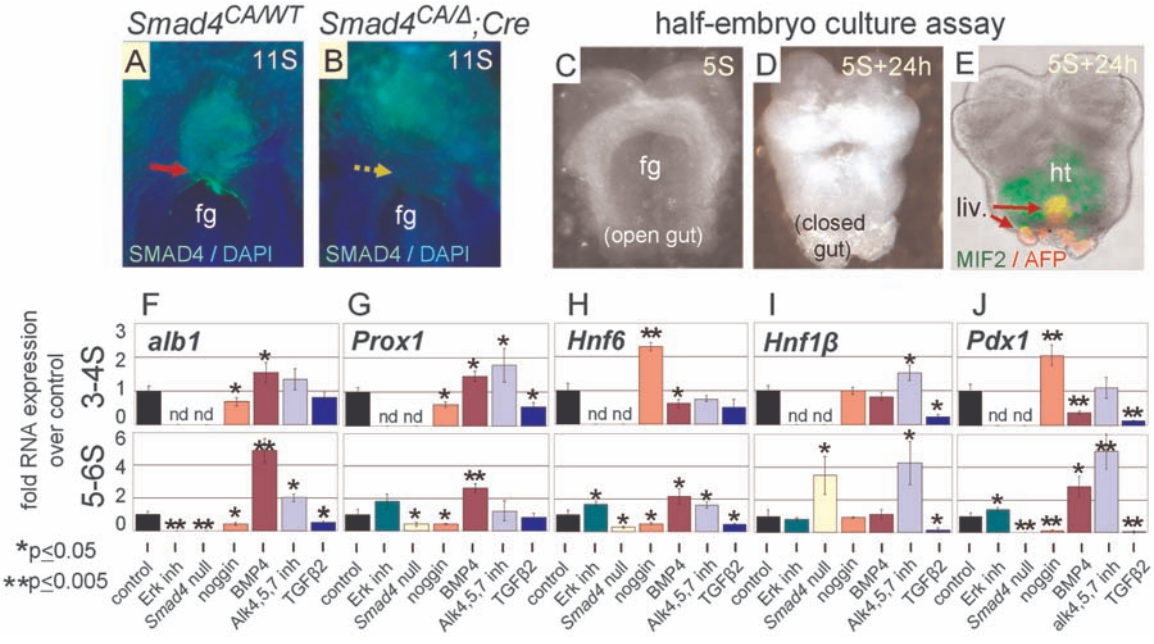

Fig. 2. Genetic and pharmacologic perturbation of signaling pathways. (**A** and **B**) Whole-mount IF of designated genotypes. Red arrow indicates presence of SMAD4 in ventral foregut endoderm; dashed arrow indicates lack of SMAD4. DAPI, 4′,6′-diamidino-2-phenylindole. (**C** to **E**) Images of 5S half embryo before (C) or after (D and E) culture. (**F** to **J**) qRT-PCR on endoderm from half embryos ± inhibitors or from *FoxA3*^{cre};*SMAD4*$^{CA/\Delta}$ (*Smad4* null) embryos at 11S compared with that from 11S wild-type embryos. Each sample (n = 2 to 8) was analyzed in triplicate; *$P \leq 0.05$ determined by t test; **$P \leq 0.005$; "nd," not determined. Error bars indicate SD calculated with the comparative Ct (ΔCt) method.

pSMAD1,5,8 began to spread laterally (Fig. 1H). At the time of activation of the liver program (7-9S), the two lateral hepatic progenitor domains had migrated ventrally, joining the midline progenitors, and thus the entire liver domain became positive for pERK and pSMAD1,5,8 (Fig. 1, F and I).

At 3-6S stages, the prospective ventral pancreas progenitors lacked activated pSMAD1,5,8 (Fig. 1, G and H). However, by the 7-8S stages, the lateral cells moved ventrally and were in the domain of pSMAD1,5,8 (Fig. 1I). In summary, the ventral pancreatic progenitors are initially negative for BMP signaling and, several hours later, become positive.

BMP signaling via pSMAD1,5,8 utilizes SMAD4, which is a partner for TGFβ-activin signaling via phosphorylated SMAD2,3. Because TGFβ2 is expressed in the foregut and its receptors are expressed in the endoderm (*22*, *26*), we investigated pSMAD2. Notably, during all stages, we detected pSMAD2 throughout the ventral foregut endoderm (Fig. 1, J to L). Similarly, SMAD4 was expressed throughout the ventral foregut endoderm, as well as in the cardiac mesoderm (Fig. 1, M to O). In the dorsal endoderm, we detected SMAD4 and pSMAD2, but not pERK or pSMAD1,5,8 (Fig. 1, J to L, N, and O). Several hours later (11S), ventral SMAD4 expression was confined to the ventral-medial endodermal domain, extending anteriorly to the pharyngeal region of the foregut (Fig. 2A).

To investigate the role of each pathway, we used genetic and pharmacologic perturbants. We used a *FoxA3*^{CRE} transgene, which becomes functional in the ventral foregut endoderm at the 5-6S stage (*17*, *27*) and a *Smad4* conditional allele (*Smad4*^{CA}) (*28*) to impair SMAD1,5,8 (BMP) and SMAD2,3 (TGFβ) signaling. As anticipated, ventral foregut expression of SMAD4 was completely ablated in *FoxA3*^{CRE};*Smad4*^{CA}/*Smad4*$^{\Delta}$ embryos, although persisted in the pharyngeal region (Fig. 2, A and B). We also developed a new half-embryo culture system that allows foregut development (*24*). Briefly, yolk sacs and tissues caudal to the first somite were removed from 2-6S embryos, and the anterior half embryos were cultured 24 hours while floating. These half embryos reproducibly underwent gut tube closure, then induction of early liver and pancreatic markers, and formed a large, beating heart (Fig. 2, C to E). We processed the ventral gut domain for mRNA analysis by quantitative reverse transcription polymerase chain reaction (qRT-PCR). Gene expression in 24-hour cultures was normalized to that of the gene for glyceraldehyde-3-phosphate dehydrogenase, *Gapdh*, and compared with that in ventral foregut tissues isolated from intact embryos at 5S, 9S, and 13S stages, with the 5S stage as a reference. *Foxa2* expression, a marker of foregut endoderm (*27*), was consistent throughout the embryonic stages and in 24-hour half-embryo cultures, whereas *Pdx1, Hnf1b, Hnf6*, *Prox1*, and *alb1* were activated in half embryos to levels observed in 9-13S native embryos (fig. S3). Thus, the half-embryo explants recapitulate the induction of the earliest known genes for the pancreatic and hepatic programs.

Treating half embryos isolated at the 3-4S stage with the BMP inhibitor noggin suppressed induction of the hepatocyte early gene *alb1*, whereas exogenous BMP4 treatment slightly enhanced *alb1* induction (Fig. 2F). With half embryos isolated at the 5-6S stage, stronger effects were observed (Fig. 2F). Similarly, noggin inhibited *Prox1* induction, whereas BMP4 enhanced it (Fig. 2G). Consistent with the latter results, the embryos in which *Smad4* had been deleted in the endoderm at 5-6S exhibited a complete loss of *alb1* induction and impaired *Prox1* induction (Fig. 2, F and G), although some *Afp*-positive cells were eventually produced (see Fig. 3F below). Thus, BMP signaling initially is prohepatic with this experimental system, as seen in our previous studies and elsewhere (*1*, *20*, *21*).

Treating half embryos isolated at 3-4S with noggin induced the pancreatic beta cell early gene, *Pdx1*, and treatment with BMP4 inhibited it (Fig. 2J), which together imply a reciprocal effect compared with liver induction, as we saw previously (*18*, *20*). Similarly, at the 3-4S stage, *Hnf6* was induced by noggin and inhibited by BMP (Fig. 2H).

In contrast, half-embryo cultures established several hours later, at the 5-6S stage, consistently exhibited the opposite phenotype. Noggin suppressed *Pdx1* and *Hnf6* expression, whereas exogenous BMP4 enhanced it (Fig. 2, H and J). These results were confirmed by genetics, as deletion of *Smad4* at 5-6S wiped out *Pdx1* induction and impaired *Hnf6* induction (Fig. 2, H and J), which underscored the rapidity with which programming signals naturally change in their inductive effects. The latter findings are consistent with studies on endoderm explants from later-stage chick embryos (*29*).

The gene expression phenotypes in the *FoxA3*^{CRE};*Smad4*^{CA}/*Smad4*$^{\Delta}$ embryos were accompanied by profound organogenic defects. Immunofluorescence staining revealed virtually no Pdx1-positive cells at embryonic day 9.5 (E9.5) in the ventral gut, nor was there morphological evidence of a ventral pancreatic bud (Fig. 3, C and D). By E10.5, a few ventral Pdx1-positive cells were evident (Fig. 3, G and H). Liver development was also impaired (Fig. 3, E and F). However, there was only a weak effect of *Smad4* deletion on dorsal pancreatic development (Fig.

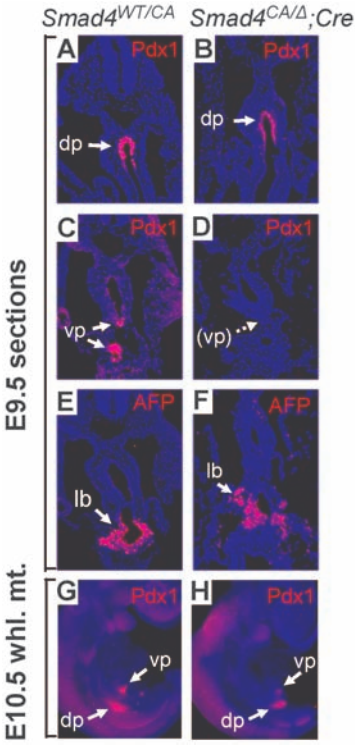

Fig. 3. Defective ventral pancreatic development in embryos deficient for *Smad4* in the endoderm. (**A** to **F**) Transverse IF sections for Pdx1 or AFP (red), and DAPI. (**G** and **H**) Whole-mount IF for Pdx1 with DAPI. d.p., dorsal pancreas; lb, liver bud.

Fig. 4. TGFβ signaling restrains the specification of ventral pancreatic progenitors. (**A**, **C**, and **E**) Whole-mount X-gal staining (blue) for pancreatic progenitors. (**B**, **D**, and **F**). Sagittal sections, counterstained for Ki-67 (brown). (**G**) Dynamic network inducing the earliest genes for liver and pancreas specification. Arrows, positive signaling; blunt-ended arrows, negative. The thicker lines for BMP and thinner lines for TGFβ at 5-6S indicate BMP as the dominant *Smad4*-dependent pathway for *alb1*, *Hnf6*, and *Pdx1*.

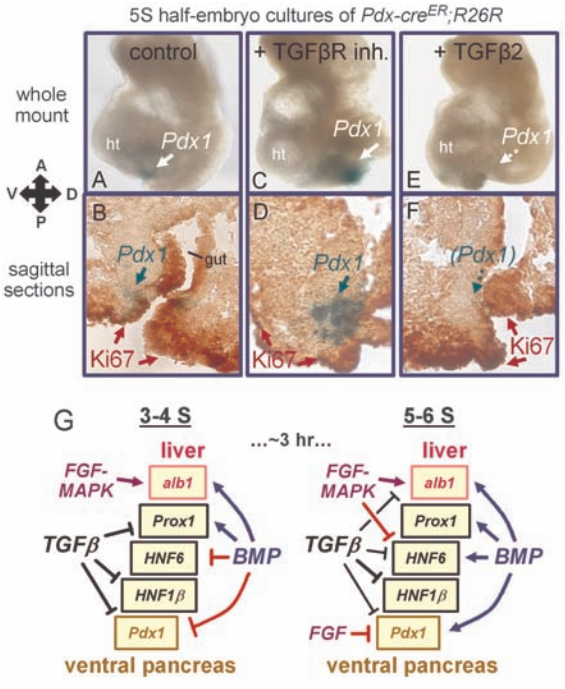

3, A, B, G, and H), consistent with our observation that pSMAD1,5,8 was not observed in the dorsal endoderm (Fig. 1, G to I). Another study used $Pdx1^{CRE}$, which is activated after 7-8S, to delete a conditional *Smad4* allele, and no phenotype was seen during dorsal or ventral pancreatic development (*30*). Taken together, it appears that BMP-SMAD4 signaling is crucial solely for a several-hour period of ventral pancreatic development, from the 5-6S stage to the 7-8S stage, when *Pdx1* becomes activated.

To assess the role of activated pSMAD2,3 (TGFβ signaling) throughout the foregut endoderm (Fig. 1, J to L), we treated half embryos at 3-4S and 5-6S stages with SB431542, an inhibitor of the activin receptor–like kinases (ALK) 4,5,7, and also treated half embryos with exogenous TGFβ2. TGFβ signaling was strongly inhibitory to pancreatic *Pdx1* and *Hnf1b* and modestly inhibitory to the hepatic *alb1* and *Hnf6* at 5-6S (Fig. 2, F to J). Because *Hnf1b* was strongly induced in the *Smad4* null embryos and was not affected by the other signaling pathways, it appears that *Hnf1b* suppression could be a primary effect of TGFβ signaling.

The extensive inhibitory effect of TGFβ signaling suggested that it could be restraining cell type specification in the foregut. To test this, we marked nascent pancreatic progenitor cells by pulsing pregnant females from a $Pdx1^{cre\text{-}ER}$ × *Rosa26R* cross (*31*) with tamoxifen at E7.5, isolating $Pdx1^{cre\text{-}ER}$;*Rosa26R* embryos at E8.25 and setting up 5-6S half-embryo cultures with or without the ALK4,5,7 inhibitor or exogenous TGFβ2. The ALK4,5,7 inhibitor greatly increased the number of $Pdx1^{CRE}$-positive cells along the gut endoderm, and excess TGFβ2 virtually prevented their appearance (Fig. 4, A, C, and E). To determine whether the ALK4,5,7 inhibitor markedly changed the proliferative rate of the $Pdx1^{CRE}$-positive cells, we sectioned the embryo halves sagittally and stained for Ki-67. Extensive Ki-67–positive cells were seen within the gut endoderm, but in both the treated and untreated tissues, $Pdx1^{CRE}$;*Rosa26R*–positive cells exhibited little or no staining (Fig. 4, B, D, and F). Furthermore, the ALK4,5,7 inhibitor did not induce apoptosis (fig. S4). Taken together, the data indicate that continuous TGFβ signaling within the foregut endoderm restrains the number of ventral pancreas cells that are specified.

During foregut closure, the movement of undifferentiated ventral endoderm cells ventrally and caudally, away from pancreas-inhibitory FGF signaling from the cardiac mesoderm, is necessary for pancreatic specification (*32*). We speculate that TGFβ signaling restrains lateral endoderm specification until the cells move sufficiently far from the heart and into a BMP signaling domain, with the latter then becoming the dominant SMAD4-dependent pathway leading to pancreatic induction.

Our findings underscore the importance of a detailed understanding of the signaling events for cell type specification. In particular, it would be crucial to modulate the timing of BMP and TGFβ signaling to optimize for pancreatic progenitors from stem cells. Our work also suggests possible flexibility in hepatic programming, in that the prospective lateral hepatic progenitors receive FGF signaling before that for BMP, whereas the prospective medial hepatic progenitors receive BMP signaling before that for FGF. Regardless of this marked difference, descendants of both progenitor cell types activate *Afp* and *Hnf4* in the nascent liver bud (*23*).

Finally, we find that the signals that induce the earliest hepatic and pancreatic genes operate in parallel, independently tracking to different gene targets that together are crucial for cell specification (Fig. 4G). The parallel model helps explain incomplete cell programming in stem cell studies, in that, if a key signal is not provided or not provided at the appropriate time, various markers of correct differentiation could still be induced, but not all of them. A careful investigation of the inductive networks at each step of hepatocyte or beta cell differentiation should allow prospective cell derivation that is useful for research and therapies.

References and Notes

1. V. Gouon-Evans *et al.*, *Nat. Biotechnol.* **24**, 1402 (2006).
2. E. Kroon *et al.*, *Nat. Biotechnol.* **26**, 443 (2008).
3. K. S. Zaret, M. Grompe, *Science* **322**, 1490 (2008).
4. U. Ahlgren, J. Jonsson, H. Edlund, *Development* **122**, 1409 (1996).
5. G. Deutsch, J. Jung, M. Zheng, J. Lóra, K. S. Zaret, *Development* **128**, 871 (2001).
6. R. Gualdi *et al.*, *Genes Dev.* **10**, 1670 (1996).
7. M. F. Offield *et al.*, *Development* **122**, 983 (1996).
8. Z. Burke, G. Oliver, *Mech. Dev.* **118**, 147 (2002).
9. C. Haumaitre *et al.*, *Proc. Natl. Acad. Sci. U.S.A.* **102**, 1490 (2005).
10. P. Jacquemin, F. P. Lemaigre, G. G. Rousseau, *Dev. Biol.* **258**, 105 (2003).
11. L. Lokmane *et al.*, *Development* **135**, 2777 (2008).
12. B. Sosa-Pineda, J. T. Wigle, G. Oliver, *Nat. Genet.* **25**, 254 (2000).
13. S. K. Kim, M. Hebrok, D. A. Melton, *Development* **124**, 4243 (1997).
14. N. Le Douarin, *J. Embryol. Exp. Morphol.* **12**, 651 (1964).
15. V. A. McLin, S. A. Rankin, A. M. Zorn, *Development* **134**, 2207 (2007).
16. J. M. Wells, D. A. Melton, *Development* **127**, 1563 (2000).
17. A. Calmont *et al.*, *Dev. Cell* **11**, 339 (2006).

18. W. S. Chung, C. H. Shin, D. Y. Stainier, *Dev. Cell* **15**, 738 (2008).
19. J. Jung, M. Zheng, M. Goldfarb, K. S. Zaret, *Science* **284**, 1998 (1999).
20. J. M. Rossi, N. R. Dunn, B. L. Hogan, K. S. Zaret, *Genes Dev.* **15**, 1998 (2001).
21. D. Shin *et al.*, *Development* **134**, 2041 (2007).
22. F. Chen *et al.*, *Development* **134**, 2969 (2007).
23. K. D. Tremblay, K. S. Zaret, *Dev. Biol.* **280**, 87 (2005).
24. Materials and methods are available as supporting material on *Science* Online.
25. Y. Furuta, D. W. Piston, B. L. Hogan, *Development* **124**, 2203 (1997).
26. M. C. Dickson, H. G. Slager, E. Duffie, C. L. Mummery, R. J. Akhurst, *Development* **117**, 625 (1993).
27. C. S. Lee, J. R. Friedman, J. T. Fulmer, K. H. Kaestner, *Nature* **435**, 944 (2005).
28. G. C. Chu, N. R. Dunn, D. C. Anderson, L. Oxburgh, E. J. Robertson, *Development* **131**, 3501 (2004).
29. M. Kumar, N. Jordan, D. Melton, A. Grapin-Botton, *Dev. Biol.* **259**, 109 (2003).
30. N. Bardeesy *et al.*, *Genes Dev.* **20**, 3130 (2006).
31. G. Gu, J. Dubauskaite, D. A. Melton, *Development* **129**, 2447 (2002).
32. R. Bort, J. P. Martinez-Barbera, R. S. Beddington, K. S. Zaret, *Development* **131**, 797 (2004).
33. We thank E. Robertson for *Smad*^{CA} mice; K. Kaestner for *FoxA3*^{cre} mice; A. Hines for help with breeding; the Fox Chase Cancer Center (FCCC) Laboratory Animal Facility; F. Roegiers, E. Robertson, H. Fan, R. Lake, and D. Freedman-Cass for comments on the manuscript; and E. Pytko for help in its preparation. E.W. was a Postdoctoral Fellow of the Swedish Research Council. The work was funded by NIH grants R37GM36477 and U01DK072503 to K.S.Z. K.S.Z. is on a Scientific Advisory Board for Johnson & Johnson in the area of embryonic stem cells.

Supporting Online Material

www.sciencemag.org/cgi/content/full/324/5935/1707/DC1
Materials and Methods
Figs. S1 to S4
Table S1
References

3 April 2009; accepted 20 May 2009
10.1126/science.1174497

MicroRNA-92a Controls Angiogenesis and Functional Recovery of Ischemic Tissues in Mice

Angelika Bonauer,[1] Guillaume Carmona,[1] Masayoshi Iwasaki,[1] Marina Mione,[2] Masamichi Koyanagi,[1] Ariane Fischer,[1] Jana Burchfield,[1] Henrik Fox,[1,3] Carmen Doebele,[1] Kisho Ohtani,[1] Emmanouil Chavakis,[1,3] Michael Potente,[1,3] Marc Tjwa,[4] Carmen Urbich,[1] Andreas M. Zeiher,[3] Stefanie Dimmeler[1]*

MicroRNAs (miRs) are small noncoding RNAs that regulate gene expression by binding to target messenger RNAs (mRNAs), leading to translational repression or degradation. Here, we show that the miR-17~92 cluster is highly expressed in human endothelial cells and that miR-92a, a component of this cluster, controls the growth of new blood vessels (angiogenesis). Forced overexpression of miR-92a in endothelial cells blocked angiogenesis in vitro and in vivo. In mouse models of limb ischemia and myocardial infarction, systemic administration of an antagomir designed to inhibit miR-92a led to enhanced blood vessel growth and functional recovery of damaged tissue. MiR-92a appears to target mRNAs corresponding to several proangiogenic proteins, including the integrin subunit alpha5. Thus, miR-92a may serve as a valuable therapeutic target in the setting of ischemic disease.

MicroRNAs (miRs) are small noncoding RNAs that regulate a wide range of physiological and pathophysiological processes (*1*–*4*). The conserved miR-17~92 cluster, consisting of miR-17, miR-18a, miR-19a, miR-20a, miR-19b-1, and miR-92a (*3*), shows up-regulated expression in tumors (*5*–*7*), and its overexpression in tumor cells promotes tumor angiogenesis (*8*). The proangiogenic functions of the miRs encoded by the cluster have been attributed to miR-18a and miR-19a, which promote tumor angiogenesis by suppressing the release of soluble anti-angiogenic factors by tumor cells, thereby affecting endothelial cells (ECs) in a paracrine manner (*8*). Inhibition of miR processing by genetic knockdown of Dicer expression impairs EC functions and angiogenesis (*9*–*12*), and several miRs stimulate [let-7f (*11*), miR-27b (*11*), and miR-130 (*13*)] or inhibit [miR-221 and miR-222 (*14*)] angiogenesis in vitro or regulate vascular development [miR-126 (*15*, *16*)]. However, the postnatal function of individual endothelial miRs in vivo under pathophysiological conditions remains unclear (*17*).

Our microRNA expression profiling study revealed that human ECs express the miR-17~92 cluster, and particularly its member miR-92a (fig. S1), whose specific role in angiogenesis is unknown. In contrast to the proangiogenic effects of miR-18a and miR-19a in tumor angiogenesis (*8*), we found that forced overexpression of miR-92a in human ECs using a precursor molecule (termed pre92) [fig. S2A (*18*)] blocked sprout formation in a three-dimensional model of angiogenesis (Fig. 1, A and C), inhibited vascular network formation in matrigel assays (Fig. 1, B and C), reduced EC migration (fig. S2B), and impaired EC adhesion to fibronectin (Fig. 1D). Overexpression of miR-92a did not affect EC proliferation or viability (fig. S3). When human umbilical vein endothelial cells (HUVECs) were implanted in a matrigel plug in nude mice in vivo, pre92 reduced the number of invading cells and formation of in vivo perfused lectin-positive vessels (Fig. 1, E and F, and fig. S4A). In addition, the hemoglobin content (a surrogate marker of perfusion) was significantly lowered in the explanted matrigel plugs (fig. S4B). Likewise, overexpression of miR-92a induced severe defects in intersegmental vessel formation in zebrafish (fig. S5). These results indicate that overexpression of miR-92a blocks angiogenesis and vessel formation in vitro and in vivo.

We next investigated whether inhibition of miR-92a can enhance vessel growth. Indeed, inhibition of endothelial miR-92a in human ECs by 2′O-methyl antisense oligoribonucleotides increased sprout formation in vitro (fig. S6), leading us to test in vivo models. To inhibit miR-92a in vivo, we designed single-stranded RNA oligonucleotides complementary to specific miRs, also known as antagomirs, that are chemically modified for improved stability and cell delivery (*19*). Consistent with the hypothesis that inhibition of miR-92a augments angiogenesis, systemic application of antagomirs, specifically targeting miR-92a (antagomir-92a), enhanced the number of invading cells and in vivo perfused lectin-positive vessels in implanted matrigel plugs in mice (Fig. 2A and figs. S7 and S8). To control for off-target effects of single-stranded RNA oligonucleotides and to confirm the specificity of antagomir-92a, we used two different control antagomirs, neither of which affected plug vascularization (fig. S7).

To further characterize the in vivo role of miR-92a in angiogenesis, we used a mouse hindlimb ischemia model to study whether the expression level of miR-92a in skeletal muscle changes in response to ischemic injury. Ischemic injury significantly increased miR-92a expression, with a maximal effect seen within 1 to 3 days after injury (Fig. 2B). We next tested whether antagomir-92a can promote neovascularization in ischemic limbs. Mice systemically injected with antagomir-92a exhibited a significant reduction in toe necrosis in comparison with mice treated with a control antagomir or phosphate-buffered saline (PBS) (fig. S9). Recovery of blood flow was increased in the antagomir-92a–treated mice, consistent with the hypothesis that the reduced necrosis was due to improved neovascularization in the ischemic limb (Fig. 2C). Likewise, the number of capillaries and smooth muscle actin-positive arterioles was increased after antagomir-92a treatment (fig. S10), indicating that antagomir-92a improves perfusion and the functional recovery of ischemic limbs. To

[1]Institute for Cardiovascular Regeneration, Centre of Molecular Medicine, Goethe-University Frankfurt, 60590 Frankfurt, Germany. [2]Italian Foundation for Cancer Research Institute of Molecular Oncology Foundation, 02139 Milan, Italy. [3]Division of Cardiology, Department of Medicine III, Goethe-University Frankfurt, 60590 Frankfurt, Germany. [4]Leibniz AG, Institute for Cardiovascular Regeneration, Goethe-University Frankfurt, 60590 Frankfurt, Germany.

*To whom correspondence should be addressed. E-mail: dimmeler@em.uni-frankfurt.de

test the specificity of antagomir-92a, we studied its effect on the expression of miR-92a, the closely related miR-92b, and members of the miR-17~92 cluster, namely miR-18a and miR-19a, and the unrelated miR-93. Whereas a single intravenous injection of antagomir-92a in mice significantly suppressed miR-92a expression in nonischemic and ischemic limbs, this treatment only slightly and nonsignificantly reduced the expression of miR-92b and had no effect on the expression of the other miRs studied (Fig. 2D).

miR-92a also was up-regulated after induction of acute myocardial infarction (fig. S11). Therefore, we investigated the effect of antagomir-92a treatment on recovery of heart function in a mouse model of acute myocardial infarction. We intravenously injected antagomir-92a or a control antagomir at days 0, 2, 4, 7, and 9 after occlusion of the left coronary artery, and then determined left ventricular (LV) function by Millar catheterization at day 14. Compared with controls, antagomir-92a treatment improved LV systolic and diastolic function, as evidenced by increases of maximum and minimum rate of rise of left ventricular pressure (dp/dt_{max} and dp/dt_{min}), and significantly reduced end-diastolic pressure and tau (Fig. 3, A and B, fig. S12, and table S1). Furthermore, antagomir-

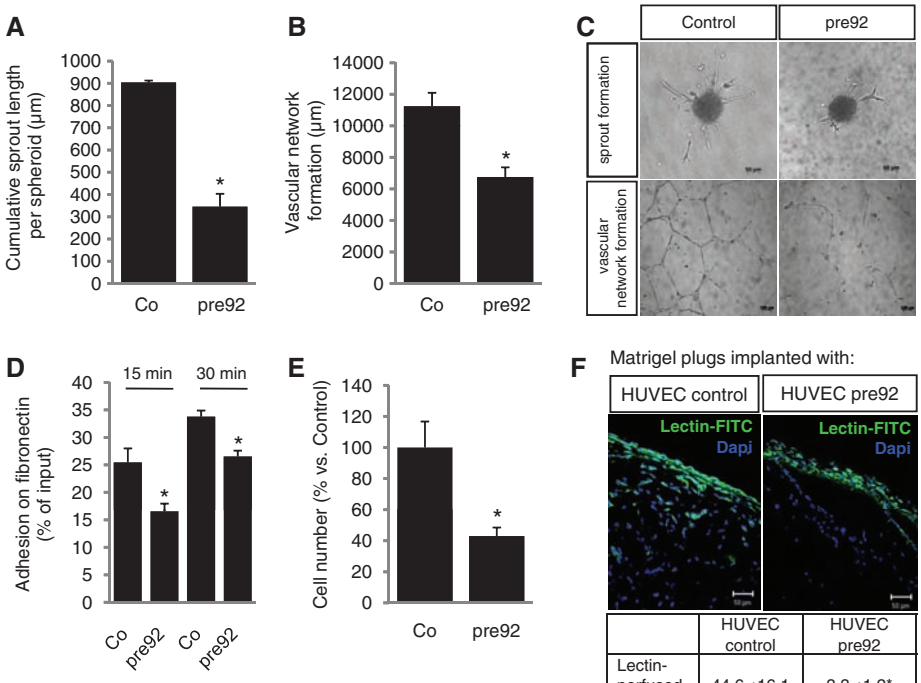

	HUVEC control	HUVEC pre92
Lectin-perfused vessels	44.6 ±16.1	3.3 ±1.2*

Fig. 1. Effect of overexpression of miR-92a on angiogenesis in human ECs. (**A**) Inhibition of sprout formation in spheroids (n = 10 spheroids per experiment, n = 3 experiments) and (**B**) matrigel assays in vitro (n = 3 experiments). Representative micrographs are shown in (**C**). (**D**) Effect of miR-92a overexpression on adhesion of ECs to fibronectin (n = 4 experiments). (**E** and **F**) HUVECs were transfected with pre92 or control pre-miR and 1 × 10^6 cells were implanted in matrigel plugs in vivo. (E) After 6 days, invading cells were detected in hematoxylin and eosin sections (n = 5 to 6 plugs). (F) Vessels were identified and counted after intravenous infusion of fluorescein isothiocyanate (FITC)–conjugated lectin (n = 8 high-power fields). Due to the implantation of HUVECs, baseline vascularization is higher compared with Fig. 2A. Data are mean ± SEM. *P < 0.05 versus control (Student's t test).

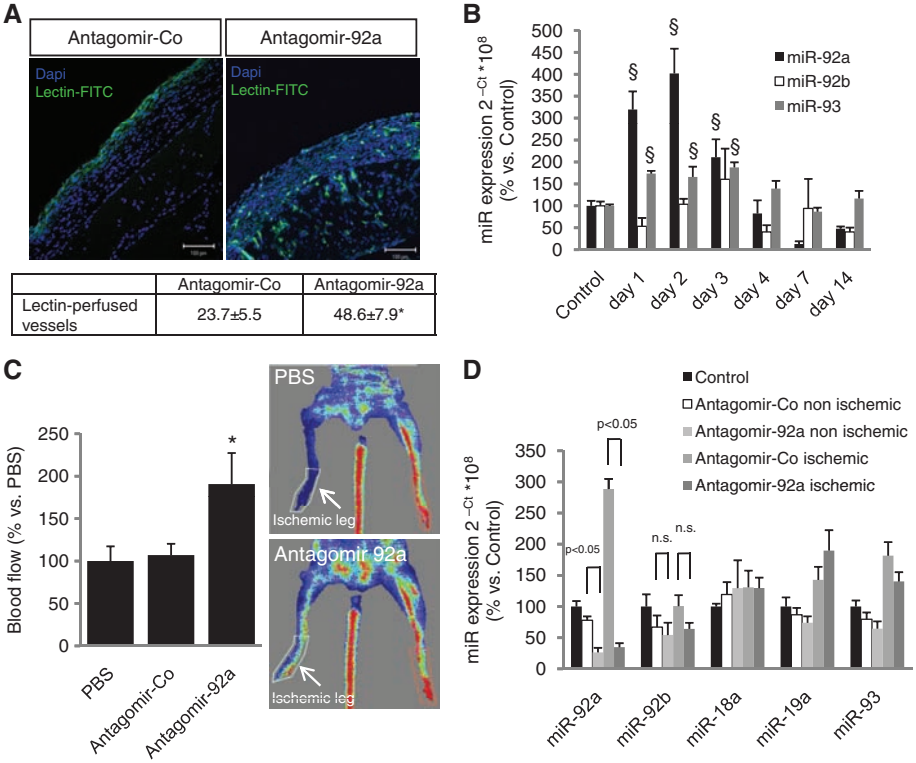

	Antagomir-Co	Antagomir-92a
Lectin-perfused vessels	23.7±5.5	48.6±7.9*

Fig. 2. Inhibition of miR-92a enhances angiogenesis and neovascularization in mice. (**A**) Effect of systemic infusion of antagomirs targeting miR-92a [8 mg per kg of body weight (mg/kg bw), n = 6 plugs] or control antagomirs (antagomir-Co, n = 5 plugs) at days 1, 3, and 5 in each mouse on the number of lectin-perfused vessels in matrigel plugs in vivo. *P < 0.05 versus antagomir-Co (t test). (**B**) Expression of miR-92a, miR-92b, and miR-93 was detected in ischemic muscle tissue compared with nonischemic control muscle at various days after ischemia. n = 3 mice each, §P < 0.05 versus control [analysis of variance (ANOVA)]. (**C**) miR-92a was inhibited by injecting antagomir-92a (8 mg/kg bw, injected at days 0, 2, 4, 7, and 9) after induction of hind-limb ischemia. At day 14, laser Doppler–derived blood flow was determined (n = 4 to 8 mice per group). *P < 0.05 versus PBS (t test). Representative images are shown in the right panel. (**D**) Antagomir-92a (8 mg/kg bw, injected intravenously once, directly after induction of ischemia) specifically reduced miR-92a expression in ischemic and nonischemic muscle tissue at 2 days after induction of hind-limb ischemia. Expression of miRs was determined by real-time polymerase chain reaction as indicated in antagomir-92a or control antagomir-treated mice and was compared with nontreated controls. n = 4 mice. Data are mean ± SEM (ANOVA).

92a treatment reduced the infarct size by 39 ± 15.5% ($P = 0.05$) (fig. S13), suppressed the number of apoptotic cells (fig. S14), and significantly augmented the number of in vivo perfused lectin-positive vessels, particularly in the infarct border zone (Fig. 3C and fig. S15). Antagomir-92a treatment also increased the number of smooth muscle actin-positive vessels (fig. S15). Control experiments for specificity confirmed that antagomir-92a suppressed the expression of miR-92a but did not affect expression of another miR (miR-24) in the heart (Fig. 3D). By using Cy3-labeled antagomir-92a to visualize biodistribution, we found that antagomir-92a was taken up by vascular cells, but also by other cells of the limb and heart (figs. S16 and S17). Consistently, antagomir-92a treatment inhibited miR-92a expression in the endothelium and in other cells of the heart, such as cardiac myocytes (figs. S18 to S20).

We next analyzed putative miR-92a targets predicted by defined criteria (*20*) using the TargetScan and miRanda software. The in silico predicted targets included mRNAs encoding several regulators of endothelial cell functions and vessel growth, such as the integrin subunits α5 and αv, which mediate cell-matrix interactions and cell migration (*21*–*23*). Additional predicted proangiogenic targets included the mRNAs encoding the histone deacetylase SIRT1 (*24*, *25*), the small guanosine triphosphate–binding protein Rap-1, an angiogenesis-mediating protein involved in integrin signaling (*26*), the sphingosine-1-phosphate receptor 1 ($S1P_1$) (*27*), and the mitogen-activated kinase kinase 4 (MKK4). Using an Affymetrix mRNA gene expression array, we confirmed that expression of the mRNAs for integrin subunits α5 (ITGA5) and αv, $S1P_1$, and MKK4 was reduced in response to miR-92a overexpression, whereas Rap-1 mRNA expression was unaffected in human ECs (Fig. 4A). Interestingly, the mRNA expression profile also revealed a down-regulation of endothelial NO-synthase (eNOS), which controls vascular tone and is essential for postnatal neovascularization (*28*, *29*). We confirmed that ITGA5 and eNOS protein levels were significantly reduced in HUVECs overexpressing miR-92a (Fig. 4B and fig. S21, A and B). Conversely, inhibiting miR-92a by antagomir-92a treatment in mice increased the expression of ITGA5 mRNA and protein in the vasculature of skeletal muscle tissue (figs. S21C and S22).

Given the pivotal role of ITGA5 in vascular development and angiogenesis (*21*, *22*) (fig. S23A) and its regulation by inhibition or overexpression of miR-92a, we investigated whether ITGA5 is a direct target of miR-92a. The 3′ untranslated region (3′UTR) of the ITGA5 mRNA contains one conserved predicted binding site for miR-92a (Fig. 4C). We therefore cloned a fragment of the ITGA5 3′UTR sequence downstream of a luciferase construct and examined luciferase activity after cotransfection with miR-92a in human embryonic kidney (HEK) cells. Indeed, miR-92a overexpression reduced luciferase activity (Fig. 4C), which strongly suggests that ITGA5 mRNA

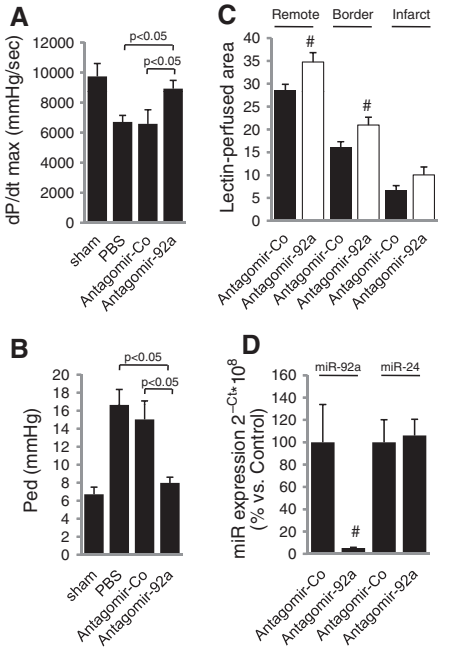

Fig. 3. Inhibition of miR-92a enhances recovery after acute myocardial infarction in mice. (**A** and **B**) 8 mg/kg bw antagomir-92a ($n = 8$ mice), control antagomirs ($n = 6$ mice), or PBS ($n = 7$ mice) were injected at days 0, 2, 4, 7, and 9 after induction of myocardial infarction. On day 14, cardiac catheterization was performed for functional analysis (dp/dt_{max} and end-diastolic pressure) compared with sham controls ($n = 5$ mice) (Mann-Whitney *U* test). (**C**) Capillary density was determined after intravenous infusion of FITC-conjugated lectin and was quantified in the remote, border, and infarct regions of the hearts by automatic quantification of lectin-positive pixels per total pixels ($\times 10^4$). Quantification of $n = 6$ high-power fields per region per group. #$P < 0.05$ versus antagomir-Co (*t* test). (**D**) miR-92a expression in hearts 6 days after antagomir-92a treatment ($n = 8$ mice) compared with control antagomirs ($n = 3$ mice). miR-24 expression was detected as control. Data are mean ± SEM. #$P < 0.05$ versus control antagomirs (Mann-Whitney *U* test).

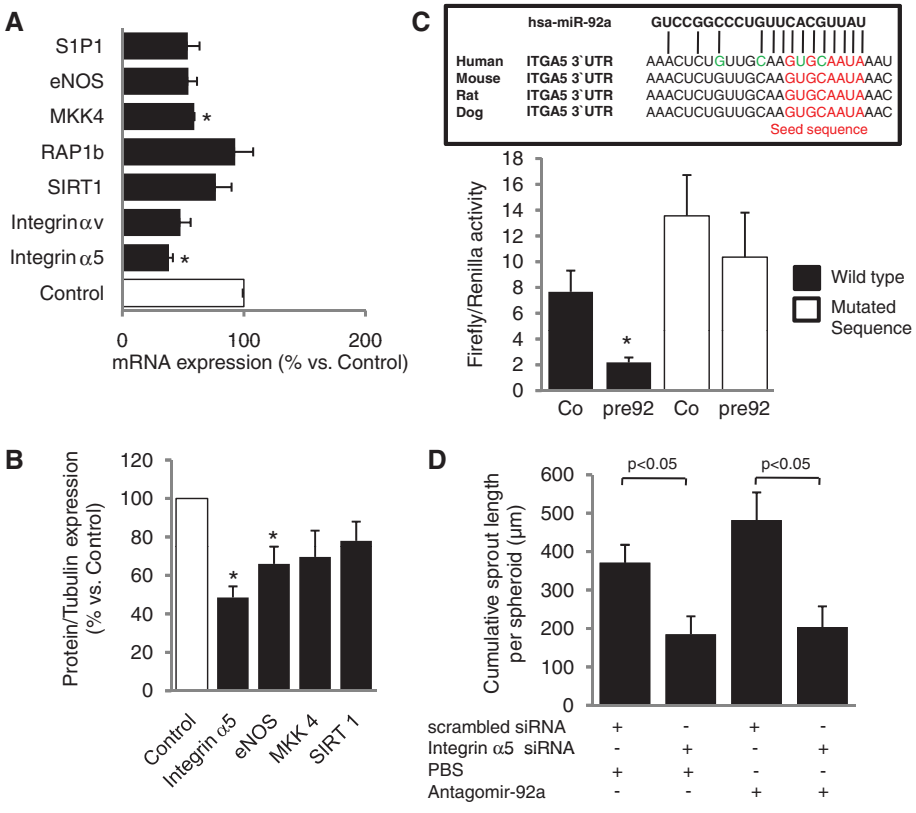

Fig. 4. Identification of miR-92a targets. (**A** and **B**) Expression analysis of genes regulated in pre-miR-92 overexpressing human ECs. (A) Results of Affymetrix mRNA expression profiles at 48 hours after pre92 transfection compared with controls ($n = 4$ to 5 experiments) (see also table S2). (B) Protein expression in human EC determined by Western blotting using antibodies against ITGA5, eNOS, MKK4, and SIRT1 ($n = 3$ to 4 experiments). ITGA5 down-regulation was confirmed by fluorescence-activated cell sorting (fig. S21). (**C**) (Top) Schematic illustration of miR-92a seed sequence in the integrin α5 3′UTR. Green indicates the mutated nucleotides. (Bottom) Luciferase normalized to Renilla activity measured in homogenates of HEK cells transfected with the wild-type or mutated luciferase constructs and pre-miR-92a or scrambled controls. Mutation of the target sequence resulted in a higher basal expression, indicating stabilization possibly by protecting against endogenous miR-92a. $n = 5$ to 6 experiments. (**D**) Effect of ITGA5 siRNA and antagomir-92a on spheroid sprout formation of HUVECs compared with scrambled siRNA, $n = 4$ experiments. The efficiency of ITGA5 siRNA is illustrated in fig. S25. Data are mean ± SEM. *$P < 0.01$ in (A), and $P < 0.05$ versus controls in all other panels (Student's *t* test).

is a direct target of miR-92a. Mutation of the target sequence prevented down-regulation of luciferase activity by pre-miR-92a (Fig. 4C). To determine whether the reduced expression of ITGA5 by miR-92a contributes to the inhibition of sprout formation and neovascularization, we inhibited ITGA5 expression by small interfering RNA (siRNA) in human ECs or used ITGA5$^{+/-}$ mice and found that antagomir-92a induced sprouting and that rescue of necrosis was reduced when ITGA5 was down-regulated, respectively (Fig. 4D and fig. S23B). Conversely, overexpression of ITGA5 partially rescued the miR-92a–mediated suppression of sprout formation in human ECs (fig. S24).

To explore whether the effect of miR-92a on mRNA expression levels can be mimicked by silencing ITGA5 expression, we compared the gene expression patterns in HUVECs overexpressing miR-92a versus HUVECs depleted of ITGA5. As predicted, several putative direct miR-92a targets such as MKK4 or $S1P_1$ were not affected by ITGA5 siRNA (table S2, yellow box). However, the expression levels of a second group of genes, which were down-regulated by miR-92a despite the lack of target sequences in their 3′UTR, were also reduced by siRNA against ITGA5 (table S2, red box). Hence, these genes might be secondarily regulated as a consequence of ITGA5 down-regulation. The most prominent example was the regulation of eNOS expression, which was down-regulated by miR-92a and ITGA5 siRNA, indicating that eNOS down-regulation in response to miR-92a overexpression may occur secondarily as a consequence of ITGA5 mRNA degradation.

We have identified miR-92a as an endogenous repressor of the angiogenic program in ECs, and we have shown in two mouse models that a reagent designed to inhibit the actions of this microRNA enhances the functional recovery of ischemic tissue. The mRNA encoding integrin subunit alpha5 is one of several candidate targets of miR-92a. The relevance of this potential target is evidenced by the severe vascular defects seen in mice genetically deficient in this integrin subunit (*21*). Although our studies have focused on ECs, we cannot formally exclude the possibility that miR-92a has effects on other cell types in the cardiovascular system. Indeed, apoptosis in the heart was reduced by antagomir-92a treatment. However, antagomir-92a did not affect apoptosis of cardiomyocytes in vitro (fig. S14B), suggesting that the antiapoptotic activity of antagomir-92a in vivo is mediated by an indirect mechanism. The capacity of miR-92a to target various downstream effectors might offer a therapeutic advantage to interfere with the complex modulation of vessel growth, maturation, and functional maintenance in ischemic diseases.

References and Notes

1. Y. Zhao *et al.*, *Cell* **129**, 303 (2007).
2. E. van Rooij, E. N. Olson, *J. Clin. Invest.* **117**, 2369 (2007).
3. A. Ventura *et al.*, *Cell* **132**, 875 (2008).
4. D. P. Bartel, *Cell* **116**, 281 (2004).
5. A. Ota *et al.*, *Cancer Res.* **64**, 3087 (2004).
6. L. He *et al.*, *Nature* **435**, 828 (2005).
7. L. Venturini *et al.*, *Blood* **109**, 4399 (2007).
8. M. Dews *et al.*, *Nat. Genet.* **38**, 1060 (2006).
9. A. J. Giraldez *et al.*, *Science* **308**, 833 (2005).
10. W. J. Yang *et al.*, *J. Biol. Chem.* **280**, 9330 (2005).
11. A. Kuehbacher, C. Urbich, A. M. Zeiher, S. Dimmeler, *Circ. Res.* **101**, 59 (2007).
12. Y. Suarez, C. Fernandez-Hernando, J. S. Pober, W. C. Sessa, *Circ. Res.* **100**, 1164 (2007).
13. Y. Chen, D. H. Gorski, *Blood* **111**, 1217 (2008).
14. L. Poliseno *et al.*, *Blood* **108**, 3068 (2006).
15. S. Wang *et al.*, *Dev. Cell* **15**, 261 (2008).
16. J. E. Fish *et al.*, *Dev. Cell* **15**, 272 (2008).
17. A. Kuehbacher, C. Urbich, S. Dimmeler, *Trends Pharmacol. Sci.* **29**, 12 (2008).
18. Materials and methods are available as supporting material on *Science* Online.
19. J. Krutzfeldt *et al.*, *Nature* **438**, 685 (2005).
20. A. Grimson *et al.*, *Mol. Cell* **27**, 91 (2007).
21. J. T. Yang, H. Rayburn, R. O. Hynes, *Development* **119**, 1093 (1993).
22. S. E. Francis *et al.*, *Arterioscler. Thromb. Vasc. Biol.* **22**, 927 (2002).
23. C. Urbich *et al.*, *Arterioscler. Thromb. Vasc. Biol.* **22**, 69 (2002).
24. M. Potente *et al.*, *Genes Dev.* **21**, 2644 (2007).
25. S. Imai, C. M. Armstrong, M. Kaeberlein, L. Guarente, *Nature* **403**, 795 (2000).
26. M. Chrzanowska-Wodnicka, A. E. Kraus, D. Gale, G. C. White 2nd, J. Vansluys, *Blood* **111**, 2647 (2008).
27. J. H. Paik, S. Chae, M. J. Lee, S. Thangada, T. Hla, *J. Biol. Chem.* **276**, 11830 (2001).
28. R. M. Palmer, A. G. Ferrige, S. Moncada, *Nature* **327**, 524 (1987).
29. T. Murohara *et al.*, *J. Clin. Invest.* **101**, 2567 (1998).

30. We thank M. Muhly-Reinholz, T. Röxe, N. Reinfeld, and F. Pezzimenti for expert technical assistance and W.-K. Hofmann for performing the mRNA array. This work is supported by the Deutsche Forschungsgemeinschaft (Di 600/6-3, Exc 147/1), the Alfried Krupp Foundation (A.B.), the Landes-Offensive zur Entwicklung Wissenschaftlich- ökonomischer Exzellenz (LOEWE) (C.D.), the European Research Council (Angiomir), and the Leducq Foundation (J.B. and M.K.). A.B., C.U., A.M.Z., and S.D. have applied for a patent relating to this work.

Supporting Online Material

www.sciencemag.org/cgi/content/full/1174381/DC1
Materials and Methods
Figs. S1 to S25
Tables S1 and S2
References

13 October 2008; accepted 13 May 2009
Published online 21 May 2009;
10.1126/science.1174381
Include this information when citing this paper.

Mitochondrial STAT3 Supports Ras-Dependent Oncogenic Transformation

Daniel J. Gough,[1]* Alicia Corlett,[1]*† Karni Schlessinger,[1]‡ Joanna Wegrzyn,[2] Andrew C. Larner,[2] David E. Levy[1]§

Signal transducer and activator of transcription 3 (STAT3) is a latent cytoplasmic transcription factor responsive to cytokine signaling and tyrosine kinase oncoproteins by nuclear translocation when it is tyrosine-phosphorylated. We report that malignant transformation by activated Ras is impaired without STAT3, in spite of the inability of Ras to drive STAT3 tyrosine phosphorylation or nuclear translocation. Moreover, STAT3 mutants that cannot be tyrosine-phosphorylated, that are retained in the cytoplasm, or that cannot bind DNA nonetheless supported Ras-mediated transformation. Unexpectedly, STAT3 was detected within mitochondria, and exclusive targeting of STAT3 to mitochondria without nuclear accumulation facilitated Ras transformation. Mitochondrial STAT3 sustained altered glycolytic and oxidative phosphorylation activities characteristic of cancer cells. Thus, in addition to its nuclear transcriptional role, STAT3 regulates a metabolic function in mitochondria, supporting Ras-dependent malignant transformation.

Signal transducers and activators of transcription (STATs) mediate cellular differentiation, proliferation, survival, and immune function (*1*). Tyrosine-phosphorylated STATs undergo phosphotyrosine–Src homology 2 (SH2) domain interactions, leading to nuclear translocation and expression of target genes (*2*). STAT3 mediates acute phase responses to cytokines such as interleukin-6 (*3*–*6*) and has been linked to cancer development (*7*). Deregulated tyrosine kinase oncoproteins can target constitutive STAT3 phosphorylation (*8*), resulting in gene expression associated with tumor cell survival and proliferation. Augmented STAT3 activity is associated with multiple human tumors, and STAT3 inhibition can mediate tumor regression (*9*). However, additional STAT3 functions that are inconsistent with functioning solely as a transcription factor have been described (*10*).

Ablation of STAT3 impairs malignant transformation by protein tyrosine kinase oncoproteins, such as anaplastic lymphoma kinase (ALK) and v-Src (*11*, *12*). To determine whether oncogenes that lack tyrosine kinase activity also require STAT3, we examined cellular transformation by activated Ras (H-RasV12, where V12 indicates valine-12) (*13*). Although previous evidence suggested that Ras

[1]Department of Pathology and New York University Cancer Institute, New York University School of Medicine, 550 First Avenue, New York, NY 10016, USA. [2]Department of Biochemistry and Massey Cancer Center, Virginia Commonwealth University, Richmond, VA 23298, USA.

*These authors contributed equally to this work.
†Present address: Institute of Molecular Genetics, Academy of Sciences of the Czech Republic, Vídeňská 1083, Prague 4, Czech Republic 14220.
‡Present address: Memorial Sloan-Kettering Cancer Center, 1275 York Avenue, New York, NY 10065, USA.
§To whom correspondence should be addressed. E-mail: david.levy@med.nyu.edu

transformation was independent of STAT3 (*7*, *8*), we found that the ability of H-Ras to cause cell growth in soft agar, like that of v-src, was impaired without STAT3 (Fig. 1A). Similarly, growth of Ras-transformed tumors in mice was abrogated without STAT3 (Fig. 1B). Reconstitution of STAT3-null cells with mutated STAT3 lacking its tyrosine phosphorylation site [Tyr^{705} → Phe^{705} (Y705F)] restored growth of H-RasV12–expressing tumors (Fig. 1B) (*14*). Lack of a STAT3 tyrosine phosphorylation requirement for tumor formation by H-RasV12 is distinct from the phosphorylation requirement for v-Src transformation (*11*), but is consistent with absence of detectable tyrosine-phosphorylated STAT3 in Ras-transformed cells (fig. S1A).

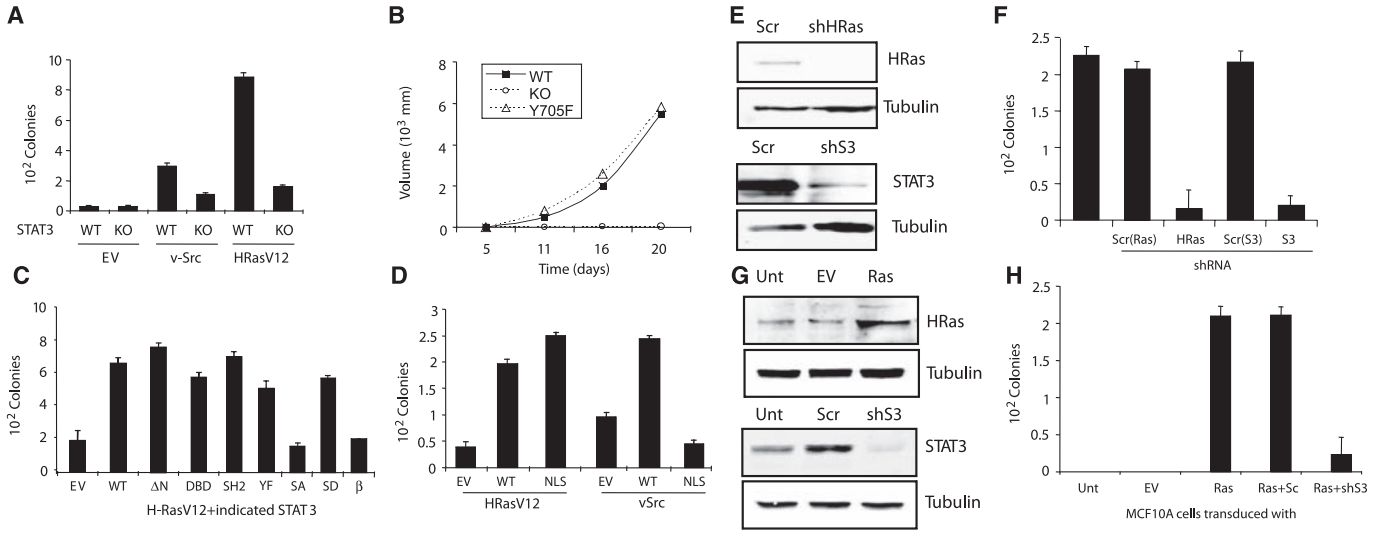

Fig. 1. STAT3 is essential for Ras transformation but not as a transcription factor. (**A**) Colony formation of WT or STAT3-deficient (KO) cells with or without v-Src or H-RasV12 plated in soft agar. EV, empty vector. (**B**) Average tumor volume formed by H-RasV12–expressing STAT3-null cells transduced with EV (KO), WT, or Y705F-mutant STAT3 (Y705F) and injected into Balb/$c^{nu/nu}$ mice (5 mice per group). (**C**) Average colony formation of H-RasV12–expressing STAT3-deficient cells stably transduced with EV, WT STAT3, or STAT3 mutants. ΔN, N-terminal 132–amino acid deletion; DBD, DNA binding domain VVV461-463AAA; SH2, SH2 domain R609K; YF, tyrosine phosphorylation site Y705F; SA, serine phosphorylation site S727A; SD, serine phosphorylation site S727D; and β, the STAT3β isoform. (**D**) Average colony formation of H-RasV12– or v-Src–expressing cells transduced with EV, WT STAT3, or STAT3 with a mutated nuclear localization signal (NLS). (**E**) Depletion of H-Ras or STAT3 protein by shRNA in T24 human bladder carcinoma cells compared with scrambled shRNA control (Scr). (**F**) Average colony formation of T24 cells depleted for STAT3 or H-Ras. (**G**) Expression of H-Ras and STAT3 in human breast epithelial MCF10A cells transduced with EV or H-RasV12 (Ras) and transfected with shRNA to STAT3 (shS3) or Scr. (**H**) Average colony formation of MCF10A cells with and without H-RasV12 and STAT3. Error bars indicate SD.

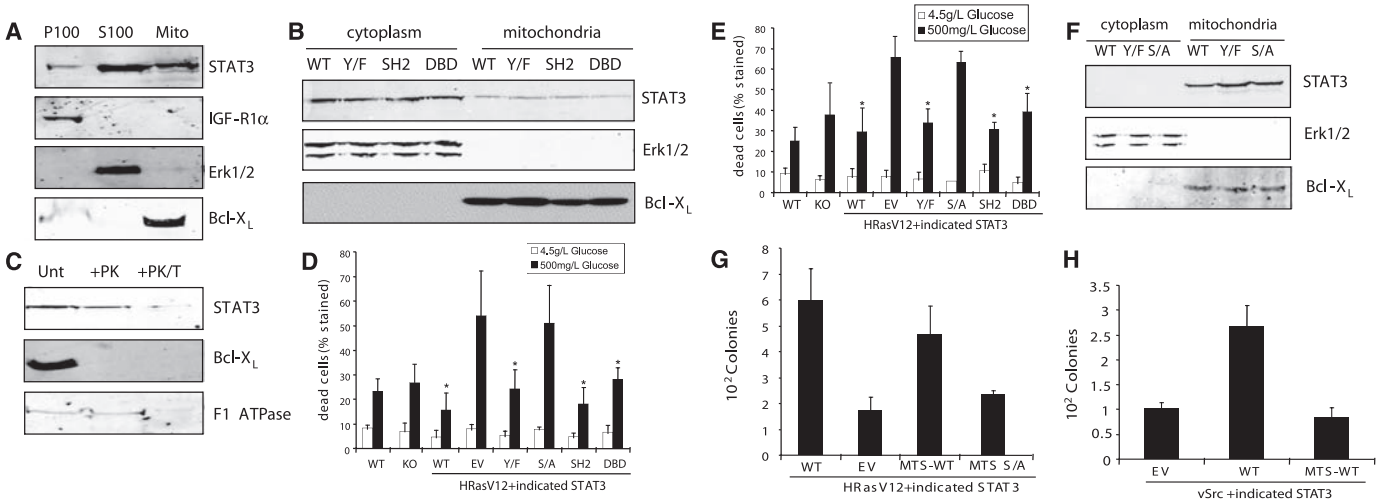

Fig. 2. Localization of STAT3 to mitochondria supports Ras transformation. (**A**) Fractionation of cells mechanically disrupted in the absence of detergent and separated into P100 (plasma membrane), S100 (organelle-free cytosol), and mitochondrial fractions. Samples probed for STAT3, IGF1-R1α, or Bcl-X_L, as indicated. (**B**) Distribution of STAT3 mutants expressed in H-RasV12–transduced cells. Erk1/2 and Bcl-X_L expression verified fraction purity. (**C**) Protease-sensitivity of proteins associated with mitochondrial membranes in absence (Unt) or presence (+PK) of proteinase K or of proteinase K and Triton X-100 (+PK/T). (**D**) Survival of H-RasV12–expressing cells after glucose depletion. Survival of STAT3-null (KO) or WT cells expressing H-RasV12 (WT) or STAT3-null cells expressing H-RasV12 reconstituted with EV or STAT3 mutants after growth in low or high glucose medium, as indicated. Asterisks indicate statistically significant differences ($P < 0.05$ by Student's *t* test) of individual conditions relative to EV. (**E**) Survival of cells exposed to 2% oxygen. (**F**) Mitochondrially targeted WT and mutant STAT3 protein expression. (**G**) Colony formation by H-RasV12–, (**H**) v-Src–, and (**I** and **J**) N– and K-Ras–expressing cell lines. Error bars indicate SD.

To further evaluate STAT3 structural requirements for Ras transformation, we reconstituted STAT3-null cells with STAT3 mutants (Fig. 1C). Versions of STAT3 inert for cytokine-activated transcription or v-Src transformation supported Ras transformation. STAT3 N-terminal, DNA-binding, SH2 domains and tyrosine phoshorylation site were not required. However, mutation of the serine phosphorylation site in the C terminus (S727A) or deletion of the C-terminal domain (STAT3β) abrogated cooperation between STAT3 and Ras. Replacement of S727 with phosphorylation-mimetic aspartate (S727D) restored transformation (Fig. 1C), suggesting that S727 phosphorylation is required.

The C terminus of STAT proteins and phosphorylation of S727 are implicated in transcriptional activity (*15*), but lack of a requirement for STAT3 DNA binding or SH2 domains implied that STAT3-mediated transcription was not necessary for Ras transformation. We tested whether STAT3 nuclear translocation is required to augment Ras transformation. We mutated the two nuclear localization sequences (NLS) in STAT3 (*16*), causing cytoplasmic retention (fig. S2). Cytoplasmic-restricted STAT3 restored transformation by Ras but not v-Src (Fig. 1D) . These data are consistent with dual functions of STAT3 in transformation. The tyrosine kinase oncoprotein v-Src required tyrosine-phosphorylated, transcriptionally competent nuclear STAT3 for transformation, but activated Ras required non-transcriptional, non-nuclear STAT3.

We tested whether STAT3 is required for transformation of human cells. We ablated STAT3 expression by short hairpin RNA (shRNA) knockdown in the T24 cell line derived from a spontaneous H-Ras–transformed human bladder cell carcinoma (*17*). Ablation of STAT3 expression impaired T24 colony formation to the same extent as shRNA ablation of Ras expression (Fig. 1, E and F). Similarly, transformation of the normal human mammary epithelial cell line MCF10A by H-RasV12 depended on expression of STAT3 (Fig. 1, G and H). Neither T24 nor MCF10A cells required STAT3 for proliferation or survival during adherent growth.

Activated Ras signals primarily through stimulation of MAPK, PI3K, and RalGDS pathways (*18*). We interrogated Ras signaling biochemically and by using Ras-effector domain mutants (fig. S1). Ras-mediated activation of RalA was the only effector function showing dependence on STAT3, but activation of this pathway did not explain STAT3 dependence of Ras-mediated transformation (fig. S3). Because STAT3 has been documented in discrete cytoplasmic bodies (*19*), we fractionated cytosol into plasma-membrane, organelle-free cytoplasmic, and organelle fractions and probed for STAT3. STAT3 was detected in all three fractions, with the greatest amounts found in cytosol (S100) but a distinct presence in the organelle fraction, which was mostly mitochondria (Fig. 2A). Mitochondrial STAT3 was also detected in primary liver tissue, non-transformed MCF10A mammary epithelial cells, and T24 bladder carcinoma cells (fig. S4). We fractionated STAT3 knockout cells reconstituted with mutant forms of STAT3. The presence of STAT3 in mitochondria did not require tyrosine phosphorylation or intact SH2 or DNA binding domains, mirroring the lack of requirement of these domains for Ras transformation (Fig. 2B).

To further assess STAT3 mitochondrial localization, we tested its protease sensitivity with or without detergent. Proteins associated with outer mitochondrial membranes are expected to be protease-sensitive, whereas internal proteins are degraded only after membrane disruption with detergent (*20*). Incubation of purified mitochondria with proteinase K readily removed Bcl-X expressed on the outer mitochondrial membrane, but STAT3 and F1 adenosine triphosphatase (F1 ATPase), an internal mitochondrial protein, were retained unless mitochondria were treated with both protease and detergent (Fig. 2C). Therefore, like F1 ATPase, STAT3 appears to be an internal mitochondrial protein.

Given the presence of STAT3 in mitochondria and the dependence of tumor cells for glucose due to high glycolytic activity (*21*), we probed for metabolic defects in RasV12-expressing cells engineered to express STAT3 mutants. Activated Ras increased dependence on high glucose medium in the absence of STAT3 (Fig. 2D). Reconstitution of cells with STAT3 suppressed this sensitivity, and the structure-function relation between STAT3 and cell survival mirrored that for transformation. That is, tyrosine phosphorylation and intact SH2 and DNA binding domains were not required for protection from cell death, but S727 was essential (Fig. 2D). Similarly, RasV12-expressing cells lacking STAT3 were more sensitive to glucose restriction when cultured in reduced oxygen concentrations, requiring S727 for protection but not other STAT3 domains implicated in cytokine signaling (Fig. 2E). In contrast, cells with or without functional STAT3 were equally viable when cultured in the presence of high glucose medium, demonstrating that mitochondrial STAT3 is not essential for normal cell viability.

To determine if mitochondrial STAT3 was sufficient to support Ras transformation, we reconstituted STAT3-null cells with STAT3 artificially targeted exclusively to mitochondria. We transfected Ras-expressing STAT3-null cells with wild-type (WT) or mutant versions of STAT3 fused with a mitochondrial targeting sequence (MTS) derived from cytochrome c oxidase subunit VIII, an integral mitochondrial protein (*22*). Cytoplasmic and mitochondrial extracts from stably transfected cells confirmed the exclusive presence of STAT3 in mitochondria, with approximately equal abundance of WT and tyrosine- or serine-phosphorylation–deficient mutants (Fig. 2F). STAT3 expressed exclusively in mitochondria supported anchorage-independent growth, but S727 was required (Fig. 2G). In contrast, mitochondrially restricted STAT3 did not support v-Src–driven anchorage-independent growth (Fig. 2H), consistent with our previous finding that v-src requires nuclear functions of STAT3 (*11*). Cellular transformation by activated N- or K-Ras also required STAT3, and impaired transformation without STAT3 was reversed by STAT3 artificially restricted to mitochondria, again dependent on S727 (Fig. 2, I and J, and fig. S5). Mitochondrially restricted STAT3 supported growth of Ras-transformed cells as solid tumors in vivo, which could not grow

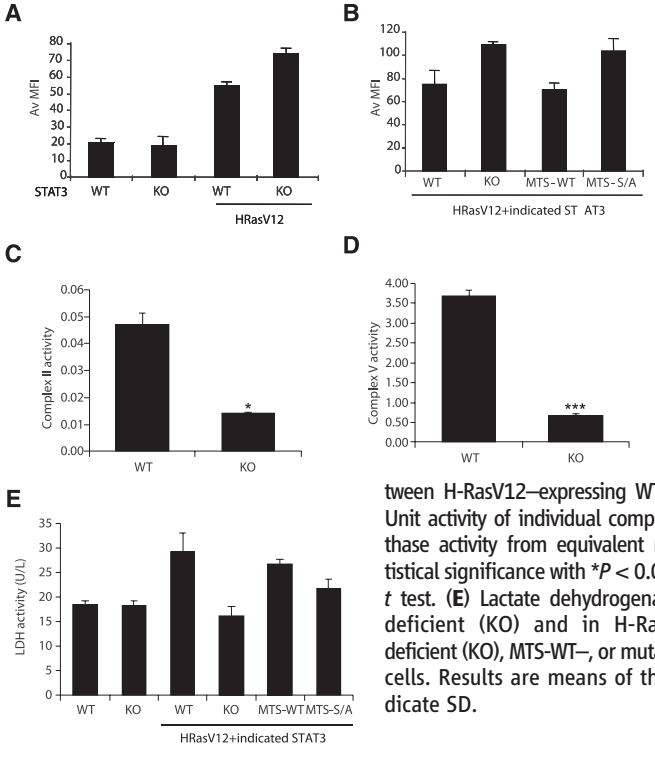

Fig. 3. Mitochondrial STAT3 augments electron transport chain activity. (**A**) Mitochondrial membrane potential measured with TMRE and recorded as mean fluorescence intensity (MFI) by flow cytometry in WT or STAT3-deficient (KO) cells with or without H-RasV12. (**B**) Mitochondrial membrane potential of H-RasV12–expressing cells with WT, vector (KO), mitochondrially targeted WT (MTS-WT), or S727A-mutant STAT3. Activities of electron transport chain complexes II (**C**) and V (**D**) compared between H-RasV12–expressing WT or STAT3-deficient (KO) cells. Unit activity of individual complexes normalized to citrate synthase activity from equivalent numbers of mitochondria. Statistical significance with $*P < 0.05$ or $***P < 0.001$ by Student's *t* test. (**E**) Lactate dehydrogenase activity in WT and STAT3-deficient (KO) and in H-RasV12–expressing WT, STAT3-deficient (KO), MTS-WT–, or mutant STAT3 (MTS-S/A)–expressing cells. Results are means of three replicates. Error bars indicate SD.

without STAT3 (fig. S6). Thus, all three major human Ras oncoproteins depended on mitochondrial STAT3 for full transforming potential.

We detected no STAT3 requirement for mitochondrial formation, maintenance, or gene expression (fig. S6, A to C). However, loss of STAT3 led to a 50% reduction in cellular ATP levels (fig. S6D) and altered sensitivity to mitochondrial inhibitors (fig. S6, E to G). Therefore, we examined mitochondrial function in the presence and absence of STAT3. Transformed cells exhibited increased mitochondrial membrane potential (Fig. 3A), which is considered a characteristic of cancer cells (*23*). Although normal cells exhibited no dependence on STAT3 for mitochondrial membrane potential, the absence of STAT3 reproducibly accentuated the increased polarization of H-RasV12–expressing cells (Fig. 3A), and this accentuated polarization was reverted by mitochondrially restricted STAT3 expression (Fig. 3B). Like transformation, this mitochondrial STAT3 function required S727. Because mitochondrial membrane potential is maintained by oxidative phosphorylation, we measured activities of each enzyme complex of the electron transport chain (Fig. 3, C and D, and fig. S8). Mitochondrial function was impaired without STAT3, with significantly reduced activity of succinate oxidoreductase (complex II) and ATP synthase (complex V). Additionally, lactate dehydrogenase activity was increased in transformed cells, and this increased activity required mitochondrial STAT3, which is largely dependent on S727 (Fig. 3E).

These data demonstrate a transformation-specific function for mitochondrial STAT3, in addition to its previously characterized nuclear roles. Although previous data implicated a Ras-STAT3 axis in transformation, those cases were in the context of activated tyrosine kinases, such as NPM-ALK (*12*), RET (*24*), or autocrine cytokine signaling (*25*), requiring STAT3 function in the nucleus. Mitochondrial STAT3 appears to contribute to Ras-dependent cellular transformation by augmenting electron transport chain activity, particularly that of complexes II and V, accompanied somewhat paradoxically by shifted energy production to favor fermentation. Impaired complex V activity may contribute to a build-up of protons, causing enhanced mitochondrial membrane polarization without STAT3. STAT3 loss increased sensitivity to the small molecule inhibitors of oxidative phosphorylation, rotenone and antimycin A (fig. S4, C and D), but protected cells from the proton channel inhibitor oligomycin (fig. S4E). The reduced sensitivity of STAT3-null cells to oligomycin underscores that STAT3 is not simply a general survival factor for transformed cells, but rather has specific effects on mitochondrial function. In spite of transformation-specific functions of mitochondrial STAT3 documented here, STAT3 also accumulated in mitochondria of nontransformed cells and primary tissues (fig. S4) and recently was shown to modulate respiration in mouse heart tissue (*26*). Therefore, the metabolic shift important for tumor growth mediated by mitochondrial STAT3 may reflect exploitation of a normal function. If so, mitochondrial STAT3 function could provide an attractive target for therapeutic approaches to cancer.

References and Notes

1. D. E. Levy, C. K. Lee, *J. Clin. Invest.* **109**, 1143 (2002).
2. D. E. Levy, J. E. Darnell Jr., *Nat. Rev. Mol. Cell Biol.* **3**, 651 (2002).
3. Z. Zhong, Z. Wen, J. E. Darnell, *Science* **264**, 95 (1994).
4. R. Raz, J. E. Durbin, D. E. Levy, *J. Biol. Chem.* **269**, 24391 (1994).
5. C. Lutticken *et al.*, *Science* **263**, 89 (1994).
6. S. Akira *et al.*, *Cell* **77**, 63 (1994).
7. J. F. Bromberg *et al.*, *Cell* **98**, 295 (1999).
8. C. L. Yu *et al.*, *Science* **269**, 81 (1995).
9. G. Inghirami *et al.*, *Cell Cycle* **4**, 1131 (2005).
10. S. P. Gao, J. F. Bromberg, *Sci. STKE* **2006**, pe30 (2006).
11. K. Schlessinger, D. E. Levy, *Cancer Res.* **65**, 5828 (2005).
12. R. Chiarle *et al.*, *Nat. Med.* **11**, 623 (2005).
13. Materials and methods are available as supporting material on *Science* Online.
14. Single-letter abbreviations for the amino acid residues are as follows: A, Ala; C, Cys; D, Asp; E, Glu; F, Phe; G, Gly; H, His; I, Ile; K, Lys; L, Leu; M, Met; N, Asn; P, Pro; Q, Gln; R, Arg; S, Ser; T, Thr; V, Val; W, Trp; and Y, Tyr.
15. C. Schindler, D. E. Levy, T. Decker, *J. Biol. Chem.* **282**, 20059 (2007).
16. N. C. Reich, L. Liu, *Nat. Rev. Immunol.* **6**, 602 (2006).
17. E. Taparowsky *et al.*, *Nature* **300**, 762 (1982).
18. N. Mitin, K. L. Rossman, C. J. Der, *Curr. Biol.* **15**, R563 (2005).
19. P. B. Sehgal, *Semin. Cell Dev. Biol.* **19**, 329 (2008).
20. H. Lorenz, D. W. Hailey, J. Lippincott-Schwartz, *Nat. Methods* **3**, 205 (2006).
21. O. Warburg, *Science* **123**, 309 (1956).
22. R. Rizzuto *et al.*, *J. Biol. Chem.* **264**, 10595 (1989).
23. V. R. Fantin, J. St-Pierre, P. Leder, *Cancer Cell* **9**, 425 (2006).
24. I. Plaza-Menacho *et al.*, *J. Biol. Chem.* **282**, 6415 (2007).
25. S. P. Gao *et al.*, *J. Clin. Invest.* **117**, 3846 (2007).
26. J. Wegrzyn *et al.*, *Science* **323**, 793 (2009); published online 8 January 2009 (10.1126/science.1164551).

27. We thank A. Pellicer, L. Feig, C. Der, R. Jove, S. Watowich, and M. Philips for gifts of reagents and helpful discussions. This work was supported by NIH grant R01AI28900 and the NYSTEM Foundation.

Supporting Online Material

www.sciencemag.org/cgi/content/full/324/5935/1713/DC1
Materials and Methods
SOM Text
Figs. S1 to S8
References

2 February 2009; accepted 11 May 2009
10.1126/science.1171721

Synthetic Heterochromatin Bypasses RNAi and Centromeric Repeats to Establish Functional Centromeres

Alexander Kagansky,[1]* Hernan Diego Folco,[1]*† Ricardo Almeida,[1]* Alison L. Pidoux,[1] Abdelhalim Boukaba,[1]‡ Femke Simmer,[1]§ Takeshi Urano,[2] Georgina L. Hamilton,[1] Robin C. Allshire[1]‖

In the central domain of fission yeast centromeres, the kinetochore is assembled on CENP-A^{Cnp1} nucleosomes. Normally, small interfering RNAs generated from flanking outer repeat transcripts direct histone H3 lysine 9 methyltransferase Clr4 to homologous loci to form heterochromatin. Outer repeats, RNA interference (RNAi), and centromeric heterochromatin are required to establish CENP-A^{Cnp1} chromatin. We demonstrated that tethering Clr4 via DNA-binding sites at euchromatic loci induces heterochromatin assembly, with or without active RNAi. This synthetic heterochromatin completely substitutes for outer repeats on plasmid-based minichromosomes, promoting de novo CENP-A^{Cnp1} and kinetochore assembly, to allow their mitotic segregation, even with RNAi inactive. Thus, the role of outer repeats in centromere establishment is simply the provision of RNAi substrates to direct heterochromatin formation; H3K9 methylation-dependent heterochromatin is alone sufficient to form functional centromeres.

It is unclear what features define the chromosomal location where histone H3 is replaced by the centromere-specific histone H3 variant CENP-A to allow kinetochore assembly (*1*). Kinetochores in many organisms are surrounded by heterochromatin (*2*). In fission yeast (*Schizosaccharomyces pombe*), heterochromatin that formed on the outer repeats (*otr*, composed of *dg* and *dh* elements) flanks the central domain chromatin, in which canonical H3 is replaced by CENP-A^{Cnp1}, which promotes kinetochore assembly (*3*–*7*). Outer repeat heterochromatin on minichromosomes is necessary to allow de novo establishment of CENP-A^{Cnp1} chromatin and kinetochore protein recruitment (*8*); it also contributes to centromere function by ensuring robust cohesion between sister-centromeres (*9*, *10*). Heterochromatin is

[1]Wellcome Trust Centre for Cell Biology, School of Biological Sciences, The University of Edinburgh, 6.34 Swann Building, Edinburgh EH9 3JR, Scotland, UK. [2]Department of Biochemistry, Shimane University Faculty of Medicine, 89-1 Enya-cho, Izumo 693-8501, Japan.

*These authors contributed equally to this work.
†Present Address: Ludwig Institute for Cancer Research, Cellular and Molecular Medicine, University of California, San Diego, 9500 Gilman Drive, La Jolla, CA 92093–0660, USA.
‡Present Address: Laboratory of Cancer Epigenetics, Faculty of Medicine, Free University of Brussels, 808 route de Lennik, 1070 Brussels, Belgium.
§Present Address: Department of Molecular Biology, Radboud University Nijmegen Medical Centre, 6500 HB Nijmegen, The Netherlands.
‖To whom correspondence should be addressed. E-mail: robin.allshire@ed.ac.uk

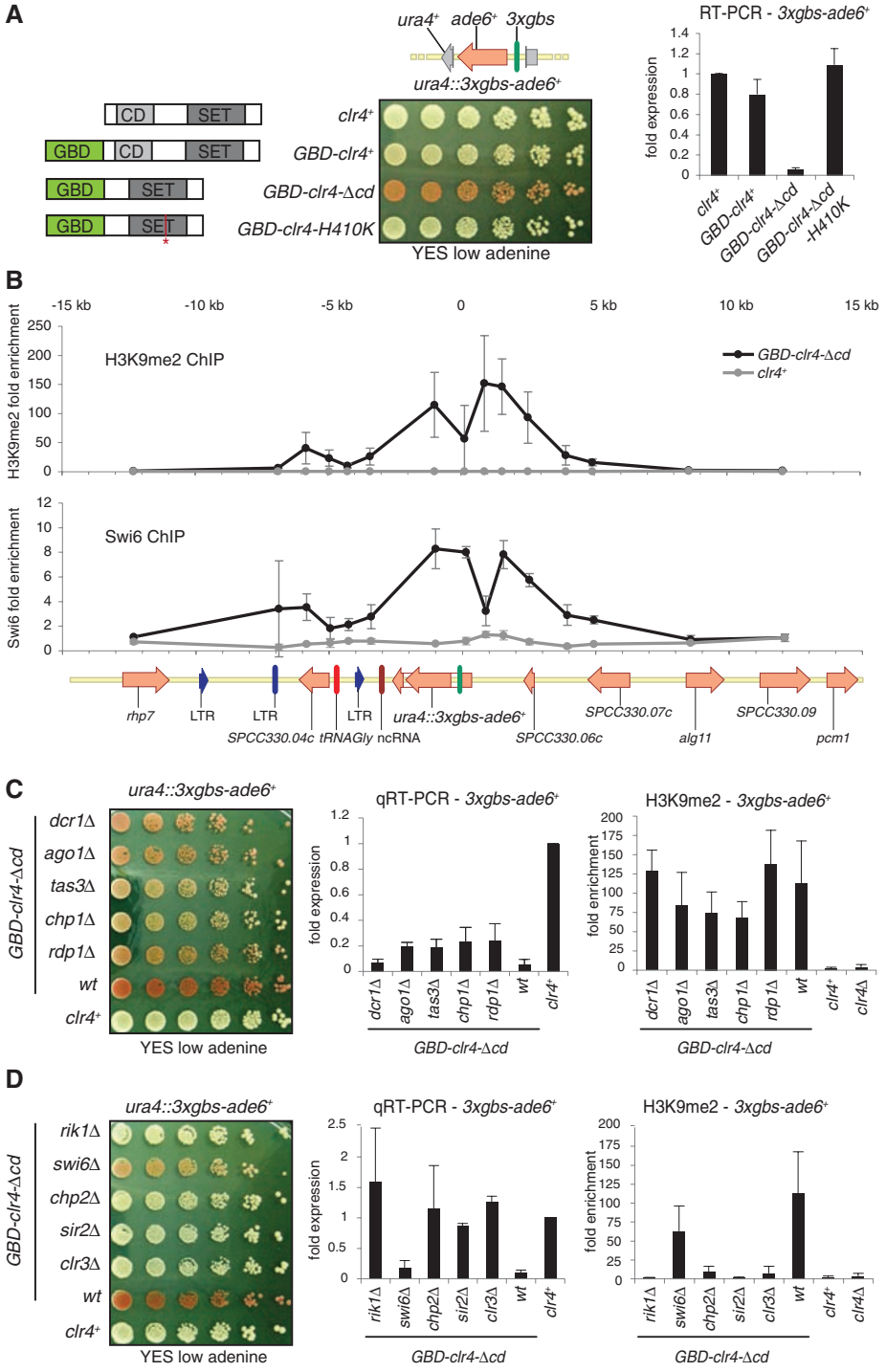

Fig. 1. Tethered Clr4 silences transcription, forms a 10-kb domain of heterochromatin, and requires HDACs, Rik1, and Chp2, but not RNAi. (**A**) (Left) Clr4 fusion proteins used. Gal4 DNA–binding, chromo-, and SET domains, and H410K (asterisk) mutation, are indicated. (Middle) Plating assay on low adenine of cells expressing the indicated Clr4 proteins and containing the *3xgbs-ade6*$^+$ reporter inserted at *ura4*$^+$. *ade6*$^+$-expressing cells form white colonies; *ade*$^-$- and *ade6*$^+$-repressed cells form red colonies. (Right) Quantitative reverse transcription polymerase chain reaction (RT-PCR) showing *3xgbs-ade6*$^+$ transcript levels (error bar, SD; $n = 3$ replicates). (**B**) ChIP analysis with antibodies to H3K9me2 or Swi6 of 25-kb region surrounding *ura4::3xgbs-ade6*$^+$ in presence of Clr4 or GBD-clr4-Δcd. Genomic features are depicted at bottom. (**C**) Plating assay on low adenine of cells with the indicated genes deleted, expressing Clr4 or GBD-clr4-Δcd with the *ura4::3xgbs-ade6*$^+$ reporter (left). Shown are quantitative RT-PCR for 3xgbs-*ade6*$^+$ transcript levels (middle) and quantitative ChIP for H3K9me2 levels on *ura4::3xgbs-ade6*$^+$ in the indicated strains (error bar, SD; $n = 3$ replicates). (**D**) As above, with indicated mutants.

formed by the action of RNA interference (RNAi)–directed chromatin modification on noncoding outer repeat transcripts to create methyl-H3K9 binding sites for the chromodomain proteins Swi6, Chp1, Chp2, and Clr4. Thus, RNAi components, histone deacetylases (HDACs), the Clr4 H3K9 methyltransferase, and chromodomain proteins all contribute to heterochromatin integrity (*11*, *12*).

Active RNAi, Clr4 methyltransferase, and the Swi6 (HP1) chromodomain protein are necessary to form heterochromatin on outer repeats and establish CENP-A^{Cnp1} chromatin over the adjacent central domain on newly introduced centromeric DNA plasmids (*8*). To test whether artificially tethering Clr4 to a euchromatic locus can promote heterochromatin assembly, and whether this alone is sufficient to establish a functional centromere, the DNA-binding domain of the *Saccharomyces cerevisiae* Gal4 protein (GBD) was fused to (Fig. 1A) the N terminus of the gene encoding wild-type Clr4 (*GBD-clr4*), Clr4-Δcd lacking the chromodomain (*GBD-clr4-Δcd*), and Clr4-H410K, a catalytically inactive SET-domain mutant (*GBD-clr4-Δcd-H410K*). These GBD-to-Clr4 fusions are produced, providing the only source of Clr4 protein (fig. S1A), and were tested in combination with the following reporters: three Gal4-binding sites (*3xgbs*) upstream of *ade6*$^+$ inserted at the *ura4* (*ura4::3xgbs-ade6*$^+$) (Fig. 1A) or *arg3* loci or 10× *gbs* upstream of *ura4*$^+$ (fig. S1, B and C).

Full *ade6*$^+$ expression results in white colonies, whereas silencing causes pink and/or red colonies to form. The GBD-Clr4-Δcd fusion protein clearly represses the *ura4::3xgbs-ade6*$^+$ (Fig. 1A) and other reporters (fig. S1, B and C), indicating that this silencing is reporter gene– and locus-independent. It is dependent on Clr4 catalytic activity because no repression occurred with the H410K mutant (Fig. 1A); therefore, repression does not result from indirect recruitment of Clr4-associated repressive factors. Although the GBD-Clr4 full-length fusion protein is recruited to the reporter (fig. S2A), it is unable to mediate repression (Fig. 1A). Deletion of the Clr4 chromodomain affects endogenous heterochromatin, and this may release limiting factors for participation in silencing at the tethering site (fig. S2A). Consistent with this, full-length GBD-Clr4 fusion protein can silence the reporter in *dcr1*Δ cells (fig. S2B). Analyses of antibodies to H3K9me2 and Swi6 chromatin immunoprecipitation (ChIP) demonstrate that in cells expressing GBD-Clr4-Δcd protein, H3K9 is dimethylated on, and Swi6 recruited to, a region of approximately 10 kb, including and surrounding the *ura4::3xgbs-ade6*$^+$ reporter (Fig. 1B). Consequently, genes neighboring the reporter are also repressed in cells expressing GBD-Clr4-Δcd (fig. S3). This synthetic heterochromatin is established de novo and maintained independent of RNAi because the reporter remains largely repressed and assembled in H3K9me2 chromatin in cells lacking Dcr1, Ago1,

Tas3, Chp1, or Rdp1 (Fig. 1C and fig. S4). Moreover, no *ade6*$^{+}$ or *ura4*$^{+}$ reporter gene homologous small interfering RNA (siRNA) were detected (fig. S5). Silencing and H3K9me2 levels are maintained in *dcr1*Δ cells (Fig. 1C); thus, although Ago1 associates with *3xgbs-ade6*$^{+}$ (fig. S5C), the contribution of it and other RNAi components may only be as bound physical entities. In contrast, silencing is highly dependent on chromatin factors Rik1 (Clr4-associated), Chp2 (a Swi6-related protein), and Sir2 and Clr3 HDACs, which must act independent of RNAi (Fig. 1E and fig. S4). Synthetic heterochromatin is essentially insensitive to loss of Swi6; this is consistent with the reported role for Swi6 in RNAi-dependent silencing, whereas Chp2 acts with Clr3 to mediate RNAi-independent transcriptional repression (*13*). In cells producing only mutant histone H3K9R or H3K9A proteins, *3xgbs-ade6*$^{+}$ is expressed, indicating that the Clr4 substrate H3K9 is critical for silencing by tethered Clr4 activity (fig. S6).

Intact heterochromatin on the outer repeats is necessary for the establishment of CENP-A^{Cnp1} chromatin on adjacent central-domain DNA (*8*). Other features of centromeric outer repeats, such as protein-binding sites (*14*) or noncoding RNA (*15*), could act in combination with heterochromatin to promote CENP-A^{Cnp1} incorporation. To determine whether heterochromatin alone is sufficient, we substituted the outer repeats on a plasmid with three Gal4-binding sites, or no sites, in close proximity to the central domain, generating the plasmids p3x*gbs*-cc2 and p0x*gbs*-cc2, respectively (Fig. 2 and fig. S7). GBD-Clr4-Δcd associates with the plasmid-borne Gal4 sites, and H3K9me2 was detected over these and extending into nearby regions, suggesting that a 6-kb domain of heterochromatin was formed (Fig. 2A and fig. S7). In support of this, the underlying plasmid-borne marker genes were silenced (fig. S8). Both CENP-A^{Cnp1} and CENP-C^{Cnp3} associated with the central core of the p3x*gbs*-cc2 plasmid, but only in cells expressing GBD-Clr4-Δcd (Fig. 2B), and CENP-A^{Cnp1} was also detected at the extremities of the 8.5-kb central domain, but not on other regions of the plasmid (fig. S9). Thus, the synthetic heterochromatin domain formed by Clr4 methyltransferase bound to these Gal4 sites is sufficient to promote the assembly of CENP-A^{Cnp1} across, and recruit other kinetochore proteins to, the central domain.

Only plasmids carrying Gal4 sites formed white and/or sectored colonies when combined with GBD-Clr4-Δcd (Fig. 2C) (*16*), indicating that a functional centromere, capable of mitotic segregation, had formed. Similar results were obtained with Gal4 sites on the opposite side of cc2 (pcc2-3x*gbs*) (fig. S9). Both 3xgbs plasmids exhibit approximately twofold greater mitotic stability than pH′-cc2, which contains native outer repeat heterochromatin on a similarly sized functional minichromosome (fig. S9). This indicates that the function of natural outer repeat DNA at a plasmid-borne centromere can be substituted by artificially recruiting Clr4 to DNA. From using this sensitive plasmid-based assay, we conclude that centromeric outer repeats have no hidden unknown features, and apart from its role in directing heterochromatin assembly the primary outer repeat DNA sequence is dispensable with respect to establishing centromere-kinetochore function.

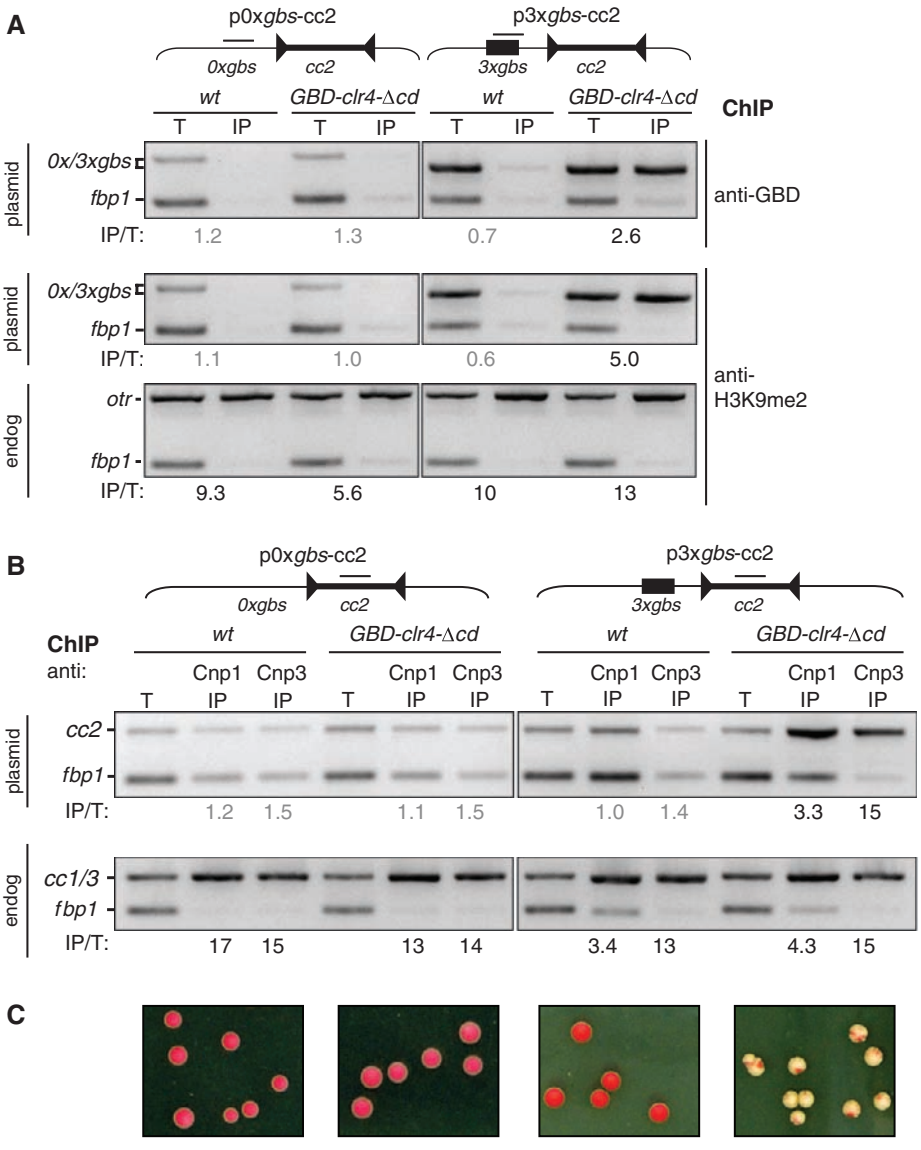

Fig. 2. Tethered Clr4 promotes CENP-A^{Cnp1} deposition, kinetochore assembly, and centromere activity. (**A**) ChIP with antibody to GBD (top) and antibody to H3K9me2 (middle and bottom) of wild-type and *GBD-clr4-Δcd* cells transformed with p0x*gbs*-cc2 or p3x*gbs*-cc2, as indicated. Enrichment values [immunoprecipitate/total (IP/T)] were calculated from the intensity of the *0xgbs* or *3xgbs* band normalized to the control *fbp1* locus. Gray values indicate no enrichment. H3K9me2 levels on endogenous centromeric *otr* repeats are shown at bottom. (**B**) ChIP with antibody to Cnp1 and antibody to Cnp3 of wild-type and *GBD-clr4-Δcd* cells transformed with p0x*gbs*-cc2 or p3x*gbs*-cc2, as indicated. Enrichment values (IP/T) were calculated from the intensity of the plasmid *cc2* band (top) or the endogenous *cc1/3* central cores (middle), normalized to the control *fbp1* locus (*16*). (**C**) Colonies from strains indicated in (B) transformed with p0x*gbs*-cc2 or p3x*gbs*-cc2 grown on low adenine. Plasmid mitotic stability is determined by colony color: white/red sectors indicates stable and uniform red indicates complete loss (*16*).

Centromeric outer repeats may just provide a double-stranded RNA substrate for RNAi to direct H3K9 methylation and centromeric heterochromatin formation. To test whether synthetic heterochromatin is completely RNAi-independent, p3x*gbs*-cc2 was transformed into wild-type, *dcr1*Δ, and *rik1*Δ cells expressing GBD-Clr4-Δcd. GBD-Clr4-Δcd was bound to the *3xgbs* in all strains (Fig. 3A), whereas

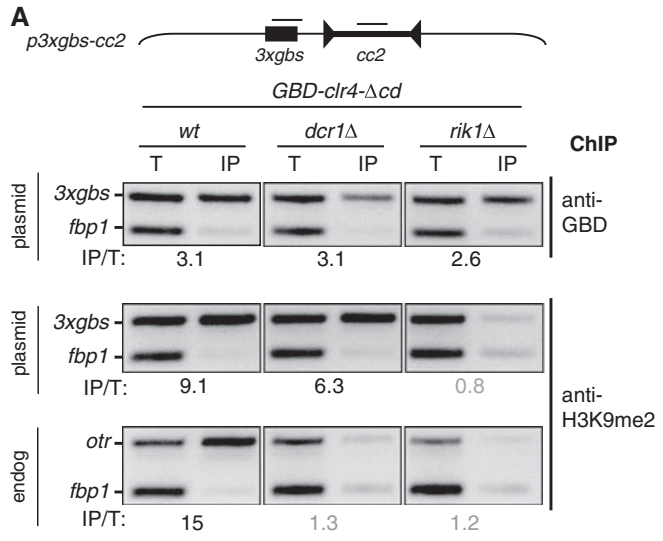

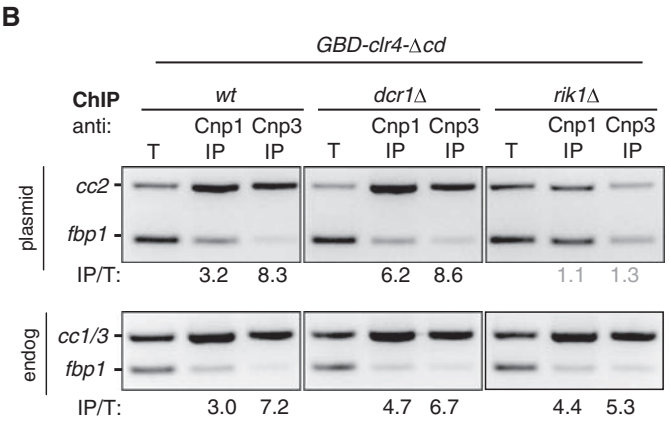

C

Host strain	Plasmid	Size (kb)	Minichromosome loss rate (%)	Colonies counted
wt	*pH'-cc2*	19.3	30.7	531
GBD-clr4-Δcd	*p3xgbs-cc2*	18.2	16.9	656
GBD-clr4-Δcd	*pcc2-3xgbs*	19.2	15.9	372
GBD-clr4-Δcd	*p0xgbs-cc2*	17.8	100.0	>500
GBD-clr4-Δcd dcr1Δ	*p3xgbs-cc2*	18.2	11.3	480

Fig. 3. Synthetic heterochromatin allows establishment of functional centromeres in cells lacking RNAi. (**A**) ChIP with antibody to GBD (top) and antibody to H3K9me2 (middle and bottom) of *wt*, *dcr1*Δ, and *rik1*Δ cells expressing *GBD-clr4-Δcd* cells transformed with p3x*gbs*-cc2. Enrichment values (IP/T) were calculated as described in (*16*). Gray values indicate no enrichment. H3K9me2 levels on endogenous centromeric *otr* repeats are shown at bottom. (**B**) ChIP with antibody to Cnp1 and antibody to Cnp3 on identical cells as in (A). Levels on endogenous centromeric cc1/3 sequences are shown (bottom). (**C**) Loss rate of indicated plasmid-based minichromosomes in indicated host strains expressing Clr4 or GBD-clr4-Δcd. pH′-cc2 containing natural outer repeat heterochromatin is included for comparison (*3*). pcc2-3*xgbs* has the 3x*gbs* to the right of *cc2* (fig. S9).

H3K9me2 was detected over this region in wild-type and *dcr1*Δ but not *rik1*Δ cells. This confirms that the establishment of H3K9me2 modified chromatin by tethered Clr4 occurs independent of RNAi but depends on Rik1. In support of this, silencing with full-length GBD-Clr4 only occurred upon deletion of Dcr1 (fig. S2B). Anti-CENP-A^{Cnp1} and CENP-C^{Cnp3} ChIP indicated that recruitment of GBD-Clr4-Δcd to the plasmids' Gal4 sites allowed the establishment of CENP-A^{Cnp1} chromatin on, and recruitment of CENP-C^{Cnp3} to, the central core of p3x*gbs*-cc2 in wild-type and *dcr1*Δ cells but not *rik1*Δ cells (Fig. 3B). The minichromosome with the Gal4 sites exhibited mitotic stability when combined with GBD-Clr4-Δcd in *dcr1*Δ cells (Fig. 3C and fig. S9). We conclude that the requirement for outer repeats and RNAi in the de novo establishment of functional heterochromatin to promote CENP-A^{Cnp1} and kinetochore assembly, and form mitotically active centromeres, on plasmid-based minichromosomes, can be fully substituted by Clr4-tethered synthetic heterochromatin formed adjacent to a central domain.

Three Gal4-binding sites, which directly recruit Clr4 methyltransferase activity, can replace the normal requirement for at least 2.1 kb of centromeric outer repeat DNA adjacent to a central domain on naïve plasmids to form active centromeres (*3*, *7*, *8*). This synthetic heterochromatin is therefore functional in that it generates sufficient sister-centromere cohesion and promotes assembly of CENP-A^{Cnp1} in place of histone H3 to provide a foundation for kinetochore formation. This indicates that no other contribution of the outer repeats is required in terms of their primary DNA sequence in this plasmid-based establishment assay. RNAi components were previously shown in similar assays to be necessary for CENP-A^{Cnp1} chromatin establishment (*8*). By artificially recruiting Clr4 activity, we have bypassed RNAi and rule it out as being directly involved in promoting CENP-A^{Cnp1} deposition. Thus, the noncoding outer repeat transcripts themselves and the resulting siRNA are not required to form a mitotically functional minichromosomal centromere. It remains to be determined how heterochromatin promotes CENP-A^{Cnp1} incorporation. Recent analyses suggest that the acetylated state of histones is important and HDAC inhibitors rescue CENP-A^{Cnp1} chromatin assembly defects (*4*, *17*). Synthetic heterochromatin placed close to a central domain may provide a favorable chromatin environment to attract key remodeling and modifying factors. Ultimately, similar manipulations as described here may improve the efficiency of human artificial chromosome formation.

References and Notes

1. R. C. Allshire, G. H. Karpen, *Nat. Rev. Genet.* **9**, 923 (2008).
2. B. A. Sullivan, G. H. Karpen, *Nat. Struct. Mol. Biol.* **11**, 1076 (2004).
3. M. Baum, V. K. Ngan, L. Clarke, *Mol. Biol. Cell* **5**, 747 (1994).
4. T. Hayashi *et al.*, *Cell* **118**, 715 (2004).
5. A. L. Pidoux, W. Richardson, R. C. Allshire, *J. Cell Biol.* **161**, 295 (2003).
6. K. Takahashi, E. S. Chen, M. Yanagida, *Science* **288**, 2215 (2000).
7. K. Takahashi *et al.*, *Mol. Biol. Cell* **3**, 819 (1992).
8. H. D. Folco, A. L. Pidoux, T. Urano, R. C. Allshire, *Science* **319**, 94 (2008).
9. P. Bernard *et al.*, *Science* **294**, 2539 (2001).
10. N. Nonaka *et al.*, *Nat. Cell Biol.* **4**, 89 (2002).
11. M. Buhler, D. Moazed, *Nat. Struct. Mol. Biol.* **14**, 1041 (2007).
12. S. I. Grewal, S. Jia, *Nat. Rev. Genet.* **8**, 35 (2007).
13. M. R. Motamedi *et al.*, *Mol. Cell* **32**, 778 (2008).
14. H. Nakagawa *et al.*, *Genes Dev.* **16**, 1766 (2002).
15. T. A. Volpe *et al.*, *Science* **297**, 1833 (2002).
16. Materials and methods are available as supporting material on *Science* Online.
17. Y. Fujita *et al.*, *Dev. Cell* **12**, 17 (2007).

18. We are grateful to the following colleagues for strains and reagents: M. Baum, L. Clarke, K. Scott, J. Partridge, J. Ma, S. Grewal, D. Moazed, K. Takahashi, M. Yanagida, and S. A. White. This research was supported by a European Molecular Biology Organization–Long-Term Fellowship (to F.S.), a Medical Research Council Strategic Grant (G0301153 to R.C.A.), and a Wellcome Trust Programme grant (065061/Z to R.C.A.). R.C.A. is a Wellcome Trust Principal Research Fellow.

Supporting Online Material

www.sciencemag.org/cgi/content/full/324/5935/1716/DC1
Materials and Methods
SOM Text
Figs. S1 to S9
Tables S1 and S2
References

9 February 2009; accepted 14 May 2009
10.1126/science.1172026

Diversity and Complexity in DNA Recognition by Transcription Factors

Gwenael Badis,[1]* Michael F. Berger,[2,3]* Anthony A. Philippakis,[2,3,4]* Shaheynoor Talukder,[1,5]* Andrew R. Gehrke,[2]* Savina A. Jaeger,[2]* Esther T. Chan,[5]* Genita Metzler,[6] Anastasia Vedenko,[7] Xiaoyu Chen,[1] Hanna Kuznetsov,[6] Chi-Fong Wang,[8] David Coburn,[1] Daniel E. Newburger,[2] Quaid Morris,[1,5,9,10] Timothy R. Hughes,[1,5,10]† Martha L. Bulyk[2,3,4,11]†

Sequence preferences of DNA binding proteins are a primary mechanism by which cells interpret the genome. Despite the central importance of these proteins in physiology, development, and evolution, comprehensive DNA binding specificities have been determined experimentally for only a few proteins. Here, we used microarrays containing all 10–base pair sequences to examine the binding specificities of 104 distinct mouse DNA binding proteins representing 22 structural classes. Our results reveal a complex landscape of binding, with virtually every protein analyzed possessing unique preferences. Roughly half of the proteins each recognized multiple distinctly different sequence motifs, challenging our molecular understanding of how proteins interact with their DNA binding sites. This complexity in DNA recognition may be important in gene regulation and in the evolution of transcriptional regulatory networks.

The interactions between transcription factors (TFs) and their DNA binding sites are an integral part of the gene regulatory networks that control development, core cellular processes, and responses to environmental perturbations. However, only a handful of sequence-specific TFs have been characterized well enough to identify all the sequences that they can and, just as importantly, cannot bind. Computational analysis of microarray readout of chromatin immunoprecipitation experiments (ChIP-chip) suggests extensive use of low-affinity binding sites in yeast (*1*), and computational models of gene expression during fly embryonic development suggest that low-affinity binding sites contribute as much as high-affinity sites (*2*).

The availability of TF binding data spanning the full affinity range would improve our understanding of the biophysical phenomena underlying protein-DNA recognition and would also improve accuracy in analyzing cis regulatory elements. Here we report the comprehensive determination of the DNA binding specificities of 104 known and predicted mouse TFs with the use of the universal protein binding microarray (PBM) technology (*3*). These TFs represent 22 different DNA binding domain (DBD) structural classes that are the major DBD classes found in metazoan TFs.

We created N-terminal glutathione *S*-transferase (GST) fusion constructs of the DBDs of 104 known and predicted mouse TFs (fig. S1 and table S1) (*4*). Five of these proteins—Max, Bhlhb2, Gata3, Rfx3, and Sox7—were also represented as full-length fusions to N-terminal GST, yielding a total set of 109 nonredundant proteins represented by 115 samples (*5*). Each protein was used in two PBM experiments (*6*, *7*) (figs. S2 to S4 and table S2). DNA binding site motifs were initially derived by the Seed-and-Wobble algorithm (*3*, *8*); Seed-and-Wobble first identifies the single 8-mer (ungapped or gapped) with the greatest PBM enrichment score (E score) (*3*) and then systematically tests the relative preference of each nucleotide variant at each position, both within and outside the seed (*5*). Later analyses incorporated additional motif-finding algorithms, including RankMotif++ (*9*) and Kafal (*5*).

Beyond simply providing a DNA binding site motif, these data provide a rank-ordered listing of the preference of a protein for every gapped and ungapped *k*-mer "word," where *k* is the number of informative nucleotide positions in the binding site. This data set consists of 9.6 million measurements, from which we can derive binding data for 22.3 million ungapped and gapped 8-mers (up to 12 positions) for each protein. For each of the 8-mers for each protein, we report its E score, median signal intensity Z score, and false discovery rate *Q* value (*5*). We found that the average number of ungapped 8-mers considered "bound" at a *Q* value threshold of 0.001 varied across classes, ranging from 65 for the MADS class factor SRF to 871 for the E2F class.

For TFs that had previously known binding site motifs, we observed general agreement with earlier motif data (fig. S5 and table S3) (*5*). Comparisons to dissociation constant data (*10*) for Max and for the yeast TF Cbf1 (*3*) indicate that words with higher E scores are generally bound with higher affinity (*3*) (fig. S6). Confirmation by electrophoretic mobility shift assays (EMSAs) for three newly characterized proteins and one recently characterized protein (*11*) —Zfp740, Osr2, Sp100, and Zfp161 (ZF5) (*12*), respectively—is shown in fig. S7.

To examine correlations among the proteins' DNA binding specificities and to identify DNA sequences that distinguish the binding profiles of different TF families, we hierarchically clustered the *k*-mers that met a stringent binding threshold (E score $\geq$ 0.45) for at least one of the proteins. We used E scores because they are robust to differences in protein concentration and thus facilitate comparison of *k*-mer data across arrays (*3*); we consider them as a proxy for relative affinities. Different DBD classes generally recognize distinct portions of sequence space (Fig. 1A and fig. S8). However, even proteins with up to 67% amino acid sequence identity exhibited distinct DNA binding profiles. For example, although Irf4 and Irf5 both bind the same highest-affinity sites (8-mers containing CGAAAC), they prefer different lower-affinity sites (TGAAAG versus CGAGAC) (Fig. 1B). We verified for five TFs that the full-length protein displays a virtually identical spectrum of 8-mer preferences to that of the DBD and that the spectrum is distinct from other proteins of the same structural class (figs. S2 and S9).

Our data set includes most members of three TF structural classes in mouse: (i) Sox and Sox-related, (ii) IRF, and (iii) AP-2. In an extreme case, we find no evidence that the binding profiles of the AP-2 class members are different from each other (fig. S9B), consistent with reports that the human counterparts of AP-2α, AP-2β, and AP-2γ all bind GCCNNNGGC (*13*). In contrast, members of the IRF class all appeared to have different binding profiles (fig. S9L).

The Sox and Sox-related family presents an intriguing instance of highly conserved DBDs with closely related but distinct binding preferences. We found marked differences in the binding specificities of the Sox (*14*), Tcf/Lef (*15*, *16*), and Hbp1/Bbx (*17*) families (Fig. 1C). In most cases, our data are roughly consistent with known binding sequences (Fig. 1C), although there are also clear differences: Hpb1 and Bbx have been described as preferring WRAATGGG (*17*), whereas in our data, Hbp1 and Bbx prefer TGAATG and have lesser preference for AATGGG. Our data confirm that there are at least four different varieties of Sox and Sox-related DNA binding specificity (Fig. 1C) and suggest that there are subtle variations among Sox proteins (Fig. 1B).

Several TFs had two distinct sets of high-scoring *k*-mers. For example, the nuclear receptor

[1]Banting and Best Department of Medical Research, University of Toronto, Toronto, ON M5S 3E1, Canada. [2]Division of Genetics, Department of Medicine, Brigham and Women's Hospital and Harvard Medical School, Boston, MA 02115, USA. [3]Committee on Higher Degrees in Biophysics, Harvard University, Cambridge, MA 02138, USA. [4]Harvard–Massachusetts Institute of Technology (MIT) Division of Health Sciences and Technology, Harvard Medical School, Boston, MA 02115, USA. [5]Department of Molecular Genetics, University of Toronto, Toronto, ON M5S 1A8, Canada. [6]Department of Biology, MIT, Cambridge, MA 02139, USA. [7]Department of Biology, Wellesley College, Wellesley, MA 02481, USA. [8]Department of Physics, MIT, Cambridge, MA 02139, USA. [9]Department of Computer Science, University of Toronto, Toronto, ON M5S 3G4, Canada. [10]Terrence Donnelly Centre for Cellular and Biomolecular Research, University of Toronto, Toronto, ON M5S 3E1, Canada. [11]Department of Pathology, Brigham and Women's Hospital and Harvard Medical School, Boston, MA 02115, USA.

*These authors contributed equally to this work.
†To whom correspondence should be addressed. E-mail: t.hughes@utoronto.ca (T.R.H.); mlbulyk@receptor.med.harvard.edu (M.L.B.)

hepatic nuclear factor 4 alpha [Hnf4a; C4 zinc finger (ZnF) DBD] exhibits strong binding to both sequences containing GGTCCA and sequences containing GGTCCA (Fig. 2A), whereas all four other C4 ZnF TFs that we examined bind only to GGTCA. We confirmed binding of Hnf4a to both variants by EMSA (fig. S10). TFs that can recognize two distinctly different DNA sequences have been noted before (*18*). We

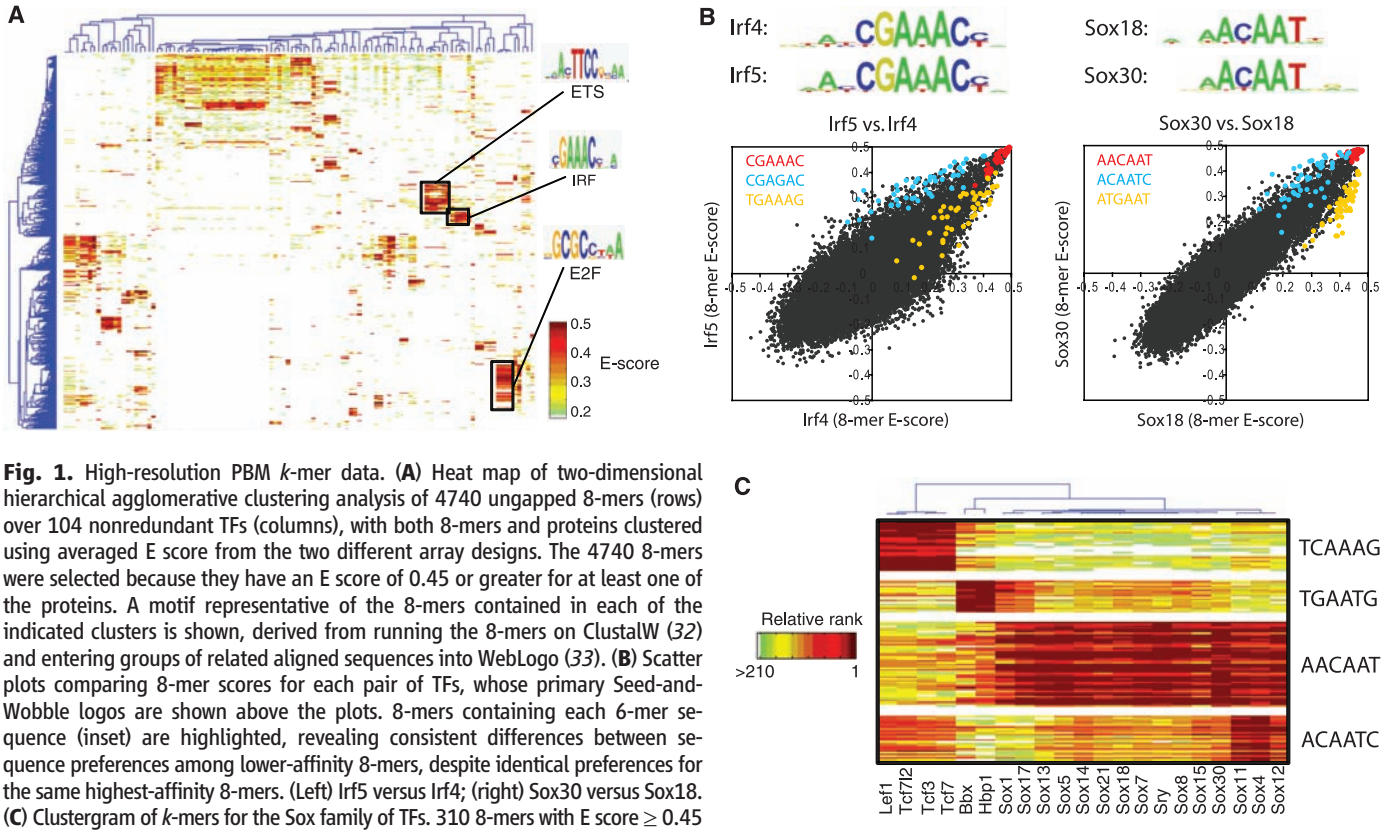

Fig. 1. High-resolution PBM *k*-mer data. (**A**) Heat map of two-dimensional hierarchical agglomerative clustering analysis of 4740 ungapped 8-mers (rows) over 104 nonredundant TFs (columns), with both 8-mers and proteins clustered using averaged E score from the two different array designs. The 4740 8-mers were selected because they have an E score of 0.45 or greater for at least one of the proteins. A motif representative of the 8-mers contained in each of the indicated clusters is shown, derived from running the 8-mers on ClustalW (*32*) and entering groups of related aligned sequences into WebLogo (*33*). (**B**) Scatter plots comparing 8-mer scores for each pair of TFs, whose primary Seed-and-Wobble logos are shown above the plots. 8-mers containing each 6-mer sequence (inset) are highlighted, revealing consistent differences between sequence preferences among lower-affinity 8-mers, despite identical preferences for the same highest-affinity 8-mers. (Left) Irf5 versus Irf4; (right) Sox30 versus Sox18. (**C**) Clustergram of *k*-mers for the Sox family of TFs. 310 8-mers with E score $\geq$ 0.45 for at least one of the 21 Sox and Sox-related TFs were hierarchically clustered according to their relative ranks for each TF, and then the rows, corresponding to *k*-mers, were rearranged to group together 8-mers with shared sequence patterns.

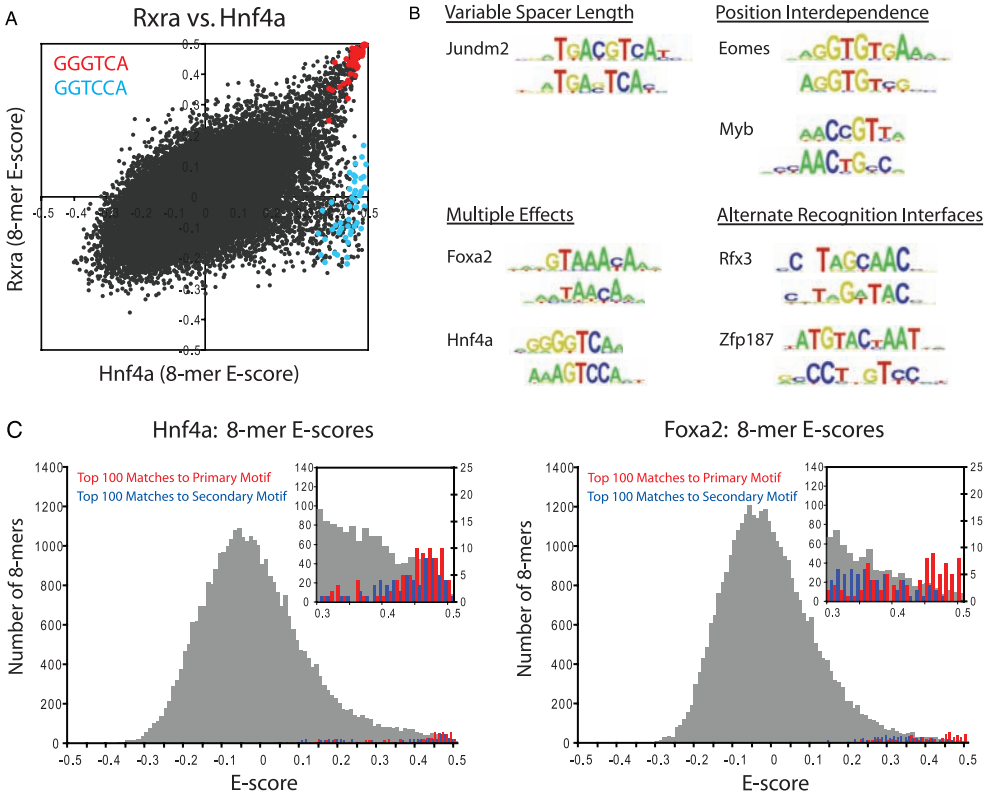

Fig. 2. TF binding site secondary motifs. (**A**) Scatter plot comparing 8-mer E scores for closely related TFs. Hnf4a and Rxra (two C4 zinc finger DBDs) both exhibit strong binding to 8-mers containing GGGTCA (red), whereas Hnf4a shows specific binding to an additional set of 8-mers containing GGTCCA (blue). (**B**) Examples of motifs from different categories of secondary motifs. (**C**) Histograms of E scores for all 8-mers (gray), the top 100 8-mer matches to the primary motif (red), and the top 100 8-mer matches to the secondary motif (blue). 8-mers were scored for matches to PWMs according to the GOMER (*27*) scoring framework. Insets provide a magnified display of the tails of the distributions; *y*-axis labels along the right of each inset refer to the red and blue bars. On the basis of the 8-mer scores, the primary and secondary Hnf4a motifs are essentially interchangeable (left), whereas Foxa2 shows a clear preference for 8-mers corresponding to its primary motif (right).

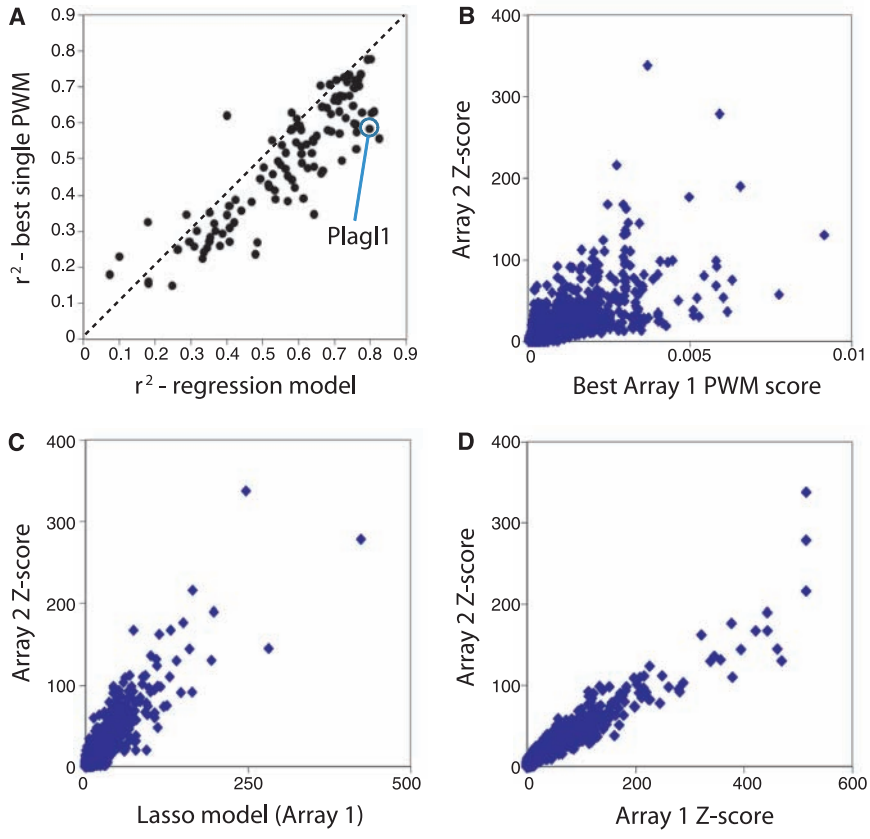

Fig. 3. Multiple-motif models typically better represent the binding profiles than do single-motif models. (**A**) Considering all TFs in this study, in general, multiple-motif models are a better representation of the data than are single-motif models. Variance in 8-mer median intensity (Z score) on Array 2 explained by our PWM regression model (*x* axis) compared to GOMER (*27*) scores for the single best PWM model obtained (best is defined as highest variance explained) over all 8-mers, with models derived from Array 1; the GOMER scoring framework calculates binding probabilities over the 8-mers according to PWMs (*27*). Each point represents one of the TFs analyzed. (**B**) The GOMER score for the best PWM derived from Array 1 is compared to the Z scores from Array 2, for Plagl1 as a case example. Each point is a single 8-mer; all 32,896 8-mers are shown. (**C**) Same as (B), except that the Array 1 regression model scores [which are a linear combination, built by using the least absolute shrinkage and selection operator (Lasso) algorithm (*34*), of GOMER scores from individual motifs] are compared to the Z scores from Array 2. (**D**) 8-mer Z scores for Plagl1 derived from Array 1 compared to the Z scores from Array 2. Each point is a single 8-mer; all 32,896 8-mers are shown.

hypothesized that the existence of secondary motifs may be a general phenomenon, and therefore, we searched for alternate binding preferences throughout our entire data set.

To aid in the identification of secondary binding preferences, we further developed our Seed-and-Wobble algorithm to search specifically for motifs that represent the *k*-mers of high signal intensity that are not explained well by the primary motif; we refer to these as the secondary motifs. A further iteration can be employed to search for a tertiary motif. As an initial test case, we examined PBM data for the human TF Oct-1 (*3*); the PBM-derived Oct-1 primary motif corresponded to the full Oct-1 DNA binding site motif, whereas the secondary and tertiary motifs corresponded to the binding site motifs of the POU_{HD} and POU_S domains (*19*), respectively (fig. S11). Analysis of 100 simulated long, 14–base pair (bp) motifs (*5*) indicated that Seed-and-Wobble was highly successful in identifying the simulated motifs and that essentially all of the secondary motifs we found in analyzing the real PBM data were unlikely to be attributable to a motif-finding artifact due to long motifs (*5*).

We observed clear secondary DNA binding preferences for nearly half of our 104 mouse TFs. Their secondary motifs fell into four different categories (Fig. 2B and supporting online material text), which we annotated manually. We confirmed binding to the secondary motifs by 6 TFs—Hnf4a, Nkx3.1, Myb, Mybl1, Foxj3, and Rfxdc2—by EMSAs (fig. S10).

We found 19 clear cases of "position interdependence" TFs, which exhibited strong interdependence (*20*) among the nucleotide positions of their binding sites. Position interdependencies frequently spanned more than just dinucleotides; for example, estrogen related receptor alpha has a strong preference for binding either CAAGGTCA or AGGGGTCA, but not CAGGGTCA or CGGGGTCA. Interdependent nucleotide positions were not always adjacent to each other; for example, Myb (fig. S10) exhibited strong interdependence at positions separated by 1 nucleotide,

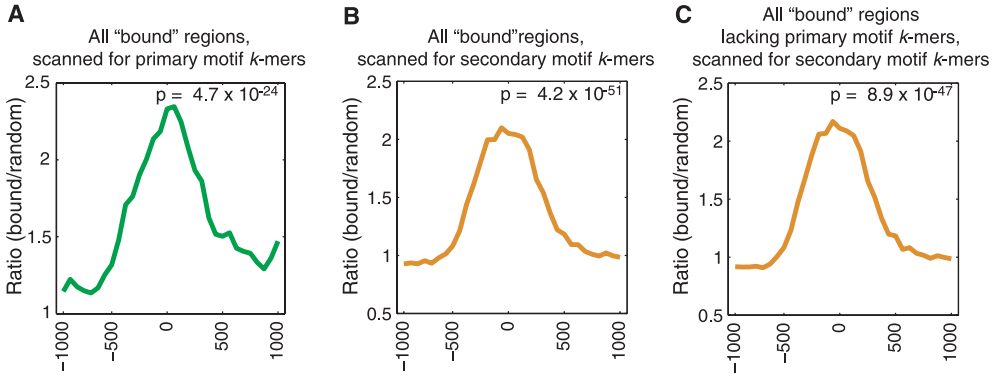

Fig. 4. Enrichment of primary versus secondary motif sequences bound in vitro within genomic regions bound in vivo. Relative enrichment of *k*-mers corresponding to the primary versus secondary Seed-and-Wobble motifs within (**A**) and (**B**) all bound genomic regions in ChIP-chip data or (**C**) those bound regions lacking primary motif *k*-mers, as compared to randomly selected sequences, was calculated (*5*) for Hnf4a (Gene Expression Omnibus accession number GSE7745). ChIP-chip "bound" peaks were identified according to the criteria of that study (*28*). A window size of 500 bp with a step size of 100 bp was used. The GOMER thresholds used are 2.958×10^{-7} and 8.419×10^{-7}, corresponding to 9 primary and 20 secondary 8-mers scanned, respectively, for Hnf4a. *P* values for enrichment of 8-mers within the bound genomic regions shown in each panel were calculated for the interval from −250 to +250 by the Wilcoxon-Mann-Whitney rank sum test, comparing the number of occurrences per sequence in the bound set versus the background set.

with preference for binding either AACCGTCA or AACTGCCA. Although position interdependence has been observed (*21*–*25*), that this phenomenon occurs on such a broad scale was not known and has important implications because commonly used TF binding site models assume mononucleotide independence.

One protein, the mouse transcriptional regulator Jundm2, which is a member of the basic leucine zipper structural class, bound to a "variable spacer length" motif (fig. S12). "Multiple effects" motifs appeared to display a combination of position interdependence and variable distances separating different parts of their motifs; at least 16 TFs fell into this category.

Finally, at least five secondary motifs in the "alternate recognition interfaces" category were not readily explainable by either a variable spacer length or position interdependence. This category is the most intriguing, as it suggests that some TFs recognize their DNA binding sites through multiple, completely different interaction modes, either through alternate structural features or by switching between alternate conformations. Support for this hypothesis comes from the co-crystal structure of human Rfx1 bound to DNA, which indicated that Rfx1 uses β strands and a connecting loop to interact with the major groove of one half-site and an α helix to interact with the minor groove of the other half-site (*26*). It is likely that Rfx3, Rfx4, and Rfxdc2 use this same mechanism of alternative DNA recognition modes (fig. S13).

For several TFs, the secondary motifs were bound nearly as well as the primary motifs, whereas in most cases, the motifs represented different affinity classes. For example, the top 20 8-mers that matched Hnf4a's primary motif were fairly evenly intermingled [$P = 0.037$ by Wilcoxon-Mann-Whitney U test, using GOMER (generalizable occupancy model of expression regulation) (*27*) scoring of motifs] with those that matched its secondary motif (Fig. 2C, left). In contrast, for Foxa2, the secondary motif represented lower-affinity binding sequences ($P = 1.94 \times 10^{-6}$) (Fig. 2C, right).

We further considered the possibility that some proteins' DNA binding specificities might be represented best by multiple motifs. We applied a linear regression approach (*5*) to learn weighted combinations of position weight matrices (PWMs) generated from several different motif-finding algorithms. We found that the binding profiles for all but 15 proteins were represented best by more than one motif (Fig. 3 and fig. S14). Some of these multiple motifs did not appear to represent different protein-DNA interaction properties described above, but nevertheless, they captured different subsets of the *k*-mer data.

We explored the in vivo usage of the secondary motifs by considering their TF occupancy. We calculated the relative enrichment of 8-mers corresponding to the primary versus secondary Seed-and-Wobble motifs within genomic regions bound in ChIP-chip data, as compared with randomly selected sequences (*5*) for Hnf4a (Fig. 4 and fig. S15, A, C, and D). As expected, Hnf4a-bound regions are enriched for matches to 8-mers corresponding to the primary motif for Hnf4a PBM data, with the greatest enrichment toward the centers of the bound regions (Fig. 4A). Hnf4a-bound regions are also enriched for matches to 8-mers corresponding to the secondary motif (Fig. 4B). Hnf4a secondary motif 8-mers are enriched even among those Hnf4a-bound regions that lack primary motif 8-mers (Fig. 4C), suggesting that the secondary motif can recruit Hnf4a to genomic loci independently of the primary motif. We observed similar results for Bcl6 (*28*) (fig. S15).

Our characterization of 104 TFs from 22 different structural classes revealed a prevalence of complexity and richness in DNA binding preferences, both across and within classes. The breadth of the observed "secondary motif" phenomenon had not been described before, and it has important implications for understanding how proteins interact with their DNA binding sites and for genome analysis.

Further experiments and analyses are needed to determine whether the same TF exerts different gene regulatory effects through distinct sequence motifs, as well as to determine whether TF-specific differences among members of a TF family (*29*) contribute to differences in binding in vivo and to distinct physiological functions. Although TFs bind a rich spectrum of *k*-mers not fully captured even by multiple PWMs, using a multiple-motif model is of practical consequence because most genome analysis tools employ PWMs. Algorithms that consider the quantitative nature of *k*-mer binding data in scoring candidate regulatory elements need to be developed.

Finally, these PBM data are likely to be highly informative for well-conserved homologs in other organisms. Generating [or inferring (*29*)] PBM data for all regulatory factors in all major model organisms is an important goal, as such *k*-mer data probably will be useful for improved prediction and analysis of regulatory elements, including the identification of direct versus indirect TF binding sites from ChIP data (*30*). Moreover, such data would aid in understanding the evolution of cis regulatory elements and transcriptional regulatory networks.

References and Notes

1. A. Tanay, *Genome Res.* **16**, 962 (2006).
2. E. Segal, T. Raveh-Sadka, M. Schroeder, U. Unnerstall, U. Gaul, *Nature* **451**, 535 (2008).
3. M. F. Berger *et al.*, *Nat. Biotechnol.* **24**, 1429 (2006).
4. M. Z. Li, S. J. Elledge, *Nat. Genet.* **37**, 311 (2005).
5. Materials and methods are available as supporting material on *Science* Online.
6. M. L. Bulyk, X. Huang, Y. Choo, G. M. Church, *Proc. Natl. Acad. Sci. U.S.A.* **98**, 7158 (2001).
7. S. Mukherjee *et al.*, *Nat. Genet.* **36**, 1331 (2004).
8. M. F. Berger, M. L. Bulyk, *Nat. Protocols* **4**, 393 (2009).
9. X. Chen, T. R. Hughes, Q. Morris, *Bioinformatics* **23**, i72 (2007).
10. S. J. Maerkl, S. R. Quake, *Science* **315**, 233 (2007).
11. V. Matys *et al.*, *Nucleic Acids Res.* **34**, D108 (2006).
12. S. V. Orlov *et al.*, *FEBS J.* **274**, 4848 (2007).
13. J. M. Bosher, N. F. Totty, J. J. Hsuan, T. Williams, H. C. Hurst, *Oncogene* **13**, 1701 (1996).
14. S. Mertin, S. G. McDowall, V. R. Harley, *Nucleic Acids Res.* **27**, 1359 (1999).
15. M. van de Wetering, M. Oosterwegel, D. Dooijes, H. Clevers, *EMBO J.* **10**, 123 (1991).
16. A. Travis, A. Amsterdam, C. Belanger, R. Grosschedl, *Genes Dev.* **5**, 880 (1991).
17. S. G. Tevosian *et al.*, *Genes Dev.* **11**, 383 (1997).
18. K. Pfeifer, T. Prezant, L. Guarente, *Cell* **49**, 19 (1987).
19. J. D. Klemm, M. A. Rould, R. Aurora, W. Herr, C. O. Pabo, *Cell* **77**, 21 (1994).
20. P. V. Benos, M. L. Bulyk, G. D. Stormo, *Nucleic Acids Res.* **30**, 4442 (2002).
21. P. V. Benos, A. S. Lapedes, G. D. Stormo, *Bioessays* **24**, 466 (2002).
22. M. L. Bulyk, P. L. Johnson, G. M. Church, *Nucleic Acids Res.* **30**, 1255 (2002).
23. M.-L. Lee, M. Bulyk, G. Whitmore, G. Church, *Biometrics* **58**, 981 (2002).
24. T. K. Man, G. D. Stormo, *Nucleic Acids Res.* **29**, 2471 (2001).
25. Y. Barash, G. Elidan, N. Friedman, T. Kaplan, paper presented at the Proceedings of the 7th Annual International Conference on Computational Molecular Biology (RECOMB), Berlin, 10 to 13 April 2003.
26. K. S. Gajiwala *et al.*, *Nature* **403**, 916 (2000).
27. J. A. Granek, N. D. Clarke, *Genome Biol.* **6**, R87 (2005).
28. S. M. Ranuncolo *et al.*, *Nat. Immunol.* **8**, 705 (2007).
29. M. F. Berger *et al.*, *Cell* **133**, 1266 (2008).
30. C. Zhu *et al.*, *Genome Res.* **19**, 556 (2009).
31. D. E. Newburger, M. L. Bulyk, *Nucleic Acids Res.* **37**, D77 (2009).
32. R. Chenna *et al.*, *Nucleic Acids Res.* **31**, 3497 (2003).
33. G. E. Crooks, G. Hon, J. M. Chandonia, S. E. Brenner, *Genome Res.* **14**, 1188 (2004).
34. R. Tibshirani, *J. R. Stat. Soc. Ser. B Methodol.* **58**, 267 (1996).

35. This project was supported by funding from the Canadian Institutes of Health Research (MOP-77721 and postdoctoral fellowship to G.B.); Genome Canada through the Ontario Genomics Institute, the Ontario Research Fund, and the Canadian Institute for Advanced Research (to T.R.H.); NSF (to M.F.B.); the Canadian Foundation for Innovation and Ontario Research Fund (to Q.M.); and grant R01 HG003985 from NIH/National Human Genome Research Institute (to M.L.B.). We thank L. Peña-Castillo, A. Cheung, M. Chan, S. Bhinder, F. Bréard, P. Qureshi, S. Mnaimneh, M. Kekis, F. Khalid, J. Holroyd, D. Terterov, and K. Robasky for technical assistance and S. Gisselbrecht, K. Struhl, and S. Sunyaev for critical reading of the manuscript. PBM data are available at http://the_brain.bwh.harvard.edu/pbms/webworks/ and also via the publicly available UniPROBE database (*31*).

Supporting Online Material

www.sciencemag.org/cgi/content/full/1162327/DC1
Materials and Methods
SOM Text
Figs. S1 to S15
Tables S1 to S3
References

25 June 2008; accepted 1 May 2009
Published online 14 May 2009;
10.1126/science.1162327
Include this information when citing this paper.

Genomic Footprints of a Cryptic Plastid Endosymbiosis in Diatoms

Ahmed Moustafa,[1]* Bánk Beszteri,[2]* Uwe G. Maier,[3] Chris Bowler,[4,5] Klaus Valentin,[2] Debashish Bhattacharya[1,6]†

Diatoms and other chromalveolates are among the dominant phytoplankters in the world's oceans. Endosymbiosis was essential to the success of chromalveolates, and it appears that the ancestral plastid in this group had a red algal origin via an ancient secondary endosymbiosis. However, recent analyses have turned up a handful of nuclear genes in chromalveolates that are of green algal derivation. Using a genome-wide approach to estimate the "green" contribution to diatoms, we identified >1700 green gene transfers, constituting 16% of the diatom nuclear coding potential. These genes were probably introduced into diatoms and other chromalveolates from a cryptic endosymbiont related to prasinophyte-like green algae. Chromalveolates appear to have recruited genes from the two major existing algal groups to forge a highly successful, species-rich protist lineage.

Diatoms are well-studied members of the putative supergroup Chromalveolata [fig. S1 and supporting online material (SOM) text] and comprise unicellular, photosynthetic, dominant taxa in the marine phytoplankton. Diatoms are central to understanding oceanic primary production and biogeochemistry (*1*). Much effort is currently being expended to develop some taxa as models for genetic and genomic research as well as sources for biofuel (*2*) and nanotechnology (*3*). We conducted a phylogenomic analysis of the diatom proteome using complete genome data from *Thalassiosira* and *Phaeodactylum*. This procedure identified 2423 and 2533 (2423/2533) *Phaeodactylum* and *Thalassiosira* genes, respectively (this order of results is used throughout the paper and SOM), that are derived from red or green algal sources. Contrary to the expectation of the chromalveolate hypothesis (*4*), however, >70% of these genes are of green (not red) lineage provenance (Fig. 1, table S1, and fig. S7). This green gene contribution constitutes ≈16% of the diatom proteome. Two of the major topological classes that were uncovered are shown in fig. S2. The first class (fig. S2A) contains 442/442 trees in which both red and green algae are present, but there is robust bootstrap support for the green algae plus diatom (and other chromalveolates) clade. Of these trees, 144/133 show the green algal and diatom sequences to diverge within the Plantae kingdom, which is composed of green algae and plants, glaucophytes, and red algae (*5*, *6*). An example is phytoene desaturase (fig. S2A), which is an early enzyme in plastid carotenoid biosynthesis. It was previously reported that 5 of the 16 genes in this photoprotective pathway are of green algal origin (*7*), and their occurrence in chromalveolates probably ensures a high photosynthetic efficiency under fluctuating light (*8*). The remaining 298/309 trees indicate an independent origin of the gene in the donor green algae, with respect to other Plantae. A second major class of trees shows an independent gene origin in prasinophytes relative to other green algae and plants, before being transferred to diatoms and other chromalveolates (Fig. 2). The absence of red algal homologs in some trees in this class may be explained by gene loss in the reduced nuclear genome of the red algal representative in our database, *Cyanidioschyzon merolae* (SOM text). An example tree from this class is a member of the isoprenylcysteine carboxyl methyltransferase superfamily (fig. S2B). We found four genes that encode the following gene products: naphthoate synthase (GenBank GI number 219114006), heme oxygenase (GenBank GI number 219117865), pyruvate dehydrogenase (GenBank GI number 219119135), and GUN4-like protein (GenBank GI number 219127880), which are retained in red algal plastid genomes but absent from this red-derived organelle genome in diatoms. These sequences are present in the diatom nucleus but are of green algal derivation. This suggests that red plastid–encoded genes were lost if green homologs were already present in the host nucleus.

To identify the putative sources of the diatom green genes, we examined their distribution among the green lineages (Viridiplantae). The Viridiplantae comprise two well-supported phyla, the Chlorophyta (most green algae, such as *Chlamydomonas*, in the core chlorophytes and the prasinophytes) and the Streptophyta (charophyte green algae and all land plants; Fig. 2A). The prasinophytes include the world's smallest eukaryotes (the picoeukaryote *Ostreococcus*; cell diameter ≈1 μm), which are part of a morphologically diverse group of paraphyletic lineages diverging at the base of the Chlorophyta (*9*). We found that 637/716 diatom green genes (36/41%) trace their origin to the prasinophytes in our data set (*Micromonas* and *Ostreococcus*; Mamiellales clade) of which 167/175 are shared with other Chlorophyta (71/67 genes; *Chlamydomonas* and *Volvox*) or Streptophyta (23/40 genes; *Arabidopsis*, *Oryza*, *Physcomitrella*, and *Zea*) or by both phyla (73/68 genes; Fig. 2B). These 167/175 genes have a putative ancient origin in Viridiplantae. Streptophyte- and core chlorophyte–specific donors account for 192/177 and 145/170 genes, respectively (Fig. 2C). Many of these genes may ancestrally have been present in the Viridiplantae and lost by prasinophytes and/or other green lineage members, whereas the remainder represent independent horizontal gene transfers (HGTs) into streptophytes and core chlorophytes. In spite of the reduced nuclear genome of the prasinophytes in our study (≈9000 protein-encoding genes) as compared to the larger genomes of core chlorophytes and streptophytes (≈15,000 and ≈30,000 protein-encoding genes, respectively), 470/541 genes are shared exclusively between prasinophytes and diatoms (Fig. 2, B and C), of which 462/502 (98 and 93%) are present in expressed sequence tag (EST) libraries from *Phaeodactylum* and *Thalassiosira*. Because of their specific affiliation with picoprasinophytes, these genes are unlikely to represent missing sequences from *Cyanidioschyzon*. This diatom green gene set may therefore be gene recruitments via HGT in picoprasinophytes that were later trans-

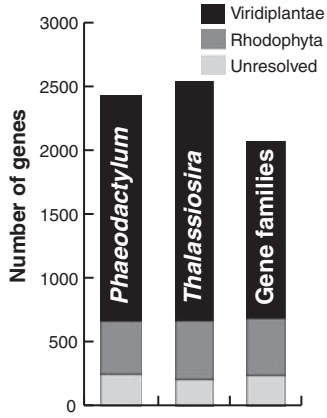

Fig. 1. Diatom genes of a red or green algal origin that were identified using phylogenomic analysis of complete genome data. Each bar represents the total number of algal genes in the corresponding diatom species. The "gene families" bar indicates the total number of transferred genes in both diatoms after clustering the data into gene families through single-linkage hierarchical clustering. The "unresolved" category indicates that red and green algae are sisters of each other in the tree and monophyletic with diatoms (and other chromalveolates).

[1]Interdisciplinary Program in Genetics, University of Iowa, Iowa City, IA 52242, USA. [2]Alfred Wegener Institute for Polar and Marine Research, Am Handelshafen 12, 27570 Bremerhaven, Germany. [3]Zellbiologie, Philipps-Universität Marburg, Marburg, Germany. [4]CNRS UMR8186, Department of Biology, Ecole Normale Supérieure, 46 rue d'Ulm, 75005 Paris, France. [5]Stazione Zoologica Anton Dohrn, Villa Comunale, I-80121 Naples, Italy. [6]Department of Biological Sciences and the Roy J. Carver Center for Comparative Genomics, University of Iowa, Iowa City, IA 52242, USA.

*These authors contributed equally to this work.
†To whom correspondence should be addressed. E-mail: debashi-bhattacharya@uiowa.edu

ferred to the diatom (chromalveolate) nucleus. These sequences could hold clues to the evolution of prasinophyte green algae and their great success in different aquatic environments (*10*).

The fourfold higher abundance of green versus red genes in diatoms raises questions about the timing of the transfer of the green genes and whether these sequences were introduced via a single or multiple endosymbioses, or by unprecedented levels of HGT in chromalveolates. In order to address this issue, we determined the distribution of diatom green genes among chromalveolates using complete genome data. Here, the distinction between gene origins via endosymbiotic gene transfer (EGT) (*11*) versus HGT reflects whether the genes can be traced back to a point source (prasinophyte-like algae) and are found in most if not all chromalveolates, versus sporadic gene origin in particular lineages and from multiple different sources, respectively. Neither of these outcomes is proof but rather argues for or against one hypothesis. Using this approach, we find that 85% of the green genes can be traced back to the ancestor of both diatoms and other Stramenopiles (Fig. 3). Diatoms share 46/55 green genes with the obligate parasites apicomplexans and 54/63 genes with the plastid-lacking ciliates. Analysis of genome data from the distantly related photosynthetic coccolithophorid *Emiliania huxleyi*, which is a haptophyte sister to cryptophytes (fig. S1), identified >400 green genes shared with diatoms. The inclusion of ESTs from dinoflagellates and cryptophyte algae shows that even when these partial data are used, 10 and 3% of the diatom green genes are shared with these groups, respectively (fig. S3). Given these results, we suggest that despite extensive gene losses among nonphotosynthetic lineages such as ciliates and apicomplexans, the most likely explanation is that a large proportion of the diatom green genes is of an ancient provenance and predate the split of cryptophytes and haptophytes from other chromalveolates.

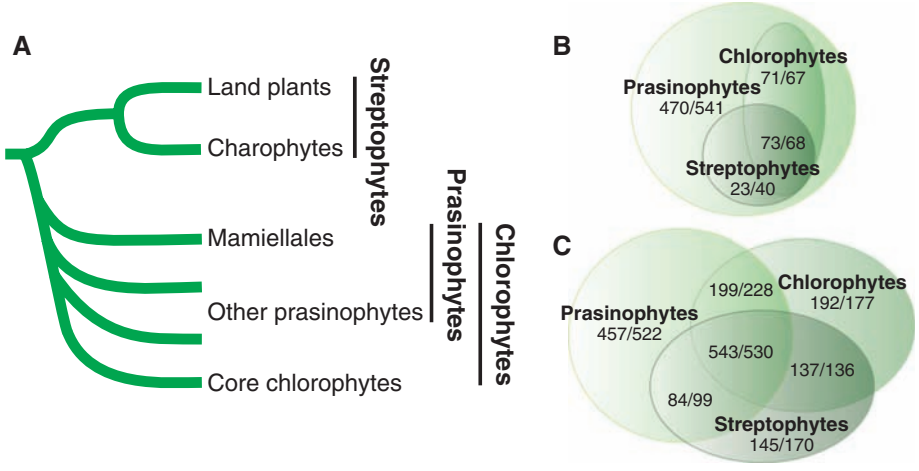

Fig. 2. Phylogenetic distribution of diatom genes of green algal origin among Viridiplantae. (**A**) Schematic tree that illustrates well-accepted phylogenetic relationships within the green lineage. (**B**) Venn diagram depicting the distribution of diatom green genes of prasinophyte origin. These genes support a specific sister-group relationship between prasinophytes and diatoms (and other chromalveolates). The two broad categories of gene sharing are as follows: (i) the gene is exclusive to prasinophytes (470/541), and (ii) the gene is shared with other Viridiplantae. (**C**) Venn diagram depicting the distribution of all diatom green genes among Viridiplantae. Here, 192/177 genes are of chlorophyte origin, whereas 145/170 genes are apparently derived from streptophytes. It should be noted that these are provisional values and will be affected by the strength of the phylogenetic signal in any given protein or the absence of data from particular groups; that is, some apparently streptophyte-specific diatom green genes may simply be explained by the loss of the genes in other Viridiplantae (such as prasinophytes).

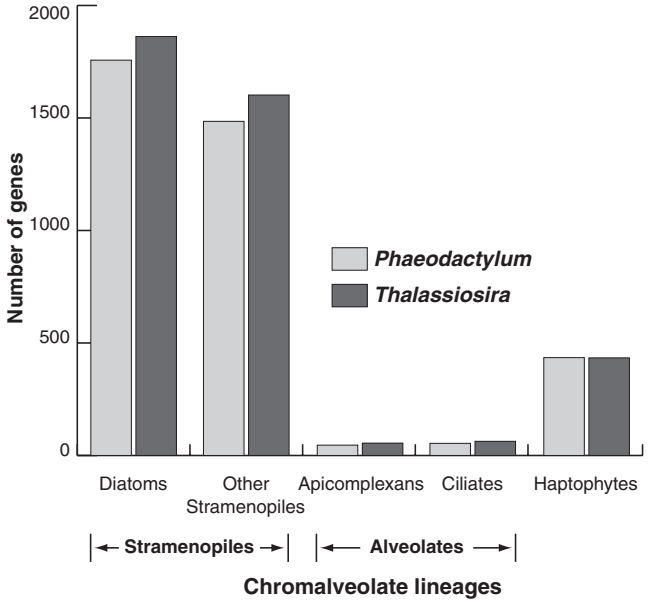

Fig. 3. The distribution of diatom green genes among different chromalveolates. The value for each major chromalveolate lineage represents the number of proteins that satisfy two phylogenetic criteria: (i) monophyly of diatoms and the chromalveolate lineage in question, and (ii) monophyly of this clade with Viridiplantae. The category "other Stramenopiles" includes the pelagophyte *Aureococcus anophagefferens* and the oomycetes *Phytophthora capsici*, *P. ramorum*, and *P. sojae*, which have complete nuclear genome data available. Data from the remaining taxa in this category are organelle- or EST-derived.

Taken together, our results provide evidence of a prasinophyte-like endosymbiont in the common ancestor of chromalveolates. As discussed above, prasinophytes are an anciently diverged paraphyletic group of green algae (*12*) that was present early on in chromalveolate evolution. In the fossil record, prasinophytes are widely distributed by the Early Cambrian (*13*). These cells may well have been an abundant prey source for the chromalveolate ancestor. The alternative explanation of chromalveolate polyphyly would imply an unprecedented number of independent gains (≈400) of the same green genes by diatoms and haptophytes. Therefore, our results provide strong support for a shared evolutionary history for these disparate chromalveolate lineages. In substantiated cases of serial endosymbiosis, the most recent endosymbiont provides the plastid, whereas the nuclear genome bears the footprints of past events. The dinoflagellates provide several independent examples of this phenomenon with the replacement of the broadly distributed red algal (peridinin-containing) plastid in different taxa with one of green, cryptophyte, or diatom origin (*14*, *15*). Therefore, the presence of a red algal–derived plastid in most photosynthetic chromalveolates is most easily explained by the green algal endosymbiosis having predated the red algal capture (*7*, *16*, *17*).

A different interpretation of our green gene data is that these sequences did not derive from EGT and HGT but rather support a bona fide sister-group relationship between chromalveolates and green algae. Under this scenario, the chromalveolate ancestor contained a plastid of primary endosymbiotic origin [cyanobacterial (*18*)] that was shared with the green lineage and subsequently replaced by one of secondary (red algal) derivation. Although possible, this scenario is highly implausible because it not only argues against Plantae monophyly, which has been supported by recent phylogenomic studies (*6*, *19*), but more importantly, demands that the vast majority of chromalveolate nuclear genes with nonplastid functions

(actin and tubulins) be directly related to Viridiplantae. Although most single- and multigene trees clearly demonstrate Viridiplantae monophyly (*20*), they do not, however, support a specific affiliation between greens and chromalveolates. There is no reason to expect that this phylogenetic signal would have been lost from chromalveolate genomes while being retained by Viridiplantae. Therefore, given the known proclivity of endosymbiosis to drive intracellular gene transfer (*21*, *22*) and the absence of evidence for a specific phylogenetic relationship between Viridiplantae and chromalveolates, outside of the 16% reported here, we suggest that the green "footprint" in chromalveolates (although substantial) probably reflects a combination of EGT and HGT rather than a host affiliation.

The rise to prominence in the oceans by diatoms and other chromalveolates such as dinoflagellates and haptophytes after the end-Permian mass extinction (250 million years ago) has been interpreted as the victory of red plastid lineages over the predominant green plastid taxa such as prasinophytes. Changing nearshore ocean chemistry is thought to underlie this globally important phenomenon (*13*, *23*). In contrast to current thinking, our findings show that chromalveolates were already green before they acquired the red plastid. Although ancient, these two endosymbioses that were supplemented by subsequent HGTs supplied chromalveolates such as diatoms [≈100,000 extant species (*24*)] with the genetic potential to become some of the most ecologically successful and dominant marine primary producers on our planet.

References and Notes

1. C. B. Field, M. J. Behrenfeld, J. T. Randerson, P. Falkowski, *Science* **281**, 237 (1998).
2. G. C. Dismukes, D. Carrieri, N. Bennette, G. M. Ananyev, M. C. Posewitz, *Curr. Opin. Biotechnol.* **19**, 235 (2008).
3. N. Kroger, N. Poulsen, *Annu. Rev. Genet.* **42**, 83 (2008).
4. T. Cavalier-Smith, *J. Eukaryot. Microbiol.* **46**, 347 (1999).
5. A. Reyes-Prieto, D. Bhattacharya, *Mol. Phylogenet. Evol.* **45**, 384 (2007).
6. N. Rodriguez-Ezpeleta *et al.*, *Curr. Biol.* **15**, 1325 (2005).
7. R. Frommolt *et al.*, *Mol. Biol. Evol.* **25**, 2653 (2008).
8. S. Coesel, M. Obornik, J. Varela, A. Falciatore, C. Bowler, *PLoS One* **3**, e2896 (2008).
9. M. Turmel, M. C. Gagnon, C. J. O'Kelly, C. Otis, C. Lemieux, *Mol. Biol. Evol.* **26**, 631 (2008).
10. E. Derelle *et al.*, *Proc. Natl. Acad. Sci. U.S.A.* **103**, 11647 (2006).
11. W. Martin, H. Brinkmann, C. Savonna, R. Cerff, *Proc. Natl. Acad. Sci. U.S.A.* **90**, 8692 (1993).
12. J. Steinkötter, D. Bhattacharya, I. Semmelroth, C. Bibeau, M. Melkonian, *J. Phycol.* **30**, 340 (1994).
13. P. G. Falkowski, A. H. Knoll, *Evolution of Primary Producers in the Sea* (Elsevier Academic, Amsterdam, 2007).
14. K. Ishida, B. R. Green, *Proc. Natl. Acad. Sci. U.S.A.* **99**, 9294 (2002).
15. T. Tengs *et al.*, *Mol. Biol. Evol.* **17**, 718 (2000).
16. J. Petersen, R. Teich, H. Brinkmann, R. Cerff, *J. Mol. Evol.* **62**, 143 (2006).
17. A. Reyes-Prieto, A. Moustafa, D. Bhattacharya, *Curr. Biol.* **18**, 956 (2008).
18. M. M. Hauber, S. B. Muller, V. Speth, U. G. Maier, *Bot. Acta* **107**, 383 (1994).
19. F. Burki, K. Shalchian-Tabrizi, J. Pawlowski, *Biol. Lett.* **4**, 366 (2008).
20. H. S. Yoon *et al.*, *BMC Evol. Biol.* **8**, 14 (2008).
21. W. Martin *et al.*, *Proc. Natl. Acad. Sci. U.S.A.* **99**, 12246 (2002).
22. A. Reyes-Prieto, J. D. Hackett, M. B. Soares, M. F. Bonaldo, D. Bhattacharya, *Curr. Biol.* **16**, 2320 (2006).
23. H. R. Thierstein, J. R. Young, *Coccolithophores: From Molecular Processes to Global Impact* (Springer, Berlin, 2004).
24. F. E. Round, R. M. Crawford, D. G. Mann, *The Diatoms: Biology and Morphology of the Genera* (Cambridge Univ. Press, Cambridge, 1990).

25. D.B. was supported by grants from NSF and NIH (EF 04-31117 and R01ES013679, respectively). A.M. was supported by an Institutional National Research Service Award (T 32 GM98629) from NIH. U.G.M. thanks the Deutsche Forschungsgemeinschaft (grant SFB-TR1) for support. We thank T. Mock for providing tiling array–generated diatom transcripts and J. E. DeReus at the High Performance Computing Facility at the University of Iowa for technical support.

Supporting Online Material

www.sciencemag.org/cgi/content/full/324/5935/1724/DC1
Materials and Methods
SOM Text
Figs. S1 to S7
Tables S1 and S2
References

3 March 2009; accepted 22 May 2009
10.1126/science.1172983

Solution Nuclear Magnetic Resonance Structure of Membrane-Integral Diacylglycerol Kinase

Wade D. Van Horn,[1]* Hak-Jun Kim,[1,2]* Charles D. Ellis,[1] Arina Hadziselimovic,[1] Endah S. Sulistijo,[1] Murthy D. Karra,[1] Changlin Tian,[1,3] Frank D. Sönnichsen,[4] Charles R. Sanders[1]†

Escherichia coli diacylglycerol kinase (DAGK) represents a family of integral membrane enzymes that is unrelated to all other phosphotransferases. We have determined the three-dimensional structure of the DAGK homotrimer with the use of solution nuclear magnetic resonance. The third transmembrane helix from each subunit is domain-swapped with the first and second transmembrane segments from an adjacent subunit. Each of DAGK's three active sites resembles a portico. The cornice of the portico appears to be the determinant of DAGK's lipid substrate specificity and overhangs the site of phosphoryl transfer near the water-membrane interface. Mutations to cysteine that caused severe misfolding were located in or near the active site, indicating a high degree of overlap between sites responsible for folding and for catalysis.

Escherichia coli diacylglycerol kinase (DAGK) is encoded by the *dgkA* gene and catalyzes the direct phosphorylation of diacylglycerol (DAG) by Mg(II)–adenosine triphosphate (MgATP) to form phosphatidic acid as part of the membrane-derived oligosaccharide (MDO) cycle (*1*–*3*). In Gram-positive organisms, the *dgkA* homolog encodes an undecaprenol kinase, indicating a role in oligosaccharide assembly or in related signaling pathways (*4*). The DAGK homolog in *Streptococcus mutans* is known to be a virulence factor for smooth-surface dental caries (*5*). DAGK was among the first integral membrane enzymes to be solubilized, purified, and mechanistically characterized (*6*). The wild-type protein is very stable (*7*, *8*) and can spontaneously insert into lipid bilayers to adopt its functional fold (*9*, *10*). Paradoxically, DAGK resembles many disease-linked human membrane proteins because it is highly susceptible to mutation-induced misfolding (*10*–*12*). DAGK functions as a 40-kD homotrimer, with a total of nine transmembrane (TM) helices and three active sites (*13*).

The structure of DAGK was determined using solution nuclear magnetic resonance (NMR) methods (*14*) under conditions in which the enzyme is a functional homotrimer solubilized in ~100-kD dodecylphosphocholine micelles; this work extends other solution NMR studies of >20-kD multispan membrane proteins (*15*–*22*). The backbone structure of the helical TM domain of DAGK (residues 26 to 121) was precisely determined by the data (Fig. 1, fig. S1, and table S4); however, motions associated with the N terminus (residues 1 to 25) have hindered determination of its conformation beyond confirming the presence of two stable amphipathic helices.

DAGK's structure bears no resemblance to that of the water-soluble DAGK (*23*) (Fig. 1). The three-fold symmetry axis lies at the center of a parallel left-handed bundle formed by the second transmembrane (TM2) helices of the three subunits. TM2 has previously been proposed to play a central role in DAGK's folding and stability (*24*, *25*) and contains several highly conserved residues (Fig. 1), particularly near the

[1]Department of Biochemistry and Center for Structural Biology, Vanderbilt University, Nashville, TN 37232, USA. [2]Korea Polar Research Institute, Incheon 406-840, Korea. [3]School of Life Science, University of Science and Technology of China, Hefei, Anhui 230026, P. R. China. [4]Otto Diels Institute for Organic Chemistry, Christian Albrechts University of Kiel, D-24098 Kiel, Germany.

*These authors contributed equally to this work.
†To whom correspondence should be addressed. E-mail: chuck.sanders@vanderbilt.edu

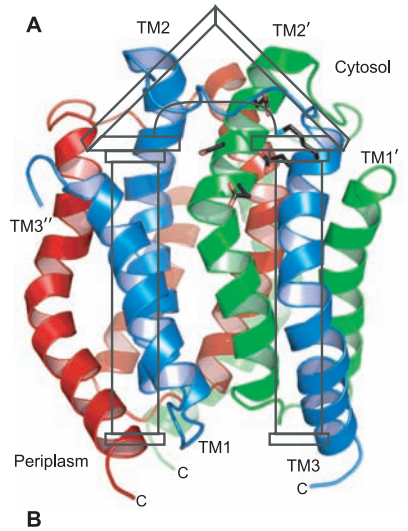

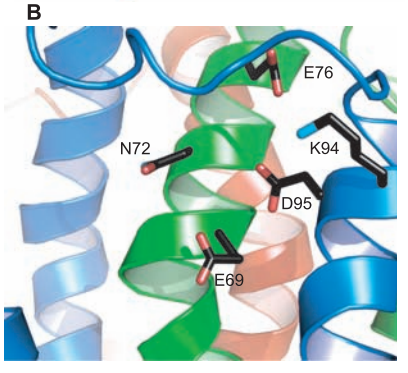

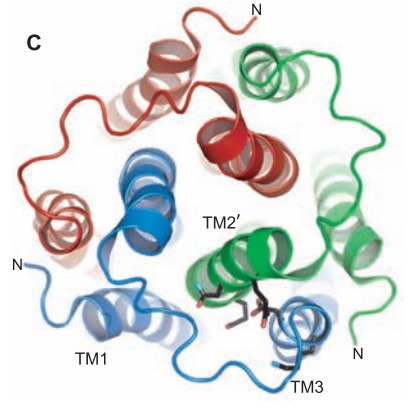

Fig. 1. Structure of diacylglycerol kinase. All panels represent the same conformer from the ensemble of structures (fig. S1). Omitted from this figure is the N terminus (residues 1 to 25), which was not precisely determined, although it is known to comprise two short α helices that extend over residues 6 to 14 and 17 to 23. (**A**) Ribbon diagram of DAGK with inscribed portico viewed from the membrane plane. DAGK's five most highly conserved residues are shown (for a single portico only). (**B**) Ribbon diagram viewed from the membrane plane, showing a close-up of the region of the active site containing DAGK's most highly conserved residues (*35*). (**C**) Ribbon diagram viewed from the cytosol, showing side chains for DAGK's five most highly conserved residues (for a single portico only). The connecting loops between the first and second TM segments have been omitted from view so that the organization of the TM helices can more easily be discerned.

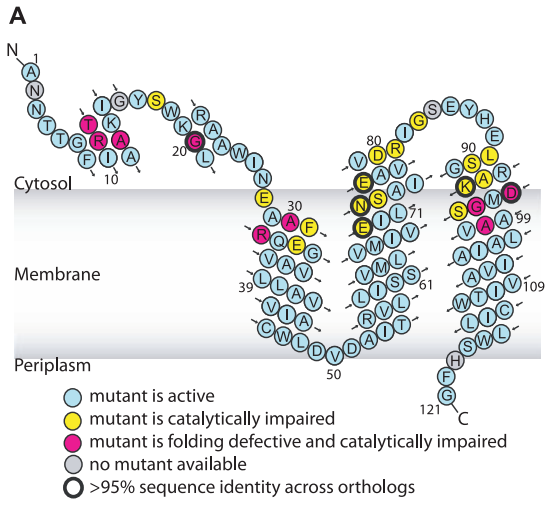

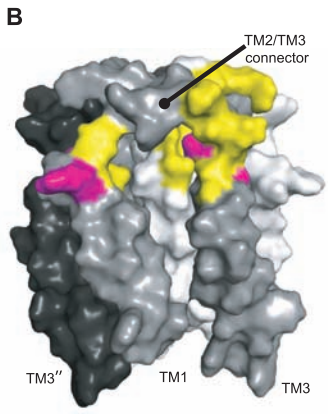

Fig. 2. Identification of sites critical for catalysis and/or for folding, based on the functional analysis of mutants generated by systematically replacing each residue in a cysteineless mutant form of DAGK (*7*) with cysteine (*35*). (**A**) Sites labeled blue designate cysteine mutants that exhibited at least 20% of wild-type activity. Yellow labels indicate sites for which mutants were observed to fold but exhibited less than 20% catalytic activity. Mutation to cysteine at the pink sites resulted in forms of DAGK that were both inactive and misfolded, both in native *E. coli* membranes and after purification and application of normally effective refolding protocols. (**B**) Surface-filled representation of DAGK. Highlighted residues are for a single portico site only (residues are highlighted only for TM1, TM3, and TM2′). Omitted from the surface representations are the imprecisely determined N termini (residues 1 to 25). Specific activities for each mutant are listed in table S1. Details of the folding behavior of mutants that exhibit <15% of wild-type activity are given in table S2. Sites that are indicated as being conserved with >95% identity were identified on the basis of multiple sequence alignment (figs. S2 and S3).

membrane-cytoplasm interface. Characterization of a series of cysteine-replacement mutants for sites in TM2 showed that mutations in this segment often resulted in a marked reduction in catalytic function (Fig. 2 and table S1), underscoring the importance of TM2 to DAGK folding and catalysis.

DAGK is seen to be a domain-swapped homotrimer (Fig. 1C). TM3 makes virtually no contact with TM2 from the same subunit. Instead, it packs against the hairpin formed by the first and second TM segments from an adjacent subunit (TM1′ and TM2′). Domain swapping may contribute to the high stability of wild-type DAGK (*7*, *8*). Conversely, domain swapping may illuminate why DAGK mutants are often difficult to refold after denaturation (*11*).

A distinctive feature of the DAGK structure is a membrane-submerged cavity that resembles a portico (Figs. 1A and 2B and fig. S1). TM1 and TM3 serve as the pillars that bound the entry, terminating at an inner wall formed by TM2′ from a neighboring subunit, and crowned by an overhanging cornice comprising the connecting loop between TM2 and TM3. The portico, and in particular the cornice, contains a majority of the residues seen to be functionally essential in our mutagenesis studies (Fig. 2). Each portico contains critical residues that are contributed by two different subunits, consistent with a previous mutagenesis study that showed that each active site is shared between subunits (*13*). Titrations of DAGK with its substrates (MgATP and DAG), product (phosphatidic acid), and a nonhydrolyzable ATP analog (β,γ-methyleneadenosine 5′-triphosphate, AMP-PCP) were monitored by NMR. Saturable changes in NMR resonances upon ligand binding (Fig. 3 and fig. S5) confirmed that the portico includes the lipid substrate binding site of DAGK. The overhanging cornice likely blocks lateral diffusion into the active site of lipids with head groups larger than DAG and phosphatidic acid. On the other hand, the spaciousness of the lower part of the portico explains the lack of specificity of DAGK with respect to the acyl chain composition of diglyceride substrates (*26*). Interactions of membrane enzymes with membranous substrates more typically involve gated internal cavities within the protein or well-structured grooves that confer high specificity for specific substrates (*27*–*29*), although the active site of the homodimeric β barrel outer-membrane phospholipase A also exhibits a portico-like architecture, consistent with the lack of specificity of this enzyme in terms of substrate acyl chains (*27*, *30*).

NMR resonances for three residues located just under the cornice on TM1 and TM2′ exhibited shifts in response to the binding of nucleotides and lipids (Fig. 3). These sites are likely proximal to the site of ATP-to-DAG phosphoryl transfer, consistent with the observed proximity to the cornice of many of the highly conserved and functionally critical residues. We suggest that a second role for the cornice in the active site may

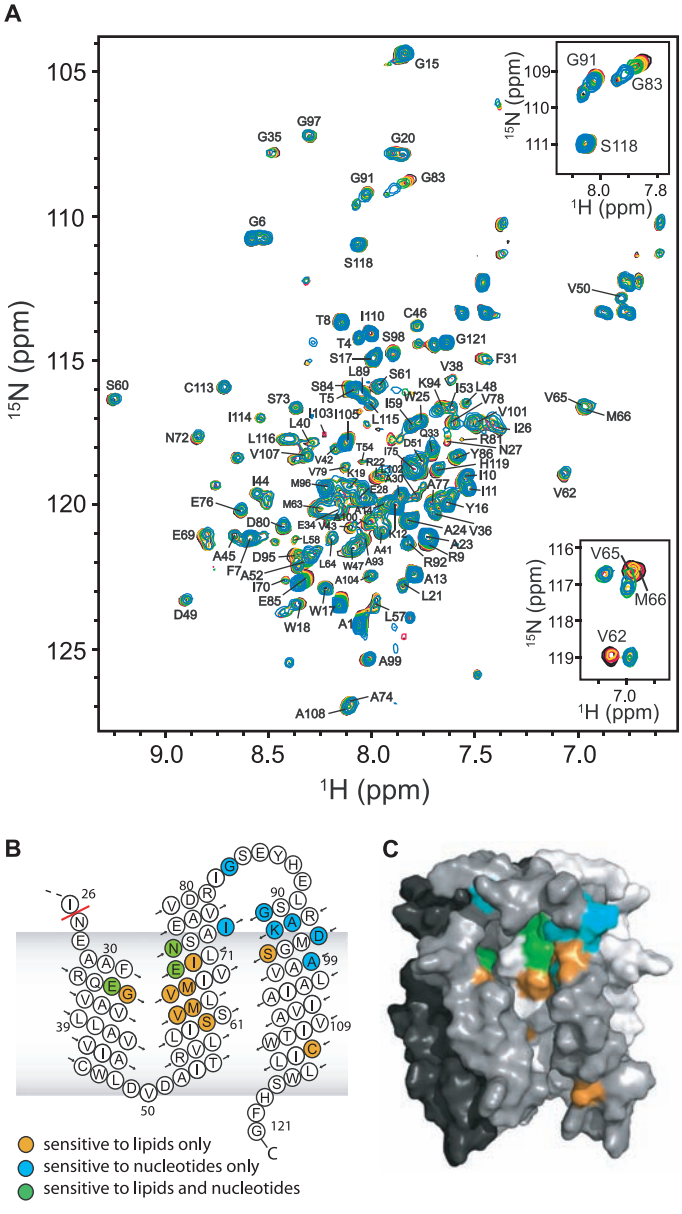

Fig. 3. NMR mapping of the substrate binding sites (*35*). (**A**) Example of 800-MHz ^{1}H,^{15}N-TROSY (transverse relaxation-optimized spectroscopy) NMR spectra used to monitor titration of wild-type DAGK by a substrate, product, or substrate analog. Shown are the overlaid spectra for titration of DAGK by MgAMP-PCP at concentrations of 0 mM (black), 2 mM (red), 4 mM (yellow), 8 mM (green), and 16 mM (blue). Resonances are labeled on the basis of their residue assignments (*36*). Unlabeled peaks reflect the 10% of resonances for which assignments were not completed. NMR data for titrations of DAGK with DAG, phosphatidic acid, and MgATP are shown in fig. S5. Insets: Selected peaks from the MgAMP-PCP titration (upper panel) and from a separate DAG titration (lower panel; see full spectra in fig. S5). The MgAMP-PCP data illustrate fast-exchange NMR conditions in which DAGK peaks gradually change position during the titration, reflecting population-weighted averages between free and complexed forms. In contrast, the data from the DAG titration (lower panel) illustrate slow exchange behavior, where the free enzyme peaks disappear and peaks representing the complex appear at new positions, with contour intensities reflecting the relative populations of the free and complexed states. (**B**) Summary of active-site mapping, highlighting residues associated with TROSY resonances that exhibit large and saturable changes in positions in response to substrate, product, or analog binding. (**C**) Structure of DAGK with residues highlighted for which TROSY resonances exhibited significant and saturable changes in chemical shift upon binding. In blue are residues that are perturbed by addition of MgATP or MgAMP-PCP ($\Delta\delta$ > 0.02 ppm); in orange are those perturbed by addition of DAG ($\Delta\delta$ > 0.025 ppm). Residues for which resonance positions are perturbed by both nucleotide and lipid titrations are in green.

be to seal off the substrate-filled active site from water (to avoid ATP hydrolysis), a catalytic imperative that is usually satisfied in water-soluble phosphotransferases, such as adenylate kinase, by global-domain motions that close the active site upon substrate binding (*31*). DAGK appears not to undergo a global conformational change, as revealed by observation of only modest and highly localized changes in NMR resonance positions for DAGK upon forming either binary complexes with its substrates or a ternary complex with DAG and MgAMP-PCP (Fig. 3 and fig. S5).

As alluded to above, we systematically examined the functional consequences of mutating each residue in DAGK to cysteine to gain insight into structure-function relationships beyond what can be deduced either from multiple sequence alignment or from a previous phenotype-based random mutagenesis study (*32*). Mutants that resulted in >85% loss of catalytic activity (table S1) were further characterized to reveal two categories of defects (Fig. 2 and table S2). One set of mutations do not disrupt protein folding but result in loss of catalytic function. These residues are either directly in the active site or play specific local structural roles in support of the active site. Other mutations to cysteine result in misfolding so severe that in vivo expression levels were seen to be reduced (Fig. 2 and table S2), often to an undetectable level. In cases where purification was possible, such mutants were typically observed to be aggregation-prone (table S2). Although cysteine-scanning mutagenesis is a commonly used in studies of membrane proteins (*33*), we are unaware of previous documentation of a set of mutants analogous to the misfolding-prone variants described in this work.

A remarkable feature of the DAGK structure is the close proximity between the active site and a majority of residues for which mutations to cysteine result in severe misfolding (Fig. 2 and table S2). This is in contrast with enzymes, such as those of the TIM barrel superfamily (*34*), where the active site is set within a robust structural framework that is tolerant of major remodeling of catalytic residues. Given that numerous diseases, such as cystic fibrosis, are associated with inherited or sporadic mutations that result in single–amino acid changes in membrane protein sequence (*12*), our results serve as a warning that even for a structurally well-characterized membrane protein, knowledge regarding the location of a disease-promoting mutation site cannot a priori be used to reliably predict the exact nature of the molecular defect that is linked to disease etiology (i.e., local active-site disruption versus catastrophic misfolding).

The observation that most of the residues important for avoiding misfolding of DAGK are located at the DAGK active site offers insight regarding why the portico has not been adapted by evolution to orthologous functions. Although DAGK has been shown to be a highly efficient catalyst in its microbial physiological niche (*3*), intimate linkage between activity and folding may help to explain why this enzyme is an evolutionary orphan.

References and Notes

1. E. P. Kennedy, *Proc. Natl. Acad. Sci. U.S.A.* **79**, 1092 (1982).
2. C. R. Raetz, K. F. Newman, *J. Bacteriol.* **137**, 860 (1979).
3. P. Badola, C. R. Sanders, *J. Biol. Chem.* **272**, 24176 (1997).
4. M. Lis, H. K. Kuramitsu, *Infect. Immun.* **71**, 1938 (2003).
5. Y. Shibata *et al.*, *Microbiology* **155**, 557 (2009).
6. J. P. Walsh, R. M. Bell, *Methods Enzymol.* **209**, 153 (1992).
7. F. W. Lau, J. U. Bowie, *Biochemistry* **36**, 5884 (1997).
8. Y. Zhou, J. U. Bowie, *J. Biol. Chem.* **275**, 6975 (2000).
9. M. Lorch, P. J. Booth, *J. Mol. Biol.* **344**, 1109 (2004).
10. J. K. Nagy, C. R. Sanders, *Biochemistry* **43**, 19 (2004).
11. B. M. Gorzelle *et al.*, *Biochemistry* **38**, 16373 (1999).
12. C. R. Sanders, J. K. Myers, *Annu. Rev. Biophys. Biomol. Struct.* **33**, 25 (2004).
13. F. W. Lau, X. Chen, J. U. Bowie, *Biochemistry* **38**, 5521 (1999).
14. See supporting material on *Science* Online. Briefly, the backbone structure of micellar DAGK at pH 6.5 was determined using ^{1}H-^{1}H nuclear Overhauser effect–derived distances, backbone torsion angle restraints from chemical shifts, residual dipolar couplings, and paramagnetic relaxation effect–derived

distances. These NMR restraints were also supplemented by a limited number of intersubunit inter-residue distance restraints derived from disulfide mapping measurements that used single-cysteine mutant forms of DAGK. Care was taken to avoid possible motional complications to the disulfide mapping–derived distances. The structure was calculated using standard restrained molecular dynamics and simulated annealing protocols.

15. K. Oxenoid, J. J. Chou, *Proc. Natl. Acad. Sci. U.S.A.* **102**, 10870 (2005).
16. Y. Zhou *et al.*, *Mol. Cell* **31**, 896 (2008).
17. M. Bayrhuber *et al.*, *Proc. Natl. Acad. Sci. U.S.A.* **105**, 15370 (2008).
18. S. Hiller *et al.*, *Science* **321**, 1206 (2008).
19. B. Liang, L. K. Tamm, *Proc. Natl. Acad. Sci. U.S.A.* **104**, 16140 (2007).
20. D. Ma *et al.*, *Proc. Natl. Acad. Sci. U.S.A.* **105**, 16537 (2008).
21. K. A. Baker, C. Tzitzilonis, W. Kwiatkowski, S. Choe, R. Riek, *Nat. Struct. Mol. Biol.* **14**, 1089 (2007).
22. J. H. Chill, J. M. Louis, C. Miller, A. Bax, *Protein Sci.* **15**, 684 (2006).
23. D. J. Miller, A. Jerga, C. O. Rock, S. W. White, *Structure* **16**, 1036 (2008).
24. J. K. Nagy, F. W. Lau, J. U. Bowie, C. R. Sanders, *Biochemistry* **39**, 4154 (2000).
25. A. W. Partridge, R. A. Melnyk, D. Yang, J. U. Bowie, C. M. Deber, *J. Biol. Chem.* **278**, 22056 (2003).
26. J. P. Walsh, L. Fahrner, R. M. Bell, *J. Biol. Chem.* **265**, 4374 (1990).
27. R. E. Bishop, *Biochim. Biophys. Acta* **1778**, 1881 (2008).
28. M. K. Lemberg, M. Freeman, *Mol. Cell* **28**, 930 (2007).
29. D. Martinez Molina *et al.*, *Nature* **448**, 613 (2007).
30. H. J. Snijder *et al.*, *Nature* **401**, 717 (1999).
31. S. Kumar, B. Ma, C. J. Tsai, H. Wolfson, R. Nussinov, *Cell Biochem. Biophys.* **31**, 141 (1999).
32. J. Wen, X. Chen, J. U. Bowie, *Nat. Struct. Biol.* **3**, 141 (1996).
33. H. R. Kaback, M. Sahin-Toth, A. B. Weinglass, *Nat. Rev. Mol. Cell Biol.* **2**, 610 (2001).
34. N. Nagano, C. A. Orengo, J. M. Thornton, *J. Mol. Biol.* **321**, 741 (2002).
35. Single-letter abbreviations for amino acid residues: A, Ala; C, Cys; D, Asp; E, Glu; F, Phe; G, Gly; H, His; I, Ile; K, Lys; L, Leu; M, Met; N, Asn; P, Pro; Q, Gln; R, Arg; S, Ser; T, Thr; V, Val; W, Trp; Y, Tyr.
36. K. Oxenoid, H. J. Kim, J. Jacob, F. D. Sonnichsen, C. R. Sanders, *J. Am. Chem. Soc.* **126**, 5048 (2004).

37. We thank J. Bowie for providing the DAGK expression system, many of the mutants used in this work, and much discussion; M. Voehler, B. Gorzelle, P. Power, C. Kang, and J. Jacob for technical assistance; and K. Oxenoid, L. Kay, S. Prosser, M.-D. Tsai, T. Iverson, J. Meiler, A. Forster, J. Battiste, W. Chazin, and members of the Sanders lab for discussion. Supported by NIH training grant T32 NS007491 (W.V.H.) and National Institute of General Medical Sciences grant RO1 GM47485. C.R.S. is a consultant for Anatrace Inc. (now owned by Affymetrix), a company that markets high-purity biological detergents, including some of the detergents used in sample preparation in this work. The coordinates for DAGK have been deposited as PDB entry 2kdc in the Protein Data Bank. This work is dedicated to the fond memory of Anne Karpay.

Supporting Online Material

www.sciencemag.org/cgi/content/full/324/5935/1726/DC1
Materials and Methods
Figs. S1 to S8
Tables S1 to S4
References

2 February 2009; accepted 7 May 2009
10.1126/science.1171716

Germline P Granules Are Liquid Droplets That Localize by Controlled Dissolution/Condensation

Clifford P. Brangwynne,[1,2,3] Christian R. Eckmann,[1] David S. Courson,[3] Agata Rybarska,[1] Carsten Hoege,[1] Jöbin Gharakhani,[2,3] Frank Jülicher,[2,3] Anthony A. Hyman[1,3]*

In sexually reproducing organisms, embryos specify germ cells, which ultimately generate sperm and eggs. In *Caenorhabditis elegans*, the first germ cell is established when RNA and protein-rich P granules localize to the posterior of the one-cell embryo. Localization of P granules and their physical nature remain poorly understood. Here we show that P granules exhibit liquid-like behaviors, including fusion, dripping, and wetting, which we used to estimate their viscosity and surface tension. As with other liquids, P granules rapidly dissolved and condensed. Localization occurred by a biased increase in P granule condensation at the posterior. This process reflects a classic phase transition, in which polarity proteins vary the condensation point across the cell. Such phase transitions may represent a fundamental physicochemical mechanism for structuring the cytoplasm.

Starting from the fertilized egg, the cells of a developing embryo differentiate to give rise to somatic tissues, as well as maintaining an immortal germ line that will generate sperm and oocytes. Germ-cell specification is mediated in part by ribonucleoprotein granules assembled from RNA and RNA-binding proteins, although the precise function of these granules remains unknown (*1*, *2*). In *Caenorhabditis elegans*, the germ granules are called P granules. P granules are initially distributed uniformly throughout the unpolarized one-cell embryo. Upon symmetry breaking, the embryo polarizes along the anterior-posterior (AP) axis: Cortical and cytoplasmic flows develop (*3*), the polarity proteins PAR-1 and PAR-2 appear on the posterior cortex, and P granules become localized to the posterior half of the cell (Fig. 1A and movie S1; all embryos are ~50 μm long); the embryo then divides, giving rise to a P granule–containing progenitor germ cell and a non–P granule–containing somatic sister cell. Two processes have been proposed to mediate this posterior localization: (i) P granule migration by cytoplasmic flow (*4*–*6*) and (ii) subsequent disassembly or degradation of remaining anterior P granules (*5*–*8*). However, evidence supporting either of these mechanisms is sparse.

To study P granule localization in the one-cell embryo, we used three-dimensional (3D) particle tracking to monitor the movement and fluorescence levels of P granules labeled with green fluorescent protein (GFP)–tagged PGL-1 (*9*, *10*) or GLH-1 (*9*, *11*), both constitutive P granule components. We found that some P granules move into the embryo posterior; however, close to the cortex there was a flux of P granules into the anterior that was of similar magnitude to the posteriorly directed flux (Fig. 1, D to F). This behavior closely matched the overall flow behavior of cytoplasmic material such as yolk granules (*6*), quantified by particle imaging velocimetry (PIV) (Fig. 1, B and C) (*9*). P granules cannot preferentially localize to the posterior by convection in the surrounding cytoplasm alone. Thus, flows have little or no role in P granule localization (*9*).

We next examined intensity changes of individual P granules during localization. We found that P granule size is spatiotemporally controlled (Fig. 2A). We determined the average rate of relative intensity change of a population of P granules, ξ, at different points in space and time (*9*); negative ξ indicates P granule dissolution (i.e., shrinkage) and positive ξ indicates P granule condensation (i.e., growth). Before symmetry breaking, ξ was negative across the entire embryo, indicating overall P granule dissolution (fig. S1). After the onset of symmetry breaking, ξ stayed negative in the anterior but became positive in the posterior of the embryo, indicating posterior condensation [Fig. 2, B (WT, wild type) and C]. As predicted from this analysis, if we delayed symmetry breaking using RNA interference (RNAi) to deplete the centrosomal protein SPD-5 (*12*), ξ stayed negative across the whole embryo, and P granules appeared to dissolve completely [Fig. 2B, *spd-5(RNAi)*]. When these embryos eventually broke symmetry, P granules appeared to form de novo, in the vicinity of posterior PAR proteins (Fig. 2D and figs. S5 and S6). This occurred concomitant with a depletion of soluble P granule components from the anterior cytoplasm (Fig. 2E), and in the absence of notable cytoplasmic flows (movie S3). As with WT embryos, the rate of P granule condensation peaked before leveling off. The maximum of the posterior growth rate in *spd-5(RNAi)* embryos was three times as high as that in WT embryos, which

[1]Max Planck Institute for Molecular Cell Biology and Genetics, 01307 Dresden, Germany. [2]Max Planck Institute for the Physics of Complex Systems, 01187 Dresden, Germany. [3]Marine Biological Laboratory, Woods Hole, MA 02543, USA.

*To whom correspondence should be addressed. E-mail: hyman@mpi-cbg.de

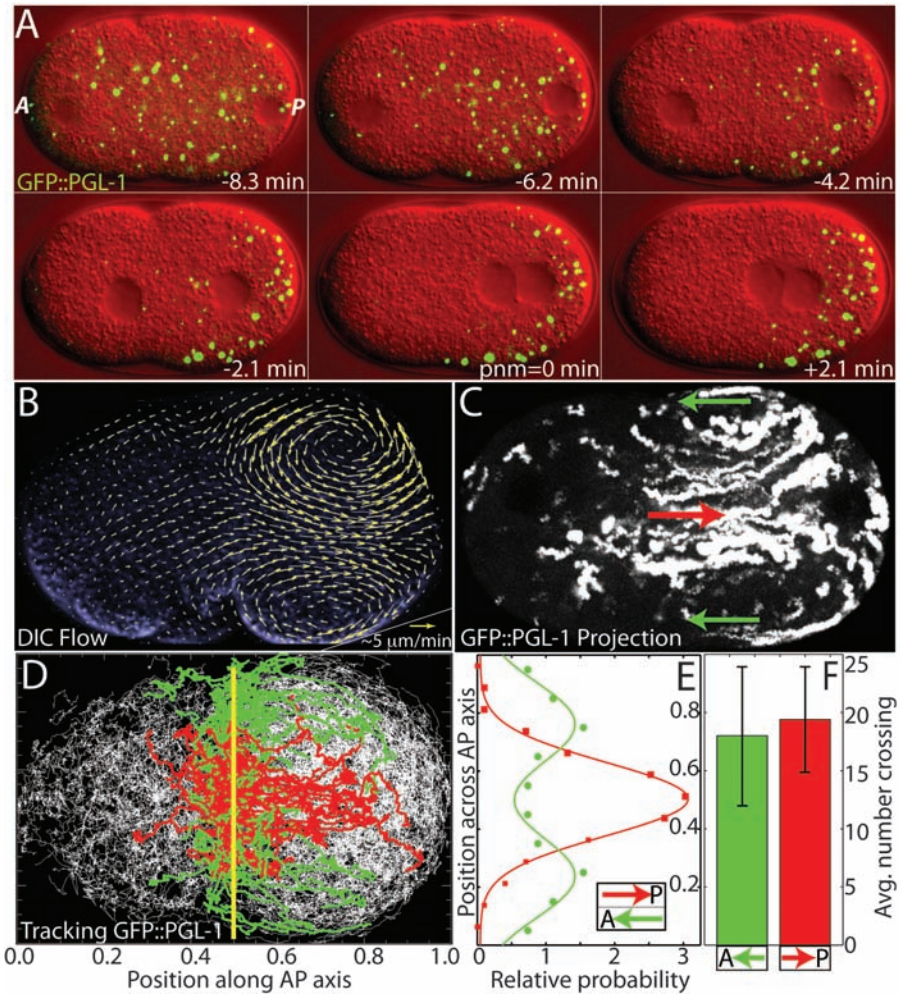

Fig. 1. P granule localization is not due to cytoplasmic flow. (**A**) Fluorescent images of GFP::PGL-1 (green) superimposed on differential interference contrast (DIC) (red). Time relative to pronuclear meeting (pnm). A, anterior; P, posterior. (**B** and **C**) The movement of P granules is similar to the movement of yolk granules. (B) Cytoplasmic flow field from PIV analysis of a single embryo (blue DIC image) during symmetry breaking. Yellow arrows indicate flow direction and magnitude. (C) Maximum-intensity projection of confocal stacks of GFP::PGL-1 P granules in the one-cell embryo during symmetry breaking; first frame, –8 min, 7 s pnm; last frame, –3 min, 30 s pnm; P granules in center of embryo move posteriorly (red arrow), and P granules near cortex move anteriorly (green arrows). (**D**) Overlay of P granule trajectories (white) from five GFP::PGL-1 embryos. Trajectories crossing into the posterior are shown in red, and those crossing into the anterior are in green. (**E**) Probability distribution of the location perpendicular to the AP axis of P granules crossing the midpoint [yellow line in (D)] into anterior (green) versus posterior (red). (**F**) The average flux per embryo (mean ± SEM, $n = 5$) indicates negligible net flux.

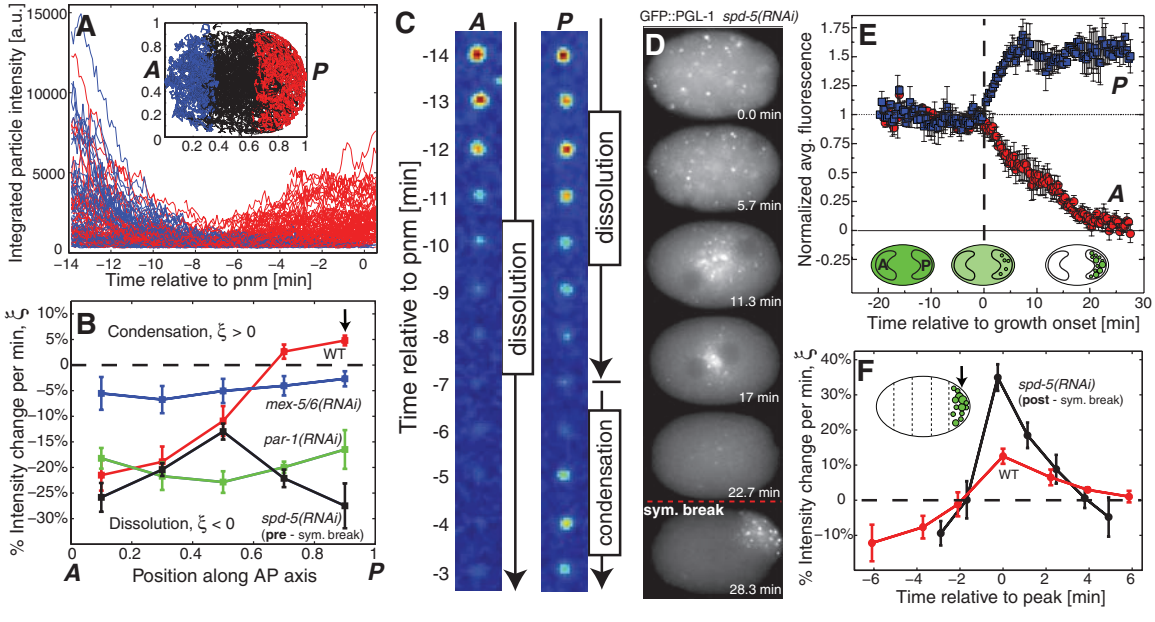

Fig. 2. Spatiotemporal changes in P granule size. (**A**) P granules throughout the one-cell embryo are initially dissolving; blue and red traces are intensities of individual GFP::PGL-1–labeled P granules in the anterior and posterior, respectively. Trajectories in the middle (black) are omitted for clarity. (**B**) *mex-5(RNAi)* ($n = 5$ embryos, blue curve) abrogates the anterior dissolution seen in WT GFP::PGL-1 embryos ($n = 8$, red curve), whereas *par-1(RNAi)* ($n = 6$, green curve) gives rise to dissolution throughout the embryo, as with *spd-5(RNAi)* embryos before symmetry breaking ($n = 8$, black curve). Data are shown as the mean ± SEM. (**C**) Example anterior (A) and posterior (P) GFP::PGL-1–labeled P granule (each recentered), showing anterior dissolution, and posterior dissolution followed by condensation. (**D**) Time sequence of GFP::PGL-1 embryo treated with *spd-5(RNAi)* for >24 hours to delay symmetry breaking. P granules completely dissolve, but then re-form upon symmetry breaking. (**E**) Fluorescence intensity in anterior (A) versus posterior (P) regions of a confocal slice through the middle of the embryo, after complete P granule dissolution in *spd-5(RNAi)* GFP::PGL-1 embryos. Regions of measurements indicated (mean ± SEM, $n = 8$). (**F**) The growth rate of P granules in the embryo posterior (arrow).

may reflect a higher concentration of soluble components due to complete dissolution (Fig. 2F) (*9*). These observations suggest a localization mechanism in which the condensation point is lowered in the posterior, causing condensation of components released by dissolved anterior P granules (see below).

A clue to the molecular control of this behavior comes from the proteins MEX-5 and PAR-1, which are implicated in the degradation of P granule components and P granule stability (*6*–*8*). The MEX-5 concentration is high throughout the embryo before symmetry breaking (*13*, *14*), when we found negative values of ξ across the AP axis [Fig. 2B, *spd-5(RNAi)*]. Upon symmetry breaking, PAR-1 reduces the concentration of MEX-5 in the posterior (*13*–*15*); the resulting MEX-5 concentration gradient was opposite to the dissolution/condensation gradient, ξ (fig. S3). Thus, high MEX-5 levels correlate in space and time with P granule dissolution. Consistent with this, when we depleted embryos of MEX-5, the value of ξ approached zero across the embryo, indicating weakened P granule dissolution [Fig. 2B, *mex-5/6(RNAi)*]. In embryos depleted of PAR-1, which have uniform, high levels of MEX-5 (*13*–*15*), the value of ξ was strongly negative across the AP axis [Fig. 2B, *par-1(RNAi)*], and P granules dissolved throughout (*6*) (movie S6). Thus, PAR-1 and MEX-5 may localize P granules mainly by controlling their dissolution and condensation, rather than by spatially regulating degradation.

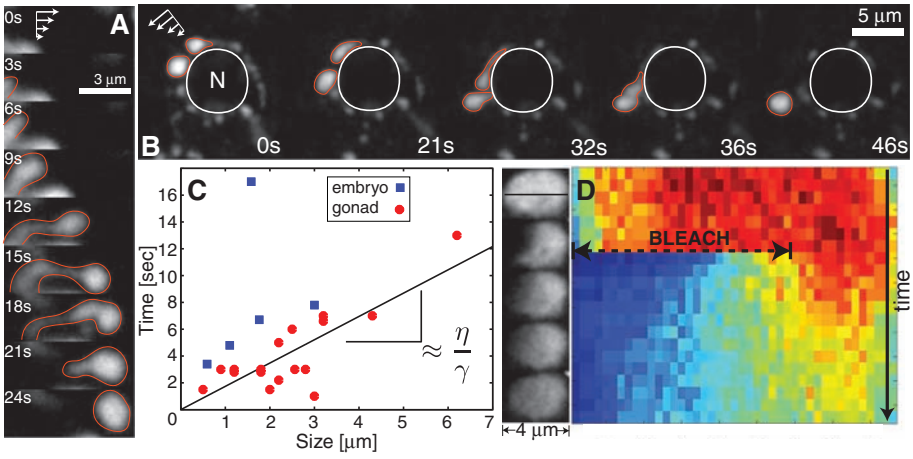

Fig. 3. P granules behave like liquids. (**A**) Jetting P granule (red outline) from a dissected GFP::PGL-1 germline nucleus (lower left, not visible). Shear direction, white arrows. (**B**) Dripping P granules (red outline) from a dissected GFP::PGL-1 germ line. Nucleus (N), white line. (**C**) Time scale of drop breakup and fusion events in dissected germline and early embryos, as a function of droplet size. The black line is a linear fit, yielding a ratio of viscosity to surface tension (η/γ) ≈ 2 s/μm. (**D**) Fluorescence recovery after photobleaching (FRAP) of a large nuclear-associated GFP::PGL-1–labeled P granule from an eight-cell embryo (upper left sequence; top to bottom = 20 s). Kymograph is along the black line in left sequence. Red denotes high intensity and blue, background intensity. The intensity decreases in the unbleached region (fluorescence loss in photobleaching, FLIP) as the bleached region recovers. From exponential fits, in the bleached region τ_{FRAP} = 4.7 s, and in the unbleached region τ_{FLIP} = 5.7 s.

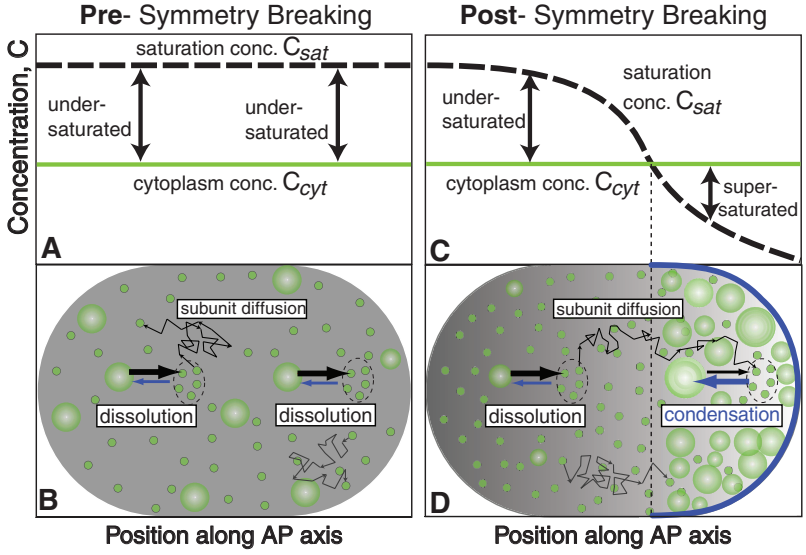

Fig. 4. Proposed mechanism of P granule localization. (**A**) Concentration of soluble components versus position along AP axis (posterior to right). Before symmetry breaking, the condensation point C_{sat} (dashed black line) is high across the embryo. The cytoplasmic concentration of P granule components C_{cyt} (green line) is much lower than C_{sat}, and the embryo is undersaturated with P granule components everywhere. (**B**) Undersaturation leads to dissolution of P granules (large green spheres) into diffusing components (small green circles). (**C**) Symmetry breaking decreases C_{sat} in the posterior, below C_{cyt}. (**D**) Consequently, posterior P granules condense from soluble components, whereas anterior P granules continue dissolving. The spatial dependence of C_{sat} arises from gradients in polarity proteins, including MEX-5 (gray) and PAR-1 (blue).

Our results thus far imply that localization of P granules depends on the ability of subunits to transition between a soluble form and a condensed phase, which appears to be spherical. P granules became nonspherical when they reattached to the nucleus at the four-cell stage, when they appeared similar to liquid drops wetting a surface (fig. S8 and movie S9). Together with the observation that P granules occasionally fused with one another, this suggests that the protein/RNA mixture comprising P granules may behave as a liquid. Indeed, the modularity and weak RNA affinity exhibited by RNA-binding proteins (*16*) would enable rapid molecular rearrangements that could give rise to liquid-like behavior.

For a simple liquid (e.g., water), applied shear stresses induce flows, unlike an elastic solid, which maintains a constant deformed shape under stress (*17*). We induced shear stresses across the large nuclear-associated P granules within the tube-like worm gonad (fig. S2) (*9*). P granules flowed off nuclei, dripped, and often fused into one larger drop; these are classic liquid behaviors (Fig. 3, A and B, and movies S7 to S9). Germ granules in zebrafish may show similar behaviors (*18*).

Liquids exhibit such flow behavior owing to fast internal molecular rearrangements. Consistent with this, when we selectively bleached half of large GFP::PGL-1 P granules at the eight-cell stage, we observed fluorescence recovery on a rapid time scale, τ = 5.9 ± 0.6 s (SEM, n = 5 GFP::PGL-1 P granules); concomitantly, the adjacent unbleached region decreased in fluorescence intensity, suggesting rapid diffusion within the granule (Fig. 3D). Similar observations were made with GFP::GLH-1 embryos (movie S12). Using the length scale of these large granules, L ~ 4 μm, we obtained a diffusion coefficient on the order of $D \sim L^2/\tau \sim$ 1 μm^2/s. By making the simplifying assumption that they behave as equilibrium Newtonian liquids, we could use the Stokes-Einstein relation to obtain a rough estimate of P granule viscosity, η ≈ 1 Pa·s (*9*). This is ~1000 times as large as the viscosity of water, similar to that of glycerol, and comparable to values seen in

colloidal liquids (*19*). Bleaching experiments in early one-cell embryos revealed that components of these P granules (≤1 μm diameter) typically turned over in less than 30 s (fig. S7), suggesting that P granule droplets exist in dynamic equilibrium with soluble components, much as conventional liquids do.

Surface tension is another important parameter controlling the behavior of liquid drops. To quantify P granule surface tension, we measured the time scale of P granules undergoing both fusion and droplet breakup events (Fig. 3, A and B). This time scale increased approximately linearly with the droplet size, as expected for liquids (Fig. 3C). The slope of this line establishes the ratio of viscosity to surface tension, η/γ (*9*). Thus, together with our estimate of P granule viscosity ($\eta \approx 1$ Pa·s), we could make an order of magnitude estimate of the surface tension, γ, between P granules and the cytoplasm, $\gamma \sim 1$ μN/m, which is smaller than the air-water surface tension by a factor of $\sim 10^5$. Such small values are expected for macromolecular liquids (*9*); for example, colloidal liquids typically have $\gamma \sim 0.1$ μN/m and below (*19*, *20*). The surface energetic barrier to P granule formation thus should be small, which may explain their ability to rapidly form upon symmetry breaking (*9*).

The dissolution and condensation behavior we observed, together with the liquid-like nature of P granules, supports a simple physical picture for P granule localization based on the theory of demixing phase transitions in fluids (*21*). Before symmetry breaking, the concentration at which soluble P granule components are saturated, C_{sat}, is uniform and high; the concentration of soluble P granule components, C_{cyt}, is lower than this; P granules are thus undersaturated, causing dissolution throughout the embryo, similar to evaporation of water droplets at high temperature (Fig. 4, A and B). Symmetry breaking causes the posterior value of C_{sat} to decrease below C_{cyt}, and the posterior becomes supersaturated with P granule components; thus, P granule droplets begin condensing, much as air becomes supersaturated with water vapor as temperature is decreased, and water droplets condense. This posterior condensation occurs even while the anterior remains undersaturated, and anterior P granules continue dissolving. This gives rise to a diffusive flux of P granule components into the posterior, thereby clearing out anterior components. The gradient in the condensation point, C_{sat}, along the AP axis appears to be set by gradients in polarity proteins, including MEX-5 and PAR-1 (Fig. 4, C and D). Although protein degradation may also play a role, it appears here that polarity proteins function largely by spatially regulating the P granule "dew point."

We propose that P granule localization exemplifies a general mechanism for organizing the cytoplasm that arises from collections of weakly "sticky" molecules, including other ribonucleoprotein assemblies (e.g., P bodies, Cajal bodies, or stress granules) (*16*, *22*). Such phase structuring may represent a primordial mechanism for functional self-assembly of relatively unevolved molecular assemblies in the early stages of the evolution of life.

References and Notes

1. G. Seydoux, R. E. Braun, *Cell* **127**, 891 (2006).
2. S. Strome, R. Lehmann, *Science* **316**, 392 (2007).
3. S. Q. Schneider, B. Bowerman, *Annu. Rev. Genet.* **37**, 221 (2003).
4. S. N. Hird, J. G. White, *J. Cell Biol.* **121**, 1343 (1993).
5. S. N. Hird, J. E. Paulsen, S. Strome, *Development* **122**, 1303 (1996).
6. R. J. Cheeks *et al.*, *Curr. Biol.* **14**, 851 (2004).
7. C. DeRenzo, K. J. Reese, G. Seydoux, *Nature* **424**, 685 (2003).
8. C. A. Spike, S. Strome, *Curr. Biol.* **13**, R837 (2003).
9. See supporting material on *Science* Online.
10. I. Kawasaki *et al.*, *Cell* **94**, 635 (1998).
11. M. E. Gruidl *et al.*, *Proc. Natl. Acad. Sci. U.S.A.* **93**, 13837 (1996).
12. D. R. Hamill, A. F. Severson, J. C. Carter, B. Bowerman, *Dev. Cell* **3**, 673 (2002).
13. J. R. Tenlen, J. N. Molk, N. London, B. D. Page, J. R. Priess, *Development* **135**, 3665 (2008).
14. A. A. Cuenca, A. Schetter, D. Aceto, K. Kemphues, G. Seydoux, *Development* **130**, 1255 (2003).
15. C. Schubert, R. Lin, C. de Vries, R. Plasterk, J. Priess, *Mol. Cell* **5**, 671 (2000).
16. B. M. Lunde, C. Moore, G. Varani, *Nat. Rev. Mol. Cell Biol.* **8**, 479 (2007).
17. K. E. Kasza *et al.*, *Curr. Opin. Cell Biol.* **19**, 101 (2007).
18. M. J. Strasser *et al.*, *BMC Dev. Biol.* **8**, 58 (2008).
19. D. G. Aarts, M. Schmidt, H. N. Lekkerkerker, *Science* **304**, 847 (2004).
20. M. Daoud, C. E. Williams, S. N. Lyle, Eds., *Soft Matter Physics* (Springer, Berlin, 1999).
21. J. D. Gunton, M. S. Miguel, P. S. Sahni, in *Phase Transitions and Critical Phenomena,* C. Domb, M. S. Green, Eds. (Academic Press, London, 1983), vol. 8.
22. P. Anderson, N. Kedersha, *J. Cell Biol.* **172**, 803 (2006).

23. We thank T. Mitchison for advice and discussion, together with students of the MBL Physiology Course 2008; and S. Grill, N. Goehring, and members of the Hyman and Eckmann Laboratories for helpful comments. We thank S. Hell, R. Medda, and B. Harke for assistance with stimulated emission depletion microscopy. Some strains used in this study were obtained from the Caenorhabditis Genetics Center. C.P.B. is supported by a fellowship from the Helen Hay Whitney Foundation.

Supporting Online Material

www.sciencemag.org/cgi/content/full/1172046/DC1
Materials and Methods
SOM Text
Figs. S1 to S8
References
Movies S1 to S12

9 February 2009; accepted 8 May 2009
Published online 21 May 2009;
10.1126/science.1172046
Include this information when citing this paper.

Ventral Tegmental Area BDNF Induces an Opiate-Dependent–Like Reward State in Naïve Rats

Hector Vargas-Perez,[1]* Ryan Ting-A Kee,[2] Christine H. Walton,[3] D. Micah Hansen,[3] Rozita Razavi,[1] Laura Clarke,[2] Mary Rose Bufalino,[2] David W. Allison,[3] Scott C. Steffensen,[3] Derek van der Kooy[1,2]

The neural mechanisms underlying the transition from a drug-nondependent to a drug-dependent state remain elusive. Chronic exposure to drugs has been shown to increase brain-derived neurotrophic factor (BDNF) levels in ventral tegmental area (VTA) neurons. BDNF infusions into the VTA potentiate several behavioral effects of drugs, including psychomotor sensitization and cue-induced drug seeking. We found that a single infusion of BDNF into the VTA promotes a shift from a dopamine-independent to a dopamine-dependent opiate reward system, identical to that seen when an opiate-naïve rat becomes dependent and withdrawn. This shift involves a switch in the γ-aminobutyric acid type A ($GABA_A$) receptors of VTA GABAergic neurons, from inhibitory to excitatory signaling.

The ventral tegmental area (VTA) serves as an anatomical locus controlling the switch from an opiate-nondependent to an opiate-dependent state (*1*, *2*). In nondependent rats, opiate reward is mediated by a dopamine-independent neural system, involving the brainstem tegmental pedunculopontine nucleus (TPP) (*3*). Once chronically exposed to opiates and in a state of withdrawal, opiate reward switches to a dopamine-dependent system (*3*). It has been observed that the switch between the two motivational systems is due to a switch in γ-aminobutyric acid type A ($GABA_A$) receptor functioning in VTA GABAergic neurons, from an inhibitory to an excitatory signaling state (fig. S1) (*2*).

Brain-derived neurotrophic factor (BDNF) is capable of producing this change in GABAergic response, from inhibitory to excitatory, as has been observed in the hippocampus during epileptic seizures (*4*) and in the spinal cord during neuropathic pain (*5*). BDNF is present in the VTA (*6*), and its TrkB receptors are present on both GABA (fig. S2) and dopamine VTA neurons (*7*, *8*). Chronic exposure to drugs of abuse increase BDNF levels in VTA neurons

[1]Department of Molecular Genetics, University of Toronto, 160 College Street, Toronto, Ontario M5S 3E1, Canada. [2]Institute of Medical Science, University of Toronto, 160 College Street, Toronto, Ontario M5S 3E1, Canada. [3]Department of Psychology, Brigham Young University, Provo, UT 84602, USA.

*To whom correspondence should be addressed. E-mail: vargashector@yahoo.com

(*6*). Furthermore, BDNF infusions into the VTA dramatically enhance several behavioral effects of drugs, including psychomotor sensitization (*6*, *9*) and drug seeking (*6*, *10*). We hypothesized that, along with the changes in structural plasticity induced by BDNF in VTA dopaminergic neurons (*11*), increasing BDNF levels in the VTA would induce a switch to a drug-dependent motivational state in drug-nondependent rats due to the effects of BDNF on GABAergic neurons.

First, we examined whether BDNF protein and mRNA levels in the VTA were increased in opiate-dependent rats. Sixteen hours after withdrawal from repeated daily exposure to heroin (0.5 mg/kg, subcutaneously) for 8 days [see supporting online material (SOM)], BDNF protein ($F_{3,37} = 7.63$, $P < 0.05$) and BDNF mRNA ($F_{3,19} = 4.04$, $P < 0.05$) levels in the VTA increased by 150% ($P < 0.05$) and 193%, respectively, of the control drug-naïve rats ($P < 0.05$). However, there were no increases in BDNF either when rats received a single injection of heroin ($P > 0.05$) or 15 days after withdrawal from repeated heroin exposure ($P > 0.05$) (fig. S3).

To explore whether BDNF alone was sufficient to cause a change in the neurobiological substrates mediating opiate reward, we next performed place conditioning procedures on rats after single bilateral intra-VTA BDNF (0.25 μg each) infusions (*10*). Place conditioning procedures (*12*) (see SOM) were performed 3 days after BDNF infusions (*10*). During training, we administered four alternating injections of intraperitoneal morphine (10 mg/kg) and vehicle to the rats over 8 days. The dopamine receptor antagonist alpha-flupenthixol (0.8 mg/kg) (or its saline vehicle) was injected intraperitoneally 2.5 hours before each conditioning trial. Testing was performed drug-free between 48 and 72 hours after the final conditioning session. After VTA BDNF ($n = 10$ animals) [but not the saline vehicle phosphate-buffered saline (PBS) ($n = 20$)] infusion, antagonism of the dopaminergic system blocked the rewarding effects of acute systemic morphine in drug-nondependent rats ($F_{1,59} = 5.3$, $P < 0.05$, interaction of morphine and BDNF treatment). Infusion of BDNF outside of the VTA (due to cannulae misplaced rostral, ventral, or lateral to the VTA) (fig. S4) did not allow the dopamine antagonist to block the rewarding effects of morphine in nondependent rats ($t_{10} = 4.65$, $P < 0.05$, $n = 11$) (Fig. 1A). It is possible that intra-VTA BDNF modifies the ability of opiates to produce conditioned place preferences, making them easier to block. However, neither BDNF ($n = 7$) nor PBS ($n = 7$) alone had any effect on the sizes of the conditioned

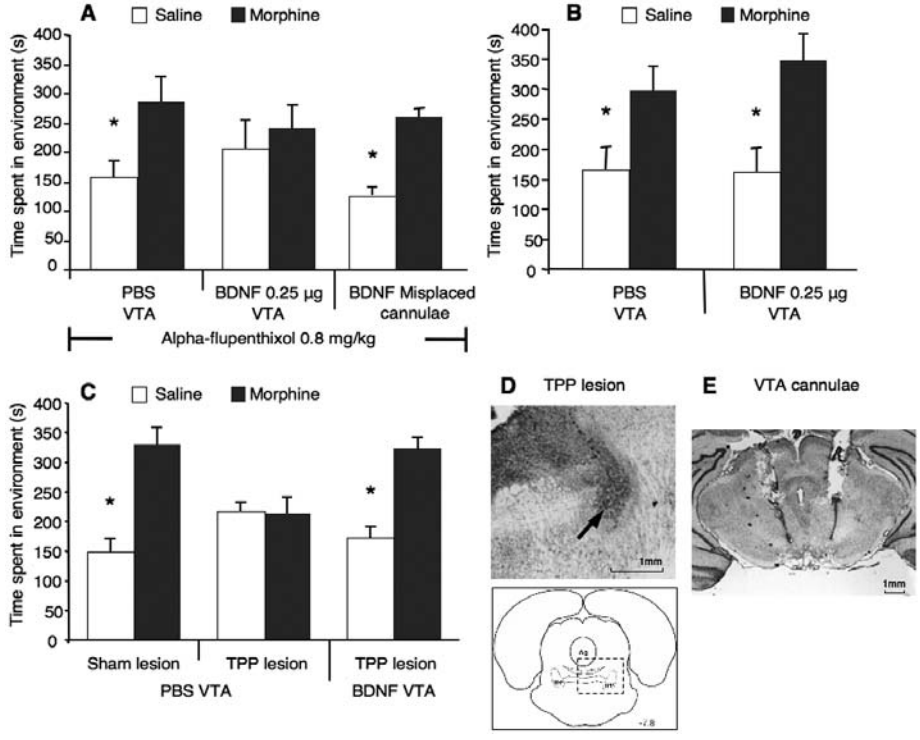

Fig. 1. Motivational effects of a single intra-VTA BDNF infusion in drug-nondependent rats. (**A**) Blockade of the dopaminergic system with neuroleptics (alpha-flupenthixol, 0.8 mg/kg) blocked the rewarding effects of morphine (10 mg/kg) in nondependent rats after a single intra-VTA BDNF (0.25 μg) infusion, but not after intra-VTA PBS infusion (*$P < 0.05$). The same treatment failed to block the rewarding effects of morphine in nondependent rats when BDNF was infused rostral, ventral, or lateral to the VTA because of missed cannulae placements (*$P < 0.05$). Error bars indicate SE of the mean. (**B**) Intra-VTA BDNF alone did not affect the sizes of the conditioned place preferences produced by acute morphine administration in drug-nondependent rats (*$P < 0.05$). (**C**) BDNF restored the rewarding properties of acute morphine administration in drug-nondependent TPP-lesioned rats (*$P < 0.05$). (**D**) Cresyl violet–stained coronal section showing one side of a bilateral TPP lesion and (below) a schematic of the anatomical region from which the section displayed was taken. The arrow indicates the TPP lesion area. (**E**) Cresyl violet–stained coronal section of a typical bilateral intra-VTA cannula placement.

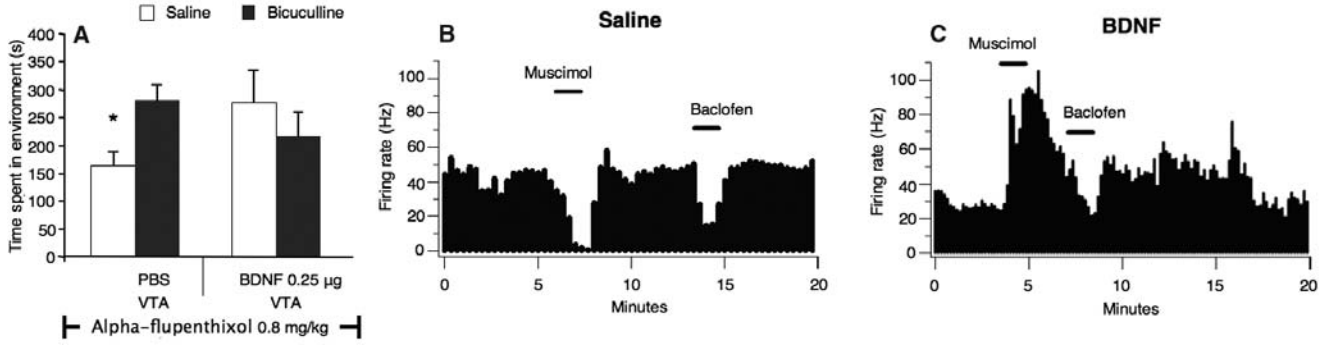

Fig. 2. Motivational and electrophysiological effects of a single intra-VTA BDNF infusion in drug-nondependent rats. (**A**) Blockade of the dopaminergic system with alpha-flupenthixol blocked the rewarding effects of an intra-VTA–administered $GABA_A$ receptor antagonist bicuculline (50 ng) in nondependent rats after a single intra-VTA BDNF infusion, but not after intra-VTA PBS infusion (*$P < 0.05$). (**B** and **C**) Single-unit extracellular recordings of VTA GABAergic neurons showing the effects of two current applications of muscimol (+50 nA) and baclofen (+50 nA) on the firing rate of representative VTA GABAergic neurons. In saline-treated rats, muscimol always decreased the firing rate of the VTA GABAergic neurons, whereas in BDNF-treated rats, muscimol enhanced the firing rate. Conversely, in both saline-treated and BDNF-treated rats, baclofen moderately decreased the firing rate of these VTA GABA neurons, as in this example.

place preferences produced by morphine [$F_{1,27}$ = 12.84, $P < 0.05$, main effect of the morphine treatment only in both BDNF ($P < 0.05$) and PBS ($P < 0.05$) groups] (Fig. 1B).

To investigate whether BDNF in the VTA changes opiate reward from a dopamine-independent (TPP-dependent) to a dopamine-dependent reward system, we examined the effects of intra-VTA BDNF in TPP-lesioned rats (*13*, *14*). In drug-nondependent rats, bilateral TPP (n = 12) [but not sham (n = 14)] lesions blocked the rewarding properties of morphine ($F_{1,51}$ = 14.29, $P < 0.05$, interaction of lesion and morphine treatment). However, after BDNF infusion (n = 12), TPP lesions did not block morphine reward ($P < 0.05$) in drug-nondependent rats, similar to sham-lesioned rats, where morphine also caused reward ($P < 0.05$) ($F_{1,51}$ = 47.87, $P < 0.05$, main effect of morphine only), but opposite to TPP-lesioned rats infused with PBS, where morphine reward was blocked ($P < 0.5$) ($F_{1,47}$ = 17.14, $P < 0.05$, interaction of BDNF and morphine treatment) (Fig. 1C).

To examine whether the $GABA_A$ receptors on VTA GABAergic neurons (*15*) are involved in the change in opiate reward system after intra-VTA BDNF infusion, we explored the effects of intra-VTA infusion of the $GABA_A$ receptor antagonist bicuculline. In drug-nondependent rats, intra-VTA bicuculline (50 ng) produced a robust rewarding effect through a non-dopaminergic, TPP-dependent reward system ($P < 0.05$). However, in drug non-dependent rats infused with intra-VTA BDNF (n = 11) [but not PBS (n = 8)], alpha-flupenthixol now blocked the rewarding effects of bicuculline ($P > 0.05$) ($F_{1,37}$ = 5.88, $P < 0.05$, interaction of BDNF and bicuculline). (Fig. 2A). To study the physiological effects of BDNF on $GABA_A$ inhibition of VTA GABA neurons, we evaluated the response of VTA GABA neurons to in situ administration of the $GABA_A$ agonist muscimol. Single-unit extracellular recordings of VTA GABAergic neurons (*16*) (four to five cells from rat) revealed that a shift from inhibitory to excitatory $GABA_A$ receptor signaling was observed in a subset of GABAergic neurons. Iontophoretic application of muscimol excited 42% [12 out of 31 (12/31)] of VTA GABAergic neurons in intra-VTA BDNF-infused rats (n = 8) compared with intra-VTA PBS (n = 8) infused controls, where 100% (29/29) of the VTA GABAergic neurons were inhibited by muscimol (Mann-Whitney U test, $P < 0.05$) (Fig. 2, B and C). This shift is very similar to that seen in a previous study with opiate-dependent rats, where 44% of VTA GABAergic neurons switched to excitatory $GABA_A$ receptor signaling (*2*). In BDNF-treated rats (16.6 ± 8.9%, n = 11), as in control PBS-treated rats (19.5 ± 9.26%, n = 7), the $GABA_B$ receptor agonist baclofen was still able to inhibit those GABA neurons that had been excited by muscimol (t_{17} = 0.216, $P > 0.05$) (Fig. 2, B and C), suggesting very specific effects of BDNF on $GABA_A$ receptor signaling on the VTA GABAergic neurons themselves.

The intra-VTA alterations that lead to this transformation are unclear. BDNF may change the anion gradient by reducing the level of the potassium-chloride co-transporter KCC2, so that the GABAergic neuron intracellular chloride concentration increases (*6*, *17*). $GABA_A$ receptor activation would then result in anions flooding out of the neuron, making the neuron's membrane potential more positive, or depolarized, relative to the resting membrane potential. Also, BDNF might elevate intracellular carbonic anhydrase levels, favoring HCO_3^- efflux and resulting in a depolarizing response in VTA GABAergic neurons (fig. S1) (*2*).

The present work suggests that BDNF in the VTA induces a transition to a drug-dependent motivational state, a crucial issue in drug addiction research. Other studies have found that BDNF levels within the mesolimbic system progressively increase after cocaine withdrawal (*18*). Intra-VTA BDNF infusion produces long-lasting enhancement of cocaine seeking (*18*) and locomotor stimulation (*6*, *9*), and it increases the rewarding effects of cocaine itself (*9*). Conversely, cocaine-conditioned place preference was reduced in heterozygous BDNF knockout mice (*9*), and inhibiting BDNF activity reduces amphetamine-induced dopamine release (*19*). Our findings complement research in animal and clinical studies suggesting that VTA BDNF is implicated in the pathogenesis of drug addiction (*20*).

References and Notes

1. S. R. Laviolette, D. van der Kooy, *Eur. J. Neurosci.* **13**, 1009 (2001).
2. S. R. Laviolette, R. A. Gallegos, S. J. Henriksen, D. van der Kooy, *Nat. Neurosci.* **7**, 160 (2004).
3. S. R. Laviolette, K. Nader, D. van der Kooy, *Behav. Brain Res.* **129**, 17 (2002).
4. C. Rivera *et al.*, *J. Cell Biol.* **159**, 747 (2002).
5. J. A. Coull *et al.*, *Nature* **438**, 1017 (2005).
6. C. A. Bolaños, E. J. Nestler, *Neuromol. Med.* **5**, 69 (2004).
7. S. Numan, K. B. Seroogy, *J. Comp. Neurol.* **403**, 295 (1999).
8. C. Hyman *et al.*, *J. Neurosci.* **14**, 335 (1994).
9. B. A. Horger *et al.*, *J. Neurosci.* **19**, 4110 (1999).
10. L. Lu, J. Dempsey, S. Y. Liu, J. M. Bossert, Y. Shaham, *J. Neurosci.* **24**, 1604 (2004).
11. S. E. Hyman, R. C. Malenka, E. J. Nestler, *Annu. Rev. Neurosci.* **29**, 565 (2006).
12. A. Bechara, D. van der Kooy, *Behav. Neurosci.* **106**, 351 (1992).
13. T. E. Kippin, D. van der Kooy, *Eur. J. Neurosci.* **18**, 2581 (2003).
14. H. Vargas-Perez *et al.*, *Eur. J. Neurosci.* **25**, 3713 (2007).
15. S. R. Laviolette, D. van der Kooy, *Eur. J. Neurosci.* **20**, 2179 (2004).
16. S. C. Steffensen, R. S. Lee, S. H. Stobbs, S. J. Henriksen, *Brain Res.* **906**, 190 (2001).
17. H. Wake *et al.*, *J. Neurosci.* **27**, 1642 (2007).
18. J. W. Grimm *et al.*, *J. Neurosci.* **23**, 742 (2003).
19. M. Narita, K. Aoki, M. Takagi, Y. Yajima, T. Suzuki, *Neuroscience* **119**, 767 (2003).
20. S. J. Tsai, *Med. Hypotheses* **68**, 410 (2007).

21. This work was funded by the Canadian Institutes of Health Research. S.C.S. received funding from NIH (grant AA13666).

Supporting Online Material

www.sciencemag.org/cgi/content/full/1168501/DC1
SOM Text
Figs. S1 to S4
References

13 November 2008; accepted 14 May 2009
Published online 28 May 2009;
10.1126/science.1168501
Include this information when citing this paper.

Patch Clamp Systems

The Ion-Flux-HT and IonFlux-16 Automated Patch Clamp Systems for ion-channel drug discovery offer gains in throughput, workflow simplicity, and affordability. These new systems combine Fluxion's proprietary microfluidic technology with integrated electronics to automate the traditional patch clamp assay. Applications include primary and secondary screening, lead optimization, and toxicology screening. The Ion-Flux-HT system includes 64 amplifiers and delivers between 8,000 and 10,000 assays per day at a cost of just 30 cents per data point using 384-well plates. The IonFlux-16 includes 16 amplifiers and uses a 96-well plate format. It delivers 2,000 data points per day at an affordable cost. The systems make use of a plate reader format for simplicity and integration with existing automated liquid handlers. The IonFlux technology automates cell manipulation, trapping, sealing, whole-cell formation, and precise voltage protocols.

Fluxion Biosciences
For information 650-241-4747
www.fluxionbio.com

Dry Baths

New compact, rapid-heating, microprocessor-controlled dry baths are suitable for a wide range of tasks in most laboratories, including clinical, histology, and molecular biology applications. They provide a heating speed from ambient temperature to 100°C in 12 minutes. With dimensions of 15 cm by 15 cm by 13.5 cm, they save bench space. They offer precise, accurate control of integral high-wattage heaters via a digital microprocessor control panel. The block chamber is constructed from molded aluminum, so the baths offer heat uniformity because of the perfect contact with the base of the interchangeable blocks, while retaining heating efficiency because the molded construction does not warp over time. A user calibration function allows easy calibration to suit in-house standards and requirements, while an RS232 port can export block temperature activity. Data-logging software that links to a computer can also be supplied.

Cleaver Scientific
For information 44-(0)-1788-565-300
www.cleaverscientific.com

TIRF Microscopy

The Laser TIRF 3 is a total internal reflection fluorescence (TIRF) microscopy system for reproducible examinations of near-cell membrane dynamic processes and interactions of single molecules in cell-free systems with high time resolution. The Laser TIRF 3 can be combined with other procedures and techniques, such as atomic force microscopy, for use in the biosciences, biophysics, biochemistry, and molecular. The technical features of TIRF 3 provide users with a wide variety of experimental possibilities. The TIRF slider is available in two versions, with manual or motorized angle setting. The new laser module offers a flexible choice of dyes. It can be equipped with up to four different solid-state lasers. Additional features include high time resolution, reproducible angle settings, and reproducible depths of penetration.

Carl Zeiss
For information +49-(0)-3641-642770
www.zeiss.de/micro

Weighing Terminal

The IND226x weighing terminal has received a full range of approvals for worldwide use in the chemical and pharmaceutical industries, uniting safety, productivity, and quality. The weighing terminal's stainless steel housing can withstand the toughest operating and cleaning conditions in chemical and pharmaceutical facilities. Exact container filling is ensured by the seven-segment LED display and integrated over/under control weighing mode. The IND226x is compatible with all of Mettler Toledo's analog weighing platforms. It is equipped with a mountable serial data interface and an interface converter for connection to computers and printers via an RS232 interface. This capability makes the unit usable remotely in hazardous areas. Its power supply options allow for its use in a wide range of application areas, including mobile weighing with a rechargeable battery.

Mettler Toledo
For information 800-638-8537
www.mt.com

pH Electrodes

Jenway Performance pH electrodes reduce analysis time through rapid equilibration compared with conventional pH electrodes with silver chloride reference systems, and increase the reproducibility of results following exposure to extremes of pH and temperature. Two new glass-bodied models include a 12-mm general purpose model and a 4.5-mm semimicro-electrode with 90-mm reach for small volume samples. Both provide high levels of accuracy in general solutions and biological samples containing Tris buffers. The electrodes' faster response times in pH buffers allow for rapid calibration. The general purpose model is recommended for a wide range of applications, including chemical production, environmental monitoring, food processing, and pharmaceutical manufacturing. The semimicro version is suited to the measurement of volumes smaller than 500 µl, commonly required in biochemistry laboratories.

Bibby Scientific
For information +44-(0)-1785-812121
www.bibby-scientific.com

Electronically submit your new product description or product literature information! Go to **www.sciencemag.org/products/newproducts.dtl** for more information.

Newly offered instrumentation, apparatus, and laboratory materials of interest to researchers in all disciplines in academic, industrial, and governmental organizations are featured in this space. Emphasis is given to purpose, chief characteristics, and availabilty of products and materials. Endorsement by *Science* or AAAS of any products or materials mentioned is not implied. Additional information may be obtained from the manufacturer or supplier.

POSITIONS OPEN

FACULTY POSITION
Medical Oncology Division
USC/Norris Comprehensive Cancer Center
The University of Southern California

The USC/Norris Comprehensive Cancer Center is seeking a faculty member to hold and conduct an active program in translational research in the area of breast cancer. The prospective candidate will be appointed at the **ASSISTANT/ASSOCIATE PROFESSOR** level in the Department of Medicine, Keck School of Medicine at the University of Southern California, Los Angeles, and will be expected to be an integral participant and member of the Women's Cancer Program at the Cancer Center. There is a competitive startup and salary package with excellent benefits.

Extensive Cancer Center core facilities for translational research are available, and their use by the candidate for innovative bench research and correlative and/or clinical trials will be encouraged. The patient population at Norris Cancer Hospital, University Hospital, and LAC+USC Medical Center is a diverse and outstanding resource for the conduct of clinical and correlative trials. At the USC Keck School of Medicine and USC/Norris Comprehensive Cancer Center, significant growth in clinical and translational research, in laboratory space resources, and in faculty recruitment will occur in the next five years as a high priority of the University of Southern California.

Minimum qualifications: translational and/or basic research experience and clinical expertise in the area of breast cancer with a preference for clinical/translational trials and/or drug development. Candidates must be Board-certified or equivalent in medical oncology. Background in clinical and/or translational research, possession of a valid California medical license at the time of appointment, and knowledge of scientific research methods will be required. Knowledge of federal guidelines related to conducting clinical trials and tissue-based research and knowledge of quality assurance as well as excellent spoken and written communication skills are required. Candidates should be ready to function as independent investigators with multidisciplinary teams of mentors available. Applicants should electronically submit curriculum vitae, and request three letters of reference to be sent, to:

Michael F. Press, M.D., Ph.D.
c/o Isabel Lora at e-mail: admedone@ccnt.usc.edu

The University of Southern California is an Equal Opportunity Employer committed to excellence through diversity and strongly encourages applications from all qualified applicants, including women and minorities.

RESEARCH MICROBIOLOGIST

Project description: A Research Microbiologist position is available in the Environmental Sciences and Biotechnology Department at the Savannah River National Laboratory (**website: http://srnl.doe.gov**) for a highly motivated individual with demonstrated experience in microbiology, molecular biology, and biogeochemistry. The successful candidate will join a multidisciplinary team of investigators conducting transitional research to elucidate and understand the expressed activities and ecology of microorganisms in support of U.S. Department of Energy missions. The successful candidate will participate in a wide variety of projects ranging from the microbial ecology of contaminated environments to the genetics, physiology, and scale-up of biological energy production.

Qualifications: The position requires a completed B.S. or M.S. degree in a relevant field and demonstrated experience in classical microbiological techniques, molecular biology, microscopy, and analytical chemistry. The successful candidate must possess excellent written and oral communication skills.

How to apply: Qualified applicants are encouraged to submit a cover letter, detailed curriculum vitae, and reference **job number PR-EX-2009-00141** to the SRNL Recruiting Office at **e-mail: srnlresearchrecruiting@srnl.doe.gov.**

Savannah River National Laboratory is an Equal Opportunity Employer, Minorities/Females/Persons with Disabilities/Veterans. U.S. citizenship is required. This appointment is open to all qualified U.S. citizens without regard to race, color, age, religion, sex, national origin, physical or mental disability, or status as a Vietnam-era veteran or disabled veteran.

POSITIONS OPEN

ASSISTANT OR ASSOCIATE PROFESSOR
Center of Excellence for Infectious Diseases

The newly created Center of Excellence for Infectious Diseases at the Paul L. Foster School of Medicine, Texas Tech University Health Sciences Center, El Paso, Texas, is seeking candidates for tenure-track faculty positions at Assistant or Associate Professor level. This is part of a state-funded initiative to enhance research in infectious diseases. The Center is primarily interested in investigators with research interests in molecular immunology, host-pathogen interactions, vaccine development, and animal models for translational studies.

Successful candidates are expected to develop and maintain independently funded research programs in infectious diseases or a related field. The position reports to the co-directors of the Center of Excellence for Infectious Diseases.

Minimum qualifications: M.D. or Ph.D. degree in a related field and at least three years of postdoctoral experience with a strong publication record.

Preferred qualifications: Candidates with funded grant support and experience in emerging infectious diseases and cutting edge technologies are particularly encouraged to apply.

The Center offers competitive salary and startup packages, newly constructed laboratory space, BSL-2 and BSL-3 laboratories, and a supportive interactive environment. Interested candidates must apply online at **website: http://jobs.texastech.edu, requisition #77147** by submitting curriculum vitae, a short write-up of research interests, and three letters of recommendation. For further information, please e-mail or contact:

Manjunath Swamy, M.D.
E-mail: manjunath.swamy@ttuhsc.edu or
Premlata Shankar, M.D.
E-mail: premlata.shankar@ttuhsc.edu
Co-Directors of the Center of Excellence for Infectious Diseases

The positions are open until filled. Application review will begin immediately.

Texas Tech University Health Sciences Center is an Equal Opportunity/Affirmative Action Employer.

STANFORD UNIVERSITY
Neuroscience Virus Core Facility Director

The Stanford Institute for Neuro-Innovation and Translational Neurosciences (SINTN) seeks an outstanding and entrepreneurial molecular biologist/virologist to establish and direct a core facility to generate viral vectors and distribute them to Stanford neuroscientists. The successful candidate will have a Ph.D. and/or M.D., and several years of postdoctoral experience with a strong track record in molecular biology and cell culture, ideally involving the generation and use of viruses (e.g. lentiviruses, AAVs). Salary will be commensurate with experience. Please submit a curriculum vitae, statement of research experience and have 3 letters of recommendation sent to: **Kristy Verhines, email: ksn@stanford.edu.**

Stanford University is committed to increasing representation of women and members of minority groups on its staff and particularly encourages applications from such candidates.

POST-DOCTORAL POSITIONS are available to study the molecular mechanisms regulating IgG and complement mediated neutrophil recruitment and effector functions using in vitro and in vivo approaches. Strong background in cell biology/immunology and small animal experimentation especially intravital microscopy is desired. Publication(s) in international journals is a prerequisite. Please send CV and names of 3 references to: **Tanya Mayadas, Ph.D., Associate Professor of Pathology, Brigham and Women's Hospital and Harvard Medical School, 77 Avenue Louis Pasteur, NRB 752O, Boston, MA 02115. E-mail: tmayadas2@rics.bwh.harvard.edu; fax: (617) 525-4333.**

LOOKING UP IN A DOWN MARKET:

CAMBRIDGE, OXFORD, AND LONDON

The science job market in the London–Oxford–Cambridge triangle, after 10 years of rising public investment in the United Kingdom's science base, has never been stronger. But the shockwaves of the financial crisis are undermining the biotech industry and pharma restructuring is hitting R&D, while academia is refocusing research with a translational bent. **By Nuala Moran**

Like the curate's egg, the scene for science jobs and recruitment in the London–Oxford–Cambridge triangle is good in parts—the good being those areas that, as yet, have escaped the fallout from the financial catastrophe and the restructuring of the pharmaceutical industry; the bad being those that have not.

To take the prime example of a bad part, the United Kingdom's biotechnology sector, based in the triangle, has been hard hit by the seizure in the capital markets. In a survey of 295 companies carried out by the UK BioIndustry Association in March, 78 percent said they had found it more difficult to raise cash in the previous 12 months. More than a third of companies trying to raise equity financing failed to do so, while a further 47 percent were not able to obtain all the financing they required.

With fewer products in the pipeline and sources of funding drying up, some biotechs are shutting their doors. Others are cutting back to conserve cash and try to hang on until the financing position improves. Companies in the region that have announced staff cuts include Oxford-based Summit Corporation, a zebrafish genomics specialist; Alizyme of Cambridge, which is developing treatments for gastrointestinal diseases; and Silence Therapeutics of London, an siRNA company.

Meanwhile, the pharmaceutical industry worldwide is undergoing the most thorough restructuring and consolidation in its history. While many of the pharma job cuts of the past two years have involved sales and marketing divisions, the UK's previously strong position in pharmaceutical R&D and manufacturing has left it especially exposed to these shifts.

To cite two examples, GlaxoSmithKline, the largest UK-based pharmaceutical company, has announced the closure of three UK R&D sites in the past two years. And with Pfizer and Wyeth accounting for over 6,000 jobs in the UK, employees are braced for the job losses that will likely flow from their recent merger.

Accompanying these macroeconomic factors, changes such as the push to interdisciplinary and translational research, as well as the addition of innovation and technology transfer to the research and teaching remits of universities, are changing the nature and practice of academic research and of science-related jobs.

The Fallout from Pharma

David Rees, senior vice president of medicinal chemistry at Astex Therapeutics, a fragment-based drug discovery specialist based in Cambridge, keeps a keen eye on the recruitment market in the city. Medicinal chemistry has continued »

Changes such as the push to interdisciplinary and translational research are changing the nature and practice of academic research and of science-related jobs.

UPCOMING FEATURES

Bioentrepreneurship — July 17

BS/MS - Choosing the Right Graduate Program — August 14

Postdoc Survey — August 28

"Pharma wants people who are adaptable, and are prepared to collaborate and interact with the public and private sectors."

long been a specialty where skills are in short supply, but speaking in March, Rees said there are far fewer job vacancies than 12 months ago. "There are many more people looking for jobs because of downsizing in pharma."

Whereas Astex and its biotech peers would previously have taken doctoral students straight from university, "It is now possible to recruit people from pharma with lots of experience in chemistry," says Rees.

As a consequence, some salaries are falling. "Astex is maintaining salary levels—which have always been competitive with pharma—but contract research organizations (CROs) are paying less." Some CROs are employing staff on short-term contracts to work on specific projects.

A curious factor is a shift in the perception of risk. Whereas scientists in big pharma previously expected to have secure jobs for life, Rees believes they now have no greater sense of job security than those in biotech.

"There still aren't many unemployed chemists, but people do accept the need to change company more often, and they may need to look at a move as a way to reinvigorate their skill set," advises Rees.

The CEO of another development-stage Cambridge biotech, **Tim Brears** of Xention, a discovery company specializing in ion channels, agrees that the recruitment market in the city suddenly has a very different feel. "We always expect quite a few applications when we advertise, but since the pharma downsizing began we are getting deluged."

Pharma Changing Its Requirements

The restructuring of the pharmaceutical industry may be happening under the cover of the global financial crisis, but it was sparked by factors that are particular to the sector. These include patent expirations, the rise of competition from generics, a downward pressure on drug prices, increasing scrutiny from regulators and health technology assessment bodies, pressure to move research offshore, and the crisis in R&D productivity.

Ann Gales, a partner at the high-level recruitment consultancy Heidrick and Struggles in London, advises that these pressures are reflected in the kinds of people pharma now wants to recruit. "Requirements are changing in response to the environment. Pharma wants people who are adaptable, and are prepared to collaborate and interact with the public and private sectors," says Gales.

There is no less focus on scientific expertise. "Science is still the key strength, but on the more commercial end of the business there is a need for people who can engage with the payers and are comfortable in dealings with regulators, health technology assessment bodies such as NICE [the UK's National Institute for Health and Clinical Excellence], clinicians, and patient groups."

Meanwhile, for those embarking on a career in the industry, a first degree in science leaves a wide number of career avenues open. But there is no doubt that scientists now need to offer commercial skills as well. "As the two sides of pharmaceutical companies get closer together, staff need to work in multifunctional teams, both internally and externally," says Gales.

Public Investment Continues to Create Jobs

After 10 years of rising public funding, the UK's science base has never been stronger. One manifestation of this investment is the Diamond Light Source near Oxford, the largest science facility to be built in the UK in the past 40 years. The synchrotron opened just over two years ago and is still in the process of building up its operations. Professor **Trevor Rayment,** physical sciences director, says 161 staff are employed in physical sciences; at the full capacity of 15 beam lines, this will rise to between 400 and 500.

Most recruits are academics, but there is a need for hybrid skills. "You have to be capable of handling a big machine, and need to enjoy troubleshooting and getting it to work well. And although our scientists have their own projects, the emphasis is on providing a service to our users," says Rayment.

While public spending on science is at an all-time high, this has been justified as an investment in the knowledge economy. Inevitably, this has repercussions in terms of the pressures universities are coming under to adopt a more commercial focus in their research, professionalize technology transfer, and collaborate with industry.

Universities such as Oxford, Cambridge, University College London (UCL), and Imperial College pride themselves on their commercial edge, and as a movement it is becoming hard for academic researchers to resist, as several recent initiatives highlight.

For instance, beyond generalist technology transfer, the Biotechnology and Biological Sciences Research Council (BBSRC) is now funding Innovation and Knowledge Centres to promote early commercialization of research in specific fields. An example is Cambridge University's center specializing in manufacturing technologies for photonics and electronics. This combines research with business development, market analysis, and commercialization skills.

Another scheme is bringing industrial "moles" into the heart of academe through Industrial Impact Fellowships. Researchers from industry join existing projects and programs with a brief to support translation of research. Science Minister Paul Drayson says, "Fellows of this scheme will get to share their experience, skills, and contacts directly with researchers—which is essential to bring innovations from research to market rapidly." continued »

CREDIT: COURTESY OF S. MARTIN, TMO RENEWABLES, LTD.

EMBL EMBL-EBI

Part of the European Molecular Biology Laboratory (EMBL), the European Bioinformatics Institute (EBI) is located on the Wellcome Trust Genome Campus at Hinxton, near Cambridge and provides cutting-edge research, service and training in the field of bioinformatics. The EBI is a vibrant and multicultural science institute, including access to outstanding students and post-doctoral scientists from around Europe and highly developed computational facilities and support.

Group Leader

We are seeking a dynamic computational biologist, with a proven track record, to establish a new research group to complement our current programme.

As a global centre for biological data, EMBL-EBI hosts the very large sequence, structure and expression data resources in Europe as well as eight dedicated research groups. At the EBI, research is pursued in many different aspects of biology, exploiting and helping to interpret the biological data held in the databases. Currently research topics include sequence analysis, computational genomics, phylogeny, structural biology, regulatory control networks, functional genomics, neurobiology and literature/text mining. In addition, research activities are an important part of several of the large data resource teams, which also provide services.

We are keen to expand our research into the areas of comparative genomics, human variation, biomedical informatics and novel algorithms/statistical approaches, but will favour outstanding candidates from any area of computational biology. The candidate will join a strong and supportive group of research group leaders and will interact closely with the large database teams, benefiting from their technical expertise and scientific knowledge.

An initial contract of 5 years will be offered to the successful candidate. This can be renewed, depending on circumstances at the time of review.

Further information on the position can be obtained from the Director of the EMBL-EBI Janet Thornton (**doffice@ebi.ac.uk**).

To apply, please email a cover letter, CV (in English), three written references and a concise description of research interests and future plans quoting ref. no. S/09/052/EBI in the subject line, to: **applications@ebi.ac.uk**

EMBL is an inclusive, equal opportunity employer offering attractive conditions and benefits appropriate to an international research organisation.

www.embl.org
www.ebi.ac.uk

By importing skills from outside, this program is attempting to make up for the perceived deficit of entrepreneurial skills and business knowledge inside universities. But universities are also offering courses in entrepreneurship to their researchers. A leading example is Imperial College's Entrepreneurship Hub, which teaches all science and technology undergraduates entrepreneurship skills and provides training for faculty and researchers in venture creation.

The Push to Translational Research

In medicine in particular, there is a push to create a translational research chain from laboratory bench, through drug discovery and development, and into the clinic. This new direction is prompting the major reorganization of the leading medical schools and teaching hospitals at Imperial College, UCL, and Cambridge, among others. The aim is to create American-style academic health science centers, such as that at Harvard, that integrate research, education, and clinical care.

Alongside this large-scale restructuring are programs to fill in the gaps in the translational research chain. For example, Imperial College and King's College London recently won funding for an Integrative Mammalian Biology program, in which researchers will be trained in the use of computer models of human physiology to replace the use of animals in experiments.

One step that exemplifies how the pressure to translate research through to the market is forcing the pace of multidisciplinary research is the formation in April of the Center for Stem Cells and Regenerative Medicine at UCL. The list of specialties that will be brought together is deep and broad: beyond a swathe of biological sciences, they include physical scientists, chemists, mathematicians, engineers, and material scientists from 130 research groups in several faculties, hospitals, and research institutes.

Professor **Claudio Stern,** chair of the center's steering committee, says UCL has many scientists in the field of stem cells, but they were working in relative isolation from each other. "The enhanced communication will greatly improve the flow of information between basic and clinical scientists that is absolutely crucial for this field to move forward." continued »

Featured Participants

Alizyme
www.alizyme.com

Astex Therapeutics
www.astex-therapeutics.com

Biotechnology and Biological Sciences Research Council
www.bbsrc.ac.uk

Bluewater Bio
www.bluewater.bio.com

Cambridge University
www.cam.ac.uk

Cancer Research UK
www.cancerresearchuk.org

Diamond Light Source
www.diamond.ac.uk

GlaxoSmithKline
www.gsk.com

Heidrick and Struggles
www.heidrick.com

Imperial College
www.imperial.ac.uk

King's College London
www.kcl.ac.uk

National Institute for Health and Clinical Excellence
www.nice.org.uk

Oxford University
www.ox.ac.uk

Pfizer
www.pfizer.com

Silence Therapeutics
www.silence-therapeutics.com

Summit Corporation
www.summitplc.com

TMO Renewables
www.tmo-group.com

UK BioIndustry Association
www.bioindustry.org

University College London
www.ucl.ac.uk

Wyeth
www.wyeth.com

Xention
www.xention.com

Postdoctoral Fellow – Computational Genomics

Salary range £28,000 to £34,433 per annum dependent on experience

The Wellcome Trust Sanger Institute is a world leader in genomic research, with an expanding scientific programme dedicated to understanding gene function in health and disease.

A post-doctoral bioinformatician is sought for a cutting edge research programme in the Cancer Genome Project. The fellow will focus on the application of new sequencing technologies to identify genetic variants in cancer genomes, including the development of novel algorithms for sequence analysis and mutation calling, informatic analysis of mutational patterns and cancer gene identification.

Essential Skills:

- PhD which includes a substantial component in bioinformatics or computer science (or equivalent experience).
- Experience in the analysis and manipulation of large datasets, such as accessing data via MySQL or commonly used bioinformatics APIs.
- Proven record of writing analysis programs and scripts to rapidly investigate scientific questions
- Ability to work independently to carry out data analysis
- Excellent attention to detail and good communication skills

Ideal Skills:

- Interest/previous experience in genomic analysis

Other information: The Wellcome Trust Sanger Institute operates at the forefront of genomics, sequencing and analyses of a wide range of genomes from single cell pathogens to higher vertebrates, with an emphasis on genomes relevant to human medicine and welfare. The Cancer Genome Project at the Institute has led the way in the systematic analysis of cancer genomes by using the human genome sequence and high throughput mutation detection techniques to identify somatically acquired sequence variants/mutations and hence identify genes critical in the development of human cancers. The ideal candidate would be from a programming background interested in applying their knowledge in the field of genomics. They will be able to work independently, enjoy collaborating with different teams, assimilate tasks easily and generate scripts quickly to analyse genomic data whilst supporting the research of the team and producing publications.

Benefits: Salary range £28,000 to £34,433 per annum dependent on experience. The Institute has excellent purpose built facilities on the Genome Campus, Hinxton on the outskirts of Cambridge. We offer a comprehensive range of benefits including a final salary pension scheme and excellent on-site facilities. Further details can be found on our website **https://jobs.sanger.ac.uk**.

This is a fixed-term contract for 3 years. To submit your CV and apply for this job please go to **https://jobs.sanger.ac.uk**, to register and apply on line.

wellcome trust sanger institute

UNIVERSITY OF OXFORD

www.ox.ac.uk/jobs

Sir William Dunn School of Pathology

Graduate Research Assistant

Grade 6 £25,623 - £30,594 pa

We are seeking to appoint a Research Assistant in the laboratory of Professor Elizabeth Robertson, FRS, WT-PRF, located at the Sir William Dunn School of Pathology.

The post-holder must have a good first degree or equivalent and laboratory experience in animal models, molecular biology, and/or tissue culture. You should have a keen interest in developmental biology and immunology. We are seeking an enthusiastic and highly motivated scientist with good organisational and communication skills to be actively involved in research projects.

Please quote reference LR/09/013.

Post-Doctoral Research Assistant

Grade 7 28,839 - £35,469 pa

We are seeking to appoint a post-doctoral Research Associate in a Wellcome Trust funded laboratory with research interests in mammalian developmental biology located at the Sir William Dunn School of Pathology.

Under the direction of Professor Elizabeth Robertson FRS, WT-PRF, the programme focuses on defining the molecular cues responsible for cell allocation and tissue morphogenesis in the developing mammalian embryo. We have exploited transgenic and ES cell technologies to investigate the key signalling pathways and transcriptional networks that regulate expansion of diverse progenitor cell populations. Candidates with experience in gene targeting construct design, high resolution imaging, cell sorting, microarrays, CHIP, and/or proteomic approaches would be especially welcome. We are seeking a well trained and ambitious scientist with good organisational and communication skills.

Please quote reference LR/09/014.

Please send your CV and the contact details of three references to the Administrator, Sir William Dunn School of Pathology, South Parks Road, Oxford OX1 3RE, or email administration@path.ox.ac.uk.

Informal enquiries welcome - please email Prof Robertson at elizabeth.robertson@path.ox.ac.uk **(www.path.ox.ac.uk/dirsci).**

The closing date is Friday 24 July 2009.

Committed to equality and valuing diversity

UNIVERSITY OF CAMBRIDGE

A world of opportunities

www.cam.ac.uk/jobs/

Research Associate – influenza research

The Pathogen Evolution Group
LoT applies*
£27,183-£35,469 per annum

We invite applications for a postdoctoral Research Associate to work in the Department of Zoology, University of Cambridge, UK, on the development of new analytical techniques for quantifying the evolutionary selection pressures on influenza viruses. We aim to better understand their evolutionary dynamics and to inform control strategies. The project, which is funded by the Human Frontier Science Program, is start as soon as possible.

The candidate should have a PhD in computational biology, computer science, virology, epidemiology, a related subject or equivalent and should have excellent programming skills in C++, Python, Java or Lisp and ideally other languages.

*The appointment will be for a period of up two years in the first instance.

Informal email enquiries may be made to Prof. Derek Smith at am688@cam.ac.uk

To apply see:
http://www.zoo.cam.ac.uk/zooone/administration/vacancy.html
Please quote reference: PF05226.
Closing date: Friday 31 July 2009.
Interviews as soon as possible thereafter.

The University is committed to Equality of Opportunity.

"We've been recruiting over the past two years, and when I look at our ranks, about one-third of staff are from the pharmaceutical sector."
—Hamish Curran

The immediate payoff was a commercialization deal in age-related macular degeneration in which Pfizer became the first big pharma company to make a move into the use of embryonic stem cells as the basis for a tissue regeneration therapy.

The Triple Whammy: Multidisciplinarity, Translation, Commercialization

So how are these huge shifts in the research firmament—multidisciplinarity, translational research, and commercialization—affecting one of the largest funders of basic biomedical science in the country, Cancer Research UK?

"We are not turning away from basic research—that is still at the core of what we do," says **Simon Vincent,** the charity's head of personal awards. However, he adds, "The nature of basic science is changing, and this is influencing the kind of people we are looking to recruit."

In particular, the charity is moving up the development pathway, and has begun to establish drug discovery and development capabilities. "This means we are recruiting more synthetic chemists, for example," says Vincent.

Indeed, in this move to secure the foundations of drug development, CRUK has needed to bridge several skills gaps. An example is bioinformatics, a specialty in which it has set up groups in Cambridge and London. "This is a reflection of the impact of genomics on the way we do basic biology," Vincent says.

In November 2008 CRUK announced its GBP1.5 billion science strategy for 2009–2014, under which it will establish 20 centers of excellence linking research, patient care, public engagement, and prevention. "We are putting more emphasis on translation—that is our clear objective. We will only work with universities to establish a center if there is a commitment from academic groups and clinical departments to get involved," explains Vincent.

The centers will not require new specializations, but Vincent says there will be a need to cultivate researchers who are capable of seeing patients in the clinic and then applying their observations in the lab.

Speaking in March, Vincent said CRUK was actively recruiting, and there was no sign as yet of an increase in applications as a result of fallout from the pharma and biotech sector.

However, as a charity, CRUK is seeing a fall in donations as the economy contracts, Vincent says. "It has had an impact; we are expecting a 4 percent fall this year. But we are not cutting programs."

Cleantech: A New Source of Science Jobs

The sudden contraction in some parts of the science jobs market may undermine existing career plans of those in pharma and biotech and require a rethink by new graduates trying to get on the first rung of the ladder. But avenues are opening up elsewhere. The UK's emerging cleantech sector holds prospects for people with pharmaceutical experience, according to **Hamish Curran** CEO of TMO Renewables, a cellulosic biofuels specialist. "We've been recruiting over the past two years, and when I look at our ranks, about one-third of staff are from the pharmaceutical sector."

The company was founded in 2002 to develop second generation biofuels and is currently testing its first demonstration plant. Curran, himself a veteran of the oil industry, advises that cleantech projects require a new mix of skills. "There has to be a marriage between engineering and biology to build a bioprocess plant that can operate 24 hours a day."

Similarly, sustaining microbial populations is central to the R&D activity of Bluewater Bio, a wastewater treatment specialist. The London-based company is in the process of optimizing technology discovered in South Korea for removing organic material from wastewater, to suit environmental conditions and wastewater standards in the UK and elsewhere in Europe. "We have a formula, but we need to understand more about the effects of changing the operating parameters on the process," says **Garry Hoyland,** technical director.

There is increasing public investment in the field, too. A notable example is the GBP27 million Sustainable Bioenergy Centre set up with the aim of replacing petrol with biofuels. In another initiative the BBSRC has joined with 10 companies to develop the technologies required to replace petrochemicals through biorefining.

Potential recruits should be aware that cleantech is opening up a new interface between disciplines, says **Tim Barnes,** executive director of UCL Advances, the technology transfer and commercialization arm of University College London. This is reflected in the kinds of expertise that employers of science graduates are looking for. "Just look at the problems we are trying to solve: developing a hydrogen-powered car covers a range of different disciplines—many aspects of which aren't really to do with engineering," says Barnes. Those interested in working in the field need to demonstrate they can network and operate across disciplinary barriers.

Traditionally 25 percent of the UCL's numerate graduates have gone to work in the City of London's financial services sector, a market that has dried up overnight. "Science graduates at any level are finding it tough to get jobs," says Barnes who advises that one tack is to complete another course.

The university is helping by offering discounts on fees for its postgraduate courses. As well as increasing skills levels, it hopes that the best students will be attracted into research.

This would be at least one positive outcome of the current financial crisis.

Nuala Moran is a freelance writer based in Cheshire, United Kingdom.

DOI: 10.1126/science.opms.r0900073

CREDIT: COURTESY OF TMO RENEWABLES, LTD.

MRC | Laboratory of Molecular Biology

Cambridge

Postdoctoral Scientist

£25,622 - £27,223 per annum

We are seeking a Postdoctoral Scientist to work in the Group of Dr Ingo Greger, to investigate signalling properties of neuronal and recombinant AMPA-type glutamate receptors. The project will involve analysis of native AMPA receptors from hippocampus, as well as assaying recombinant, structure-guided receptor mutants in heterologous expression systems.

Applicants should have a PhD in biological and/or physical sciences, and experience in electrophysiological recording techniques applied to ligand-gated ion channels. A strong interest in synaptic signalling and ion-channel function is essential. A background in calcium imaging techniques would be advantageous.

You will be awarded an MRC Career Development Fellowship, which is a three year training and development position for a postdoctoral scientist who has recently completed their doctoral studies or is moving into a new research discipline.

Your salary is supported by a flexible pay and reward policy, 30 days' annual leave entitlement, an optional MRC final salary pension scheme and excellent on site sports and social facilities.

This position is subject to pre-employment screening.

Applications for this role must now be made online at http://jobs.mrc.ac.uk inputting reference LMB09/257. If you do not have internet access or experience technical difficulties please call 01793 301280.

Closing date: 23 July 2009.

For further information about the MRC please visit www.mrc.ac.uk

The Medical Research Council is an Equal Opportunities Employer

ANNOUNCEMENTS

Department of Veterans Affairs

Office of Research and Development

Biomedical Laboratory Research and Development Service

2008 William S. Middleton Award

Was presented to:
Stephen G. Waxman, M.D., Ph.D.
VA Connecticut Healthcare System, West Haven, CT

The Middleton Award is Biomedical Laboratory Research and Development Service's highest scientific honor, awarded annually to a senior VA investigator for accomplishments in areas of prime importance to the VA's research mission.

Dr. Waxman was especially honored for his contributions to our understanding of the causes and treatment of neurological disorders including spinal cord injury, multiple sclerosis and chronic neuropathic pain. The award also recognizes his exemplary record of service to the VA and to the biomedical profession.

New Faculty and post-doctoral appointments in The University of Queensland

Centre for Advanced Imaging (CAI) in Brisbane, Australia

A range of faculty and post-doctoral positions are available in the newly established Centre for Advanced Imaging (www.uq.edu.au/cai) at The University of Queensland. Talented researchers are sought to build internationally recognized research programs in areas of animal, translational and clinical imaging research using PET and MRI. Applications are sought from researchers with expertise in areas of imaging including, but not restricted to, image analysis relevant to functional imaging, tractography or computational anatomy, molecular imaging and the use of imaging to study brain disorders such as epilepsy and cerebrovascular disease in clinical populations or in animal models.

Appointments may be made for up to 5 years initially, with renewal beyond that dependent on performance. Applicants should hold a Ph.D. or equivalent. Applications from more senior candidates and for candidates with clinical training will also be considered. The level of appointment will be commensurate with the candidate's level of experience, and a competitive start-up package will be provided. There is also the possibility of joint appointments at the Queensland Brain Institute and the University of Queensland Centre for Clinical Research.

At the CAI, The University of Queensland aims to create, under the leadership of Professor David Reutens, a world-class integrated imaging research facility which is multidisciplinary and multimodal, with facilities for human and animal high field MRI and PET and molecular probe development for PET and MRI. Other active research programs at the CAI include MR microscopy; imaging applications of nanomaterials; structural biology of biometallic proteins, chemistry and metabonomics with EPR and NMR; and MR engineering. With a student population of over 35,000, The University of Queensland has an international reputation in medical research and education and also has strong programs in mathematics, physics, computer science and engineering.

To apply please send a cover letter, a CV, a statement of research interests, and arrange to have 3 letters of recommendation sent to the Search Committee.

Applications should be sent either by email to k.michalski@uq.edu.au, or by regular mail to Ms Kate Michalski, Queensland Brain Institute, The University of Queensland, St Lucia, QLD 4072, Australia.

Applications should be received by 17 August 2009 to assure full consideration.

The University Of Queensland AUSTRALIA | cai centre for advanced imaging

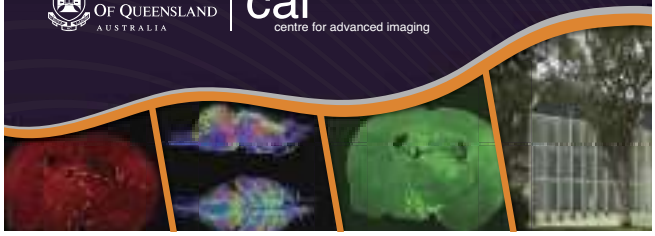

Clinical Chair in Translational Medicine

University of East Anglia

Norwich

The University of East Anglia (UEA) is an internationally renowned campus based university that provides top quality academic, social and cultural facilities to over 13,000 students. The School of Medicine was established in 2000 and with its strong links with the Norfolk and Norwich University Hospitals NHS Foundation Trust, Institute of Food Research and John Innes Centre, has an impressive track record of internationally recognised research and of attracting substantial research funding. UEA is now seeking to appoint an exceptional clinical scientist to the new post of Clinical Chair in Translational Medicine. The successful candidate will join established groupings of both laboratory and social researchers with access to state of the art facilities both at the University and on the hospital site. This is a hugely exciting opportunity to play a major role in shaping the clinical research undertaken across the whole of the Faculty of Health over the coming decade.

The Role:

- To contribute to the clinical research strategy and the expansion of postgraduate research.
- To develop and lead a programme of high calibre research in an area related to the School of Medicine's current research strengths.
- To develop external relationships with basic scientists in the Faculty's partner organisations and encourage collaborative working with the Trust to increase the number of clinically active academics.

The Candidate:

- An exceptional clinical academic with an active research profile of distinction and a track record of peer reviewed and published papers and of securing external funding.
- Strong intellect and commitment to innovation; s/he will be a visionary and strategic thinker, able to spot opportunities and assess risks.
- Well developed leadership skills with a commitment to the facilitation of clinical/translational research within an integrated academic-clinical unit.

For further information and a candidate brief containing application details please see www.odgers.com/25956 or contact us quoting reference CS/25956S. Closing date for applications is 17th July.

11 Hanover Square,
London W1S 1JJ
0845 1309005
www.odgersberndtson.co.uk

ODGERS BERNDTSON
Executive Search
51 offices in 24 countries

Associate or Full Professor

The Institute of Human Virology (IHV) and the Institute for Genome Sciences (IGS), in conjunction with the Marlene and Stewart Greenebaum Cancer Center at the University of Maryland School of Medicine, are searching for a faculty candidate to direct a new Division of Oncological Genomics. The new division will be located in the IHV and, coupled with full appointments in IHV and IGS, will have the ability to recruit junior faculty to support its mission. The appointment will be either at the Associate or Full Professor level, commensurate with experience.

The successful candidate will have extramural funding and a track record of conducting independent and collaborative research using approaches that include genomics and bioinformatics, as well as an interest in the field of cancer. The candidate will work closely with tumor cell biologists, molecular biologists, immunologists, and epidemiologists in the IHV to identify high-risk individuals and cancers that may have an infectious etiology. Particular emphasis will be placed on cancer associated with adventitious agents, especially viruses, and the candidate will use appropriate genomics and bioinformatics approaches to identify such agents in tumors, in the tumor microenvironment, and in individuals at high risk for specific cancers. The qualified individual will have publications utilizing genomics that may be applicable to human cancer. The cancers of interest in this institute are those occurring in the context of HIV or Hepatitis C infection and include cancer of the lung, kidney, liver, ovary, prostate, brain, leukemia, lymphoma and epithelial cells. The qualified individual will have familiarity with genomic applications such as transcriptional profiling, genotyping, tiling arrays, exon throughput assays, methylation, real time PCR, microRNA analyses and automated high throughput assays, and be aware of technology leading to detection of other agents, including possibly novel ones.

IHV and IGS offer excellent laboratory facilities, competitive salary and startup packages, and access to numerous resources within the School of Medicine, including state-of-the-art BSL3/ABSL3 facilities and a large-scale DNA sequencing and analysis core in a strong academic environment.

The faculty search committee will be co-chaired by **Dr. Robert Gallo**, Director of IHV, and **Dr. Claire Fraser-Liggett**, Director of IGS.

Please submit a letter of interest, CV, and three references to: **Oncologic Genomics Faculty Search Committee, c/o Beth Peterson, Institute of Human Virology, 725 West Lombard Street, S307, Baltimore, MD 21201; bpeterson@ihv.umaryland.edu**.

The University of Maryland, Baltimore is an Equal Opportunity, Affirmative Action Employer. Minorities, women, veterans and individuals with disabilities are encouraged to apply.

Postdoctoral Associate Stem Cell Research

Stony Brook University's Department of Physiology and Biophysics is seeking a postdoctoral associate to study the signaling in embryonic and mesenchymal stem cells.

Required qualifications: Ph.D. or equivalent in the biological sciences with prior experience in cell signaling with at least two years of postdoctoral training preferred. The function and regulation on Wnt signaling will be explored by using molecular biological, biochemical, and microscopic techniques.

For a full position description, application procedures, or to apply online, visit *www.stonybrook.edu/jobs* (JOBS Reference #: HS-R-5848-09-06-S).

To apply, submit a cover letter and résumé to: *wangh@pharm.stonybrook.edu,* or mail to: Dr. Hsien-yu Wang, Associate Professor of Research, Department of Physiology and Biophysics, Health Sciences Center BST T5-180, Stony Brook University Stony Brook, NY 11794-8661

Fax: (631) 444-3432

Equal Opportunity/Affirmative Action Employer. Women, people of color, individuals with disabilities, and veterans are encouraged to apply.

STONY BROOK

Our work is someone's hope. Join us.

At Merck, we believe in putting patients first in all we do. This commitment, along with our focus on developing novel medicines and vaccines that address unmet patient needs, distinguishes us as one of the world s leading research-driven pharmaceutical companies.

Our Basic Research Biology teams are therapeutic area based teams supporting target identification biology, In Vitro target validation, disease-relevant cellular biology, compound mechanism of action studies, and target-related safety and toxicity. Successful candidates will engage in drug discovery and basic research efforts with a focus in biology.

To be considered for any of these opportunities, please visit our career site at **www.merckcareers.jobs/SCIENCE** to create a profile and submit your resume for any of the open positions that may be of interest. To view these opportunities, please visit our career site and search under keywords: BRB.

Merck is an equal opportunity employer, M/F/D/V – proudly embracing diversity in all of its manifestations.

BASIC RESEARCH BIOLOGY OPPORTUNITIES

Rahway, NJ

Ph.D. Scientists & Research Associates

- Experience investigating physiological pathways, ideally metabolic pathways, using In Vivo Models and/or primary cell based systems.
- Exploratory Biomarker, mass spectroscopy experience.
- Experience with pharmacological tools to evaluate In Vivo efficacy and tolerability.
- Experience with cell signaling.

Boston, MA

Ph.D. Scientists & Research Associates

Experience with Musculoskeletal & Respiratory Research, Exploratory Pharmacology, Exploratory Biomarkers and Oncology Research required.

Ph.D. Scientists

Background in Molecular Profiling & Research Informatics and Statistical Genetics required.

Research Associates

Background in In Vivo & In Vitro Sciences required.

West Point, PA

MS or Ph.D. in Neuroscience or related discipline required.

Montreal, Canada

Ph.D. in Microbiology, Biochemistry, Molecular Biology or another relevant biological science required.

www.merckcareers.jobs/SCIENCE

MERCK

SOOCHOW UNIVERSITY

Faculty Positions in Biomaterials and Engineering

Soochow University, founded in 1900 in Suzhou, Jiangsu Province, is a premier university in China. The University is committed to excellence in education, research and innovation. A major expansion of its multidisciplinary research programs is underway across many scientific areas including physics, chemistry, materials sciences, textile engineering and design, life sciences, and medicine. A complete listing of open positions is available at **http://rsc.suda.edu.cn/zpxx.asp?type=15**.

The National Engineering Lab for Silk Exploration Research and Innovation (NELab SERI), Soochow University, invites applications for faculty positions at the levels of **Associate** and **Full Professors** in the following areas: Bio/Functional Materials; Mesoscopic and Nano Materials and Devices; Computational Biophysics; Biosensor and Bioelectronics; Imaging and Spectroscopy Techniques; Textile Engineering and Design; Bio/Medical Chemistry; Synthetic and Supramolecular Chemistry; Surface Sciences and Optics.

Candidates should have a Ph.D. with an outstanding track record, and demonstrate a strong commitment to excel in research and teaching in the above areas. They should possess leadership qualities and are expected to establish their respective research strengths in the Lab. Candidates with outstanding potential and promise will also be considered even if their fields of specialization do not fall within any of the above categories. Successful candidates will be provided with competitive relocation and salary packages, generous start-up funds, and state-of-the-art research facilities.

The recruitment will start immediately and continue until all the vacancies are filled. Outstanding individuals should send their detailed curriculum vitae, a brief research plan and a statement of research interests, and full names and contacts of three referees to: **Mr. Zhen Li, HR Department, Soochow University, Box 428, 50 Donghuan Rd, Suzhou, Jiangsu, 215021, China; Email: sdrcjl@suda.edu.cn; Tel: 86-512-67503045; Fax: 86-512-67503248; http://www.suda.edu.cn/**.

Associate Director for Basic Science
University of Illinois at Chicago Cancer Center

The University of Illinois at Chicago (UIC) Cancer Center is recruiting an outstanding cancer scientist for the key senior leadership position of Associate Director for Basic Science. He/she will have the opportunity to continue to pursue individual laboratory interests while providing scientific direction and guidance to the center's three robust basic science programs: carcinogenesis and chemoprevention, experimental therapeutics and imaging, and tumor cell biology.

This administrative position (25%) reports directly to the UIC Cancer Center Director and will play a key role in shaping the center's scientific direction and achieving its overall goals, including building cancer translational research. He/she will work closely with the associate directors for clinical science and for cancer control and population science.

Specific administrative responsibilities include: i) oversight of intra and inter research program interactions and collaborations; ii) developing program focus, its evaluation and enhancement; iii) guiding and influencing recruitment of new investigators; iv) resource allocation; v) oversight for cancer center basic science shared resources; and vi) involvement in preparing an application for an NCI Cancer Center Support Grant.

Significant institutional resources are available to support this leadership position (dedicated laboratory space, pilot project funds, salary and start-up funds).

The successful candidate must have a PhD and/or MD with a minimum of seven years of cancer research experience, including evidence of substantial scholarly contributions and active, consistent peer-reviewed cancer research funding. Strong leadership, interpersonal, and communication skills are required to advance interdisciplinary and translational cancer research among cancer investigators in the six health science colleges that contribute to the cancer center.

Some administrative experience in an NCI-designated cancer center, an interest in translational cancer research, and a global perspective on cancer research are also desirable.

Academic rank will be determined based on the candidate's credentials and experience. An academic department appointment will be in the most appropriate health science college.

For fullest consideration, submit a cover letter, resume and three (3) references by July 15, 2009 to: jsylvest@uic.edu. UIC is an AA/EOE.

UIC Cancer Center
UNIVERSITY OF ILLINOIS AT CHICAGO
COLLEGE OF MEDICINE

icm
Institut du Cerveau et de la Moelle épinière

Brain and spinal cord research Institute (Paris-France), international institute of neurosciences, ***recruits***

Junior and Senior group leaders

The ICM, will open in the Pitié-Salpétrière university hospital in Autumn 2010. The institute - 22 000 sqm - will host 600 researchers, cutting edge cores facilities, a neuroimaging platform (MRI 3T, MRI 7T, animal MRI 11.7 T), a large clinical research center, animal housing and a biotechnological spin off companies area.

The scientific program aims at developing multidisciplinary research projects of excellence with an emphasis on the discovery of new treatments for diseases of the nervous system.

Deadline: September 5, 2009

Further information and application file on:
http://www.icm-institute.org/job

Weill Cornell Medical College

EXPERIMENTAL PATHOLOGY FACULTY POSITIONS

The Department of Pathology and Laboratory Medicine of the Weill Cornell Medical College invites applications for faculty positions in experimental pathology. Candidates are expected to develop and maintain productive, independent, externally funded research programs in basic mechanisms of human disease which fall within the broad areas of molecular oncology and cancer genetics.

Candidates may hold an MD, a PhD, or combined MD and PhD degrees but must possess a sufficient amount of post-doctoral research training to develop an independent research program. Teaching responsibilities will include graduate and medical students.

The Department offers a supportive intellectual environment in which several mid-level and senior scientists direct well-funded independent research programs in molecular oncology, immunobiology, and vascular biology. Modern research laboratory facilities, excellent core facilities, and competitive start-up packages are available.

Interested applicants should submit a curriculum vitae, representative recent publications, and a brief description of past scientific accomplishments, future research plans, and career objectives, as well as the names of three individuals familiar with the applicant and the applicant's research program. Applications will be accepted until all positions are filled. Please submit via email to **rubinma@med.cornell.edu** or to:

Dr. Mark A. Rubin
Vice Chairman for Experimental Pathology
Department of Pathology and Laboratory Medicine
Weill Cornell Medical College
1300 York Avenue, Box #69
New York, New York 10065

Weill Cornell Medical College is an Equal Opportunity/Affirmative Action Employer. Women and minority candidates are encouraged to apply.

USDA ars Agricultural Research Service
www.ars.usda.gov

"The premier food and agricultural research agency of USDA"

ASSISTANT AREA DIRECTOR

(Agricultural Administrator, GS-0401-15)

Pacific West Area Salary Range of $131,873.00 to $153,200.00
Midwest Area Salary Range of $111,760.00 to $145,290.00

Applications must be received by **July 21, 2009**

The USDA, Agricultural Research Service (ARS) is seeking highly qualified candidates for two permanent full-time leadership positions of Assistant Director for the Pacific West and Midwest Areas, located in Albany, California and Peoria, Illinois, respectively. The Assistant Director is a key member of a Senior Management Team that:

- Implements problem-solving research that provides an abundant, nutritious and safe food supply, protects the environment, and generates sustainable bioproducts and biofuels.
- Leads a large, talented cadre of scientists in an eight-state region.
- Works collaboratively with scientists and administrators within ARS, the Land-Grant Universities, State Agricultural Experiment Stations, other governmental agencies (Federal, state, local), Non-Governmental Organizations, private industry, and other stakeholder groups in the region, nation, and around the world.
- Manages human, fiscal and physical resources.

Candidates seeking a challenging leadership position that contributes to a secure and sustainable agricultural future are encouraged to apply. Applicants must have professional knowledge of research methods related to the biological sciences, environmental sciences, agricultural engineering, food technology or chemistry; knowledge of cooperative and user oriented programs directed toward agricultural research; and excellent leadership and communication skills.

Join us in Advancing the Health and Wealth of the Nation and Its Peoples, Solving Problems, Expanding Knowledge, Delivering Answers

To apply, print a copy of the vacancy announcement from the ARS Careers Website at **http://www.ars.usda.gov/Careers/Careers.htm** (Pacific West Area - **ARS-X9W-0188**) or (Midwest Area - **ARS-X9W-0194**) and follow the application directions provided. For questions about these positions, call **(510) 559-6015** (Pacific West Area) OR **(309) 681-6633** (Midwest Area).

USDA/ARS is an Equal Opportunity Employer and Provider.

International Programme for Advanced Study on the Environment and Climate
Istituto Nazionale di Geofisica e Vulcanologia (www.ingv.it)
Centro Euro-Mediterraneo per i Cambiamenti Climatici (www.cmcc.it)

The International Programme for Advanced Study on the Environment and Climate (PISAC) of the Istituto Nazionale di Geofisica e Vulcanologia (INGV) is currently seeking applications from distinguished scholars for visitor positions, from 6 months up to 12 months. Senior and junior positions are available depending on qualifications.

The PISAC is an interdisciplinary effort focusing on climate change issues from a scientific, historical and socioeconomic perspective. The Program is carried out in cooperation with the Centro Euro-Mediterraneo per i Cambiamenti Climatici (CMCC). The CMCC is an Italian Research Consortium consisting of several Italian public and private research institutions involved in climate-related research, including INGV. Research objectives of CMCC include investigating climate variability and climate change by developing and using models of the Earth System.

Interested individuals are expected to have documented experience in climate research and being motivated to share their expertise and to interact with local scientists. They will benefit from the high performance computing facility and the Earth System Models available to CMCC. Possible research themes include process studies on climate variability and change from seasonal to decadal to century timescales, the carbon cycle, atmospheric chemistry, and ocean data assimilation. Individuals seeking a location for a sabbatical would be suitable applicants.

This is an open call. Applications will be evaluated quarterly. The next deadlines are: 31 August 2009, 30 November 2009, 28 February 2010, and 31 May 2010. In your application, please include a curriculum vitae and a brief research proposal.

Please send your application by email to :
Loredana Amato, email : amato@bo.ingv.it
INGV - Viale Aldo Moro 44
40127 Bologna, Italy

POSITIONS OPEN

Washington University in St. Louis School of Medicine

The Department of Radiation Oncology at the Washington University School of Medicine in Saint Louis, Missouri, seeks qualified applicants for the position of **DIRECTOR, CANCER BIOLOGY DIVISION.** The position is a tenure-track faculty appointment at the rank of **ASSOCIATE** or **FULL PROFESSOR.** Successful candidates must demonstrate significant experience in developmental therapeutics in cancer research and will be expected to establish an innovative research program, provide education and mentorship, and participate in service activities within the medical school at the senior leadership level.

Applicants should forward a cover letter, curriculum vitae, three references, and a description of research to:

Dennis E. Hallahan, M.D.
Elizabeth H. and James S. McDonnell III
Distinguished Professor and Department Head
Department of Radiation Oncology
4511 Forest Park Boulevard, Suite 200
St. Louis, Missouri 63108

HARVARD UNIVERSITY. The Department of Psychology anticipates making one tenure-track appointment at the **ASSISTANT PROFESSOR** level to begin July 1, 2010. The Department conducts experimental research in several areas, including cognition, brain, and behavior; psychopathology and clinical psychology; developmental psychology; and social psychology. Faculty and students in the Department have access to a recently opened state-of-the-art brain imaging facility located nearby the Department.

We are particularly interested in individuals who are working in the areas of judgment and decision making/neuroeconomics, developmental cognitive neuroscience, or human behavioral genetics/brain genomics.

Candidates should expect to have completed the requirements for the Ph.D. prior to appointment and to have demonstrated a promise of excellence in both research and teaching. Teaching duties will include offerings at both undergraduate and graduate levels.

Candidates should submit curriculum vitae and representative reprints and should have at least three letters of recommendation sent to: **Psychology Search Committee, Harvard University, Department of Psychology, WJH 230, 33 Kirkland Street, Cambridge, MA 02138.** The closing date for applying is October 1, 2009.

Applications from women and members of minority groups are strongly encouraged. Harvard University is an Affirmative Action/Equal Opportunity Employer.

POSTDOCTORAL POSITION available immediately to study the molecular mechanisms of T lineage development and transformation using both zebrafish and murine models. Available projects include: (1) executing a zebrafish genetic screen to identify genes controlling T cell development and transformation; (2) understanding the basis for blockade of T cell development by ribosomal protein L22 deficiency (*Immunity* **26:**759-772, 2007); or (3) investigating the role of signal strength in ab/gd lineage commitment (*Immunity* **22:**595-606, 2005). Experience in protein-RNA interactions and/or zebrafish genetics desirable but not essential. The successful applicant will enjoy a competitive salary and will have access to subsidized housing and child care as well as an active postdoctoral association. Curriculum vitae and three references should be sent to: **David L. Wiest, Ph.D., Fox Chase Cancer Center, 333 Cottman Avenue, Philadelphia, PA 19111-2497. Fax: 215-728-2412. E-mail: david.wiest@fccc.edu.** *Equal Opportunity Employer.*

MAX-PLANCK-GESELLSCHAFT

Alexander von Humboldt
Stiftung/Foundation

Call for nominations

Max Planck Research Award 2010

The International Research Award of the Alexander von Humboldt Foundation and the Max Planck Society

The Alexander von Humboldt Foundation and the Max Planck Society jointly confer the Max Planck Research Award on exceptionally highly-qualified German and foreign scientists. The researchers are expected to have already achieved international recognition and to continue to produce outstanding academic results in international collaboration – not least with the assistance of this award. Funding for the award is provided by the Federal Ministry of Education and Research.

Every year, two research awards are conferred on internationally renowned academics. One of the awards should be given to a researcher working in Germany and the other to a researcher working abroad. As a rule, each Max Planck Research Award is endowed with 750,000 Euros. Nominations of qualified female academics are especially welcome.

On an annually-alternating basis, the call for nominations addresses areas within the natural and engineering sciences, the life sciences, and the humanities.

The Max Planck Research Award 2010 will be awarded in the area of life sciences in the field of

Human Evolution

The Rectors/Presidents and Deans of German universities or research organisations are eligible to nominate candidates. Nominations must be submitted by the Rectors/Presidents of the universities or research organisations to the Administrative Headquarters of the Max Planck Society or the Alexander von Humboldt Foundation. Direct applications by candidates themselves are not possible. The deadline for nominations is **26 October 2009.**

Please find further information at either www.humboldt-foundation.de or www.mpg.de.

Max-Planck-Gesellschaft
Hofgartenstraße 8
D-80539 München
phone: +49-(0)89-2108-1265
Fax: +49-(0)89-2108-2240
E-mail: maxplanck-fp@gv.mpg.de

Alexander von Humboldt-Stiftung
Jean-Paul-Straße 12
D-53173 Bonn
phone: +49-(0)228/833-197
Fax: +49-(0)228/833-212
E-mail: leilani.orate@avh.de

The 7th Okazaki Biology Conference "The Evolution of Symbiotic Systems"

Kakegawa, Japan, January 11-14, 2010

The Okazaki Biology Conferences (OBC) hosted by the National Institute for Basic Biology (NIBB), one of Japan's leaders in promoting international cooperation in the field of biology, are international conferences dedicated to providing opportunities to create new international networks of scientists as well as to facilitate the development of future areas of research in the biological sciences. They accomplish these goals by providing both a forum for the presentation and discussion of frontier research and an opportunity to discuss and map out the future direction of the field with researchers from around the world. The conferences are held in relaxing intimate settings that allow participants to get the most out of the time spent.

The theme of the 7th OBC will be "The Evolution of Symbiotic Systems". Symbiosis is a biological phenomenon involving dynamic changes of the genome, metabolism, and signaling network, and a unified comprehension of these interactions is required when studying symbiotic organisms. In the Conference, we will explore a new direction of the fundamental science "Symbiotic systems" using a great variety of living species and bridge the gap between scientists studying various examples of these systems. Organized by **Masayoshi Kawaguchi** (NIBB).

NIBB is calling for speakers to contribute to this conference. Traveling and lodging expenses will be provided for those selected.

For more information please see the link to the 7th OBC homepage below.

Registration Process and Deadline: Please use the link below to download the application form and email the completed form to **obc7@nibb.ac.jp** by **August 10th, 2009**.

National Institute for Basic Biology
TEL: +81 (0)564-55-7596
E-mail: obc7@nibb.ac.jp
URL: http://www.nibb.ac.jp/obc/7th/

NIBB

McMaster University

CANADA EXCELLENCE RESEARCH CHAIR IN MICROBIOME RESEARCH
HAMILTON, ONTARIO, CANADA

Farncombe Family Digestive Health Research Institute
Faculty of Health Sciences
McMaster University

THE OPPORTUNITY
McMaster University has been invited to submit an application for a Canada Excellence Research Chair (CERC) in Microbiome Research. The CERC program was created to recognize that Canada's future prosperity depends on its ability to attract the highest calibre of researchers and scholars to this country. This prestigious program will award the chairholder and their research teams with up to $10 million over seven years to conduct research in areas of strategic importance to Canada. More information on the CERC program can be found at http://www.cerc.gc.ca/

QUALIFICATIONS OF THE POTENTIAL APPLICANT
We are seeking an internationally recognized expert in the field of the intestinal microbiota and probiotics. The successful applicant will work within a large group of scientists expert in host physiology, immunology and mucosal vaccine development, behavior, diabetes and obesity, and to exploit the therapeutic potential of the microbiota in these fields. Applicants must have proven expertise in molecular identification and manipulation of the intestinal microbiota and/or probiotics and must be full professors, or associate professors who are expected to be promoted to the full professor level within one or two years as of November 2009. Alternatively, if they come from outside the academic sector, applicants must possess the necessary qualifications to be appointed at these levels.

The closing date for application is August 31, 2009. The selected candidate will be expected to participate in compiling the final application to the Canadian government (due November 15, 2009). If successful, the start date for the Chair will be July 1, 2010 (negotiable), and will be at the rank of Full Professor in the Department of Medicine.

Qualified applicants should send their Curriculum Vitae to:

John L. Wallace, PhD, MBA, FRSC
Director, Farncombe Family Digestive Health Research Institute
McMaster University
1200 Main Street West, HSC-3N9
Hamilton, Ontario, L8N 3Z5, Canada
Tel: (+1) 905-525-9140, extension 22591
Fax: (+1) 905-528-9862
wallacejohn@mcmaster.ca
http://farncombe.mcmaster.ca

Note: ***All qualified candidates are encouraged to apply. However, Canadian citizens and permanent residents will be considered first for these positions. McMaster University is strongly committed to employment equity within its community, and to recruiting a diverse faculty and staff. The University encourages applications from all qualified candidates, including women, members of visible minorities, Aboriginal peoples, members of sexual minorities and persons with disabilities.***

NW182195RM

POSITIONS OPEN

PH.D. RESEARCH MICROBIOLOGIST

Project description: A Senior Research Microbiologist position is available in the Environmental Sciences and Biotechnology Department at the Savannah River National Laboratory (**website: http://srnl.doe.gov**) for an individual with training in molecular microbiology and biogeochemistry. The successful candidate will join a multidisciplinary team of investigators whose primary focus will be the discovery, development, and implementation of biological processes for the remediation of organic pollutants, metals, and mixed wastes in soils and groundwater. We are keenly interested in applicants that can combine approaches (e.g., stable isotope biogeochemistry, fluorescent in situ hybridization, microanalytical and imaging technologies, genomics) to elucidate cellular metabolism and ecophysiological adaptations as they pertain to microbial interactions during detoxification and stabilization of soils in contaminated environments.

Qualifications: Candidates must have a completed Ph.D. with postdoctoral experience in microbiology, molecular biology, and biogeochemistry. The successful candidate must have a clear ability to obtain funding and maintain a productive research program.

How to apply: Qualified applicants are encouraged to submit a cover letter, detailed curriculum vitae, and reference **job number PR-EX-2009-00143** to the SRNL Recruiting Office at **e-mail: srnlresearchrecruiting@srnl.doe.gov.**

This appointment is open to all qualified U.S. citizens without regard to race, color, age, religion, sex, national origin, physical or mental disability, or status as a Vietnam-era veteran or disabled veteran. U.S. Department of Energy security clearance is required for this position.

POSTDOCTORAL POSITION available to study the molecular mechanism of hepatocyte growth factor–mediated inhibition of lung fibrosis. Experimental approach will involve studies of regulation of gene expression by microRNAs in a mouse model of lung fibrosis and cell culture model of epithelial-mesenchymal transition. The successful applicant will have the opportunity to utilize several cutting-edge technologies using outstanding core facilities at the University of Pittsburgh School of Medicine. Our laboratory has significant collaborations with both basic and clinical science departments. Candidates should have experience in molecular biology. Additional experience in microarray analysis, lentivirus-mediated gene transfer, or immunofluorescence microscopy is highly desirable. Strong written and verbal skills in English are essential. This research is funded by NIH. Please send a brief cover letter, curriculum vitae, and the names and telephone numbers of two references to: **Dr. Prabir Ray, Department of Medicine/Pulmonary Division, University of Pittsburgh School of Medicine, MUH 628 NW, 3459 Fifth Avenue, Pittsburgh, PA 15213. E-mail: rayp@pitt.edu; website: http://www.dept-med.pitt.edu/paccm.**

POSTDOCTORAL POSITION (100 percent, multiyear) in mouse genetics and neurodegenerative disease available immediately at University of California, Davis to use mouse models to study the genetic, cellular, molecular, and mitochondrial mechanisms of neurodegenerative disease. Expertise in cloning, conditional knockouts, and overexpression of genes required. Salary depends upon experience (NIH scale). Send curriculum vitae to **e-mail: gcortopassi@ucdavis.edu. Website: http://cortopassilab.ucdavis.edu.**

UCD is an Affirmative Action/Equal Opportunity Employer.

POSITIONS OPEN

FACULTY POSITIONS in Children's Nutrition Research

The Children's Nutrition Research Center of the Baylor College of Medicine announces the availability of **TENURE-TRACK POSITIONS** in nutrition at the molecular, cellular, and whole organism levels, including translational human nutrition research. Although positions are not limited to these areas, specific interests are fetal, neonatal, and early childhood nutrition (including fundamental mechanisms for the developmental origins of adult health and disease) and obesity (including fundamental adipose tissue biology, regulation of appetite and satiety, development of eating and physical activity behaviors, and prevention/intervention studies).

The level of appointment will be consistent with the candidate's qualifications. Candidates should have a record of achievement through publications in peer-review journals and successful competition for extramural funding. In addition to a strong independent research program, the successful candidate will be expected to have significant potential for research collaboration with existing research programs within the Children's Nutrition Research Center.

Interested candidates should submit their curriculum vitae, a statement of research interests, and three letters of recommendation to: **Dennis M. Bier, M.D., Director, Children's Nutrition Research Center, Baylor College of Medicine, 1100 Bates, Houston, TX 77030-2600.**

Baylor College of Medicine is an Equal Access/Equal Opportunity/Affirmative Action Employer.

SENIOR GENOMICS SCIENTIST

Are you interested in systems genetics?

Do you want to make an impact on genomics research?

At RTI International, you can use your experience, creativity, and bioinformatics skills to address cutting-edge problems in genetics and genomics.

Qualifications include: motivation to establish an independent research program; demonstrated ability to secure funding; experience with development of data visualization tools; experience with analysis of complex data sets.

To learn more and apply, visit **website: http://www.rti.org/job11323.**

We are proud to be an Equal Employment Opportunity/Affirmative Action Employer, Minorities/Females/Persons with Disabilities/Veterans.

The **Center for Genomics and Bioinformatics (CGB) at Indiana University, Bloomington,** carries out independent research in the fields of functional genomics, environmental toxicology, ecology and evolution. The CGB has recently acquired an Illumina sequencer to partner with its Roche Titanium sequencer. We seek a **Bioinformatics Staff Scientist** (at the level of **RESEARCH ASSOCIATE**) to handle the data from these platforms, and to develop programs to analyze the data.

The ideal candidate will have strong programming skills in PERL, C++ and possibly Java. Understanding of basic biological language would be an asset. Ability to design and develop algorithms would also be highly preferred. We require a Masters degree in Computer Science or equivalent. For more details, visit our website: **http://cgb.indiana.edu/careers/**.

Applications received by July 31, 2009 will be assured full consideration for an immediate start date. Send questions to **email:job@cgb.indiana.edu.** Submit a curriculum vitae and a description of your background and interests, and have three (3) letters of recommendation sent to: **Bioinformatics Staff Scientist CGB-015, Center for Genomics and Bioinformatics, Indiana University, 1001 E. 3rd St., Bloomington, IN 47405.**

Indiana University is an Affirmative Action Equal Opportunity Employer.

POSITIONS OPEN

ASSISTANT PROFESSOR
Plant Virology

The Plant Pathology Department at the University of Wisconsin-Madison invites applications for a tenure-track faculty position in Plant Virology at the assistant professor level. Research will focus on the biology of plant viruses and their interaction with plants. We expect the incumbent to interact with other programs to bridge basic and applied research. The incumbent will mentor graduate and undergraduate students and support the university's teaching and training missions. The 9-month appointment carries a 70% research / 30% teaching distribution of effort. Requirements include a Ph.D. in plant pathology, virology, or related discipline; a strong foundation in the principles and concepts of plant pathology and relevant research experience; effective oral and written communication skills; and a positive attitude for teamwork, including the ability to lead and motivate. To apply, submit a curriculum vitae, a cover letter with a statement of research and teaching interests, a copy of undergraduate and graduate transcripts, and three letters of reference to: **Professor Amy Charkowski, Plant Pathology Search Chair, 1630 Linden Dr., Madison, WI 53706.**

Applications received by August 21, 2009 are assured full consideration; review of applications will continue until a suitable candidate is identified.

The University of Wisconsin is an Equal Opportunity/Affirmative Action Employer. Unless confidentiality is requested in writing, information regarding applicants must be released upon request. Finalists cannot be guaranteed confidentiality.

For job details see **website: http://www.ohr.wisc.edu/pvl/pv_060664.html**

POSTDOCTORAL FELLOW (29UC3649)

The University of Cincinnati is currently accepting applications for a Postdoctoral Fellow. The postdoctoral fellow will participate in ongoing research projects using inducible transgenic mouse models created in the Ophthalmic Research Laboratories in the Department of Ophthalmology.

Job description: to examine the molecular and cellular mechanism(s) of ocular surface morphogenesis during embryonic development and pathogenesis of diseases using binary inducible transgenic mouse lines that are currently available in the Ophthalmic Research Laboratories in the Department of Ophthalmology.

Minimum qualifications: Ph.D. in life sciences or M.D.

Ideal qualifications: Individuals with a strong background in molecular biology, molecular genetics, or protein chemistry are preferred.

To apply for position (**29UC3649**), please see **website: http://www.jobsatuc.com.**

The University of Cincinnati is an Affirmative Action/Equal Opportunity Employer. UC is a smoke-free work environment.

MARKETPLACE

INTERNATIONAL SCIENCE & ENGINEERING
VISUALIZATION CHALLENGE

CALL FOR ENTRIES

ENTRY DEADLINE: SEPTEMBER 15, 2009

SCIENCE AND ENGINEERING'S MOST POWERFUL STATEMENTS
ARE NOT MADE FROM WORDS ALONE

When the left brain collaborates with the right brain, science emerges with art to enhance communication and understanding of research results—illustrating concepts, depicting phenomena and drawing conclusions.

The National Science Foundation (NSF) and the journal *Science*, published by the American Association for the Advancement of Science, invite you to participate in the seventh annual International Science & Engineering Visualization Challenge. The competition recognizes scientists, engineers, visualization specialists and artists for producing or commissioning innovative work in visual communication.

Winners in each category will be published in the February 19, 2010 issue of *Science* and *Science* Online, and will be displayed on the NSF Web site.

Award Categories

- Photographs/Pictures
- Illustrations/Drawings
- Informational/Explanatory Graphics
- Interactive Media
- Non-Interactive Media

COMPLETE ENTRY INFORMATION:
WWW.NSF.GOV/NEWS/SCIVIS

PCR ARRAYS

Try A Starter Pack Today!

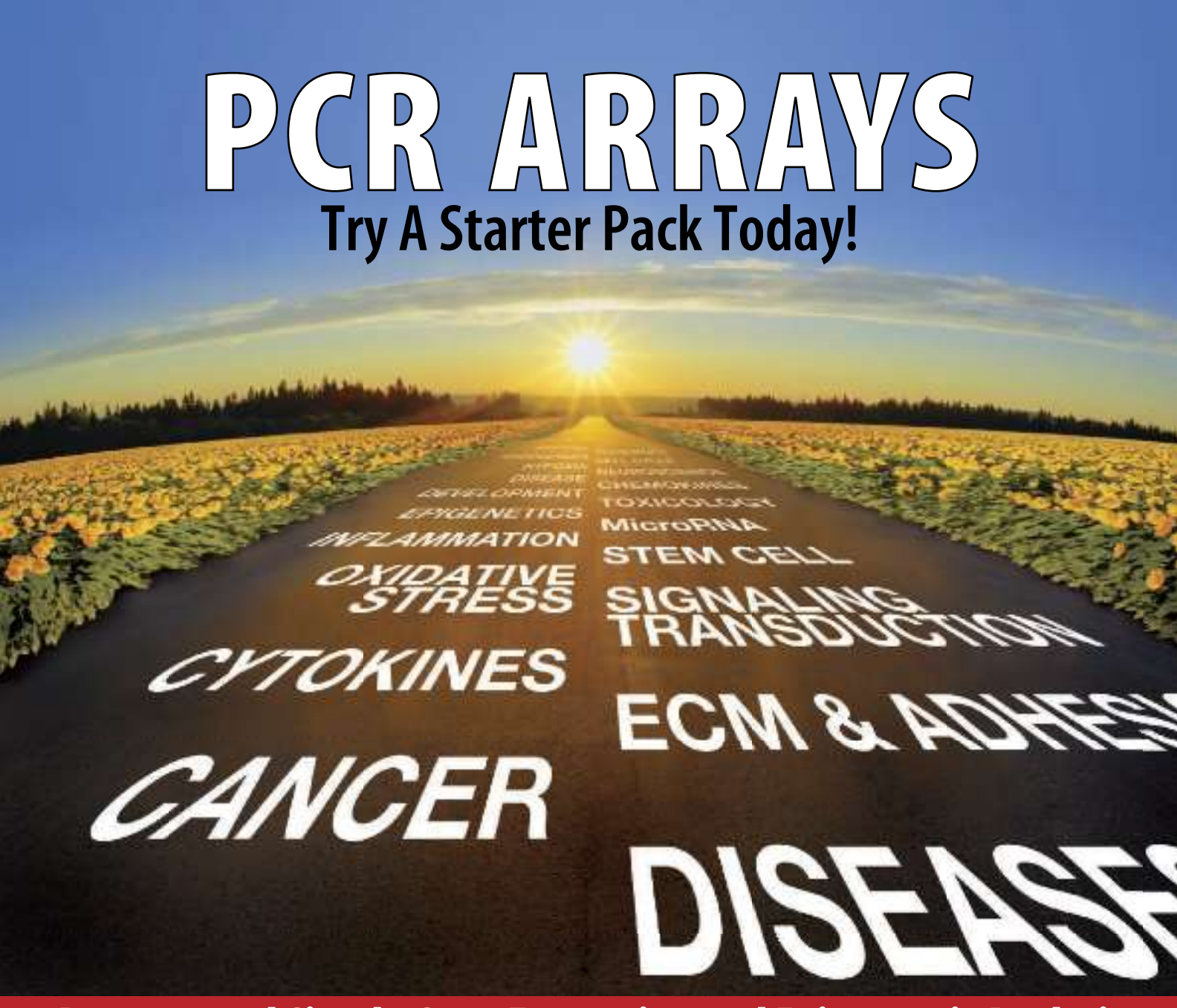

Accurate and Simple Gene Expression and Epigenomic Analysis

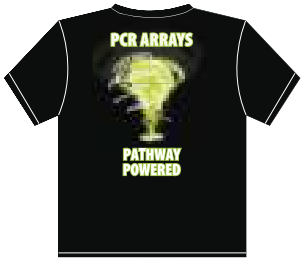

PCR ARRAY STARTER PACK OFFER

Offer Details: ***www.SABiosciences.com/Science5.php***

FREE PCR ARRAY T-Shirt* and PCR ARRAY Handbook!

ACT NOW! Offer Ends 24th of July 2009

* With your order of a PCR Array Starter Pack; while supplies last

SABiosciences™